National Research Council Canada

Conseil national de recherches Canada

NRC · CNRC

Canadian Journal of Fisheries and Aquatic Sciences

Journal canadien des sciences halieutiques et aquatiques

ISSN 0706-652X / CJFSDX 52(2) 233–437(1995)

The *Canadian Journal of Fisheries and Aquatic Sciences*, previously published as *Contributions to Canadian Biology* 1901–1925, *Contributions to Canadian Biology and Fisheries* 1926–1934, *Journal of the Biological Board of Canada* 1934–1937, and *Journal of the Fisheries Research Board of Canada* 1938–1979, is issued monthly to form annual volumes of 12 numbers plus Supplements.

Editorial policy: The *Journal* publishes original research articles, critical reviews, perspectives (essays of opinion or hypothesis), and comments. Papers may concern cells, organisms, populations, ecosystems, or processes that affect aquatic production systems, and they should lead to identifiable conclusions or synthesis, which variously may amplify, modify, question, or redirect accumulated knowledge embodied in contemporary perceptions of a particular state of fisheries and aquatic sciences. They should demonstrate clearly a contribution to knowledge beyond the confirmation state. Originality should relate to more than the particular (a certain year, place, taxon, or chemical compound) such that existing understanding is reformulated or extended.

Manuscripts for publication should be submitted to **Dr. D.G. Cook**, Canadian Journal of Fisheries and Aquatic Sciences, Research Journals, National Research Council of Canada, Ottawa, ON K1A 0R6, Canada (613-993-2209; fax: 613-952-7656; e-mail: cjfas@journals.lan.nrc.ca).

Submissions in English or French are acceptable. The information must be original, that is, not copyrighted, published, or submitted elsewhere except in abstract form or unless by written consent of the Editor. NRC accepts no responsibility for statements or opinions expressed by a contributor. Acceptance of an advertisement, announcement, or other material does not imply endorsement by either the *Journal*'s Editors or NRC. The use of proprietary names does not imply endorsement of the product or company.

Correspondence concerning accepted manuscripts and corrected proofs should be sent to Research Journals, National Research Council of Canada, Ottawa, ON K1A 0R6, Canada.

Instructions to Authors are published once a year in the first issue of each volume; copies can be obtained from the Publishing Office.

Microfilm: Issues from 1934 through the current volume can be purchased on 16- or 35-mm microfilm. Photocopies of individual articles or issues can be purchased from University Microfilms International, 330 North Zeeb Road, Ann Arbor, MI 48106, U.S.A.

Publié sans interruption depuis 1901, le *Journal canadien des sciences halieutiques et aquatiques* a paru sous plusieurs titres : *Contributions to Canadian Biology* 1901–1925, *Contributions to Canadian Biology and Fisheries* 1926–1934, *Journal of the Biological Board of Canada* 1934–1937, et *Journal of the Fisheries Research Board of Canada* 1938–1979. Le *Journal* paraît tous les mois, formant ainsi un volume de 12 numéros, et offre en plus jusqu'à deux suppléments par année.

Politique de rédaction : Le *Journal* publie des articles fondés sur une recherche de originale, des critiques, des essais portant sur une opinion ou une hypothèse (perspectives) et des commentaires. Les textes peuvent avoir trait aux cellules, aux organismes, aux populations, aux écosystèmes ou aux processus qui influent sur les systèmes de production aquatique. Ils doivent aboutir à des conclusions ou synthèses précises qui, de diverses façons, peuvent accroître, modifier, remettre en question ou réorienter le bagage actuel des connaissances et perceptions dans une discipline donnée des sciences aquatiques. Ils doivent clairement démontrer qu'ils contribuent aux connaissances en faisant plus que corroborer des faits. L'originalité doit dépasser le caractère particulier (une année, un endroit, un taxon ou un composé chimique donné) et tenir à une épuration ou à une reformulation des connaissances actuelles.

Les auteurs doivent addresser leurs **manuscrits** à **D.G. Cook**, Journal canadien des sciences halieutiques et aquatiques, Revues scientifiques, Conseil national de recherches du Canada, Ottawa, ON K1A 0R6, Canada (613-993-2209); télécopieur : 613-952-7656; courrier électronique : cjfas@journals.lan.nrc.ca).

Les contributions peuvent être en anglais ou en français. Elles doivent être originales, c.-à.-d. qu'elles ne doivent pas avoir fait l'objet d'un copyright, avoir été publiées ou soumises ailleurs, sauf sous forme abrégée ou avec le consentement du rédacteur. Le CNRC ne se tient en aucune façon responsable des opinions exprimées par un collaborateur ou des déclarations que pourrait faire ce dernier. La pubication d'annonces publicitaires, d'avis et autres n'implique pas l'endossement de leur contenu par les directeurs du *Journal* ou du CNRC. L'utilisation des noms de marques de commerce ne signifie aucunement une sanction du produit en question ou de la compagnie qui le fabrique.

La correspondance ayant trait aux manuscrits acceptés et les **épreuves corrigés** doivent être envoyées aux Revues scientifiques, Conseil national de recherches du Canada, Ottawa, ON K1A 0R6, Canada.

Recommendations aux auteurs sont publiés une fois par année dans le premier numéro de chaque volume. On peut s'en procurer une copie, sur demande, au Bureau des publications.

Microfilms : On peut acheter sur microfilms de 16 ou 35 mm tous les numeeros depuis 1934. Des photocopies d'articles ou de numéros individuels sont aussi en vente auprès de University Microfilms International, 330 North Zeeb Road, Ann Arbor, MI 48106, É.-U.

U.S. second-class postage paid at Champlaing, N.Y., and at additional mailing offices. U.S. POSTMASTER: Send address changes to **Canadian Journal of Fisheries and Aquatic Sciences**, c/o USACAN Media Distrinution Center, P.O. Box 2888, Plattsburg, NY 12901, USA.

Courrier de seconde classe des É.-U. payé à Champlain, N.Y., et d'autres centres de courrier. MAÎTRE DE POSTE des É.-U. : Faire parvenir les corrections d'adresse à **Journal canadien des sciences halieutiques et aquatiques**, a/s du Service de distribution médias USACAN Inc., C.P. 2888, Plattsburg, NY 12901, É.-U.

Volume 52, Number 2, February 1995

Canadian Journal of Fisheries and Aquatic Sciences

Published by the National Research Council of Canada

Volume 52, numéro 2, février 1995

Journal canadien des sciences halieutiques et aquatiques

Publié par le Conseil national de recherches du Canada

Editor / directeur scientifique **D.G. Cook**

Assistant to the Editor / adjointe au directeur scientifique **M.M. Milne**

Consulting Editor / rédacteur-conseil **P.E.K. Symons** (Victoria, B.C.)

Consulting Editor / rédactrice-conseil **N. Moir** (Nepean, Ont.)

Editorial Board / conseil des rédaction

S.E. Campana, *DFO/MPO, Dartmouth*
E.M.P. Chadwick, *DFO/MPO, Moncton*
L.M. Dickie, *DFO/MPO, Dartmouth*
G.S. Jamieson, *DFO/MPO, Nanaimo*
J.R.M. Kelso, *DFO/MPO, Sault Ste. Marie*
J.D. Neilson, *DFO/MPO, St. Andrews*
L.S. Parsons, *DFO/MPO, Ottawa*
R.M. Peterman, *Simon Fraser University*
J.C. Roff, *University of Guelph*
D.M. Rosenberg, *DFO/MPO, Winnipeg*
P. Schwinghamer, *DFO/MPO, St. John's*
(Deputy editor / rédacteur adjoint)
C.J. Walters, *University of British Columbia*
W.G. Warren, *DFO/MPO, St. John's*
N.H.F. Watson, *DFO/MPO, Halifax*

Research Journals / Revues scientifiques

Editor-in-chief / directeur général **Bruce P. Dancik**

Assistant Editor-in-chief / directeur général adjoint **Iain E.P. Taylor**

Publishing Office / Bureau des publications

(Fax / télécopieur : 613-952-7656; e-mail / courrier électronique : research.journals@nrc.ca)

Director / directrice **Aldyth Holmes**

Business Manager / gestionnaire des affaires **Paul McClymont**

Production Manager / gestionnaire de la production **Susan R. Strahlendorf**

Senior Publication Officer / agent principal de publication **Mike Boroczki**

Publication Officer (French manuscripts) / agente de publication (manuscrits français) **Ginette Fortier (613-993-9117)**

Advertising / annonces publicitaires **Hoda Jabbour (613-993-9085)**

Reprints / tirés à part **Eileen Fink (613-993-0151)**

Subscriptions / abonnements **Helen Goulet (613-993-9084)**

© National Research Council of Canada 1995. World rights reserved.

NRC grants **permission*** to individuals who wish to quote short exerpts and reproduce figures, tables, or photographs from articles in this Journal, provided that the source of such material is fully acknowledged. As a courtesy the consent of authors of such material should be obtained.

Authorization to photocopy items for internal or personal use, or the internal or personal use of specific clients, is granted by NRC for libraries and other users registered with the Copyright Clearance Center (CCC) Transactional Reporting Service, provided that the base fee of $3.00 per copy is paid directly to CCC, 21 Congress Street, Salem, MA 01970, USA. 0315-1468/95 $3.00 + 0.00.

*The above permission does not extend to other kinds of copying, such as copying for general distribution, for advertising, or promotional purposes, for creating new collective works (e.g., using published illustrations in a review article), or for resale. For such copying, arrangements must be made with the NRC.

© Conseil national de recherches du Canada 1995. Tous droits réservés.

Le CNRC accorde aux particuliers la **permission de citer*** de brefs extraits et de reproduire des figures, des tableaux, ou des photographies d'articles du Journal, à la condition que la source soit indiquée explicitement. Dans le cas, il convient, par courtoisie, d'obtenir le consentement des auteurs.

Le CNRC autorise les bibliothèques et autres utilisateurs inscrits au Copyright Clearance Center (CCC) Transactional Reporting Service à photocopier les documents destinés à un usage interne ou personnel, ou à l'usage interne ou personnel de clients particuliers, à la condition que le tarif de base de 3 $ par copie soit payé directement au CCC, 21 Congress Street, Salem, MA 01970, É.-U. 0315-1468/95 3,00 $ + 0,00.

*La présente permission ne s'applique pas à d'autres genres de reproduction, notamment la reproduction en vue d'une distribution générale, à des fins de publicité ou de promotion, pour la création de nouveaux travaux collectifs (p. ex., l'emploi d'illustrations publiées dans une synthèse), ou pour la revente. Dans ces cas, il faut prendre les dispositions qui s'imposent en communiquant avec le CNRC.

This journal is indexed or abstracted in / Ce journal est signalé ou résumé dans

Aquatic Sciences and Fisheries Abstracts, Biological & Agricultural Index, CAB Abstracts (Centre for Agriculture and Biosciences), Chemical Abstracts, Current Awareness in Biological Sciences, Current Contents, FAO Freshwater and Aquaculture Contents Tables, FAO Marine Science Contents Tables, Geo Abstracts, GEOBASE, Meteorological and Geoastro physical Abstracts, Oceanic Abstracts, and Science Citation Index

Variation in the relationship between otolith weight and age: implications for the estimation of age of two tropical damselfish (*Pomacentrus moluccensis* and *P. wardi*)

D.G. Worthington, P.J. Doherty, and A.J. Fowler

Abstract: The weight of otoliths may provide an objective and economic method of ageing fish. To investigate this potential, populations of two species of fish (*Pomacentrus moluccensis* and *P. wardi*) were sampled from the lagoons of seven coral reefs within the Great Barrier Reef, Australia. The weight of otoliths increased with age throughout the life of both species. Two factors appeared to have the potential to undermine the use of otolith weight to estimate the age of individuals. First, overlap in the range of otolith weight among fish of different ages caused normally distributed errors in the subsequent estimation of age by otolith weight. Second, variation among reefs in the relationship between otolith weight and age biased subsequent age determinations. Both these types of error also affected the estimation of the age structure of the populations. Random errors in age determination resulted in the smoothing of the age structure whilst bias either shifted or compressed the age structure. While smoothing of an age structure will not compromise the results of several types of analysis, bias will be detrimental to most. Consequently, randomization methods were used to estimate the power of tests to detect variation in the relationship between otolith weight and age. Our results show that by frequently recalibrating the relationship between otolith weight and age, it can be used as an objective and economic method of age determination with the potential to be as reliable as counting annuli in sectioned otoliths.

Résumé : Nous montrons que la mesure du poids d'un otolithe peut constituer une méthode objective et économique pour déterminer l'âge des poissons, et peut être aussi fiable que le dénombrement des anneaux de croissance sur les sections d'otolithes. Le poids des otolithes augmente tout au long de la vie chez deux poissons de récifs coralliens (*Pomacentrus moluccensis* et *P. wardi*) trouvés dans des lagons de la Grande Barrière, en Australie. Deux facteurs ont toutefois limité l'emploi du poids des otolithes pour estimer l'âge : le chevauchement de la fourchette de poids des otolithes entre des poissons d'âges différents causait des erreurs suivant une distribution normale dans l'estimation subséquente de l'âge et la variation de la relation d'un récif à l'autre biaisait les déterminations subséquentes des âges. Les estimations de la structure d'âge étaient aplanies par les erreurs distribuées normalement chez les individus dont on déterminait l'âge, tandis que le biais décalait ou comprimait la structure d'âge. Le lissage d'une structure d'âge ne compromet pas les résultats de divers types d'analyses, mais le biais réduit la validité de la plupart des analyses. En conséquence, nous avons eu recours à la randomisation afin d'estimer la puissance des tests de détecter la variation dans la relation entre le poids de l'otolithe et l'âge. Cela permet de penser qu'un réétalonnage de la relation est possible si l'on détermine l'âge d'un petit nombre de poissons à l'aide de méthodes différentes.
[Traduit par la Rédaction]

Received November 11, 1993. Accepted July 7, 1994.
J12169

D.G. Worthington,[1] P.J. Doherty, and A.J. Fowler. Australian Institute of Marine Science, PMB 3, Townsville MC, QLD, 4810, Australia.

[1] Author to whom correspondence should be addressed at: NSW Fisheries Research Institute, P.O. Box 21, Cronulla, NSW 2230, Australia.

Introduction

Methods of stock assessment that require information on the age structure of populations form the basis of fisheries management (see review by Megrey 1989). Age structures have traditionally been estimated by interpreting annual marks in the scales or otoliths of fish (e.g., Francis et al. 1992). Differences in the interpretation of annuli by the same reader and among readers can affect the apparent age of individual fish and, as a result, the estimated age structure of a population (Boehlert and Yoklavich 1984). Similarly, the time-consuming procedures required to section and prepare otoliths may restrict the size of the sample that can be aged and, hence, affect the precision of the estimated age structure. Consequently, more reliable estimates of age structure could be produced by a more objective and economic method of determining the age of individual fish.

One alternative method of ageing that has the potential to be both objective and economic uses the weight of otoliths to assign an age to a fish (Boehlert 1985; Pawson 1990; Fletcher 1991). This method first requires a knowledge of the relationship between the age of a fish and the weight of its otolith. As otoliths may increase in weight throughout the life of a fish (Fowler and Doherty 1992) and appear not to be greatly resorbed (Mugiya and Watabe 1977), there may be a direct relationship between otolith weight and age. If the relationship between otolith weight and age can be estimated, a calibration curve (Snedecor and Cochran 1989) can be established, and subsequently used to estimate the age of a larger sample of fish. In common with traditional methods of ageing, the use of otolith weight may result in both random errors and bias in age determination. In contrast, because of the reduced processing time (see Boehlert 1985), the use of otolith weight may allow larger samples to be aged, thus reducing sampling error.

Errors in age determination can have considerable influence on subsequent stock assessment models (Lai and Gunderson 1987; Tyler et al. 1989; Bradford 1991). Consequently, variability in the determination of age by annuli has been well investigated for many species (e.g., Boehlert and Yoklavich 1984; Kimura and Lyons 1991), and several techniques have been developed to compare this variability among different methods (Kimura et al. 1979; Beamish and Fournier 1981; Chang 1982) and compensate for any systematic errors (Hoenig and Heisey 1987; Richards et al. 1992). In contrast, no study has yet used these techniques to investigate variability in age determination using otolith weight, or compared such variability to that when age is determined by annuli (see also Boehlert 1985). This comparison is particularly relevant in tropical regions where the less seasonal environment can increase the ambiguity of structures in the otolith.

Populations of damselfish have been extensively studied on the Great Barrier Reef (GBR), Australia (see review by Doherty and Williams 1988). Damselfish are small (<100 g) benthic fishes that, in general, move less than a few metres after settlement to the reef. As a result, populations on different coral reefs are completely isolated, except for the potential exchange of larvae, enabling discrete populations to be easily sampled at a range of spatial scales. One study described samples of *Pomacentrus moluccensis* and *P. wardi* from a complex of seven coral reefs, and related present patterns in age structure among the reefs to past patterns in recruitment (Doherty and Fowler 1994). It was possible to estimate the age structure of these populations, from the Capricorn–Bunker region in the southern GBR, using sectioned otoliths that displayed an interpretable pattern of increments validated as being formed annually (Fowler and Doherty 1992). In locations further north (i.e., almost 1000 km, in the Central Region of the GBR) the opaque regions that form annuli in the otolith of both species are less clear, and few *P. wardi* can be aged (Fowler and Doherty 1992). Consequently, we wished to investigate the potential of alternative ageing techniques. The sample of fish from the Capricorn–Bunker region enabled an examination of the utility and limitations of using otolith weight to estimate age.

Two factors were considered to have the potential to undermine the use of otolith weight to estimate age. First, the range in otolith weight for fish of a given age may cause an overlap in otolith weights for fish of different ages. This would reduce the ability of otolith weight to discriminate between different age-classes and could affect the frequency and magnitude of random errors in age determination. Second, there may be variation in the relationship between otolith weight and age. For example, spatial variation in the slope or elevation of the relationship could bias subsequent age determinations if the relationship from one area were applied in another. Here, we assess the influence of the above two factors on the potential of otolith weight to estimate the age of individual fish and the age structure of populations. This was done by comparing the ages and age structures estimated by otolith weight with those determined by annuli for both *P. mollucensis* and *P. wardi*.

Methods

Collection of fish and analysis of otoliths

During September and October 1989, all *P. mollucensis* and *P. wardi* were collected from 10 small patch reefs (i.e., each with a surface area of approximately 100 m^2) within the lagoons of seven coral reefs in the Capricorn–Bunker region of the southern GBR, Australia (152°E, 23–24°S). The patch reefs were chosen from throughout the lagoon of each reef to provide a representative sample that would encompass any variation in the relationship between otolith weight and age within the reefs. Rotenone poison was released within barrier nets that encircled each patch reef, and fish were collected by hand (see Doherty and Fowler 1994).

Sagittal otoliths were removed from each fish and both were weighed to the nearest 0.01 mg. There were no consistent differences between left and right otoliths, and all weights reported here are for the right sagittae. One otolith of each fish was then cut to produce a thin (400 μm), transverse section using the methods described in Fowler and Doherty (1992). Sections were examined using a compound microscope with transmitted light (at ×60 magnification) and opaque zones of the annuli were counted.

Fig. 1. Mean, standard error (vertical bars), and range (horizontal bars) of otolith weight for each age-class of *P. moluccensis* and *P. wardi* on two reefs. The two reefs are those with the most different slopes for the relationship between otolith weight and age for each species.

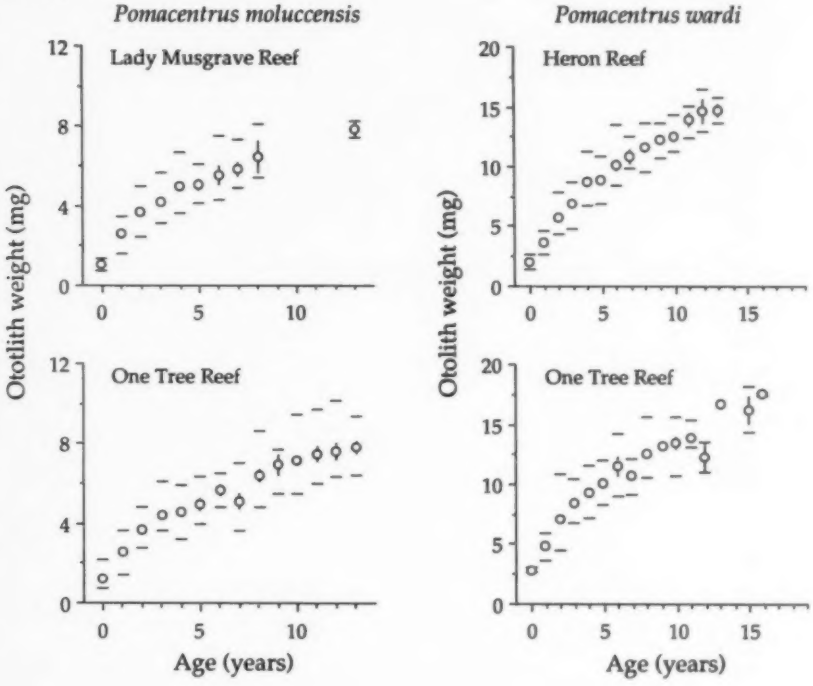

All age determinations from annuli were done by one of us (A.J.F.), and the resulting estimates are referred to as "true" ages, while those determined by otolith weight are referred to as "estimated" ages.

Relationship between otolith weight and age

The relationship between otolith weight and age was described using linear regression with otolith weight as the dependent variable and age the independent. Both variables were transformed to $\log_e (x + 1)$ to enable the data to conform to assumptions of linearity, normality, and homogeneous variance. The relationship between otolith weight and age was compared among reefs using analysis of covariance (ANCOVA). A random sample of fish was taken from reefs with greater than the minimum sample size to make the analysis balanced. The specific differences among reefs in the slope of the relationship between otolith weight and age were investigated by the Tukey–Kramer method (Snedecor and Cochran 1989).

Estimation of age by otolith weight

When transformed, there was a linear relationship between otolith weight and age, and an approximately normal distribution of otolith weights for fish of each age. This enabled the use of linear calibration (Snedecor and Cochran 1989) to estimate the age of fish from the weight of its otolith, instead of nonparametric procedures (such as the age–length key; see Kimura 1977). To estimate the age of a fish from the weight of its otolith, a continuous variable (i.e., otolith weight) must be transformed to a discrete variable (i.e., age-class). Initially, otolith weight was used to estimate age on a continuous scale. These continuous ages were then rounded to the nearest integer to produce the discrete variable of age-class. Errors in the determination of age by otolith weight resulted in the estimation of some continuous ages less than zero, which were subsequently classified as 0^+ individuals.

The best conditions for the estimation of age from otolith weight will occur when a strong relationship exists between the two variables. If the relationship between otolith weight and age is weak, or if an inappropriate calibration relationship is used, conditions for the estimation of age will deteriorate. The strongest relationship between otolith weight and age for either species was from *P. wardi* on Wistari Reef (see Results). In contrast, the weakest relationship between otolith weight and age for either species was from *P. wardi* on One Tree Reef (see Results). Use of each of these relationships to estimate the age of individuals on the same reef allowed an assessment of the range of errors in ageing caused simply by overlap in otolith weight among different age-classes. To assess the possible effects of using an inappropriate calibration relationship, we estimated the age structure of *P. wardi* on Heron Reef by the relationship derived from One Tree

Table 1. Sample size and mean otolith weight (standard error in parentheses) and range for different age-classes of *P. moluccensis* and *P. wardi* for the total sample of fish collected from seven reefs.

	Pomacentrus moluccensis			*Pomacentrus wardi*		
True age	*n*	Otolith weight (mg)	Range	*n*	Otolith weight (mg)	Range
0	145	1.16 (0.02)	0.60–2.20	83	2.19 (0.06)	1.11–3.63
1	273	2.41 (0.03)	1.40–3.73	104	4.33 (0.09)	2.16–6.54
2	160	3.45 (0.05)	2.24–6.18	173	6.33 (0.08)	4.03–10.85
3	142	4.07 (0.05)	2.85–6.18	183	7.64 (0.09)	4.73–15.22
4	103	4.66 (0.08)	3.13–6.71	83	8.82 (0.13)	6.20–11.60
5	70	4.88 (0.11)	3.51–8.65	82	9.64 (0.14)	6.61–12.39
6	64	5.37 (0.10)	4.02–7.63	67	10.72 (0.16)	7.80–14.18
7	84	5.54 (0.10)	3.60–7.42	79	11.24 (0.14)	8.81–13.61
8	49	6.18 (0.15)	4.36–8.60	78	11.92 (0.14)	9.07–15.64
9	17	6.23 (0.21)	4.88–7.70	33	12.19 (0.20)	10.03–14.34
10	83	6.74 (0.10)	4.85–9.50	32	13.24 (0.30)	10.70–17.84
11	26	6.96 (0.21)	5.36–9.70	29	13.65 (0.31)	9.64–17.61
12	17	7.09 (0.26)	5.94–10.10	26	14.47 (0.30)	11.04–18.09
13	20	7.48 (0.26)	5.60–9.84	9	15.56 (0.39)	13.62–17.27
14	1	9.30	—	1	17.32	—
15	6	8.97 (0.95)	6.10–11.70	4	16.10 (0.77)	14.37–18.13
16	1	7.50	—	2	17.67 (0.04)	17.63–17.70
17	2	8.58 (0.92)	7.66–9.50	1	17.68	—
18	0	—	—	1	19.05	—

Reef. The slope of the relationship from these reefs were the most different for either species, and there were also differences in the intercept of the two relationships.

Three indices of ageing error were used to assess the differences between each true and estimated age, and were then averaged over all individuals within each true age-class, and over all age-classes (see also Kimura and Lyons 1991). First, the coefficient of variation (CV; Chang 1982) was calculated as the standard deviation of true and estimated ages divided by their mean. Second, bias was defined as the true age minus the estimated age. Both the CV and bias are zero when all individuals are correctly aged, and increase as the frequency and magnitude of ageing errors increase. The third index used was the percent agreement that simply identifies the percentage of ages estimated by otolith weight that agreed with the true age.

Ability to detect differences in the relationship between otolith weight and age

When using linear calibration, the most common cause of bias is the use of an inappropriate relationship (Snedecor and Cochran 1989). Considering the potential for variation in the relationship between otolith weight and age, it would be appropriate to confirm the relationship between otolith weight and age when sampling a new site, or resampling an existing site. If this involved ageing large numbers of fish, it would compromise the economy of the method. An alternative approach would be to age a small number of fish from a new sample to determine if the relationship between otolith weight and age for these individuals was different from the standard relationship used previously. Consequently, it would be desirable to know the ability of tests (i.e., their power) to detect differences in the slope of the relationship between otolith weight and age. We investigated this question using randomization by treating the relationship derived from One Tree Reef for *P. wardi* as a standard, and estimating the power of tests to detect the relationships from Heron or Fitzroy Reef. These reefs were chosen as they represented the two most different slopes (One Tree and Heron) and the two most similar slopes that were still significantly different (One Tree and Fitzroy). Five hundred random selections of 5, 10, 20, 30, 50, and 100 individuals from Heron and Fitzroy reefs were used to estimate the slope of the relationship between otolith weight and age for each reef. Each of these slopes was then compared with the slope from the complete sample from One Tree Reef using a *t*-test. The frequency of significant tests then represents the conditional power of the test. Tests with higher power have a greater ability to detect the specified differences in slope of the relationship.

Results

Relationship between otolith weight and age

A total of 1263 *P. moluccensis* (ranging in age from 0 to 17 years old) and 1070 *P. wardi* (ranging 0 to 18 years old) were collected from the seven reefs. The average weight of otoliths of both species increased with age for all the ages sampled, although there was a considerable range in otolith weight within each age-class (Fig. 1, Table 1).

Table 2. Summary of parameters from regressions of otolith weight on age (i.e., otolith weight = $a + b$.age) to be used for linear calibration. ANCOVA tests the significance of differences in the slope (i.e., b) of the relationship among reefs, and vertical lines join slopes that are not significantly different. The coefficient of determination is shown as r^2, and F refers to the ratio of the mean squares due to the regression and the residual.

Reef	n	b	a	r^2	F
Pomacentrus moluccensis					
One Tree	177	0.48	0.94	86.2	1089
Fairfax	199	0.49	0.90	87.7	1405
Llewellyn	147	0.50	0.86	86.0	893
Wistari	162	0.50	0.81	92.4	1936
Heron	205	0.53	0.83	90.4	1922
Fitzroy	216	0.54	0.78	89.1	1751
Lady Musgrave	157	0.57	0.84	84.9	868
ANCOVA: $F_{6,1015} = 3.2$; $P < 0.01$					
Pomacentrus wardi					
One Tree	194	0.49	1.51	84.2	1028
Fitzroy	164	0.56	1.26	87.9	1126
Lady Musgrave	110	0.60	1.36	87.8	776
Fairfax	95	0.61	1.30	91.2	968
Llewellyn	156	0.62	1.19	88.8	1216
Wistari	171	0.63	1.21	95.8	4021
Heron	180	0.65	1.13	94.4	3007
ANCOVA: $F_{6,651} = 9.5$; $P < 0.001$					

Consequently, the range of otolith weights overlapped among separate age-classes for both species. For example, individuals of *P. moluccensis* with an otolith weight of approximately 6 mg were found in age-classes from 2 to 13. Furthermore, the range and variability in otolith weight within an age-class increased with age for both species (Table 1). As a result, the overlap in otolith weights among age-classes also increased with age.

There was a highly significant relationship between otolith weight and age for both species on each reef (Table 2). Otolith weight explained 86.0–92.4% of the variation in age of *P. moluccensis*, and 84.3–95.8% of the variation in age of *P. wardi*. The slope of the relationship between otolith weight and age differed among reefs for both species (Table 2). That is, the average growth in weight of the otolith varied among reefs. For example, the otoliths of *P. wardi* from One Tree Reef grew in weight at a significantly slower rate than on all other reefs (Table 2, Fig. 1). Similarly, the growth in weight of otoliths of *P. moluccensis* from One Tree Reef was significantly slower than those from Fitzroy and Lady Musgrave reefs (Table 2, Fig. 1). Apparently, the growth in weight of the otolith of both species is consistently slower on some reefs than others.

Estimation of age by otolith weight

Using an appropriate relationship

When the relationship from Wistari Reef was used to estimate the age of *P. wardi* individuals from the same reef, most (61%) of the individuals were estimated to be the same age as determined by annuli. Only 11% of individuals were estimated to be greater than 1 year different from the true age. Estimated ages were most reliable and least biased in the young age-classes (Table 3). For example, 35 of the 37 individuals in the 0 age-class were correctly aged, and there was little bias. In contrast, one 12-year-old fish was estimated to be 9, and most were under aged. The average CV across all age-classes was 5.4%. There was no significant difference between the estimated and true age structures for Wistari Reef (Kolmogorov–Smirnov test, $P > 0.05$; Fig. 2*b*), although it is clear that the peaks and troughs evident in the true-age structure have been smoothed by the use of otolith weight (Fig. 2*b*).

Table 3. Comparison of age determinations from annuli and otolith weight for *P. wardi* on Wistari Reef. Otolith weight was used to estimate age with the relationship derived from fish on Wistari Reef.

True age	Count	Range of estimates	Percent agreement	CV (%)	Bias (years)
0	37	0–2	95.2	3.4	0.10
1	20	1–2	80.0	5.7	0.20
2	16	1–4	62.5	10.0	0.38
3	18	2–4	61.1	6.4	0.28
4	4	4–6	25.0	12.3	1.00
5	8	4–7	75.0	4.1	0.13
6	12	4–7	50.0	6.1	−0.08
7	15	5–9	26.7	8.4	0.00
8	16	6–9	50.0	5.2	−0.38
9	7	7–10	28.6	6.3	−0.29
10	2	11–11	0.0	6.2	1.00
11	4	9–13	0.0	9.0	−0.50
12	9	9–13	22.2	9.2	−1.33
13	2	12–14	0.0	5.1	0.0
14	1	14	100.0	0.0	0.0

When the relationship from One Tree Reef was used to estimate the age of *P. wardi* individuals from that reef, 36% of the individuals were estimated to be the same age as determined by annuli. Of those incorrectly aged, 90% were within 2 years of the age determined by annuli, although one 12-year-old fish was estimated to be 6 years old based on the weight of its otolith. The CV for each age-class was consistently greater than the Wistari example (compare Tables 3 and 4) and the average CV across all age-classes was 10.5%. Similar to the example from Wistari Reef, there was no significant difference between the estimated and true age structures for One Tree Reef (Kolmogorov–Smirnov test; $P > 0.05$). Once again, it is clear that the peaks and troughs evident in the true age structure have been smoothed by the use of otolith weight (Fig. 2*b*). In particular, the proportion of fish in the troughs of 4-, 6- and 9-year-old fish were increased, and the peaks of 2-, 3- and 8-year-old fish were reduced (Fig. 2*b*).

As well as the above examples, age structures were estimated for both species on each reef using the appropriate relationship between otolith weight and age (Fig. 2).

Fig. 2. Age structures of (a) *P. moluccensi* and (b) *P. wardi* from all reefs sampled. Bars show true age structure determined from annuli in sectioned otoliths and lines show estimated age structure from the relationship between otolith weight and age for each reef.

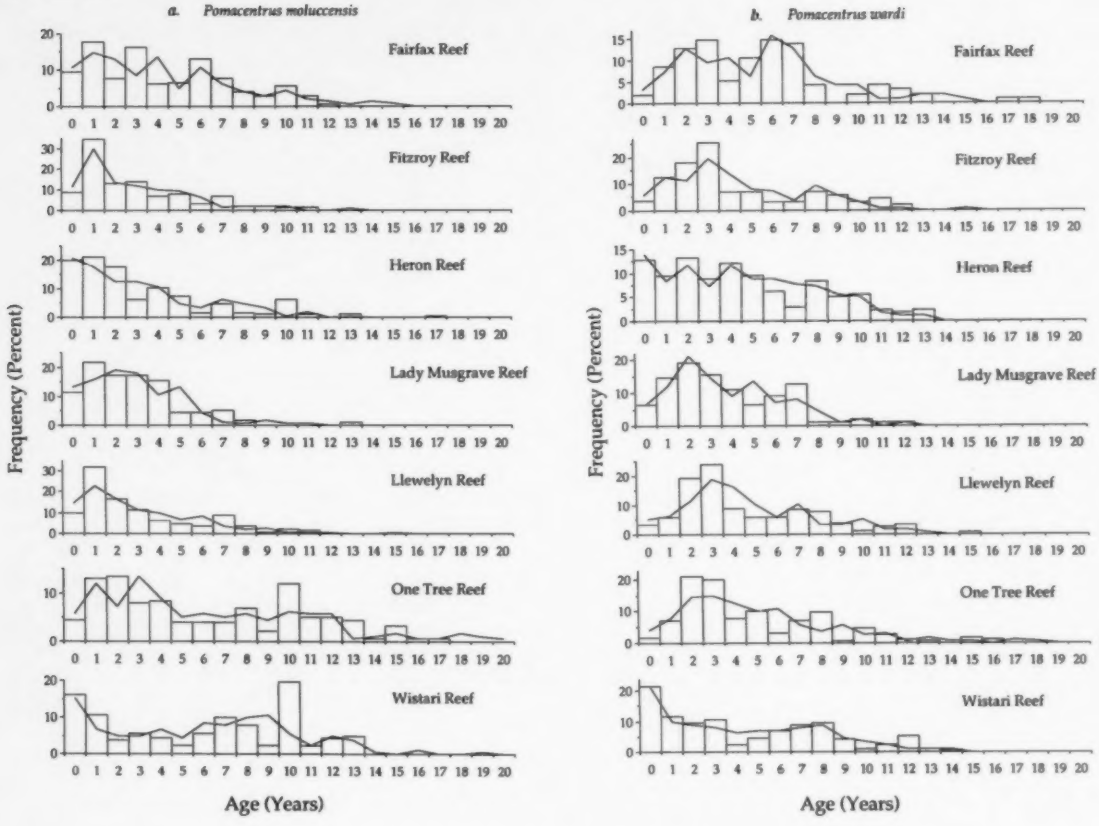

In general, it is apparent that the use of otolith weight smooths the true age structure. This is shown most clearly by the strength of all relatively abundant age-classes (e.g., 10-year-olds of *P. moluccensis* from One Tree and Wistari reefs; Fig. 2*a*) being underestimated by otolith weight. Conversely, the strength of most weak age-classes is overestimated by otolith weight. Despite this, there was no significant difference among the true and estimated age structures for any reef (Kolmogorov–Smirnov tests, $P > 0.05$). It also appears that the differences in age structure among reefs were maintained when otolith weight was used to estimate age (Fig. 2).

Using an inappropriate relationship

When the relationship from One Tree Reef was used to estimate the age of individuals from Heron Reef, 28% of the individuals were estimated to be the same age as determined by annuli. Sixty percent of the individuals were estimated to be younger than the true age. This negative bias in estimation increased with age (Table 5), because the relationship used to estimate age had a lower slope than the appropriate relationship. The average CV across all age-classes was 15.7%. There was a significant difference between the true age structure of Heron Reef and that estimated using the calibration relationship from One Tree Reef (Fig. 3; Kolmogorov–Smirnov test, $P < 0.01$). Despite this, the age structures are of the same general shape, although the peaks evident in the true age structure have been smoothed by the use of otolith weight, and there has been a reduction in the average age of individuals.

Ability to detect differences in the relationship between otolith weight and age

When trying to detect a difference in the slope of two relationships as great as that between One Tree and Heron reefs for *P. wardi* (Table 2), only small numbers of fish (e.g., 10–20) would need to be aged from the new sample to allow a powerful test (i.e., power of 85–95%) against the previously used standard relationship (Fig. 4). In contrast, to detect differences in the slope of two relationships as small as those between One Tree and Fitzroy reefs for *P. wardi* (Table 2), a much larger number (e.g., 80–100) of fish would need to be aged from the new sample to allow a powerful test (Fig. 4). Consequently, the size of the subsample of fish aged to achieve a given power is dependent on the difference in slopes that it is desired to

Table 4. Comparison of age determinations from annuli and otolith weight for *P. wardi* on One Tree Reef. Otolith weight was used to estimate age with the relationship derived from fish on One Tree Reef.

True age	Count	Range of estimates	Percent agreement	CV (%)	Bias (years)
0	3	0–0	100.0	0.0	0.00
1	14	0–1	64.3	16.8	−0.36
2	41	0–6	51.2	14.3	0.27
3	39	2–5	38.5	12.5	0.54
4	15	2–7	26.7	14.4	0.27
5	20	3–7	30.0	11.1	0.15
6	6	4–11	33.3	15.9	1.17
7	14	4–8	21.4	12.8	−1.14
8	19	6–13	21.1	9.4	0.32
9	1	9	100.0	0.0	0.00
10	9	6–13	11.1	12.9	−0.56
11	5	9–12	20.0	7.5	−0.80
12	2	6–10	0.0	27.1	−4.00
13	1	15	0.0	9.4	2.00
14	0	—	—	—	—
15	3	11–17	0.0	11.0	−1.00
16	2	17–17	0.0	4.0	1.00

Table 5. Comparison of age determinations from annuli and otolith weight for *P. wardi* on Heron Reef. Otolith weight was used to estimate age with the relationship derived from fish on One Tree Reef.

Age (from annuli)	Count	Range of estimates	Percent agreement	CV (%)	Bias (years)
0	23	0–0	100.0	0.0	0.00
1	17	0–1	11.8	41.6	−0.88
2	24	0–3	16.7	24.7	−0.71
3	16	1–4	25.0	19.9	−0.81
4	22	2–6	31.8	14.5	−0.23
5	17	2–6	11.8	19.6	−1.06
6	11	3–10	9.1	19.0	−0.82
7	5	5–8	20.0	13.8	−1.00
8	15	5–10	20.0	12.8	−1.07
9	9	6–10	11.1	11.2	−1.22
10	10	6–11	10.0	14.6	−1.80
11	4	8–12	25.0	8.0	−0.75
12	3	9–14	0.0	11.4	−0.67
13	4	10–13	25.0	9.8	−1.75

detect and, in turn, that will be dependent on the desired degree of accuracy and precision in the subsequent age determination and age structure. Improvements in power could be achieved by taking a size-structured sample of fish for ageing (i.e., a selection of large and presumably old fish, and a selection of small and presumably young fish). If this were done, it would result in a more reliable estimate of the relationship between otolith weight and age for a given number of fish sampled.

Discussion

Relationship between otolith weight and age

The average weight of otoliths increased with age throughout the life of both *P. moluccensis* and *P. wardi*. This implies that otolith weight may provide a rapid and economic method of ageing, as suggested in many previous studies (e.g., Templeman and Squires 1956; Boehlert 1985; Reznik et al. 1989; Pawson 1990; Fletcher 1991). Several of these authors have emphasised that the average weight of otoliths in old fish continues to increase unlike other variables (e.g., standard length, weight, otolith length, etc.). Indeed, growth of otoliths appears to be somewhat decoupled from other somatic growth rates, and may simply be more closely related to time and age (Reznik et al. 1989). Consequently, otolith weight provides a more accurate estimate of age than these other parameters (e.g., Fletcher 1991) and, in some circumstances, may provide a more reliable estimate of age than annuli in sectioned otoliths (e.g., when interpretation of annuli is ambiguous).

Many previous studies have investigated the relationship between otolith weight and age, and cited its strength and apparent potential for age determination. Reported coefficients of determination range from otolith weight explaining 95% of the variation in age of splitnose rockfish (*Sebastes diploproa*) (Boehlert 1985) to 51% of the variation in age of Pacific hake (*Merluccius productus*) (Beamish 1979). Most studies report otolith weight explaining 80–95% of the variation in age (e.g., Radtke et al. 1985; Beckman et al. 1991; Wilson et al. 1991; Fletcher 1991). In this study, otolith weight explained 84–96% of the variation in age of *P. moluccensis* and *P. wardi*. That is, values spanned the range commonly reported for the relationship between otolith weight and age. Unfortunately, the coefficient of determination is not the best index on which to assess the utility of otolith weight to estimate age, as it does not directly incorporate information on the slope of the relationship. This is important as more reliable estimates of age will be possible when there is little variation in otolith weight within age-classes and large variation among age-classes. That is, there is a tight fit of observations to a relationship with a high slope. Consequently, the ratio of the mean squares due to the regression and the residual, which is traditionally used to assess the significance of a regression relationship, is a more appropriate index of the potential of otolith weight to estimate age.

Estimation of age by otolith weight

Overlap in the range of otolith weights for fish from adjacent age-classes contributed to the errors in ageing. Overlap was approximately symmetrical among adjacent age-classes, and consequently mainly resulted in normally distributed errors in the estimation of age. Nonetheless, variability in otolith weight did increase with age, causing an increase in the overlap of otolith weights of fish from older age-classes. This resulted in decreased precision of ages estimated for older fish, a result similar to that reported for the use of annuli (Kimura and Lyons 1991). Within the age structure, such ageing errors led to the loss of incorrectly aged individuals from an age-class

Fig. 3. Age structures of *P. wardi* from Heron Reef. Bars show true age structure determined from annuli in sectioned otoliths and lines show estimated age structure from the relationship between otolith weight and age from One Tree Reef.

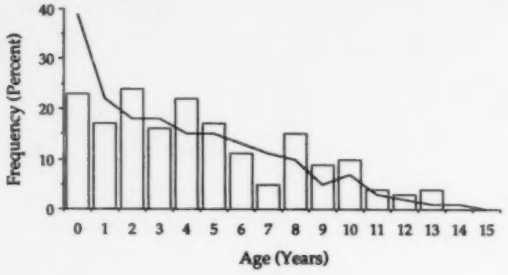

Fig. 4. Results of simulations to estimate the power to detect a significant difference between the slopes of two relationships between otolith weight and age of *P. wardi*. Values are given for differences in slope as large as those between One Tree and Heron reefs (open circles) and One Tree and Fitzroy reefs (filled circles).

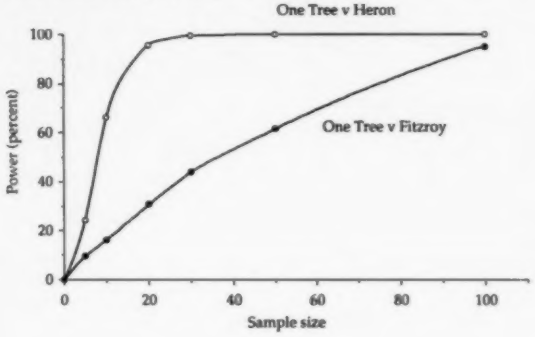

and the addition of incorrectly aged individuals from adjacent age-classes. The frequency of incorrectly aged individuals lost and gained by an age-class in this way is dependent on both the size of the error and the abundance of each age-class. For example, Kimura and Lyons (1991) noted "if two adjacent year-classes have absolute strengths of 10 and 100 fish, a 10% imprecision of ±1 year will add 5 fish from the strong year-class to the weak one (a 50% change) but only one-half a fish from the weak year-class to the strong (a 0.5% change)". That is, the true peaks and troughs in an age structure can be smoothed by normally distributed ageing errors (see also Richards et al. 1992). Overlap in otolith weight among age-classes will be the most common cause of such errors when using otolith weight to estimate age.

In contrast with overlap in otolith weight among age-classes, spatial variation in the relationship between otolith weight and age biased subsequent estimates of age. For example, if a relationship with a lower elevation than the true relationship is used, the ages of all fish will be underestimated, resulting in the shifting of the age structure. A calibration line with a lower slope than the true relationship will underestimate the age of old fish more than young fish, resulting in the compression and (or) shifting of the age structure (e.g., Table 5). Once again, biases similar to these are frequently reported when using annuli to estimate age (Boehlert and Yoklavich 1984). Regardless, any biases in ageing can seriously modify age structures, with resultant implications for subsequent analyses (Lai and Gunderson 1987; Bradford 1991). Consequently, it is important to use an appropriate calibration relationship to estimate age from otolith weight.

Whilst errors in the determination of age will occur when using otolith weight, a great deal of the subjectivity of age determination can be removed. This is obviously desirable when it can be stated that traditional techniques of age determination are "as much an art as a science" (Williams and Bedford 1974). Determining age by annuli involves the counting of marks in otoliths, the interpretation of which may change among replicate readings, as a reader becomes more experienced or among different readers. Once an appropriate relationship between otolith weight and age has been determined, subjective errors can only be introduced during the estimation of the weight of an otolith. This process will obviously be less subjective than interpretation of annuli for most species. As a consequence, there will be little if any variation among replicate estimates of age for the same otolith. Errors in the determination of age by otolith weight will be dominated by objective errors simply caused by the relationship between otolith weight and age. Perhaps most importantly, such objective ageing errors will be more easily quantified and corrected (see Richards et al. 1992) than errors in interpretation of annuli that differ among readers and through time.

Throughout this paper we have assumed that the initial annuli counts represented the true age of each individual. This is almost certainly untrue. Errors in the interpretation of annuli in otoliths are frequent and there can be substantial variability both among and within readers of the same otolith (e.g., Boehlert and Yoklavich 1984). Similarly, there can be spatial or temporal variation in the interpretability of a species' otoliths (Fowler and Doherty 1992). Errors caused by such factors may complicate the use of otolith weight to estimate age, as the method is constrained by the reliability of the initial age estimates used for calibration. That is, if imprecise or biased estimates of age are used for calibration, the use of otolith weight to estimate age will be similarly affected. As a consequence, the use of known-age fish for calibration may greatly increase the reliability of subsequent age determinations using otolith weight. Alternatively, in any sample of fish to be used for calibration, extra effort can be used to ensure some consensus of opinion among separate readers of the annuli.

The CV has been previously used as an index of the precision of a set of age determinations (e.g., Chang 1982; Campana and Moksness 1991; Kimura and Lyons 1991). For example, Kimura and Lyons (1991) compared the precision of age determination using annuli for several species. CVs ranged from 3% for the relatively short-lived Pacific hake to 13% for sablefish (*Anoplopoma fimbria*), which

was difficult to age due to "unresolved" marks in its otoliths (Kimura and Lyons 1991). In the central GBR, similar estimates for *P. moluccensis* are approximately 8%, but can vary greatly with latitude (Fowler 1990; Fowler and Doherty 1992). CVs comparing ages determined by otolith weight to the true age in this study ranged from 5 to 16%. It must be remembered that the examples that produced these values were chosen to represent the best and worst cases, and in practice, CVs between these limits might be expected. Nonetheless, these data indicate the potential of otolith weight to be as reliable in the determination of the age of *P. moluccensis* and *P. wardi* as the use of annuli in sectioned otoliths.

Potential uses of otolith weight

The utility of otolith weight as an estimator of age will be dependent on how the age data will be used. Some types of analysis will be particularly sensitive to any ageing errors. For example, hind-casting rates of recruitment from age structures, by methods such as sequential population analysis, may be particularly sensitive to any type of ageing error (Bradford 1991). Other types of analysis will be more sensitive to particular types of ageing error. For example, underageing bias has potentially great effects on estimates of growth and yield-per-recruit (Lai and Gunderson 1987). In contrast, some methods of analysis will be reasonably robust to different types of ageing error. Estimation of rates of mortality from catch curves should be affected little by the smoothing of normally distributed ageing errors (Brander 1974, but see Barlow 1984). In all these respects, errors in ageing by otolith weight are no different from errors in ageing by annuli in otoliths.

Perhaps one of the most obvious uses for the relationship between otolith weight and age would be for monitoring the age structure of populations. Provided there were not large random errors or bias in the determination of age, such a monitoring program could provide estimates of spatial and temporal variation in parameters such as longevity and mortality, and estimate levels of recent recruitment. One way to ensure that age determinations were not biased by using an inappropriate relationship between otolith weight and age would be to age a subsample of any new collection of fish. This would enable a test between a previously used standard relationship and that from the new collection. Our preliminary results suggest that large differences in the slope of two relationships can be detected with a small number of fish. The procedures for optimising the subsampling of fish from new collections will be very similar to those for the use of age–length keys (Kimura 1977; Lai 1987).

Providing significant biases can be eliminated by recalibration of the relationship between otolith weight and age, it appears that otolith weight may provide a reliable estimate of age for many fish species. For some species and (or) places, otolith weight may even provide an estimate of age as reliable as annuli in sectioned otoliths. This is particularly true for species that are difficult to age using annuli, provided an initial calibration equation can be determined. In addition, the ability to age larger samples of fish using otolith weight can provide a more precise estimate of the true age structure of a population than a smaller sample with fewer ageing errors (Worthington et al. 1995). That is, the sampling error encountered by ageing small numbers of fish may outweight the advantages of a more reliable ageing method, particularly in species with many age-classes. At worst, otolith weight can be used as a check on ages determined by annuli, especially in old fish or species with otoliths that are difficult to interpret. Essential to the use of otolith weight (or any ageing technique) is a knowledge of the potential variability and bias in the determination of true age (see Richards et al. 1992). If this were possible, otolith weight could provide a rapid, easy, and economic method of objective age determination.

Acknowledgments

Many people helped with the sampling involved in this study. We thank them all. Doug Ferrell, Dave Williams, and Nokome Bentley provided comments on the manuscript. This is contribution 728 from the Australian Institute of Marine Science.

References

Barlow, J. 1984. Mortality estimation: Biased results from unbiased ages. Can. J. Fish. Aquat. Sci. **41**: 1843–1847.

Beamish, R.J. 1979. Differences in the age of Pacific Hake (*Merluccius productus*) using whole otoliths and sections of otoliths. J. Fish. Res. Board Can. **36**: 141–151.

Beamish, R.J., and Fournier, D.A. 1981. A method for comparing the precision of a set of age determinations. Can. J. Fish. Aquat. Sci. **38**: 982–983.

Beckman, D.W., Stanley, A.L., Render, J.H., and Wilson, C.A. 1991. Age and growth-rate estimation of sheepshead *Archosargus probatocephalus* in Louisiana waters using otoliths. Fish. Bull. U.S. **89**: 1–8.

Boehlert, G.W. 1985. Using objective criteria and multiple regression models for age determination in fishes. Fish. Bull. U.S. **83**: 103–117.

Boehlert, G.W., and Yoklavich, M.M. 1984. Variability in age estimates in *Sebastes* as a function of methodology, different readers, and different laboratories. Calif. Fish Game, **70**: 210–224.

Bradford, M.J. 1991. Effects of ageing errors on recruitment time series estimates from sequential population analysis. Can. J. Fish. Aquat. Sci. **48**: 555–558.

Brander, K. 1974. The effect of age-reading errors on the statistical reliability of marine fishery modelling. *In* The ageing of fish. *Edited by* T.B. Bagenal. Unwin Brothers Ltd., Surrey. pp. 103–107.

Campana, S.E., and Moksness, E. 1991. Accuracy and precision of age and hatch date estimates from otolith microstructure examination. ICES J. Mar. Sci. **48**: 303–316.

Chang, W.Y.B. 1982. A statistical method for evaluating the reproductibility of age determination. Can. J. Fish. Aquat. Sci. **39**: 1208–1210.

Doherty, P.J., and Fowler, A.J. 1994. An empirical test of recruitment-limitation in a coral reef fish. Science. (Wash., D.C.), **263**: 935-939.

Doherty, P.J., and Williams, D.McB. 1988. The replenishment of coral reef fish populations. Oceanogr. Mar. Biol. Annu. Rev. **26**: 487–551.

Fletcher, W.J. 1991. A test of the relationship between otolith weight and age for the pilchard *Sardinops neopilchardus*. Can. J. Fish. Aquat. Sci. **48**: 35–38.

Fowler, A.J. 1990. Validation of annual growth increments in the otoliths of a small, tropical coral reef fish. Mar. Ecol. Progr. Ser. **64**: 25–38.

Fowler, A.J., and Doherty, P.J. 1992. Validation of annual growth increments in the otoliths of two species of damselfish from the southern Great Barrier Reef. Aust. J. Mar. Freshwater Res. **43**: 1057–1068.

Francis, R.I.C.C., Paul, L.J., and Mulligan, K.P. 1992. Ageing of adult snapper (*Pagrus auratus*) from otolith annual ring counts: validation by tagging and oxytetracycline injection. Aust. J. Mar. Freshwater Res. **43**: 1069–1089.

Hoenig, J.M., and Heisey, D.M. 1987. Use of a log-linear model with the EM algorithm to correct estimates of stock composition and to convert length to age. Trans. Am. Fish. Soc. **116**: 232–243.

Kimura, D.K. 1977. Statistical assessment of the age–length key. J. Fish. Res. Board Can. **34**: 317–324.

Kimura, D.K., and Lyons, J.J. 1991. Between-reader bias and variability in the age determination process. Fish. Bull. U.S. **89**: 53–60.

Kimura, D.K., Mandapat, R.R., and Oxford, S.L. 1979. Method, validity, and variability in the age determination of yellowtail rockfish (*Sebastes flavidus*), using otoliths. J. Fish. Res. Board Can. **36**: 377–383.

Lai, H.L. 1987. Optimum allocation for estimating age composition using age–length key. Fish. Bull. U.S. **85**: 179–183.

Lai, H.L., and Gunderson, D.R. 1987. Effects of ageing errors on estimates of growth, mortality and yield per recruit for walleye pollock (*Theragra chalcogramma*). Fish. Res. **5**: 287–302.

Megrey, B.A. 1989. Review and comparison of age-structured stock assessment models from theoretical and applied points of view. Am. Fish. Soc. Symp. **6**: 8–48.

Mugiya, Y., and Watabe, N. 1977. Studies on fish scale formation and resorption II. Effect of estradiol on calcium homeostasis and skeletal tissue resorption in the goldfish, *Carassius auratus*, and the killifish, *Fundulus heteroclitus*. Comp. Biochem. Physiol. A, **57**: 197–202.

Pawson, M.G. 1990. Using otolith weight to age fish. J. Fish Biol. **36**: 521–531.

Radtke, R.L., Fine, M.L., and Bell, J. 1985. Somatic and otolith growth in the oyster toadfish (*Opsanus tau* L.). J. Exp. Mar. Biol. Ecol. **99**: 259–275.

Reznik, D., Lindbeck, E., and Bryga, H. 1989. Slower growth results in larger otoliths: An experimental test with guppies (*Poecilia reticulata*). Can. J. Fish. Aquat. Sci. **46**: 108–112.

Richards, L.J., Schnute, J.T., Kronlund, A.R., and Beamish, R.J. 1992. Statistical models for the analysis of ageing error. Can. J. Fish. Aquat. Sci. **49**: 1801–1815.

Snedecor, G.W., and Cochran, W.G. 1989. Statistical methods. 7th ed. The Iowa State University Press, Ames, Iowa.

Templeman, W., and Squires, H.J. 1956. Relationship of otolith lengths and weights in the haddock *Melanogrammus aeglefinus* (L.) to the rate of growth of the fish. J. Fish. Res. Board Can. **13**: 467–487.

Tyler, A.V., Beamish, R.J., and McFarlane, G.A. 1989. Implications of age determination errors to yield estimates. Can. Spec. Publ. Fish. Aquat. Sci. **108**: 27–35.

Williams, T., and Bedford, B.C. 1974. The use of otoliths for age determination. *In* The ageing of fish. *Edited by* T.B. Bagenal. Unwin Brothers Ltd., Surrey. pp. 114–123.

Wilson, C.A., Dean, J.M., Prince, E.D., and Lee, D.W. 1991. An examination of sexual dimorphism in Atlantic and Pacific blue marlin using body weight, sagittae weight, and age estimates. J. Exp. Mar. Biol. Ecol. **151**: 209–225.

Worthington, D.G., Fowler, A.J., and Doherty, P.J. 1995. Determining the most efficient method of age determination for estimating the age structure of a fish population. Can. J. Fish. Aquat. Sci. **52**. (In press)

Development of salinity tolerance in underyearling smolts of Atlantic salmon (*Salmo salar*) reared under different photoperiods

Åse I. Berge, Arne Berg, Hans Jørgen Fyhn, Trygg Barnung, Tom Hansen, and Sigurd O. Stefansson

Abstract: Groups of Atlantic salmon (*Salmo salar*), first fed in mid-February 1989, were reared under continuous light (LL) at 12–15°C until late June. One group remained on LL, while the FEB, MAR, and MAY groups were subjected to segments of a simulated naturally increasing photoperiod (61°N), with initial daylength corresponding to February 1, March 15, and May 1, respectively. The MAR and FEB groups developed important smolt characters (increase in gill Na^+,K^+-ATPase activity, hypoosmoregulatory ability, and salinity tolerance) during the experiment whereas LL and MAY groups showed only incomplete changes in smolt status. The combination of continuous light during first feeding and early parr stages with a subsequent reduction to short daylength followed by a segment of simulated natural photoperiod allow important parts of the parr–smolt transformation to be completed. The period of exposure to short photoperiod is critical for the synchronization of smolt characters in underyearling Atlantic salmon.

Résumé : Des groupes de saumons atlantiques (*Salmo salar*), en début de phase d'alimentation à la mi-février 1989, ont été élevés en éclairement continu (LL) à 12–15°C jusqu'à la fin de juin. Un groupe est demeuré en LL, tandis que les groupes de février, de mars et de mai ont été soumis à des conditions simulant des phases naturelles de photopériode ascendante (61°N), la durée du jour au départ correspondant respectivement à celles du 1er février, du 15 mars et du 1er mai. On a vu apparaître dans les groupes de mars et de février des caractères importants de smoltification (augmentation de l'activité de la Na^+,K^+-ATPase branchiale, adaptation à un milieu hypoosmotique et tolérance à la salinité) pendant l'expérience, tandis que le groupe LL et le groupe de mai ne présentaient que des modifications incomplètes en ce sens. La combinaison de l'éclairement continu pendant le début de l'alimentation et de la phase de tacon, d'une réduction par la suite de la durée de l'éclairement puis d'une phase de photopériode naturelle simulée permet l'accomplissement d'une partie importante de la transformation du tacon en smolt. La période d'exposition à une courte photopériode joue un rôle critique dans la synchronisation des caractères du smolt chez le saumon atlantique de moins de 1 an.

[Traduit par la Rédaction]

Introduction

According to Mills (1989), a smolt is a "fully silvered salmon migrating to sea". To reach this smolt state, juvenile salmon have to complete a developmental process called smolting, smoltification, or parr–smolt transformation. Salmonid smoltification is defined as the orchestration of simultaneous or consecutive morphological, behavioural, and biochemical changes that transform a darkly pigmented, bottom-dwelling parr into a pelagic, silvery smolt prepared for the transition into seawater (Hoar 1963; Folmar and Dickhoff 1980; McCormick and Saunders 1987).

In a natural environment, photoperiod, thermal regime, and river flow synchronize this spectrum of processes that constitute parr–smolt transformation. In culture, juvenile Atlantic salmon (*Salmo salar*) are often deprived of important

Received November 23, 1993. Accepted July 14, 1994.
J12173

Å.I. Berge, A. Berg, T. Barnung, and T. Hansen. Institute of Marine Research, Section for Aquaculture, Matre Aquaculture Research Station, N-5198 Matredal, Norway.
H.J. Fyhn. Department of Zoology, University of Bergen, Allégt. 41, N-5007 Bergen, Norway.
S.O. Stefansson.[1] Department of Fisheries and Marine Biology, University of Bergen, Bergen High Technology Center, N-5020 Bergen, Norway.

[1] Author to whom correspondence should be addressed.

Fig. 1. Experimental photoperiod regimes for rearing underyearling smolts of Atlantic salmon. The LL group was maintained on continuous light. The MAY, MAR, and FEB groups experienced a reduction in daylength corresponding to May 1, March 15, and February 1, respectively, followed by a simulated natural increase.

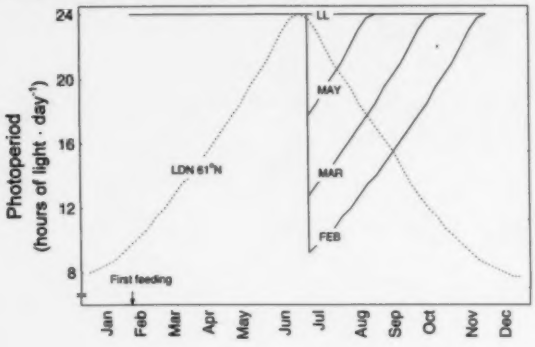

natural environmental cues. Extended daylength has a growth-promoting effect on juvenile Atlantic salmon (Saunders et al. 1985; McCormick et al. 1987; Stefansson et al. 1989); hence, continuous light has been extensively used in culture as a means to increase growth rate. Although increased growth rate is one of the major events of parr–smolt transformation, other than natural photoperiods may seriously affect the parr–smolt transformation (Saunders et al. 1985; McCormick et al. 1987; Björnsson et al. 1989; Stefansson et al. 1991).

Associated with the elevated growth rate during smolting are metabolic changes that often result in a reduction in condition coefficient (Farmer et al. 1978; Wedemeyer et al. 1980; Sheridan et al. 1983; McCormick and Saunders 1987; Hoar 1988). Another major event during parr–smolt transformation is the preadaptive increase in hypoosmoregulatory ability, which is necessary for a successful transition of juvenile salmonids from freshwater to seawater (Wedemeyer et al. 1980; McCormick and Saunders 1987). The increased hypoosmoregulatory ability has been related to an increase in gill Na^+,K^+-ATPase activity (Zaugg and McLain 1970; Boeuf and Harache 1982; Boeuf et al. 1985; McCormick et al. 1987), although any causal relationship between the two has been questioned (Saunders et al. 1989; Saunders and Harmon 1990).

By manipulating photoperiod and temperature, it has been possible to obtain smolting in underyearling spring chinook (*Oncorhynchus tshawytscha*) (Zaugg et al. 1986; Clarke et al. 1989), coho (*O. kisutch*) (Clarke et al. 1978, 1989; Brauer 1982; Clarke and Shelbourn 1986), and sockeye salmon (*O. nerka*) (Clarke et al., 1978). In a preliminary study, Stefansson et al. (1992) demonstrated that Atlantic salmon possess the potential to develop hypoosmoregulatory ability as underyearlings, but the relationship between photoperiod, hypoosmoregulatory ability, and other aspects of the smolting process in underyearlings has not been fully documented. In the present experiment, photoperiod and temperature manipulation have been applied to Atlantic salmon from first feeding in an attempt to induce parr–smolt transformation during the first year of life.

Materials and methods

Fish stock and rearing conditions

Eggs of Atlantic salmon from the hatchery stock at Matre Aquaculture Research Station were pooled and incubated at 5–6°C. The fish were first fed in mid-February 1989 at a temperature of 12°C. In early May the temperature was elevated 1° daily up to 16°C and kept stable until the start of the experiment in late June. During the experimental period the fish were reared at ambient temperature, fluctuating between 11 and 14°C during June–August, decreasing to 8°C in early October, and maintained at 8–9°C throughout the study. The fish were reared under continuous light from first feeding until the start of the experiment.

The experimental tanks were 1 m^2 square, gray, covered fiberglass tanks with a rearing volume of 350 L. Water flow was kept at 15 $L \cdot min^{-1}$. Light was supplied by two 18-W fluorescent daylight tubes installed in the tank cover. Light intensity at the bottom was approximately 270 lx as measured by a custom-made hemispherical photometer (Hansen 1990). A computer program (Hansen 1990) generated a simulated natural light regime including twilight periods. All groups were fed commercial dry feed (Skretting Tess Elite, sizes 2.0 and 3.0) in excess from automatic feeders every 5 min 12 h a day during the photophase.

Experimental design

On June 26, four experimental light regimes were initiated (Fig. 1). One group, LL, remained on constant light, while three groups were reared on various segments of a simulated naturally increasing photoperiod of 61°N. The daylength of one group, MAY, was initially reduced to correspond to May 1, reaching summer solstice on August 20. Accordingly, the daylength of the two other groups, MAR and FEB, was initially reduced to correspond to March 15 and February 1, respectively, reaching summer solstice on October 5 and November 16. When the MAY, MAR, and FEB groups reached continuous light, they were maintained on this light regime throughout the experiment. All groups consisted of two replicate tanks, each containing 470 fish. To follow individual growth rate, 113 fish in each tank were tagged with passive integrated transponder (PIT) tags intraperitoneally near the midventral line and posterior to the pectoral fins (Prentice et al. 1986). Every third week (on June 20, July 11, August 1, August 24, September 14, October 5, October 26, and November 14), all tagged fish were measured for fork length and body weight to the nearest 0.1 cm and 0.1 g. Growth rate was calculated for the tagged subpopulation as millimetres per day according to the formula $(l_2 - l_1)(t_2 - t_1)^{-1}$ where l_1 and l_2 are fork lengths at times t_1 and t_2. Condition coefficient (K) was calculated as $K = 100\ w \cdot l^{-3}$ where w is the individual weight and l is the fork length of the corresponding fish.

Every third week, untagged fish were sacrificed for determination of specific gill Na^+,K^+-ATPase activity, plasma Na^+ levels, and salinity tolerance. Fifteen to 17 fish were sampled from each group and for each parameter

Fig. 2. Growth rate of juvenile Atlantic salmon reared under four different photoperiods. Vertical lines indicate SEM. Different letters indicate statistical differences ($p < 0.05$). Open bars, LL; medium-shaded bars, MAY; lightly shaded bars; dark-shaded bars, MAR; dark-shaded bars, FEB.

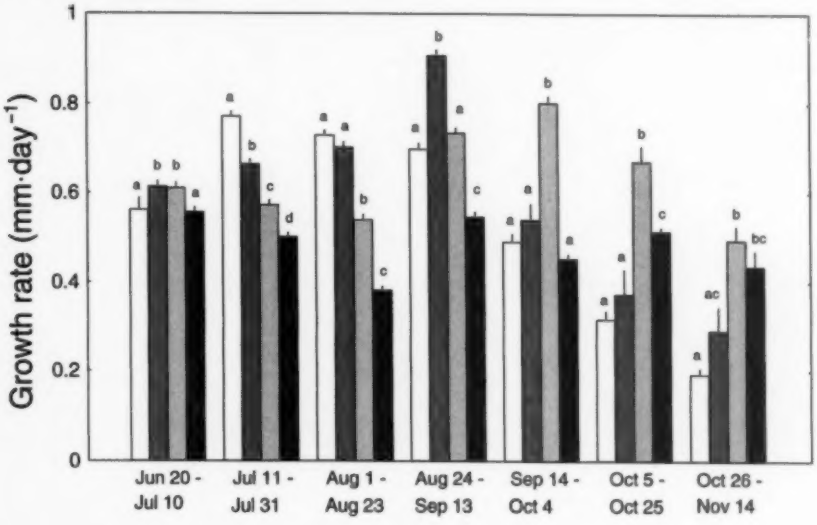

studied. Gill filaments were collected for determination of Na^+,K^+-ATPase activity on July 10, July 31, August 21, September 11, October 2, October 24, November 13, and December 4. Between 0.05 and 0.2 g of gill tissue was sampled from each fish. On July 10, all gill arches on both sides were taken to obtain the prescribed amount of gill tissue. As the fish grew larger the number of sampled gill arches was reduced correspondingly in all sampled fish. The gill tissue was immersed in SEI (102.70 g sucrose·L^{-1}, 7.44 g $Na_2EDTA·L^{-1}$, 6.80 g Imidazol·L^{-1}, and 1.0 M HCl for final pH adjustment, pH = 7.1 at 37°C), immediately frozen at −80°C, and stored from 3 to 6 weeks until analysis by the procedure of Zaugg (1982), modified by Sigholt et al. (1989). ATP was supplied to the enzyme preparation and incubated at 37°C. The concentration of inorganic phosphate (Pi) released as a product of the enzyme activity ($ATP \rightarrow ADP + P_i$) was determined by the method of Fiske and Subbarow (1925). The colour reaction was automated using a reaction time of 10 min at 37°C. Protein in the enzyme preparation was determined by the method of Bradford (Bradford 1976; Hammond and Kruger 1988).

Seawater challenge tests (35‰, 24 h) to assess hypoosmoregulatory ability were conducted on June 27, July 11, July 31, August 22, September 11, October 2, October 24, November 15, and December 7, according to the method of Clarke and Blackburn (1977). The fish were starved for 24 h prior to the test. The 35‰ seawater was obtained by adding ocean salt to 28–30‰ well water and the static water was continuously aerated. At the end of each challenge test, blood was collected from the caudal vein of surviving fish following the procedure of Stefansson et al. (1989). The samples were centrifuged at 4000 × *g* and plasma was stored at −80°C for subsequent analysis of plasma Na^+. On June 28 and July 11, two or three blood samples were pooled before analysis.

Salinity tolerance tests (40‰, 96 h), based on the ability of salmon smolts to withstand hypersaline water for 96 h, were run according to Stefansson and Hansen (1989) on June 27, July 11, July 31, August 22, September 12, October 2, October 31, November 15, and December 11. A 40‰ salinity was obtained as described for the seawater challenge test, with continuous aeration. Dead fish were collected daily and weight and length recorded. After 96 h, surviving fish were measured for weight and length.

To study the effects of salinity on gill Na^+,K^+-ATPase activity and continued seawater exposure on plasma ion levels during the final stages of smolting, extended seawater challenge tests (35‰, 24 and 96 h) were performed 3 weeks after the groups showed high or increasing survival (>60%) in the salinity tolerance tests (40‰, 96 h). As the different groups developed seawater tolerance at different times according to photoperiod treatment, these tests were extended to 96 h for the LL and MAY groups on September 12, for the MAR group on October 2, and for the FEB group on October 24. Plasma Na^+ levels and gill Na^+,K^+-ATPase activity were measured after exposure to 35‰ for 24 and 96 h. Further, gill Na^+,K^+-ATPase activity was also measured in the FEB group after 14 days of seawater exposure.

Statistical methods

To assess for normality of distributions of the measured parameters, a Wilk–Shapiro test of normality was applied. Variances were tested using an Fmax test, while one-way ANOVA followed by a Student–Newman–Keuls test was applied to determine differences among experimental groups. A significance level of 0.05 was used throughout the study.

Fig. 3. Fork length of juvenile Atlantic salmon reared under four different photoperiods. The vertical lines indicating SEM may be obscured by symbols. Different letters indicate statistical differences ($p < 0.05$). Squares, LL; triangles, MAY; diamonds, MAR; circles, FEB.

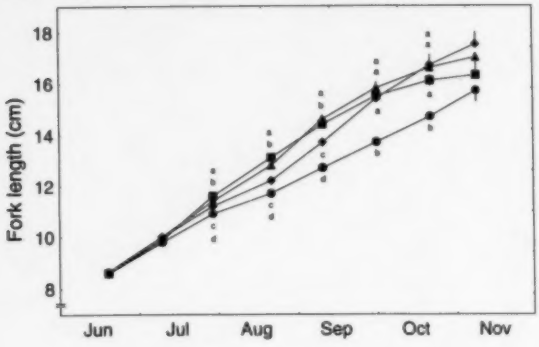

Fig. 4. Condition coefficient of juvenile Atlantic salmon reared under four different photoperiods. The vertical lines indicating SEM may be obscured by symbols. Different letters indicate statistical differences ($p < 0.05$). Symbols as in Fig. 3.

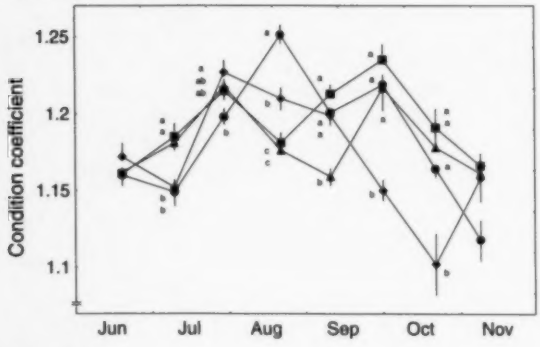

Results

Growth rate and condition factor

Replicates were not significantly different and were combined in all cases. From late June until late October, there were significant differences in growth rate (millimetres per day) between groups according to photoperiod (Fig. 2). The LL and MAY groups had higher growth rate ($p < 0.05$) from mid-July to early August and late August to mid-September, respectively, and consequently had the greatest mean fork length through August and September (Fig. 3). Growth rate in the MAR and FEB groups decreased until mid-August. From late August, growth rate in these groups increased with increasing photoperiod. The MAR group had higher growth rate than the other groups ($p < 0.05$) in early October and the largest fish in November. Although growth rate in the FEB group increased from late August to late October, this group had the shortest mean fork length from late July through October ($p < 0.05$). Following peak growth rates, growth rate declined in all groups.

Fig. 5. Specific gill Na^+,K^+-ATPase activity of juvenile Atlantic salmon reared under four different photoperiods. The vertical lines indicating SEM may be obscured by symbols. Different letters indicate statistical differences ($p < 0.05$). Symbols as in Fig. 3.

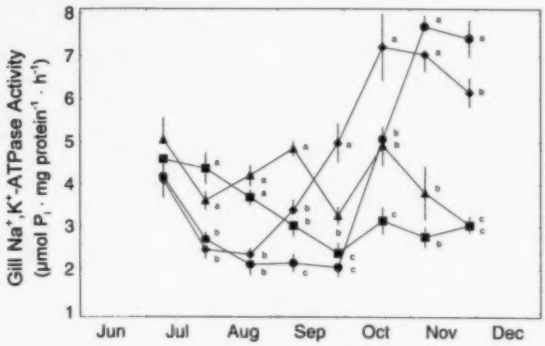

The condition coefficient increased in all groups between late June and early August. Condition coefficients of the LL and MAY groups never showed the expected decline associated with smolting, remaining above 1.15 (Fig. 4). In the MAR and FEB groups, condition coefficient decreased from early August and late August, respectively. The MAR group had lower ($p < 0.05$) condition coefficient than the other groups through October, reaching a level of 1.10 in late October, while the FEB group reached its lowest observed level in mid-November when growth samplings were terminated.

Gill Na^+,K^+-ATPase activity

Specific gill Na^+,K^+-ATPase activity declined in all groups following the initiation of the experimental photoperiods in late June (Fig. 5). The MAR and FEB groups experienced the sharpest decrease ($p < 0.05$), reaching a level of about 2.2 μmol Pi·mg protein^{-1}·h^{-1} in late August. Gill Na^+,K^+-ATPase activity remained low until late August in the MAR group and early October in the FEB group, followed by a more than threefold increase ($p < 0.05$) in enzyme activity, reaching a peak activity of approximately 7.2 in late October and 7.6 in mid-November, respectively. Gill Na^+,K^+-ATPase activity in the MAY group fluctuated throughout the experiment, but changes were significant only in the period early July to early October. The LL group showed a significant decrease in gill Na^+,K^+-ATPase activity from early July to late October.

All groups significantly increased their gill Na^+,K^+-ATPase activity during the prolonged seawater challenge tests (Table 1). The LL group had a 45% increase after 96 h, while gill Na^+,K^+-ATPase in the MAY group increased by 20%. The MAR group had a 48% increase, and the FEB group experienced a 60% increase after 96 h of seawater exposure. No further increase in gill Na^+,K^+-ATPase activity was measured in the FEB group after 14 days in 35‰ seawater.

Plasma Na^+ levels after 24 h in seawater

At the commencement of the experimental photoperiods in late June, plasma Na^+ levels of about 215 mM after

exposure to 35‰ salinity for 24 h indicated a failure to hypoosmoregulate (Fig. 6). In the MAR and FEB groups, plasma Na^+ levels remained high until late August followed by a decrease ($p < 0.05$) to levels between 165 and 170 mM in mid-September and late October, respectively. Plasma levels remained low in these groups throughout the study. In the MAY and LL groups, plasma Na^+ decreased to levels of approximately 180 mM during July ($p < 0.05$) with subsequent significant fluctuations between 175 and 195 mM during the following months. The MAR and FEB groups showed significantly lower plasma Na^+ levels than MAY and LL from mid-November to the end of the experiment.

During the prolonged seawater challenge tests the LL and FEB groups significantly reduced plasma Na^+ levels from 24 to 96 h. The MAR group also showed a decrease, while the MAY group showed an increase in plasma Na^+ levels (Table 2). No morphological signs of osmotic disturbance were observed among the fish in 35‰ salinity, even after continued exposure (96 h).

Salinity tolerance

Survival in 40‰ salinity for 96 h was low in all groups during the first 5 weeks of the experiment (Fig. 7). From late July, survival in the LL and MAY groups increased rapidly until late August, with subsequent survival fluctuating between 60 and 100%. Similarly, survival in the MAR and FEB groups increased in late August and mid-September, respectively, remaining high (>90%) throughout the experiment.

Morphological signs of salinity stress were observed among surviving fish in the MAY and LL groups, even at times of high survival. The most evident signs were skin darkening, sluggish behaviour, and fin necrosis ("erosions"). No morphological signs of salinity stress were observed in the MAR and FEB groups after they reached 90–100% survival.

Discussion

Growth rate and size relations

All fish sampled in the present experiment belonged in the upper growth mode, representing the potential smolts of the population (Thorpe et al. 1982). As a reduction in daylength affects lower and upper mode fish differently (Thorpe et al. 1989), a sufficient number of upper mode fish (>8.0 cm, potential 0+ smolt) for monitoring growth and physiological changes was present in the population in late June when experimental photoperiods were initiated. The reduction in daylength caused an initial reduction in growth rate of the FEB and MAR groups, with a subsequent increase to levels exceeding those of the LL and MAY groups during the latter half of the experiment (Fig. 2). All groups reached a size (15–17 cm, Fig. 3) typical of Atlantic salmon smolts (Hoar 1976) between mid-October and mid-November. Similar photoperiod-induced growth changes have been reported for potential 1+ Atlantic salmon smolts (McCormick et al. 1987; Stefansson et al. 1989, 1991; Björnsson et al. 1989; Solbakken et al. 1994).

Gill Na^+,K^+-ATPase activity

An increase in gill Na^+,K^+-ATPase activity as would be expected in Atlantic salmon smolts (Boeuf and Harache

Table 1. Specific gill Na^+,K^+-ATPase activity (μmol Pi·mg $protein^{-1}$·h^{-1}) and mean fork length during prolonged seawater challenge tests (24 h, 96 h, and 14 days in 35‰ seawater). Fish from groups LL and MAY were transferred to seawater tests on September 11. Groups MAR and FEB were transferred on October 2 and October 24, respectively. Results are given as mean values (SEM). Mean values not followed by the same letter within each group are statistically different ($p < 0.05$).

	0 h			24 h			96 h			14 days		
Group	*n*	Fork length (cm)	Gill ATPase activity	*n*	Fork length (cm)	Gill ATPase activity	*n*	Fork length (cm)	Gill ATPase activity	*n*	Fork length (cm)	Gill ATPase activity
LL	16	14.2 x (0.24)	3.02 a (0.25)	10	14.3 x (0.29)	3.34 a (0.13)	10	13.7 x (0.17)	4.37 b (0.38)			
MAY	16	14.3 x (0.24)	4.84 a (0.18)	10	14.7 x (0.27)	4.98 a (0.25)	9	14.0 x (0.26)	5.60 a (0.43)			
MAR	14	15.3 x (0.27)	4.97 a (0.46)	9	14.9 x (0.38)	6.01 ab (0.51)	8	14.3 x (0.27)	7.37 b (0.91)			
FEB	16	14.2 x (0.18)	5.06 a (0.29)	7	15.3 y (0.23)	6.67 b (0.45)	10	14.5 x (0.12)	8.11 c (0.44)	8	16.0 y (0.42)	7.90 c (0.27)

Table 2. Plasma Na^+ levels and fork length of underyearling Atlantic salmon during the prolonged seawater challenge tests (24 and 96 h in 35‰ seawater). Fish from groups LL and MAY were transferred to seawater tests on September 11 and groups MAR and FEB on October 2 and 24, respectively. Results are given as mean values (SEM). Mean values not followed by the same letter in the same group are statistically different ($p < 0.05$).

	24 h			96 h		
Group	n	Fork length (cm)	Plasma Na^+ (mM)	n	Fork length (cm)	Plasma Na^+ (mM)
LL	16	14.2 x (0.19)	182.8 a (2.26)	10	13.6 y (0.17)	174.0 b (1.72)
MAY	16	14.6 x (0.21)	173.5 a (2.68)	10	14.0 x (0.24)	178.2 a (2.94)
MAR	15	14.7 x (0.29)	166.0 a (1.93)	13	14.2 x (0.22)	160.5 a (3.48)
FEB	16	14.9 x (0.20)	168.8 a (1.72)	10	14.5 x (0.12)	157.3 b (2.52)

Fig. 6. Plasma Na^+ after 35‰ 24-h seawater challenge tests of juvenile Atlantic salmon reared under four different photoperiods. The vertical lines indicating SEM may be obscured by symbols. Different letters indicate statistical differences ($p < 0.05$). Symbols as in Fig. 3.

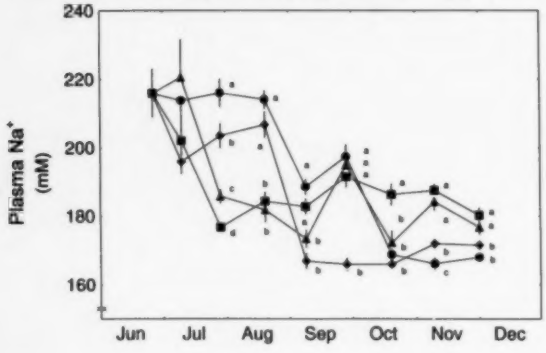

Fig. 7. Survival in 40‰ 96-h salinity tolerance tests of juvenile Atlantic salmon reared under four different photoperiods. The vertical lines indicating SEM may be obscured by symbols. Different letters indicate statistical differences ($p < 0.05$). Symbols as in Fig. 3.

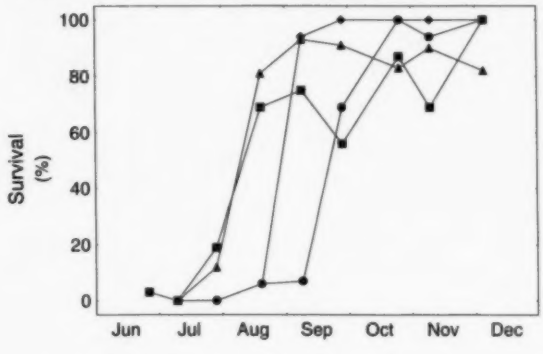

1982; Boeuf et al. 1985; McCormick et al. 1987; Hoar 1988) was seen in the MAR and FEB groups (Fig. 5). In the MAY and LL groups the expected increase typical of smolting was absent, suggesting that a minimum period of exposure to short daylength is necessary for underyearling Atlantic salmon to complete parr–smolt transformation. These results agree with previous findings for underyearling coho, spring chinook (Clarke and Shelbourn 1986; Clarke et al. 1989), and masu salmon (*O. masou*, Okumoto et al. 1989) that a certain minimum time of exposure to short photoperiods is needed to complete smolting. Accordingly, Clarke and Shelbourn (1986) stated that the initiation of the smolting process occurs under short daylength conditions. The longer exposure to short daylengths in the FEB group explains why this group showed delayed development of gill Na^+,K^+-ATPase activity compared with the MAR group. The delayed development may be the result of a direct effect of short daylength on the activity of this enzyme. Alternatively the delayed development of gill Na^+,K^+-ATPase may have been an indirect result of continued exposure to short photoperiod, reducing growth rate and delaying smolting. This agrees with Björnsson et al. (1989) who showed that short photoperiods delay growth and smolting in Atlantic salmon. The decreasing temperature may also have delayed the increase of gill Na^+,K^+-ATPase activity, either directly or through an effect on growth rate.

Increasing or elevated levels of gill Na^+,K^+-ATPase activity coincided with periods of rapid growth (compare Figs. 2 and 5), indicating that high growth rate may be important for the development of gill Na^+,K^+-ATPase activity in underyearling Atlantic salmon. Accordingly, all groups had elevated gill Na^+,K^+-ATPase activity in early July, when growth rate was still relatively high as a consequence of the growth-stimulating effect of exposure to continuous light until late June. The subsequent decline in growth rate may be related to the effect of continued exposure to constant light experienced by the LL group, and which eventually causes a decrease in growth rate (Saunders et al. 1985; Stefansson et al. 1989; Solbakken et al. 1994), or the reduction in daylength for the remaining groups. A relationship between photoperiod, growth rate, and parr–smolt transformation has been reported for several anadromous salmonids (Komourdjian et al. 1976; Clarke et al. 1978, 1981; Brauer 1982; Björnsson et al. 1989). The increase in gill Na^+,K^+-ATPase activity, coinciding with high growth rate, may have been a consequence of

the action of growth hormone (GH). Björnsson et al. (1989) concluded that GH plays an important role in stimulating growth and increasing hypoosmoregulatory ability during parr–smolt transformation. Further, GH increases concurrently with activation of Na^+,K^+-ATPase activity in coho (Björnsson et al. 1987; Richman and Zaugg 1987) and Atlantic salmon (McCormick et al. 1987; Björnsson et al. 1989; Boeuf et al. 1994).

Elevated gill Na^+,K^+-ATPase activity coincided with decreasing condition coefficient in the MAR and FEB groups, suggesting that important parts of parr–smolt transformation were synchronized in these two groups. A negative correlation between condition coefficient and plasma GH levels has been observed in smolting 1+ Atlantic salmon (Stefansson et al. 1991).

As the different groups were subjected to extended exposure to 35‰ seawater around the time of peak in smolt status, all groups significantly increased their gill Na^+,K^+-ATPase activity (Table 1). The increase after 96 h of seawater exposure was greatest in the FEB group and least in the MAY group. The MAR and FEB groups increased their gill Na^+,K^+-ATPase activity after 96 h of seawater exposure to levels similar to those observed in freshwater 3 weeks later. The observed increase agrees with earlier reports on the stimulation of gill Na^+,K^+-ATPase activity in juvenile salmonids exposed to seawater (Zaugg and McLain 1970; Giles and Vanstone 1976; Saunders and Henderson 1978; McCormick et al. 1989). However, the period of seawater exposure required to induce increased gill Na^+,K^+-ATPase activity differs between experiments. In the present study, gill Na^+,K^+-ATPase activity of the FEB group showed no further increase from 96 h to 14 days in seawater, suggesting that the fish were fully acclimated within 4 days of seawater exposure. However, it has not been documented whether this also applies to the other groups. The MAY group showed a lower percentage increase in gill Na^+,K^+-ATPase activity than the other groups, suggesting that the rate of increase of enzyme activity may depend on the developmental state of the fish at the time of seawater transfer. Again, the stimulation of Na^+,K^+-ATPase activity in seawater may be a direct effect of salinity on enzyme activity, or indirectly through growth. Growth rate in the MAR and FEB groups was peaking, while in the LL and MAY groups the growth rate was rapidly declining at the time of extended seawater exposure.

Plasma Na^+ levels in seawater

Plasma Na^+ levels after 24 h of 35‰ seawater exposure were affected by photoperiod treatment (Fig. 6). All groups increased hypoosmoregulatory ability during the experiment, although the LL and MAY groups never attained high gill Na^+,K^+-ATPase activity. In the FEB and MAR groups, there was a relationship between decrease in plasma Na+ levels and increase in gill Na^+,K^+-ATPase activity. However, the decrease in plasma Na^+ levels occurred in advance of the development of high gill Na^+,K^+-ATPase activity in freshwater. The ability of salmonids to adapt to seawater in advance of parr–smolt transformation has formerly been demonstrated by Wagner (1974) in steelhead trout (*O. mykiss*) and by McCormick et al. (1987) in Atlantic salmon, suggesting that the inducibility of gill Na^+,K^+-ATPase activity on seawater exposure precedes the increase in enzyme activity of fish that are maintained in freshwater. Observations on gill Na^+,K^+-ATPase activity of the MAR and FEB groups after seawater exposure (Table 1) support this hypothesis, since both groups were capable of significantly increasing their gill Na^+,K^+-ATPase activity within 96 h of seawater exposure at the same time as these groups maintained low plasma Na^+ levels following the seawater challenge test. Although the LL and MAY groups also increased their gill Na^+,K^+-ATPase levels upon seawater exposure, they did not reach the same high gill Na^+,K^+-ATPase levels as did the MAR and FEB groups, suggesting that these groups lacked the ability to regulate plasma Na^+ below the critical level of 170 mM as found in smolts of Atlantic salmon (McCormick et al. 1989).

Hypoosmoregulation is thought to be related to growth rate through the action of GH (Björnsson et al. 1989), and a relationship between growth rate and hypoosmoregulatory ability may explain why the LL and MAY groups managed to regulate plasma Na^+ to some extent in seawater. An increased ability to regulate plasma Na^+ coincided with increasing or elevated growth rate in all groups. Although mean length was low at the time of peak Na^+ regulation of the LL group in late July, the high growth rate at this time demonstrates the important effect of growth rate on plasma Na^+ regulation. Accordingly, as growth rate subsequently decreased in the LL group, hypoosmoregulatory ability did not improve despite the increase in size (compare Figs. 2, 3, and 6).

The LL, MAR, and FEB groups showed a decrease in plasma Na^+ levels from 24 to 96 h of seawater exposure, although significantly only in the LL and FEB groups (Table 2). This further suggests a connection between plasma Na+ regulation and gill Na^+,K^+-ATPase activity through the stimulation of this enzyme in seawater. Accordingly, the MAY group showed the least ability to increase gill Na^+,K^+-ATPase activity in seawater and consequently showed no ability to decrease plasma Na^+ from 24 to 96 h in 35‰ seawater.

Gill Na^+,K^+-ATPase has been assumed to play an important role in hypoosmoregulation of several salmonid species (Zaugg and McLain 1970; Boeuf and Harache 1982; Boeuf et al. 1985; McCormick et al. 1987). This relationship has recently been questioned, since Atlantic salmon have been shown to hypoosmoregulate well in seawater even at times of low gill Na^+,K^+-ATPase activity (Saunders and Harmon 1990; Solbakken et al. 1994). The present experiment shows that gill Na^+,K^+-ATPase can be induced in seawater, suggesting why hypoosmoregulatory ability on exposure to seawater may precede the development of gill Na^+,K^+-ATPase in freshwater, supporting the assumption that gill Na^+,K^+-ATPase plays an important role in hypoosmoregulation of underyearling Atlantic salmon.

Salinity tolerance

Although the MAR and FEB groups were delayed in developing salinity tolerance compared with the LL and MAY groups, these groups eventually showed a higher and more consistent survival (Fig. 7). High survival in the MAY, MAR, and FEB groups coincided with decreasing

plasma Na^+ levels, and a similar tendency, although not as clear, was seen in the LL group. It is therefore suggested that the same mechanisms regulating plasma Na^+ also influence survival in 40‰ seawater.

Survival after 96 h in 40‰ salinity was not a reliable way to assess smolt status in the present experiment with underyearling Atlantic salmon. Fully smolted Atlantic salmon survive 100% and show no signs of osmotic disturbance in hypersaline water, even after 1 week of exposure to 40‰ salinity (Å. Berge and S.O. Stefansson, unpublished observations). The morphological signs of severe osmotic stress (e.g., necrosis of tissue along fin margins as fin tissue becomes dehydrated) observed among surviving fish in the LL and MAY groups suggest that although survival was high after 96 h in 40‰ seawater, these fish were not competent osmoregulators and would have died after continued exposure to hypersaline water.

Conclusions

Photoperiod manipulation may be used to stimulate parr–smolt transformation in underyearling Atlantic salmon. Photoperiod treatment affected gill Na^+,K^+-ATPase activity, ability to regulate plasma Na^+ levels in seawater, salinity tolerance, growth rate, and condition coefficient of potential 0+ smolts. The MAR and FEB groups achieved important aspects of smolt status, while the LL and MAY did not, supporting the view that juvenile Atlantic salmon have to experience a period of short daylength to complete smolting. Elevated gill Na^+,K^+-ATPase levels and development of hypoosmoregulatory ability coincided with the period of increased growth rate in each group. Our results suggest that once juvenile Atlantic salmon have reached the required minimum size for smolting, growth rate may be more important than actual size for the development of gill Na^+,K^+-ATPase activity, plasma Na^+ regulation, and survival in saline waters.

References

Björnsson, B.Th., Yamauchi, H. Nishioka, R.S., Deftos, L.J., and Bern, H.A. 1987. Effects of hypophysectomy and subsequent hormonal replacement therapy on hormonal and osmoregulatory status of coho salmon, *Oncorhynchus kisutch*. Gen. Comp. Endocrinol. **68**: 421–430.

Björnsson, B.Th., Thorarensen, H., Hirano, T., Ogasawara, T., and Kristinsson, J.B. 1989. Photoperiod and temperature affect plasma growth hormone levels, growth, condition factor and hypoosmoregulatory ability of juvenile Atlantic salmon (*Salmo salar*) during parr–smolt transformation. Aquaculture, **82**: 77–91.

Boeuf, G., and Harache, Y. 1982. Criteria for adaptation of salmonids to high salinity seawater in France. Aquaculture, **28**: 163–176.

Boeuf, G., Le Roux, A., Gaignon, J.L., and Harache, Y. 1985. Gill (Na^+,-K^+)-ATPase activity and smolting in Atlantic salmon (*Salmo salar* L.) in France. Aquaculture, **45**: 73–81.

Boeuf, G., Marc, A.M., Prunet, P., LeBail, P.-Y., and Smal, J. 1994. Stimulation of parr–smolt transformation by hormonal treatment in Atlantic salmon (*Salmo salar* L.). Aquaculture, **121**: 195–208.

Bradford, M.M. 1976. A rapid and sensitive method for the quantitation of microgram quantities of protein utilizing the principle of protein-dye binding. Anal. Biochem. **72**: 248–254.

Brauer, E.P. 1982. The photoperiod control of coho salmon smoltification. Aquaculture, **28**: 105–111.

Clarke, W.C., and Blackburn, J. 1977. A seawater challenge test to measure smolting of juvenile salmon. Fish. Mar. Serv. Res. Dev. Tech. Rep. **705**: 11 pp.

Clarke, W.C., and Shelbourn, J.E. 1986. Delayed photoperiod produces more uniform growth and greater seawater adaptability in underyearling coho salmon (*Oncorhynchus kisutch*). Aquaculture, **56**: 286–299.

Clarke, W.C., Shelbourn, J.E., and Brett, J.R. 1978. Growth and adaptation to sea water in underyearling sockeye (*Oncorhynchus nerka*) and coho (*O. kisutch*) salmon subjected to regimes of constant or changing temperature and day length. Can. J. Zool. **56**: 2413–2421.

Clarke, W.C., Shelbourn, J.E., and Brett, J.R. 1981. Effect of artificial photoperiod cycles, temperature and salinity on growth and smolting in underyearling coho (*Oncorhynchus kisutch*), chinook (*O. tshawytscha*) and sockeye (*O. nerka*) salmon. Aquaculture, **22**: 105–116.

Clarke, W.C., Shelbourn, J.E., Ogasawara, T., and Hirano, T. 1989. Effect of initial daylength on growth, seawater adaptability and plasma growth hormone levels in underyearling coho, chinook and chum salmon. Aquaculture, **82**: 51–62.

Farmer, G.J., Ritter, A., and Ashfield, D. 1978. Seawater adaptation and parr–smolt transformation of juvenile Atlantic salmon, *Salmo salar*. J. Fish. Res. Board Can. **35**: 93–100.

Fiske, C.H., and Subbarow, Y. 1925. The colorimetric determination of phosphorus. J. Biol. Chem. **66**: 375–400.

Folmar, L.C., and Dickhoff, W.W. 1980. The parr–smolt transformation (smoltification) and seawater adaptation in salmonids. Aquaculture, **21**: 1–37.

Giles, M.A., and Vanstone, W.E. 1976. Changes in ouabain-sensitive adenosine triphosphatase activity in gills of coho salmon (*Oncorhynchus kisutch*) during parr–smolt transformation. J. Fish. Res. Board Can. **33**: 54–62.

Hammond, J.B.W., and Kruger, J. 1988. The Bradford method for protein quantitation. Methods Mol. Biol. **3**: 25–32.

Hansen, E.H. 1990. Bruk av kunstig lys og lysmanipulering for styrt produksjon av laksefisk. Dr. ing. thesis, Norwegian Electric Power Research Institute (EFI), Norwegian Institute of Technology (NTH), University of Trondheim. (In Norwegian)

Hoar, W.S. 1963. The endocrine regulation of migratory behavior in anadromous teleosts. Proc. XVI Int. Congr. Zool. **3**: 14–20.

Hoar, W.S. 1976. Smolt transformation, evolution, behaviour and physiology. J. Fish. Res. Board Can. **33**: 1234–1252.

Hoar, W.S. 1988. The physiology of smolting salmonids. *In* Fish physiology. Vol. XIB. *Edited by* W.S. Hoar, and D.J. Randall. Academic Press, New York, N.Y. pp. 275–343.

Komourdjian, M.P., Saunders, R.L., and Fenwick, J.C. 1976. Evidence of the role of growth hormone as part of a "light-pituitary axis" in growth and smolting of Atlantic salmon (*Salmo salar*). Can. J. Zool. **54**: 544–551.

McCormick, S.D., and Saunders, R.L. 1987. Preparatory physiological adaptations for marine life of salmonids: osmoregulation, growth and metabolism. Am. Fish. Soc. Symp. **1**: 211–229.

McCormick, S.D., Saunders, R.L., Henderson, E.B., and Harmon, P.R. 1987. Photoperiod control of parr–smolt transformation in Atlantic salmon (*Salmo salar*): changes in salinity tolerance, gill Na^+,K^+-ATPase activity, and plasma thyroid hormones. Can. J. Fish. Aquat. Sci. **44**: 1462–1468.

McCormick, S.D., Moyes, C.D., and Ballantyne, J.S. 1989. Influence of salinity on the energetics of gill and kidney of Atlantic salmon (*Salmo salar*). Fish Physiol. Biochem. **6**: 243–254.

Mills, D.H. 1989. Ecology and management of Atlantic salmon. Chapman and Hall, London.

Okumoto, N., Ikuta, K., Aida, K., Isao, H., and Hirano, T. 1989. Effects of photoperiod on smolting and hormonal secretion in masu salmon, *Oncorhynchus masou*. Aquaculture, **82**: 63–76.

Prentice, E.F., Park, D.L., Flagg, T.A., and McCutheon, S. 1986. A study to determine the biological feasibility of a new fish tagging system, 1985–1986. U.S. Department of Commerce, NOAA, NMFS, Northwest and Alaska Fisheries Center, Seattle, Wash.

Richman, N.H., III., and Zaugg, W.S. 1987. Effects of cortisol and growth hormone on osmoregulation in pre- and desmoltified coho salmon (*Oncorhynchus kisutch*). Gen. Comp. Endocrinol. **65**: 189–198.

Saunders, R.L., and Harmon, P.R. 1990. Influence of photoperiod on growth of juvenile Atlantic salmon and development of salinity tolerance during winter–spring. Trans. Am. Fish. Soc. **119**: 689–697.

Saunders, R.L., and Henderson, E.B. 1978. Changes in gill ATPase activity and smolt status of Atlantic salmon (*Salmo salar*). J. Fish. Res. Board Can. **35**: 1542–1546.

Saunders, R.L., Henderson, E.B., and Harmon, P.R. 1985. Effects of photoperiod on juvenile growth and smolting of Atlantic salmon and subsequent survival and growth in sea cages. Aquaculture, **45**: 55–66.

Saunders, R.L., Specker, J.L., and Komourdjian, M.P. 1989. Effects of photoperiod on growth and smolting in juvenile Atlantic salmon (*Salmo salar*). Aquaculture, **82**: 103–117.

Sheridan, M.A., Allen, W.V., and Kerstetter, T.H. 1983. Seasonal variations in the lipid composition of steelhead trout, *Salmo gairdneri*, associated with parr–smolt transformation. J. Fish Biol. **23**: 125–134.

Sigholt, T., Järvi, T.J., and Lofthus, R. 1989. The effect of constant 12-hour light and simulated natural light on growth, cardiac–somatic index and smolting in the Atlantic salmon (*Salmo salar*). Aquaculture, **82**: 127–136.

Solbakken, V., Hansen, T., and Stefansson, S.O. 1994. Effects of photoperiod and temperature on growth and parr–smolt transformation in Atlantic salmon (*Salmo salar* L.) and subsequent post-smolt performance in seawater. Aquaculture, **121**: 13–27.

Stefansson, S.O., and Hansen, T. 1989. The effect of spectral composition on growth and smolting in Atlantic salmon (*Salmo salar*) and subsequent growth in sea cages. Aquaculture, **82**: 155–162.

Stefansson, S.O., Nævdal, G., and Hansen, T. 1989. The influence of three unchanging photoperiods on growth and parr–smolt transformation in Atlantic salmon, *Salmo salar* L.J. Fish Biol. **35**: 237–247.

Stefansson, S.O., Björnsson, B.Th., Hansen, T., Haux, C., Taranger, G.L., and Saunders, R.L. 1991. Growth, parr–smolt transformation, and changes in growth hormone of Atlantic salmon (*Salmo salar*) reared under different photoperiods. Can. J. Fish. Aquat. Sci. **48**: 2100–2108.

Stefansson, S.O., Berg, A.E., Hansen, T., and Saunders, R.L. 1992. The potential for development of salinity tolerance in underyearling Atlantic salmon (*Salmo salar*). World Aquacult. **23**: 52–55.

Thorpe, J.E., Talbot, C., and Villareal, C. 1982. Bimodality of growth and smolting in Atlantic salmon, *Salmo salar* L. Aquaculture, **28**: 123–132.

Thorpe, J.E., Adams, C.E., Miles, MS., and Keay, D.S. 1989. Some influences of photoperiod and temperature on opportunity for growth in juvenile Atlantic salmon, *Salmo salar* L. Aquaculture, **82**: 119–126.

Wagner, H.A. 1974. Photoperiod and temperature regulation of smolting in steelhead trout (*Salmo gairdneri*). Can. J. Zool. **52**: 219–234.

Wedemeyer, G.A., Saunders, R.L., and Clarke, W.C. 1980. Environmental factors affecting smoltification and early marine survival of anadromous salmonids. Mar. Fish. Rev. **42**: 1–14.

Zaugg, W.S. 1982. A simplified preparation for adenosine triphosphatase determination in gill tissue. Can. J. Fish. Aquat. Sci. **39**: 215–217.

Zaugg, W.S., and McLain, L.R. 1970. Adenosine triphosphatase in gills of salmonids: seasonal variations and salt water influence in coho salmon, *Oncorhynchus kisutch*. Comp. Biochem. Physiol. **35**: 587–596.

Zaugg, W.S., Bodle, J.E., Manning, J.E., and Wold, E. 1986. Smolt transformation and seaward migration in 0-age progeny of adult spring chinook salmon (*Oncorhynchus tshawytscha*) matured early with photoperiod control. Can. J. Fish. Aquat. Sci. **43**: 885–888.

A maximum likelihood approach for estimating growth from tag–recapture data

You-Gan Wang, Mervyn R. Thomas, and Ian F. Somers

Abstract: The Fabens method is commonly used to estimate growth parameters k and l_∞ in the von Bertalanffy model from tag–recapture data. However, the Fabens method of estimation has an inherent bias when individual growth is variable. This paper presents an asymptotically unbiassed method using a maximum likelihood approach that takes account of individual variability in both maximum length and age-at-tagging. It is assumed that each individual's growth follows a von Bertalanffy curve with its own maximum length and age-at-tagging. The parameter k is assumed to be a constant to ensure that the mean growth follows a von Bertalanffy curve and to avoid overparameterization. Our method also makes more efficient use of the measurements at tag and recapture and includes diagnostic techniques for checking distributional assumptions. The method is reasonably robust and performs better than the Fabens method when individual growth differs from the von Bertalanffy relationship. When measurement error is negligible, the estimation involves maximizing the profile likelihood of one parameter only. The method is applied to tag–recapture data for the grooved tiger prawn (*Penaeus semisulcatus*) from the Gulf of Carpentaria, Australia.

Résumé : La méthode de Fabens est couramment utilisée pour estimer les paramètres de croissance k et l_∞ dans le modèle de von Bertalanffy à partir des données de marquage–recapture. Toutefois, cette méthode présente un biais inhérent lorsque la croissance individuelle est variable. Notre étude présente une méthode asymptotiquement sans biais qui utilise une approche du maximum de vraisemblance tenant compte de la variabilité individuelle tant dans la longueur maximale que dans l'âge au marquage. On pose que la croissance de chaque individu suit une courbe de von Bertalanffy avec sa propre longueur maximale et son âge au marquage. On pose également que le paramètre k est constant pour faire en sorte que la croissance moyenne suive une courbe de von Bertalanffy et pour éviter le surparamétrage. Notre méthode utilise aussi de façon plus efficace les mesures au marquage et à la recapture et comporte des techniques de diagnostic qui permettent de vérifier les hypothèses de répartition. Cette méthode est raisonnablement robuste et donne de meilleurs résultats que la méthode de Fabens lorsque la croissance individuelle diffère de la relation de von Bertalanffy. Lorsque l'erreur de mesure est négligeable, l'estimation passe par la maximisation de la vraisemblance du profil d'un seul paramètre. La méthode est appliquée aux données sur le marquage et la recapture de la crevette tigrée verte (*Penaeus semisulcatus*) dans le golfe de Carpentarie, en Australie.

[Traduit par la Rédaction]

Introduction

In fisheries research, the von Bertalanffy equation is often used to describe the relationship between age and length:

$$[1] \qquad l(t) = l_\infty(1 - e^{-k(t-t_0)})$$

in which l_∞, k, and t_0 are parameters. Equation [1] is often assumed to be the mean length of a fish at age t that is randomly selected from the population. Such a curve will be referred to as the *mean growth curve* of the population.

Tag–recapture is one of the most important methods for estimating growth parameters (k, l_∞), especially for species that cannot be aged directly. If we let L_M and L_R denote an individual's length at mark (tag) and length at recapture after time T, respectively, the growth can be expressed as

$$[2] \qquad L_R - L_M = (l_\infty - L_M)(1 - e^{-kT}).$$

Estimation of l_∞ and k based on [2] using least squares is known as the Fabens method (Fabens 1965), which is widely used for analyzing tag–recapture data where age is unknown. Note that the Fabens method assumes that the parameters in [2] are the same as the population growth parameters for all individuals, i.e., each individual's growth follows an identical von Bertalanffy curve. However, biological evidence generally shows that individual variability

Received July 29, 1993. Accepted July 21, 1994.
J12027

Y.-G. Wang and M.R. Thomas. IPP & P Biometrics Unit, CSIRO Cunningham Laboratory, St Lucia, Queensland 4067, Australia.
I.F. Somers. CSIRO, Division of Fisheries, P.O. Box 120, Cleveland, Queensland 4163, Australia.

in growth is the norm. For example, the variability in size of old fish clearly indicates that the maximum lengths are not the same for all fish. However, it is well known that estimation from the Fabens method produces biased estimates when individual growth is variable (see Sainsbury 1980; Maller and deBoer 1988; Francis 1988). In particular, Francis (1988) examined the different meanings of [1] and [2] and concluded that the k and l_∞ parameters from tag–recapture and length-at-age analyses were not comparable.

Kirkwood and Somers (1984) modified the Fabens method by assuming that each individual has its own maximum length, $L(\infty)$, which has a normal distribution. They suggested using maximum likelihood to find parameter estimates. However, as Maller and deBoer (1988) pointed out, their normally distributed error term meant the method was effectively a weighted least-squares method (weighted by a function of time-at-liberty), which was not all that different from the least-squares method of Fabens. Somers and Kirkwood (1991) improved on their 1984 method by assuming a truncated normal distribution for $L(\infty)$ and adding a measurement error to the model.

One of the main advantages of the Fabens equation is that it does not require the knowledge of the age-at-tagging. However, this advantage disappears when individual growth varies. This is because the variance of the increment will depend on the age-at-tagging, and the estimation will be biassed if the variance structure is not taken into account in the estimation. In the present study, we generalize the classical von Bertalanffy growth model by assuming that the maximum length, $L(\infty)$, varies among individuals with a mean of l_∞. The unknown age-at-tagging and parameter t_0 are both treated as random variables. The parameter t_0 cannot be estimated from tagging data unless the absolute ages are known for some individual. To ensure that the mean growth of the population follows a von Bertalanffy curve and to avoid overparameterization, we assume that k is a constant. We then describe a maximum likelihood approach that takes account of both individual variability in $L(\infty)$ and age-at-tagging based on distribution theory; the method should, therefore, be asymptotically unbiassed.

We investigate the robustness of the maximum likelihood approach to individual deviations from the von Bertalanffy curves using a simulation study. To verify the distributional assumptions of the model, we also introduce a new transformation that allows us to examine the variability in $L(\infty)$ and the age-at-tagging. Our maximum likelihood (ML) approach makes full use of measurements at both tag and recapture.

The ML estimation procedure and the diagnostic technique are illustrated with tagging data for the grooved tiger prawn (*Penaeus semisulcatus*) in the northwestern Gulf of Carpentaria, and the results are compared with those obtained with the methods of Fabens (1965) and Somers and Kirkwood (1991).

Maximum likelihood estimation

From [1] we can write the size at mark (tag), L_M, and the size at recapture, L_R, as

$$[3] \qquad L_M = L(\infty)(1 - e^{-kA})$$

$$[4] \qquad L_R = L(\infty)(1 - e^{-k(A+T)})$$

where A is the age at tag (since birth) minus t_0. Here $L(\infty)$, t_0, and the age-at-tag (since birth) are assumed to be random. As one can see, the effect of age-at-tag (since birth) and t_0 is indistinguishable and we only need to consider the effect of A. Therefore, for brevity, we will call A the (relative) age-at-tagging without mentioning "minus t_0".

Let $f(\cdot)$ and $g(\cdot)$ be the density functions of $L(\infty)$ and $1 - e^{-kA}$, respectively. For an animal with observed size-at-tag (mark) l_M and observed size-at-recapture l_R, the likelihood of (l_M, l_R) is

$$[5] \qquad h(l_M, l_R) = \frac{1}{l_R - e^{-kT} l_M} f(u) g(l_M / u)$$

in which $u = (l_R - e^{-kT} l_M)/(1 - e^{-kT})$ if we assume independence of $L(\infty)$ and A (Appendix 1). Note that $f(u)$ is a density function with mean l_∞ in [5].

We will use the uppercase letters for random variables and the lowercase letters for the corresponding observations.

For convenience, we will denote the density of A as $p(\cdot)$. The relationship between $g(\cdot)$ and $p(\cdot)$ is

$$[6] \qquad g(y) = \frac{1}{k(1-y)} p\left(\frac{-1}{k} \log(1-y)\right).$$

Although most of the tagged animals are usually not recaptured, the size-at-tagging for those animals provides age information for the study. If the recatchability is independent of their size, we can also take account of the likelihood contributed by those that are not recaptured. This is because the age distribution for those not recaptured will theoretically be the same as that for those recaptured. The corresponding likelihood is the marginal density function of L_M and can be evaluated from the joint likelihood of (L_M, L_R) ([5]):

$$[7] \qquad \int x^{-1} f(x) g(l_M / x) \mathrm{d}x.$$

The overall likelihood can thus be obtained from the product of [5] for those animals that are recaptured and [7] for those animals that are not recaptured. However, if the recatchability is dependent on the size, the likelihood should be based on [5] alone.

The overall likelihood may then be expressed as a function of the parameters of the probability density functions $f(\cdot)$ and $p(\cdot)$. These parameters are then estimated by standard maximisation of the likelihood function. Asymptotic standard errors can be estimated from the inverse of the Hessian at the optimum using the well-known large-sample properties of maximum likelihood estimators (Cox and Hinkley 1974). The accuracy of large-sample approximations to the distribution of maximum likelihood estimators depends on how quadratic the log–likelihood function is at and near the optimum. Most modern statistical software will allow this issue to be investigated using contouring techniques and profile likelihood plots.

In maximizing the right-hand side of [5] the estimates of the parameters in $f(\cdot)$ are independent of those in $g(\cdot)$ or $p(\cdot)$ when a value of k is specified. Therefore, the estimation can be based on maximizing the profile likelihood with respect

to the parameter k only. This greatly reduces the complexity and computation (cf. the application section).

The success of maximum likelihood estimation depends on having appropriate distributional families for $f(\cdot)$ and $p(\cdot)$. We now consider empirical validation of the functional forms assumed for $f(\cdot)$ and $p(\cdot)$.

From [3] and [4] we have

$$[8] \qquad L(\infty) = L_R + \frac{e^{-kT}}{1-e^{-kT}}(L_R - L_M)$$

and

$$[9] \qquad A = \frac{-1}{k}\log\left[1 - \frac{L_M}{L(\infty)}\right].$$

Therefore, for a given k, one can calculate $L(\infty)$ and A for each individual, using (L_M, L_R). We may then display the empirical distribution of $L(\infty)$ and A by histograms or kernel density estimates. This display allows us to validate the functional forms assumed for $f(\cdot)$ and $p(\cdot)$. Values of $L(\infty)$ and A for several values of k must be generated to determine the appropriate distributions. This diagnostic technique is illustrated below in the application to the estimation of growth of tiger prawns from tag–recapture data.

Effect of measurement error

It is realistic to assume the existence of measurement error, and to study and quantify its effect on the estimation and inference in order to decide whether to incorporate it into the model.

The observed sizes at tag and recapture can be written as

$$\hat{L}_I = L_I + \epsilon_I, \qquad I = M, R.$$

Here $\hat{L}_I$ stands for the observed length, and L_I represents the expected length *for the given animal*, conditional on the values of $L(\infty)$ and A for the animal in question. Assume that ϵ_M and ϵ_R are independent and normally distributed with mean 0 and variance σ^2. For an animal with the observation $(\hat{l}_M, \hat{l}_R)$ the likelihood conditional on $(\epsilon_M = x, \epsilon_R = y)$ is $h(\hat{l}_M - x, \hat{l}_R - y)$. Integrating this with respect to the density of (ϵ_M, ϵ_R), we obtain the unconditional likelihood function $(\hat{l}_M, \hat{l}_R)$

$$[10] \qquad \iint \frac{e^{-(x^2+y^2)/2\sigma^2}}{2\pi\sigma^2} h(\hat{l}_M - x, \hat{l}_R - y)\,dx\,dy.$$

When σ^2 is small, this likelihood can be written (using a Taylor series expansion) as

$$h(\hat{l}_M, \hat{l}_R) + c\sigma^2$$

where $c = \partial h^2(x,y)/\partial x^2 + \partial^2 h(x,y)/\partial y^2$ evaluated at $(x,y) = (\hat{l}_M, \hat{l}_R)$, which is independent of σ. With the measurement error contributing $c\sigma^2$ to the likelihood, its effect may be ignored when σ^2 is small. For example, in the prawn study, the measurement can be accurate to within 0.5 mm, which is small relative to the growth of about 1 mm·week^{-1} (see the application section).

In practice, the growth of an individual fish may be affected by many factors such as water temperature, salinity, food availability, disease and parasites, etc. Therefore, it is more realistic to assume that ϵ_M and ϵ_R are correlated because of the model error. Our conclusion still holds in that case but the derivation is more complicated.

Simulation studies

We investigated the sensitivity of the technique to individual growth curves that deviate markedly from the von Bertalanffy relationship. We generated growth data that had the following properties: (1) the mean growth curve of the population is von Bertalanffy, (2) the deviation of individuals from the mean growth curve is an increasing function of time, and (3) individual growth curves deviate from the von Bertalanffy relationship. This was achieved using the following simulation strategy.

(*a*) Generate a deterministic population mean growth curve.

(*b*) Generate a deviation function $\delta(t)$ where $\delta(t)$ is a deterministic function. $\delta(t)$ specifies the functional form of individual deviations from the mean growth curve.

(*c*) Sample a random deviation term for each individual, R. R is sampled from a distribution with zero mean.

(*d*) Generate the individual growth curve as $L(t) = l(t) + \delta(t)R$. Since R has zero mean, the average of the individual growth curves will be von Bertalanffy. If $\delta(t)$ is chosen to be any function of t that is not simply proportional to $l(t)$, then each individual growth curve will show systematic deviation from the von Bertalanffy relationship.

(*e*) Sample measurement error for each observation, i.e., compute individual length as $L(t) + \epsilon(t)$. Sample different ϵ for each length at mark and length at recapture for each individual.

The *mean growth curve* of the population is assumed to be $l(t) = 100(1 - e^{-0.5t})$. The function $\delta(t)$ is taken to be (1) $1 - e^{-0.8t}$ (von Bertalanffy), (2) $1/(1 + e^{-0.8t})$ (logistic), (3) $\exp(-e^{-0.8t})$ (Gompertz), and (4) $(1 - e^{-0.8t})^2$ (Richards) and R is taken to be distributed as normal $N(0,100)$. The measurement error $\epsilon(t)$ is assumed to be normal $N(0,\sigma_\epsilon^2)$ and the values of σ_ϵ^2 are taken to be 0, 4, and 16. Individual growth curves generated in this way differ from the von Bertalanffy relationship (even in case (1)), but the mean growth curve *does not*.

The time-at-liberty is taken to be uniformly distributed on (0.5,2.5), and A is taken to be a gamma distribution $\Gamma(2,1)$. The estimates are based on 100 simulations and the total number of recaptures is 100 in each simulation. The results in Table 1 show that the new maximum likelihood is quite robust to the individual's deviation from the von Bertalanffy curve, and, as one might expect, the bias increases as the measurement error increases. Overall, the estimates are much better than those of the Fabens method, especially when the measurement error is not very large. Similar results were obtained when $e^{-0.8t}$ was replaced by $e^{-0.3t}$ and $e^{-0.5t}$ in function $\delta(t)$, respectively.

Application to prawn study

To illustrate the method, we use a tag–recapture dataset for the grooved tiger prawn (*Penaeus semisulcatus*), which was obtained from experiments carried out in 1984 in the northwestern Gulf of Carpentaria, Australia (Somers and

Table 1. Growth parameter estimates (and their standard deviations) from 100 simulations using new maximum likelihood (ML) and Fabens methods when the population growth curve follows a von Bertalanffy curve with $k = 0.5$ and $l_\infty = 100$ but individuals *do not* follow a von Bertalanffy curve. The variance of the measurement error is taken to be 0 (no error), 4 (moderate), and 16 (large).

Deviation type	Maximum likelihood		Fabens	
	l_∞	k	l_∞	k
		$\sigma_\epsilon^2 = 0$		
von Bertalanffy	100.7 (2.2)	0.49 (0.036)	107.5 (3.0)	0.39 (0.032)
Logistic	105.7 (4.4)	0.43 (0.057)	128.4 (7.6)	0.25 (0.034)
Gompertz	104.0 (3.8)	0.44 (0.050)	128.7 (8.2)	0.24 (0.036)
Richards	97.9 (3.5)	0.55 (0.070)	122.5 (8.8)	0.28 (0.046)
		$\sigma_\epsilon^2 = 4$		
von Bertalanffy	98.0 (3.3)	0.55 (0.077)	125.6 (9.0)	0.26 (0.042)
Logistic	98.9 (3.9)	0.53 (0.076)	125.7 (9.5)	0.26 (0.038)
Gompertz	98.4 (3.7)	0.54 (0.079)	125.1 (8.1)	0.26 (0.041)
Richards	94.1 (2.8)	0.64 (0.075)	121.9 (8.6)	0.28 (0.052)
		$\sigma_\epsilon^2 = 16$		
von Bertalanffy	91.2 (2.1)	0.76 (0.062)	119.8 (7.9)	0.29 (0.052)
Logistic	92.0 (2.5)	0.72 (0.075)	121.0 (9.1)	0.29 (0.051)
Gompertz	91.5 (2.3)	0.74 (0.070)	120.0 (8.7)	0.30 (0.048)
Richards	90.6 (1.5)	0.78 (0.039)	115.9 (7.9)	0.32 (0.063)

Kirkwood 1991). As with most crustaceans, this species could not be aged directly.

To account for individual variability in $L(\infty)$, Somers and Kirkwood (1991) estimated their growth from these data by a modification of the Fabens method. To be consistent with their study, we analyzed only prawns that (*a*) from inshore releases, (*b*) were at liberty for at least 14 days, and (*c*) had no bopyrid parasites. Each sex was analysed separately.

The 115 male and 131 female *P. semisulcatus* recaptures in the selected dataset had mean carapace lengths (CL) at tag of 27.6 and 29.6 mm, respectively. Mean time at liberty was 13.6 weeks, but ranged as high as 80.9 weeks. The largest size at recapture was 39.8 mm CL for males and 49.0 mm CL for females. To specify appropriate distributions for $L(\infty)$ and age-at-tagging, we chose a few reasonable values of k and examined the empirical distributions obtained from [8] and [9]. In this prawn example, the normal and gamma distributions suited $L(\infty)$ and age-at-tagging, respectively. The parameters were then estimated by numerical maximization of the likelihood function given by [5] and [6] as follows.

(*a*) Choose an initial estimate for k (e.g., 0.05·week^{-1} for the prawn datasets).

(*b*) Calculate $L(\infty)$ and A for each individual using [8] and [9].

(*c*) Estimate the mean l_∞ and variance σ^2 (the maximum likelihood estimates for the normal distribution of $L(\infty)$) from the individual $L(\infty)$ obtained from (*b*).

(*d*) Estimate α and β (the parameters for the gamma distribution for age) from the individual ages A obtained in (*b*), using the approximation method of Thom (Johnson and Kotz 1970). The gamma density function is $x^{\alpha-1}e^{-x/\beta}/\{\beta^\alpha\Gamma(\alpha)\}$. There is no analytical solution for obtaining the parameter estimates for the gamma distribution.

(*e*) Calculate the likelihood based on [5] and [6], using the parameters obtained from (*c*) and (*d*).

(*f*) Use one of the standard numerical techniques for choosing an improved value of k (repeating (*b*) through (*e*)) until the likelihood obtained from (*e*) is maximized (e.g., we used the direct-search method of Nelder and Mead (1965)).

The computation involved is essentially the same as a one-parameter-optimization problem although there are five parameters in the objective function. (The program is written in Fortran and is available from the first author)

The estimates of l_∞, σ^2, k, α, β for males are 36.0, 4.2, 0.081, 15.4, and 1.2, respectively, and for females are 46.6, 15.7, 0.,060, 11.6, and 1.5, respectively. The density of $L(\infty)$ was also chosen to be log–normal, and the estimates of l_∞ and k did not differ substantially (37.3 and 0.075 for males and 46.3 and 0.075 for females). It was then decided that the normal density for $L(\infty)$ was more appropriate based on visual examination. The normal density functions of $L(\infty)$ and A are superimposed on the frequency plot (see Figs. 1 and 2). Comparison of the density functions of $L(\infty)$ and A with the frequency plots indicates a reasonably good fit, with the possible exception of $L(\infty)$ for females (Fig. 2*a*). The range of $L(\infty)$ for females is much greater than for males. Nevertheless, the variation in $L(\infty)$ is evident. Another point of note is that $L(\infty)$ was greater for animals at liberty the longest. Of the individuals at

Fig. 1. Diagnostic frequency distributions for recaptured male *P. semisulcatus* with respect to (*a*) maximum carapace length showing fitted normal distribution and (*b*) age at release showing fitted gamma distribution.

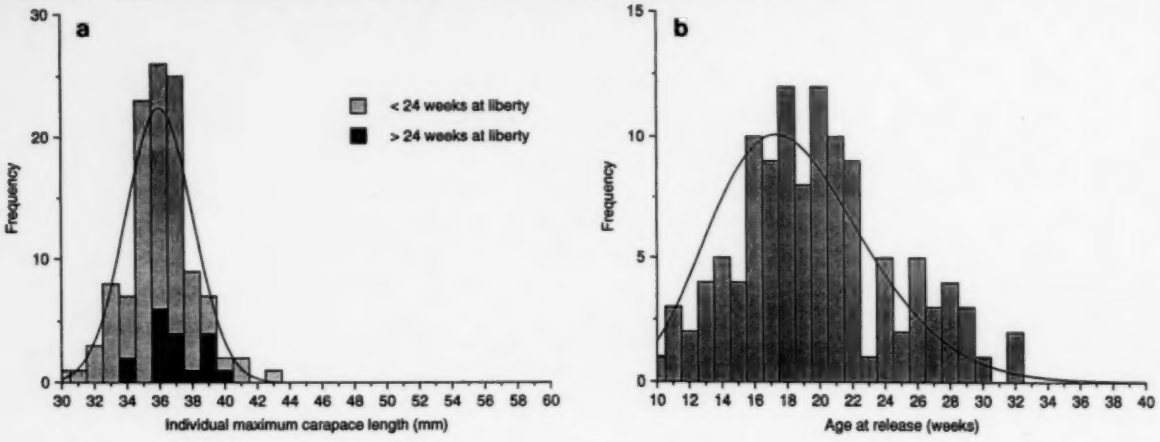

Fig. 2. Diagnostic frequency distributions for recaptured female *P. semisulcatus* with respect to (*a*) maximum carapace length showing fitted normal distribution and (*b*) age at release showing fitted gamma distribution.

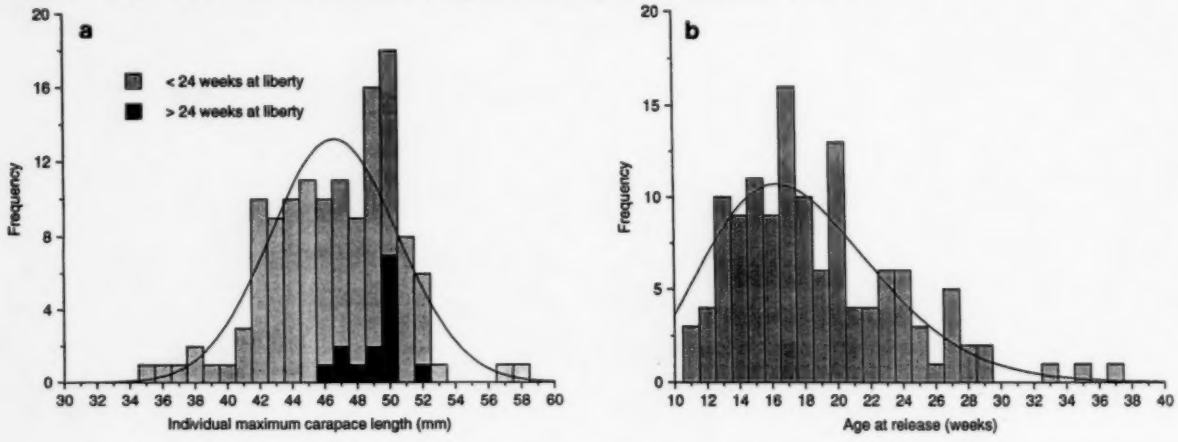

liberty for 24 weeks or more, 16 of 18 males (Fig. 1*a*) and 13 of 14 females (Fig. 2*a*) had $L(\infty)$ greater than the mean $L(\infty)$ for their sex.

The parameter values for k and l_∞ differ from those obtained by Somers and Kirkwood (1991), which are similar to those obtained by the Fabens method (Table 2). For both male and female *P. semisulcatus*, the new k values are 30–40% higher and the $l\infty$ values 4–10% lower in the present study.

To more easily interpret the differences between the maximum likelihood and the Fabens method, growth of *P. semisulcatus* was projected forward and backward from the mean size at tag for both males and females (Fig. 3). Over the average time-at-liberty for the selected dataset (just over 3 months), the two methods give similar results: the models begin to diverge from about 4 months at liberty, but diverge almost immediately when projecting back in time.

Discussion

The assignment of a specific growth curve for individuals is essential in analysing tag–recapture data. The Fabens (1965) approach presumes that individuals follow the same growth curve and individual variability is ignored. We described a maximum likelihood approach that generalizes the Fabens method by taking account of both variabilities in maximum length and age-at-tagging. It seems reasonable to assume that each fish grows according to its own von Bertalanffy curve when the mean growth of the population is thought to follow a von Bertalanffy curve.

The assumption that each fish follows its own von Bertalanffy curve may not be the case in practice. If necessary, an aquarium study can provide a series of recapture data for this test, although the growth parameters of fish in the laboratory may be different from those in the field. The choice of the growth curves is often quite subjective,

Table 2. Comparison of growth parameter estimates for *P. semisulcatus* using new maximum likelihood (ML), Somers and Kirkwood (1991) (S & K), and Fabens methods.

	ML (variable $L(\infty)$ and age)		S & K (variable $L(\infty)$)		Fabens (constant $L(\infty)$)	
Sex	l_∞	k	l_∞	k	l_∞	k
Male	36.0	0.081	37.5	0.062	37.8	0.056
Female	46.6	0.060	51.5	0.043	51.7	0.043

and we recommend using a pragmatic decision based on previous study and experience rather than goodness of fit. On the other hand, it is reassuring that the simulation study shows reasonable robustness of our maximum likelihood estimates to the deviation of individual growth from von Bertalanffy growth curves, and overall it provides better estimates than the Fabens method. The Fabens method performs slightly better as the measurement error becomes larger, but still not as good as the ML method.

The present study focussed on a case (growth of tiger prawns) where the measurement error was negligible. The measurements were accurate to within 0.5 mm, which is small relative to the growth of about 1 mm·week^{-1}. In cases where measurement error is a significant proportion of expected growth, the estimation should be based on the likelihood function [10], which is expected to be robust to the measurement error. It may be worthwhile in future work to investigate the maximum likelihood approach incorporating such measurement errors.

While some attention has been given to addressing the effect of variability in $L(\infty)$, little has been given to variation in age-at-tagging (cf. Kirkwood and Somers 1984; Hampton 1991). Our approach based on the joint probability density function of length at mark, length at recapture, and A ([5]), as pointed out by Sainsbury (1980), "is clearly the correct way of approaching the problem" (his notation T is equivalent to our A). The parameter k, however, is assumed to be a constant in this study. Otherwise, the likelihood function would be integrated with respect to the density of k, and as noted by Sainsbury (1980), the computation involved in the estimation would be expensive to perform. With modern computing facilities, further generalization of our current work is possible; however, as Hampton's (1991) simulation studies suggested, it is not necessary to accommodate the additional complexity of a variable k. We concur with Hampton and have chosen k to be a constant after considering the following. Firstly, there is usually a high correlation between the estimates of l_∞ and k. Overparameterization is a possible problem if we let both k and $L(\infty)$ be random when analysing tagging data, as there are only two data points for each fish. Secondly, in contrast with variation in $L(\infty)$, variation in k means that the mean growth of the population would no longer follow a von Bertalanffy curve (Sainsbury 1980; Crowder and Hand 1990, p. 147). The population growth would also depend on the distribution of k, which adds extra parameters, and the expressions involved would be much more complicated (cf. Xiao 1994). In this case, other growth curves might be more appropriate considering the principle of optimal complexity. Thirdly, maximum length and t_0 play more important roles than k when we have to extrapolate the growth. Therefore, it appears to be unwarranted to allow k to vary as well as $L(\infty)$. On the other hand, if there is evidence that the von Bertalanffy curve does not adequately describe the mean growth of the population, it may be better to consider using other growth curves such as the generalized von Bertalanffy curve (introducing a power parameter).

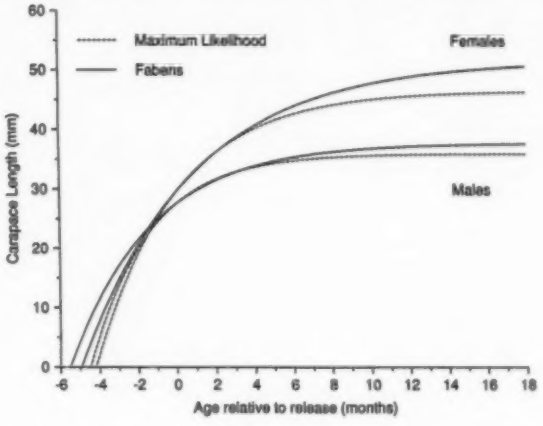

Fig. 3. von Bertalanffy growth curves for tagged male and female *P. semisulcatus* using parameters estimated from the new maximum likelihood and Fabens methods.

The ML approach taken by Somers and Kirkwood (1991) is based on the individual length increment $L_R - L_M$. It assumes that $L(\infty)$ has a normal distribution, truncated at L_M to keep $L(\infty)$ at least as large as L_M. In our approach, $L(\infty)$ is always larger than L_R (see [8]). In fact, we can show that Somers and Kirkwood's (1991) approach is a special case of our more general case. Their notation L_τ is for the size-at-tagging and corresponds to our L_M rather than L_R. From [8], a general expression for the conditional density of $L(\infty)$, given $L_M = l$, can be obtained using distribution theory:

$$[11] \qquad f(x|l) \propto x^{-1} f(x) g\left(\frac{l}{x}\right), \qquad x \geq l.$$

The proportionality sign $\propto$ indicates that a constant independent of x has been omitted; it may be determined from the fact that $\int_l^\infty f(x|l)dx = 1$, and $g(\cdot)$ is the density of $\rho = 1 - e^{-kA}$. In particular, if we let A have the density $\propto$

$e^{-kx}/(1 - e^{-kz})$, or equivalently, let the density of ρ, $g(y)$, take an improper density form, $\propto y^{-1}$ (for those who are not familiar with improper density, see Raiffa and Schlaifer 1961), then

$$f(x|l_M) = \frac{f(x)}{\int_{l_M}^{\infty} f(y)dy}, \qquad x \geq l_M.$$

As one can see, the conditional density of $L(\infty)$ is the density of $L(\infty)$ but left truncated at l_M, i.e., the conditional density of $f(x|L(\infty) \geq l_M$. Note that, in general, the conditional density also depends on the density of A because the observed length contains information both in $L(\infty)$ and A. So the Somers and Kirkwood (1991) approach is a special case of our technique, in which $f(\cdot)$ is assumed to be a normal and $g(y) \propto y^{-1}$. Although their method accounts for individual variability in $L(\infty)$, the parameter estimates may still be biassed because of the variation in A. The estimates for their method do not differ markedly from those of the Fabens method (Table 2), which also takes an asymmetric approach in its treatment of L_M and L_R. An efficient analysis should use L_M and L_R equally. Note that it would also be possible to let $L(\infty)$ be truncated at size at recapture L_R, since the increment can also be written as $(L(\infty) - L_R)(e^{kT} - 1)$.

The likelihood function [5] is derived under the independence of the $L(\infty)$ and age. This assumption can be achieved if we assume that the distribution of $L(\infty)$ is identical over all age classes, or equivalently, conditional on the mean length of the *population* (which is a function of age), and that the distribution of $L(\infty)$ for the population is identical over the length or age range considered (Xiao 1994). Sainsbury (1980) gave an extensive discussion on the implications about this assumption. Another practical concern is that one may have cases where $l_R \leq l_M$, which can easily happen with modest measurement error if animals are old or if times-at-liberty are short. This should not arise if the times-at-liberty are long enough. In our case, the times-at-liberty were greater than 2 weeks.

In comparison with the model of Somers and Kirkwood (1991), our method makes full use of individual measurements, not just the increments, which improves the estimate. The parameter estimates are markedly different from those of either Fabens (1965) or Somers and Kirkwood (1991). The illustration of the ML method using the prawn dataset not only shows its ease of use but also suggests what revised parameter estimates might mean. The description of the growth of *P. semisulcatus* over the range of data collected during the tag–recapture study is effectively the same for both methods. This should not be surprising because both models have been fitted with the same data over this range. That the individual parameter estimates can be so different while the curves are so similar over this range can be attributed to the high negative correlation between k and $L(\infty)$, as was clearly demonstrated by Kirkwood and Somers (1984). Thus the important implications of the revised model are for where growth is extrapolated beyond the range of the observations. For example, the two models differ by about 20% in the estimates of the average age of the prawns at time of tagging (Fig. 3). In this case, both models may in fact be incorrect, as comparison with spawning times and population structure for the species implies an average age-at-tagging of about 6 months (Somers and Kirkwood 1991). Again it should not be surprising that a simple growth model may not describe growth over the entire life cycle of species such as prawns, which inhabit completely different biotic and abiotic environments in their larval, juvenile, and adult stages.

Another important implication for the difference in parameter estimates is where k and l_∞ are used independently of each other or where researchers are trying to compare growth between species or between regions. In these cases, the parameters from the revised model will be more stable and less biassed than those from the Fabens method. Even so, because of the high negative correlation of k and $L(\infty)$, it still may be more appropriate to compare biological reference points (e.g., size at 1 year) rather than growth parameters in the models.

An important assumption that one must make when using tag–recapture data to describe growth is that the growth is the same for both tagged and untagged fish. Tagged *P. semisulcatus* at liberty for long periods (e.g., >24 weeks) have, in general, grown larger than predicted from the model (Figs. 1*a* and 2*a*).

Possibly, tagging temporarily retards the growth of *P. semisulcatus*, as suggested by Penn (1975) for the penaeid *P. latisulcatus*. Hill and Wassenberg (1985) found that tagged *P. esculentus* moulted more often but grew less between moults. They concluded that this was an adaptation to repair wounds. Nonetheless, the net growth of tagged and untagged prawns over the 10 weeks of their experiments was the same. But care should always be exercised in extrapolating to the untagged population. Seasonal growth is another possible factor that could have contributed to the apparent discrepancy in $L(\infty)$ with respect to time-at-liberty. Most of the prawns in this case were tagged and released in autumn, and those with relatively short times-at-liberty experienced the coldest water temperatures. However, as the tagging experiments were in tropical waters with temperatures no lower than 24°C, it is unlikely that there was marked seasonal growth. Any bias in the estimates will also contribute to the discrepancies. Bias may arise from factors such as measurement error (the effect being more significant for animals at liberty the shortest) or size-dependent survival (the fastest growing animals surviving longest). Nevertheless, our ML approach has the potential to be further developed to account for seasonal effect and measurement error, if they are deemed important for the species in question.

Acknowledgements

We are grateful to R.I.C.C. Francis at the Fisheries Research Centre, Wellington, New Zealand, W.S. Hearn at the CSIRO Division of Fisheries, Hobart, Tasmania, Australia, and our colleague P. Jones at the Biometrics Unit for their useful comments on earlier versions of the manuscript. We are also thankful for the comments given by the referees and the associate editor.

References

Cox, D.R., and Hinkley, D.V. 1974. Theoretical statistics. Chapman and Hall, London.

Crowder, M.J., and Hand, D.J. 1990. Analysis of repeated measures. Chapman and Hall, London.

Fabens, A.J. 1965. Properties and fitting of the von Bertalanffy growth curve. Growth **29**: 265–289.

Francis, R.I.C.C. 1988. Are growth parameters estimated from tagging and age–length data comparable? Can. J. Fish. Aquat. Sci. **45**: 936–942.

Hampton, J. 1991. Estimation of southern bluefin tuna *Thunnus maccoyii* growth parameters from tagging data, using von Bertalanffy models incorporating individual variation. Fish. Bull. U.S. **89**: 577–590.

Hill, B.J., and Wassenberg, T.J. 1985. A laboratory study of the effect of streamer tags on mortality, growth, moulting and duration of nocturnal emergence of the tiger prawn *Penaeus esculentus* (Haswell). Fish. Res. **3**: 223–235.

Johnson, N.I., and Kotz, S. 1970. Continuous univariate distributions — 1. Houghton Mifflin, Boston, Mass. pp. 188–189.

Kirkwood, G.P., and Somers, I.F. 1984. Growth of the two species of tiger prawn, *Penaeus esculentus* and *Penaeus semisulcatus*, in the western Gulf of Carpentaria. Aust. J. Mar. Freshwater Res. **35**: 703–712.

Maller, R.A., and Deboer, E.S. 1988. An analysis of two methods of fitting the von Bertalanffy curve to capture–recapture data. Aust. J. Mar. Freshwater Res. **39**: 459–466.

Nelder, J.A., and Mead, R. 1965. A simplex method for function minimization. Comput. J. **7**: 308–313.

Penn, J.W. 1975. Tagging experiments with the western king prawn *Penaeus latisulcatus* Kishinouye. *In* First Australian national prawn seminar. *Edited by* P.C. Young. Australian Government Publishing Service, Canberra, Australia. pp. 84–103.

Raiffa, H., and Schlaifer, R. 1961. Applied statistical theory. Harvard Business School, Cambridge, Mass.

Sainsbury, K.J. 1980. Effect of individual variability on the von Bertalanffy growth equation. Can. J. Fish. Aquat. Sci. **37**: 241–247.

Somers, I.F., and Kirkwood, G.P. 1991. Population ecology of the grooved tiger prawn, *Penaeus semisulcatus*, in the north-western Gulf of Carpentaria, Australia: growth, movement, age structure and infestation by the bopyrid parasite *Epipenaeon ingens*. Aust. J. Mar. Freshwater Res. **42**: 349–467.

Xiao, Y. 1994. von Bertalanffy growth models with variability in, and correlation between, k and L_∞. Can. J. Fish. Aquat. Sci. **51**: 1585–1590.

Appendix 1: Derivation of the likelihood function

Denote $1 - e^{-kA}$ as ρ. We have

[A1] $L_M = L(\infty)\rho$

[A2] $L_R = L(\infty)[1 - (1 - \rho)e^{-kT}]$.

We can express $L(\infty)$ and ρ in terms of L_M and L_R as follows:

$$L(\infty) = \frac{L_R - e^{-kT}L_M}{1 - e^{-kT}}, \qquad \rho = \frac{L_M(1 - e^{-kT})}{L_R - e^{-kT}L_M}.$$

Therefore the likelihood of (l_M, l_R) is $h(l_M, l_R) = f(u)g\left(\frac{l_M}{u}\right)\|D\|$,

where $u = (l_R - e^{-kT}l_M)/(1 - e^{-kT})$ and D is the corresponding Jacobian matrix of the transformation with respect to (l_M, l_R). From [A1] and [A2]:

$$D = \begin{pmatrix} \partial L(\infty)/\partial l_M & \partial L(\infty)/\partial l_R \\ \partial\rho/\partial l_M & \partial\rho/\partial l_R \end{pmatrix} = \begin{pmatrix} -e^{-kT}/(1 - e^{-kT}) & 1/(1 - e^{-kT}) \\ (1 - e^{-kT})L_R/(L_R - e^{-kT}L_M)^2 & -(1 - e^{-kT})L_M/(L_R - e^{-kT}L_M)^2 \end{pmatrix}.$$

Therefore, we have (the absolute value of the determinant is taken) $\|D\| = (l_R - e^{-kT}l_M)^{-1}$.

A stock survey technique using the time to capture individual fish on longlines

David A. Somerton and Bert S. Kikkawa

Abstract: Longline catches per unit of effort (CPUE) from research surveys are often assumed to vary in proportion to fish abundance. This assumption, however, may be invalid if the abundance of the target species is high enough to saturate the gear or if the abundance of nontarget species is high enough to exclude the target species from capture. We examine a new approach to surveying fish populations with longlines that is based on time-to-capture data measured with small, fish-activated timing devices attached to every hook. A new measure of relative abundance, λ, is developed that is immune to the effects of gear saturation and interspecific competition for hooks. Two estimators of λ are compared by using capture-time data collected during summer 1987–1991 for pelagic armorhead (*Pseudopentaceros wheeleri*). Both estimators are shown to be unbiased if the underlying assumptions are true and fairly robust to the observed departures from these assumptions.

Résumé : On considère souvent que les prises à la palangre par unité d'effort (PUE) effectuées pendant les campagnes de recherche varient en proportion de l'abondance des poissons. Cette hypothèse peut toutefois être invalide si l'abondance de l'espèce ciblée est assez élevée pour saturer l'engin ou si l'abondance des espèces non visées est assez forte pour exclure l'espèce cible. Nous décrivons une nouvelle méthode permettant de faire des relevés des populations de poissons à la palangre. Cette méthode mesure à l'aide de petits dispositifs fixés à chaque hameçon et activés par le poisson, le temps écoulé jusqu'à la capture. Nous avons élaboré une nouvelle mesure de l'abondance relative, λ, qui est insensible aux effets de la saturation de l'engin et à la concurrence interspécifique pour les hameçons. Nous comparons deux estimateurs de λ en utilisant les données sur le temps écoulé jusqu'à la capture recueillies pendant l'été, de 1987 à 1991, pour la tête-casquée (*Pseudopentaceros wheeleri*). Nous montrons que les deux estimateurs ne sont pas biaisés si les hypothèses de base sont vraies, et sont assez robustes pour supporter les écarts observés par rapport à ces hypothèses.

[Traduit par la Rédaction]

Introduction

Fish stock assessments are often based on the assumption that changes in the catch per unit of effort (CPUE) obtained in stock surveys are proportional to changes in population size. When longlines are the sampling gear, however, the assumption of proportionality is tenuous because longlines are highly susceptible to the effects of gear saturation and interspecific competition for hooks. Gear saturation occurs when the local density of fish is so high or the fishing time so long that the proportion of hooks remaining unoccupied and baited approaches zero before the longline is retrieved. The primary effect of this is that longline CPUE tends to increase asymptotically rather than proportionately with fish abundance and at high levels of abundance becomes an insensitive indicator of change (Ricker 1975). Interspecific competition for hooks occurs when several species attack the gear simultaneously such that the CPUE of a target species is reduced by the catch of other species (Rothschild 1967). A new index of relative abundance, one immune to the problems of gear saturation and hook competition, is therefore needed to increase the utility of longlines as a stock assessment tool.

Herein we examine an index that has these properties because it is based not on the total number of fish caught during a longline soak, as is the case with CPUE, but rather on the rate at which they are caught relative to the number of hooks remaining during each instant of the soak. Estimation of this index, λ, requires measurements of capture time or the time between the start of fishing and the capture of each fish. Obtaining such measurements remained problematical until development of the hook timer, which is a small, fish-activated timing device attached to each hook (Somerton et al. 1989). This study is a first attempt to develop an index of relative abundance based on the capture times measured with hook timers.

Received October 14, 1991. Accepted July 14, 1994.
J11270

D.A. Somerton[1] **and B.S. Kikkawa**. Honolulu Laboratory, Southwest Fisheries Science Center, National Marine Fisheries Service, NOAA, 2570 Dole Street, Honolulu, HI 96822-2396, USA.

[1] Present address: Alaska Fisheries Science Center, National Marine Fisheries Service, NOAA, 7600 Sand Point Way NE, Seattle, WA 98125, USA.

Two estimators of λ are examined, a regression estimator and a maximum likelihood estimator, both of which are adaptations of estimators used with time-to-failure data (Kalbfleisch and Prentice 1980). The performances of these two estimators are assessed, relative to each other and to CPUE, using capture times measured for pelagic armorhead (*Pseudopentaceros wheeleri*) on the Southeast Hancock Seamount (latitude 29°N, longitude 179°E).

Estimators of λ

The regression and the maximum likelihood estimators of λ are developed by modeling the fate of individual hooks over time subsequent to the set of a longline. For both estimators, λ can be considered as the probability that a hook will stop fishing, or be deactivated, during any instant of time. Initially we assume that the capture of a fish is the only process that can deactivate a hook.

The regression estimator of λ is based on the familiar exponential model used to describe fish mortality (Ricker 1975). Assuming that λ does not vary during a longline soak, then the exponential model can be expressed as

$$[1] \qquad \frac{dN_t}{N_t dt} = -\lambda$$

which upon integration becomes

$$[2] \qquad N_t = N_0 e^{-\lambda t}$$

where N_0 is the initial number of baited hooks and N_t is the number surviving to time t. If all fish strikes result in a capture, then the cumulative catch by time t (C_t) is

$$[3] \qquad C_t = N_0(1 - e^{-\lambda t}).$$

Additionally, if λ can be considered as a sum of components attributable to individual species or species groups, then the cumulative catch of each species is

$$[4] \qquad C_{i,t} = N_0 \frac{\lambda_i}{\lambda}(1 - e^{-\lambda t})$$

where λ_i is the component attributed to species i. To estimate λ_i for each of n species, n equations similar to Eq. [4] are simultaneously fit to cumulative catch and capture-time data using nonlinear regression.

The maximum likelihood estimator of λ is based on the exponential probability model. According to this model, if the hooks suffer a constant probability of being struck by a fish, λ, then the probability that a strike will occur during a small interval about the capture time (τ) is expressed as

$$[5] \qquad P(t = \tau) = \lambda e^{-\lambda t}.$$

If the soak time were long enough to allow all hooks to be struck, then the likelihood function would simply be the product of N_0 expressions like Eq. [5] evaluated at the appropriate capture times. In practice, however, two modifications are usually required. First, capture times for some hooks might be unknown and the corresponding probabilities incalculable because the hooks were retrieved before being struck by a fish. Although for these hooks the probabilities cannot be specified explicitly, they can at least be bounded by integrating Eq. [5] up to the time when each baited hook was retrieved:

$$[6] \qquad P(t \geq \tau) = e^{-\lambda t}$$

where τ is the retrieval time. Second, the value of λ for an individual species (λ_1; subscript 1 henceforth indicates the target species) is usually more important for stock assessment purposes than the value for all species combined; therefore, the effects of competing species must be separated from those of the target species. This can be accomplished by considering the strikes by nontarget species as simply another process that results in unknown capture times. As in the case of early retrieval, the probabilities for the target species cannot be specified explicitly when nontarget species strike the hooks, but the probabilities can be bounded by evaluating Eq. [6] at the capture time of the nontarget species. Incorporating both the capture times of the target species and those of the nontarget species, the likelihood function can be expressed as

$$[7] \qquad L(\lambda) = \lambda_1^{n_1} e^{-\lambda_1 \sum_{i=1}^{n_1} t_{1,i}} e^{-\lambda_1 \sum_{i=1}^{n_2} t_{2,i}} e^{-\lambda_1 \sum_{i=1}^{n_3} t_{3,i}}$$

where n_1 and n_2 are the number of target and nontarget fish that are caught, n_3 is the number of baited hooks retrieved, and $t_{1,i}$, $t_{2,i}$, and $t_{3,i}$ are the ith capture times for target and nontarget fish and the ith soak time for baited hooks. The maximum likelihood estimator is then derived by setting the derivative of the logarithm of Eq. [7] equal to zero and solving for λ_1:

$$[8] \qquad \lambda_1 = \frac{n_1}{\sum_{i=1}^{n_1} t_{1,i} + \sum_{i=1}^{n_2} t_{2,i} + \sum_{i=1}^{n_3} t_{3,i}}.$$

One important feature of this estimator is that, unlike the regression estimator, it requires estimates of the soak times of hooks recovered with bait.

Application of the estimators

The two estimators of λ were applied to data collected by the National Marine Fisheries Service, Honolulu Laboratory, on survey cruises to the Southeast Hancock Seamount conducted each summer during 1987–1990. The sampling gear used was a bottom longline consisting of 30 rigid poles (droppers), each with five equally spaced hooks on short leaders, attached at 18-m intervals along a 600-m groundline (Shiota 1987). Installed in each leader was a hook timer that was activated when a fish struck the hook and indicated the time (in whole minutes) since the strike (Somerton et al. 1989). To maintain constant catchability, all longlines were set perpendicular to the depth contours and fished with the same bait (squid), hook size (No. 20 circle), soak time (1 h), and fishing time (08:00–17:00).

Several types of data were collected during deployment and retrieval of each longline. A depth profile of the bottom was made with a recording fathometer while the longline was set. In addition, the actual fishing depths of the shallow anchor, the midpoint, and the deep anchor were measured by using maximum depth recorders attached to the groundline. For each dropper, the times at release and recovery were recorded. For each hook, the species of any captured fish was recorded as well as the presence of any bait, the activation state of the hook timer (tripped or untripped), and any indicated time.

The fishing depth of each hook was estimated by first fixing on the recorded depth profile, the measured maximum depth of each anchor and the midpoint of the longline. The depth of each dropper was then interpolated at 15 equidistant points between the measured depths of each anchor and the midpoint. All hooks on each dropper were assumed to be at the same depth.

The total elapsed time between release and recovery of a hook included three components: (1) the time between release and bottom contact when fishing presumably began (sink time), (2) the time between bottom contact and a fish strike (capture time), and (3) the time between a fish strike and hook recovery (clock time). The capture time of each fish was not measured and instead was estimated as the difference between the total elapsed time and the sum of the measured clock time and the estimated sink time.

The sink time and soak time (i.e., the time the hook remains in contact with the bottom) for each hook were estimated in two stages. First, sink and soak times were occasionally measured at each anchor and at the midpoint of the longline with time–depth recorders (TDR) having a 30-s sampling interval. Sink time was measured as the time between TDR release and bottom contact; soak time was measured as the time the TDR remained in contact with the bottom. Stepwise multiple regression was used to develop functional relationships to predict sink and soak times from depth and various powers of dropper number (ordered from 1 at the shallow anchor to 30 at the deep anchor). Using the best relationship obtained (in both cases, this was linear with respect to depth and parabolic with respect to dropper number), sink and soak times were then estimated for each hook.

Data collected for each hook were frequently incomplete because either the clock time or the identity of the striking fish was unknown. Because estimates of λ would be biased if hooks with such incomplete data were discarded, we used several methods to account for the unknown data, depending on whether the clock time or the species identity were unknown.

Clock times were unknown when hook timers were tripped near the surface during deployment (early) or at recovery (late) or when they suffered one of several possible malfunctions (Somerton et al. 1989). Most of the timers that were classified as being tripped early or late were observed being tripped; the remainder were identified as early if the clock time was within 3 min of the total elapsed time or as late if the clock time was less than 3 min (armorhead only strike near the bottom and at least 5 min was required for a hook to sink or rise from the bottom). Hooks with late times and intact baits were considered untripped. All other hooks with unknown clock times within each of four hook condition categories (i.e., armorhead, other species, empty hooks, and baited hooks) were allocated among valid clock times by prorating them over the observed capture-time frequency distribution for the appropriate hook condition category.

Species identity was unknown when hooks had apparently been struck by a fish but the fish was not retained. Included in this category were cases in which the hook was recovered with bait and a tripped timer or without bait irrespective of the timer condition. Capture times for the two hook condition categories with unknown species identity (empty hooks and baited hooks) were allocated among the two hook conditions with known species identity (armorhead, other species) in proportion to their relative abundance in the same time interval.

Armorhead catch per hook ($\bar{U}$) and each of the two estimators of λ were calculated as weighted averages over four depth strata (<265, 265–300, 301–400, and 401–500 m). The weighted means ($\bar{X}$) were expressed algebraically:

$$[9] \qquad \bar{X} = \frac{\sum_{i=1}^{4} X_i A_i}{\sum_{i=1}^{4} A_i}$$

where X_i is the stratum mean of the estimator and A_i is the bottom area of the stratum. Variances of the regression and maximum likelihood estimates of $\bar{X}$ were estimated:

$$[10] \qquad \mathrm{Var}\,(\bar{X}) = \frac{\sum_{i=1}^{4} A_i^2 \,\mathrm{Var}\,(X_i)}{\left(\sum_{i=1}^{4} A_i\right)^2}$$

where Var (X_i) is the within-stratum variance.

Within-stratum variances were estimated by using bootstrapping (Efron and Gong 1983) to include error in the estimates of capture and soak times. These variance estimates were calculated as follows. First, the data for each hook in each depth strata were sampled with replacement to generate a new data set with the same sample size (number of hooks) as the original. Second, estimation errors, computed as described below, were added to the estimates of capture and soak times associated with each hook. Third, the regression and maximum likelihood estimators of λ_i were then calculated as before. Third, steps 1 and 2 were repeated 100 times, and the variance among the 100 independent estimates of λ_i was then calculated for each stratum. Fourth, Var $(\bar{X})$ was then estimated by using Eq. [10].

Estimation error was added to the capture and soak times as follows. Error in the estimates of capture time was assumed to be identical to the error in the estimates of sink time because the other components of time used in the estimate, that is, elapsed time and clock time, were measured without appreciable error. Estimation-error deviates for both capture and soak times were assumed to be normal random variables with a mean of zero and a standard deviation (SD) equal to the SD of the residuals about the multiple regression equations predicting sink or soak time from depth and dropper number.

Robustness of the regression and the maximum likelihood estimators to departures from the assumptions of the underlying models were examined by using Monte-Carlo simulation. Three cases were simulated: (1) when all assumptions of the underlying models were valid, (2) when soak times were not constant but varied among hooks, and (3) when λ was not constant but varied with time over the soak duration. In all three cases, a simulation consisted of generating a sample data set, as described below, and then estimating

λ by applying either the regression or the maximum likelihood estimator. The simulations were replicated 100 times. Significance of any bias in the estimates of λ was then tested by comparing the mean of the estimated values of λ with the parametric value by using a *t*-test.

For case 1, λ was set at a value of 0.02 (the observed 4-year mean for armorhead), the soak time was set at 60 min, and, for simplicity, only one species was allowed to strike the hooks. Capture times were generated as follows. The number of fish caught during each 1-min interval was calculated as a binomial random variable with the probability of success equal to $1 - e^{-\lambda}$ (Eq. [3]) and the number of trials equal to the number of baited hooks. The number of baited hooks in each interval was calculated as the number in the previous interval minus the catch.

For case 2, the simulation was identical to case 1, except that the soak time experienced by each hook was variable. Variable soak times were included in the simulation as follows. Over the duration of a simulated longline soak, the number of baited hooks remaining in each time interval was calculated as the number in the previous interval minus both the catch and the number removed from the bottom. The number removed from the bottom in each interval was modeled as a binomial random variable with the probability of success equal to the empirical removal probability and the number of trials equal to the initial number of baited hooks. The removal probability distribution was constructed from the estimated soak times for all hooks set during the stock assessments.

For case 3, the simulation was again identical to case 1, except that λ was allowed to vary with time over a fixed soak time (60 min). The temporal variation in λ used in the simulated longline sets was chosen to mimic the observed pattern obtained by approximating λ within each 1-min interval as $\ln(1 - C_t/N_t)$ (Eq. [3]) where C_t is the catch of all species at time t, and N_t is the number of baited hooks at time t. Values of N_t were estimated as $N_{t-1} - C_{t-1} - R_{t-1}$ where R_{t-1} is the number of baited hooks removed at time t. To obtain a smoother approximation to the pattern of variability in λ over time, a segmented straight-line model, with three segments and variable intersections, was fit to the λ and time data (Gallant and Fuller 1973). Predicted values of λ were then scaled by a constant chosen so that the unweighted average of λ over the soak duration equaled 0.02. In the simulation, λ for each 1-min interval was then predicted by using the scaled model.

Bias in the likelihood estimates of λ due to bias in the estimates of soak time was examined as follows. The maximum likelihood estimator (Eq. [8]) was first simplified by assuming no interspecific competition for hooks and a constant soak time:

$$[11] \qquad \lambda = \frac{n_1}{\sum_i t_i + n_3 T}$$

where $\sum t_i$ is the sum of all capture times, T is the fixed soak time, and the other symbols are as defined earlier. Indicating the biased soak time and the resulting biased estimate of λ (i.e., T^*, λ^*), the magnitude of the bias in λ can then be expressed as

Fig. 1. Average capture-time frequency distribution for the hook conditions of armorhead, other species, empty hooks, and baited hooks. Frequencies, expressed as a percentage of all hooks set within a hook condition and time category, represent a measure of catch rate.

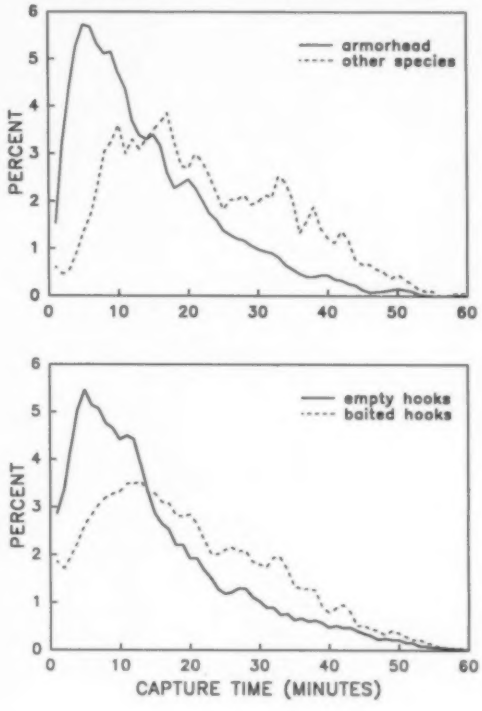

$$[12] \qquad \frac{\lambda^* - \lambda}{\lambda} = \frac{n_3(T - T^*)}{\sum_i t_i + n_3 T^*}$$

$$= -\frac{n_3 T}{\sum_i t_i + n_3 T^*} \frac{T^* - T}{T}$$

$$= -\frac{B}{\left(\frac{\sum_i t_i}{n_3 T}\right) + B + 1}$$

where B is the bias in soak time. The value of $\sum t_i / n_3 T$ is completely determined when λ and T are specified and is calculated using a deterministic version of the simulation model (case 1) previously described.

Results and discussion

The capture-time frequency distributions for pelagic armorhead and all other species as well as for baited and empty hooks with tripped timers all show a similar pattern in which the catch rate increases with time to some maximum and then decreases steadily until the end of the soak (Fig. 1). Although, to our knowledge, the initial increase in

Fig. 2. Regression estimates (triangles) and maximum likelihood estimates (circles) of armorhead λ for each of four survey years.

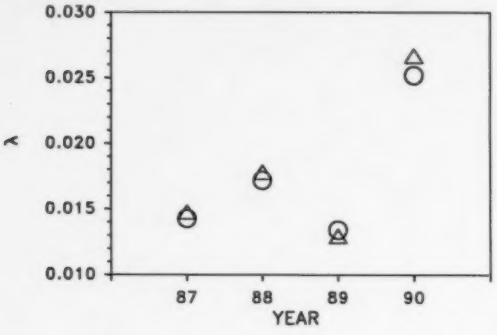

Fig. 3. Variance of the regression estimates (triangles) and the maximum likelihood estimates (circles) of armorhead λ for each of four survey years.

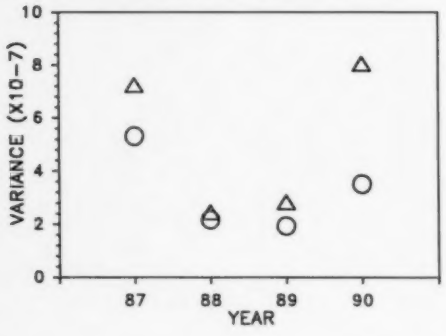

the catch rate of a longline has not been demonstrated before, the subsequent decline is a well-known characteristic of longlines. Note that the peak in the armorhead catch rate occurs earlier than that for other species. Because dogfish (*Squalis misukurii*) are the primary component of the other species category, we interpret this difference as indicative of a difference in mode of feeding. That is, armorhead are pelagic feeders that primarily rely on sight (Seki and Somerton 1994), while dogfish are demersal feeders that primarily rely on smell (Wilson and Seki 1994).

The regression and the maximum likelihood estimates of λ for each year were quite similar and lacked any tendency for one to be larger than the other (Fig. 2). The two estimates, however, differed in precision and, over the 4 years, the average variance of the maximum likelihood estimates was 30.8% less than it was for the regression estimates (Fig. 3).

The similarity of the two estimates is consistent with results of the case 1 Monte-Carlo simulations which demonstrated that neither of the estimates was significantly biased (*t*-test, $P < 0.05$). Case 1 simulations, however, considered idealized longline sets in which λ was constant over the soak duration, all hooks experienced an identical soak duration, and all strikes resulted in a fish capture and a

Fig. 4. Approximate estimates of λ for each 1-min interval averaged over all cruises. A smooth approximation to the fluctuation in λ over time (solid line) was obtained by fitting a segmented straight-line model to the data.

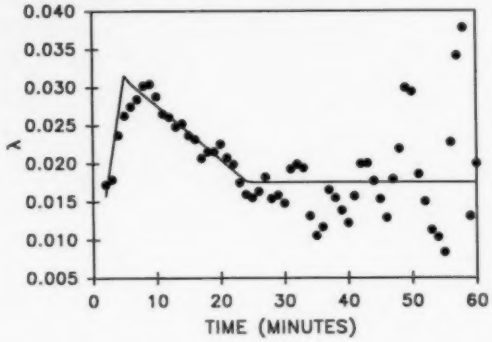

valid time. Since these assumptions were violated during the stock assessments, further Monte-Carlo simulations were performed to examine the potential for bias.

The first assumption examined, that is, the constancy of λ over the duration of a longline set, potentially influences both the regression and the maximum likelihood estimates. Averaged over the four stock assessments, approximate λ estimates for each minute were not constant but increased from 0.017/min at 2 min to a maximum of 0.030/min at 9 min and then decreased to about 0.017/min at 25 min where they remained on average for the remainder of the soak, but with considerable minute-to-minute fluctuation due to small sample sizes (Fig. 4). This pattern is similar to that of catch rate (Fig. 1); however, unlike catch rate, λ estimates depend on the number of hooks still fishing at each instant and therefore are not constrained to decline with time. When a smoothed approximation to this pattern of λ variation was included in the Monte-Carlo simulation, the means of the regression estimates (0.022) and the maximum likelihood estimates (0.021) were not significantly different (*t*-test, $P > 0.05$) than the value of λ (0.020) averaged over the soak time. Thus, for armorhead the observed departure from a constant λ did not result in a detectable bias.

The reasons why λ varies with time are unclear. One possible explanation is that λ varies in proportion to fish density in the immediate vicinity of the longline and this density changes with time because of the attraction of fish by the bait and the catch of fish by the longline. Another, but less likely, explanation is that λ does not vary in strict proportion to fish density but instead changes with time because of the initial diffusion of the bait's odor and its subsequent dissipation.

Regardless of the mechanism, temporal variation in λ can occur and may in some cases invalidate the use of constant λ estimators. We considered various approaches for dealing with this problem, including the use of models with time-varying λ and the use of time-specific estimates of λ (Fig. 4). These approaches were abandoned, however, because λ must be a simple number rather than a function of time to be useful as an index of relative abundance.

Fig. 5. Soak time probability distribution or the proportion of all hooks set that were retrieved per minute.

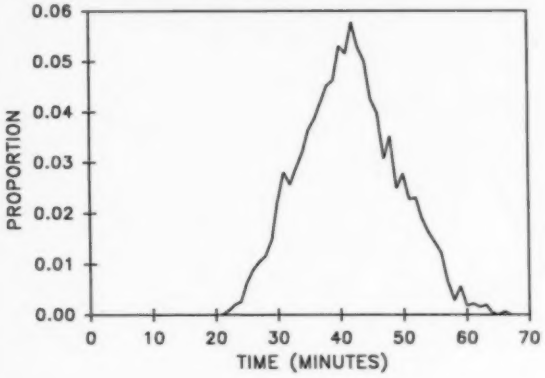

Fig. 6. Estimated percent bias in the maximum likelihood estimate of λ as a function of the bias in soak time and the true value of λ. Calculations are based on Eq. [12] with a true soak time of 60 min.

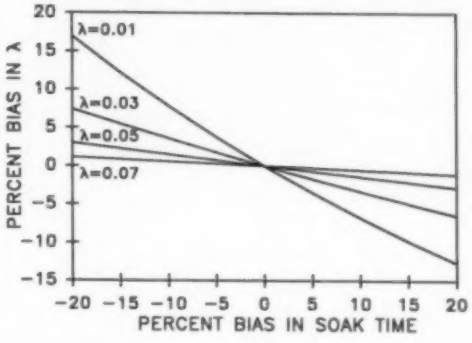

The second assumption examined, that is, the constancy of the soak time among hooks, potentially influences only regression estimates because likelihood estimates require explicit specification of the soak times. In our case, soak time averaged 43 min but varied considerably (Fig. 5) because of variation in fishing depth, sinking speed, and retrieval speed. To examine the likely effect of such variation in soak time in the Monte-Carlo simulation, hooks were removed from the bottom according to the observed soak time distribution. The resulting mean regression estimate of λ (0.019) was not significantly different (*t*-test, $P > 0.05$) than the value used in the simulation. Therefore, any bias in the regression estimate due to variation in soak times is too small, for armorhead, to be detectable.

Although soak time variability cannot influence maximum likelihood estimates of λ, because soak times must be explicitly specified, such estimates of λ are subject to bias if the estimates of soak time are biased. The likely magnitude of such bias will depend on the true values of λ and soak time. For armorhead, bias was examined for a λ of 0.01–0.09 and a soak time of 60 min, values approximating those observed or expected during the stock assessments (Fig. 6). In general, when λ is low and a high proportion of the hooks are retrieved with bait, bias in the estimates of soak time produces a corresponding bias of opposite sign in the likelihood estimates. When λ is high and a low proportion of hooks are retrieved with bait, bias in soak time estimates produces negligible bias in the λ estimates. Thus, the utility of the maximum likelihood estimator is diminished greatly if soak time cannot be measured accurately and if the proportion of the hooks recovered with intact bait is high. Since the average value of λ was 0.02 for armorhead, any bias in the estimates of soak time could have an appreciable effect on the estimated value of λ.

Perhaps the greatest limitation to the use of capture-time data in developing an index of relative abundance, at least for armorhead, is the prevalence of unknown capture times or species identities. Capture times were unknown for 32% of the apparent strikes (Table 1). Since hooks with unknown times cannot be eliminated without inducing a bias, they were accounted for in the estimates by simply prorating them over the time distribution of the appropriate catch category (i.e., armorhead, other species, empty hooks, baited hooks; Fig. 1). Such a procedure rests on the assumption that the processes producing the valid times are applicable to the hooks with invalid or missing times in the same catch category. The reasonableness of this assumption, however, varies with catch category. For example, when a fish is captured, it is fairly certain that the timer has been tripped by the captured fish and it is therefore reasonable to assign a capture time to a hook with a fish using the capture times for other hooks from the same species category. But when an empty hook or a bait is returned, the timer could have been tripped by a fish strike or by snagging some object during gear deployment or retrieval. Because of this uncertainty, it is possible that simple proration is inappropriate for the last two catch categories.

Species identity was unknown for 70% of the apparent fish strikes and therefore posed a greater problem than the unknown capture times (Table 1). The procedure used for allocating hooks with unknown species identity between the catch categories of armorhead and other species is based on the assumption that, once a hook is struck by a fish, the probabilities of capture, escaping without bait removal, and escaping with bait removal are the same for all species. However, this may not be true. For example, the capture-time distribution for empty hooks (Fig. 1) was similar to that for armorhead, while the distribution for baited hooks was similar to that for other species, suggesting that armorhead are more prone to removing a bait after striking a hook than are the other species. We attempted to account for such species differences in the probability of leaving intact bait by regressing the number of baited and empty hooks against the number of armorhead and other species on each longline set and then using the estimated constants in an allocation scheme. However, this approach is also problematical because it must be based on the identities of the species captured. Further, it is possible that some species are adept at stealing bait and avoiding capture. In our case, for example, the blunthead puffer (*Sphoeroides pachygaster*) appeared to be such a species because it was rarely caught but invariably stuffed with bait.

Table 1. All hooks recovered on each of the four stock survey cruises (excluding those set at depths of >500 m) categorized by hook conditions (armorhead, other species, empty hooks, baited hooks) and by time condition (valid, invalid, not tripped). The percentage of all observations within each category is also shown.

Hook condition category	No. of hooks		
	Valid time	Invalid time	Not tripped
1987			
Armorhead	282	131	3
Other species	157	70	16
Empty	599	438	535
Bait	180	265	910
1988			
Armorhead	921	187	25
Other species	103	26	7
Empty	864	209	380
Bait	538	226	1114
1989			
Armorhead	589	78	15
Other species	244	40	24
Empty	1391	193	440
Bait	654	173	1049
1990			
Armorhead	835	139	2
Other species	181	35	10
Empty	1453	275	503
Bait	506	157	747
Overall percentages			
Armorhead	15	3	0
Other species	4	1	0
Empty	24	6	10
Bait	10	5	21

Unknown capture times and species identities not only have the potential of biasing estimates of λ, they also complicate the calculation of variance because the true sample sizes are unknown due to the allocation scheme used to account for the missing data. For example, if the proportion of all hooks with unknown data were increased, the effective sample size would decrease. However, the sample size used in the bootstrapping procedure would remain constant because of the allocation of the unknown data, and the estimated variance would progressively underestimate the true variance. Unfortunately, we do not know how to correct this problem.

Although unknown capture times and species identities were problematical in our study, their prevalence appears to be lower in other studies that have used hook timers. In his study of tuna and billfish using pelagic longlines, Boggs (1992) found a relatively low incidence of unknown capture time and species identity. This was also true for the study of sablefish (*Anoplopoma fimbria*) conducted by Sigler (1993) using bottom longlines.

Fig. 7. Armorhead $\bar{U}$ (number caught per 1000 hooks) and armorhead λ (average of the regression and maximum likelihood estimates) for stock assessments, 1987–1990.

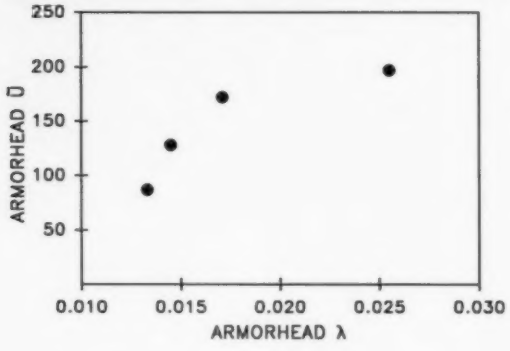

Superiority of the regression or the maximum likelihood estimator is equivocal. The maximum likelihood estimator appears to be better because it is easier to calculate and has a smaller variance. However, unlike the regression estimator, the maximum likelihood estimator requires estimates of soak time and, at least for armorhead, soak time is the most difficult of all data to estimate precisely. This imprecision in the estimates of soak time is due to the fact that soak time cannot be practically measured for all hooks and instead must be predicted from a limited number of observations. Variation in the speed of longline retrieval, due to weather conditions or a variety of operational problems, can result in a considerable bias in the predicted values of soak time which, in turn, could result in biased estimates of λ.

The primary motivation for using λ, rather than $\bar{U}$, as an index of relative abundance is that λ increases linearly with fish density, while $\bar{U}$ increases at a diminishing rate. When $\bar{U}$ is plotted against λ, such a curvilinear relationship is evident in the armorhead time series, even though the density of armorhead varied by only a factor of 2 (Fig. 7) and gear saturation averaged only 0.62 (i.e., 1 minus the proportion of total hooks set that is recovered with bait). At the higher saturation levels that would occur at higher population densities, the nonlinearity would be more pronounced. For example, although $\bar{U}$ appears to be responsive to changes in λ at levels of $\lambda < 0.02$, if density increased to $\lambda > 0.03$, say, then the slope of the curve would be considerably less and $\bar{U}$ would be an insensitive index of changes in density. For armorhead, this point is especially important because the population has been overfished to only 1% of its initial abundance (Somerton and Kikkawa 1992), and if management efforts to restore the stock are effective, the densities that might be achieved would render $\bar{U}$ ineffective for stock assessment.

Although gear saturation and its consequent effects on CPUE are not unique to longlines, the process of saturation is perhaps more subtle for longlines than for other types of

fishing gear, and the initial but influential stages of gear saturation may be generally unrecognized. For example, saturation would probably be defined by most as the absence of baited hooks upon retrieval of the gear. However, most fish species sampled with longlines are spatially distributed in patches whose dimensions are small relative to the length of the longlines, and such patchiness may lead to localized saturation of the longlines. Thus, saturation effects on CPUE could be significant even when a substantial proportion of the hooks may remain baited when the gear is retrieved. We therefore believe that gear saturation is more pervasive on longline stock surveys than is likely perceived and that using the hook timers and the parameter estimation techniques described herein effectively minimize the effects of gear saturation.

Acknowledgements

We thank Dan Kimura for his help in formulating the maximum likelihood estimator of λ and Ana Parma, Jeff Polovina, and Laura Richards for reviewing the manuscript and offering helpful suggestions.

References

Boggs, C.H. 1992. Depth, capture time and hooked longevity of longline-caught pelagic fish: timing bites of fish with chips. Fish. Bull. **90**: 642–658.

Efron, B., and Gong, G. 1983. A leisurely look at the bootstrap, the jackknife and cross-validation. Am. Stat. **37**: 36–48.

Gallant, A.R., and Fuller, W.A. 1973. Fitting segmented polynomial regression models whose joint points have to be estimated. J. Am. Stat. Assoc. **68**: 144–147.

Kalbfleisch, J.D., and Prentice, R.L. 1980. The statistical analysis of failure time data. John Wiley & Sons, New York, N.Y.

Ricker, W.E. 1975. Computation and interpretation of biological statistics of fish populations. Bull. Fish. Res. Board Can. **191**.

Rothschild, B.J. 1967. Competition for gear in a multiple-species fishery. J. Cons. Perm. Int. Explor. Mer **31**: 102–110.

Seki, M.P., and Somerton, D.A. 1994. Feeding ecology and daily ration of the pelagic armorhead, *Pseudopentaceros wheeleri*, at Southeast Hancock Seamount. Environ. Biol. Fishes **39**: 73–84.

Shiota, P.M. 1987. A comparison of bottom longline and deep-sea handline for sampling bottom fishes in the Hawaiian Archipelago. Honolulu Lab., Southwest Fish. Sci. Cent. Natl. Mar. Fish. Serv. NOAA, Honolulu, HI 96822-2396, USA. Southwest Fish. Sci. Cent. Admin. Rep. H-87-5.

Sigler, M.F. 1993. Stock assessment and management of sablefish *Anoplopoma fimbria* in the Gulf of Alaska. Ph.D. dissertation, University of Washington, Seattle, Wash.

Somerton, D.A., and Kikkawa, B.S. 1992. Population dynamics of pelagic armorhead *Pseudopentaceros wheeleri* on Southeast Hancock Seamount. Fish. Bull. **90**: 756–769.

Somerton, D.A., Kikkawa, B.S., and Wilson, C.D. 1989. Hook timers to measure the capture time of individual fish. Mar. Fish. Rev. **50**(2): 1–5.

Wilson, C.D., and Seki, M.P. 1994. Biological and population characteristics of *Squalis Mitsukurii* from a seamount in the central north Pacific Ocean. Fish. Bull. **92**: 851–864.

Historical versus recent levels of organochlorine contaminants in lamprey larvae of the St. Lawrence River basin, Québec

Claude B. Renaud, Klaus L.E. Kaiser, and Michael E. Comba

Abstract: This study shows that persistent organochlorine contaminants, including PCBs, reached higher concentrations in lamprey of the St. Lawrence River basin 40 years ago. A comparison was made of the concentrations of 22 organochlorine pesticides and 93 polychlorinated biphenyl (PCB) congeners in formalin-preserved lamprey ammocoetes collected between 1947-1950 and in 1990 in the St-François and Ste-Anne rivers, St. Lawrence River basin, Québec. Eight pesticides (β-BHC, α-Chlordane, γ-Chlordane, *p,p'*-DDD, *o,p'*-DDE, *p,p'*-DDE, *p,p'*-DDT, and Heptachlor) reached higher concentrations in the earlier period, with Mirex being the only pesticide found in higher concentrations in 1990. Seventeen PCB congeners (24(27), 28, 98(84), 101, 110(77), 128, 129, 141, 149, 151, 158, 174, 177, 180, 183, 187(182), and 198) had higher concentrations in the 1947–1950 period compared with 1990. A significant inverse relationship was found between the concentration of the various PCB congeners and sampling date. The concentrations of DDT have decreased significantly, while its metabolites, DDD and DDE, have increased significantly over the last 40 years.

Résumé : Cette étude a permis de démontrer que les contaminants organochlorés persistants, y compris les BPCs, atteignaient des concentrations plus élevées dans les lamproies du bassin fluvial du St-Laurent il y a 40 ans. Nous avons comparé les concentrations de 22 pesticides organochlorés ainsi que les concentrations de 93 congénères de biphényles polychlorés (BPCs) dans des ammocètes de lamproies préservées dans le formol, échantillonnées en 1947–1950 et en 1990 dans les rivières St-François et Ste-Anne, bassin du fleuve St-Laurent, Québec. Huit pesticides (β-BHC, α-Chlordane, γ-Chlordane, *p,p'*-DDD, *o,p'*-DDE, *p,p'*-DDE, *p,p'*-DDT, et Heptachlor) affichaient des concentrations plus élevées dans la période antérieure et le Mirex fut le seul pesticide à atteindre une plus haute concentration en 1990. Dix-sept congénères de BPCs (24(27), 28, 98(84), 101, 110(77), 128, 129, 141, 149, 151, 158, 174, 177, 180, 183, 187(182) et 198) affichaient des concentrations plus élevées dans la période 1947–1950 comparativement à 1990. Une relation inverse statistiquement significative existe entre la concentration des divers congénères de BPCs et la date d'échantillonnage. La concentration du DDT a diminué de façon significative tandis que ses métabolites, le DDD et le DDE, ont augmenté de façon significative au cours des 40 dernières années.

Introduction

The purpose of this study was to test the hypothesis that the freshwater environment has changed with regards to organochlorine contaminants over the last 40 years or so. We are aware of only two studies (MacGregor 1974; Neidermyer and Hickey 1976) that have used formalin-preserved museum specimens for historical trend analysis of organochlorine contaminants. One problem with using historical museum wet collections for pesticide analyses has always been that the history of the preservative(s) used for a given collection was either not or poorly documented, making any analytical results unreliable (Rick 1975). For example, if a preservative had extracted pesticide contaminants into solution, an unknown amount of contaminants would be lost upon changing the preservative. Such was not the case in this study. Whereas fishes usually are initially fixed in a formaldehyde solution and then transferred into alcohol for permanent storage, the late V.D. Vladykov kept his lamprey collections permanently in 4–5% formalin (Vladykov 1949, 1950, 1952). He donated his historical lamprey collections to the Canadian Museum of Nature (CMN) in October 1968 (Accession No. 68-278). The

Received August 26, 1993. Accepted July 14, 1994.
J12067

C.B. Renaud. Ichthyology Section, Research Division, Canadian Museum of Nature, P.O. Box 3443, Station D, Ottawa, ON K1P 6P4, Canada.
K.L.E. Kaiser and M.E. Comba. Lakes Research Branch, National Water Research Institute, P.O. Box 5050, 867 Lakeshore Rd., Burlington, ON L7R 4A6, Canada.

Fig. 1. Localities in the St. Lawrence River basin, Québec, where the lamprey ammocoete samples were collected.

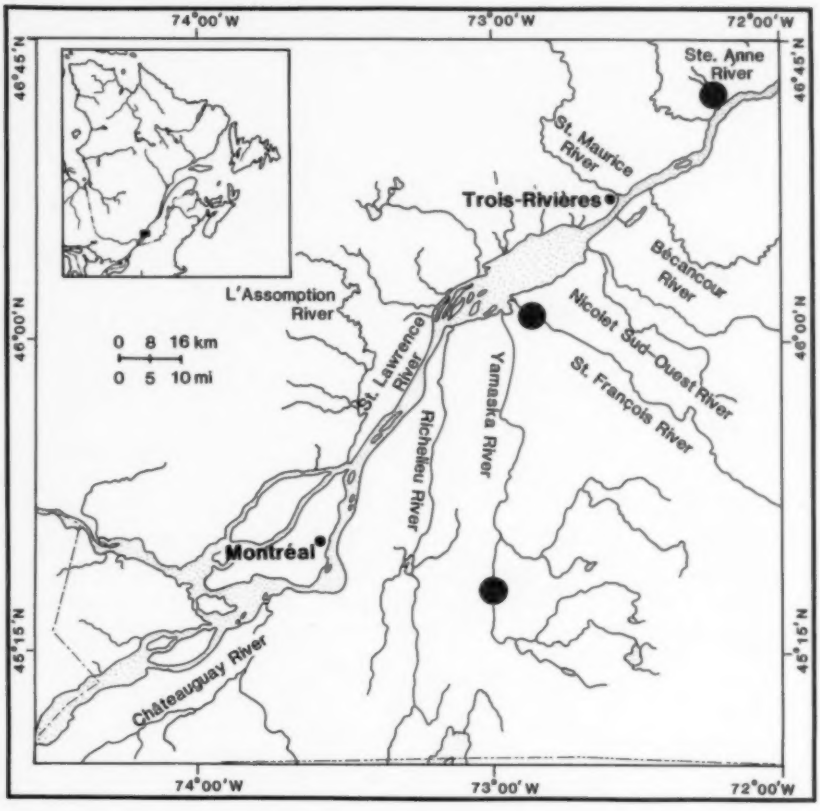

Vladykov collections, all still in the original 4–5% formalin preservative, were used in this study. Lamprey collections were made in 1990 for comparative purposes.

This is the first study of organochlorine contaminants using lamprey larvae, although other studies involving adults of the sea lamprey (*Petromyzon marinus*) have been completed (Kaiser and Valdmanis 1978; Kaiser 1982).

Materials and methods

Sampling and identifications

The eight historical larval lamprey (ammocoete) samples, totalling 48 specimens of two species (the northern brook lamprey (*Ichthyomyzon fossor*) and the American brook lamprey (*Lampetra appendix*)), came from CMN collections (catalog Nos. NMC86-0901 to 86-0906, 86-0908, and 86-0909). These were collected between 1946 and 1959 in the following three rivers of the St. Lawrence River basin in Québec: Yamaska near St-Césaire, St-François near Pierreville, and Ste-Anne at Sainte-Anne-de-la-Pérade (Fig. 1). The method of capture was not documented, but according to Vladykov (1952), ammocoetes from these localities were commonly collected using either a shovel or a dredge. The four recent ammocoete samples, totalling 18 specimens of the same two species, were collected from the same sites in the St-François and Ste-Anne rivers in July 1990, at depths ranging from 0.01 to 1.50 m, using a Smith-Root type VII DC-electrofisher. Despite intensive electrofishing efforts, no ammocoete specimens were collected at the Yamaska locality in 1990. The 1990 samples were put directly into 5% formalin upon collection according to Vladykov (1950, 1952). They were identified to species using Vladykov (1950) and Lanteigne (1988), and their total length was measured to the nearest 0.5 mm.

Chemical analyses

Chemical analyses were conducted for 22 organochlorine pesticides (Tables 1 and 2) as well as polychlorinated biphenyls (PCBs) (118 congeners grouped in 93 congener–congener combinations). The lampreys from a given sample were sliced into approximately 5-mm segments to ensure optimal extraction and air-dried to a constant weight (normally 3 days), after which their combined weight was determined to the nearest 0.01 g. The lamprey segments were then immersed in 20 mL of concentrated hydrochloric acid until dissolved (normally 5 days) and homogenized with an Ultra Turrax homogenizer for 15 min. This procedure was chosen, as previous investigators experienced difficulty with the extraction of lamprey skin (Kaiser

and Valdmanis 1978). The acid solution was placed into a 1-L separatory funnel to which 75 mL of deionized water (preextracted with hexane) was added. The acid–water solution was extracted with 3× 50-mL washes of dichloromethane and the solvent extract eluted through sodium sulphate. The final sample extract was reduced to ~2 mL using rotary and atmospheric evaporation. Separation of lipid and contaminant was achieved using gel permeation chromatography (GPC). The 2-mL sample was fractionated by elution with 50:50 hexane–dichloromethane through a column (2 × 50 cm) of preswelled Biobeads S-X3 resin. Fraction 1 (first 100 mL) contained the lipid portion of the sample that was dried and weighed to the nearest 0.0001 g. The amount of lipid recovered using GPC/acid extraction was the same as that using GPC/soxhlet extraction and 13% higher than the lipid recovered with a Büchi model 810 fat extractor and 2:1 chloroform–methanol. There was no further recovery of lipid (<5% of total lipid) in subsequent GPC/soxhlet extracts of lamprey samples using 9:1 dichloromethane–methanol. The second 100-mL aliquot (GPC fraction 2) contained all the organochlorine contaminants of interest. This fraction was evaporated to ~2 mL and fractionated further by elution through a 1 × 20 cm column of activated silica gel (fired at 350°C) yielding fractions A (50 mL of hexane) and B (50 mL of 1:1 dichloromethane–hexane). Both fractions were rotary evaporated to ~5 mL with 1 mL of toluene as keeper. The final sample volume of 1 mL was obtained by atmospheric evaporation. Fraction A contained the PCB components, pentachlorobenzene, hexachlorobenzene, Aldrin, Mirex, and *t*-Nonachlor. Fraction B contained α-, β-, and γ-BHC, Heptachlor, Heptachlor epoxide, α- and γ-Chlordane, α- and β-Endosulfan, Endrin, Dieldrin, *o,p′*- and *p,p′*-DDE (90%), *o,p′*- and *p,p′*-DDD, and *o,p′*- and *p,p′*-DDT.

The formalin preservative solutions from both the historical and recent lamprey collections for each river were pooled and extracted with 3 × 100-mL hexane washes in a 2-L separatory funnel. The hexane extracts were dried with anhydrous sodium sulphate, reduced to ~2 mL by rotary evaporation, fractionated on silica gel, and analysed for organochlorine contaminants.

Extracts were analysed with a HP 5890 gas chromatograph with dual capillary columns and electron capture detectors. Two fused silica high-performance capillary columns (i) 30-m HP-5 (Hewlett Packard) and (ii) 30-m DB-1 (Chromatographic Specialties, Brockville, Ont.) with 0.25-mm interval diameter and 0.11-μm phase thickness were used. Samples (2 μL) were injected automatically into a split/splitless injector (250°C), operated with a splitless hold time of 0.2 min. Initial chromatography conditions were 65°C, isothermal for 2 min, 10°C/min to 110°C, 3°C/min to a final temperature of 280°C, isothermal 5-min hold. The carrier gas was hydrogen.

Quantitation of organochlorines was based on dual-column confirmation and acceptance of the averaged signal responses when each deviated less than 30% from the mean. Compound identification was ascertained by verification with performance standards, compliance with specified fractionation procedures, and continuous monitoring with method spikes. Quantitative values were assigned according to response factors based on instrument performance standards and retention time matching for the compounds of concern. Acceptance windows were ±0.05 min on both columns. Quantitation procedures and standard reliability were checked regularly through quality control samples and participation in interlaboratory quality assurance studies. Contaminant concentrations are expressed in parts per billion (ppb) (nanograms per gram) of lipid sample weight. The nominal detection limits (Comba et al. 1993*a*, 1993*b*) varied between 0.1 and 10.0 ng/g lipid analysed, depending on the PCB congener, and between 0.1 and 1.0 ng/g lipid analysed for the other organochlorines. Spiked control samples ($n = 5$), without sample matrices, were analysed in the same manner as samples except that they were soxhlet-extracted instead of acid-extracted. Recoveries of organochlorine residues (Comba et al. 1993*a*) were consistently greater than 90 and 109% ± 21 (SD) for total PCB after all three methods of treatment (soxhlet, GPC, silical gel). Monochloro PCBs had the lowest recovery at 56% ± 11 (PCB 1) and 68% ± 8 (PCB 3). Recoveries of organochlorines based on acid-extracted samples are generally 13–20% lower than those based on soxhlet-extracted samples (Renaud et al. 1995).

The observation of Mirex in pre-1960 samples was confirmed with a Hewlett Packard 5971A mass selective detector. Compound identification was made according to Onuska et al. (1980) by monitoring the ion responses at *m/z* 546, *m/z* 238, and *m/z* 272 with quantitative comparison of the ion ratio *m/z* 238/272 and retention time response to that of Mirex (±0.08 min).

PCBs were measured as individual congeners according to the IUPAC structure and numbers assigned by Ballschmitter (Ballschmitter and Zell 1980). Congener identification and gas chromatographic separation were based on the dual capillary column procedure established at the 1985 PCB Workshop in Grosse Ile, Michigan. Initial quantitation of PCB congeners was carried out using the primary Green Bay mass balance standard (Swackhamer 1988), obtained through the University of Minnesota. The Green Bay PCB standard is a mixture of Aroclors 1232, 1248, and 1262 (item Nos. E107, E108, and E130) from the Quality Assurance Branch, U.S. Environmental Protection Agency, Cincinnati, Ohio, in the ratio 25:18:18. Individual congener concentrations were calibrated by Mullin (M.D. Mullin, Great Lakes Research Station, Grosse Ile, Mich., personal communication at PCB Workshop, June 1985) for this PCB standard. Response factors were provided by Mullin for the individual and coeluting congeners and were similar to published values (Mullin et al. 1984). Twenty-three coeluting PCB combinations, 4(10), 12(13), 16(32)*, 24(27), 48(47)*, 60(56), 70(76), 64(41)71, 66(95)*, 98(84), 107(123), 110(77), 134(143), 135(144), 138(163)*, 167(185), 171(156), 172(197), 176(130), 178(126)*, 187(182), 195(208), and 203(196), were quantified using the mixed response factors for specified standard concentrations. With the exception of 4(10), the individual response factors differ by less than 50%. Therefore, a shift in the proportions of the coelutants should not result in any large error. Congener pairs indicated with an asterisk are separated in the majority of samples, but were recombined for continuity. Congeners 10, 77, 98, 126, 143, 163, and 208 are minor constituents in PCB mixtures. Presently, the

Table 1. Concentration of organochlorine contaminants (ppb), based on lipids, in the lamprey ammocoete *Ichthyomyzon fossor* from the Yamaska River, near St-Césaire, Québec, in the 1946–1959 period. The mean, standard deviation, and range are given for the total length. BDL = below sample detection limit.

Sample collection date	28 Sept. 1946	25–28 Aug. 1949	26 Aug. 1949	26–28 Aug. 1949	Oct. 1959
Specimens in sample	9	7	22	2	2
Total length (mm)	149.5 ± 16.8 (119.5–175.5)	113.9 ± 42.9 (22.0–147.0)	106.9 ± 18.1 (78.0–140.0)	103.0 ± 26.9 (84.0–122.0)	125.0 ± 14.1 (115.0–135.0)
Sample lipid weight (g)	2.22	1.86	9.10	0.08	0.20
Aldrin	32	72	4	250	14
Dieldrin	BDL	BDL	61	250	BDL
Endrin	BDL	BDL	BDL	BDL	BDL
α-BHC	17	65	120	60	110
β-BHC	17	23	58	150	140
γ-BHC (= Lindane)	10	44	61	160	130
α-Chlordane	21	220	470	290	260
γ-Chlordane	18	180	440	200	160
o,p'-DDD	320	690	780	790	900
p,p'-DDD	1500	1500	1700	1600	2200
o,p'-DDE	62	35	53	83	78
p,p'-DDE	210	250	8	590	300
o,p'-DDT	460	280	180	820	960
p,p'-DDT	5700	2200	170	8000	5000
α-Endosulfan	29	28	210	63	BDL
β-Endosulfan	19	39	78	180	110
Heptachlor	29	7	33	6	6
Heptachlor epoxide	12	28	140	78	66
Hexachlorobenzene	12	9	BDL	8	17
Pentachlorobenzene	3	3	BDL	BDL	5
Mirex	BDL	BDL	BDL	61	12
PCBs	1700	2700	2900	15000	4600
t-Nonachlor	27	110	75	140	72

PCBs with IUPAC Nos. 23, 36, 57, 62, 68, 73, 94, 96, 102, 106, 109, 111, 113, 117, 119, 120, 125, 140, 142, 145, 148, 150, 152, 160, 161, 162, 164, 165, 168, 184, and 192 have no quantitative standard confirmation.

Statistical treatment of data

The presentation of the data is such that they do not lend themselves readily to statistical analysis. Twelve samples, varying in size from 1 to 22 specimens of a given lamprey species ($\bar{X}$ = 5.5, SD = 5.9), were analysed as aggregates. In view of this pooling of specimens of a given species, we do not have a precise idea of the individual variation within a species. In comparing historical versus recent organochlorine concentrations in ammocoete samples from the St-François and Ste-Anne rivers, the two rivers for which we have comparative data, we opted for a conservative approach by considering as different only those concentrations with nonoverlapping ranges. All 22 organochlorine pesticides and 93 PCB congeners were compared. Some of the PCB congeners were not resolved due to coelution in the capillary columns and were therefore considered together. For the sake of calculations, concentrations below the sample detection limit (nominal detection limit/sample lipid weight) were treated as zero. This procedure may result in significant underestimates of some contaminant concentrations only in cases where the sample lipid weight is low. A single sample, from 1990, was identified as having a low lipid weight. In this sample, the following organochlorine residues had concentrations below the detection limit: Endrin, *o,p'*-DDT, and PCB congeners 24(27), 54, 103, 107(123), 128, 129, 132, 158, 173, 176(130), 198, 200, and 209. However, the concentrations for these residues in at least some of the other samples from 1990, for which the lipid weights were adequate, were either also below the detection limit or significantly lower than in the 1947–1950 samples, except for PCB congeners 103, 107(123), 132, and 200. These latter congeners had similar ranks in the Spearman's rank correlation coefficient test (see below). The procedure was therefore deemed to have a conservative effect, if any, on the results.

A two-sided Spearman's rank correlation coefficient test was used to compare the weighted concentrations of the 93 PCB congeners in the historical versus recent ammocoete samples from the St-François and Ste-Anne rivers. The chosen level of significance was $P \leq 0.05$. The weighted mean of means method gives proportionately more weight to larger samples (Simpson et al. 1960). A *G*-test of goodness of fit for single classification frequency distributions (Sokal and Rohlf 1981) was used to compare the weighted frequency distributions of PCB homologues in the historical

Table 2. Ranges in concentration of organochlorine contaminants (ppb), based on lipids, in the lamprey ammocoetes *Ichthyomyzon fossor* and *Lampetra appendix* from the St-François and Ste-Anne rivers, Québec, in the 1947–1950 period versus 1990. The mean, standard deviation, and range are given for the total length. BDL = below sample detection limit.

Collection date	1947–1950	1990
No. of samples	3	4
Total no. of specimens	6	18
Total length (mm)	73.1 ± 8.3 (58.5–81.5)	94.0 ± 27.3 (63.0–162.0)
Sample lipid weight (g)	0.02–0.06	0.01–1.12[a]
Aldrin	270–380	64–860
Dieldrin	420–520	85–550
Endrin	BDL	BDL
α-BHC	85–170	29–240
β-BHC	290–340	21–150
γ-BHC (=lindane)	130–590	19–290
α-Chlordane	520–550	70–380
γ-Chlordane	500–520	36–290
o,p'-DDD	850–1100	79–1200
p,p'-DDD	1100–1400	140–1000
o,p'-DDE	190–220	3–100
p,p'-DDE	370–730	61–200
o,p'-DDT	56–550	BDL–120
p,p'-DDT	2200–3900	52–1400
α-Endosulfan	300–370	52–480
β-Endosulfan	180–1000	30–690
Heptachlor	120–180	5–70
Heptachlor epoxide	BDL–110	15–280
Hexachlorobenzene	BDL–40	12–100
Pentachlorobenzene	BDL–3	3–15
Mirex	BDL	2–50
PCBs	12 000–14 000	1600–33 000
t-Nonachlor	240–430	58–250

[a] One of the 1990 samples consisted of a single specimen and had a very low weight making the results less precise.

versus recent ammocoete samples from the St-François and Ste-Anne rivers. The chosen level of significance was $P \leq 0.05$.

A two-sided Mann–Whitney *U*-test was used to compare the weighted ratios of DDD/∑DDT (i.e., [*o,p'*-DDD] + [*p,p'*-DDD]/[*o,p'*-DDD] + [*p,p'*-DDD] + [*o,p'*-DDE] + [*p,p'*-DDE] + [*o,p'*-DDT] + [*p,p'*-DDT]), DDE/∑DDT, and DDT/∑DDT in the historical versus recent ammocoete samples from the St-François and Ste-Anne rivers. The chosen level of significance was $P \leq 0.05$. These ratios have been proposed by Kaiser (1982) for elucidating temporal trends in organochlorine contaminant concentrations.

A two-sided Mann–Whitney *U*-test was used to compare the weighted lipid content in the historical versus recent ammocoete samples from the St-François and Ste-Anne rivers. The chosen level of significance was $P \leq 0.05$. A two-sided Mann–Whitney *U*-test was also used to compare the total lengths of the six specimens from the historical samples with the 18 specimens from the recent samples from the St-François and Ste-Anne rivers. This test serves to compare the approximate age, and therefore the exposure, of the two groups. The chosen level of significance was $P \leq 0.05$.

A Power function test was performed, as recommended by Peterman (1990), whenever a null hypothesis was accepted.

Results

Yamaska, St-François, and Ste-Anne rivers

Analysis of the original formalin preservative solutions for both the historical and recent samples revealed only trace amounts of PCB congeners in some of the solutions. All the other organochlorines investigated were not detected. The quantities of PCBs found, expressed in terms of concentration based on sample lipid amount, were an order of magnitude below the nominal detection limits. The jars containing the lamprey samples, both historical and recent, were not air-tight. Significant losses of compounds with high Henry's Law constants (e.g., mono- and dichlorobiphenyl congeners) were ruled out, however, because only trace amounts of PCBs were detected in some of the formalin solutions. The low solubility of lower chlorinated PCB homologues (K_{ow} in the order of 10^5) would restrict any extensive removal of PCBs through volatilization.

One out of 12 samples did not reach a final constant air-dried weight. The sample in question came from a 1949 Yamaska River collection and consisted of 22 specimens (Table 1). Retaining this sample means that the calculation "percentage of lipid per sample" may be slightly underestimated. However, its lipid content, based on body dry weight, was 36.1%, well within the overall range across the 12 samples of 7.7–46.2%.

Endrin was not detected (nominal detection limit 1.0 ng/g lipid analysed) in either the 1946–1959 or the 1990 ammocoete samples (Tables 1 and 2). Of the pre-1960 samples, Mirex was detected and confirmed by mass spectrometry in two out of five samples from the Yamaska River only (Table 1).

St-François and Ste-Anne rivers

A two-sided Mann–Whitney *U*-test was used to compare the weighted lipid content in the historical versus recent ammocoete samples from the St-François and Ste-Anne rivers. The null hypothesis, H_0: $\Delta = 0$, was accepted at $P = 0.09$. The power of this result was determined using a Monte Carlo simulation (Peterman 1990). The power was 0.14 based on 300 iterations. In order to increase the power value to the conventional level of 0.80, 45 times more samples would have been required.

A two–sided Mann–Whitney *U*-test used to compare the total lengths of the six specimens from the historical samples with the 18 specimens from the recent samples from the same two rivers (Table 2) was significant at $P = 0.02$. The null hypothesis, H_0: $\Delta = 0$, was therefore rejected.

A comparison of concentrations for 22 organochlorine pesticides and total PCBs in ammocoete samples from the St-François and Ste-Anne rivers in 1947–1950 versus 1990 revealed that eight pesticides (β-BHC, α-Chlordane, γ-Chlordane, *p,p'*-DDD, *o,p'*-DDE, *p,p'*-DDE, *p,p'*-DDT,

Fig. 2. Distribution of PCB homologues, expressed as percentages, in the historical (1947–1950) and recent (1990) lamprey ammocoete samples, based on the weighted means of their concentrations, from the St. François and Ste-Anne rivers, St. Lawrence River basin, Québec.

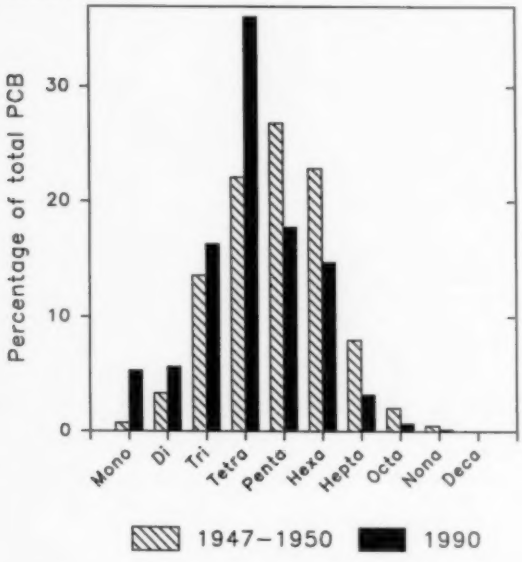

and Heptachlor) had higher concentrations in the 1947–1950 period and only one, Mirex, was found in higher concentrations in 1990 (Table 2). In fact, Mirex was not detected (nominal detection limit = 0.4 ng/g lipid analysed) in the St-François and Ste-Anne river samples of 1947–1950 (Table 2).

A two-sided Spearman's rank correlation coefficient test, comparing the weighted concentrations of the 93 PCB congeners between the historical and recent ammocoete samples from the St-François and Ste-Anne rivers, gave an $r_S = -0.44$. This r_S value, although not very high, is significant at $P \leq 0.001$, and therefore, the null hypothesis that there is no correlation between the two groups was rejected. The negative correlation coefficient means that there is an inverse relationship between the concentration of the various PCB congeners and the sampling date.

PCB congeners 3, 86, and 209 were not detected (nominal detection limits 7.0, 0.5, and 1.0 ng/g lipid analysed, respectively) in the 1947–1950 period whereas congener 54 (nominal detection limit 0.4 ng/g lipid analysed) was not detected in 1990. Seventeen congeners (24(27), 28, 98(84), 101, 110(77), 128, 129, 141, 149, 151, 158, 174, 177, 180, 183, 187(182), and 198) had higher concentrations in the 1947–1950 period compared with 1990. These higher concentrated congeners, except for 77 (a minor coelutant of 110), have either one (28), two (24, 27, 101, 110, 128, 129, 141, 158, and 180), three (84, 98, 149, 151, 174, 177, 182, 183, and 187), or four (198) orthosubstituted chlorines. PCB congeners with chlorine at the ortho positions have a lower probability for coplanarity (Kaiser 1975; Clarke et al. 1989), and as such, a decreased chance of being metabolised. Congeners with chlorine substitution at the 2,4,5 positions of one or both phenyl rings demonstrate higher bioaccumulation in fish (Gagnon et al. 1990) and in beluga whales when substituted on either the 2,4 or 2,4,5 of both phenyl rings (Béland et al. 1993). Although most of the observed higher concentrated congeners fall into these categories, their only common feature was chlorine substitution at the ortho positions. No PCB congeners had higher concentrations in 1990.

Table 3. Range and weighted means (in parentheses) of contaminant ratios in three historical (1947–1950) versus four recent (1990) lamprey larvae samples from the St-François and Ste-Anne rivers, Québec.

Contaminant ratio	1947–1950	1990	Significance (P)
DDD/∑DDT	0.31–0.40 (0.33)	0.53–0.57 (0.55)	0.000
DDE/∑DDT	0.08–0.15 (0.13)	0.08–0.21 (0.20)	0.001
DDT/∑DDT	0.48–0.56 (0.54)	0.23–0.36 (0.25)	0.000

A G-test used to compare the weighted frequency distributions of PCB homologues between the historical and recent ammocoete samples from the St-François and Ste-Anne rivers (Fig. 2) was significant at $P < 0.001$. The null hypothesis, H_0: $\Delta = 0$, was therefore rejected. The historical samples showed lower levels (39.8 versus 63.4%) of mono- to tetra-chlorobiphenyl congeners and higher levels (60.2 versus 36.6%) of penta- to nona-chlorobiphenyl congeners relative to the recent samples (Fig. 2). The deca isomer was not detected in the historical samples and it represented only 0.03% of the total PCB lipid burden in the recent samples.

A two-sided Mann–Whitney U-test was used to compare the weighted ratios of DDD/∑DDT, DDE/∑DDT, and DDT/∑DDT in the historical versus recent ammocoete samples from the St-François and Ste-Anne rivers. All three ratios were significantly different at $P = 0.001$ or better (Table 3). The null hypothesis, H_0: $\Delta = 0$, was therefore rejected in all three cases.

Discussion

The trace amounts of PCBs lost to the formalin preservative could not have accounted for the low concentrations of PCBs in the recent samples relative to the historical samples. This, together with the fact that none of the organochlorine pesticides investigated was detected in the formalin solutions, means that formalin-preserved museum material can be used for historical trend analyses of organochlorine contaminants.

In a 1-month period, between 27 July and 30 August 1949, Vladykov and his assistants collected 732 ammocoetes at the Yamaska River locality, near St-Césaire (Vladykov 1952). Our lack of success in collecting ammocoetes at the same locality in 1990 may be related to the extensive use of the selective herbicide Atrazine on the

corn fields along the Yamaska River (R.J. Maguire, National Water Research Institute, Burlington, Ont., personal communication). The corn fields are very close to river's edge, and the Atrazine washes out into the river following heavy rains and presumably kills the phytoplankton, the main food source for ammocoetes according to Moore and Beamish (1973). Atrazine would not have had an effect in the 1940–1950s because it was not patented until 1960. The Yamaska is a very polluted river and, in particular, fishes in the St-Césaire area have had high levels of total DDT and PCBs (Harvey 1979). Additionally, severe lowering of the water level is regularly recorded during the summer in the Yamaska River, which is probably another significant factor contributing to ammocoete mortality (Lanteigne 1992). However, we have no reason to believe that this last factor was any less severe 40 years ago.

The Yamaska locality, from which two ammocoete samples, collected, respectively, in 1949 and 1959, had detectable levels of Mirex (Table 1), is roughly 75 km upstream of this river's confluence with the St. Lawrence River (Fig. 1). There are two reasons why this is significant. According to Lum et al. (1987), although Mirex has been observed in fishes and whales of the St. Lawrence River and upper estuary, its major known source is Lake Ontario and it is not believed to have been manufactured in significant quantities until 1959. However, Comba et al. (1993*c*) reported that Mirex appears to have entered the Laurentian Trough in the early 1950s, and Sergeant et al. (1993) have recently detected low levels of Mirex in biota of the upper Great Lakes.

According to Hardisty (1956), the lipid content, expressed as a percentage of body dry weight, in ammocoetes of the lamprey *Lampetra planeri*, collected between June and October and measuring 70–100 mm total length, varies from 10 to 41%. This range is comparable with what we report in this study. The historical and recent lamprey samples in this study were also collected between June and October.

According to Purvis (1970), ammocoetes of *Ichthyomyzon fossor* from Sturgeon River, Lake Superior basin, measuring 17–37, 38–74, 62–101, and 83–116 mm in total length, represent, respectively, young-of-the-year, 1+-year-old, 2+-year-old, and 3+-year-old individuals. Notwithstanding variation in growth rates based on locality and species, the 1947–1950 ammocoetes (Table 2) would therefore be on average 1–2+ years old and the 1990 ammocoetes (Table 2) would be on average 2–3+ years old. The times of exposure for the two groups are therefore broadly comparable.

Very little information exists regarding the filtration rate in ammocoetes. Rovainen and Schieber (1975) recorded a range of 21–60 $mL \cdot g^{-1} \cdot h^{-1}$ at 20°C for resting ammocoetes of the sea lamprey *Petromyzon marinus* 60–140 mm total length and weighing 0.7–3.5 g wet weight. The total lengths involved encompass most of the variation in our ammocoetes for the two time periods (Table 2), and we therefore assume that both groups had comparable filtration rates and hence intake rates.

A number of the organochlorine pesticides studied, Aldrin, Dieldrin, α- and γ-Chlordane, α- and β-Endosulfan, Heptachlor, and Mirex, were found in detectable quantities (Tables 1 and 2) prior to their U.S. patent registration dates, which vary between 1952 and 1961 (Kaiser 1984). However, commercial production and use of these compounds commonly occurred several years before the patent issues.

The lower levels of mono- to tetra-chlorobiphenyl congeners and higher levels of penta- to nona-chlorobiphenyl congeners in the historical ammocoete samples relative to the recent ammocoete samples are probably a reflection of the relatively wider use in the 1940s of the higher chlorinated biphenyl mixtures, such as the Aroclor 1254 and 1260 formulations, when their environmental significance (persistence and greater toxicity) was not widely known.

The statistically significant increase in the DDD/ΣDDT and DDE/ΣDDT ratios and the statistically significant decrease in the DDT/ΣDDT ratio between the historical versus recent ammocoete samples from the St-François and Ste-Anne rivers indicate that the original *p,p'*-DDT and *o,p'*-DDT are being replaced by their degradation products (i.e., *p,p'*-DDD, *o,p'*-DDD, *p,p'*-DDE, and *o,p'*-DDE). This observation is consistent with the restrictions on the use of DDT in the early 1970s.

In summary, based on the two rivers for which we have comparable data (Table 2), this study shows that persistent organochlorine contaminants, including PCBs, reached higher concentrations in biota of the St. Lawrence River basin 40 years ago.

Acknowledgments

Our thanks to André Landry, Ministère du Loisir, de la Chasse et de la Pêche du Québec (MLCP), Québec, for issuing C.B.R. with a collecting permit for the recent lampreys; François Chapleau, University of Ottawa, for the use of the DC-electrofisher; J. Andrew Cooper and Ian R. Jones for their assistance in the field, Susan Laurie-Bourque for drawing the map; Virginia S. Palabrica, National Water Research Institute (NWRI), Burlington, Ont., and Sean M. Backus, Backus Consulting, Stoney Creek, Ont., for the organochlorine assays; Mike Keir, Department of Fisheries and Oceans, Burlington, for part of the lipid analyses; R.J. Maguire, NWRI, Burlington, for his helpful comments; and Daniel Nadon, Canadian Museum of Nature, for the statistical analyses. This study was partially supported by a research grant to C.B.R. from the Canadian Museum of Nature.

References

Ballschmitter, K., and Zell, M. 1980. Analysis of polychlorinated biphenyls (PCB) by glass capillary gas chromatography. Fresenius Z. Anal. Chem. **302**: 20–31.

Béland, P., DeGuise, S., Girard, C., Lagacé, A., Martineau, D., Michaud, R., Muir, D.C.G., Norstrum, R.J., Pelletier, E., Ray, S., and Shugart, L.R. 1993. Toxic compounds and health and reproductive effects in St. Lawrence Beluga whales. J. Great Lakes Res. **19**(4): 766–775.

Clarke, J.U., McFarland, V.A., and Pierce, B.D. 1989. Preliminary recommendations for a congener-specific

PCB analysis in regulatory evaluation of dredged material. Misc. Pap. D-89-2, U.S. Army Engineer Waterways Experiment Station, Vicksburg, Miss.

Comba, M.E., Kaiser, K.L.E., and Backus, S.M. 1993*a*. Distribution of polychlorinated biphenyls in spottail shiners from the St. Lawrence River. Natl. Water Res. Inst. Contrib. 92-100. 46 p.

Comba, M.E., Palabrica, V.S., Backus, S.M., and Kaiser, K.L.E. 1993*b*. St. Lawrence River trace organic contaminant study. Part IV, 1989–90 and summary. Natl. Water Res. Inst. Contrib. 93-19.

Comba, M.E., Norstrom, R.J., Macdonald, C.R., and Kaiser, K.L.E. 1993*c*. A Lake Ontario – Gulf of St. Lawrence dynamic mass budget for Mirex. Environ. Sci. Technol. **27**: 2198–2206.

Gagnon, M.M., Dodson, J.J., Comba, M.E., and Kaiser, K.L.E. 1990. Congener-specific analysis of the accumulation of polychlorinated biphenyls (PCBs) by aquatic organisms in the maximum turbidity zone of the St. Lawrence estuary, Quebec, Canada. Sci. Total Environ. **97/98**: 739–759.

Hardisty, M.W. 1956. Some aspects of osmotic regulation in lampreys. J. Exp. Biol. **33**: 431–447.

Harvey, G. 1979. Les métaux lourds et les composés organochlorés dans la chair des poissons du bassin versant de la Yamaska. Rapp. tech. Minist. Loisir Chasse Pêche Qué. 06-30.

Kaiser, K.L.E. 1975. On the optical activity of polychlorinated biphenyls. Environ. Pollut. **7**: 93–101.

Kaiser, K.L.E. 1982. Early trend determination of organochlorine contamination from residue ratios in the sea lamprey (*Petromyzon marinus*) and its lake whitefish (*Coregonus clupeaformis*) host. Can. J. Fish. Aquat. Sci. **39**: 571–579.

Kaiser, K.L.E. 1984. Organic contaminants in the environment: research progress and needs. Environ. Int. **10**: 241–250.

Kaiser, K.L.E., and Valdmanis, I. 1978. Organochlorine contaminants in a sea lamprey (*Petromyzon marinus*) from Lake Ontario. J. Great Lakes Res. **4**: 234–236.

Lanteigne, J. 1988. Identification of lamprey larvae of the genus *Ichthyomyzon* (Petromyzontidae). Environ. Biol. Fishes, **23**: 55–63.

Lanteigne, J. 1992. Status of the northern brook lamprey, *Ichthyomyzon fossor*, in Canada. Can. Field-Nat. **106**: 7–13.

Lum, K.R., Kaiser, K.L.E., and Comba, M.E. 1987. Export of Mirex from Lake Ontario to the St. Lawrence estuary. Sci. Total Environ. **67**: 41–51.

MacGregor, J.S. 1974. Changes in the amount and proportions of DDT and its metabolites, DDE and DDD, in the marine environment off southern California, 1949–72. Fish. Bull. **72**: 275–293.

Moore, J.W., and Beamish, F.W.H. 1973. Food of larval sea lamprey (*Petromyzon marinus*) and American brook lamprey (*Lampetra lamottei*). J. Fish. Res. Board Can. **30**: 7–15.

Mullin, M.D., Pochini, C.M., McCrindle, S., Romkes, M., Safe, S.H., and Safe, L.M. 1984. High-resolution PCB analysis: synthesis and chromatographic properties of all 209 PCB congeners. Environ. Sci. Technol. **18**: 468–476.

Neidermyer, W.J., and Hickey, J.J. 1976. Chronology of organochlorine compounds in Lake Michigan fish, 1929–66. Pestic. Monit. J. **10**: 92–95.

Onuska, F.I., Comba, M.E., and Coburn, J.A. 1980. Quantitative determination of Mirex and its degradation products by high resolution capillary gas chromatography/mass spectrometry. Anal. Chem. **52**: 2272–2275.

Peterman, R.M. 1990. Statistical power analysis can improve fisheries research and management. Can. J. Fish. Aquat. Sci. **47**: 2–15.

Purvis, H.A. 1970. Growth, age at metamorphosis, and sex ratio of northern brook lamprey in a tributary of southern Lake Superior. Copeia **1970**: 326–332.

Renaud, C.B., Kaiser, K.L.E., Comba, M.E., and Metcalfe-Smith, J.L. 1995. Comparison between lamprey ammocoetes and bivalve molluscs as biomonitors of organochlorine contaminants. Can. J. Fish. Aquat. Sci. **52**: 000–000.

Rick, A.M. 1975. Use of museum specimens in toxic chemical research. Can. Wildl. Serv. Occas. Pap. **21**.

Rovainen, C.M., and Schieber, M.H. 1975. Ventilation of larval lampreys. J. Comp. Physiol. A Sens. Neural Behav. Physiol. **104**: 185–203.

Sergeant, D.B., Munawar, M., Hodson, P.V., Bennie, D.T., and Huestis, S.Y. 1993. Mirex in the North American Great Lakes: new detections and their confirmation. J. Great Lakes Res. **19**: 145–157.

Simpson, G.G., Roe, A., and Lewontin, R.C. 1960. Quantitative zoology. Harcourt, Brace and World, Inc., New York, N.Y.

Sokal, R.R., and Rohlf, F.J. 1981. Biometry. The principles and practice of statistics in biological research. 2nd ed. W.H. Freeman and Co., New York, N.Y.

Swackhamer, D.L. 1988. Quality Assurance Plan, Green Bay Mass Balance Study. I. PCBs and Dieldrin. Prepared for U.S. Environmental Protection Agency, Great Lakes National Program Office, Chicago, Ill.

Vladykov, V.D. 1949. Quebec lampreys (Petromyzonidae) I. — List of species and their economical importance. Dep. Fish. Prov. Que. **26**: 7–67.

Vladykov, V.D. 1950. Larvae of the eastern American lampreys (Petromyzonidae) I. — Species with two dorsal fins. Nat. Can. (Qué.), **77**: 73–95.

Vladykov, V.D. 1952. Distribution des lamproies (Petromyzonidae) dans la province de Québec. Nat. Can. (Qué.), **79**: 85–120.

Comparison between lamprey ammocoetes and bivalve molluscs as biomonitors of organochlorine contaminants

Claude B. Renaud, Klaus L.E. Kaiser, Michael E. Comba, and Janice L. Metcalfe-Smith

Abstract: Lamprey ammocoetes were determined to be as suitable as adult bivalve molluscs for monitoring persistent organochlorine contaminants in the freshwater environment. Ammocoetes of four lamprey species and adults of three bivalve mollusc species, collected from the same seven rivers of the St. Lawrence River basin in Québec, were assayed for 21 organochlorine pesticides and for polychlorinated biphenyl (PCB) congeners. All organochlorine compounds assayed were detected in one or more of the 15 lamprey samples whereas Aldrin, β-BHC, and PCB congeners 1, 3, 12(13), 29, 54, 189, 191, and 199 were not detected in any of the nine bivalve samples. Nine pesticides (Aldrin, Dieldrin, γ-BHC, α-Chlordane, γ-Chlordane, *o,p'*-DDD, *p,p'*-DDD, *p,p'*-DDT, and α-Endosulfan) had higher concentrations in the lampreys. PCB congeners 167(185) and 209 had higher concentrations in bivalves. PCBs accounted for 96.6–99.4% of the organochlorine lipid burden in bivalves, but only 33.4–76.8% in lampreys. On average, ammocoetes had 44 times more lipids per body dry weight than did bivalves. The differences observed in concentrations and types of organochlorine compounds found in the two taxa may be due to differences in the amounts (observed) and types (postulated) of body lipids they each possess.

Résumé : Cette étude a démontré que les ammocètes de lamproies sont aussi appropriées que les mollusques bivalves adultes comme baromètres des niveaux de contaminants organochlorés persistants dans le milieu dulçaquicole. Les concentrations de 21 pesticides organochlorés ainsi que celles de congénères de biphényles polychlorés (BPCs) furent déterminées chez des ammocètes de quatre espèces de lamproies et des adultes de trois espèces de mollusques bivalves, échantillonnés de façon sympatrique dans sept rivières du bassin fluvial du St-Laurent au Québec. Tous les composés organochlorés évalués furent décelés dans un ou plus des 15 échantillons de lamproies. Par contre, l'Aldrin, le β-BHC et les congénères de BPCs 1, 3, 12(13), 29, 54, 189, 191 et 199 n'ont été décelés dans aucun des neuf échantillons de bivalves. Neuf pesticides (Aldrin, Dieldrin, γ-BHC, α-Chlordane, γ-Chlordane, *o,p'*-DDD, *p,p'*-DDD, *p,p'*-DDT et α-Endosulfan) affichaient de plus hautes concentrations chez les lamproies. Les congénères 167(185) et 209 affichaient de plus hautes concentrations chez les bivalves. Les BPCs comptaient pour 96,6–99,4 % du fardeau lipidique d'organochlorés chez les bivalves, mais seulement 33,4–76,8 % chez les lamproies. Les ammocètes avaient en moyenne 44 fois plus de lipide par unité de poids corporel sec que les bivalves. Nous formulons l'hypothèse que les différences observées chez les deux taxons quant aux concentrations et aux types de composés organochlorés retrouvés, sont dues à des différences dans les montants (observés) et les types (postulés) de tissus lipidiques qu'ils possèdent.

Received August 26, 1993. Accepted July 14, 1994.
J12068

C.B. Renaud. Ichthyology Section, Research Division, Canadian Museum of Nature, P.O. Box 3443, Station D, Ottawa, ON K1P 6P4, Canada.
K.L.E. Kaiser and M.E. Comba. Lakes Research Branch, National Water Research Institute, P.O. Box 5050, 867 Lakeshore Rd., Burlington, ON L7R 4A6, Canada.
J.L. Metcalfe-Smith. Rivers Research Branch, National Water Research Institute, P.O. Box 5050, 867 Lakeshore Rd., Burlington, ON L7R 4A6, Canada.

Introduction

Adult freshwater bivalve molluscs have long been used as biomonitors of organochlorine contaminants (Bedford et al. 1968; Godsil and Johnson 1968; Curry 1977–1978; Leard et al. 1980; Hartley and Johnston 1983; Kauss et al. 1983; Elder and Mattraw 1984; Kauss and Hamdy 1985; Pugsley et al. 1985; Metcalfe and Charlton 1990; Muncaster et al. 1990). Lamprey larvae (ammocoetes), like adult freshwater bivalve molluscs, are fairly long-lived (usually 3–8 years, exceptionally 18 years), relatively sedentary freshwater organisms, that spend the better part of their lives partially to completely burrowed in substrates and filter-feeding on microorganisms (Hardisty and Potter 1971; Moore and Mallatt 1980; Potter 1980). These characteristics make them particularly well suited to act as biomonitors of organochlorine contaminants. In view of this similarity in their ecology, the purpose of this study was to test the hypothesis that lamprey ammocoetes are as suitable as adult bivalve molluscs for monitoring organochlorines in the freshwater environment.

Materials and methods

Sampling and identifications

Between 16 July and 30 August 1990, 144 lamprey ammocoetes (15 samples) belonging to four species (*Ichthyomyzon fossor*, *I. unicuspis*, *Lampetra appendix*, and *Petromyzon marinus*) were collected with a Smith-Root type VII DC-electrofisher, and 32 adult bivalve molluscs (nine samples) belonging to three species (*Elliptio complanata*, *Lampsilis radiata*, and *L. ventricosa*) were collected by hand. The ammocoetes and bivalves were collected at depths ranging from 0.01 to 1.5 m from the following seven rivers of the St. Lawrence River basin in Québec: Châteauguay north–northwest of Athelstan, Richelieu at Saint-Roch-de-Richelieu, St-François northwest of Pierreville, Nicolet Sud-Ouest at Mitchell, Bécancour at Bécancour, St-Maurice at Trois-Rivières and L'Assomption south of L'Assomption (Fig. 1). The lamprey samples were put directly into 5% formalin upon collection; the molluscs were individually wrapped in acetone-washed aluminium foil and put on dry ice. The reason for the different treatments of the two taxa was that some of the lamprey samples were compared in terms of organochlorine residues with historical lamprey samples preserved in 5% formalin and are the subject of another paper (Renaud et al. 1995). The ammocoetes were identified to species using Vladykov (1950) and Lanteigne (1988) and their total length was measured to the nearest 0.5 mm. The bivalves were identified to species using Clarke (1981) and their shell length was measured to the nearest 0.1 mm.

Chemical analyses

Chemical analyses were conducted for 21 organochlorine pesticides (Table 1) as well as polychlorinated biphenyls (PCBs) (107 congeners grouped in 81 congener–congener combinations). The lamprey samples were prepared as in Renaud et al. (1995). The bivalves were shucked and the soft tissues were homogenized in a Waring stainless steel blender until liquefied. A 50-g soft tissue wet weight subsample (in one case, only 15 g was available) was taken from each of the homogenates. The dry weight of the subsample was based on a 90% mean soft tissue moisture content (J.L. Metcalfe-Smith, unpublished data). An amount of anhydrous sodium sulphate equal to the subsample wet weight was added and blended into the homogenate. The prepared sample was placed in a glass extraction thimble and soxhlet-extracted with dichloromethane for 8 h. The final sample extract was reduced to ~2 mL using rotary and atmospheric evaporation.

Separation of lipid and contaminant for lampreys and bivalves was achieved as in Renaud et al. (1995). The amount of lipid recovered from lampreys using GPC/acid extraction was the same as that using GPC/soxhlet extraction and 13% higher than the lipid recovered with a Bucchi model 810 fat extractor and 2:1 chloroform–methanol. There was no further recovery of lipid (<5% of total lipid) in subsequent GPC/soxhlet extracts of lamprey samples using 9:1 dichloromethane–methanol. Recovery of lipid from bivalves with the fat extractor was significantly greater than with dichloromethane and GPC/soxhlet (21% of the amount using the fat extractor) or after combination with the 9:1 dichloromethane–methanol – GPC/soxhlet (60%) lipid fraction. Differences in body lipids of the two taxa are discussed later. The formalin preservative solutions from the lamprey collections were treated as in Renaud et al. (1995).

Extracts were analysed with a HP 5890 gas chromatograph as described in Renaud et al. (1995). Recovery efficiencies and method reproducibility for soxhlet/GPC/silica gel sample treatments are reported in Renaud et al. (1995). Recoveries of organochlorines based on acid-extracted samples are generally 13–20% lower than those based on soxhlet-extracted samples (see below). PCBs were measured as in Renaud et al. (1995).

The use of acid and soxhlet extraction procedures to treat the two taxa could influence the amounts of lipids and contaminants recovered. Comparison of the two extraction techniques, based on a two-sided Spearman's rank correlation coefficient test, made on two aliquots of a lamprey sample showed no statistical difference overall between the lipid concentrations of organochlorine residues. An $r_S = 0.94$ was calculated for the organochlorine pesticides and the null hypothesis that there is no correlation between the two groups was rejected at $P < 0.01$. The mean percent difference for recoveries of all organochlorine pesticide residues was derived from the following equation:

$$\sum_{i=1}^{n} \frac{[\text{soxhlet}]_i - [\text{acid}]_i}{[\text{soxhlet}]_i} \times 100$$

where i = organochlorine pesticides examined and amounted to 13.6% ± 48.9 (SD) and ranged between −163.9 and 71.7%. There was a tendency towards lower recoveries for Aldrin, Dieldrin, α-Chlordane, γ-Chlordane, *o,p'*-DDD, *p,p'*-DDD, *p,p'*-DDT, and α-Endosulfan and greater recoveries for γ-BHC using the acid procedure. The differences noted, however, do not have a significant effect on the conclusions reached in this study because the concentrations of all of the above pesticides except γ-BHC were higher in the lampreys compared with the bivalves. PCB congener concentrations obtained with each procedure were also

Fig. 1. Localities where the lamprey ammocoetes and adult bivalve molluscs were collected in the St. Lawrence River Basin, Québec.

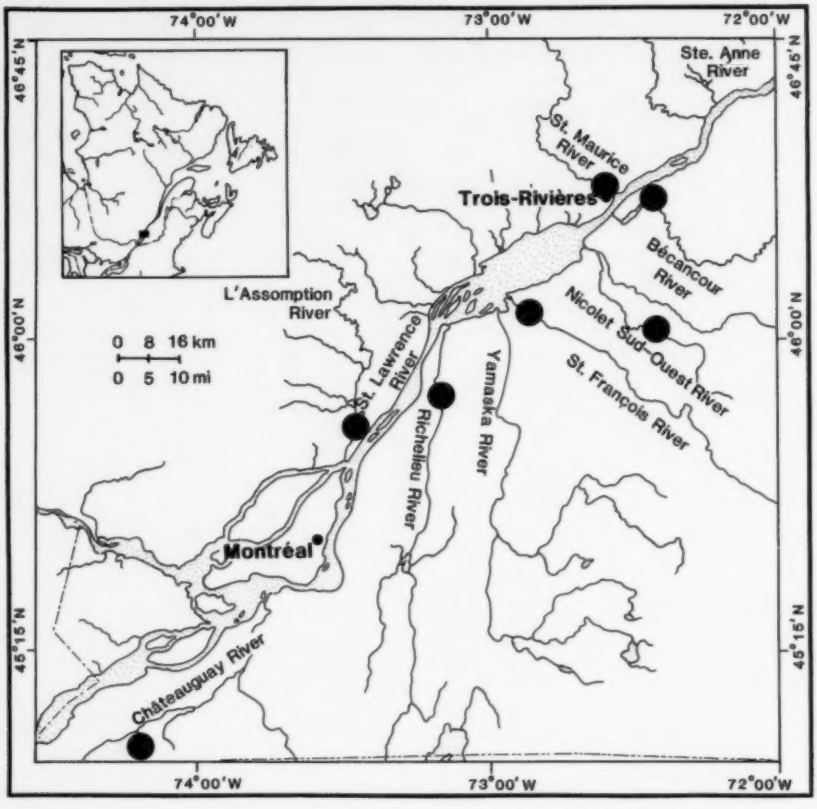

significantly correlated. An $r_S = 0.86$ was calculated and the null hypothesis that there is no correlation between the two groups was rejected at $P < 0.01$. The mean percent difference for recoveries of all PCB congener residues amounted to 19.9% ± 32.5 and ranged between −96.0 and 62.5%. There was a tendency towards lower recoveries of congeners 167(185) and 209 using the acid procedure. Therefore, we cannot be sure whether the higher concentrations for these PCB congeners noted in the bivalves in this study are due to the extraction procedure or are taxon-based.

Statistical treatment of data

The presentation of the data is such that they do not lend themselves readily to statistical analysis. Samples varying in size from 1 to 42 specimens of a given lamprey species ($\bar{X} = 9.6$, SD = 13.2) and from one to five specimens of a given bivalve species ($\bar{X} = 3.6$, SD = 1.7) were analyzed as aggregates. In view of this pooling of specimens of a given species, we do not have a precise estimate of the individual variation within a species. In our comparison of organochlorine concentrations between lampreys and bivalves, we opted for a conservative approach by considering as different only those concentrations with nonoverlapping ranges. All 21 organochlorine pesticides and 81 PCB congeners were compared. Some of the PCB congeners were not resolved due to coelution in the capillary columns and were therefore considered together. For the sake of calculations, concentrations below the sample detection limit (=nominal detection limit/sample lipid weight) were treated as zero and trace concentrations were treated as half the nominal detection limit for the particular compound. This procedure may result in significant underestimates of some contaminant concentrations only in cases where the sample lipid weight is low. In this study, only three lamprey samples were considered to have low lipid levels, one each from the Richelieu, St-François, and L'Assomption rivers. None of the organochlorine residues with trace concentrations or concentrations below the sample detection limit in these three samples had higher concentrations in the other lamprey samples compared with the bivalves, and as such, introduction of approximated values was deemed to have a conservative effect on the results.

A two-sided Spearman's rank correlation coefficient test was used to compare the weighted concentrations of the 81 PCB congeners in the lamprey versus bivalve samples. The chosen level of significance was $P \leq 0.05$. The weighted mean of means method gives proportionately more weight to larger samples (Simpson et al. 1960). A *G*-test of goodness

of fit for single classification frequency distributions (Sokal and Rohlf 1981) was used to compare the weighted frequency distributions of PCB homologues in the lamprey versus bivalve samples. The chosen level of significance was $P \leq 0.05$.

Lipid burdens of organochlorine contaminants in both lampreys and bivalves were calculated by summing the concentrations of all compounds for each of the seven localities. In cases where more than one taxon was represented per locality for either lampreys or bivalves, a weighted mean of means was calculated. A two-sided Spearman's rank correlation coefficient test was used to compare the river rankings in the two taxa. The chosen level of significance was $P \leq 0.05$.

A Power function test was performed, as recommended by Peterman (1990), whenever a null hypothesis was accepted.

Results

Analysis of the formalin preservative solutions in the lamprey samples revealed no detectable amounts of PCBs or of the other organochlorines investigated.

In the 15 lamprey ammocoete samples, the percent lipid per sample, based on body dry weight, varied between 14.5 and 50.5%, with weighted mean of means 21.9%. In contrast, in the nine bivalve mollusc samples, the percent lipid per sample, based on body dry weight (without the shell), varied between 0.2 and 1.2%, with weighted mean of means 0.5%. Therefore, on average, ammocoetes had 44 times more lipid per body dry weight than did bivalves. Three out of 15 lamprey samples did not reach a final constant air-dried weight. Two of the samples came from the St-Maurice River and consisted of 42 and 34 specimens, respectively, while the third sample came from the Châteauguay River and consisted of eight specimens. Retaining these samples means that the percentage of lipids for these samples may be slightly underestimated. However, their respective lipid contents, based on body dry weight, 18.9, 22.7, and 25.4%, were well within the overall range across the 15 lamprey samples of 14.5–50.5%.

All 21 organochlorine pesticides investigated were detected in one or more of the lamprey samples whereas two of these, Aldrin and β-BHC (nominal detection limits 0.2 and 0.5 ng/g lipid analysed, respectively), were not detected in any of the bivalve samples (Table 1). A comparison of concentrations for 21 organochlorine pesticides and total PCBs in four species of lampreys and three species of bivalves from the seven rivers investigated revealed that nine pesticides (Aldrin, Dieldrin, γ-BHC, α-Chlordane, γ-Chlordane, *o,p'*-DDD, *p,p'*-DDD, *p,p'*-DDT, and α-Endosulfan) had higher concentrations in the lampreys (Table 1).

A two-sided Spearman's rank correlation coefficient test, comparing the weighted concentrations of the 81 PCB congeners between the lamprey and bivalve samples, gave an $r_S = 0.77$. This r_S value is significant at $P \leq 0.001$, and therefore, the null hypothesis that there is no correlation between the two groups was rejected.

All PCB congeners investigated were detected in one or more of the lamprey samples whereas congeners 1, 3, 12(13), 29, 54, 189, 191, and 199 (nominal detection limits 10.0, 7.0, 1.0, 0.4, 0.4, 0.5, 1.0, and 0.5 ng/g lipid analysed, respectively) were not detected in any of the bivalve samples. PCB congeners 167(185) and 209 had higher concentrations in bivalves compared with lampreys.

A *G*-test used to compare the weighted frequency distributions of PCB homologues between the lamprey and bivalve samples (Fig. 2) was significant at $P < 0.001$. The null hypothesis, H_0: $\Delta = 0$, was therefore rejected.

A comparison between the rankings of the rivers according to increasing levels of organochlorine lipid burden (based on the 21 organochlorine pesticides and 81 PCB congeners investigated) in lampreys and bivalves revealed a certain degree of congruence between the two taxa (Table 2). Four out of the seven rivers had identical ranks

Table 1. Ranges in concentration of organochlorine contaminants (ppb), based on lipids, in the lamprey ammocoetes *Ichthyomyzon fossor*, *I. unicuspis*, *Lampetra appendix*, and *Petromyzon marinus* and in the bivalve molluscs *Elliptio complanata*, *Lampsilis radiata*, and *L. ventricosa* from the Châteauguay, Richelieu, St-François, Nicolet Sud-Ouest, Bécancour, St-Maurice, and L'Assomption rivers, Québec, and collected between 16 July and 30 August 1990. The mean, standard deviation, and range are given for the total length. BDL = below sample detection limit.

Taxon	Lamprey ammocoetes	Bivalve molluscs
No. of samples	15	9
Total no. of specimens	144	32
Total length (mm)	85.1 ± 26.4 (32.5–162.0)	92.2 ± 11.7 (72.0–123.6)
Sample lipid weight (g)	0.04–2.34[a]	0.01–0.04
Aldrin	9–480	BDL
Dieldrin	31–800	1–14
Endrin	BDL–330	BDL–7
α-BHC	BDL–80	BDL–4
β-BHC	BDL–200	BDL
γ-BHC (=lindane)	7–150	BDL–3
α-Chlordane	16–520	BDL–6
γ-Chlordane	10–310	BDL–4
o,p'-DDD	23–700	BDL–15
p,p'-DDD	42–1200	1–10
o,p'-DDE	2–160	BDL–3
p,p'-DDE	19–560	6–130
o,p'-DDT	BDL–190	BDL–15
p,p'-DDT	31–520	BDL–9
α-Endosulfan	24–260	1–8
β-Endosulfan	5–340	BDL–7
Heptachlor	BDL–340	BDL–2
Heptachlor epoxide	3–160	1–3
Hexachlorobenzene	8–110	8–86
Pentachlorobenzene	1–68	6–55
Mirex	BDL–11	BDL–55
PCBs	200–23 000	4400–42 000

[a]Three of the lamprey samples consisted of one or two specimens only and had very low weights making the results less precise.

Table 2. Rankings of seven rivers of the St. Lawrence River Basin, Québec, according to the summed weighted concentrations of 128 organochlorine compounds (ppb), based on lipids, in two taxa.

River	Lamprey ammocoetes	Ranking	Bivalve molluscs	Ranking
Bécancour	607	1	4 486	1
Châteauguay	1 230	2	25 245	6
Nicolet Sud-Ouest	1 953	3	7 162	3
St-Maurice	2 330	4	5 869	2
Richelieu	3 482	5	19 518	5
St-François	4 931	6	9 640	4
L'Assomption	13 933	7	42 081	7

Fig. 2. Distribution of PCB homologues, expressed as percentages, in the lamprey ammocoete versus adult bivalve mollusc samples, based on the weighted means of their concentrations, from seven rivers in the St. Lawrence River Basin, Québec.

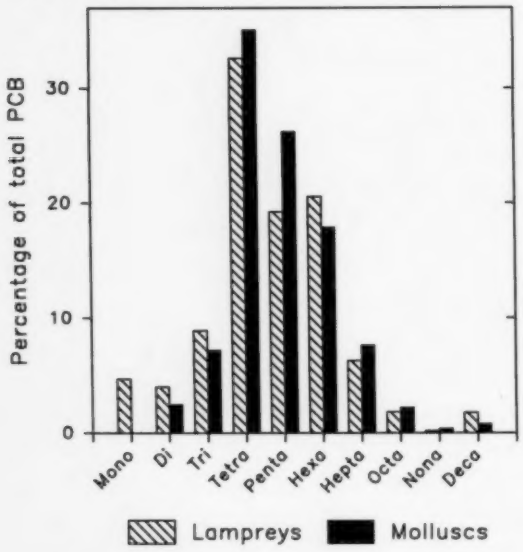

in both taxa. The cleanest river in terms of organochlorine residues based on both lampreys and bivalves was the Bécancour and the most polluted one the L'Assomption. A two-sided Spearman's rank correlation coefficient test, comparing the weighted lipid burdens in lampreys versus bivalves in the seven rivers (Table 2), gave an $r_S = 0.57$. This r_S value is significant at $P = 0.18$, and therefore, the null hypothesis that there is no correlation between the two groups was accepted. However, a Power function test on these data revealed that the power was <0.37, according to a table in Cohen (1969). The number of rivers required to increase the power value to the conventional level of 0.80 would be 21. In other words, to be reasonably confident that the noncorrelation we observed is true, a significantly greater number of rivers would need to be sampled. The bivalves always had greater contaminant lipid burdens than the lampreys for a given river (Table 2), mainly because of PCBs. PCBs accounted for 96.6–99.4% of the organochlorine lipid burden in the bivalves, but only 33.4–76.8% in the lampreys.

Discussion

Justification for lumping species in one taxon and comparing them with those of another taxon is based on the studies of Bedford et al. (1968) and Muncaster et al. (1990) who found generally little or no differences in the concentrations of various organochlorine contaminants in, respectively, seven and six species of freshwater bivalves belonging to a number of genera. One of the species in Bedford et al. (1968) and two of the species in Muncaster et al. (1990) were common to our study.

The fact that none of the organochlorine contaminants investigated was detected in the formalin solutions means that lampreys preserved in formalin may be used as biomonitors.

Lipid content in bivalves is highly variable. According to Kauss and Hamdy (1985), specimens of *E. complanata*, 65–72 mm shell length, have on average 1% lipid based on body wet weight (without the shell) and a mean water content of 84%. This means that the lipid content, expressed as a percentage of dry weight, in an average individual would be 6.2%. This value is 12.4 times higher than what is reported here for the mean of means of subsamples. On the other hand, Muncaster et al. (1990) determined that the mean water content in specimens of the same species and length was 89%, a value very close to the one used here (see Materials and methods). Furthermore, they determined the lipid content expressed as a percentage of dry weight to vary from 1.8 to 3.4% with mean 2.6%. Although substantially lower, this value is still 5.2 times higher than what is reported here for the mean of means of subsamples. These differences in lipid content may be due to a seasonal effect. The lipid content, expressed as a percentage of dry weight, in *E. complanata* collected from 12 sites in the Cornwall–Massena corridor on 23–25 June 1992 varied from 2.5 to 5.6% with mean 3.7% (J.L. Metcalfe-Smith, unpublished data) whereas *E. complanata* collected from 14 sites in the same area in September 1991 varied from 0.2 to 2.0% with mean 0.6% (M.E. Comba, unpublished data). According to Hardisty (1956), the lipid content, expressed as a percentage of dry weight, in ammocoetes

of the lamprey *Lampetra planeri*, collected in July and August and measuring 70–100 mm total length, varies from 15 to 40%. This range is comparable with what is reported in this study.

According to Moore and Beamish (1973), ammocoetes of *P. marinus* from Shelter Valley Creek, Lake Ontario basin, measuring 0–35, 36–70, and >71 mm in total length, represent, respectively, young-of-the-year, 1- to 2-year-old, and 3- to 6-year-old individuals. Nothwithstanding variation in growth rates based on locality and species, the ammocoetes in this study (Table 1) would therefore be on average at least 3 years old. We feel confident that this assumption is sound because 107 of the 144 ammocoetes in this study were *P. marinus* ranging in total length from 32.5 to 155.0 mm with mean 79.1 and standard deviation 23.3. According to Magnin and Stańczykowska (1971), the bivalves *E. complanata* and *L. radiata* from Lac des Deux Montagnes and Lac Saint-Louis in the Montréal area, with a shell length >70 mm, are at least 8 years old. It would seem logical to assume that the bivalves in this study (Table 1) are at least 8 years old because 29 of the 32 bivalves were either *E. complanata* or *L. radiata* ranging in shell length from 72.0 to 123.6 mm with mean 90.8 and standard deviation 11.3. However, since the bivalves in Lac Saint-Louis are stunted (J.L. Metcalfe-Smith, unpublished data), it is likely that many of the bivalves in the present study were younger than 8 years.

The filtration rate for *P. marinus* ammocoetes 101–111 mm total length and weighing 1.6 g wet body weight was determined by Mallatt (1982) to be 8–64 $mL \cdot g^{-1} \cdot h^{-1}$ ($\bar{X}$ = 28) at 12.5°C. Additionally, Mallatt (1982) estimated the filtration rate in completely burrowed ammocoetes to be half their unimpeded rate (i.e., without a sand plug), or about 15 $mL \cdot g^{-1} \cdot h^{-1}$. Rovainen and Schieber (1975) also recorded a comparable range in filtration rate of 21–60 $mL \cdot g^{-1} \cdot h^{-1}$ at 20°C for resting ammocoetes of *P. marinus* 60–140 mm total length and weighing 0.7–3.5 g wet weight. Lewandowski and Stańczykowska (1975) calculated that the bivalves *Anodonta piscinalis* (60–64 mm shell length), and *Unio tumidus* (48–54 mm shell length) filter an average 14.3 $mL \cdot g^{-1} \cdot h^{-1}$. This value is based on the wet weight of the mollusc with the shell. The actual weight of the specimens and the temperature at which the experiment was conducted were not reported. Given that we do not have a measure of the variation in filtration rate in the bivalves, all that can be inferred is that the filtration rate, and consequently the intake rate, appears to be higher in lampreys. Additionally, lamprey larvae can filter on average 82% of algal cells over a range of concentrations of 1–75 mg/L, concentrations that should include those they experience in nature (Mallatt 1982). Many suspension feeders, including bivalves, begin to perform inefficiently when concentrations exceed 1–10 mg/L, rejecting particles (Mallatt 1982). Therefore, the higher retention efficiencies in ammocoetes, coupled with their higher filtration rates, give them higher intake rates than those in bivalves.

The differences observed in concentrations and types of organochlorine compounds found in the two taxa are hypothesized to be mainly due to differences in the amounts and types of body lipids they each possess. Randall et al. (1991) have drawn attention to the fact that different lipid extraction procedures lead to different measurable pollutant concentrations. In this study, we used slightly different lipid extraction procedures for lampreys and bivalves. However, the magnitude of the differences in the pollutant levels noted are such that intertaxa differences in the percentage of the three general pools in which lipids are classified (i.e., neutral, membrane-bound polar, or covalently bound) could only partially explain those differences. Alternatively, lampreys and bivalves may have different detoxifying and (or) elimination capabilities.

In summary, given the similarities between the river rankings, based on the organochlorine lipid burdens of lamprey larvae and bivalves, we consider lamprey larvae to be as suitable as bivalves for monitoring of persistent organochlorine contaminants in the freshwater environment. They may even be superior to bivalves because they bioaccumulate a wider array of organochlorine compounds. Adding another biomonitor will prove very useful in areas where one taxon occurs and not the other, and also will serve as a test of the reliability of results in areas where both occur.

Acknowledgments

Our thanks to André Landry, Ministère du Loisir, de la Chasse et de la Pêche du Québec (MLCP), Québec, for issuing C.B.R. with a collecting permit for lampreys; François Chapleau, University of Ottawa, for the use of the DC-electrofisher; Gilles Roy and Jean Leclerc, MLCP, Rosemont, and Michel Lafleur, MLCP, Trois-Rivières, for their help in identifying some collection sites; J. Andrew Cooper and Ian R. Jones for their assistance in the field; Susan Laurie-Bourque for drawing the map; Virginia S. Palabrica, National Water Research Institute, Burlington, Ont., and Sean M. Backus, Backus Consulting, Stoney Creek, Ont., for the organochlorine assays; and Daniel Nadon and Judy Busnarda, Canadian Museum of Nature, for the statistical analyses. This study was partially supported by a research grant to C.B.R. from the Canadian Museum of Nature.

References

Bedford, J.W., Roelofs, E.W., and Zabik, M.J. 1968. The freshwater mussel as a biological monitor of pesticide concentrations in a lotic environment. Limnol. Oceanogr. **13**: 118–126.

Clarke, A.H. 1981. The freshwater molluscs of Canada. National Museum of Natural Sciences, National Museums of Canada, Ottawa, Ont.

Cohen, J. 1969. Statistical power analysis for the behavioral sciences. Academic Press, Inc., New York, N.Y.

Curry, C.A. 1977–1978. The freshwater clam (*Elliptio complanata*), a practical tool for monitoring water quality. Water Pollut. Res. Can. **13**: 45–52.

Elder, J.F., and Mattraw, Jr., H.C. 1984. Accumulation of trace elements, pesticides, and polychlorinated biphenyls in sediments and the clam *Corbicula manilensis* of the Apalachicola River, Florida. Arch. Environ. Contam. Toxicol. **13**: 453–469.

Godsil, P.J., and Johnson, W.C. 1968. Pesticide monitoring

of the aquatic biota at the Tule Lake National Wildlife Refuge. Pestic. Monit. J. **1**: 21–26.

Hardisty, M.W. 1956. Some aspects of osmotic regulation in lampreys. J. Exp. Biol. **33**: 431–447.

Hardisty, M.W., and Potter, I.C. 1971. The behaviour, ecology and growth of larval lampreys. *In* The biology of lampreys. Vol. 1. *Edited by* M.W. Hardisty and I.C. Potter. Academic Press, New York, N.Y. pp. 85–125.

Hartley, D.M., and Johnston, J.B. 1983. Use of the freshwater clam *Corbicula manilensis* as a monitor of organochlorine pesticides. Bull. Environ. Contam. Toxicol. **31**: 33–40.

Kauss, P.B., and Hamdy, Y.S. 1985. Biological monitoring of organochlorine contaminants in the St. Clair and Detroit rivers using introduced clams, *Elliptio complanatus*. J. Great Lakes Res. **11**: 247–263.

Kauss, P.B., Suns, K., and Johnson, A.F. 1983. Monitoring of PCBs in water, sediments and biota of the Great Lakes — some recent examples. *In* Physical behavior of PCBs in the Great Lakes. *Edited by* D. Mackay, S. Paterson, S.J. Eisenreich, and M.S. Simmons. Ann Arbor Science Publishers, Ann Arbor, Mich. pp. 385–409.

Lanteigne, J. 1988. Identification of lamprey larvae of the genus *Ichthyomyzon* (Petromyzontidae). Environ. Biol. Fishes, **23**: 55–63.

Leard, R.L., Grantham, B.J., and Pessoney, G.F. 1980. Use of selected freshwater bivalves for monitoring organochlorine pesticide residues in major Mississippi stream systems, 1972–73. Pestic. Monit. J. **14**: 47–52.

Lewandowski, K., and Stańczykowska, A. 1975. The occurrence and role of bivalves of the family Unionidae in Mikołajskie Lake. Ekol. Pol. **23**: 317–334.

Magnin, E., and Stańczykowska, A. 1971. Quelques données sur la croissance, la biomasse et la production annuelle de trois mollusques Unionidae de la région de Montréal. Can. J. Zool. **49**: 491–497.

Mallatt, J. 1982. Pumping rates and particle retention efficiencies of the larval lamprey, an unusual suspension feeder. Biol. Bull. (Woods Hole), **163**: 197–210.

Metcalfe, J.L., and Charlton, M.N. 1990. Freshwater mussels as biomonitors for organic industrial contaminants and pesticides in the St. Lawrence River. Sci. Total Environ. **97/98**: 595–615.

Moore, J.W., and Beamish, F.W.H. 1973. Food of larval sea lamprey (*Petromyzon marinus*) and American brook lamprey (*Lampetra lamottei*). J. Fish. Res. Board Can. **30**: 7–15.

Moore, J.W., and Mallatt, J.M. 1980. Feeding of larval lamprey. Can. J. Fish. Aquat. Sci. **37**: 1658–1664.

Muncaster, B.W., Hebert, P.D.N., and Lazar, R. 1990. Biological and physical factors affecting the body burden of organic contaminants in freshwater mussels. Arch. Environ. Contam. Toxicol. **19**: 25–34.

Peterman, R.M. 1990. Statistical power analysis can improve fisheries research and management. Can. J. Fish. Aquat. Sci. **47**: 2–15.

Potter, I.C. 1980. Ecology of larval and metamorphosing lampreys. Can. J. Fish. Aquat. Sci. **37**: 1641–1657.

Pugsley, C.W., Hebert, P.D.N., Wood, G.W., Brotea, G., and Obal, T.W. 1985. Distribution of contaminants in clams and sediments from the Huron–Erie corridor. I — PCBs and octachlorostyrene. J. Great Lakes Res. **11**: 275–289.

Randall, R.C., Lee, II, H., Ozretich, R.J., Lake, J.L., and Pruell, R.J. 1991. Evaluation of selected lipid methods for normalizing pollutant bioaccumulation. Environ. Toxicol. Chem. **10**: 1431–1436.

Renaud, C.B., Kaiser, K.L.E., and Comba, M.E. 1995. Historical versus recent levels of organochlorine contaminants in lamprey larvae of the St. Lawrence River basin, Québec. Can. J. Fish. Aquat. Sci. **52**: 000–000.

Rovainen, C.M., and Schieber, M.H. 1975. Ventilation of larval lampreys. J. Comp. Physiol. A Sens. Neural Behav. Physiol. **104**: 185–203.

Simpson, G.G., Roe, A., and Lewontin, R.C. 1960. Quantitative zoology. Harcourt, Brace and World, Inc., New York, N.Y.

Sokal, R.R., and Rohlf, F.J. 1981. Biometry. The principles and practice of statistics in biological research. 2nd ed. W.H. Freeman and Co., New York, N.Y.

Vladykov, V.D. 1950. Larvae of the eastern American lampreys (Petromyzonidae) I. — Species with two dorsal fins. Nat. Can. (Qué.), **77**: 73–95.

Effects of late-season catch and release angling on anaerobic metabolism, acid–base status, survival, and gamete viability in wild Atlantic salmon (*Salmo salar*)

Richard K. Booth, James D. Kieffer, Kevin Davidson, Alex T. Bielak, and Bruce L. Tufts

Abstract: The effects of catch and release angling on muscle physiology, survival and gamete viability were examined in wild Atlantic salmon (*Salmo salar*), just prior to spawning. Lactate in the white muscle increased to 37.4 $\mu mol \cdot g^{-1}$ after angling and recovered within 4 h. Muscle pH decreased from 7.46 at rest to 6.80 following angling, but returned to resting levels within 2 h. White muscle concentrations of PCr, ATP, and glycogen were depleted by 74, 46, and 73%, respectively, following angling. ATP and PCr returned to resting levels within 2 h, but glycogen did not recover until 12 h. The absence of significant changes in blood glucose indicated that the stress response was minimal in salmon angled under these conditions (6°C). There were also no mortalities among 20 salmon that were angled and transported to the hatchery. Multi-sea-winter (MSW) salmon (>63 cm) required a longer period to angle to exhaustion than grilse (<63 cm), but the physiological disturbance was less in MSW salmon. The survival of eggs from angled and nonangled salmon was 98 and 97%, respectively. Together, these results support the strategy of a late-season catch and release fishery for Atlantic salmon.

Résumé : Nous avons examiné les effets de la pêche sportive avec remise à l'eau sur la physiologie musculaire, la survie et la viabilité des gamètes chez des saumons atlantiques (*Salmo salar*) sauvages, juste avant la ponte. La concentration de lactate dans les muscles blancs est montée à 37,4 $\mu mol \cdot g^{-1}$ après la capture et s'est rétablie au bout de 4 h. Le pH des muscles a baissé, passant de 7,46 au repos à 6,80 après la capture, mais est revenu au niveau de repos dans les 2 h. Les concentrations de PCr, d'ATP et de glycogène dans les muscles blancs se sont appauvries respectivement de 74, 46 et 73 % après la capture. Les concentrations de PCr et d'ATP sont revenues au niveau de repos au bout de 2 h, mais le glycogène ne s'est rétabli qu'après 12 h. L'absence de changements significatifs dans la teneur en glucose du sang indique que la réaction au stress était minime chez les saumons capturés et remis à l'eau dans ces conditions (6 °C). On n'a pas observé non plus de mortalité parmi les 20 saumons qui ont été capturés et transportés à la pisciculture. Les saumons pluribermains (> 63 cm) ont combattu plus longtemps avant l'épuisement que les grilses (< 63 cm), mais la pertubation physiologique était moindre chez les saumons pluribermarins. La survie des oeufs chez les saumons capturés et non capturés était respectivement de 98 et 97 %. Les résultats obtenus appuient donc la stratégie d'établissement d'une saison tardive de pêche avec remise à l'eau pour le saumon atlantique.

[Traduit par la Rédaction]

Received January 20, 1994. Accepted August 5, 1994.
J12240

R.K. Booth, J.D. Kieffer, and B.L. Tufts.[1] Department of Biology, Queen's University, Kingston, ON K7L 3N6, Canada.
K. Davidson and A.T. Bielak. Department of Fisheries and Oceans, Fish Habitat and Enhancement Division, Moncton, NB E1C 9B6, Canada.

[1] Author to whom correspondence should be addressed.

Introduction

According to Pearse (1988), recreational angling has traditionally accounted for the majority of Canada's harvest of freshwater fish. To reduce the effect of recreational angling on declining fish stocks, managers have implemented a number of conservation-oriented management strategies. One of these measures, which has been actively promoted over the past several years, is nonconsumptive or "catch and release" angling.

The Atlantic salmon (*Salmo salar*) is one of Canada's most important recreational fish and is highly regarded for its apparent capacity for burst exercise during angling. In recent years, population declines have resulted in reductions in both the commercial and recreational Atlantic salmon fisheries. In most regions of eastern Canada the commercial fishery for Atlantic salmon has been closed entirely. Within the recreational fishery (excluding Quebec), legislation now requires anglers to release all multi-sea-winter (MSW) salmon (i.e., salmon >63 cm in length). Voluntary release of angled salmon <63 cm (i.e., grilse) is also being actively promoted by conservation groups in an attempt to further conserve and enhance salmon stocks. At present, however, our knowledge of the biological effects of catch and release is limited, particularly for the Atlantic salmon.

One of the most severe forms of exhaustive exercise for a fish is to be caught by angling. To date, however, there have been no studies examining the biological effects of angling in wild Atlantic salmon in their natural habitat. Laboratory studies have shown that exhaustive exercise results in a marked physiological disturbance in salmonids (Milligan and Wood 1986*a*, 1986*b*; Wood et al. 1983; Tufts et al. 1991; Wood 1991). Several studies have also reported significant delayed mortality in fish following exhaustive exercise (Black 1958; Beggs et al. 1980; Graham et al. 1982; Wood et al. 1983). The exact cause of mortality after severe exercise is not fully understood, but according to Wood et al. (1983), mortality may be related to the magnitude of the physiological disturbance within the muscle. In contrast, other investigators have found that exhaustive exercise was not associated with significant postexercise mortality (Wydoski et al. 1976; Schwalme and MacKay 1985; Tufts et al. 1991). The reasons for these apparently conflicting results regarding postexercise survival are not clear. It has been demonstrated, however, that specific exogenous and (or) endogenous factors such as training (Pearson et al. 1990), air exposure (Ferguson and Tufts 1992), and temperature (Kieffer et al. 1994) may influence the magnitude of the physiological disturbance after exhaustive exercise. Notably, Ferguson et al. (1993) have also recently shown that body size is an important determinant of the acid–base and metabolite status in the muscle of exhaustively exercised rainbow trout (*Oncorhynchus mykiss*). Although existing catch and release legislation is mainly oriented towards the MSW individuals which may reach extremely large sizes, the importance of factors such as body size in the physiological disturbance associated with angling in Atlantic salmon is presently unknown.

On many rivers in eastern Canada, current regulations permit angling of Atlantic salmon into the late fall, close to the spawning season. Late-season extensions are also being proposed for a number of salmon rivers which currently do not have extended seasons. According to Jonsson et al. (1991), gonad development proceeds throughout the spawning migration in salmon. In species such as rainbow trout and brown trout (*Salmo trutta*), it has been shown that acute stresses during the reproductive cycle may adversely affect gamete quality (Carragher et al. 1989; Campbell et al. 1992). At present, however, it is not known whether the stress associated with angling results in any deleterious effects on gamete viability in wild salmon which are caught and released just prior to spawning. Indeed, the absence of such information has contributed to controversy regarding the rationale for seasons in this economically important sport fishery.

In view of the importance of catch and release as a management strategy in the Atlantic salmon fishery, a thorough investigation of the potential biological effects of catch and release angling on this species is clearly warranted. The purpose of this study was therefore to (*i*) examine the magnitude of the physiological disturbance in different sizes of wild Atlantic salmon angled in the late season, (*ii*) assess survival under these conditions, and (*iii*) investigate the effects of angling on gamete viability.

Materials and methods

Animals

Male Atlantic salmon were obtained during their fall spawning migration (October 1992) from the New Brunswick Department of Natural Resources and Energy fish monitoring barrier, North Branch of the Main Southwest Miramichi River near Juniper, New Brunswick. To minimize the impact of our experiments on the reproductive potential of the river's adult salmon population, only male MSW salmon (65–84 cm fork length (FL), $N = 8$) and grilse (50–61 cm FL, $N = 34$) were sacrificed for the physiology experiments. Another group of both male and female MSW salmon were used to assess gamete viability after angling. The adult salmon used in the spawning experiments were eventually released in the same river. All of the animals were collected by either funnel trap or seining methods and held in large ($1 \times 1 \times 3$ m) live-boxes anchored in the river. The experiments were conducted in a typical holding pool for wild salmon where the width ranged between 5 and 10 m and the maximum depth was about 2 m. The water temperature was 6 ± 1°C.

Experimental protocol

To obtain resting (control) samples, grilse were collected and held in live-boxes for at least 24 h. Individual fish were then transferred with minimal disturbance to smaller wooden boxes continuously supplied with aerated water where they were held for an additional 12 h prior to sampling. Resting fish were anaesthetized individually by stopping the water flow and adding a buffered solution of tricaine methanesulfonate (MS-222, final concentration 0.25 $g \cdot L^{-1}$) to the box. Once anaesthetized (about 2 min), the fish were removed from the box and a 2-mL blood sample was taken by caudal puncture. Plasma was separated from the corpuscular component by 3 min of centrifugation. Following centrifugation, 500 μL of plasma was removed and placed

in a 1.5-mL Eppendorf tube with an equal volume of 8% perchloric acid. Plasma samples were then frozen in liquid nitrogen for transport and later analyses. Immediately after blood sampling, a section of white muscle was removed from the epaxial musculature approximately 6 cm prior to the dorsal fin, and well above the lateral red muscle band. Tissue was clamped in precooled tongs and immediately frozen in liquid nitrogen. The elapsed time between removal from anaesthetic, blood sampling, and tissue collection was less than 30 s. We chose to anaesthetize the fish prior to sampling because this method has been shown to reduce any metabolic and acid–base changes associated with the handling of a conscious animal (see Tang and Boutilier 1991 for a critique of this method). This is particularly important for highly labile muscle metabolites such as phosphagens and adenylates (see Dobson and Hochachka 1987). According to Davis et al. (1982), this method of anaesthesia also results in no release of corticosteroids. Fork length, to the nearest centimetre, was measured after tissue and blood sampling.

The remaining salmon and grilse were individually removed from the live-box, hooked in the top jaw, and angled to exhaustion by local anglers, using standard fly-fishing gear. It should be noted that the anglers had participated in a similar pilot study with our scientific team the previous year and consistently played the fish as they would under natural conditions until the fish were exhausted (as indicated by loss of equilibrium). Exhausted animals were immediately placed in well-aerated wooden boxes supplied with a continuous flow of river water, except for those to be sampled immediately after angling, which were placed directly into a Plexiglas box containing a concentrated and buffered solution of MS-222 (final concentration 0.25 $g \cdot L^{-1}$). Tissue and blood samples were then obtained from exercised animals using the same protocol, described above, as for the resting animals. Grilse were sampled at rest ($N = 8$) immediately following angling ($N = 6$) and at 2 h ($N = 6$), 4 h ($N = 6$), and 12 h ($N = 6$) after angling. Due to the importance of large (MSW) salmon to stock recruitment, we only killed and sampled one group of MSW salmon immediately after angling ($N = 8$).

Experiments were also carried out using adult male and female Atlantic salmon ($N = 20$ males, 20 females) to assess the effects of angling on gamete viability. These fish were divided into two separate groups that were either (i) angled or (ii) held in live-boxes and used as controls. These treatments resulted in a group of 10 angled fish and 10 control fish for each sex. The salmon were then transported to the Miramichi Salmonid Enhancement Centre, Department of Fisheries and Oceans, Newcastle, New Brunswick, for spawning. The potential effects of angling on reproduction were investigated by spawning (stripping) control and angled females with both control and angled males and measuring egg survival. Egg survival was measured as the number of fertilized eggs that reached the prehatch stage.

Analyses

Plasma metabolites and ions

Frozen plasma samples were thawed just prior to analysis and kept on ice until assays were performed. Plasma lactate and glucose concentrations were determined on 50-μL samples of neutralized plasma via the method of Lowry and Passonneau (1972) using Sigma reagents. Sodium and potassium concentrations were measured on 50-μL samples of plasma using a Corning model 410C clinical flame photometer (CIBA Corning Canada Inc.) and appropriate standards. Chloride concentrations were measured on 25-μL samples of plasma using a CMT 10 chloride titrator (Radiometer Copenhagen, Denmark).

Muscle metabolites

Sections of frozen white muscle tissue were ground into a fine powder under liquid nitrogen using a precooled mortar and pestle. Any skin fragments and tissue flakes were removed from the powder prior to analysis. Approximately 1–1.5 g of powdered tissue was added to a tared 15-mL Falcon tube containing 3 mL of 8% perchloric acid and 1 mmol $EDTA \cdot L^{-1}$. The tube containing the tissue was then reweighed and a further volume of the perchloric acid solution, equal to four times the tissue weight, was added. The mixture was then vortexed until a consistent slurry was formed (about 10 s). Next, the slurry was subjected to 5 min of acid extraction at 5°C. After the extraction period, the mixture was divided among 1.5 mL Eppendorf tubes and centrifuged for 4 min at 5°C. The supernatant was drawn off and placed in a tared 15-mL Falcon tube, the weight was recorded, and the sample was neutralized to pH 7.0 using a solution of 2 M KOH, 0.4 M KCl, and 0.4 M imidazole. The mixture was then transferred to 1.5-mL Eppendorf tubes and frozen in liquid nitrogen.

The resulting samples were analysed for lactate, phosphocreatine (PCr), and adenosine triphosphate (ATP) concentrations according to the methods of Lowry and Passonneau (1972) using Sigma reagents. Glycogen concentrations were determined using the method of Hassid and Abraham (1957).

Muscle acid–base status

White muscle tissue was powdered using the same technique as above, and acid–base status was determined using the method of Pörtner et al. (1990). Approximately 0.1 g of powdered tissue was added to 200 μL of chilled metabolic inhibitor in a tared Eppendorf tube. The metabolic inhibitor consisted of a solution of 150 mmol potassium flouride$\cdot L^{-1}$ and 6 mmol nitrilotriacetic acid$\cdot L^{-1}$. An additional 200 μL of metabolic inhibitor was then added, and the mixture was vortexed and centrifuged for 10 s. After centrifugation, a 200-μL sample was removed with a Hamilton gas-tight syringe and analysed for total CO_2 (C_{CO_2}) using a Corning model 965 CO_2 analyzer (CIBA Corning Canada Inc.). Measurements of C_{CO_2} were corrected for tissue water using the equation provided in Pörtner et al. (1990). An 80-μL sample of the supernatant was used to measure pH with a PHM 73 pH meter and associated micro-pH unit (Radiometer, Copenhagen, Denmark) maintained at 6°C. The C_{CO_2} and pH for each sample were then calculated as the means from duplicate measurements. Postexercise metabolic proton load (ΔH^+) was calculated using the formulae of Milligan and Wood (1986*b*).

Muscle nonbicarbonate buffer value

Nonbicarbonate buffer values were determined on muscle tissue taken from resting grilse using the methods of

Fig. 1. (A) PCr, (B) ATP, and (C) glycogen concentrations in the white muscle of Atlantic salmon grilse at rest and at 0, 2, 4, and 12 h following angling at 6°C. Significant differences from resting values are indicated by an asterisk ($N = 8$ for control group and $N = 6$ for angled groups).

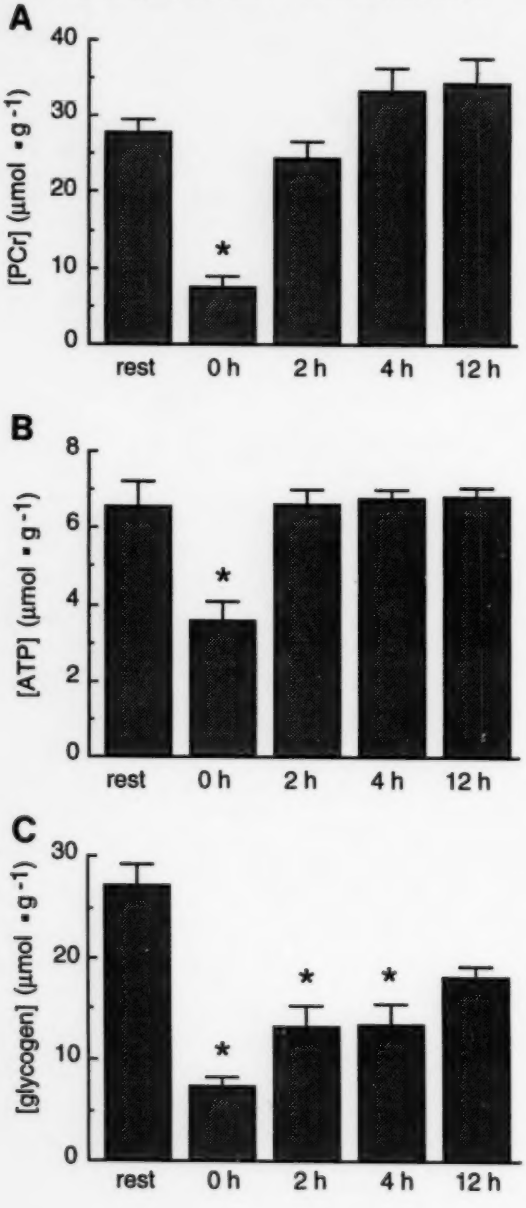

Pörtner (1990). Briefly, sections of white muscle were ground under liquid nitrogen, and 1 g of the tissue powder was diluted in fourfold volume of chilled metabolic inhibitor (150 mmol potassium flouride·L^{-1} and 6 mmol nitrilotriacetic acid·L^{-1}). The mixture was vortexed and the solution was placed into precooled tonometer vessels and equilibrated for 30 min at CO_2 concentrations of 1, 2, 5, and 9% in air, using a Wostoff gas-mixing pump (Wöstoff, Bochum, Germany). One-millilitre samples were removed after each equilibration period and analysed for pH and C_{co_2} as described above. The concentration of HCO_3 in muscle was determined from C_{co_2} using calculations for the solubility of CO_2 (alpha CO_2) and P_{co_2} provided by Heisler (1984). The nonbicarbonate buffer capacity (β) was calculated as the slope of the straight line obtained by plotting [HCO_3^-] against pH, as described in Heisler and Piiper (1971) and Pörtner (1990).

Muscle water content

A known mass of muscle tissue was placed in a tared Eppendorf tube. The sample was then placed in a drying oven at 80°C and weighed daily until there was no change in mass for any sample. Water content (%H_2O) was calculated using the following equation:

$$\%H_2O = 100 - [(100 \times \text{dry weight})/(\text{wet weight})].$$

Statistics

A one-factor analysis of variance (ANOVA) was used to determine whether there were significant differences between resting and recovery values in the time-course experiments. Significant differences between sample times were then determined using Scheffe's F-test ($P < 0.05$). Unpaired t-tests were used to determine the significance of postangling variables between grilse and MSW salmon. Unpaired t-tests were also used to determine whether there were significant differences in the egg viability between angled and control salmon in the spawning experiments. All values are reported as the mean ± 1 SE.

Results

Following angling, PCr, ATP, and glycogen concentrations in grilse fell by approximately 74, 46, and 73%, respectively (Fig. 1). PCr and ATP had fully recovered within 2 h of angling, but glycogen remained significantly lower than the resting value until the 12-h sample. However, the glycogen concentration was still 44% lower than the resting level after 12 h of recovery (Fig. 1C).

Muscle lactate levels peaked (37.4 ± 1.6 μmol·g^{-1}) in grilse immediately following angling and remained significantly higher than resting levels until 4 h of recovery (Fig. 2A). In contrast, lactate concentration in the plasma did not peak until 2 h (9.1 ± 1.0 μmol·mL^{-1}) of recovery and was still elevated after 4 h (Fig. 2B). The metabolic proton load in the muscle, like muscle lactate concentration, was greatest immediately after angling (24.5 ± 1.5 μmol·L^{-1}) and returned to resting levels within 4 h (Fig. 2C). Following angling, muscle pH was significantly reduced from 7.46 ± 0.02 to 6.80 ± 0.05, but it had fully recovered within 2 h (Fig. 2D). The mean nonbicarbonate buffer value of grilse ($N = 6$) was determined to be 35.5 ± 5.2 mmol·L^{-1}·pH $unit^{-1}$.

Angling also resulted in significant increases in plasma potassium and chloride concentrations of 11 and 34%, respectively (Table 1), but by 2 h of recovery, these variables were no longer significantly different from resting

Fig. 2. (A) White muscle lactate concentration, (B) plasma lactate concentration, (C) white muscle metabolic proton concentration, and (D) white muscle pH in Atlantic salmon grilse at rest and at 0, 2, 4, and 12 h following angling at 6°C. Significant differences from resting values are indicated by an asterisk ($N = 8$ for control group and $N = 6$ for angled groups).

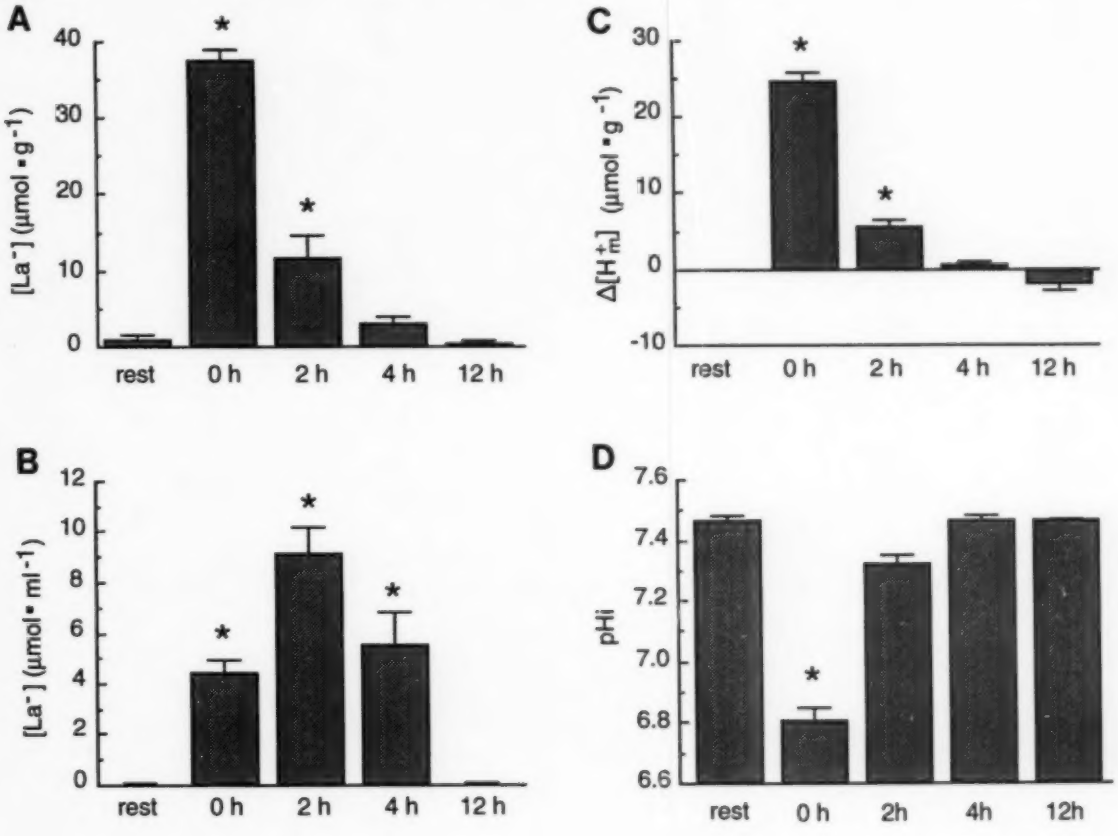

levels. Plasma sodium levels also increased slightly after angling, but these changes were not significant (Table 1). There were no significant changes in plasma glucose concentrations (2.5–2.7 mmol·L^{-1}) associated with angling in Atlantic salmon.

The weights of the MSW salmon used in this study were approximately double those of the grilse. Moreover, the MSW salmon required about twice the amount of time to angle than the grilse. However, there appeared to be consistently lower levels of energy metabolites in the white muscle of grilse as compared with MSW salmon immediately following angling (Fig. 3A). Postangling concentrations of PCr were significantly higher in MSW salmon. In addition, grilse also had significantly more lactate in their white muscle, and a lower muscle pHi, than MSW salmon after angling (Fig. 3B).

All of the salmon ($N = 20$) that were angled and transported to the hatchery for spawning survived. Moreover, there were no significant differences in the hatching success of eggs between angled (97.8 ± 0.6%) or control salmon (97.0 ± 0.9%).

Discussion

To our knowledge, this is the first detailed investigation of the physiological and reproductive effects of angling in wild Atlantic salmon. In a qualitative sense, the physiological response to angling, and the mechanisms involved in the process of recovery in Atlantic salmon, should be quite similar to those associated with other forms of exhaustive exercise in salmonids (Wood 1991). These physiological and biochemical processes have been well described (Wood and Perry 1985; Dobson and Hochachka 1987; Wood 1991; Schulte et al. 1992) and are not the main focus of this investigation. The following discussion will primarily focus on the magnitude of the physiological disturbance, the time required for recovery, and survival in wild Atlantic salmon angled in the late season (6°C) in comparison with other studies of exhaustive exercise in salmonids.

The magnitudes of the changes in PCr, ATP, and glycogen in angled Atlantic salmon (Fig. 1) were quite similar to those previously reported for rainbow trout that had been exhaustively exercised under laboratory conditions

Fig. 3. (A) White muscle concentrations of PCr, ATP, and glycogen and (B) white muscle lactate concentration and pH in grilse ($N = 6$) and MSW salmon ($N = 6$) sampled immediately after angling at 6°C. Significant differences between groups are indicated by an asterisk.

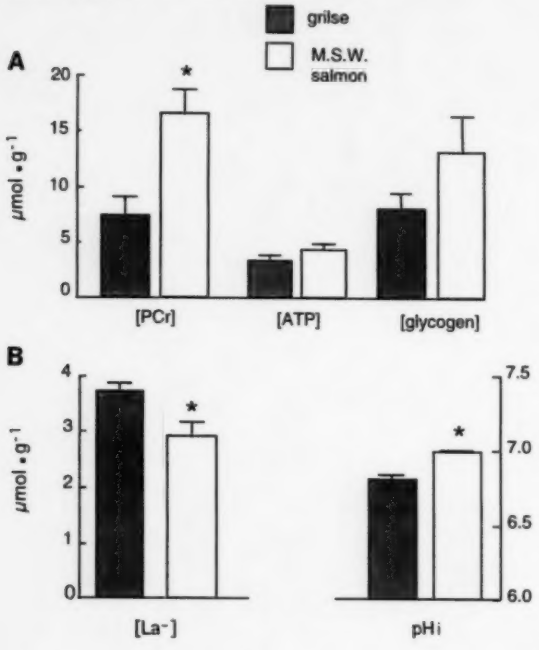

(Milligan and Wood 1986*b*; Dobson and Hochachka 1987; Schulte et al. 1992; Ferguson et al. 1993; Kieffer et al. 1994). The time required for recovery of PCr in angled Atlantic salmon (Fig. 1A) was also similar to that previously reported for rainbow trout by Schulte et al. (1992), but was markedly faster than the rate of recovery observed by Dobson and Hochachka (1987). Recovery of ATP in Atlantic salmon (Fig. 1B) was faster than that observed in recent studies on rainbow trout (Schulte et al. 1992; Kieffer et al. 1994). It is also noteworthy that there was 30% recovery in muscle glycogen within the first 2 h after angling in salmon (Fig. 1C). In comparison, most studies on rainbow trout have found that recovery of muscle glycogen is absent, or very limited, within this time period (Milligan and Wood 1986*b*; Pagnotta and Milligan 1991; Schulte et al. 1992; Kieffer et al. 1994).

Immediately following angling, muscle lactate concentrations in Atlantic salmon peaked at levels (Fig. 2A) that were similar to postexercise values in rainbow trout (Milligan and Wood 1986*b*; Pagnotta and Milligan 1991; Tang and Boutilier 1991; Schulte et al. 1992; Milligan and Girard 1993; Kieffer et al. 1994). Once again, however, recovery of muscle lactate (Fig. 2A) and muscle acid–base status (Fig. 2C and 2D) was faster in Atlantic salmon. Plasma lactate concentrations in the present study (Fig. 2B) were also less than half the levels reported in wild Atlantic salmon chased to exhaustion under laboratory conditions (Tufts et al. 1991). This difference can probably be largely

Table 1. Changes in plasma ion concentrations in grilse following angling and at various times during recovery. Significant differences ($P < 0.05$) from rest are indicated by an asterisk.

Group	$[Na^+]$ ($meq \cdot L^{-1}$)	$[K^+]$ ($meq \cdot L^{-1}$)	$[Cl^-]$ ($meq \cdot L^{-1}$)
Rest	148.3±1.8	2.2±0.2	125.8±2.8
0 h	153.8±1.2	3.6±0.1*	139.8±3.6*
2 h	160.0±3.1	2.0±0.1	131.6±1.8
4 h	150.3±3.1	2.1±0.1	124.4±1.8
12 h	145.7±2.9	1.6±0.1	121.8±2.0

explained by differences in experimental temperature (6 vs. 18°C) between these studies. Kieffer et al. (1994) have recently shown that the gradient for lactate between muscle and blood in rainbow trout during recovery from exhaustive exercise is largely determined by environmental temperature.

There are a number of factors that could account for the relatively rapid rate of recovery in Atlantic salmon. Certainly interspecific differences between the Atlantic salmon used in the present study and the rainbow trout commonly used in previous studies cannot be discounted. It is also important to consider that the majority of the previous physiological studies on exhaustive exercise in salmonids have used fish that were raised in a hatchery. Hatchery fish are rarely required to swim aerobically at high speeds or to perform bouts of anaerobic activity. In contrast, periods of high-speed aerobic swimming and (or) burst activity are probably common for salmonids in their natural environment during activities such as predator–prey interactions or while negotiating rapids or waterfalls on their migrations. Training has been shown to significantly enhance the rate of recovery in several physiological variables in salmonids following exhaustive exercise (Pearson et al. 1990). It is therefore likely that significant physiological differences probably also exist between wild and hatchery salmonids that may account for the relatively rapid recovery in Atlantic salmon following angling.

The majority of our physiological experiments were carried out on grilse. However, the current management strategy for Atlantic salmon in Canada is largely oriented towards the release of MSW salmon. MSW salmon are significantly larger than grilse and, as observed, generally require longer periods of time to land when they are angled. Recently, Ferguson et al. (1993) have shown that the magnitude of the physiological disturbance in rainbow trout following exhaustive exercise is directly related to body size and that larger individuals experience a greater disturbance after a similar period of exercise. Immediately after angling, PCr, ATP, and glycogen concentrations in MSW salmon were all greater than in grilse, although only the difference in PCr was significant (Fig. 3A). Similarly, the postangling concentration of lactate was significantly lower, and the pHi significantly higher, in the muscle of MSW salmon (Fig. 3B). Thus, the postangling values for MSW salmon suggest that the magnitude of the physiological disturbance in MSW salmon was actually less than

that in grilse. These results are somewhat surprising in view of the recent findings of Ferguson et al. (1993) and because the time required to land the MSW salmon was almost double that for grilse. Elucidation of the biological basis of these results will undoubtedly require further investigation.

A number of studies have reported significant postexercise mortality following exhaustive exercise in fish (Black 1958; Beggs et al. 1980; Graham et al. 1982; Wood et al. 1983). According to Wood et al. (1983), the cause of this delayed mortality in exhausted fish is probably related to the magnitude of certain aspects of the physiological disturbance within the muscle such as intracellular acidosis. In the present study, we observed no mortalities prior to sampling within the physiological series or among the 20 salmon that were angled and transported for spawning. Interestingly, we also found that recovery of several physiological variables within the muscle, particularly acidosis, was extremely rapid (Fig. 2). The absence of mortalities in our experiments provides the first documented evidence that "catch and release" will probably have minimal impact on the survival of Atlantic salmon angled in the late season prior to spawning. Indeed, the lack of significant increases in blood glucose levels and the minor changes in plasma ion concentrations (Table 1) following angling suggest that salmon may not even be severely stressed by angling under these conditions. Changes in plasma glucose levels and ion concentrations are generally considered to be important indicators of the relative magnitude of the stress response in fish (Wydoski et al. 1976; Ristori and Laurent 1985; Waring et al. 1992; McDonald and Robinson 1993).

Previous studies by Pickering et al. (1987) and Carragher et al. (1989) have demonstrated that stress may severely alter the levels of reproductive hormones in fish. Changes in reproductive endocrinology have been linked to suppression in ovulation (Tam and Payson 1986) and egg production (Lee and Gerking 1980) in females and milt quality in males (Weiner et al. 1986). More recently, acute stress has also been shown to affect both the egg quality (i.e., size, hatching success) and quantity (i.e., number of eggs produced) in rainbow trout (Campbell et al. 1992). In contrast, there were no significant differences in the hatching success of eggs between groups of angled and nonangled Atlantic salmon in our study. These results suggest that (i) the Atlantic salmon in our experiments were not angled during a period that may be critical for reproduction and (or) (ii) the stress associated with angling under these conditions was not severe enough to have a negative impact on gamete viability. Further studies may still be required, however, to determine whether angling in the late season affects other aspects of reproduction in Atlantic salmon such as redd defense, digging behaviour, and (or) the intensity of spawning acts.

Under current regulations, it is possible to angle and release Atlantic salmon in a number of maritime rivers until late fall, just prior to spawning. Many other salmon rivers are currently closed for angling at this time of year, and there has been considerable controversy over possible extensions to the season, arising from concerns related to potentially harmful impacts of catch and release on Atlantic salmon just prior to spawning. The present experiments indicate, however, that the likelihood of delayed mortality is minimal and there are no significant consequences on gamete viability resulting from angling and release of Atlantic salmon in the late fall.

Acknowledgements

We gratefully acknowledge financial support for this research provided by the Atlantic Salmon Federation, as well as the DFO/NSERC Science Subvention Program. In addition, logistical support provided by the New Brunswick Department of Natural Resources and Energy, particularly P. Cronin, and the Miramichi Salmon Association was greatly appreciated. Finally, we are also grateful for the excellent technical assistance of M. Hambrook, J. Hayward, J. Shaesgreen, P. Swan, and the volunteer anglers.

References

Beggs, G.L., Holeton, G.F., and Crossman, E.J. 1980. Some physiological consequences of angling stress in muskellunge, *Esox masquinongy* Mitchell. J. Fish Biol. **17**: 649–659.

Black, E.C. 1958. Hyperactivity as a lethal factor in fish. J. Fish. Res. Board Can. **15**: 573–586.

Campbell, P.M., Pottinger, T.G., and Sumpter, J.P. 1992. Stress reduces the quality of gametes produced by rainbow trout. Biol. Reprod. **47**: 1140–1150.

Carragher, J.F., Sumpter, J.P., Pottinger, T.G., and Pickering, A.D. 1989. The deleterious effects of cortisol implantation on reproductive function in two species of trout, *Salmo trutta* L. and *Salmo gairdneri* Richardson. Gen. Comp. Endocrinol. **76**: 310–321.

Davis, K.B., Parker, N.C., and Suttle, M.A. 1982. Plasma corticosteroids and chlorides in striped bass exposed to tricaine methanosulfate, quinaldine, etomidate, and salt. Prog. Fish-Cult. **44**: 205–207.

Dobson, G.P., and Hochachka, P.W. 1987. Role of glycolysis in adenylate depletion and repletion during work and recovery in teleost white muscle. J. Exp. Biol. **129**: 125–140.

Ferguson, R.A., and Tufts, B.L. 1992. Physiological effects of brief air exposure in exhaustively exercised rainbow trout (*Oncorhynchus mykiss*): implications for "catch and release" fisheries. Can. J. Fish. Aquat. Sci. **49**: 1157–1162.

Ferguson, R.A., Kieffer, J.D., and Tufts, B.L. 1993. The effects of body size on the acid–base and metabolite in the white muscle of rainbow trout before and after exhaustive exercise. J. Exp. Biol. **180**: 195–207.

Graham, M.S., Wood, C.M., and Turner, J.D. 1982. The physiological responses of rainbow trout to strenuous exercise: interactions of water hardness and environmental acidity. Can. J. Zool. **60**: 3153–3164.

Hassid, W.Z., and Abraham, S. 1957. Chemical procedures for analysis of polysaccharides. *In* Methods in enzymology. Vol. 3. *Edited by* S.P. Colwick and N.O. Kaplan. Academic press, New York, N.Y. pp. 34–37.

Heisler, N. 1984. Acid–base regulation in fishes. *In* Fish physiology. *Edited by* W.S. Hoar and D.J. Randall. Elsevier, New York, N.Y. pp. 315–392.

Heisler, N., and Piiper, J. 1971. The buffer value of rat diaphram muscle tissue determined by P_{co_2} equilibration of homogenates. Respir. Physiol. **12**: 169–178.

Jonsson, N., Jonsson, B., and Hansen, L.P. 1991. Energetic cost of spawning in male and female Atlantic salmon (*Salmo salar* L.). J. Fish Biol. **39**: 739–744.

Kieffer, J.D., Currie, S., and Tufts, B.L. 1994. Effects of environmental temperature on the metabolic and acid–base responses of rainbow trout to exhaustive exercise. J. Exp. Biol. **194**: 299–317.

Lee, R.M., and Gerking, S.D. 1980. Survival and reproductive performance in the desert pupfish, *Cyprinodon n. nevadensis* (Eigenmann and Eigenmann), in acid waters. J. Fish Biol. **17**: 507–515.

Lowry, O.H., and Passonneau, J.V. 1972. A flexible system of enzymatic analysis. Academic Press, New York, N.Y.

McDonald, D.G., and Robinson, J.G. 1993. Physiological responses of lake trout to stress: effects of water hardness and genotype. Trans. Am. Fish. Soc. **122**(6): 1146–1156.

Milligan, C.L., and Girard, S.S. 1993. Lactate metabolism in rainbow trout. J. Exp. Biol. **180**: 175–193.

Milligan, C.L., and Wood, C.M. 1986*a*. Intracellular and extracellular acid–base status and H^+ exchange with the environment after exhaustive exercise in the rainbow trout. J. Exp. Biol. **123**: 93–121.

Milligan, C.L., and Wood, C.M. 1986*b*. Tissue intracellular acid–base status and the fate of lactate after exhaustive exercise in the rainbow trout. J. Exp. Biol. **123**: 123–144.

Pagnotta, A., and Milligan, C.L. 1991. The role of blood glucose in the restoration of muscle glycogen during recovery from exhaustive exercise in rainbow trout (*Oncorhynchus mykiss*) and winter flounder (*Pseudopleuronectes americanus*). J. Exp. Biol. **161**: 489–508.

Pearse, P.H. 1988. Rising to the challenge: a new policy for Canada's freshwater fisheries. Independent report published by the Canadian Wildlife Federation, Ottawa, Ont.

Pearson, M.P., Spriet, L.L., and Stevens, E.D. 1990. Effect of sprint training on swim performance and white muscle metabolism during exercise and recovery in rainbow trout (*Salmo gairdneri*). J. Exp. Biol. **149**: 45–60.

Pickering, A.D., Pottinger, T.G., Carragher, J., and Sumpter, J.P. 1987. The effects of acute and chronic stress on the levels of reproductive hormones in the plasma of mature male brown trout, *Salmo trutta* L. Gen. Comp. Endocrinol. **68**: 249–259.

Pörtner, H.O. 1990. Measurements of intracellular buffer values after metabolic inhibition by flouride and nitrilotriacetic acid. Respir. Physiol. **81**: 275–288.

Pörtner, H.O., Boutilier, R.G., Tang, Y., and Toews, D.P. 1990. Determination of intracellular pH and P_{co_2} by flouride and nitrilotriacetic acid. Respir. Physiol. **81**: 255–274.

Ristori, M.T., and Laurent, P. 1985. Plasma catacholamines and glucose during moderate exercise in the trout: comparison with bursts of violent activity. Exp. Biol. **44**: 247–253.

Schulte, P.M., Moyes, C.D., and Hochachka, P.W. 1992. Integrating metabolic pathways in the post-exercise recovery of white muscle. J. Exp. Biol. **166**: 181–195.

Schwalme, K., and MacKay, W.C. 1985. The influence of angling-induced exercise on the carbohydrate metabolism of northern pike (*Esox lucius* L.). J. Comp. Physiol. B, **156**: 67–75.

Tam, W.H., and Payson, P.D. 1986. Effects of chronic exposure to sublethal pH on growth, egg production, and ovulation in Brook trout, *Salvelinus fontinalis*. Can. J. Fish. Aquat. Sci. **43**: 275–280.

Tang, Y., and Boutilier, R.G. 1991. White muscle intracellular acid–base status and lactate status following exhaustive exercise: a comparison between freshwater- and seawater-adapted rainbow trout. J. Exp. Biol. **156**: 153–171.

Tufts, B.L., Tang, Y., Tufts, K., and Boutilier, R.G. 1991. Exhaustive exercise in "wild" Atlantic salmon (*Salmo salar*): acid–base regulation and blood gas transport. Can. J. Fish. Aquat. Sci. **48**: 868–874.

Waring, C.P., Stagg, R.M., and Poxton, M.G. 1992. The effects of handling on flounder (*Platichthys flesus* L.) and Atlantic salmon (*Salmo salar* L.). J. Fish Biol. **41**: 131–144.

Weiner, G.S., Schreck, C.B., and Li, H.W. 1986. Effects of low pH on reproduction of rainbow trout. Trans. Am. Fish. Soc. **115**: 75–82.

Wood, C.M. 1991. Acid–base and ion balance, metabolism and their interactions, after exhaustive exercise in fish. J. Exp. Biol. **160**: 258–308.

Wood, C.M., and Perry, S.F. 1985. Respiratory, circulatory, and metabolic adjustments to exercise in fish. *In* Circulation, respiration and metabolism. *Edited by* R. Gilles. Springer-Verlag, Berlin, Germany. pp. 2–22.

Wood, C.M., Turner, J.D., and Graham, M.S. 1983. Why do fish die after severe exercise? J. Fish Biol. **22**: 189–201.

Wydoski, R.S., Wedemeyer, G.A., and Nelson, N.C. 1976. Physiological response to hooking stress in hatchery and wild rainbow trout (*Salmo gairdneri*). Trans. Am. Fish. Soc. **105**: 601–606.

Choosing fisheries harvest policies: when does uncertainty matter?

Shane W. Frederick and Randall M. Peterman

Abstract: Fisheries harvest policies are formulated under uncertainty because estimates of stock abundance and biological parameters are imprecise. However, allowable harvests are often based solely on point estimates of these quantities, essentially ignoring uncertainty. Some fishery scientists have advocated adjusting harvest levels downward to account for uncertainty, but few formal methods have been developed to determine how large these "uncertainty adjustments" should be. We describe an age-structured simulation model that explicitly incorporated uncertainty in parameters of the stock–recruitment relationship, errors in abundance estimates, and year-to-year variability in recruitment and calculated which uncertainty adjustment was optimal in terms of expected discounted yield. The optimal adjustment varied considerably, depending on the stock and harvest policy simulated. The increase in expected value from incorporating the adjustment into the harvest policy was usually small, except when we modeled a biological "threshold", where overharvests could lead to an irreversible stock collapse. Therefore, while our analysis suggests that basing harvest decisions solely on the best point estimates may often be an approximately optimal strategy, it also indicates that large adjustments may sometimes be appropriate. Consequently, fishery managers should avoid making arbitrary adjustments for uncertainty, and instead derive the optimal adjustment for each situation.

Résumé : Les politiques de prélèvement des pêches sont formulées dans l'incertitude, étant donné que les estimations de l'abondance des stocks et les paramètres biologiques sont imprécis. Toutefois, les volumes de capture autorisés sont souvent basés simplement sur des estimations ponctuelles de ces quantités, qui pour l'essentiel ne tiennent pas compte de l'incertitude. Certains halieutes préconisent de rajuster à la baisse les niveaux de capture pour tenir compte de l'incertitude, mais rares sont les méthodes formelles permettant de déterminer l'ampleur de ces « corrections d'incertitude ». Nous décrivons un modèle de simulation structurée par âge qui intégrait explicitement l'incertitude dans les paramètres de la relation stock–recrutement, les erreurs dans les estimations de l'abondance et la variabilité annuelle dans le recrutement, et qui calculait quelle correction d'incertitude était optimale pour déterminer de combien la production doit être réduite. La correction optimale variait considérablement selon le stock et la politique de prélèvement simulés. L'accroissement de valeur attendu de l'intégration de la correction à la politique de prélèvement était généralement faible, sauf lorsque nous avons modélisé un « seuil » biologique, dans les cas où une surexploitation pouvait causer un effondrement irréversible du stock. En conséquence, tandis que notre analyse montre que le fait de fonder les décisions de prélèvement uniquement sur les meilleures estimations ponctuelles peut souvent constituer approximativement la stratégie optimale, elle indique aussi que des corrections importantes se justifient parfois. Les gestionnaires des pêches devraient donc éviter d'apporter des corrections arbitraires pour tenir compte de l'incertitude, et plutôt calculer quelle doit être la correction optimale dans chaque situation.
[Traduit par la Rédaction]

Introduction

Uncertainty is a widely recognized aspect of fisheries management, but it is often ignored in practice. Allowable harvest levels are frequently based solely on the best point estimates of stock abundance and stock–recruitment parameters, without accounting for the uncertainty in those estimates (Walters 1981; Gulland 1983; Lovejoy 1988; Sainsbury 1991). This practice conflicts with the common intuition that uncertainty should dictate more conservative

Received August 4, 1993. Accepted July 14, 1994.
J12033

S.W. Frederick[1] **and R.M. Peterman.** School of Resource and Environment Management, Simon Fraser University, Burnaby, B.C. V5A 1S6, Canada.

[1] Author to whom correspondence should be addressed. Present address: Department of Social and Decision Sciences, Carnegie Mellon University, Pittsburgh, PA 15213-3890, USA.

harvesting strategies (Clark 1985) and is counter to the prevailing belief that uncertainty should be explicitly incorporated in the formation of management policy (e.g., Peterson and Smith 1981; Sissenwine 1984; Clark 1985; Brown and Patil 1986; Bergh and Butterworth 1987; Linder et al. 1987; Francis 1992; Thompson 1992).

Several approaches have been advanced to formally incorporate uncertainty into harvest policy decisions. One approach is to estimate the probabilities that various management options will cause the fish stock to fall below a predefined threshold in a specified period (Brown and Patil 1986; Linder et al. 1987; Francis 1992). A second approach is to measure the expected economic losses caused by errors in parameter estimates and to compare these losses for different harvest policies to help select one that is robust to such errors (Ruppert et al. 1985). A third approach is to use stochastic dynamic programming to directly compute the optimal harvest decision, given the management objectives, the current uncertainties, and the effect of management actions on future uncertainties (Walters 1975, 1981, 1986; Walters and Hilborn 1976; Silvert 1978; Parma and Deriso 1990).

Stochastic dynamic programming is the most sophisticated of these approaches because it explicitly calculates the decision that maximizes the chosen objective(s), and because it can formally incorporate the value of information of alternative management actions (the degree to which different harvest levels reduce future uncertainty). However, the computational demands of dynamic programming are formidable and it is often prohibitively difficult to calculate optimal policies for practical situations (Smith and Walters 1981; Walters 1981; Ludwig and Hilborn 1983; Mangel and Clark 1983; Parma and Deriso 1990).

The other approaches, which do not use formal optimization techniques, are much simpler to implement but do not provide the information the decision maker really needs; they usually focus more on describing the possible outcomes than on prescribing the optimal decision. Similarly, Clark (1985) and Walters (1986) noted that although confidence intervals often accompany the point estimates of parameters or state variables, the information they provide is rarely used, since, by themselves, they do not indicate how, or even if, the decision based on the point estimates should be modified. Without such quantitative guidelines for setting policy, managers sometimes make conservative allowances for uncertainty through arbitrary safety factors or uncertainty adjustments. For example, catch limits for groundfish stocks off the west coast of Canada are often set 25–50% lower than the estimated sustainable level when abundance estimates are highly uncertain (Tyler 1988).

Although such an approach may be intuitively appealing, it can only be justified if it improves management performance (i.e., if the benefit of reducing the risk of overfishing exceeds the cost of reducing harvests). Because there is little empirical evidence supporting this conclusion, it is worth asking whether such uncertainty adjustments are appropriate and, if so, exactly how large they should be.

In this paper, we propose a method for determining optimal uncertainty adjustments for harvest policies set in the presence of uncertainty in stock abundance estimates, uncertainty in the stock–recruitment parameters, and variability in recruitment. By computing the expected value of different uncertainty adjustments, we determined how much the harvest calculated from the best point estimates of stock abundance and stock–recruitment parameters should be adjusted to account for the uncertainty in those estimates. We first describe four concepts from decision theory that provide a useful framework for discussing harvest decisions made under uncertainty.

Determining the optimal harvest under uncertainty: perspectives from decision theory

Deterministic and Bayes equivalent decisions

A deterministic approach bases decisions solely on point estimates of parameters and state variables, with no formal consideration of uncertainty. In contrast, a "Bayes equivalent" approach (Walters 1981) explicitly accounts for parameter uncertainty by selecting the decision that maximizes expected value over the probability distributions of the uncertain quantities. An "active–adaptive" approach (Walters 1986) goes one step further — it calculates the optimal decision by considering not only the current uncertainties, but also the effect of the current decision on future uncertainties.

In this study, we consider the decision dictated by the Bayes equivalent approach to be the optimal decision. We recognize, however, that it may not always be truly "optimal" because it may impede movement toward the optimal harvest policy compared with an active–adaptive approach that explicitly includes the informative value of alternative decisions as a criterion for selecting management strategies (see Walters and Hilborn 1976; Smith and Walters 1981; Walters 1981, 1986; Parma and Deriso 1990; Hilborn and Walters 1992). Notwithstanding the fundamental conceptual differences between a Bayes equivalent and an active–adaptive approach, many stochastic dynamic programming studies in fisheries indicate that when the Bayes equivalent decision is not optimal, its expected value is usually very close to that of the true optimal strategy that involves adaptive "probing" (Walters and Hilborn 1976; Walters 1981; Parma and Deriso 1990). Furthermore, determining the Bayes equivalent solution is computationally tractable whereas obtaining the active–adaptive, optimal solution would be infeasible given the complexities included in our model — age structure, measurement errors, and multiple uncertain parameters. Thus, for the purpose of this study, ignoring the active–adaptive aspects of the problem is an appropriate and a necessary simplification.

Calculating the optimal uncertainty adjustment

The optimal harvest (H^*) in any given year is the harvest level that best achieves some chosen objective, such as long-term discounted yield. However, H^* is unknown because it is a function of quantities that we are uncertain about, such as the stock abundance and the stock–recruitment parameters. Therefore, the harvest level that is actually set will typically deviate from H^*. The loss in value caused by this deviation is the *opportunity loss* (Raiffa 1968; Jones 1977) for that decision.

Fig. 1. (A) Loss function describing the costs of deviating from the optimal harvest level (H^*). (B) Distribution describing the probability of different deviations of H from H^*, for a given harvest level (H). The distribution shown here corresponds to the deterministic harvest level (H_D). For harvests lower than H_D, the distribution would shift to the left; for harvests higher than H_D, it would shift to the right. (C) Expected opportunity loss (EOL) for each harvest level. The EVPI is the expected value of perfect information — the expected value of eliminating the uncertainty in H^*, given the costs of deviating from H^*. H_B is the Bayes equivalent harvest level.

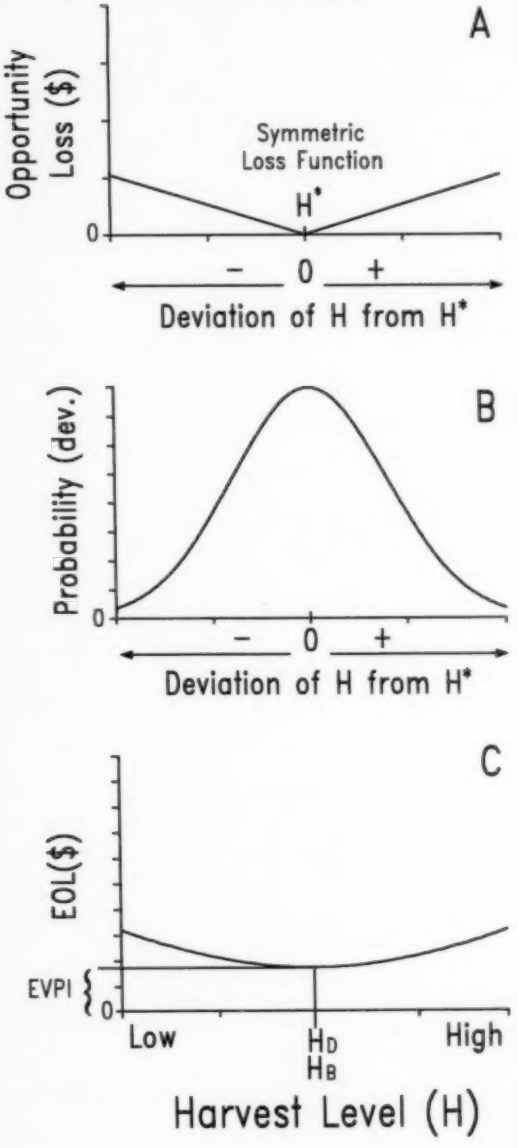

The relationship between the size of this deviation and the magnitude of the opportunity loss can be plotted as a *loss function* (Figs. 1A and 2A). The opportunity loss is zero at H^* by definition. It usually increases continuously as the harvest level that is set (H) deviates from H^*. The loss function can be linear or nonlinear, symmetric or asymmetric. For a symmetric loss function (Fig. 1A), the opportunity loss depends only on the size of the deviation — underharvests and overharvests are equally costly. But, for an asymmetric loss function (Fig. 2A), the opportunity loss depends on the direction of, as well as the size of, the deviation. In this example, overharvests are more costly than underharvests.

Because H^* is unknown, the deviation of H from H^* is unknown. Therefore, the opportunity loss corresponding to a particular harvest level (H) cannot be calculated. Nevertheless, the *expected opportunity loss* (EOL) (Raiffa 1968) *can* be calculated by multiplying the probability of each possible deviation of H from H^* (Figs. 1B and 2B) by the opportunity loss corresponding to that deviation (Figs. 1A and 2A) and then summing the products. The EOL for different harvest levels is shown in Figs. 1C and 2C. (See Appendix A for a formal mathematical description of the calculations involved.)

The harvest level that minimizes EOL is the "Bayes equivalent" harvest (H_B). This may or may not correspond to the "deterministic" harvest (H_D) — the harvest level based solely on the best *point estimate* of H^*. For a symmetric loss function (Fig. 1A), where the costs of overharvest and underharvest are equal, H_B will coincide with H_D, no matter how uncertain our estimate of H^* is (provided that this uncertainty is described by a symmetric probability distribution — see the last part of the sensitivity analyses section). However, for an asymmetric loss function (Fig. 2A), H_B will differ from H_D because the EOL can be reduced by adjusting the allowable harvest in the direction that has lower opportunity losses. For example, in Fig. 2C, H_B is lower than H_D because it pays to "hedge" against the higher costs of overharvest.

The difference between H_B and H_D is the optimal *uncertainty adjustment* ("Adjust." in Fig. 2C); it is the amount that the harvest level calculated from the best point estimates of the stock abundance and stock–recruitment parameters should be adjusted to account for the uncertainty in those estimates, given the difference in costs between overharvests and underharvests. The reduction in EOL resulting from the uncertainty adjustment is called the *expected value of including uncertainty* (EVIU) (Morgan and Henrion 1990). The EVIU must be differentiated from a more common term in decision theory — the *expected value of perfect information* (EVPI) (Raiffa 1968; Walters 1986). The EVPI is the EOL at H_B (Figs. 1C and 2C) whereas the EVIU is the difference in EOL between H_B and H_D (Fig. 2C). In other words, the EVPI is the cost of *being* uncertain whereas the EVIU is the additional cost of *ignoring* uncertainty by basing the harvest decision solely on the best point estimates of the stock abundance and the stock–recruitment parameters (hereafter referred to just as the best point estimates). Equivalently, the EVPI is the value of *eliminating* uncertainty whereas the EVIU is the value of *accounting for* uncertainty by using the additional information contained

Fig. 2. Same as Fig. 1, except the loss function is asymmetric. Because of the asymmetric loss function, the Bayes equivalent harvest level (H_B) differs from the deterministic harvest (H_D). The difference between H_B and H_D is the optimal uncertainty adjustment ("Adjust." in Fig. 2C). The value of applying this adjustment is the expected value of including uncertainty (EVIU); it is the difference in expected opportunity loss (EOL) between H_D and H_B. As in Fig. 1, the EVPI is the expected value of perfect information — the EOL at H_B.

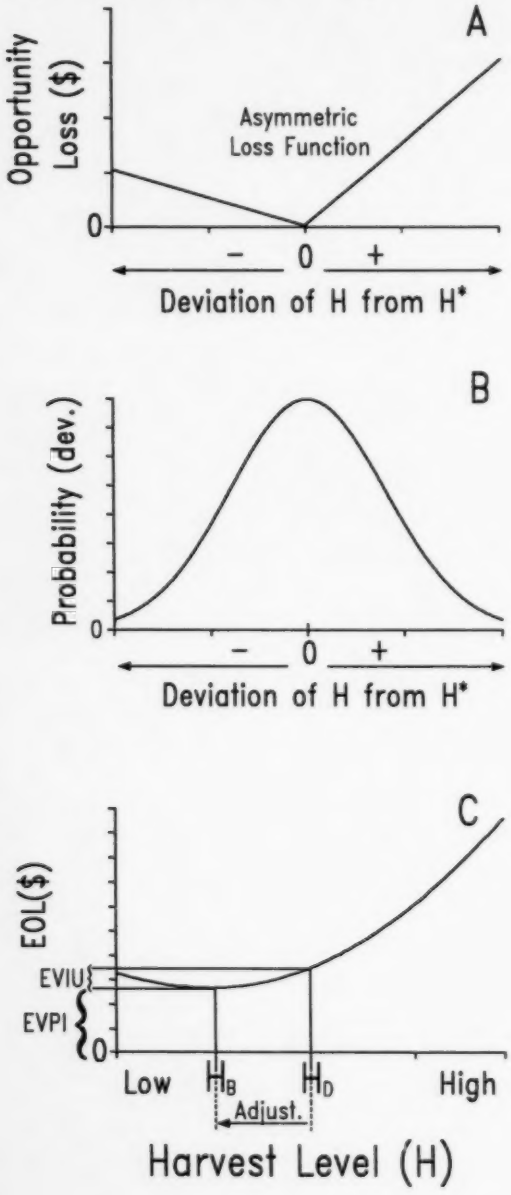

in the probability distributions of the uncertain point estimates (Morgan and Henrion 1990).

A large EVPI does not necessarily imply a large EVIU. Although eliminating uncertainty is nearly always valuable, explicitly including uncertainty may not be. For instance, for a symmetric loss function and distribution (Figs. 1A and 1B), the decision dictated by the deterministic approach (H_D) is the same as that dictated by the Bayes equivalent approach (H_B), and therefore has the same EOL (Fig. 1C). Consequently, explicitly including uncertainty does not alter the decision in this case. Conversely, for an asymmetric loss function (Fig. 2A), explicitly including uncertainty is valuable because it leads to the selection of a superior decision — one with a lower EOL and thus a higher expected value (Fig. 2C).

The preceding hypothetical examples were only intended to illustrate why uncertainty adjustments may or may not be appropriate. In practice, neither the probability distribution describing the uncertainty in H^* nor the parameters of the loss function can be easily specified, and analytical solutions may require such extreme simplifying assumptions that they will be of little practical use. Therefore, we used a Monte Carlo simulation model to numerically estimate the optimal uncertainty adjustment.

Methods

This section illustrates how to calculate the optimal uncertainty adjustment for a harvest policy that confronts several sources of uncertainty simultaneously: errors in estimates of stock abundance, uncertainty in the underlying stock–recruitment parameters, and year-to-year variability in recruitment processes. We explored uncertainty adjustments for a constant escapement policy and a constant harvest rate policy for the Atlantic menhaden (*Brevoortia tyrannus*) and the Arcto-Norwegian stock of Atlantic cod (*Gadus morhua*). We chose these two stocks simply because they were examples of fish with widely differing life history characteristics (their biological parameter values are listed in Tables 1 and 2); this paper is not directed toward the management of these stocks specifically. This is particularly true because more recent data may alter estimates of the parameters that we used in our examples.

General description of the model

The nine basic steps of the simulation model (Fig. 3), which are elaborated upon below, were as follows. (1) The optimal escapement or optimal harvest rate was estimated from the point estimates of all biological parameters and the discount rate applied to future harvests. (2) An uncertainty adjustment was chosen, which modified the harvest level calculated from the deterministic analysis. (3) The abundance of the vulnerable stock was estimated. (4) The allowable harvest was set, according to the abundance estimate, the type of harvest policy simulated, and the specified uncertainty adjustment strategy for that loop in the model. (Note that henceforth we use "harvest policy" to refer to either the constant escapement or constant harvest rate policies whereas "strategy" will refer to the amount of adjustment for uncertainty in an escapement goal or harvest rate.) (5) The stock remaining after harvest produced

Table 1. Parameter values used in the model for Atlantic menhaden (*Brevoortia tyrannus*) (taken from Ahrenholtz et al. 1987). Instantaneous natural mortality rate was 0.45.

Age (years)	Weight (kg)	Fecundity (1000's eggs) per female	Relative catchability
0	0.015	0	0
1	0.130	0	0
2	0.300	41	1
3	0.480	176	1
4	0.600	269	1
5	0.680	376	1
6	0.710	456	1
7	0.720	525	1

recruits according to a Shepherd (1982) stock–recruitment model. Uncertainty in the stock–recruitment parameters was simulated by bootstrapping the stock–recruitment data set and assigning the resulting parameter estimates to Monte Carlo trials. Interannual variability in recruitment was simulated by applying a lognormal, multiplicative random error term to the predicted recruitment. (6) The present value (PV) of the sum of harvests for each trial was calculated by discounting the dollar value of harvests to year 1, using a 5% discount rate in the baseline case. (To convert harvest in metric tons into dollar value, we assumed as a rough approximation that menhaden were worth $100 per metric ton and cod were worth $1000 per metric ton.) (7) 1000 trials were conducted for each uncertainty adjustment strategy; the expected PV for that strategy was the average PV of those 1000 trials. (8) A different uncertainty adjustment was set and the procedure was repeated. (9) The adjustment that maximized expected PV was the optimal uncertainty adjustment for that simulated stock and harvest policy. The EVIU was the increase in expected PV of the optimal adjustment strategy over the zero adjustment or deterministic strategy.

Estimating the optimal escapement

For an age-structured stock, the optimal escapement (S^*) and optimal harvest rate (F^*) are complicated functions of the recruitment parameters (a, k, and b in the Shepherd (1982) equation), natural mortality rate (M), weight at age (w_i), fecundity of females at age (f_i), relative vulnerability at age (q_i), and the discount rate applied to future harvests (r). We estimated the optimal escapement or optimal harvest rate iteratively, by using the published estimates of the relevant biological parameters (or the best-fit parameters for the stock–recruitment relationship) and by incrementally varying the escapement or harvest rate until the PV of harvests was maximized. We assumed deterministic recruitment to simplify this calculation because we found that the optimal escapement or harvest rate was virtually identical whether deterministic or stochastic recruitment was simulated, which is consistent with the results of Reed (1978), Ludwig and Varah (1979), Ludwig and Walters (1982), and Clark (1985).

Table 2. Parameter values used for Arcto-Norwegian cod (*Gadus morhua*) estimated from graphs in Cushing (1966), Garrod (1967), and Schopka and Hempel (1973). Instantaneous natural mortality rate was 0.2.

Age (years)	Weight (kg)	Fecundity (1000's eggs) per female	Relative catchability
0	0.05	0	0
1	0.1	0	0
2	0.3	0	0
3	0.5	0	0
4	1.0	0	1
5	1.6	0	1
6	2.3	0	1
7	3.0	75	1
8	4.5	225	1
9	5.9	738	1
10	7.0	1400	1
11	8.2	2460	1
12	9.4	3525	1
13	10.6	4770	1
14	11.8	5900	1
15	12.9	6450	1
16	14.0	7000	1

The deterministic analysis was used solely in the first step of the model, to calculate the best point estimate of optimal escapement or optimal harvest rate and to obtain the equilibrium age structure for initializing each Monte Carlo trial. Uncertainty was still incorporated explicitly in the simulations because the stock–recruitment parameters for each trial were randomly drawn from a bootstrap distribution, the stock was estimated with error, and the stock–recruitment process was simulated with interannual variability.

Estimating stock abundance

For each year within a Monte Carlo trial, the estimate of the stock abundance that was vulnerable to the fishery (S_{est}) was calculated by adding a normally distributed error term to the true abundance of the vulnerable stock (S). The error term was created by multiplying S by the coefficient of variation (CV) of the estimation procedure and a normally distributed random variable (w), with a mean of 0 and a variance of 1:

$$[1] \quad S_{est} = S + (S \cdot CV \cdot w).$$

The CV was varied from 0 to 0.5 in increments of 0.1 to represent a wide range of levels of uncertainty in estimates of abundance. (The average CV for trawl surveys in the Georges Bank area of the eastern United States is approximately 0.25 (Sissenwine 1984).) CV = 0 represents the special, hypothetical case where stock abundance was measured perfectly, which allowed us to dissociate the effects of uncertainty in the stock–recruitment parameters from the effects of uncertainty in abundance estimates.

Fig. 3. Flowchart showing the main components of the model.

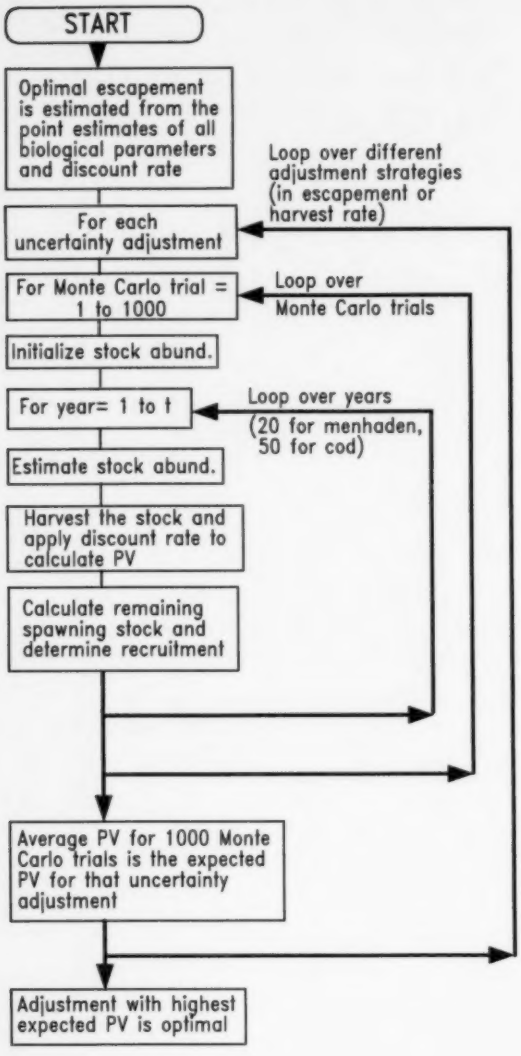
START
Optimal escapement is estimated from the point estimates of all biological parameters and discount rate
Loop over different adjustment strategies (in escapement or harvest rate)
For each uncertainty adjustment
For Monte Carlo trial = 1 to 1000
Loop over Monte Carlo trials
Initialize stock abund.
For year= 1 to t
Loop over years (20 for menhaden, 50 for cod)
Estimate stock abund.
Harvest the stock and apply discount rate to calculate PV
Calculate remaining spawning stock and determine recruitment
Average PV for 1000 Monte Carlo trials is the expected PV for that uncertainty adjustment
Adjustment with highest expected PV is optimal

Calculating the harvest

When a constant escapement policy was simulated, the stock was not harvested when S_{est} was lower than the target escapement (S_T). Otherwise, the harvest (H) was the difference between S_{est} and S_T, provided that this difference was not larger than 99% of the vulnerable stock (S):

$$[2]\quad \begin{aligned} &\text{If } S_{est} < S_T && H = 0\\ &\text{If } S_{est} - S_T \le 0.99 \cdot S && H = S_{est} - S_T\\ &\text{If } S_{est} - S_T > 0.99 \cdot S && H = 0.99 \cdot S. \end{aligned}$$

For a constant harvest rate policy, H was determined by multiplying the estimated stock abundance (S_{est}) by the target harvest rate (F_T), although H was again bounded at 99% of S:

$$[3]\quad \begin{aligned} &\text{If } F_T \cdot S_{est} \le 0.99 \cdot S && H = F_T \cdot S_{est}\\ &\text{If } F_T \cdot S_{est} > 0.99 \cdot S && H = 0.99 \cdot S. \end{aligned}$$

We bounded the harvest at 99% of the vulnerable stock for both policies because we assumed some limit to the efficiency of the fleet (that the entire vulnerable stock would not be harvested, no matter how high the allowable harvest was set). Because we modeled age-structured stocks, the numbers harvested at each age were determined on the basis of their relative abundance and catchability. We assumed equal catchability for all ages after first recruitment (see Tables 1 and 2).

Calculating spawning stock biomass

The spawning stock (S_{sp}) was represented as egg potential, which was calculated by multiplying the numbers of female fish of each age class, i, remaining after harvest (N_i) by their average fecundity at age (f_i) and then summing over all age classes:

$$[4]\quad S_{sp} = \Sigma(N_i \cdot f_i).$$

Recruitment

We modeled recruitment with the Shepherd (1982) model:

$$[5]\quad R = (aS_{sp}/[1 + (S_{sp}/k)^b])e^v$$

with the following definitions:

R is the recruitment at age 0 (in billions).

S_{sp} is the egg production (in billions).

a, k, and b are parameters estimated from nonlinear parameter estimation with $\log_e(R/S)$ as the response variable. a is the slope of the recruitment curve at the origin, k is the spawning stock level at which recruitment is reduced to half the level it would be under density-independent processes only (Shepherd 1982) (i.e., the spawning stock level at which compensatory processes reduce the recruitment to half the value that would be expected from extrapolating the slope of R/S at the origin), and b reflects the nature and intensity of compensatory processes that control the overall form or shape of the stock–recruitment relationship. When $b > 1$, the Shepherd model generates a domed stock–recruitment relationship, similar to a Ricker model. When $b = 1$, the Shepherd model is identical to a Beverton–Holt model. When $b < 1$, the Shepherd model generates a relationship where recruitment increases monotonically, without limit.

v is a normal random variable distributed $N(0,\sigma^2_{env})$ where σ^2_{env} is the variance of the residuals around the best fit curve to $\log_e(R/S)$. σ^2_{env} was reestimated for each bootstrapped data set (it averaged 0.41 for menhaden and 0.75 for cod). Because v is normally distributed, e^v is lognormally distributed, with an expectation of $\exp(\sigma^2_{env}/2)$. Thus, including environmental variability in the simulations in this manner corrected for the fact that the stock–recruitment parameters, estimated by fitting $\log_e(R/S)$, represented the geometric, rather than the arithmetic, mean of the stock–recruitment relationship.

We chose to use the Shepherd model, rather than the more common Ricker or Beverton–Holt models, because the Shepherd model allows the uncertainty in the overall shape of the stock–recruitment relationship to be directly

accounted for via the b parameter. The Ricker and Beverton–Holt models do not have this flexibility. If the basic shape of the stock–recruitment relationship is itself uncertain, assuming one of these more common models may lead to misleading measurements of uncertainty.

To incorporate uncertainty about the parameters of the Shepherd model in our analysis, we performed a simple bootstrap (randomly sampled the stock–recruitment data points, with replacement, from the original data set) to generate 1000 "new" bootstrapped data sets. For each new data set, the stock–recruitment parameters and the environmental variability term were reestimated by nonlinear parameter estimation. Each parameter set was then used as the stock–recruitment parameters for a particular Monte Carlo trial.

Simulating the different uncertainty adjustment strategies

For the constant escapement policy, the different uncertainty adjustments consisted of either increasing or decreasing the escapement from the deterministic escapement — the one calculated as optimal from the best point estimates. To simulate harvest strategies ranging from extremely conservative to extremely permissive, the adjustments were varied in 10% intervals, from increasing the deterministic escapement by 100% to decreasing it by 100% (i.e., from doubling the escapement to setting the allowable harvest to be the same as the *estimated* stock abundance, S_{est}). Note in the latter case that escapement was >0 when the true abundance of the vulnerable stock, S, was $>S_{est}$ because H was set to S_{est} and escapement = $S - H$. Adjustments that increased escapement from the deterministic level were considered conservative because allowable harvests were set lower than the level that the point estimates dictated as optimal. Conversely, adjustments that decreased escapement were considered permissive because allowable harvests were set higher.

For the constant harvest rate policy, the different uncertainty adjustments consisted of either decreasing or increasing the harvest rate from the deterministic rate — the proportion of the stock that it would be optimal to harvest if the point estimates were, in fact, the true values. For menhaden, the deterministic harvest rate was 72%, and the different uncertainty adjustments consisted of simulating different harvest rates ranging from 52 to 92% in 2% increments. Exploitation rates lower than 72% were called conservative adjustments; those higher than 72% were called permissive. For cod, the deterministic harvest rate was 15% and the different adjustments were harvest rates ranging from 5 to 25% in 1% increments. Exploitation rates lower than 15% were conservative; higher ones were permissive.

Each Monte Carlo trial was run for 20 years for menhaden and 50 years for cod. Previous explorations indicated that these periods were sufficient to generate stable results because we used the equilibrium age structures to start each run, as noted above.

Determining the optimal adjustment strategy

The expected PV for each adjustment strategy was the average PV of the 1000 trials applying that adjustment. The optimal uncertainty adjustment was the one with the largest expected PV. The EVIU was the increase in expected PV of the optimal strategy over the deterministic strategy.

Results and discussion

The expected PV for each uncertainty adjustment for each simulated stock and harvest policy is shown in Fig. 4.

Constant escapement policy

For menhaden (Fig. 4A), the deterministic escapement was optimal for the CV = 0 case, despite the considerable uncertainty in the stock–recruitment parameters. However, when uncertainty in the stock abundance estimates was included (CVs of 0.1 through 0.5), the optimal escapement became increasingly conservative (in the CV = 0.5 case, it was 80% higher than the deterministic escapement). Nevertheless, note how flat the curves in Fig. 4A are over a wide range of escapements. Thus, the expected PV was so insensitive to escapement that the optimal strategy had only a slightly higher expected PV than the deterministic strategy — ranging from a 0.4% increase in the CV = 0.1 case to a 3.2% increase for the CV = 0.5 case.

For the CV = 0 case for cod (Fig. 4B), the optimal escapement was 20% lower than the deterministic escapement. As with menhaden, the optimal escapement became more conservative as the level of uncertainty in the abundance estimates was increased, but, again, the expected PV of the deterministic strategy was nearly as high as that of the optimal adjustment strategy — within 2% in all six cases.

The decrease in performance of conservative strategies was much more marked for cod than for menhaden. Because the average stock–recruitment relationship for cod was considerably more dome shaped (the point estimate of the b parameter was 3.59 for cod, compared with 1.05 for menhaden), conservative harvest strategies not only reduced current harvests, but also often created high spawning stock abundances that reduced subsequent recruitment and, thus, future harvests. This phenomenon does not occur for stock–recruitment relationships that exhibit relatively constant or increasing recruitment with increases in stock abundance.

The performance of conservative strategies for cod was especially poor for low levels of uncertainty in the abundance estimates (low CVs). In fact, reducing the uncertainty in abundance estimates actually decreased the performance of conservative strategies (notice on the left side of Fig. 4B that performance was highest in the CV = 0.5 case, and lowest in the CV = 0 case). This counterintuitive result can easily be explained. For harvest strategies that are far too conservative or far too permissive, errors in abundance estimates may compensate for the inappropriateness of the strategy by causing the harvests to be set closer to the true optimal level. For instance, for conservative adjustments to the constant escapement policy for Arcto-Norwegian cod (Fig. 4B), high CVs in the stock estimation procedure frequently generated large overestimates of stock abundance, which increased the allowable harvests, often bringing escapements closer to the true optimal level. While the higher CVs also generated larger underestimates, the beneficial effect of the overestimates

Fig. 4. Expected present value (PV) (over 20 years for menhaden and 50 years for cod, with a 5% discount rate applied for both stocks) for each uncertainty adjustment for four different cases: (A and B) constant escapement policy for menhaden and cod; (C and D) constant harvest rate policy for menhaden and cod. "D" on the *x*-axes designates the deterministic strategy — the escapement or harvest rate that would be applied if only the point estimates were used to choose the management action. For Figs. 4A and 4B, the *x*-axis represents the amount of adjustment in the escapement goal from the deterministic strategy whereas for Figs. 4C and 4D, the *x*-axis is the constant harvest rate applied. In each graph, the six curves represent results for coefficients of variation (CV) in

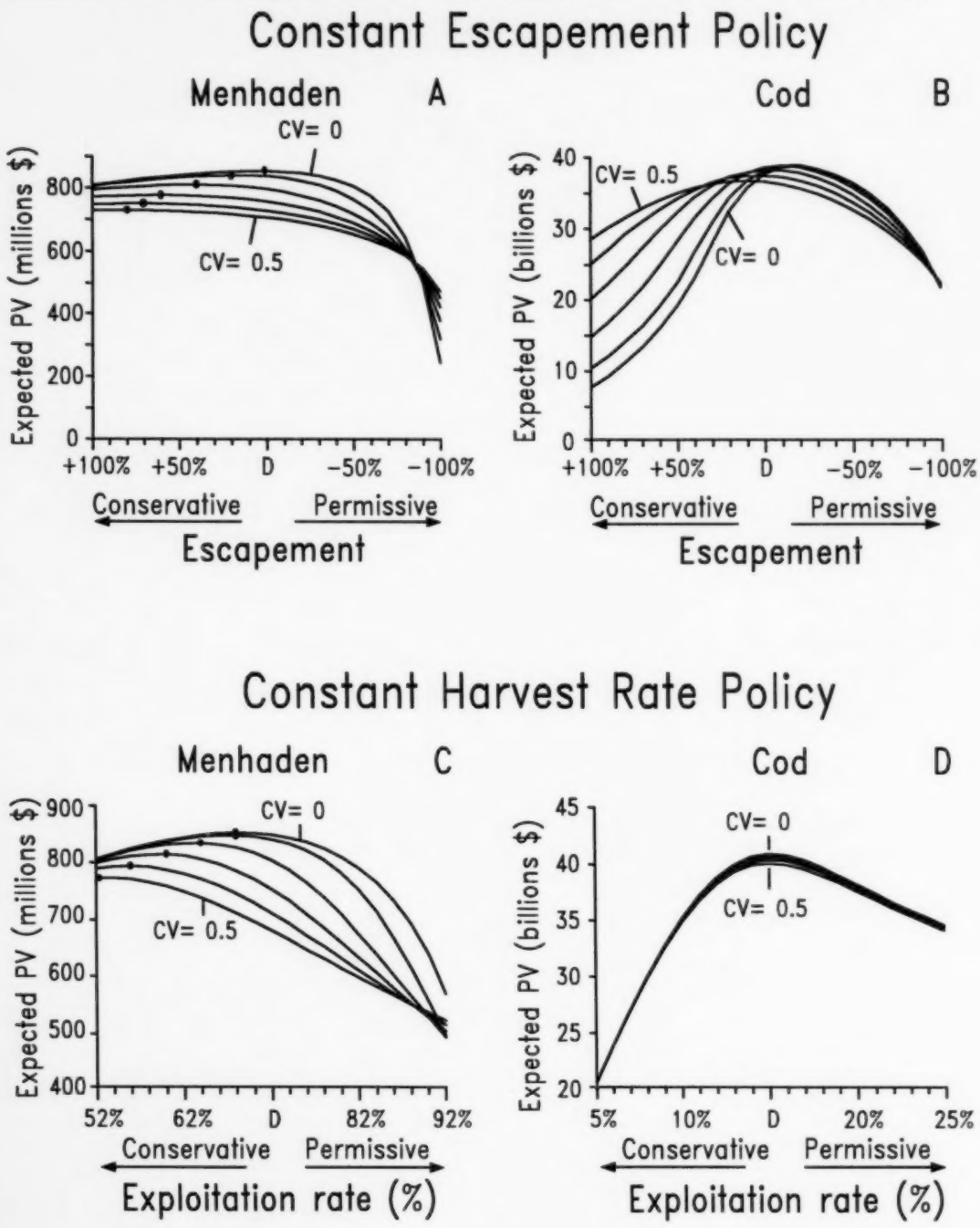

the stock abundance estimation procedure ranging from 0 to 0.5. The optimal uncertainty adjustment for a given CV of the stock estimation procedure is the one that maximizes expected PV. The respective optima for each case of CV are shown explicitly in Figs. 4A and 4C as solid dots on the curves.

was not cancelled because underestimates did not affect the resulting management action as often. That is, whenever the abundance estimate was below the target escapement, the allowable harvest was set to zero — no matter how large the underestimate.

The same phenomenon operated in reverse for menhaden. Notice on the right side of Fig. 4A that more accurate stock measurement (lower CVs) reduced the performance of extremely permissive adjustment policies. In this example, the benefits of the larger underestimates of stock abundance from the high CV cases outweighed the costs of the larger overestimates because the maximum possible harvest was bounded at 99% of the stock, regardless of how severely the stock was overestimated.

Thus, the value of improving abundance estimates depends on the context in which those estimates will be used. Reducing uncertainty in the abundance estimate is clearly beneficial when the adjustment strategy for escapement is approximately optimal (i.e., near the adjustment that generates the highest PV). The exact value of a given reduction in uncertainty can be assessed directly, by measuring the increase in performance as the CV is reduced (compare the maximum PVs of each of the CV curves in Fig. 4). However, as the adjustment strategy becomes increasingly suboptimal, the value of reducing uncertainty in the abundance estimates not only decreases, but may even become negative.

Constant harvest rate policy

The results above were for the constant escapement policy; results for a constant harvest rate policy differed. For the CV = 0 case, the optimal harvest rate for menhaden (Fig. 4C) was 68% — 4% lower than the deterministic rate of 72%. The optimal harvest rate became even more conservative as uncertainty in the stock estimates was increased; it was only 52% in the high uncertainty case (CV = 0.5). Although the increase in expected PV of the optimal adjustment strategy over the deterministic strategy was still modest, it was larger than for the constant escapement policy (for the CV = 0.5 case, the performance of the optimal adjustment strategy was 13.5% higher than the deterministic strategy).

For cod (Fig. 4D), the optimal harvest rate coincided with the deterministic rate for all levels of uncertainty in the stock estimates. More surprisingly, the expected PV was almost independent of the level of uncertainty in the stock estimates (the six curves in Fig. 4D nearly overlap one another). At the optimal harvest rate, the expected PV was only 2% higher in the CV = 0 case than in the CV = 0.5 case. This difference was much smaller than for the other three cases of Fig. 4, where the expected PV of the optimal harvest policy for the CV = 0 case was 5.7, 10.2, and 17.2% higher than it was for the CV = 0.5 case (see Figs. 4B, 4C, and 4A, respectively). In other words, in the particular case of cod managed with a constant harvest rate policy, not only was the value of including uncertainty (EVIU) negligibly small, but the value of reducing uncertainty (some fraction of the EVPI) was also very small.

This surprising result may be because we simulated cod recruiting to the fishery at age 4, although the optimal age at first entry was about 7. When the age at first capture is less than that which is required to produce maximum yield, periodic or "pulse-fishing" strategies will usually outperform strategies that aim at taking a constant harvest (see Walters 1969; Clark 1976; Botsford 1981; DeKlerk and Gatto 1981). In these cases, greater uncertainty in the abundance estimates creates more variable harvests from year to year, which may more closely simulate a pulse-fishing policy. The benefit of this system behavior may partially offset the costs of greater uncertainty, and may explain why, in this case, reducing uncertainty in the abundance estimates did not substantially improve performance.

Sensitivity analyses

Discount rate

For the analyses described above, the PV was calculated using a discount rate of 5%. We repeated these analyses using discount rates of zero and 10%, but the general conclusions were not altered. Neither the deterministic harvest level nor the optimal uncertainty adjustments were appreciably changed (the deterministic harvest level was slightly lower for a discount rate of zero, and slightly higher for a discount rate of 10%). Therefore, we would agree with Mendelssohn (1982) that for many fish stocks, the optimal harvest strategy is insensitive to the discount rate applied to future harvests. However, this generalization will not be valid for extremely unproductive stocks, whose intrinsic rates of growth are similar to, or below, the proposed discount rate (see Clark 1973), or for active–adaptive polices, since the value of future information will strongly depend on how heavily the future is discounted (Walters 1981). In those cases, the optimal strategy can be dramatically affected by the discount rate applied to future harvests.

Performance measure

To this point, we have measured the performance of alternative harvest policies solely in terms of the expected PV of the catches, but there are other measures of success. Reducing the between-year variability of harvests or the incidence of very low harvests are often important additional considerations. To address these issues, we recorded the percentage of annual harvests (over the 1000 trials) that fell below some minimum value (H_{min}), defined as 10% of the deterministic, equilibrium harvest.

The main results of this analysis are shown in Fig. 5. For a constant escapement policy (Figs. 5A and 5B), the incidence of low harvests was very high, especially for high CVs in the abundance estimates. Conservative adjustments did not reduce this high frequency because they created such a high target escapement that the allowable harvest

Fig. 5. Similar to Fig. 4, except the performance criterion is the percentage of time that the harvests fell below H_{min} (defined as 10% of the deterministic equilibrium harvest).

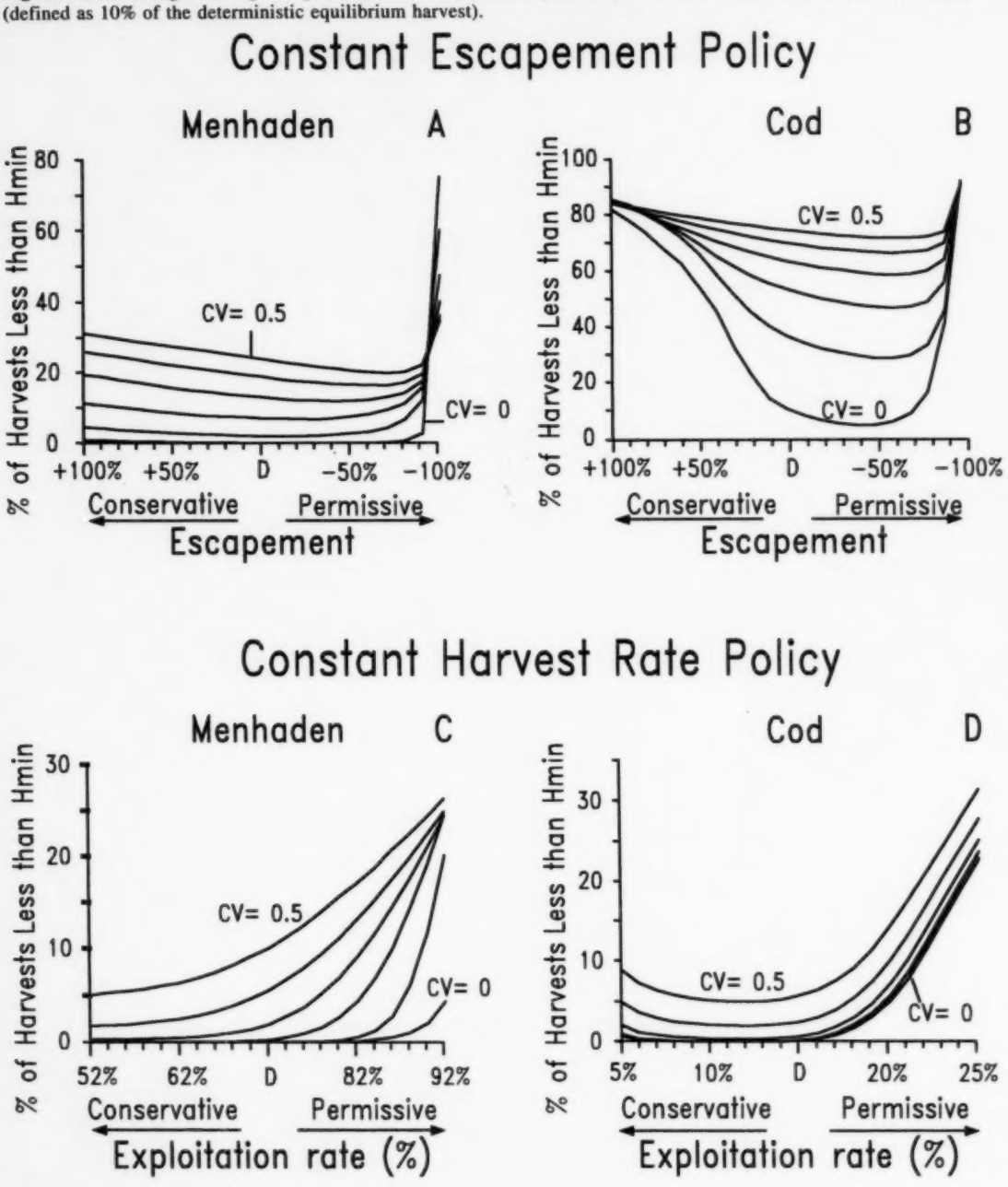

often had to be set below H_{min} just to account for natural stock fluctuations. Conversely, permissive adjustments resulted in such low target escapements that the stock was often driven below H_{min} by overharvests.

A constant harvest rate policy greatly reduced the incidence of low harvests because some harvests were always allowed, no matter how much the stock fluctuated (notice the difference in scale on the *y*-axes in Fig. 5). For the CV = 0.5 case of the deterministic strategy, switching from a constant escapement to a constant harvest rate policy reduced the incidence of low harvests from 24 to 10% for menhaden (Figs. 5A and 5C) and from 75% to 6% for cod (Figs. 5B and 5D). Furthermore, conservative adjustments drastically reduced the incidence of very low harvests

when a constant harvest rate policy was used (Figs. 5C and 5D).

Comparison of constant escapement and constant harvest rate policies

Many have discussed the apparent conflict between a constant escapement policy (usually characterized by a high average harvest but also a high interannual variability in harvests) and a constant harvest rate policy (usually associated with lower average harvests but also lower harvest variability) (e.g., Ricker 1958; Allen 1973; Gatto and Rinaldi 1976; Hall et al. 1988; Quinn et al. 1990). Although this is an accurate characterization of the two policies for stocks that are optimally managed with perfect information, it does not necessarily apply where there is observation error in stock abundance, or in the cases where pulse-fishing can improve yield. In such situations, a constant harvest rate policy may not only have a lower harvest variability than the constant escapement policy, but it may also have a higher expected discounted yield, depending on the type of fish life history and the deviation from the deterministic strategy (e.g., Fig. 6).

Broader comparisons of the harvest policies can be done by contrasting, through Fig. 4, the results of applying the *optimal escapement strategy* for a given CV case with the results of applying the *optimal harvest rate strategy* for that same CV. In this context, the optimal constant harvest rate policy for cod had a slightly higher expected yield than the optimal constant escapement policy for all cases of CV. Perhaps this is because the stock was allowed to vary more under the constant harvest rate policy, which may produce superior yields when pulse-fishing is optimal. For menhaden, the optimal constant harvest rate policy resulted in a higher expected yield in all cases where observation error was included (CV = 0.1 through CV = 0.5 cases).

When the stock abundance is observed with error, setting the allowable harvests as a constant proportion of the estimated abundance may be less likely to lead to a severe overharvest than a constant escapement policy, which sets the allowable harvest as the difference between the abundance estimate and the estimated optimal escapement. For example, consider a stock whose true, but unknown, abundance is 1000, whose optimal escapement is 500 (assume this is known), and whose harvest rate is set at 50%. If this stock is estimated at 1500, then strictly following the constant escapement = 500 policy would dictate an allowable harvest of 1000, which would, theoretically, harvest the stock to extinction. The allowable harvest dictated by the constant harvest rate = 50% policy, however, would only be 750, substantially reducing the severity of the overharvest.

Of course, when the stock estimate is reasonably accurate, the constant escapement policy is more consistent with the objective of maximizing expected yield because it protects the stock completely when it is below the optimal escapement and fully exploits it when it exceeds the optimal escapement. On average, however, our results suggest that substantial observation error may make the constant harvest rate policy superior to the constant escapement policy in terms of maximizing expected yield. This may be yet another reason to favor a constant harvest rate policy, in addition to its lower harvest variability noted by the authors above, its superior performance for risk averse performance criteria (Deriso 1985; Hilborn 1985; Walters and Ludwig 1987), and its superiority for mixed-stock fisheries whose component stocks exhibit uncorrelated (or

Fig. 6. Expected present value (PV) of the constant escapement policy (broken line) and the constant harvest rate policy (solid line) for menhaden and cod. The top *x*-axis scale of each graph corresponds to the constant harvest rate policy whereas the bottom *x*-axis scale corresponds to the constant escapement policy. An intermediate level of uncertainty in the abundance estimates (CV = 0.3) was used for these comparisons.

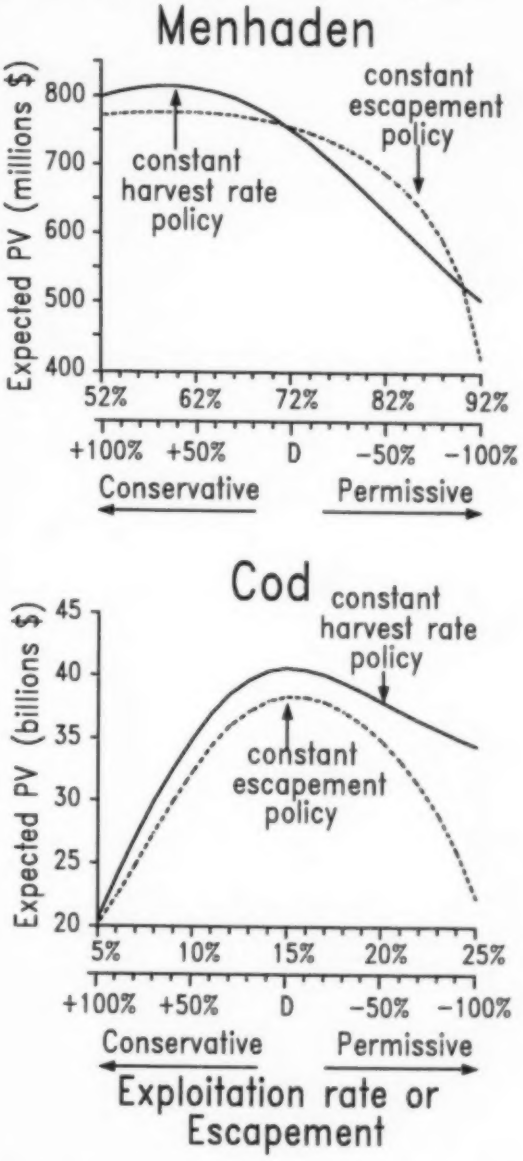

Fig. 7. Results of the "threshold" and "no-threshold" cases for menhaden for constant escapement and constant harvest rate policies. The *x*-axes are as defined in Fig. 4. Solid dots designate the expected present value (PV) for the optimal strategy for each case. Open circles designate the expected PV if the optimal strategy *for the wrong case* was applied (see text for explanation). Plus signs on the curves show the expected PV for the deterministic strategy. These comparisons were for a medium level of uncertainty in the abundance estimates (CV = 0.3).

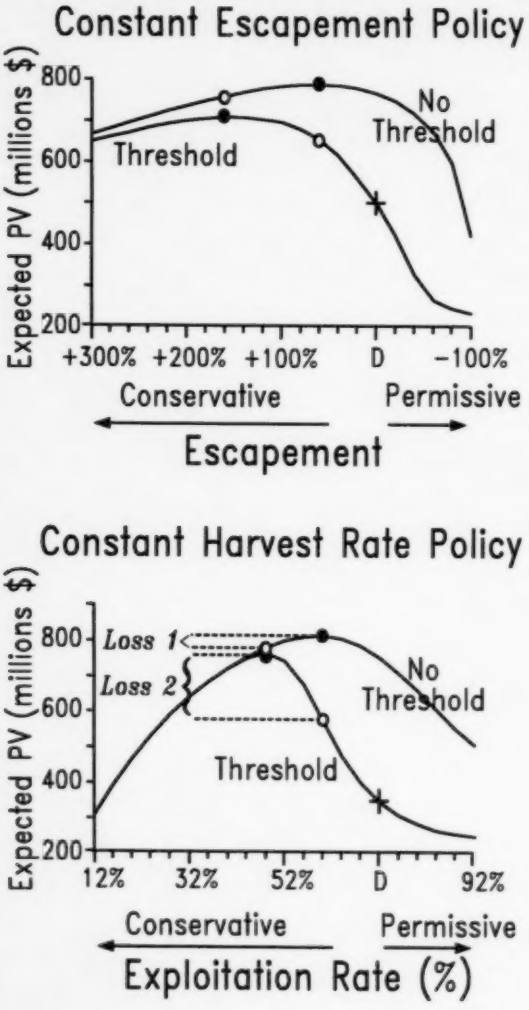

only slightly correlated) natural variability in recruitment (Hilborn 1985).

Autocorrelated observation errors and residuals in recruitment

As a simplification, our initial model assumed that estimation errors were independent from year to year and that there was no autocorrelation structure in the residuals of recruitment from the underlying stock–recruitment curve. We later modified the model to incorporate positive autocorrelation in estimation errors (as would result from an estimation technique such as virtual population analysis) and in recruitment variability, since stocks often show a pattern of many successive years of good recruitment, followed by several successive years of poor recruitment (Walters 1990). Neither of these modifications substantially altered the main results (Frederick 1993).

Biological "thresholds"

Because the baseline simulations assumed that some age classes were invulnerable to harvest and that only 99% of the vulnerable stock could be harvested, the probability of extinction of the simulated stock was virtually zero. However, a stock may not have to be harvested to zero for permanent commercial extinction to occur. A biological "threshold" may exist — a nonzero stock abundance below which biological processes either drive the stock to extinction, maintain it near an unproductive lower equilibrium, or substantially delay its recovery. Although there is little direct evidence for such thresholds, some mechanisms are known that could cause them, including the "Allee effect" (difficulty of finding mates at low abundance) (Allee 1931), certain forms of interspecific competition (Gilpin and Case 1976), and depensatory predation mortality (Gulland 1977; Peterman 1977). Furthermore, some stocks have not recovered from overfishing or have taken longer than expected to do so, despite reduction or elimination of fishing pressure (Paulik 1971; Clark 1974), which suggests the operation of one or more of these phenomena.

To represent a biological threshold, we modeled a situation where the recruitment dropped to zero whenever the spawning stock fell below some arbitrarily low level (which we defined as 5% of the unfished equilibrium spawning stock). The stock could fall below the critical threshold because of overharvests, many successive years of very poor recruitment, or some combination of these two factors. The stock did not necessarily go extinct once it fell below the threshold. The maturation of the immature cohorts sometimes provided enough additional spawning stock to bring the total spawning stock back above the threshold level and allow recovery. If not, the stock became extinct.

For cod, the optimal uncertainty adjustment for this threshold case was the same as for the nonthreshold case because the probability of stock extinction was extremely low, given that four age classes were invulnerable to the fishery. Thus, for cod, even following an extreme overharvest where 99% of the *vulnerable* stock was removed, there was still a high probability that the next four cohorts would, collectively, be large enough for the stock to recover.

For menhaden, however, only two age classes were invulnerable to the fishery, creating a much higher probability of stock extinction and making the effect of the simulated threshold very significant (Fig. 7). For the threshold case, the optimal adjustment strategy (leftmost solid dots in Fig. 7) was quite conservative for both the constant escapement and constant harvest rate policies; it dramatically increased the expected value compared with the deterministic strategy (indicated as "+" in Fig. 7). There was a 41% increase for the constant escapement policy, from $501 million to $708 million, and a 129% increase for

the constant harvest rate policy from $334 million to $765 million.

Therefore, for some stocks, the possibility of a biological threshold may dictate large, conservative safety factors or uncertainty adjustments. In such cases, conservative adjustments may increase *expected* PV of yields even if the probability that a threshold exists is fairly low because the cost of acting as if a threshold *does* exist when it actually *does not* is much lower than the cost of acting as if it *does not* exist when it actually *does*. To illustrate this, notice in the bottom panel of Fig. 7 that the expected PV is reduced by only $36 million (from $815 million to $779 million — Loss 1) if the optimal harvest rate for the threshold case (48%) is applied when no threshold exists whereas it is reduced by $186 million (from $765 million to $579 million — Loss 2) if the "no-threshold" optimal harvest rate (60%) is applied when a threshold actually exists.

In decision theoretic terms, these results indicate that the presence of a threshold may create such a highly asymmetric loss function (large differences in the costs between overharvesting and underharvesting) that extremely conservative uncertainty adjustments are appropriate. We emphasize that uncertainty adjustments should be justified on the basis of such asymmetries — the mere presence of uncertainty and the demonstration that estimation errors lead to losses in value are typically *not* sufficient justifications for acting conservatively, contrary to what Clark (1985, p. 241) implied. Thus, those who have advocated acting conservatively in the face of uncertainty (e.g., Kirkwood 1981; Kimura 1988; Thompson 1992) presuppose an asymmetric loss function for harvests or an asymmetric probability distribution of an uncertain quantity, although these issues are rarely addressed explicitly.

Our results presented in previous sections indicate that asymmetries may frequently exist and that they can be large in certain cases. However, they also suggest that in many situations, the loss function will be fairly symmetric, in which case a deterministic strategy will perform almost as well as the optimal adjustment strategy.

Two major exceptions to this apparent adequacy of the deterministic strategy are when declines in stock abundance resulting from overharvest are irreversible (when some critical, nonzero abundance threshold exists) or when the policy is nonfeedback, such that there is little opportunity to change the allowable harvests between years. Most managed fisheries have some feedback mechanism because the status of the stock is estimated annually (Kirkwood 1981). Therefore, the appropriateness of a deterministic harvest strategy may often rest on the likelihood and particular characteristics of possible nonzero thresholds or multiple stable states. While there is little direct evidence for such biological thresholds, there is strong indirect evidence that the component processes that can create them are common (e.g., nonlinear functional and numerical responses of predators (including humans) or density-dependent competitive interactions among species). Therefore, it is reasonable for managers to use conservative harvest adjustments to hedge against this possibility, but the justification for such an approach should rest on the asymmetric nature of the loss function or an asymmetric probability distribution and not simply on the presence of uncertainty.

Some of our results for the performance of the deterministic strategy might seem to contradict the message to be drawn from the many stock declines that have resulted from overfishing. But such collapses were not generally the result of adhering to a deterministic strategy in the face of uncertainty. Rather, they were the result of failing to keep harvests below levels even approximating those that the fishery models (deterministic or otherwise) specified as optimal. If anything, focusing excessively on uncertainty in these situations diminished the extent to which apparent stock declines motivated actions to control harvests (e.g., Saetersdal 1980).

Risk aversion

By using expected value as the primary criterion to compare the performance of alternative strategies, we have assumed a "risk-neutral" decision stance. That is, we have assumed that the strategy with the highest expected PV of harvests is preferable (has the highest utility), regardless of the particular distribution of harvests among years. For a "risk averse" manager, however, utility does not increase linearly with harvest, so maximizing expected PV may not be the appropriate performance criterion. A fisheries manager who is risk averse may often prefer a management policy with more stable harvests, even if that policy reduces the long-term average harvests.

Therefore, in some circumstances it may be better to use a risk averse performance criterion, such as the sum of the natural logarithm of harvests, rather than the sum of harvests (see Mendelssohn 1982; Deriso 1985; Ruppert et al. 1985; Walters and Ludwig 1987). We should clarify here that we use the term risk aversion in its strictest sense — to refer to a concave utility function, where the value placed on an additional unit of harvest decreases with increasing harvest. Confusion can result if the term is loosely used to mean "a strong desire to avoid bad outcomes." For example, a constant harvest rate policy is typically viewed as more risk averse than a constant escapement policy because it avoids the low or zero harvests that a constant escapement policy would often dictate. However, if risk aversion is used to imply "a strong desire to avoid a *biologically* disastrous outcome," a constant harvest rate policy may be *less* risk averse than a constant escapement policy because it may provide less protection to the stock when it is at dangerously low levels. Therefore, when using terms like risk aversion, it is important to be clear about exactly what one is "risk averse" to.

When we repeated our analyses using the natural logarithm of harvests as the performance criterion, the constant harvest rate policy outperformed the constant escapement policy more than previously indicated because it more frequently avoided the very low harvests that this performance criterion heavily penalizes. The optimal adjustment was virtually unchanged for the constant harvest rate policy, but was shifted to be more permissive for the constant escapement policy because avoiding zero harvests became so critical.

Asymmetric probability distributions

Until now we have implied that the symmetry of the loss function is the fundamental attribute determining how

much the harvests calculated from the best point estimates of stock abundance and stock–recruitment parameters should be adjusted to account for the uncertainty in these estimates. We have suggested that highly asymmetric loss functions dictate large adjustments to the deterministic strategy, that relatively symmetric loss functions dictate smaller ones, and that perfectly symmetric loss functions dictate no adjustment at all. However, if the uncertainty in the optimal harvest level (H^*) is best described by an asymmetric probability distribution, the optimal strategy may deviate from the deterministic strategy, even if the loss function describing the costs of underharvests and overharvests is perfectly symmetric.

Thus, any assumptions made about the probability distribution describing the uncertainty in H^* (and, thus, in the deviation of H from H^*) should be carefully scrutinized. Because H^* depends on the true stock abundance and the true stock–recruitment parameters, its probability distribution depends on shapes of the constituent distributions describing the uncertainty in these quantities. We made no direct assumption about the shape of the multivariate distribution of the recruitment parameters, because that was generated nonparametrically via bootstrapping. Moreover, whatever the shape of this distribution, it entered directly into the Monte Carlo simulations, so any asymmetry was accounted for. However, possible asymmetry in the distribution of errors in abundance estimates was not accounted for, since we assumed that they were normally distributed. If this assumption is strongly violated in practice, then the conclusions we drew would have to be reevaluated. However, some partial sensitivity analyses suggested that our conclusions were robust to moderate departures from this assumption.

Conclusions

Explicit representations of uncertainty, such as probability distributions, contain more information than point estimates, such as the mean. In some situations, formally including this additional information in policy analyses can reveal harvest strategies whose expected performance is much better than a deterministic strategy, which ignores uncertainty. However, uncertainty by itself is not typically a sufficient condition to warrant a departure from the deterministic strategy unless it can also be shown that the costs of overharvest and underharvest are asymmetric or that the probability density function for an uncertain component is asymmetric. The degree of asymmetry in costs will depend on the biological parameters of the stock's population dynamics and on the criteria by which performance is measured. Although it is likely that some degree of asymmetry will always be present, our results suggest that such loss functions are not always highly asymmetric, since the deterministic strategy frequently performed well, even under high levels of uncertainty.

The situation where the deterministic strategy is most likely to perform poorly is when a biological threshold exists, such that large overharvests could lead to an irreversible stock decline. In this situation, overharvests can be much more costly than underharvests, which creates a highly asymmetric loss function and, correspondingly, dictates a large conservative uncertainty adjustment.

Therefore, our results demonstrate that uncertainty "adjustments" can improve management performance under certain circumstances, but also indicate that there are no general rules for determining the appropriate adjustment in a particular situation. Our methodology does, however, provide a rational basis for determining the best approach for each situation, which may prevent uncertainty from being improperly used to justify overly permissive or overly conservative harvest policies.

Acknowledgments

We thank Milo Adkison, Jon Brodziak, Paul Fischbeck, Michael LaPointe, Ernie Love, Murdoch McAllister, Andre Punt, Brian Pyper, Daniel Read, Virginia Soehl, Thomas Soehl, Lisa Thompson, Carl Walters, and an anonymous reviewer for comments received on earlier drafts. We also thank Reo Audette and Richard Lockhart for providing statistical advice and Jack Knetsch and Michael Link for many stimulating discussions. This research was funded by Graduate Fellowships and a Special Graduate Entrance Scholarship to Shane Frederick from Simon Fraser University, by a Department of Fisheries and Oceans Subvention Grant to R.M. Peterman, and by an Operating Grant to R.M. Peterman from the Natural Sciences and Engineering Research Council of Canada.

References

Ahrenholtz, D.W., Nelson, W.R., and Epperly, S.P. 1987. Population and fishery characteristics of Atlantic menhaden (*Brevoortia tyrannus*). Fish. Bull. **85**: 569–600.

Allee, W.C. 1931. Animal aggregations: a study in general sociology. University of Chicago Press. Chicago, Ill.

Allen, K.R. 1973. The influence of random fluctuations in the stock–recruitment relationship on the economic return from salmon fisheries. Rapp. P.-v. Réun. Cons. int. Explor. Mer, **164**: 350–359.

Bergh, M.O., and Butterworth, D.S. 1987. Towards rational harvesting of the South African anchovy considering survey imprecision and recruitment variability. S. Afr. J. Mar. Sci. **5**: 937–951.

Botsford, L.W. 1981. Optimal fishery policy for size-specific, density-dependent population models. J. Math. Biol. **12**: 265–293.

Brown, B.E., and Patil, G.P. 1986. Risk analysis in the Georges Bank haddock fishery — a pragmatic example of dealing with uncertainty. N. Am. J. Fish. Manage. **6**: 183–191.

Clark, C.W. 1973. The economics of overexploitation. Science (Wash., D.C.), **181**: 630–634.

Clark, C.W. 1974. Possible effects of schooling on the dynamics of exploited fish populations. J. Cons. int. Explor. Mer, **36**: 7–14.

Clark, C.W. 1976. Mathematical bioeconomics: the optimal management of renewable resources. John Wiley, New York, N.Y.

Clark, C.W. 1985. Bioeconomic modelling and fisheries management. John Wiley, New York, N.Y.

Cushing, D.H. 1966. The arctic cod: a study of research into the British trawl fisheries. Pergamon Press Ltd., Oxford.

DeKlerk, P.D., and Gatto, M. 1981. Some remarks on periodic harvesting of a fish population. Math. Biosci. **56**: 47–69.

Deriso, R.B. 1985. Risk averse harvesting strategies. *In* Resource Management, Proceedings of the Second Ralf Yorque Workshop. *Edited by* M. Mangel. Lecture notes in biomathematics No. 61. Springer-Verlag, Berlin. pp. 65–73.

Francis, R.I.C.C. 1992. Use of risk analysis to assess fishery management strategies: a case study using orange roughy (*Hoplostethus atlanticus*) on the Chatham Rise, New Zealand. Can. J. Fish. Aquat. Sci. **49**: 922–930.

Frederick, S.W. 1993. Determining optimal fisheries harvest policies: how much does uncertainty matter? Master's thesis, School of Resource and Environmental Management, Simon Fraser University, Burnaby, B.C.

Garrod, D.J. 1967. Population dynamics of the Arcto-Norwegian cod. J. Fish. Res. Board Can. **24**: 145–190.

Gatto, M., and Rinaldi, S. 1976. Mean value and variability of fish catches in fluctuating environments. J. Fish. Res. Board Can. **33**: 189–193.

Gilpin, M.E., and Case, T.J. 1976. Multiple domains of attraction in competition communities. Nature (Lond.), **261**: 40–42.

Gulland, J.A. 1977. The stability of fish stocks. J. Cons. int. Explor. Mer, **37**: 199–204.

Gulland, J.A. 1983. Fish stock assessment: a manual of basic methods. Wiley, New York, N.Y.

Hall, D.L., Hilborn, R., Stocker, M., and Walters, C.J. 1988. Alternative harvest strategies for Pacific herring (*Clupea harengus pallasi*). Can. J. Fish. Aquat. Sci. **45**: 888–897.

Hilborn, R.B. 1985. A comparison of harvest policies for mixed stock fisheries. *In* Resource Management, Proceedings of the Second Ralf Yorque Workshop. *Edited by* M. Mangel. Lecture notes in biomathematics No. 61. Springer-Verlag, Berlin. pp. 75–87.

Hilborn, R., and Walters, C.J. 1992. Quantitative fisheries stock assessment: choice, dynamics, and uncertainty. Routledge, Chapman & Hall, Inc., New York, N.Y.

Jones, J.M. 1977. Introduction to decision theory. Richard D. Irwin, Inc., Homewood, Ill.

Kimura, D.K. 1988. Stock–recruitment curves as used in the stock-reduction analysis model. J. Cons. int. Explor. Mer, **44**: 253–258.

Kirkwood, G.P. 1981. Allowing for risks in setting catch limits based on MSY. Math. Biosci. **53**: 119–129.

Linder, E., Patil, G.P., and Vaughan, D.S. 1987. Application of event tree risk analysis to fisheries management. Ecol. Model. **36**: 15–28.

Lovejoy, W.S. 1988. Effect of stochasticity on optimal harvesting strategies in some lumped-parameter fishery models. Can. J. Fish. Aquat. Sci. **45**: 1789–1800.

Ludwig, D., and Hilborn, R. 1983. Adaptive probing strategies for age-structured fish stocks. Can. J. Fish. Aquat. Sci. **40**: 559–569.

Ludwig, D., and Varah, J. 1979. Optimal harvesting of a randomly fluctuating resource. 2. Numerical methods and results. J. Soc. Ind. Appl. Math. **47**: 185–205.

Ludwig, D., and Walters, C.J. 1982. Optimal harvesting with imprecise parameter estimates. Ecol. Model. **14**: 273–292.

Mangel, M., and Clark, C.W. 1983. Uncertainty, search and information in fisheries. J. Cons. int. Explor. Mer, **41**: 93–103.

Mendelssohn, R. 1982. Discount factors and risk aversion in managing random fish populations. Can. J. Fish. Aquat. Sci. **39**: 1252–1257.

Morgan, M.G., and Henrion, M. 1990. Uncertainty: a guide to dealing with uncertainty in quantitative risk and policy analysis. Cambridge University Press, Cambridge.

Parma, A.M., and Deriso, R.B. 1990. Experimental harvesting of cyclic stocks in the face of alternative recruitment hypotheses. Can. J. Fish. Aquat. Sci. **47**: 595–610.

Paulik, G.J. 1971. Anchovies, birds, and fishermen in the Peru current. *In* W.W. Murdoch. Environment: resources, pollution and society. *Edited by* Sinauer Associates, Inc., Sunderland, Mass. pp. 35–79.

Peterman, R.M. 1977. A simple mechanism that causes collapsing stability regions in exploited salmonid populations. J. Fish. Res. Board Can. **34**: 1130–1142.

Peterson, S., and Smith, L.J. 1981. Risk reduction in fisheries management. Ocean Manage. **8**: 65–79.

Quinn, T.J. II, Fagen, R., and Zheng, J. 1990. Threshold management policies for exploited populations. Can. J. Fish. Aquat. Sci. **47**: 2016–2029.

Raiffa, H. 1968. Decision analysis: introductory lectures on choices under uncertainty. Addison-Wesley, Reading, Mass.

Reed, W.J. 1978. The steady state of a stochastic harvesting model. Math. Biosci. **41**: 273–307.

Ricker, W.E. 1958. Maximum sustained yields from fluctuating environments and mixed stocks. J. Fish. Res. Board Can. **15**: 991–1006.

Ruppert, D., Reish, R.L., Deriso, R.B., and Carroll, R.J. 1985. A stochastic population model for managing the Atlantic menhaden (*Brevoortia tyrannus*) fishery and assessing managerial risks. Can. J. Fish. Aquat. Sci. **42**: 1371–1379.

Saetersdal, G. 1980. A review of past management of some pelagic fish stocks and its effectiveness. Rapp. P.-v. Réun. Cons. int. Explor. Mer, **177**: 505–512.

Sainsbury, K.J. 1991. Application of an experimental approach to management of a tropical multispecies fishery with highly uncertain dynamics. ICES Mar. Sci. Symp. **193**: 301–320.

Schopka, S.A., and Hempel, G. 1973. The spawning potential of populations of herring (*Clupea harengus* L.) and cod (*Gadus morhua* L.) in relation to the rate of exploitation. Rapp. P.-v. Réun. Cons. int. Explor. Mer, **164**: 178–185.

Shepherd, J.G. 1982. A versatile new stock–recruitment relationship for fisheries, and the construction of sustainable yield curves. J. Cons. int. Explor. Mer, **40**: 67–75.

Silvert, W. 1978. The price of knowledge: fisheries management as a research tool. J. Fish. Res. Board Can. **35**: 208–212.

Sissenwine, M.P. 1984. The uncertain environment of

fishery scientists and managers. Mar. Res. Econ. **1**: 1–30.

Smith, A.D.M., and Walters, C.J. 1981. Adaptive management of stock–recruitment systems. Can. J. Fish. Aquat. Sci. **38**: 690–703.

Thompson, G.G. 1992. A Bayesian approach to management advice when stock–recruitment parameters are uncertain. Fish. Bull. **90**: 561–573.

Tyler, A.V. 1988. Biological basis for management of groundfish resources of the west coast of Canada. *In* Fishery science and management: objectives and limitations. *Edited by* W.S. Wooster. Springer-Verlag, Berlin. pp. 217–232.

Walters, C.J. 1969. A generalized computer simulation model for fish population studies. Trans. Am. Fish. Soc. **98**: 505–512.

Walters, C.J. 1975. Optimal harvest strategies for salmon in relation to environmental variability and uncertain production parameters. J. Fish. Res. Board Can. **32**: 1777–1784.

Walters, C.J. 1981. Optimum escapements in the face of alternative recruitment hypotheses. Can. J. Fish. Aquat. Sci. **38**: 678–689.

Walters, C.J. 1986. Adaptive management of renewable resources. Macmillan, New York, N.Y.

Walters, C.J. 1990. A partial bias correction factor for stock–recruitment parameter estimation in the presence of autocorrelated environmental effects. Can. J. Fish. Aquat. Sci. **47**: 516–519.

Walters, C.J., and Hilborn, R. 1976. Adaptive control of fishing systems. J. Fish. Res. Board Can. **33**: 145–159.

Walters, C.J., and Ludwig, D. 1987. Adaptive management of harvest rates in the presence of a risk averse utility function. Nat. Resour. Model. **1**(2): 321–337.

Appendix A

H^* is the true, but unknown, optimal harvest level.

H_D is the best point estimate of H^*, as determined from the point estimates of stock abundance and the stock–recruitment parameters (hence called the deterministic harvest).

H is the allowable harvest level that is set by the management agency.

$L(H,H^*)$ is the opportunity loss for a particular harvest H, given the true optimal harvest, H^* (i.e., the opportunity loss corresponding to a particular deviation).

$f(H^*)$ is the probability distribution describing the uncertainty in H^*. (Note that the probability distribution describing the uncertainty in the magnitude of the deviation of H from H^* (as shown for H_D in Figs. 2B and 3B) is simply the probability distribution of the difference between H and H^*, $f(H - H^*)$.)

$\mathrm{EOL}[H,f(H^*)]$ is the expected opportunity loss (EOL) for a given harvest level, H, and a given level of uncertainty in H^*. It is calculated by multiplying the opportunity loss corresponding to a particular deviation, $L(H,H^*)$, by the probability of that deviation, $f(H - H^*)$, integrated over all possible deviations $H - H^*$:

$$\mathrm{EOL}[H,f(H^*)] = \int L(H,H^*) \cdot f(H - H^*)\, dH^*.$$

The harvest level that minimizes expected opportunity loss is the "Bayes equivalent" harvest (H_B):

$$\mathrm{EOL}[H_B,f(H^*)] = \min\,[\mathrm{EOL}(H,f(H^*)].$$

The optimal uncertainty adjustment = $H_B - H_D$.

The expected value of perfect informative (EVPI) is the expected opportunity loss at H_B:

$$\mathrm{EVPI} = \mathrm{EOL}[H_B,f(H^*)].$$

The expected value of including uncertainty (EVIU) is the difference between the expected opportunity loss at H_D and the expected opportunity loss at H_B:

$$\mathrm{EVIU} = \mathrm{EOL}[H_D,f(H^*)] - \mathrm{EOL}[H_B,f(H^*)].$$

Genetic and environmental correlates of variation in body weight of brook trout (*Salvelinus fontinalis*)

Moira M. Ferguson, Arunas P. Liskauskas, and Roy G. Danzmann

Abstract: Families of brook trout (*Salvelinus fontinalis*) were produced from adults collected from Mykiss Lake, Algonquin Provincial Park, Ontario, and reared in the laboratory for 1 year. Egg size and hatching time explained a significant amount of variation among families in mean weight of hatched embryos. Heavier embryos were produced from larger eggs, and embryos with earlier hatching times were also larger. First-feeding alevins reared at higher densities were smaller than those at lower densities. Multilocus enzyme heterozygosity was neither a significant predictor of mean family body weight at any age nor significantly associated with body weight of juveniles within families. Analyzing each enzyme locus separately revealed significant effects for *G3PDH-1* in two families but in different directions. Fish from two mitochondrial DNA phylogenetic assemblages, A and B, differed significantly in weight as hatched embryos and first-feeding alevins. Similarly, the progeny of different males and females differed significantly in body weight at all ages sampled. Thus, parental effects were the most persistent correlates of body size of all those examined. The statistical analyses and the nested designs suggest that variation in body weight among the progeny of specific parents can partially be attributed to genetic effects.

Résumé : Nous avons produit des familles d'omble de fontaine (*Salvelinus fontinalis*) à partir d'adultes prélevés dans le lac Mykiss, dans le Parc provincial Algonquin (Ontario), et élevés en laboratoire pendant 1 an. La taille des oeufs et la durée d'incubation expliquaient une partie importante de la variation du poids moyen des embryons éclos entre les familles. Les embryons les plus lourds provenaient des oeufs les plus gros, et les embryons qui éclosaient plus tôt étaient aussi plus gros. Les alevins en début d'alimentation qui étaient élevés à de fortes densités étaient plus petits que ceux élevés à des densités plus faibles. L'hétérozygosité des enzymes sur plusieurs locus n'était pas un prédicteur significatif du poids corporel moyen d'une famille à un âge donné, et n'était pas non plus associée de façon significative avec le poids corporel des juvéniles au sein des familles. L'analyse séparée de chaque locus enzymatique a révélé des effets significatifs pour *G3PDH-1* dans deux familles, mais dans des directions différentes. Les poissons appartenant à deux assemblages phylogénétiques différents sur le plan de l'ADN mitochondrial, A et B, différaient de façon notable sur le plan du poids au stade d'embryons éclos et d'alevins en début d'alimentation. De même, la progéniture des divers mâles et femelles présentait des différences significatives dans le poids corporel à tous les âges échantillonnés. Ainsi, les effets parentaux étaient les plus persistants parmi tous les corrélats de la taille corporelle examinés. Les analyses statistiques et les plans emboîtés semblent indiquer que la variation du poids corporel parmi la progéniture de parents spécifiques peut être attribuée en partie à des effets génétiques.

[Traduit par la Rédaction]

Introduction

An understanding of evolutionary processes requires knowledge of the proximate and ultimate control of traits related to fitness. In many organisms, including fishes, body size is one such trait because it is correlated with survival (Adelman et al. 1955; Bagenal 1969; Marsh 1986; Ferguson and Drahushchuk 1990; Hutchings 1991; Liskauskas and Ferguson 1991). In natural populations of many salmonid species, the importance of body size may relate to early social behaviour. Intraspecific behavioural interactions are characterized by size-dependent dominance hierarchies (Cole and Noakes 1980; Abbott et al. 1985; Ferguson and Danzmann 1985; Grant 1990). Large dominant fish possibly limit the food consumption of smaller subordinates (Metcalfe 1989), thereby reducing the probability of survival. However, the relationship between body size and fitness is not a simple positive one in salmonid fishes because of variability in life-history styles (Noakes et al. 1989; Skulason et al. 1990).

Received August 26, 1993. Accepted July 21, 1994.
J12065

M.M. Ferguson, A.P. Liskauskas,[1] and R.G. Danzmann. Department of Zoology, University of Guelph, Guelph, ON N1G 2W1, Canada.

[1] Present address: Lake Huron Management Unit, Ontario Ministry of Natural Resources, 611 Ninth Avenue East, Owen Sound, ON N4K 3E4, Canada.

The body size of young salmonid fishes is the result of complex interaction among various genetic and environmental factors. Significant amounts of additive genetic variation in growth rate have been detected (e.g., Robinson and Leumpert 1984; McKay et al. 1986). Associations between heterozygosity at enzyme coding loci and body size have also been detected when sexual maturation is not a confounding factor (Liskauskas and Ferguson 1991; Ferguson 1992). However, female egg size and offspring development rate are also significant. For example, maternal egg size is often positively correlated with the size of offspring at hatching and the onset of exogenous feeding (e.g., Beacham and Murray 1990; Skulason 1990; Wood and Foote 1990; Hutchings 1991) but not necessarily in older fish (Thorpe et al. 1984). Similarly, faster development time can be associated with larger body size (Allendorf et al. 1983; Ferguson et al. 1988). Despite the acknowledged significance of all these factors, few studies have addressed their relative importance within a single controlled experiment.

We examined the association between maternal egg size, offspring development time, heterozygosity at enzyme coding loci, as well as parental background and the body weight of brook trout (*Salvelinus fontinalis*) families reared in a controlled laboratory environment for 1 year. We also determined whether families produced by females from different mitochondrial DNA (mtDNA) haplotype assemblages differed in body size. We tested for such an association because mtDNA is a sensitive indicator of female genetic history (Billington and Hebert 1991) due to its maternal transmission (Moritz et al. 1987). mtDNA has the potential to mark maternally controlled traits due to associations with nuclear maternal loci that are clonally inherited (Solter 1988). Offspring from different mtDNA matriarchal lineages might differ in body size if maternal genetic effects are determinants of body size. Family groups were produced from mature fish collected from a naturalized population in Mykiss Lake, Algonquin Provincial Park, Ontario. This population was chosen because body size is of adaptive significance in these fish (Liskauskas and Ferguson 1990, 1991).

Materials and methods

Experimental matings

Twenty female and 18 male sexually mature brook trout (2–4 years old) were collected from Mykiss Lake (45°41N, 78°14W), Algonquin Provincial Park, Ontario (see Liskauskas and Ferguson 1990, 1991 for details). Eggs and sperm were removed from each fish by abdominal compression, placed in dry plastic containers, and transported to the University of Guelph packed on wet ice. Subsamples of gametes from single males and females were combined on October 31, 1988, to produce 30 full- and half-sib families (Table 1). The families were reared in the common environment of a vertical incubating rack at 6°C. Each was thinned to approximately 100–150 embryos once they had developed eye pigment for determination of hatching time (see below). Excess embryos were placed in other sections of the same incubating rack. After hatching (101 days from fertilization), each family (embryos from the hatching experiment as well as the excess, total average density = 288, range = 125–546) was placed into a 30-L tank. Each family was thinned to approximately 125 first-feeding alevins at 121 days (range = 122–125) and further thinned to 40 older alevins at 257 days. All families were housed in a single room on commercial trout food (fish fed four to eight times throughout the day depending on age) and under natural photoperiod for approximately 1 year. The common water supply to all tanks varied between 6 and 12°C depending on the season. Unfortunately, it was not possible to rear each family in more than one tank. Even though extreme care was taken to minimize environmental variation among tanks, density did vary (especially before first-feeding) and was therefore considered in the statistical analyses described below.

Egg size

We used the data on female egg diameter previously reported by Liskauskas and Ferguson (1990), as the same adult females were used in the present experiment. There, a subsample of 20 unfertilized eggs from each female was water hardened, preserved in 10% buffered formalin, stored for 2 months, and measured (nearest 0.1 mm) on the largest axis with vernier callipers.

Development time

Hatching time was used as a measure of development time. The embryos were monitored every 24 h over a 15-day hatching period (beginning at 68 days from fertilization); hatched embryos were removed, counted, and placed in an adjacent section of the incubating tray. Mean hatching time for each family was based on an average of 117 embryos (range = 74–158).

Body size

Ten fish from each family were collected (age from fertilization in parentheses, developmental terminology follows Balon 1980) just after hatching (99–100 days, designated hatched embryos), as 121-day first-feeding alevins (alevins have started to feed exogenously but have not developed scales), and as older alevins (182 days) and killed with an overdose of 2-phenoxyethanol. They were preserved in 10% buffered formalin until they were weighed (wet weight, nearest 0.1 mg) and measured (fork length, nearest 0.1 mm). At the termination of the experiment (378 days), all remaining juveniles (an individual who has developed scales but has not yet developed gametes) from each family were killed and 10 from each were weighed and measured; no fish matured during the study. These, and all others, were stored at −80°C until analyzed for variation at enzyme coding loci (see below). Fish were denied food for 24 h before each collection.

Enzyme coding loci

Twenty-five juveniles from each family (if available) were thawed, weighed, and analyzed for polymorphism at 11 loci. The brook trout parents used in the present experiment had detectable polymorphism at *AAT-1,2*, *CK-2*, *G3PDH-1*, *GPI-1*, *IDHP-3*, *LDH-3*, *LDH-4*, *MDH-B1,2*, *MEP-1*, *PGM-1*, and *6PGD* based on a survey of 44 enzyme coding loci with horizontal starch gel electrophoresis (Liskauskas and Ferguson 1990, 1991). Six hundred and eighty-six progeny were screened for protein variation at those loci known

Table 1. Association (Pearson product-moment correlation, *r*) between multilocus heterozygosity and body weight (g) within families of brook trout reared in the laboratory for 1 year. The identity and age (in parentheses) of the male and female parents as well as which families were used in various statistical analyses are also given.

	Parent						Used in analysis[a]			
Family	♀	♂	*N*	Het	Wt	*r*	A	B	C	D
B102	11 (2)	134 (4)	26	1.53	17.19	0.146				
B103	30 (3)	129 (2)	25	0.80	16.42	0.066	×			
B104	1 (4)	133 (3)	24	2.25	17.20	−0.074				
B105	28 (3)	136 (3)	25	1.52	18.74	0.512	×	×		
B106	27 (3)	126 (3)	24	0.63	17.95	0.007				
B107	22 (3)	130 (2)	25	2.16	22.46	−0.309	×	×		
B108	31 (3)	128 (4)	22	1.00	20.83	−0.033				
B109	13 (3)	127 (2)	24	0.46	16.20	0.125	×	×		
B111	3 (3)	116 (3)	25	2.04	19.57	0.062		×		
B112	6 (3)	131 (2)	26	1.19	21.91	0.250	×			
B114	24 (4)	109 (3)	23	1.70	20.26	0.026				
B118	16 (3)	114 (4)	25	2.04	15.16	−0.044			×	×
B119	23 (3)	121 (4)	23	0.00	19.34	—		×	×	×
B120	18 (3)	118 (3)	24	0.58	17.17	0.344	×		×	
B123	30 (3)	134 (4)	24	1.58	13.93	0.152	×		×	×
B125	28 (3)	133 (3)	25	0.00	18.08	—	×		×	×
B126	27 (3)	136 (3)	25	2.16	18.22	−0.067		×	×	×
B127	22 (3)	126 (3)	16	3.31	9.13	−0.522	×		×	×
B128	31 (3)	130 (2)	25	2.00	17.44	—		×	×	×
B129	13 (3)	128 (4)	25	2.04	20.72	0.075	×		×	×
B130	14 (3)	127 (2)	22	0.00	16.64	—		×	×	×
B132	6 (3)	116 (3)	25	1.60	18.85	0.369	×	×	×	×
B133	17 (3)	131 (2)	25	2.20	19.60	0.037			×	×
B134	24 (4)	132 (2)	23	3.26	19.16	−0.014				
B135	26 (3)	109 (3)	22	2.63	24.10	−0.062			×	×
B136	29 (3)	102 (3)	25	0.00	16.10	—			×	×
B137	19 (3)	111 (2)	15	0.60	10.37	0.063			×	×
B138	16 (3)	105 (3)	13	1.31	8.58	0.088				
B140	18 (3)	121 (4)	24	0.33	18.08	−0.271	×	×		
B141	5 (3)	118 (3)	11	1.73	10.55	0.377				×

[a]Analyses: A = nested ANOVA (female, male{female}); B = nested ANOVA (male, female{male}); C = multiple regression of mean family heterozygosity, hatching time, egg size, and rearing density on mean family body weight; D = nested ANOVA (mtDNA assemblage, family {mtDNA assemblage}).

to be polymorphic based on the combination of genotypes in the parents. Multilocus heterozygosity was calculated from the number of heterozygous loci per fish. Individuals with more than one allele at each of the duplicated loci (*MDH-B1,2*, and *AAT-1,2*) were considered heterozygotes at a single duplicated locus. This was necessary because it is difficult to assign variant alleles to one particular locus.

mtDNA

mtDNA was isolated from the livers of excess juveniles from the rearing experiment according to the protocol of Chapman and Powers (1984). The livers from several fish within a family were combined to obtain adequate amounts of tissue and mtDNA for a large number of restriction digests. This is valid because full-sibs will all have the haplotype of their mother. Partially purified mtDNA was digested with 58 restriction endonucleases (Danzmann et al. 1991). The mtDNA fragments were separated on 0.8% agarose (Boehringer Mannheim) gels and visualized by UV irradiation after ethidium bromide staining. Restriction fragment length polymorphisms were detected with *Asn* I, *Ban* II, *Hind* III, *Nco* I, *Nde* I, *Nhe* I, *Nsi* I, and *Pst* I. Five haplotypes (designated 1, 7, 8, 9, and 10 by Bernatchez and Danzmann 1993) were detected and haplotypes showing less than 0.1% sequence divergence were grouped together resulting in two major mtDNA phylogenetic assemblages (haplotypes 9 and 10 = assemblage A; haplotypes 1, 7, and 8 = assemblage B) that differ on average by approximately 0.3–0.4% site divergence (Nei and Tajima 1983).

Statistics

Within families

The association between the number of heterozygous loci per fish (multilocus heterozygosity) and juvenile body weight within each of the 25 families with detectable polymorphism

was tested with the Pearson product-moment correlation coefficient (r). Here and below, probability values were adjusted to minimize Type I error and take into account the number of simultaneous tests (Cooper 1968). The analysis of multilocus heterozygosity, as such, assumes that the effects of individual loci are equal and additive. The sexes were combined because they did not differ significantly for any measure as determined by separate factorial ANOVAs (family, sex, family × sex as sources of variation). This also applies to all statistical tests involving juvenile body weight described below. Multiple regression was used to determine whether individual loci contributed significantly to the heterozygosity – body weight associations by determining the significance and direction of the partial regression coefficient. Here, each locus was considered an independent variable and body weight the dependent variable. Heterozygotes at a particular locus were assigned a value of 1 and homozygotes a value of 0. This second approach allows the effects of individual loci to be unequal and nonadditive (Bush et al. 1987; Diehl 1988; Koehn et al. 1988).

Among families

All among-family analyses were based on those families produced from 3-year-old females to remove effects attributable to female age (Table 1). Four females were either 2 or 4 years old (fish aged as described by Liskauskas and Ferguson 1990). Even though the male parents of these families varied in age, male age had no detectable effect on body weight of progeny sampled at any age. One-way ANOVAs of male age (independent variable) and mean family body weight at any age (dependent variable) were not significant (all P-values >0.4).

Multiple regression was used to determine if mean family heterozygosity, female egg size, hatching time, and rearing density (independent variables) explained a significant amount of variation in mean family body weight (dependent variable) at each of the four sampling times. We recorded exact densities for each family at 100 days (after hatching) and 121 days (initiation of exogenous feeding) but not for the older alevin (182 days) and juvenile (378 days) collections. We used the closest available estimates based on exact densities at 246 and 265 days for the third and fourth collections. Although not exact, these estimates should reflect relative densities after family sizes were equalized at 121 and 257 days. The highly significant correlation between densities at 246 and 265 days suggests that the relative densities do remain similar (Pearson $r = 0.691$, $t = 3.45$, df = 13, $P = 0.004$). If the overall regression equation with all four variables included was not significant, a backward elimination procedure (Draper and Smith 1981) was incorporated until all variables in the regression equation were significant. We used a subset of 15 full-sib families produced from matings between different females and males (Table 1). The remaining 10 families produced from 3-year-old females were excluded because they had at least one parent in common with those used above. In order to maximize the number of different parents used in the analysis, a subset of 11 families must be used (B125, B126, B127, B128, B129, B130, B132, B133, B135, B136, and B137). The remaining four families can be compiled with slightly different combinations (i.e., B103 or B123; B118 or 138; B140 + B141 or B119 + B120; B118 or B138). However, analyses of variant family sets produced qualitatively the same results (data not shown); the same variables remained significant in specific analyses. We predicted that the progeny from families with greater heterozygosity, larger eggs, earlier hatching times, and lower rearing densities would be heavier.

We tested if the progeny of different males and females differed in body weight at each of the four sampling times (hatched embryo, first-feeding alevin, older alevin, juvenile) with nested ANOVAs (Table 1). Six pairs of maternal half-sib families (single female crossed with two males × 6) were used to test if males produced progeny of different sizes in a common female genetic background and egg size (ANOVA sources of variation: female, male nested within female). We excluded the four half-sib families produced by females 27 and 31 because they shared the same male parents as families produced by females 13, 22, and 28; nested ANOVA requires indepedence among families. The body size of first-feeding alevins was standardized to a density of 220 fish per tank because density was a significant predictor of body size at this age (details given below). The following formula was used:

$$\text{ABW} = (220 \text{ fish/density})^{b} \times \text{BW}$$

where ABW is adjusted body weight, density is the number of fish in a particular family, b is the slope from the regression of density on body size, and BW is observed body weight in grams (Koehn and Shumway 1982).

Five pairs of paternal half-sib families (single male with two females × 5) were used to test if females produced progeny of different sizes in a common male genetic background (ANOVA sources of variation: male, female nested within male). The half-sib families sired by males 118, 126, 128, and 131 were excluded from the analysis for reasons given above. The body size of first-feeding alevins was adjusted as described for the maternal half-sib families. In a similar fashion, the body size of hatched embryos was adjusted to a common egg size (mean of all females) because egg size was a significant predictor of body size at this age (details given below).

Nested ANOVAs (ANOVA sources of variation: mtDNA assemblage, family within mtDNA assemblage) were used to determine if individual fish from two mtDNA assemblages differed in mean body weight at each of the four sampling times. For reasons discussed above, this analysis was based on a subset of 15 full-sib families (five families from assemblage A and 10 families from assemblage B) produced from matings between different females and males (Table 1). This subset of families maximizes the number of families from assemblage A. Family within mtDNA assemblage was used as the error term when testing for effects of mtDNA assemblage (Sokal and Rohlf 1981). We determined if mtDNA assemblage was confounded by variation in egg size, hatching time, and rearing density in two ways. First, we determined if families from the two mtDNA assemblages differed significantly for any of these measures with two-sample t-tests. Second, each measure was used as a covariate in separate ANCOVAs of family body size means. The assumption of parallelism was met in all cases.

Fig. 1. Mean body weights and standard errors of brook trout belonging to two mtDNA assemblages and sampled as hatched embryos (99–100 days from fertilization), first-feeding alevins (121 days), older alevins (182 days), and juveniles (378 days).

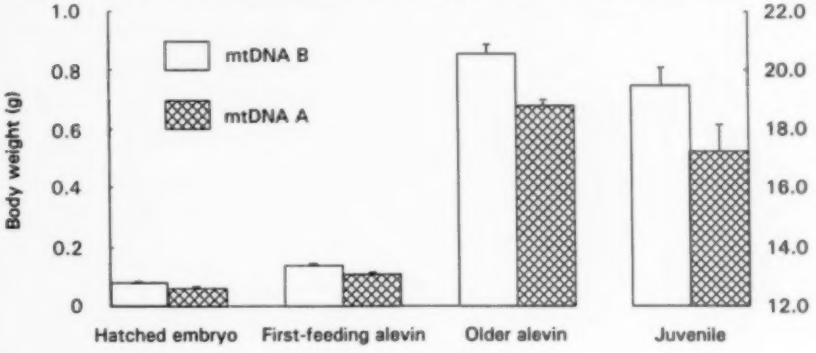

Results

The subset of 15 families produced from 3-year-old females differed in hatching time ($F[14,1689] = 56.65$, $P < 0.001$) with a mean of 10.37 days from the start at 68 days (range = 8.77–11.98). Similarly, the 15 female parents of these families produced eggs of significantly different diameters ($F[15,285] = 18.16$, $P < 0.001$) with a mean of 0.51 cm (range = 0.49–0.54). Both egg diameter and hatching time accounted for significant amounts of variation in the body weight of hatched embryos ($P_{1\text{-tail}} = 0.019$, $P_{1\text{-tail}} = 0.025$, respectively, $R^2 = 0.420$). Families produced from larger eggs and those that hatched earlier were heavier. Rearing density was a significant predictor of the body size of first-feeding alevins ($P_{1\text{-tail}} = 0.044$, $R^2 = 0.209$) but not for older alevins and juveniles; densities were more equal among families at these latter stages. The bivariate correlations (Pearson r) among mean family heterozygosity, egg size, hatching time, and rearing density were all non-significant (all P-values >0.3).

Average number of heterozygous loci per fish was not a significant predictor of mean family body weight at any age (all P-values >0.3). Furthermore, the relationship between multilocus heterozygosity and the body weight of individual juveniles within families was not significant (Table 1). Overall, 16 families showed a positive association and nine showed a negative association.

Multiple regression with individual loci indicated that the mean weights of homozygotes and heterozygotes at *G3PDH-1* differed significantly in two families; homozygotes were significantly heavier in B107 and heterozygotes heavier in B105. All other loci did not account for significant amounts of variation in body size of juveniles.

The progeny of different males crossed to common females (male nested within female) differed ($P < 0.001$) in body weight at all ages (hatched embryos: $F[6,108] = 14.76$; first-feeding alevins: $F[6,108] = 19.32$, controlled for rearing density; older alevins: $F[6,108] = 5.33$; juveniles: $F[6,108] = 7.13$). Similarly, different females crossed to common males (female nested within male) produced progeny of different sizes (hatched embryos: $F[5,90] = 72.17$, $P < 0.001$, controlled for egg size; first-feeding alevins: $F[5,90] = 17.61$, $P < 0.001$, controlled for rearing density; older alevins: $F[5,90] = 6.08$, $P < 0.001$; juveniles: $F[5,90] = 3.52$, $P = 0.006$). The relative magnitude of the F-values in both sets of analyses indicates that the parental effects are stronger in younger fish. Analysis of body length gave equivalent results for these and all other analyses (data not shown).

Families from the two mtDNA assemblages differed in body weight as hatched embryos ($F[1,13] = 7.75$, $P = 0.015$) and first-feeding alevins ($F[1,13] = 6.42$, $P = 0.025$), marginally so as older alevins ($F[1,13] = 4.00$, $P = 0.067$), and not as juveniles ($F[1,13] = 0.84$, $P = 0.377$) (Fig. 1). Families with assemblage B haplotypes were significantly heavier than those with assemblage A haplotypes. Female (family) effects were detected in all cases ($P < 0.001$). Families from the two mtDNA assemblages did not differ in egg size, rearing density, and hatching time at any age (all P-values >0.4). Furthermore, the body lengths of the females (data from Liskauskas and Ferguson 1990) used to produce the families in the two mtDNA assemblages did not differ significantly ($P > 0.8$). ANCOVAs of family means with either rearing density, egg size, or hatching time as covariates of body size indicated that families from the two mtDNA assemblages still differed in body size as hatched embryos (rearing density: $F[1,12] = 6.77$, $P = 0.023$; egg size: $F[1,12] = 8.97$, $P = 0.011$; hatching time: $F[1,12] = 4.94$, $P = 0.046$) and first-feeding alevins (rearing density: $F[1,12] = 5.57$, $P = 0.036$; egg size: $F[1,12] = 6.46$, $P = 0.026$; hatching time: $F[1,12] = 4.88$, $P = 0.047$).

Discussion

Parental effects were the most persistent correlates of progeny body size of all those examined because they were detectable throughout the entire year of the experiment. Several lines of evidence suggest that variation in body weight among the progeny of specific parents can partially be attributed to genetic effects. First, we detected significant effects of males mated to common females in the nested design. Here, egg size and female genetic component were controlled for and therefore, differences in progeny body sizes are most likely attributable to genetic differences

among males. Adjustment of body size controlling for density in first-feeding alevins still resulted in significant differences. Second, the progeny of females mated to common males differed in body size even when egg size and rearing density were controlled for statistically when necessary. Third, the rearing environments of the different families throughout the year of the experiment (identical tanks, similar ration, common water supply, and same photoperiod) were controlled, suggesting that some of the variation among families is genetic.

Maternal egg size was associated with the body weight of hatched embryos. Families produced from larger eggs were heavier. The importance of egg size on the size of young salmonid fishes at the onset of exogenous feeding is well established (Fowler 1972; Thorpe et al. 1984; Wood and Foote 1990; Hutchings 1991). However, Skulason (1990) observed effects in older fish among four morphs of Arctic char (*Salvelinus alpinus*) reared in captivity and attributed this to the relatively low water temperatures of the experiment. Smaller morphs produced smaller eggs which in turn resulted in smaller progeny at the onset of exogenous feeding. Even though the effects of egg size are relatively short term in most species, variation in progeny body size at first feeding can have long-lasting effects on the fitness of mothers and offspring alike. For example, Hutchings (1991) observed that survival of brook trout throughout the first 50 days of exogenous feeding was linearly related to egg size. Decreased food abundance significantly increased the mortality among offspring produced from the smallest eggs but had a negligible effect on those from the largest eggs. Furthermore, variable size at first feeding can have long-lasting effects on the size of young salmonid fishes (Allendorf et al. 1983; Elliott 1984).

Earlier hatching families were larger than later hatching families shortly after hatching. The association between hatching time and body size observed here, as well as work with rainbow trout (*Oncorhynchus mykiss*) (Allendorf et al. 1983; Ferguson et al. 1985; Danzmann et al. 1989), suggests that hatching time provides important information on the relative timing of developmental events. No such associations would have been detectable if hatching time was not a valid measure of developmental rate as has been suggested (Balon 1980). However, the use of hatching time as a landmark of the developmental process is probably invalid when applied to interspecific comparisons because the degree of morphological differentiation at hatching varies among species.

We observed that hatched embryos and first-feeding alevins from mtDNA assemblage B were significantly larger than those from assemblage A. These differences are biologically meaningful because they remain when egg size, rearing density, and hatching are controlled for statistically. The differences in body size between families belonging to different mtDNA haplotype assemblages do not indicate that nucleotide variation in the mtDNA molecule has a direct causal effect on the phenotype. It is unlikely that the mtDNA molecule controls body size directly because of the limited number and function of its genetic elements (Moritz et al. 1987). Furthermore, studies that have controlled for confounding nuclear effects have not detected direct effects of mtDNA genotypes on fitness in rainbow trout (Forbes and Allendorf 1991). mtDNA variation may be associated with body size because of historical associations with nuclear loci with direct effects. For example, if females share particular chromosomal regions which affect body size because of common ancestry, they might also be expected to have more mtDNA haplotypes in common than they would with more distantly related females with different sets of nuclear genes affecting growth. We have used a similar argument to explain the mtDNA variation among female rainbow trout spawning in different seasons (Ferguson et al. 1993).

Multilocus enzyme heterozygosity was not a correlate of body size of young brook trout within or among families. This stands in contrast with the significant positive association detected in young-of-the-year fish collected from Mykiss Lake just after they had started to feed exogenously (Liskauskas and Ferguson 1991). A first explanation for the apparent disparity relates to differences among studies in the breeding structure of the brook trout examined and the implications of this to the likelihood of detecting associations between multilocus heterozygosity and fitness traits. Unlike the analysis of families presented here, the wild fish examined by Liskauskas and Ferguson (1991) were probably the progeny of many males and females, as individuals were captured after young had dispersed from redd sites. Data on Mykiss Lake suggest that the single breeding population is moderate (180–200 spawning adults; Dr. Mark Ridgway, Harkness Fisheries Laboratory, OMNR, personal communication). The dependency of a detectable association between multilocus heterozygosity and body weight on breeding structure is consistent with the hypothesis that the enzyme loci are not responsible for phenotypic attributes studied (i.e., associative overdominance) (Zouros and Foltz 1987). Associative overdominance predicts that the enzyme polymorphism – fitness association is greater in progeny groups produced from large numbers of parents rather than families because the association between the scored enzyme loci and those controlling the traits measured is greater (Zouros and Foltz 1987). Under the direct involvement of the enzyme loci, the relationship between specific genotypes and relative fitness should be consistent among progeny groups (among families, pooled gamete versus families) due to the consistent metabolic roles of the gene products. Ferguson (1992) also observed that full-sibs do not show the positive associations between multilocus and single-locus heterozygosity and body size detectable in larger pooled gamete matings.

The lack of a consistent association between multilocus heterozygosity and juvenile body weight within families of Mykiss Lake brook trout may also be a function of sampling age. Previous work with rainbow trout indicates that the positive associations detectable in 6-month-old fish are absent at 1 year, the age at which the juveniles in the present study were sampled (Ferguson 1992). Declines in growth in conjunction with precocious sexual maturation of more heterozygous rainbow trout males were suggested as responsible for the lack of any association. One testable prediction from this hypothesis that can be applied to the current study is that the correlation between multilocus heterozygosity and body weight should be higher

in female progeny than in male progeny, as observed in rainbow trout (Ferguson 1992). However, there is no support for this hypothesis, as females showed a higher correlation coefficient in 14 of 25 families. Thus, differences in breeding structure between the fish examined here and those by Liskauskas and Ferguson (1991) remain the best explanation.

Genetic variation at *G3PDH-1* was associated with the body weight of juvenile brook trout in two families of Mykiss Lake brook trout. However, the differences in the relative size of homozygotes and heterozygotes among families support the hypothesis of associative overdominance in that this locus is marking a chromosomal segment with effects on body size in this population of brook trout. The suggestion that *G3PDH-1* is a marker of a chromosomal region with effects on body size is further supported in the previous analysis of the parental fishes used to produce the families studied here. Females heterozygous at *G3PDH-1* were significantly larger than homozygotes; the reverse relationship was observed in males (Liskauskas and Ferguson 1991). The localization of important chromosomal regions with effects on body size can only be accomplished with the characterization of nuclear DNA markers and the saturation of the salmonid linkage map.

Acknowledgements

We thank Dr. Leon Carl, Jim Fraser, and Greg Betteridge of the Harkness Laboratory for Fisheries Research, Algonquin Provincial Park, Ontario, for the logistical and technical support of our field work. Technical assistance was provided by Lenore Drahushchuk, Stephen Gile, and Malcolm Warner. This research was supported by funds from NSERC and Renewable Resources Research grants from the Ontario Ministry of Natural Resources. This paper benefitted greatly from the suggestions of anonymous reviewers.

References

Abbott, J.C., Dunbrack, R.L., and Orr, C.D. 1985. The interaction between size and experience in dominance relationships of juvenile steelhead trout (*Salmo gairdneri*). Behaviour, **108**: 104–113.

Adelman, H.M., Bingham, J.L., and Maatch, J.L. 1955. The effect of starvation upon brook trout of three sizes. Prog. Fish-Cult. **17**: 110–112.

Allendorf, F.W., Knudson, K.L., and Leary, R.F. 1983. Adaptive significance of differences in the tissue-specific expression of a phosphoglucomutase gene in rainbow trout. Proc. Natl. Acad. Sci. U.S.A. **80**: 1397–1400.

Bagenal, T.B. 1969. Relationship between egg size and fry survival in brown trout (*Salmo trutta* L.). Fish Biol. **1**: 349–353.

Balon, E.K. 1980. Early ontogeny of the lake charr, *Salvelinus (Cristivomer) namaycush*. *In* Charrs, salmonid fishes of the genus *Salvelinus*. *Edited by* E.K. Balon. Dr. W. Junk bv Publishers, The Hague, The Netherlands. pp. 485–562.

Beacham, T.D., and Murray, C.B. 1990. Temperature, egg size, and development of embryos and alevins of five species of Pacific salmon: a comparative analysis. Trans. Am. Fish. Soc. **119**: 927–945.

Bernatchez, L., and Danzmann, R.G. 1993. Congruence in control region sequence and restriction site variation in mitochondrial DNA of brook charr (*Salvelinus fontinalis*, Mitchill). Mol. Biol. Evol. **10**: 1002–1014.

Billington, N., and Hebert, P.D.N. 1991. Mitochondrial DNA diversity in fishes and its implications for introductions. Can. J. Fish. Aquat. Sci. **48**: 80–94.

Bush, R.M., Smouse, P.E., and Ledig, F.T. 1987. The fitness consequences of multiple-locus heterozygosity: the relationship between heterozygosity and growth rate in pitch pine (*Pinus rigida* Mill.) Evolution, **41**: 787–798.

Chapman, R.W., and Powers, D.A. 1984. A method for the rapid isolation of mitochondrial DNA from fishes. Tech. Rep. No. UM-SG-TS-84-05, Maryland Sea Grant Program, College Park, Md.

Cole, K.S., and Noakes, D.L.G. 1980. Development of early social behaviour of rainbow trout, *Salmo gairdneri* (Pisces, Salmonidae). Behav. Process. **6**: 97–112.

Cooper, D.W. 1968. The significance level in multiple tests made simultaneously. Heredity, **23**: 614–620.

Danzmann, R.G., Ferguson M.M., and Allendorf, F.W. 1989. Genetic variability and components of fitness in hatchery strains of rainbow trout. J. Fish Biol. **35**(A): 313–319.

Danzmann, R.G., Ihssen, P.E., and Hebert, P.D.N. 1991. Genetic discrimination of wild and hatchery populations of brook charr, *Salvelinus fontinalis* (Mitchill), in Ontario using mitochondrial DNA analysis. J. Fish Biol. **39**(A): 69–77.

Diehl, W.J. 1988. Genetics of carbohydrate metabolism and growth in *Eisenia foetida*. (Oligochaeta: Lumbricidae). Heredity, **61**: 379–387.

Draper, N.R., and Smith, H. 1981. Applied regression analysis. 2nd ed. John Wiley and Sons, Inc., New York, N.Y.

Elliott, J.M. 1984. Growth, size, biomass and production of young migratory trout *Salmo trutta* in a Lake District stream, 1966–83. J. Anim. Ecol. **53**: 979–994.

Ferguson, M.M. 1992. Enzyme heterozygosity and growth in rainbow trout: genetic and physiological explanations. Heredity, **68**: 115–122.

Ferguson, M.M., and Danzmann, R.G. 1985. Pleiotropic effects of a regulatory gene (*Pgm1-t*) on the social behaviour of juvenile rainbow trout (*Salmo gairdneri*). Can. J. Zool. **63**: 2847–2851.

Ferguson, M.M., and Drahushchuk, L.R. 1990. Disease resistance and enzyme heterozygosity in rainbow trout. Heredity, **64**: 413–417.

Ferguson, M.M., Danzmann, R.G., and Allendorf, F.W. 1985. Developmental divergence among hatchery strains of rainbow trout (*Salmo gairdneri*). I. Pure strains. Can. J. Genet. Cytol. **27**: 289–297.

Ferguson, M.M., Danzmann, R.G., and Allendorf, F.W. 1988. Adaptive significance of developmental rate in rainbow trout: an experimental test. Biol. J. Linn. Soc. **33**: 205–216.

Ferguson, M.M., Danzmann, R.G., and Arndt, S.K.A. 1993. Mitochondrial DNA and allozyme variation in

Ontario aquaculture rainbow trout spawning in different seasons. Aquaculture, **117**: 237–259.

Forbes, S.H., and Allendorf, F.W. 1991. Mitochondrial genotypes have no detectable effects on meristic traits in cutthroat trout hybrid swarms. Evolution, **45**: 1350–1359.

Fowler, L.G. 1972. Growth and mortality of fingerling chinook salmon as affected by egg size. Prog. Fish-Cult. **34**: 66–69.

Grant, J.W.A. 1990. Aggressiveness and the foraging behaviour of young-of-the-year brook charr (*Salvelinus fontinalis*). Can. J. Fish. Aquat. Sci. **47**: 915–920.

Hutchings, J.A. 1991. Fitness consequences of variation in egg size and food abundance in brook trout, *Salvelinus fontinalis*. Evolution, **45**: 1162–1168.

Koehn, R.K., and Shumway, S.R. 1982. A genetic/physiological explanation for differential growth rate among individuals of the American oyster *Crassostrea virginica* (Gmelin). Mar. Biol. Lett. **3**: 35–42.

Koehn, R.K., Diehl, W.J., and Scott, T.M. 1988. The differential contribution by individual enzymes of glycolysis and protein catabolism to the relationship between heterozygosity and growth rate in the coot clam, *Mulina lateralis*. Genetics, **118**: 121–130.

Liskauskas, A.P., and Ferguson, M.M. 1990. Enzyme heterozygosity and fecundity in a naturalized population of brook trout (*Salvelinus fontinalis*). Can. J. Fish. Aquat. Sci. **47**: 2010–2015.

Liskauskas, A.P., and M.M. Ferguson. 1991. Genetic variation and fitness: a test in a naturalized population of brook trout (*Salvelinus fontinalis*). Can. J. Fish. Aquat. Sci. **48**: 2152–2162.

Marsh, E. 1986. Effects of egg size on offspring fitness and maternal fecundity in the orangethroat darter, *Etheostoma spectabile* (Pisces: Percidae). Copeia, **1986**: 18–30.

McKay, L.R., Ihssen, P.E., and Friars, G.W. 1986. Genetic parameters of growth in rainbow trout, *Salmo gairdneri*, prior to maturation. Can. J. Genet. Cytol. **28**: 306–312.

Metcalfe, N.B. 1989. Differential response to a competitor by Atlantic salmon adopting alternative life-history strategies. Proc. R. Soc. Lond. B Biol. Sci. **236**: 21–27.

Moritz, C., Dowling, T.E., and Brown, W.M. 1987. Evolution of animal mitochondrial DNA: relevance for population biology and systematics. Annu. Rev. Ecol. Syst. **18**: 269–192.

Nei, M., and Tajima, F. 1983. Maximum likelihood estimation of the number of nucleotide substitutions from restriction sites data. Genetics, **105**: 207–217.

Noakes, D.L.G., Skulason, S., and Snorrason, S.S. 1989. Alternative life-history styles in salmonine fishes with emphasis on arctic charr, *Salvelinus alpinus*. *In* Alternative life-history styles of animals. *Edited by* M.N. Bruton. Kluwer Academic Publishers, Dordrecht, The Netherlands. pp. 329–346.

Robinson, O.W., and Leumpert, L.G. III. 1984. Genetic variation in weight and survival of brook trout (*Salvelinus fontinalis*). Aquaculture, **38**: 155–170.

Skulason, S. 1990. Variation in morphology, life history and behaviour among sympatric morphs of arctic charr: an experimental approach. Ph.D. thesis, University of Guelph, Guelph, Ont.

Skulason, S., Noakes, D.L.G., and Snorrason, S. 1990. Ontogeny of trophic morphology in four sympatric morphs of arctic charr *Salvelinus alpinus* in Thingvallavatn, Iceland. Biol. J. Linn. Soc. **38**: 281–301.

Sokal, R.R., and Rohlf, F.J. 1981. Biometry. 2nd ed. W.H. Freeman, San Francisco, Calif.

Solter, D. 1988. Differential imprinting and expression of maternal and paternal genomes. Annu. Rev. Genet. **22**: 127–146.

Thorpe, J.E., Miles, M.S., and Keay, D.S. 1984. Developmental rate, fecundity and egg size in Atlantic salmon, *Salmo salar* L. Aquaculture, **43**: 289–305.

Wood, C.C., and Foote, C.J. 1990. Genetic differences in the early development and growth of sympatric sockeye salmon and kokanee (*Oncorhynchus nerka*), and their hybrids. Can. J. Fish. Aquat. Sci. **47**: 2250–2260.

Zouros, E., and Foltz, D.W. 1987. The use of allelic isozyme variation for the study of heterosis. *In* Isozymes: current topics in biological and medical research. Vol. 13. *Edited by* M.C. Rattazi, J.G. Scandalios, and G.S. Whitt. Liss, New York, N.Y. pp. 1–59.

Trapping interactions of crabs and American lobster in laboratory tanks

R.J. Miller and J.T. Addison

Abstract: The relationship between trap catches of decapods and their abundance is not well established. Because it is difficult to manipulate density in the field, laboratory tanks were used to examine 10 hypotheses about the intra- and interspecific interactions of rock crab (*Cancer irroratus*), green crab (*Carcinus maenas*), and American lobster (*Homarus americanus*). The proportion of rock crabs captured did not differ among high, medium, and low densities, but the proportion captured was reduced at high densities for both green crabs and lobsters. Additional experiments demonstrated that large green and rock crabs in the tanks reduced the catch of small green and rock crabs and that the presence of lobsters reduced the catch of both crab species considerably. However, small rock crabs did not reduce the catch of large rock crabs, and neither green nor rock crabs reduced the catch of each other. Reductions in the catch of a target species caused by interactions in the field can perhaps be lessened by removing the catch from the trap at intervals of less than 24 h. Then the catches would be summed over 24 h for an index of abundance.

Résumé : La relation entre les captures au casier de décapodes et leur abondance n'est pas bien établie. Étant donné qu'il est difficile de faire varier la densité sur le terrain, on s'est servi d'aquariums pour examiner dix hypothèses sur les interactions intra- et interspécifiques du crabe commun (*Cancer irroratus*), du crabe vert (*Carcinus maenas*) et du homard américain (*Homarus americanus*). La proportion des crabes communs capturés ne différait pas selon que la densité était forte, moyenne ou basse, mais la proportion capturée était réduite aux hautes densités pour les crabes verts et les homards. Des expériences complémentaires ont révélé que la présence de crabes verts et de crabes communs de grande taille dans les aquariums causait une réduction des prises des mêmes crabes de petite taille, et que la présence de homards réduisait considérablement les prises des deux espèces de crabes. Toutefois, la présence de petits crabes communs ne réduisait pas les prises de gros crabes communs, et aucune des espèces de crabe ne réduisait les prises de l'autre espèce. Les réductions des prises d'une espèce cible causées par les interactions sur le terrain seraient peut-être diminuées si les animaux étaient retirés des casiers à des intervalles de moins de 24 h. En calculant le nombre total de prises sur 24 h, on obtient un indice de l'abondance.
[Traduit par la Rédaction]

Introduction

Crustacean population biologists continue to struggle with interpretation of trap catch rates because these rates may not be proportional to abundance of the target species. The physical design of traps influences their effectiveness and selectivity (Elner 1980; Krouse 1989; Miller 1990), but interactions between animals in and around traps are also important to the composition of the catch. For example, trap saturation (Bennett and Brown 1979; Krouse 1989; Miller 1990) might result in a smaller fraction of the population being captured if density is high than if it is low, large individuals of a species may be more catchable than small (e.g., Smith 1944; Ennis 1978; Williams and Hill 1982; Miller 1989), and the presence of a predatory species in a trap may affect the catch rate of the prey species (Richards et al. 1983; Addison 1995).

The purpose of this study was to measure, under uniform conditions in laboratory tanks, the degree to which some inter- and intraspecific interactions affect catch rates for three decapod species. A field sampling protocol is recommended that would reduce behavioral interactions between animals in and around traps and would thus allow less biased field estimates of abundance using traps. Catch rates of American lobster (*Homarus americanus*), rock crab (*Cancer irroratus*), and green crab (*Carcinus maenas*) were each measured at three densities. Then, by combining different sizes and species, the effects of lobsters on the catch of crabs, large crabs on the catch of small crabs, and green and rock crabs on the catch of each other were measured.

Trapping experiments conducted in the laboratory have clear advantages and disadvantages compared with experiments conducted in the field. In the laboratory the population is known exactly, and all individuals of that population

Received September 20, 1993. Accepted August 5, 1994.
J12096

R.J. Miller. Department of Fisheries and Oceans, Halifax Fisheries Research Laboratory, P.O. Box 550, Halifax, NS B3J 2S7, Canada.
J.T. Addison. Ministry of Agriculture, Fisheries and Food, Directorate of Fisheries Research, Fisheries Laboratory, Lowestoft, Suffolk NR33 OHT, U.K.

are exposed to bait odor and have time to reach the trap during the experiment. Thus, the laboratory tank simulates the area of attraction of a trap in the field, and the tank population simulates the target animals in that area. In the laboratory, experimental conditions are also easily replicated, and observations are easily made. However, animal densities are higher than in the field, the field environment cannot be mimicked, and one can never be certain that the experimental animals are behaving as they would in the field. Therefore, laboratory results require field confirmation.

General methods

All three species used in experiments were collected with baited traps. Green and rock crabs were collected in shallow water near Halifax during October 1991 using traps hauled at 20- to 60-min intervals. Crabs that were injured or died during the experiments were replaced by crabs caught in Halifax Harbor. Lobsters were obtained in October from a fish market, which had purchased them from fishers in the southern Gulf of St. Lawrence.

Crabs and lobsters were held in shallow tanks with flow-through seawater, usually at ambient temperature. This water was taken from a depth of 20 m in Halifax Harbor and filtered through sand under pressure. The ambient temperature decreased from 11 to 5.5°C during November–December when the experiments were being carried out. Because green crabs became inactive when the temperature dropped below 7°C, heated and ambient seawater were mixed in holding and experimental tanks during the green crab experiment in order to maintain the temperature at about 8°C. Holding tanks were partly covered to provide crabs and lobsters with reduced light levels. Initial mortality after collection (or purchase) and subsequent mortality during holding were low for all species. Rock crab mortality of 5–10% per week was highest. All three species were fed ad libitum once weekly, usually on mackerel or squid, but never with the bait used in experiments. At least 2 days lapsed between feeding and using crabs or lobsters in experiments.

Four experimental tanks were used simultaneously. These were of fiberglass construction 76 cm wide × 362 cm long and were filled to a depth of 38 cm (Fig. 1). They were covered with black plastic to reduce horizontal gradients in light level. Water, from the source that supplied the holding tanks, flowed into one end at the bottom through a diffuser and out the other end through a standpipe. Flow rates were maintained at 16 L/min giving a turnover of the tank volume every 1.1 h. Lobsters and crabs were assigned randomly to treatments, and treatments were assigned randomly to tanks. The latter was to avoid any bias due to differences among tanks, although preliminary experiments showed that catch rates were similar in all four tanks.

The same traps were used in all experiments. They were 50 × 36 × 23 cm high made of plastic-covered wire mesh with 3.4 × 3.4 cm openings (Fig. 1). An entrance funnel of nylon mesh was located in one end of the trap and was held open by an 8-cm-diameter steel entrance ring. The trap interior was divided by an all-mesh funnel into two equal compartments named the kitchen and parlor. For all three species used in the experiments, the smallest individuals were too large to escape through the wire mesh of the trap, and the largest individuals were small enough to pass through the entrance ring of the trap unhindered. One trap was set in each tank with the entrance downstream (Fig. 1). The diffuser on the inflow was adjusted such that a current of about 3 cm/s passed through the trap, over the bait, and past the entrance. A short distance downstream of the trap the unidirectional flow dispersed into a slower irregular pattern. Water flow was observed by injecting dye into the supply hose.

Several types and amounts of bait were tried during preliminary trials. From among these, redfish (*Sebastes* sp.) fillets were chosen because of their firm texture and because catches were as good as with any other bait. Several pieces totaling 70 g were placed in a perforated 0.5-L plastic container wired to the bottom of the parlor (Fig. 1).

For all experiments described below, data are presented as the mean proportion of a tank population captured by a trap. However, for statistical comparisons the individual data points were first transformed to logits (Snedecor and Cochran 1967) to eliminate correlations of mean and variance:

$$\log_e\left(\frac{g+1/2}{n-g+1/2}\right)$$

where n is the number of animals in a tank population and g is the number captured. Adding 1/2 to g makes it possible to transform zero catches. Treatments in an experiment were analyzed in one or more one-way ANOVA's and appropriate means of transformed data were compared using a Student–Newman–Keuls (S-N-K) test (Steel and Torrie 1960).

Lobsters

This experiment was designed to measure whether the catch of lobsters was proportional to density and whether trap saturation was observed.

Methods

Each day we ran one trial of 8, 14, and 24 lobsters and observed the number caught after 2, 4, 8, and 18 h in each of the parlor and kitchen portion of traps. These were "unfished" treatments which allowed us to check whether the proportion caught changed with increased density and whether lobsters escaped from the traps. A second trial of 24 lobsters was also included each day, but in this case all captures were removed following the 2-, 4-, and 8-h observations. This was a "fished" treatment and was expected to show a higher proportion caught than in the same-density unfished treatment. Each treatment was replicated 10 times. To test that the animals were responding to the bait, we ran on separate days two replicates of each treatment with unbaited traps. All experiments commenced at 15:00 and ran through to 09:00 the following day. During the course of this experiment, ambient seawater temperature varied between 9.5 and 11.0°C. The three unfished and one fished treatments were all included in a one-way ANOVA.

Fig. 1. (A) Top view of a tank used in the experiments; (B) side view of a wire trap used in the experiments.

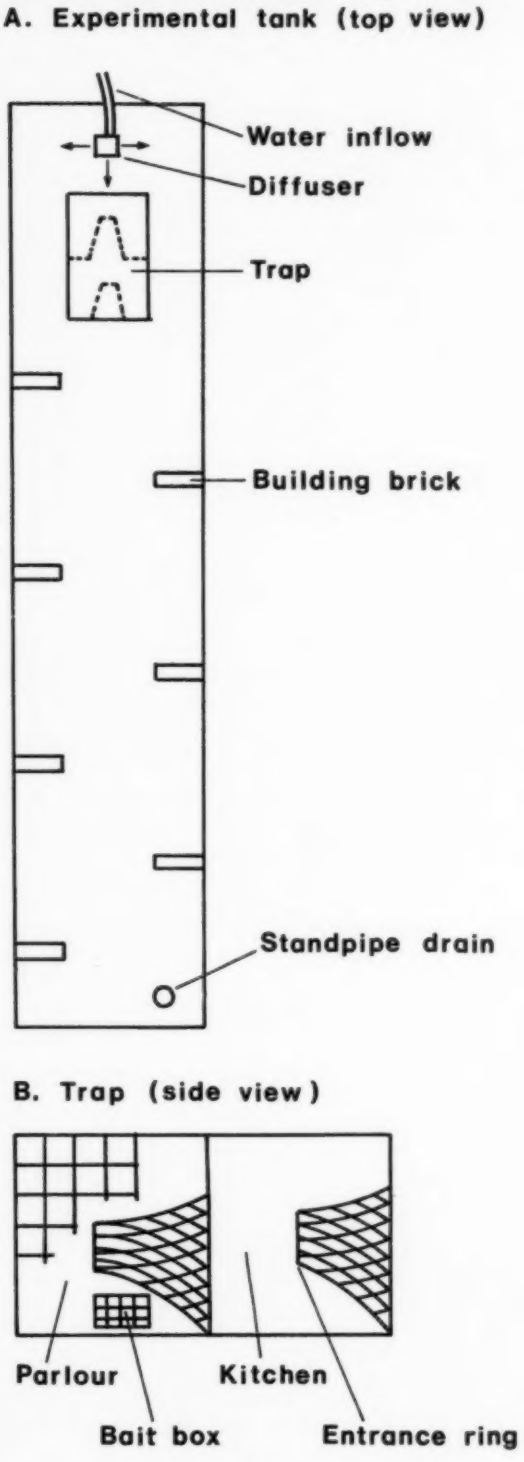

Fig. 2. Proportion of lobsters caught at three densities (mean ± SE of the mean) after 18 h.

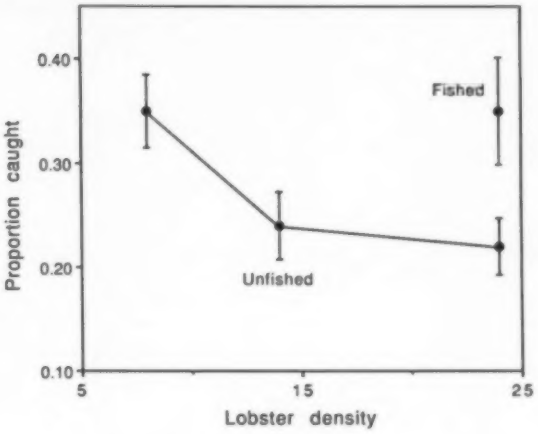

Lobsters were split into two groups. Each group was used on 2 consecutive days with treatments and lobsters reassigned among the four tanks on the second day. Lobsters were exchanged each time they had been used for 2 consecutive days until each group had been used in five replicates of each treatment with baited traps. Lobster size ranged from 66 to 73 mm carapace length (CL) (mean = 70, SD = 2 mm) with a sex ratio of 0.46 males to 0.54 females. We used only animals with both claws and both antennae intact. Claw bands were removed when animals were in experimental tanks and applied when they were kept in storage tanks.

To test if all animals were equally likely to be captured, we marked captured lobsters with color-coded rubber bands after each experiment; the different colors gave us a record of how many times each lobster was caught out of a possible five captures. This provided us with a frequency distribution of capture for 140 individual lobsters. If the frequency distribution differed from that found in a binomial distribution, then the hypothesis that all lobsters had an equal probability of capture could be rejected.

Results

The proportion of lobsters caught after 18 h in unfished traps decreased with increased density, suggesting that trap saturation affected catch rate (Fig. 2). However, the proportion caught in the fished treatment using 24 lobsters equalled that for the unfished treatment of eight lobsters, suggesting that fishing removed the effect of saturation. None of the treatment means differed significantly at 8 h (Table 1) or earlier.

The proportions caught in the baited and unbaited treatments were similar. When the results after 18 h were combined for all densities of unfished traps, 28% of lobsters in a tank population were captured in replicates using baited traps and 30% in replicates using unbaited traps.

Although each lobster was used on five occasions, there was no increase in the proportion captured over the course of the experiment, as one might expect if they learned from experience how to enter traps. Also, a chi-squared

Table 1. Mean proportions of lobsters captured (n = 10 replications). Means that are not significantly different at $P < 0.05$ are underscored (S-N-K test).

Observation time (h)	Treatment (no. of lobsters)			
	24 fished	8 unfished	14 unfished	24 unfished
18	0.35	0.35	0.24	0.22
8	0.23	0.23	0.18	0.18

Table 2. Mean proportion of small rock crabs captured at three densities and three observation time (n = 5). Means that are not significantly different at $P < 0.05$ are underscored (S-N-K test). Each observation time was analyzed separately.

	Time of observation and density of small crabs								
	18 h			8 h			4 h		
Species and size	14	22	36	14	22	36	14	22	36
Controls (small rocks only)	0.77	0.75	0.66	0.64	0.60	0.48	0.47	0.42	0.35
Small + large rocks	0.63	0.60	0.57	0.41	0.48	0.34	0.34	0.35	0.28
Small rocks + lobsters	0.29	0.38	0.32	0.17	0.23	0.27	0.13	0.14	0.19

goodness-of-fit test showed that the frequency distribution of lobster captures (0–5 times) was not significantly different from a binomial distribution (chi-square = 7.1, 5 df). Thus, we have no reason to reject the hypothesis that all individuals were equally likely to be captured during the course of the experiment, i.e., they were neither trap-happy nor trap-shy.

Counts of lobsters in the same traps at 2, 4, 8, and 18 h provided no evidence that any lobster escaped. Never was there a reduction of catch from one observation to the next, and only once was movement noted from the parlor (second compartment) to the kitchen (first compartment). It is possible that lobsters could have both entered and escaped between observations, but the above results make this unlikely.

Rock crabs

This experiment was designed to test whether the catches of small rock crabs were proportional to density and whether the presence of large rock crabs or lobsters stocked in the same tank influenced the catch of small rock crabs.

Methods

Nine treatments were replicated five times and all analyzed in a single one-way ANOVA. These treatments were 14, 22, or 36 small rock crabs alone (controls), the same densities with 10 large rock crabs added, and the same densities with five lobsters added. The control treatments were also run twice without bait. All treatments were unfished. Small rock crabs were 65-79 mm (mean = 74, SD = 4) carapace width (CW), measured as the distance between the two most lateral notches on the carapace, with a corresponding weight range of 49–88 g (mean = 73 g). Large rock crabs were 94–104 mm CW (mean = 98, SD = 3) with a weight range of 149–202 g (mean = 168 g). Lobsters were the same animals used in the lobster experiments (mean weight = 278 g). Small rock crabs, large rock crabs, and lobsters were each divided into two groups and used in experiments on alternate days. They were placed in experimental tanks at about 10:00, traps were added at 15:00, and catches were noted after 4, 8, and 18 h elapsed time. Ambient temperature varied between 7.5 and 9.2°C.

Results

The proportion of small rock crabs captured did not differ among densities. This was true for controls, when large crabs were present, and when lobsters were present and was true at 4-, 8-, and 18-h observation times (Table 2; Fig. 3). Therefore, trap saturation was not indicated for any of the three types of treatments.

Because the proportion caught was similar at all three densities, results were combined (15 trials per treatment) for comparing the effects of large crabs and lobsters in the tanks on the catch of small crabs. The proportion caught was significantly reduced when large crabs were present, and lower still with lobsters present. The lobster effect was significant at all observation times, and the large crab effect was significant at 8 and 18 h (Table 3).

Lobsters might have reduced the crab catch because they had entered the trap or because they were merely in the tank. At the 18-h observation, we were able to compare the proportion of small crabs caught when one or more lobsters had entered the trap (n = 11), the proportion caught when lobsters were in the tank but not in the trap (n = 4), and the proportion of control crabs caught with no lobsters present (n = 15). For the trials in which lobsters had entered

Fig. 3. Proportion of rock crabs caught at three densities and after three times (mean ± SE of the mean).

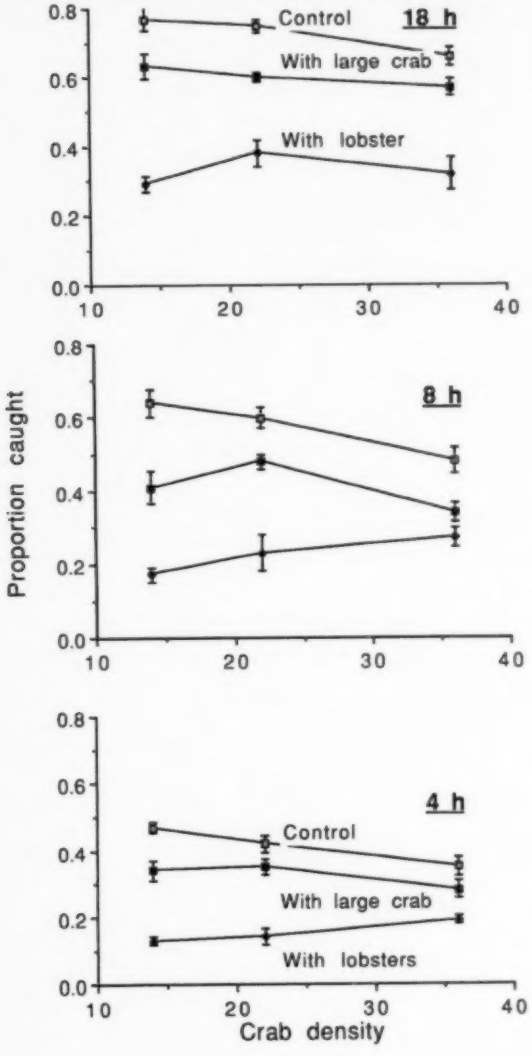

Table 3. Mean proportions of small rock crabs captured; data for three densities of small crabs combined ($n = 15$). Means that are not significantly different at $P < 0.05$ are underscored (S-N-K test).

	Treatment		
Observation time (h)	Control	With large crabs	With lobsters
18	0.73	0.60	0.33
8	0.57	0.41	0.22
4	0.41	0.32	0.15

Table 4. Mean proportions of large rock crabs captured at three densities of small rock crabs ($n = 5$). Means that are not significantly different at $P < 0.05$ are underscored (S-N-K test).

	Density of small crabs		
Observation time (h)	14	22	36
18	0.68	0.76	0.76
8	0.54	0.64	0.64
4	0.36	0.32	0.52

Table 5. Mean proportion of large rock crabs and controls captured, all densities combined ($n = 15$). Means that are not significantly different at $P < 0.05$ are underscored (S-N-K test).

	Treatment	
Observation time (h)	Controls	Large crabs
18	0.73	0.73
8	0.57	0.61
4	0.41	0.40

a trap before 18 h, at least one was also present by 8 h, and thus had time to influence crab catches. Crab catches did not differ between trials when lobsters were in the trap and the tank (proportion = 0.30) or in the tank only (proportion = 0.40). In both cases, catches were lower than for the controls (proportion = 0.73). This analysis could not be performed on treatments including large crabs in place of lobsters because they entered the trap in every trial.

The presence of lobsters changed the behavior of crabs in ways other than reducing trap entry. After 18 h (all densities combined), 92% of crabs captured in the control treatment were in the parlor end of the trap whereas in the presence of lobsters, 90% of the lobsters but only 46% of the crabs caught were in the parlor. The crabs also climbed the sides of the trap or the drain pipe to avoid the lobsters. Often, more crabs were on the trap than inside it.

The proportion of large rock crabs caught did not differ among the three densities of small rock crabs at any observation time (Table 4); thus, small rock crab density did not influence large rock crab catch. When all data for large crabs were combined, the proportion caught was not significantly different from the catch rate of small crabs in the controls (Table 5), meaning that catches of small crabs alone were as high as for large crabs.

As in the lobster experiments, successive counts of animals in the same traps at 4, 8, and 18 h could provide evidence of escape. However, there was never a reduction in catch from one observation to the next. In 5 of 51 trials (45 baited + 6 unbaited) the number of small crabs in the

Table 6. Comparison of mean proportions of small green crabs captured among three densities. Comparisons were made at each of three observations times. Means that are not significantly different ($P > 0.05$) are underscored (S-N-K test).

	Observation times and densities of small crabs								
	18 h			8 h			4 h		
Species	14	22	36	14	22	36	14	22	36
Small greens only (controls)	0.51	0.45	0.26	0.39	0.34	0.14	0.16	0.21	0.09
Small greens + lobsters	0.19	0.12	0.16	0.14	0.07	0.11	0.09	0.04	0.07

Table 7. Comparison of mean proportion of small green crabs captured with and without (control) lobsters present. Comparisons were made at each of three observation times and three densities of green crabs. Means that are not significantly different ($P > 0.05$) are underscored (S-N-K test).

	Density of small green crabs and treatments					
	14		22		36	
Observation time (h)	Control	Small greens + lobsters	Control	Small greens + lobsters	Control	Small greens + lobsters
18	0.51	0.19	0.45	0.12	0.26	0.16
8	0.39	0.14	0.34	0.07	0.14	0.11
4	0.16	0.09	0.21	0.04	0.09	0.07

parlor decreased between successive observations, indicating movement from parlor to kitchen.

Finally, bait made little if any difference in catch rates of small crabs. After 18 h, 73% of rock crabs were captured in treatments using baited traps and 62% in treatments using unbaited traps. After 8 h the respective capture rates were 68 and 47%. The transformed means were not significantly different at the 0.05 level.

Green crabs

This experiment was designed to test whether the catches of small green crabs were proportional to density and whether the presence of large green crabs or lobsters influenced the catch rate of small crabs.

Methods

We used the same experimental design as for the rock crab experiments, except that we looked for an effect of large crabs on small crabs at only one instead of three densities of small crabs. In addition, we tested for an effect of rock and green crabs on each other by including a treatment of 22 green crabs with 22 rock crabs and an additional control of 22 rock crabs only. The nine treatments in this experiment were 14 greens, 22 greens, 36 greens, 14 greens + 5 lobsters, 22 greens + 5 lobsters, 36 greens + 5 lobsters, 22 greens + 10 large greens, 22 greens + 22 rocks, and 22 rocks. Each treatment was replicated five times, and two replicates of each of the three densities of green crabs alone were run without bait. All treatments were unfished. High variance in some treatments gave low power for all tests when a single ANOVA was used; therefore, different questions were addressed with one-way ANOVAs including only a portion of the treatments.

Small green crabs were 54–66 mm CW (mean = 60, SD = 4), measured as the distance between the two most lateral notches on the carapace, with a corresponding range in weight of 48–94 g (mean = 70 g). Large green crabs were 69–76 mm CW (mean = 71, SD = 2), with a weight range of 110–152 g (mean = 122 g). Lobsters and small rock crabs were the same animals used in previous experiments. As in the rock crab experiments, small and large green crabs, small rock crabs, and lobsters were each divided into two groups and used in experiments on alternate days. Data collection was identical to that in the rock crab experiments. During this experiment, ambient water temperature in Halifax harbor fell to approximately 5.5°C, so we added varying amounts of 15°C water to both the experimental and holding tanks to ensure that the green crabs remained active. The water temperature in the experimental tanks varied between 7.0 and 8.7°C.

Results

The proportion of green crabs caught in control treatments was reduced at the highest density after 8 and 18 h, suggesting trap saturation. When lobsters were included with green crabs, the proportion captured was consistently low and did not differ among densities at any observation time (Table 6; Fig. 4).

The presence of lobsters in the tank markedly reduced the proportion of green crabs caught for the two lower densities but not the high density, where the catch was already reduced by trap saturation (Table 7). As in the case of rock crabs, the presence of lobsters affected the distribution of green crabs. After 18 h (all control densities combined), 87% of captured crabs were in the parlor end of the trap whereas in the presence of lobsters, only 33% were in the parlor. Eighty-three percent of the lobsters entered the parlor. Lobsters entered traps in 14 of 15 trials; thus, we could not differentiate between their inhibitory effect in the tank and in the trap.

The catch of small green crabs in the presence of large green crabs was significantly lower than the catch of small green crabs alone, but only after 18 h (Table 8). The presence of small rock crabs did not reduce the catch of small green crabs when compared with small green crabs alone, and the presence of small green crabs did not reduce the catch of small rock crabs compared with small rock crabs alone (Table 8).

Finally, in contrast with the lobster and rock crab experiments, the catch of green crabs was higher in baited than unbaited traps. Averaged over all three densities, 37% were captured in replicates using baited traps (n = 15) and 19% in replicates using unbaited traps (n = 6).

Discussion

Conducting these experiments in the laboratory eliminated some of the variation associated with field trapping experiments. The density, species composition, and animal sizes in the target (tank) population were known exactly, all individuals had time to reach the trap between each observation, and the experimental conditions were easily replicated. All effects of inter- and intraspecific interactions were either negative or zero relative to control catches; no interaction increased the proportion of animals captured relative to controls (Table 9).

Density effects

Density or saturation effects occur when a smaller proportion of the population available to be trapped is captured at high than at low density. Because the size of the trappable population in the field is rarely known, saturation has been demonstrated by removing the catch from traps at short time intervals and finding that the cumulative total is higher than the catch from traps not emptied. Examples for some crab species are found in Miller (1978), Roberton (1989), and Castro and DeAlteris (1990). Saturation was also implied from the results of two other types of studies. Traps fished for short soak times caught more per unit time than traps fished for long soaks when bait was unlimited (Boutilier and Sloan 1987; Smith and Jamieson 1989). Secondly, traps prestocked with one or more individuals of the target species caught less than traps not prestocked (Richards et al. 1983; Addison 1995).

Unfortunately, our results do not suggest a single quantitative relationship between catch and density. Density affected catch rate in the experiments with green crabs and with lobsters, but not with rock crabs. In previous studies, lobster catches were reduced if traps were first

Fig. 4. Proportion of green crabs caught at three densities and after three times (mean ± SE of the mean).

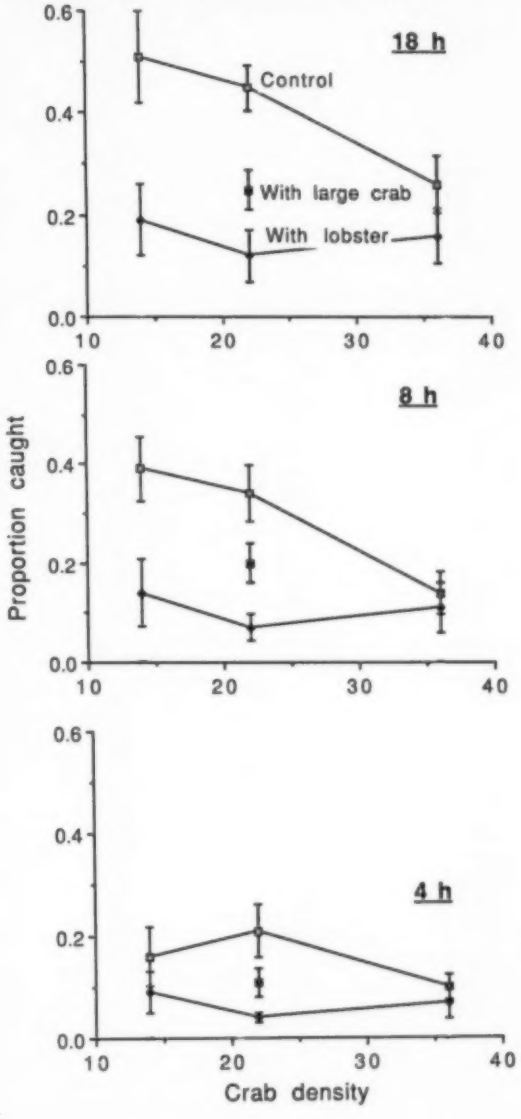

stocked with one or more lobsters (Richards et al. 1983; Addison 1995). We know of no study of trap saturation using green crabs. Our results for rock crabs differ from previous studies with rock crabs and other *Cancer* sp. Miller (1980) observed that trap catches of rock crabs peaked after a few hours and additional entrants only replaced those that escaped. Catch rate of *C. productus* slowed after a few hours, but slowed less if escape was prevented (Miller 1978), and catches of *C. magister* peaked at less than 24 h (Miller 1978; Smith and Jamieson 1989).

We are aware of only one other experimental trapping study using decapod crustaceans where density of the target species was manipulated. Yamane and Iitaka (1985)

Table 8. Mean proportion of 22 small green and 22 small rock crabs captured at three observation times. A, Small greens vs. small greens + large greens; B, small greens vs. small greens + small rocks; C, small rocks vs. small rocks + small greens. Means that are not significantly different ($P > 0.05$) are underscored (S-N-K test).

	Treatment					
	A		B		C	
Observation time (h)	Small greens	Small greens + large greens	Small greens	Small greens + small rocks	Small rocks	Small rocks + small greens
18	0.45	0.25	0.45	0.30	0.56	0.55
8	0.34	0.20	0.34	0.21	0.41	0.35
4	0.21	0.11	0.21	0.17	0.26	0.22

Table 9. Summary of interactions tested. "0", no interaction; "−", negative interaction; blank, no test performed.

	Effect on			
Effect of	Lobsters	Small rocks	Large rocks	Small greens
Lobsters	−	−		−
Small rocks		0	0	0
Large rocks		−		
Small greens		0		−
Large greens				−

stocked shrimp (*Palaeomon* sp.) in five densities in a 1 × 2 m tank and fished them in turn with traps of three designs. Because catches by all three trap types were similar, we averaged their results. At the lowest density of 20 shrimp in the tank, 72% were captured whereas at the five higher densities of 40–150 shrimp, a much lower 31–42% were captured. This does not fit the pattern observed in any of our experiments.

It might be argued that the saturation mechanism operates as follows. At some threshold density the repellent odor of lobsters or crabs already in the trap nullifies the positive attraction of the bait. However, in this study the trials using unbaited traps showed that the bait had only marginal attraction, and hence, some other feature of the trap provided attraction. The most likely explanation may be that lobsters and crabs were attracted to the trap as a shelter. Whatever the attraction, it could be countered by a repellent stimulus from the trap. Since decapods are most active at night, we presume that vision in not the important sense; we have no information on sound. In a few instances, a lobster was observed sitting in the entrance funnel of a trap with its claws facing outward, physically preventing entry of other lobsters.

Our finding that all lobsters were equally likely to enter a trap, i.e., they were neither trap-happy nor trap-shy, contrasted with the findings of Karnofsky and Price (1989) that 40% of lobsters remained invulnerable to trapping throughout 2 months of tank observations.

Species and size interactions

The above results were based on similar-sized individuals of the same species. Interactions between species and between different-sized individuals of the same species reduced catch rates substantially.

The presence of large rock crabs reduced the catch of small rock crabs, and the presence of large green crabs reduced the catch of small green crabs. Because all crabs in a tank had easy access to the trap, avoidance of large conspecifics must have been the cause. Smith and Jamieson (1989) found that the average sizes of *C. magister* captured increased with soak times from 1 to 2 days to 5 days. This was due to escape of small crabs and slower entry of large crabs. These explanations of interactions among sizes and the escape of small crabs can be added to slower walking speed (McLeese and Wilder 1958) and smaller appetite (Morrissy 1973) as reasons for lower catchability of small individuals commonly observed in field studies (Smith 1944; Williams and Hill 1982; Miller 1989).

Lobster markedly reduced catches of both crab species. Crabs obviously avoided lobsters. Predators in traps on the fishing ground were also demonstrated to greatly reduce *Cancer* crab (Richards et al. 1983; Addison 1995) and spiny lobster (Chittleborough 1974) catches. For rock crabs the experiments showed that the catch rate of crabs was reduced by the presence of lobsters in the tank only, and not necessarily in the trap itself. In tank studies, Karnofsky and Price (1989) showed that only 2% of approaches of lobsters to traps resulted in capture, suggesting that activity of lobsters around a trap could reduce the catch rate of crabs. Because there may be no resulting capture of lobsters, the inhibitory effect may remain undetected by the experimenter.

When lobsters were present in a tank, as many rock and green crabs were found on the trap, seeking to avoid the lobsters, as in the trap. Crabs also avoided the parlor end of the trap when it contained lobsters. Richards et al. (1983) found that in both laboratory and field trapping experiments, crabs were less likely to enter the parlor end of the trap and were found higher in the trap when lobsters were present. Although not seen in these short-term tank experiments, escape from traps might increase in the presence of a predator (Richards et al. 1983).

Not all interactions affected catches. The proportion of large rock crabs captured was the same over a range of

densities of small rock crabs. The addition of small rock crabs did not affect the catch of small green crabs, and vice versa.

Implications for trapping surveys

Trapping is an imprecise method for estimating decapod abundance because of the many factors influencing catches. However, there is often no suitable fishing alternative, so doing our best with the best tools available is the only solution. With these experiments, we demonstrated how catch rates were affected by density of the target species, large conspecifics, and species interactions. It was apparent that fishing for shorter soak times would help maintain a proportional relationship between catch rate and density. However, a soak time short enough to avoid saturation may give catches too small for the desired precision. To address this problem, Robertson (1989) recommended using several short soaks within 24 h, emptying the traps after each, and fitting the equation

$$C_t = C_\infty(1 - e^{-Bt})$$

where C_t is the cumulative catch at time t, C_∞ is the asymptotic catch, and B is a constant related to the rate at which the curve approaches the asymptote. Robertson (1989) suggested that B or C_∞ would be used as the density index. However, changes in catchability over 24 h (e.g., Miller 1978) can produce erratic values for C_∞ and B.

A more suitable index of abundance would be $C_\infty B$, the slope of the above equation at the origin, i.e., when t = 0. This index is equivalent to the "virtual entry rate" of Smith and Jamieson (1989). However, a changing catch rate throughout the day could still be a problem in curve fitting. Another alternative is to conduct a field experiment in which traps are fished at a range of soak times (and the catch removed) in order to determine the longest soak time possible before the catch is reduced a significant amount by saturation. Then, using this soak time, the catches are summed over 24 h for an abundance index.

The inhibitory effect of both large crabs or crab predators on either small crabs or crabs in general suggests that dominant individuals will be overrepresented in trap catches. Short soaks could reduce selectivity for dominants if they are less abundant, as is likely the case. Removing them often from the traps would decrease their interactions with less dominant individuals.

Acknowledgments

Dr. R. Rodger advised on statistical procedures. The work was carried out whilst one of us (J.T.A.) was a visiting scientist at the Halifax Fisheries Research Laboratory, Department of Fisheries and Oceans, and he thanks Dr. J.D. Pringle for provision of facilities during his visit and a stimulating environment in which to work.

References

Addison, J.T. 1995. Influence of behavioural interactions on lobster distribution and abundance as inferred from pot-caught samples. ICES Mar. Sci. Symp. No. 199.

Bennett, D.B., and Brown, C.G. 1979. The problem of pot immersion time in recording and analyzing catch-effort data from a trap fishery. Rapp. P.-v. Réun. Cons. int. Explor. Mer, **175**: 186–189.

Boutilier, J.A., and Sloan, N.A. 1987. Effects of trap design and soak time on catches of the British Columbia prawn (*Pandalus platyceros*). Fish. Res. **6**: 69–79.

Castro, K.M., and DeAlteris, J.T. 1990. Effects of trap saturation and species interaction on the capture of *Callinectes* spp. crabs in the Guayas estuary. Fish. Res. **8**: 223–232.

Chittleborough, R.G. 1974. Homerange, homing, and dominance in juvenile western rock lobsters. Aust. J. Mar. Freshwater Res. **25**: 227–234.

Elner, R.W. 1980. Lobster gear selectivity. Can. Tech. Rep. Fish. Aquat. Sci. **932**: 78–83.

Ennis, G.P. 1978. Growth curves for Newfoundland lobsters from data on molt increment and proportion molting. Can. Atl. Fish. Sci. Advis. Comm. Res. Doc. 78/29.

Karnofsky, E.B., and Price, H.J. 1989. Behavioural response of the lobster *Homarus americanus* to traps. Can. J. Fish. Aquat. Sci. **46**: 1625–1632.

Krouse, J.S. 1989. Performance and selectivity of trap fisheries for crustaceans. *In* Marine invertebrate fisheries: their assessment and management. *Edited by* J.F. Caddy. John Wiley & Sons, New York, N.Y. pp. 307–325.

McLeese, D.W., and Wilder, D.G. 1958. The activity and catchability of the lobster (*Homarus americanus*) in relation to temperature. J. Fish. Res. Board Can. **15**: 1345–1354.

Miller, R.J. 1978. Saturation of crab traps: reduced entry and escapement. J. Cons. int. Explor. Mer, **38**: 338–345.

Miller, R.J. 1980. Design criteria for crab traps. J. Cons. int. Explor. Mer, **39**: 140–147.

Miller, R.J. 1989. Catchability of American lobsters and *Cancer* crabs by traps. Can. J. Fish. Aquat. Sci. **46**: 1652–1657.

Miller, R.J. 1990. Effectiveness of crab and lobster traps. Can. J. Fish. Aquat. Sci. **47**: 1228–1251.

Morrissy, N.M. 1973. Normal (Gaussian) response of juvenile marron, *Cherax tenuimanus* (Smith) (Decapoda: Parastacidae), to capture by baited sampling units. Aust. J. Mar. Freshwater Res. **24**: 183–195.

Richards, R.A., Cobb, J.S., and Fogarty, M.J. 1983. Effects of behavioral interactions on the catchability of American lobster (*Homarus americanus*) and two species of *Cancer* crabs. Fish. Bull. **81**: 51–60.

Robertson, W.D. 1989. Factors affecting catches of the crab *Scylla serrata* (Forskal) (Decapoda: Portunidae) in baited traps: soak time, time of day and accessibility of the bait. Estuarine Coastal Shelf Sci. **29**: 161–170.

Smith, B.D., and Jamieson, G.S. 1989. A model for standardizing Dungeness crab (*Cancer magister*) catch rates among traps which experienced different soak times. Can. J. Fish. Aquat. Sci. **46**: 1600–1608.

Smith, G.F.M. 1944. The catchability of lobsters. J. Fish. Res. Board Can. **6**: 291–301.

Snedecor, G.W., and Cochran, W.G. 1967. Statistical methods. Iowa State University Press, Ames, Iowa.

Steel, R.D.G., and Torrie, J.H. 1960. Principles and procedures of statistics. McGraw-Hill, New York, N.Y.

Williams, M.J., and Hill, B.J. 1982. Factors influencing pot catches and population estimates of the portunid crab *Scylla serrata*. Mar. Biol. **71**: 187–192.

Yamane, T., and Iitaka, Y. 1985. Relation between ingress and population density. Bull. Jpn. Soc. Sci. Fish. **51**: 881–888.

Wind-induced upwelling along the west coast of North America, 1899–1988

William W. Hsieh, Daniel M. Ware, and Richard E. Thomson

Abstract: Alongshore geostrophic wind stresses (AWS) were used as an "index" of wind-induced coastal upwelling/downwelling for eight coastal stations from Baja California to Alaska for 1899–1988. For winters since around 1940, downwelling has intensified along Alaska and northern British Columbia, while upwelling has increased along Baja California. El Niño events induced strong winter coastal downwelling poleward of 40°N. During summer, upwelling has increased since around 1940 along southern British Columbia to Baja California, while from 1899 to 1940, upwelling declined along southern California to Baja California. Empirical orthogonal function analysis of the AWS showed that the first mode consisted of the AWS at the eight stations all varying in-phase, while the second mode had the northern four stations out-of-phase with the southern four stations. Off southern British Columbia, correlations between coastal sea level and AWS and between sea surface temperature and AWS were both strong during winter but insignificant during summer. In contrast, correlation between salinity and alongshore wind stress was insignificant during fall and winter, but strong during spring and moderate during summer. Summer AWS was positively correlated with both the fatness of sardine and the condition factor of herring off British Columbia.

Résumé : Les tensions du vent géostrophique le long du littoral (AWS) ont servi d'indice des remontées et des plongées des eaux côtières induites par le vent pour huit stations littorales réparties de la Basse-Californie à l'Alaska, entre 1899 et 1988. Pendant l'hiver, depuis 1940 environ, les plongées d'eau se sont intensifiées le long de l'Alaska et du nord de la Colombie-Britannique, tandis que les remontées d'eau se sont accrues le long de la Basse-Californie. Les événements El Niño ont induit une forte plongée des eaux côtières en hiver entre 40°N et le pôle. En été, les remontées d'eau se sont accrues depuis 1940 environ le long de la côte du sud de la Colombie-Britannique à la Basse-Californie, tandis que de 1899 à 1940, les remontées d'eau avaient décliné du sud de la Californie à la Basse-Californie. L'analyse empirique des fonctions orthogonales des AWS a montré que, dans le premier mode, les AWS variaient en phase aux huit stations, tandis que dans le deuxième mode, les quatre stations du nord étaient déphasées par rapport aux quatre stations du sud. Dans les eaux du sud de la Colombie-Britannique, les corrélations entre le niveau de la mer à la côte et les AWS, et entre la température superficielle et les AWS, étaient fortes pendant l'hiver mais non significatives pendant l'été. Par contre, la corrélation entre la salinité et les tensions du vent littoral n'était pas significative pendant l'automne et l'hiver, mais était forte au printemps et modérée en été. Les AWS de l'été étaient positivement corrélées avec, à la fois, la teneur en graisse des sardines et le facteur de condition des harengs dans les eaux de la Colombie-Britannique.

[Traduit par la Rédaction]

Introduction

A recent paper by Ware and Thomson (1991) examined the linkage between long-term variability in wind-induced coastal upwelling and pelagic fish biomass in the northeast Pacific Ocean. The biomass in the coastal upwelling domain along the west coast of North America (from Baja California to the northern tip of Vancouver Island) decreased by a factor of 5 in the first half of this century. Because of the strong relaxation of upwelling winds off southern California, Ware and Thomson concluded that the decline in the pelagic fish biomass was likely caused by the decline in coastal upwelling in the first half of this century. Long records of coastal winds north of California were not available to Ware and Thomson, so sea level and salinity had to be used as approximate indicators of upwelling at higher latitudes.

As monthly sea level pressure data for the Northern Hemisphere are available from the National Center for Atmospheric Research (NCAR), Boulder, Colorado, from

Received August 31, 1993. Accepted July 14, 1994.
J12073

W.W. Hsieh. Department of Oceanography, University of British Columbia, Vancouver, BC V6T 1Z4, Canada.
D.M. Ware. Department of Fisheries and Oceans, Pacific Biological Station, Nanaimo, BC V9R 5K6, Canada.
R.E. Thomson. Department of Fisheries and Oceans, Institute of Ocean Sciences, Sidney, BC V8L 4B2, Canada.

Fig. 1. Location of the 5° squares of sea level pressure data used to calculate the geostrophic wind stress at Stations A–H, situated at (137.5°W, 57.5°N), (132.5°W, 52.5°N), (127.5°W, 47.5°N), (127.5°W, 42.5°N), (122.5°W, 37.5°N), (117.5°W, 32.5°N), (117.5°W, 27.5°N), and (112.5°W, 22.5°N), respectively.

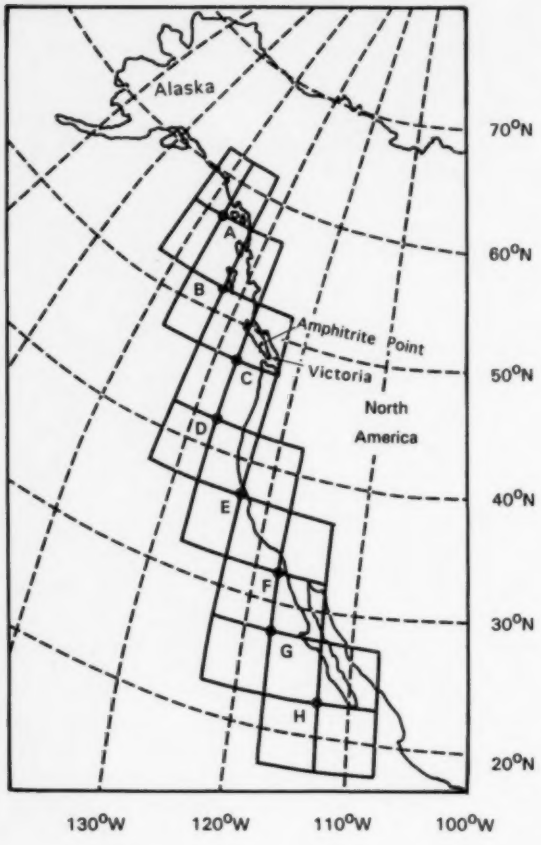

1899 to 1988, we proceeded to compute the geostrophic wind stress along the west coast of North America at various sites. The alongshore wind stress then provides a useful measure of the monthly average amount of wind-induced upwelling/downwelling along the west coast.

The goal of this paper is to provide a broad view of the changing upwelling/downwelling conditions along the west coast from Alaska to Baja California from 1899 to 1988. The outline of this paper is as follows. We describe the datasets used, then provide a detailed description of the winter and summer alongshore wind stress, and relate the variability to El Niño and longer term changes. An empirical orthogonal function (EOF) analysis of alongshore wind stress from the eight stations along the west coast is then presented. The alongshore wind stress off southern British Columbia is related to the sea level, temperature, and salinity. Finally, the relation of the wind stress to various biological time series along the west coast is shown.

Data

The NCAR monthly sea level pressure data (1899–1988) were assembled for 5° squares in the Northern Hemisphere. As the data originated from eight different sources, discontinuities had been identified with every change in source by Trenberth and Paolino (1980), who also identified many errors in the data, which were then reset as missing data. Most of the errors were in data collected over Asia, predominantly before 1922 or during World War II. Trenberth and Paolino (1981) used data since December 1924 from this dataset to study the characteristic patterns of variability of sea level pressure in the Northern Hemisphere.

Figure 1 shows the eight stations labelled A–H along the west coast of North America for which the geostrophic winds have been computed by finite-differencing the NCAR pressure data on the four surrounding squares. The wind stress was calculated from the geostrophic wind using a constant drag coefficient of 0.001. (Because wind stress is used in this paper as a relative index of upwelling, the choice of the constant drag coefficient is not critical, as a higher drag coefficient will simply linearly scale up our wind stress values. A more accurate approach would, however, use a nonconstant drag coefficient, e.g., Large and Pond 1981). The average orientation of the coastline at each station was measured from maps, and the alongshore wind stress component was then computed, with the sign convention that positive values were assigned to upwelling favorable alongshore wind stress. While this sign convention is consistent with the one used by biological oceanographers, it is opposite to the one commonly used by physical oceanographers. Seasonal values were then computed from the monthly data. Details are given in Xie and Hsieh (1991).

The resulting alongshore winds were rather well correlated with the Bakun upwelling index (available since 1946), which was expected because the Bakun index had been derived using basically the same pressure data. For instance, at Station C, the correlation between the alongshore wind stress and the corresponding Bakun upwelling index at 48°N from 1946 to 1988 was 0.84 in winter and 0.73 in summer. The two major limitations of our method for calculating the alongshore wind stress, i.e., using (a) monthly mean air pressure and (b) a constant drag coefficient, would underestimate the contribution to the monthly mean wind stress from high-frequency intense events such as storms (Thompson et al. 1993; Wright and Thompson 1983). Fewer data during the earlier part of this century would necessitate more spatial smoothing of the pressure field, which could in turn lead to a weaker geostrophic wind.

Other time series from the west coast of Vancouver Island used in this paper include monthly averaged sea level at Victoria, B.C., since 1909 and the monthly averaged sea surface temperature and salinity collected since August 1934 at the Amphitrite Point lighthouse. The only major data gaps were during March–July 1939 and the last 3 months of 1976 in the Amphitrite temperature and March–July 1939 and all of 1975–1976 (except for June–September in both years) in the Amphitrite salinity. Victoria sea level was chosen because it had the most complete

Fig. 2. (*a*) Winter alongshore wind stress (averaged over 3 months from December through February) (winter 1988 meaning December 1987 to February 1988) and (*b*) summer alongshore wind stress (averaged from June through August) for Stations A (top panel) to H (bottom panel). Upwelling alongshore winds are positive. In Fig. 2*a*, the strong winter downwelling associated with strong El Niño events is marked by solid arrowheads and that with moderate El Niño events by open arrowheads in the panel for the Station C data.

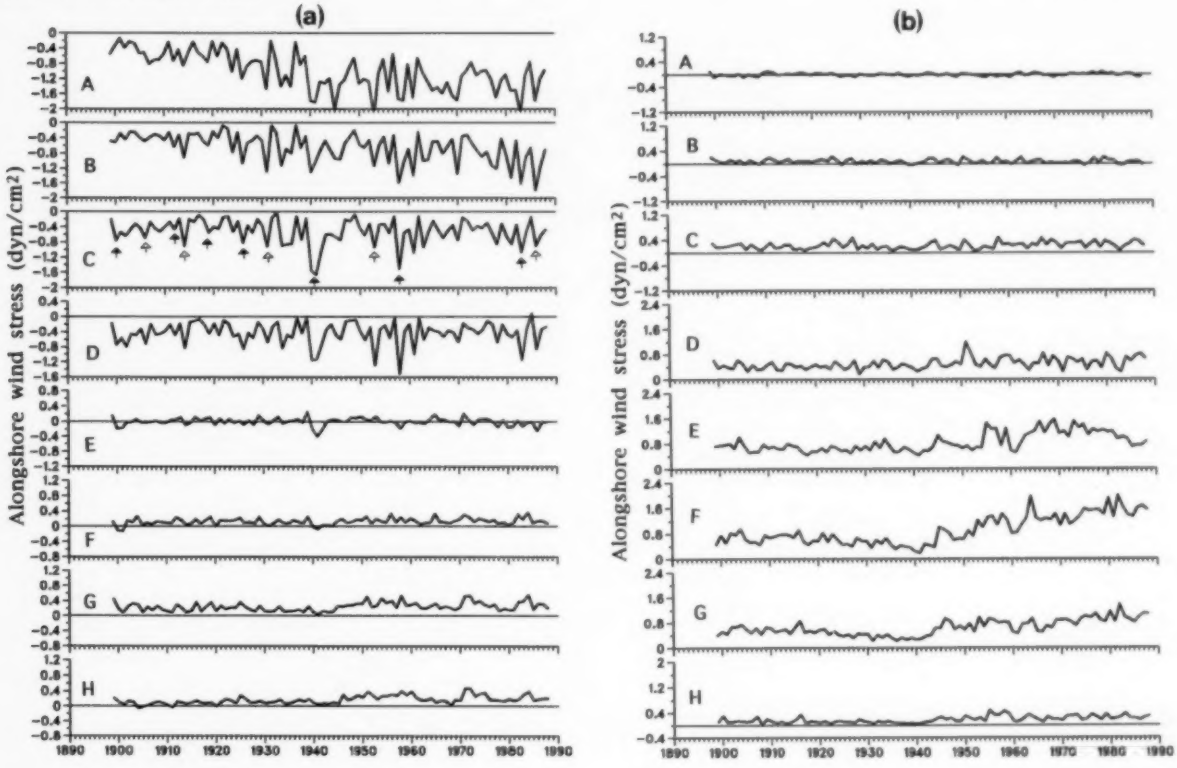

record, although Victoria is located inside the Juan de Fuca Strait. At low frequencies, Victoria sea level is highly correlated with sea level on the west coast of Vancouver Island (Thomson and Tabata 1981). We also made use of the following annual biological time series: (a) the sardine fatness index (1925–1946) and the herring condition factor (1929–1989) off southern British Columbia and (b) diatom abundance at Scripps pier, California (1920–1943), and the second quarter primary production in the southern California Bight (1920–1979) from Smith and Eppley (1982). Data are missing in the years 1930, 1932, 1938, 1944, 1956, and 1965–1969 for the age-5 herring condition factor and in 1936 for diatom abundance at Scripps pier (see Ware and Thomson 1991).

Alongshore wind stress

The winter (December–February) alongshore wind stress (Fig. 2*a*) shows generally strong downwelling winds at Stations A–D and weak upwelling winds at Stations F–H. Comparing the winds from the 1940s onward with earlier winds, we note that the downwelling winds have intensified at Stations A and B, while upwelling winds have strengthened at Stations F–H during the more recent period. At the four northern stations, intense downwelling winds were observed during El Niño events. As marked by the arrowheads in Fig. 2*a*, the sudden increase of downwelling winds observed in the winters of 1900, 1906, 1912, 1914, 1919, 1926, 1940–1941, 1953, 1958, 1983, and 1986 can all be related to El Niño events. Strong El Niño events occurred during 1899–1900, 1911–1912, 1918–1919, 1925–1926, 1940–1941, 1957–1958, 1972–1973, and 1982–1983, while moderate events occurred during 1902, 1905, 1914, 1930, 1939, 1953, 1965, 1976, and 1986–1987 (Quinn et al. 1978, 1987). During a typical El Niño, which develops in the northern summer or fall, a strong atmospheric teleconnection pattern of alternating high and low pressure cells extending from the tropics to the higher latitudes is generated by winter (Mysak 1986). In particular, the Aleutian Low is intensified during an El Niño winter, leading to an increase in the coastal downwelling winds at Stations A–D. Not all El Niño events produce strong atmospheric teleconnection patterns, however. Hamilton (1988) found that an intensified Aleutian Low was usually generated during El Niño events, but not during the El Niño winters of 1903, 1915, 1930, 1966, and 1973 (note that Hamilton's winter of 1902–1903 is equivalent to our winter of 1903, i.e., the months December 1902 to February

Fig. 3. One-month-lagged autocorrelation for the alongshore wind stress at Stations A, C, E, and G. For instance, the January value plotted is the correlation between the January and February alongshore wind stress at a particular station.

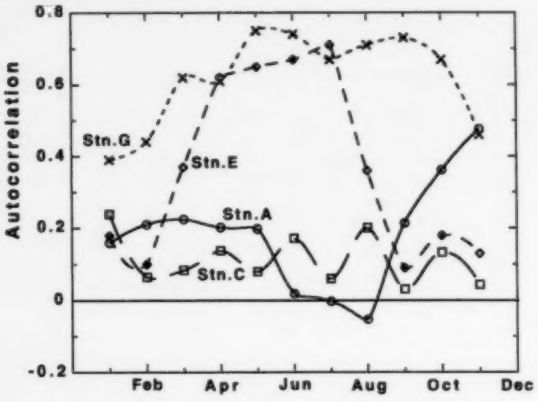

1903). The lack of strong atmospheric teleconnections during the winters of 1915 and 1930 is reflected in Fig. 2*a*, where the coastal downwelling winds at Stations A–D were weak during these winters. However, the downwelling winds were strong in the winters of 1914 and 1931, and it is not clear if these intensified winds were related to El Niño. The absence of strong teleconnections for the events of 1965–1966 and 1972–1973 explain the lack of relatively intense coastal downwelling winds from the mid-1960s to the late 1970s (except for 1970) (Fig. 2*a*). Hamilton (1988) also found an intensified Aleutian Low in the winter of 1977, but somehow this did not lead to strong coastal downwelling winds (Fig. 2*a*), although strong downwelling winds were found in winter 1978.

The summer alongshore wind stress (Fig. 2*b*) shows upwelling extending further north, as far as Station B. Again, upwelling winds intensified in the second half of the record at Stations C–H. In general, the strongest summer upwelling occurred around Station E, although since the mid-1970s, upwelling at Station F has surpassed the weakening upwelling at Station E. In the earlier half of the record, the upwelling winds declined from the turn of the century to 1940 at Stations F–H, before rising in the second half of the record. This decline in the first part of the century was used by Ware and Thomson (1991) to explain the decline in the biomass of pelagic fish off the west coast. As Ware and Thomson did not have wind data for the first part of this century north of California, they were unable to determine how far north this decline in summer upwelling winds extended. From Fig. 2*b*, it seems that this decline in the first part of this century was limited to the three southernmost stations. There is no marked change in alongshore wind behavior during El Niño events during summer, in contrast with the strong effects observed in winter at the four northern stations. This behavior is consistent with the fact that strong teleconnections conveying El Niño effects to extratropical northern latitudes occur only during the winter half of the year (Horel and Wallace 1981), a time when Westerlies are shifted sufficiently southward to blow over the equatorial heat source region and pick up the El Niño signal.

The 1-month lagged autocorrelation of the alongshore wind stress at these stations (Fig. 3) provides a measure of the memory of the wind on a 1-month time scale. In general, Station C showed the lowest 1-month lagged autocorrelation. At higher latitudes, e.g., Station A, the highest autocorrelation occurred in late fall whereas south of Station C, the autocorrelation generally rose, especially during summer. These persistence features could be explained by the dominance of the Aleutian Low pressure system at high latitudes during winter and the dominance of the North Pacific Subtropical High pressure system at the lower latitudes during summer.

EOF analysis of alongshore wind stress

EOF analysis (also known as principal components analysis) is now widely accepted as the most efficient method for compressing meteorological and oceanographic data (Preisendorfer 1988). This method usually reveals the dominant correlation patterns in the data readily. The alongshore wind stress w at station i and time t is decomposed into a sum of EOFs:

$$[1] \qquad w(i,t) = \sum_{n=1}^{M} a_n(t) e_n(i)$$

where e_n are the EOFs and a_n are the corresponding temporal amplitudes, with n denoting the mode number. The alongshore wind stress due to mode n is described by the product $a_n(t)e_n(i)$, with $a_n(t)$ determining the strength of mode n at time t and $e_n(i)$ giving the strength of mode n at station i. The modes are arranged with the first mode accounting for the largest amount of variance in w, the second mode accounting for the second largest amount of variance, etc. Before performing the EOF analysis, w at each station was normalized by the removal of its mean and division by its standard deviation.

For winter wind stress, EOF analysis showed that the first mode contained 45% of the variance and the second mode 33% of the variance. The first mode (Fig. 4) showed correlation of the alongshore winds along the entire west coast, with the correlation highest for the northernmost five stations (A–E). In contrast, the second mode (Fig. 4) showed an anticorrelation between the four northern and the four southern stations. Thus when the temporal amplitude $a_2(t)$ is positive, the product $a_2(t)e_2(i)$ in Eq. [1] is positive for the four northern stations and negative for the four southern stations, implying upwelling at the northern stations and downwelling at the southern stations. For $a_2(t)$ negative, the situation is reversed. In Fig. 5, the mode 1 temporal amplitude $a_1(t)$ generally dropped substantially during El Niño events, suggesting winter coastal downwelling (or weakened upwelling) along the west coast during El Niño events. Meanwhile, $a_2(t)$ shows a long-term decline over nearly a century, so that $a_2(t)e_2(i)$ implies a gradual increase in downwelling (or decrease in upwelling) along the northern stations, and an increase in upwelling (or decrease in downwelling) along the southern stations during

Fig. 4. First two EOF modes e_n for the winter alongshore wind stress at Stations A–H. The wind stress at each station was normalized with respect to its standard deviation.

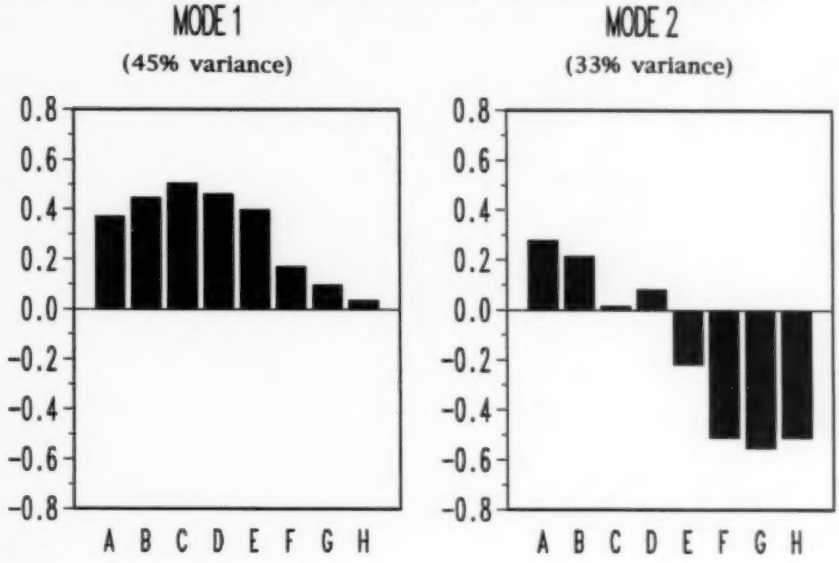

Fig. 5. Temporal amplitude a_n for the first two EOF modes for winter alongshore wind stress at Stations A–H.

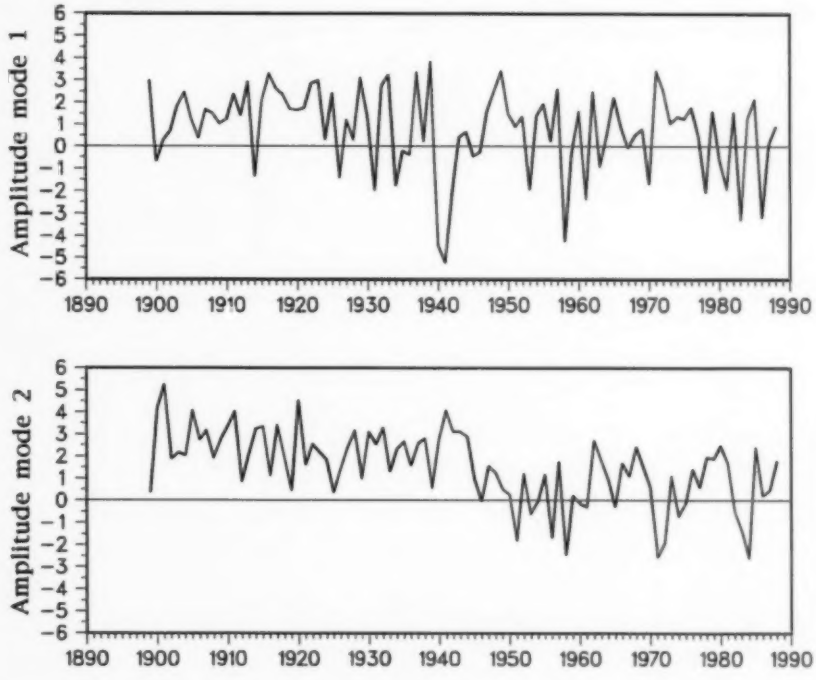

winter. Cayan (1980) computed the EOF of surface air temperature and precipitation along the west coast of the United States during winter. Interestingly, both of his mode 1 EOFs (for air temperature and for precipitation) showed the variability to be of the same sign all along the coast, while both of his mode 2 EOFs showed the variability north of about 40°N to be opposite in sign to the variability to the south. Hence, Cayan's first two EOF modes have structures similar to our EOF modes of alongshore wind stress.

Fig. 6. First two EOF modes e_n for summer alongshore wind stress at Stations A–H.

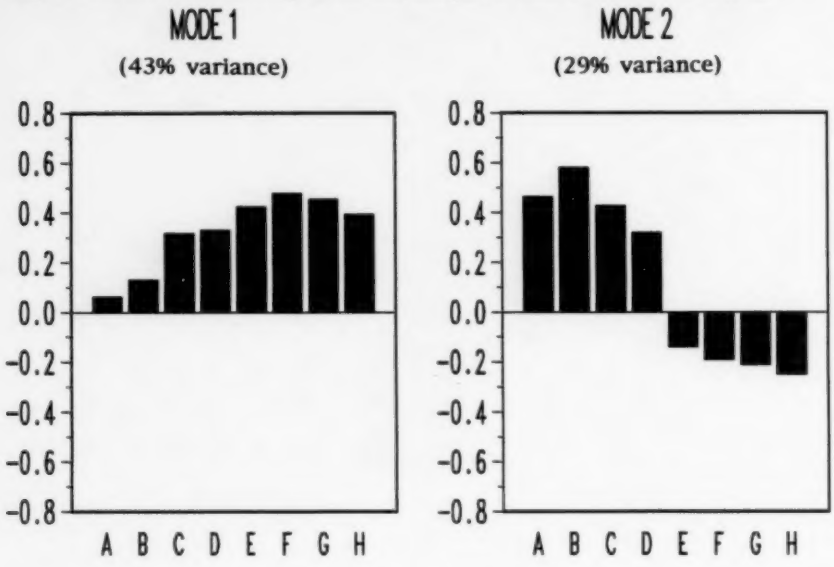

Fig. 7. Temporal amplitude a_n for the first two EOF modes for summer alongshore wind stress at Stations A–H.

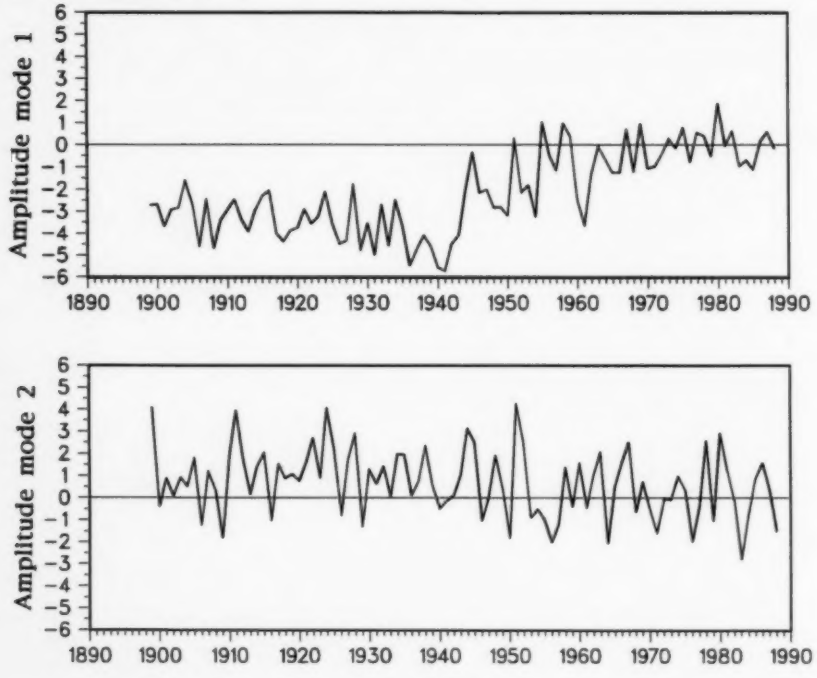

For summer wind stress, EOF analysis showed that the first and second modes contain, respectively, 43 and 29% of the variance. The first mode (Fig. 6) continues to show all eight stations positively correlated, although the highest correlation has shifted to the southernmost four stations. This shift in the correlation pattern along the coast is likely the result of the weakening and recession of the Aleutian Low and the strengthening and northward progression of the North Pacific Subtropical High as summer arrives. The second mode during summer (Fig. 6) resembles the second mode during winter (Fig. 4) in having an anticorrelated pattern, although the highest correlation

region has shifted from the southern four stations to the northern four stations. The mode 1 temporal amplitude a_1 shows a long-term decline from 1899 to 1941, followed by a long-term increase until the 1980s (Fig. 7). This pattern implies that in general, summer upwelling declined during the first four decades of this century and then increased for the next four decades.

During autumn, the anticorrelated pattern (not shown) actually edged out the correlated pattern to become the dominant mode as it accounted for 38% of the total variance (vs. 35% for the correlated pattern).

Next, we calculated the correlation coefficient between the Southern Oscillation Index (SOI) (as defined by Chelliah 1990, based on the normalized sea level pressure at Tahiti minus that at Darwin) and EOF temporal amplitudes a_n for seasonal alongshore wind stress. The winter SOI is correlated with the winter a_1, with a correlation coefficient of 0.50, significant at the 99.99% level (with the degrees of freedom estimated by the method of Davis (1976) and the significance level, at which the null hypothesis of zero correlation is disproved, estimated from subroutine PEARSN in Press et al. (1986)). The correlation is consistent with our finding in Fig. 5 that during an El Niño event, there is increased downwelling (or decreased upwelling) along the entire west coast during winter, especially at the northern stations. During spring, the correlation coefficient between SOI and a_1 dropped to 0.21, significant at the 94% level. No other correlations between SOI and a_1 or a_2 for the four seasons were above the 90% significance level. Thus, El Niño exerts influence on west coast upwelling/downwelling during winter and weakly during spring, but not during summer or autumn. The behavior is consistent with the fact that strong teleconnections conveying El Niño effects to extratropical northern latitudes occur only during the winter half of the year, as pointed out in the previous section.

Relation of wind to sea level, temperature, and salinity off British Columbia

The 1-month lagged autocorrelation of Victoria sea level peaks in summer (Fig. 8), which coincides with the poorest correlation between sea level and Station C alongshore wind stress (Fig. 8). Except during the summer, the correlation between sea level and alongshore wind stress off southern British Columbia was generally high, in contrast with the poor correlation off southern California (Strub et al. 1987). The correlation between Victoria sea level and Station C wind stress in Fig. 8 (plotted without the negative sign) was consistent with high sea level concurring with winds favorable to coastal downwelling and low sea level concurring with upwelling winds. The low correlation during summer could be explained by the fact that the Coastal Current immediately off Vancouver Island during this time is buoyancy-driven rather than wind-driven (Thomson 1981; Hickey et al. 1991), hence the drop in the correlation between coastal sea level and local wind. With the increased stability of the wind system to the south during summer (e.g., see the autocorrelation curve for Station E in Fig. 3), this wind forcing in the southern

Fig. 8. Correlations between Victoria sea level and the Station C alongshore wind stress at given months of the year (solid curve) (where the negative sign of the correlation has been omitted). The broken curve shows the 1-month-lagged autocorrelation of Victoria sea level where, e.g., the plotted April value is the correlation between the April and the May sea level values. The solid curve used sea level data during 1909–1993 whereas the broken curve used sea level and wind stress data during 1909–1988.

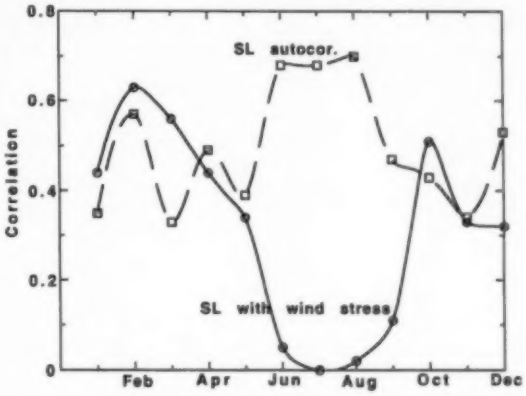

region could also propagate sea level anomalies northward into British Columbian waters by coastal trapped waves.

Correlations between the seasonal alongshore wind stress at Station C and the seasonal sea surface temperature and salinity at Amphitrite Point were computed for the period 1934–1988. In winter, a correlation of −0.63 (significant at the 99.99% level) was found between alongshore wind stress and coastal temperature. The correlation dropped to −0.27 (significant at 95%) in spring, becoming insignificant in summer, before recovering to −0.42 in autumn (significant at 99%). Hence, the strongest link between alongshore wind and coastal temperature occurred in winter, when downwelling winds produced higher coastal temperatures. There is also an effect from the high correlation between strong downwelling winter winds (intensified Aleutian Low) and the occurrence of El Niño (Emery and Hamilton 1985) that introduces anomalous warm northward advection along the west coast, resulting in higher coastal temperatures.

Between alongshore wind stress and coastal salinity, the correlation was insignificant in both fall and winter, but rose to 0.62 (significant at 99.99%) in spring, before dropping to 0.32 (significant at 98%) in summer. Thus, the strongest link between alongshore wind and coastal salinity occurred in spring, when upwelling winds brought up the more saline subsurface water, before coastal salinity became strongly influenced by river runoff during summer.

Upwelling and fisheries along the west coast

Off British Columbia

Off the west coast of Vancouver Island, alongshore winds blow toward the equator during the summer. These winds favor upwelling along the seaward margin of the continental

Fig. 9. Scatter plot of the summer alongshore wind stress (in dynes/cm^2) at Station C (off southwestern British Columbia) versus sardine fatness from 1925 to 1946. The correlation is +0.50 (significant at the 93% level).

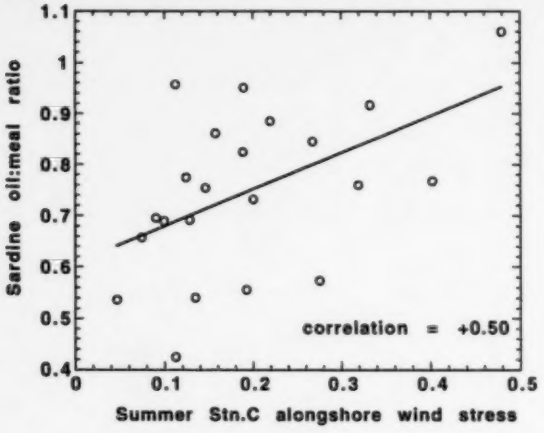

Fig. 10. Scatter plot of the summer alongshore wind stress (in dynes/cm^2) at Station C (off southwestern British Columbia) vs. the condition factor of age-5 herring from 1929 to 1988 (with 10 missing data). The correlation is +0.35 (significant at the 95% level).

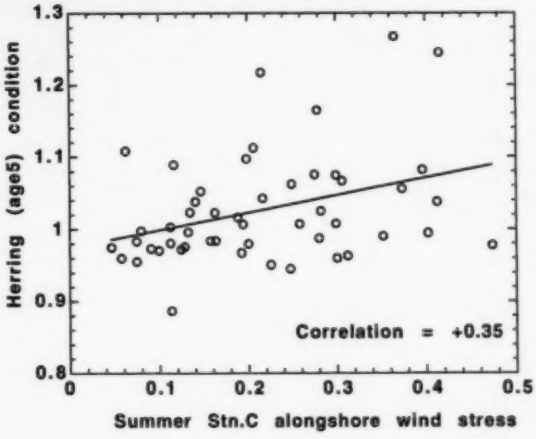

shelf (Thomson 1981), and in the Juan de Fuca eddy (Freeland and Denman 1982). This upwelling stimulates primary and secondary production, in the form of copepods and euphausiids (Robinson et al. 1993), which in turn are eaten by offshore herring stocks (Hart 1973), and historically were eaten by migratory sardines that were abundant off British Columbia in the summer in the 1930s and 1940s (Hart and Wailes 1932). Ware and Thomson (1991) found that when sardine were fished in British Columbia (from 1925 to 1946), their body fatness was positively correlated with the salinity of the mixed layer in summer and negatively correlated with sea level (these variables explained 60% of the variance in the sardine fatness time series). Ware and Thomson argued that a high summer salinity (and low sea level) indicates more upwelling, a higher nutrient load in the euphotic zone which, in turn, stimulates diatom and zooplankton production, and provides better feeding conditions for planktivores such as sardine and herring (Robinson et al. 1993).

We tested this hypothesis by determining the correlation between sardine fatness (and herring condition factor at the end of the summer) with the strength of the upwelling favorable winds from June to August with no lag. There was a significant positive correlation between summer alongshore wind stress at Station C off British Columbia and sardine fatness (Fig. 9) and the condition factor of age-5 herring (Fig. 10). We obtained similar results for age-4 and age-3 herring. These findings highlight the degree to which wind-induced upwelling can elevate the physiological condition of planktivorous fish, like herring and sardines, and allow us to extend the mechanism proposed by Ware and Thomson (1991) to another species (herring) for a much longer period of time (1929–1988).

Off southern California

The southern California Bight and Baja California are important spawning areas for the dominant pelagic fish species in the California Current region. In a detailed factor analysis of oceanographic and biological data collected in this region in 1969, Hemingway (1979) found that the standing stock of phytoplankton was strongly correlated with upwelling in April, May, and June. Consistent with Hemingway's finding, Ware and Thomson (1991) found a positive correlation between the interannual variation in second quarter wind speeds in the southern California Bight region and the abundance of diatoms measured at Scripps pier over a 26-year period. Our estimate of spring (March, April, May average) alongshore wind stress at Station F (32.5°N) is highly correlated with the estimate of second quarter (i.e., spring) wind speeds (at 30°N) used by Ware and Thomson, with a correlation coefficient of 0.61, significant at 96%. Using the same time series of diatom abundance, we expected, and subsequently found, a correlation of +0.46 (significant at 94%) between our estimates of upwelling favorable wind stress at Station F in the spring and diatom abundance. There is also a weak correlation of +0.34 (significant at 84%) between our estimate of spring wind stress and Smith and Eppley's (1982) 60-year proxy time series of second quarter primary production. These two independent tests confirm the efficacy of our wind stress time series and provide additional support for the idea that interannual variations in upwelling favorable winds produce changes in primary production in the southern California Current region.

Cury and Roy (1989) and Ware and Thomson (1991) discussed how such interannual variations in food supply can affect the productivity of pelagic fish stocks in upwelling regions. Ware and Thomson also drew attention to the strong relaxation in wind speed that occurred from 1920 to 1940 and the impact it may have had on the productivity of the southern California marine ecosystem. This relaxation of upwelling in the 1920s and 1930s is also a distinct feature of our wind stress time series. After 1940, there was a striking rise in wind stress which, up until at least 1988, has generally been above the long-term

mean. Since the mid-1970s the region of most intense summer upwelling has shifted south from Cape Mendocino (Station E) to the southern California Bight (Station F) and along Baja California (Station G). We note in passing that this shift in the west coast upwelling centre may have some causal connection with the resurgence of the California Pacific sardine population, which began about the same time (Barnes et al. 1992).

Summary and conclusion

By computing the alongshore geostrophic wind stress from the NCAR monthly air pressure data, a monthly index of coastal upwelling/downwelling has been constructed for eight stations along the west coast of North America from Alaska to Baja California for 1899–1988. While agreeing well with the Bakun index (available since 1946) in recent decades, our index extends much further back in time. For winters since around 1940, downwelling has intensified at the two northernmost stations (Alaska and northern British Columbia), and upwelling has increased at the two southernmost stations (Baja California). El Niño events were found to induce winter downwelling at the four coastal stations located north of 40°N. During summer, upwelling has increased since around 1940 at the six southernmost stations (from southern British Columbia to Baja California), most notably around California. From 1899 to 1940, there was a decline in upwelling at the three southernmost stations (from southern California to Baja California).

EOF analysis of the upwelling/downwelling at the eight stations showed that the first mode had all stations in-phase, while the second mode had the four northern stations out-of-phase with the four southern stations. Correlation of the EOF time series with the SOI also showed that El Niño exerts influence on west coast upwelling/ downwelling during winter and weakly during spring, but not during summer or autumn. For further work on El Niño related changes in the global wind-induced upwelling, see Xie and Hsieh (1995).

Off southern British Columbia, correlation between coastal sea level and alongshore wind stress was quite high except during summer, when the Coastal Current is buoyancy-driven rather than wind-driven. The correlation indicates that downwelling winds occur with high sea level. Similarly, correlation between sea surface temperature and alongshore wind stress was highest during winter, with downwelling winds concurring with high temperature. In contrast, correlation between salinity and alongshore wind stress was insignificant in both autumn and winter, but was highest in spring, with upwelling winds concurring with higher salinity.

Off British Columbia (Station C), summer alongshore wind stress was positively correlated with both the sardine fatness and the condition factor of herring. Off southern California Bight (Station F), there was also a positive correlation between spring alongshore wind stress and diatom abundance and between wind and second quarter primary production.

Acknowledgements

We thank Liusen Xie for generating the alongshore wind stress data from the NCAR pressure data file. W. Hsieh was supported by the Canadian Department of Fisheries and Oceans and NSERC subvention grants and by NSERC research grants.

References

Barnes, J.T., Jacobson, L.D., McCall, A.D., and Wolf, P. 1992. Recent population, trends and abundance estimates for the Pacific sardine (*Sardinops sagax*). Calif. Coop. Oceanic Fish. Invest. Rep. **33**: 60–75.

Cayan, D.R. 1980. Regimes and events in recent climate variables. CalCOFI Rep. **21**: 90–101.

Chelliah, M. 1990. The global climate for June–August, 1989: A season of near normal conditions in the tropical Pacific. J. Clim. **3**: 138–162.

Cury, P., and Roy, C. 1989. Optimal environmental window and pelagic fish recruitment success in upwelling areas. Can. J. Fish. Aquat. Sci. **46**: 670–680.

Davis, R.E. 1976. Predictability of sea surface temperature and sea level pressure anomalies over the north Pacific Ocean. J. Phys. Oceanogr. **6**: 249–266.

Emery, W.J., and Hamilton, K. 1985. Atmospheric forcing of interannual variability in the northeast Pacific Ocean: connections with El Niño. J. Geophys. Res. **90**: 857–868.

Freeland, H.J., and Denman, K.L. 1982. A topographically controlled upwelling center off southern Vancouver Island. J. Mar. Res. **40**: 1069–1093.

Hamilton, K. 1988. A detailed examination of the extratropical response to tropical El Niño/Southern Oscillation events. J. Clim. **8**: 67–86.

Hart, J.L. 1973. Pacific fishes of Canada. Can. Bull. Fish. Aquat. Sci. **180**.

Hart, J.L., and Wailes, G.H. 1932. The food of the pilchard off the coast of British Columbia. Contrib. Can. Biol. Fish. 7-19 Ser. A, No. 16. pp. 247–254.

Hemingway, G.T. 1979. A description of the California current ecosystem by factor analysis. Calif. Coop. Oceanic Fish. Invest. Rep. **20**: 164–177.

Hickey, B.M., Thomson, R.E., Yih, H., and LeBlond, P.H. 1991. Velocity and temperature fluctuations in a buoyancy-driven current off Vancouver Island. J. Geophys. Res. **96**: 10,507–10,538.

Horel, J.D., and Wallace, J.M. 1981. Planetary-scale atmospheric phenomena associated with the southern oscillation. Mon. Weather Rev. **109**: 813–829.

Large, W.G., and Pond, S. 1981. Open ocean momentum flux measurements in moderate to strong winds. J. Phys. Oceanogr. **11**: 324–336.

Mysak, L.A. 1986. El Niño, interannual variability and fisheries in the northeast Pacific Ocean. Can. J. Fish. Aquat. Sci. **43**: 464–497.

Preisendorfer, R.W. 1988. Principal component analysis in meteorology and oceanography. Elsevier, New York, N.Y.

Press, W.H., Flannery, B.P., Teukolsky, S.A., and Vetterling, W.T. 1986. Numerical recipes. Cambridge University Press, Cambridge.

Quinn, W.H., Zopf, D.O., Short, K.S., and Yang, R.T.W.K. 1978. Historical trends and statistics of the southern oscillation, El Niño, and Indonesian droughts. Fish. Bull. **76**: 663–678.

Quinn, W.H., Neal, V.T., and Antunez de Mayolo, S.E. 1987. El Niño occurrences over the past four and a half centuries. J. Geophys. Res. **92**: 14,449–14,462.

Robinson, C.L.K., Ware, D.M., and Parsons, T.R. 1993. Simulated annual plankton production in the northeast Pacific Coastal Upwelling Domain. J. Plankton Res. **15**: 161–183.

Smith, P.E., and Eppley, R.W. 1982. Primary production and the anchovy population in the southern California bight: comparison of time series. Limnol. Oceanogr. **27**: 1–17.

Strub, P.T., Allen, J.S., Huyer, A., and Smith, R.L. 1987. Large-scale structure of the spring transition in the coastal ocean off western North America. J. Geophys. Res. **92**: 1527–1544.

Thompson, K.R., Marsden, R.F., and Wright, D.G. 1983. Estimation of low-frequency wind stress fluctuations over the open ocean. J. Phys. Oceanogr. **13**: 1003–1011.

Thomson, R.E. 1981. Oceanography of the British Columbia coast. Supplies and Services Canada, Ottawa, Ont.

Thomson, R., and Tabata, S. 1981. Sea levels in the eastern Pacific Ocean. JSC/CCCO Workshop on Time Series of Ocean Measurements, Tokyo (11–15 May, 1981).

Trenberth, K.E., and Paolino, D.A., Jr. 1980. The Northern Hemisphere sea-level pressure data set: trends, errors and discontinuities. Mon. Weather Rev. **108**: 855–872.

Trenberth, K.E., and Paolino, D.A., Jr. 1981. Characteristic patterns of variability of sea level pressure in the Northern Hemisphere. Mon. Weather Rev. **109**: 1169–1189.

Ware, D.M., and Thomson, R.E. 1991. Link between long-term variability in upwelling and fish production in the northeast Pacific Ocean. Can. J. Fish. Aquat. Sci. **48**: 2296–2306.

Wright, D.G., and Thompson, K.R. 1983. Time-averaged forms of the nonlinear stress law. J. Phys. Oceanogr. **13**: 341–345.

Xie, L., and Hsieh, W.W. 1991. Upwelling winds along the west coast of North America, 1899–1988. Dep. Oceanogr. Manuscr. Rep. No. 58, University of British Columbia, Vancouver, B.C.

Xie, L., and Hsieh, W.W. 1995. The global distribution of wind-induced upwelling. Fish Oceanogr. **4**: 52–67.

Estimation of in-river fish passage using a combination of transect and stationary hydroacoustic sampling

Sarath G. Banneheka, Richard D. Routledge, Ian C. Guthrie, and James C. Woodey

Abstract: We describe a hydroacoustic technique that uses both transect and stationary sampling to estimate numbers of fish migrating in a river. The technique includes refinements and additions to one developed by the International Pacific Salmon Fisheries Commission to estimate sockeye (*Oncorhynchus nerka*) and pink salmon (*Oncorhynchus gorbuscha*) migrations in the Fraser River. The estimator is independent of the actual shape of the effective acoustic beam and the distribution of target strengths when the same hydroacoustic equipment and settings are used for both types of soundings. Thus, the method shares with the duration-in-beam method the advantages that equipment calibration requirements are minimal and that estimates remain valid when fish sizes vary over a wide range. We also provide formulae for the variance of the abundance estimate and illustrate the methods with example calculations of daily fish passage in the Fraser River at Mission, British Columbia. A correction procedure is proposed to compensate for bias arising from violation of the assumption that fish speed is negligible relative to boat speed.

Résumé : Nous décrivons une technique hydroacoustique qui fait appel à la fois au transect et à l'échantillonnage stationnaire pour estimer le nombre de poissons qui migrent dans un cours d'eau. Cette technique raffine et enrichit une méthode mise au point par la Commission internationale des pêcheries de saumon du Pacifique pour estimer l'ampleur des migrations du saumon rouge (*Oncorhynchus nerka*) et du saumon rose (*Oncorhynchus gorbuscha*) dans le Fraser. L'estimateur est indépendant de la forme réelle du faisceau acoustique effectif et de la distribution de la force du signal de retour lorsqu'on utilise le même matériel hydroacoustique et les mêmes réglages pour les deux types de mesures. La méthode présente donc, comme celle qui mesure la durée de passage dans le faisceau, l'avantage de nécessiter un étalonnage minimal du matériel et de donner des estimations valides même si la taille des poissons varie dans une fourchette très large. Nous présentons aussi des formules pour exprimer la variance de l'estimation de l'abondance et nous illustrons les méthodes avec des exemples de calcul du nombre de poissons qui passent dans le Fraser à Mission (en Colombie-Britannique) en une journée. Nous proposons une méthode de correction pour compenser le biais lié au non-respect de l'hypothèse selon laquelle la vitesse du poisson est négligeable par rapport à celle du bateau.
[Traduit par la Rédaction]

Introduction

For intensive management of fisheries that target large salmon runs, in-season estimates of daily escapement from commercial fishing areas and into natal rivers are critically important (Woodey 1987). These estimates contribute to the in-season assessment of total returns and allow managers to implement fishing regulations with greater certainty of achieving goals for spawning escapement and catch allocation. In-river hydroacoustic sampling is an important tool for making these estimates.

Most hydroacoustic surveys attempt to estimate the number of fish in a population that has negligible migration in or out of the survey region. In essence, these surveys extrapolate the number of fish counted in the acoustic beam to the entire survey region according to the ratio between the volume of water in the survey region and the volume sampled by the acoustic beam (e.g., Thorne and Dawson 1974). A similar method was used by Skalski et al. (1993) to estimate fish passage at a dam using a weighted sum of the numbers of fish ensonified by a beam at different depth ranges. The weights are determined by the dimensions of the beam and the dam passage ways.

A major difficulty with these methods is that the dimensions of the acoustic beam must somehow be estimated. Not only is the shape of the beam complicated by interference patterns that can produce side lobes (Clay and

Received December 23, 1993. Accepted July 14, 1994.
J12215

S.G. Banneheka and R.D. Routledge. Department of Mathematics and Statistics, Simon Fraser University, Burnaby, BC V5A 1S6, Canada.
I.C. Guthrie and J.C. Woodey. Pacific Salmon Commission, 600-1155 Robson Street, Vancouver, BC V6E 1B5, Canada.

Medwin 1977, pp. 144–146; MacLennan and Simmonds 1992, pp. 13–20; and references therein), but also the effective dimensions of an acoustic beam vary with the size, orientation, and swimming movements of fish that encounter the beam (Clay and Medwin 1977, p. 245; MacLennan and Simmonds 1992, p. 137; and references therein). Dependence on estimates of beam width also creates problems with enumerating populations that have a wide distribution of body sizes.

Usually the effective beam is assumed to be a simple cone. Crittenden et al. (1988), Thorne (1988), and others referred to therein described an empirical in situ method for simplifying the estimation of sampling volume. With this method, the time it takes fish to pass through a beam projected from a boat moving at a known velocity is used to estimate the effective beam diameter at a given depth. The method is based on the linear relationship between the number of successive echoes from individual fish (duration-in-beam) and the distance from the transducer to the fish. Crittenden et al. (1988) proposed a minimum variance unbiased estimate for the sine of the angle of the assumed cone-shaped beam by means of weighted regression through the origin. Both methods assume that fish swimming speed is small compared with the boat's speed, but Crittenden et al. (1988) provided a means for permitting variability in target strengths. Kieser and Ehrenberg (1990) also permitted this variability, through a model whose utilization requires separate measurements on the beam characteristics.

The purpose of this paper is to present a hydroacoustic sampling technique that captures the advantages of the duration-in-beam method, but that is particularly suitable for making in-river estimates of the abundance of migrating fish. The technique was developed by the International Pacific Salmon Fisheries Commission (IPSFC) in 1977 and used by the IPSFC from then until 1986 and by its successor, the Pacific Salmon Commission, since then. The application was the estimation of abundance of Fraser River sockeye (*Oncorhynchus nerka*) and pink salmon (*Oncorhynchus gorbuscha*) that pass Mission, British Columbia, during their upstream migration to spawning grounds in the Fraser River watershed (Woodey 1987). We have refined the calculation methods to improve the statistical properties of the estimate and have developed formulae for estimating the variance and bias of the estimate. With this method, a boat-mounted echo sounder that conducts shore-to-shore transects across the river is used to estimate the density of fish targets per depth interval. Stationary soundings provide an estimate of the amount of time it takes fish in each depth interval to swim through the beam. Combining these estimates yields estimates of the number of fish that pass the transect location per second. The method eliminates the need to estimate beam dimensions directly, as long as the same hydroacoustic equipment and settings are used for both the transect and stationary soundings. The sampling techniques used by the Pacific Salmon Commission are further described in the following section.

Methods

The hydroacoustic program conducted by the Pacific Salmon Commission in 1993 at Mission, British Columbia, is briefly described below. Minor technical aspects of the methods varied over time as, for example, the abating spring freshet led to declining river depths. The specific methods described below were applied on August 31. Data from this day are later used in a numerical example illustrating the calculations.

Equipment

The equipment that was used for both the transect and stationary soundings was installed on a 5.8-m aluminum vessel. A BioSonics model 105 echo sounder operating at a frequency of 50 kHz was used with a 34° (full angle) circular-beam transducer. The transducer was mounted in an aluminum stabilizer and towed from a davit 1.1 m from the starboard gunnel at a depth of 0.5 m. Settings for the equipment included a pulse rate of 15.3 ensonifications·s^{-1} and, to compensate for two-way spreading loss, a time-varied gain of 40 log R (where R = distance from transducer to target). To record the soundings, a BioSonics model 111 thermal chart recorder was used. It was set to record a 15-m depth range with 5-m depth intervals marked. This depth range encompassed the maximum river depth at the site, except during spring freshet, when the depth range was increased to 20 m. Paper speed for the recorder was 0.478 mm·s^{-1}. The equipment was serviced annually, and each day the crew checked the settings to ensure that they had not been accidentally changed.

Site

The data collection site was about 1 km upstream of the railway bridge across the Fraser River at Mission, British Columbia. River width at this site is about 437 m. This location has been used by the IPSFC and the Pacific Salmon Commission for echo sounding since 1977 because it satisfies several criteria. First, fish actively migrate at this location: the site is in a straight stretch of the river with no eddies or deep pools where fish can hold or mill about. Second, it has a rapid drop-off to deep water on both shores: there are only a few metres along each shore that cannot be sampled, and few sockeye salmon are believed to migrate this close to shore. Third, the smooth bottom is unlikely to acoustically obscure fish. Fourth, the flow of the river here is relatively even and moderately slow so that a small boat can cross the river at suitable speeds for echo sounding without being swept downstream. Finally, the site is close to a road, dock, and fuel source.

Field sampling

Two data collection activities were performed (Fig. 1). The first consisted of 215 shore-to-shore transect soundings across the river, perpendicular to the direction of fish movement. All transects used the same transect line, boat speed, and echo sounder settings. These transect soundings took about 5 min each to complete.

Second, nine stationary soundings were conducted along the transect line, using the same equipment and settings used for the transect soundings. These soundings were taken at scheduled times, with one located in each of the south, centre, and north sections of the transect line during each 8-h shift. The boat was anchored during these soundings.

Hydroacoustic data were collected over a 24-h cycle, from 5:00 a.m. to 4:59 a.m. the next morning. Transect soundings were conducted for about 18 h and stationary soundings for about 3 h. Other activities such as refuelling, changing crews, and setting anchors for the stationary soundings took up the remaining 3 h.

Data processing

After the 24-h recording session, the resulting echogram was interpreted by a trained hydroacoustics biologist. For each transect, the number of fish targets in each depth stratum was counted. For each stationary sounding, the widths of each target in each depth stratum were measured using a micrometer. Periodically, the paper speed of the recorder was verified, using marks that the echo sounder recorded on the echogram each minute.

Assumptions

(1) If there are fish present that are not part of the population of interest (e.g., other species), then these can either be distinguished on the paper record or otherwise removed from the estimates. (In the Fraser River programme, the number of resident (i.e., nonmigratory) fish was estimated by sampling when few salmon were in the river (i.e., before or after salmon runs or after commercial gillnet fisheries downstream). The target density associated with resident fish was then removed from the daily total target density to obtain an estimate of daily salmon density, which was used to estimate the salmon population. To determine the sockeye salmon component in this estimate, the species composition of these comigrating salmon was obtained from a test fishery using a variable-mesh gill net that was conducted downstream of the Mission site.)

(2) The beam has circular horizontal cross sections. (This assumption is less stringent than the more common requirement that the beam is a cone and is required because the presence of small side lobes near the transducer caused by local interference patterns (Clay and Medwin 1977, pp. 144–146; MacLennan and Simmonds 1992, pp. 13–20; and references therein) cannot be ignored, particularly in the shallow water near the shorelines at the sampling site.)

(3) The hydroacoustic beam extends to the river bottom. (In the Mission echo-sounding programme, the depth range recorded by the echo sounder encompassed the maximum depth encountered at the study site.)

(4) The records of fish echos do not overlap on the paper record. (Schooling or heavy runs could generate high local abundances that would lead to substantial numbers of overlapping records. In extreme cases, fish density can be high enough to extinguish the bottom echo signal (Foote 1990). In the present application, the local abundance of sockeye salmon was not large enough to cause significant overlapping of fish echoes.)

(5) Fish echos can be distinguished from the background noise. (The ability to distinguish fish from noise is determined by the experience of the interpreter and the selection of criteria that can be consistently applied to determine whether a target is "real" (e.g., three successive echoes).)

(6) Fish are distributed randomly with a uniform probability density over depth within each stratum. (The validity of this assumption, along with the following one, can be promoted by choosing suitably narrow depth strata.)

Fig. 1. Schematic diagram of the hydroacoustic sampling site on the Fraser River at Mission. Sampling was conducted over a 24-h period, from 5:00 a.m. to 4:59 a.m. the next morning. On the single transect line, 215 shore-to-shore transects were performed, with nine stationary soundings. River flow is into the plane of the paper, while fish movement is out, toward the reader.

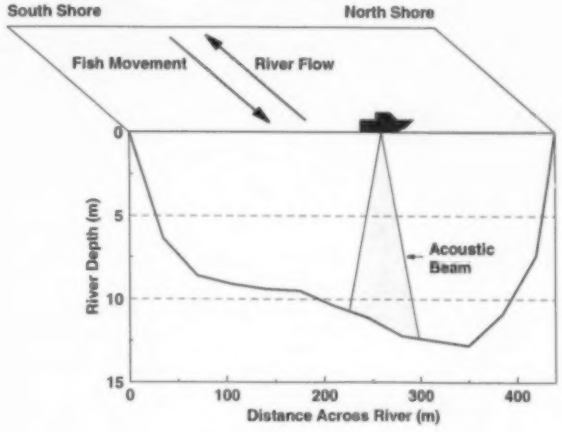

(7) Fish speeds are generated independently according to some common distribution which does not depend on depth within each stratum.

(8) Fish swimming speed is negligible relative to the boat speed. (This assumption will later be relaxed.)

(9) Fish behaviour is not altered by the survey vessel. (Although research concerning this issue is lacking, sockeye salmon likely swim too deep in the turbid waters of the Fraser River to be very susceptible to boat avoidance. For example, few migrating sockeye at the study site swim at depths above 3 m (Levy et al. 1991), and few are caught near the surface in test fishing nets downstream of Mission.)

(10) There are few fish swimming close enough to the surface and to the transducer to go undetected. (Since the large majority of sockeye at the study site migrate at depths below 3 m (Levy et al. 1991), and the minimum detection depth is likely between 1.5 and 2.5 m (R. Kieser, Pacific Biological Station, Nanaimo, BC V9R 5K6, personal communication), it is likely that few sockeye salmon were undetected.)

(11) The fish swim directly upriver. (A site should be chosen that minimizes opportunities for fish to mill about.)

(12) Fish that cross the beam in a stationary sounding are independently and uniformly distributed across the beam. (This is essentially equivalent to a key assumption in Crittenden et al. (1988).)

(13) The observations from both transect and stationary soundings, although typically systematically sampled over time, can be viewed as being randomly sampled over time. (If, for example, there are substantial daily cycles, departures from this assumption could be minimized by stratifying over shorter time intervals. Failure to do so would inflate the estimated variance.)

Fig. 2. Distance that a fish swims to cross through the acoustic beam (C) can be calculated from the radius $r(Z)$ of the beam at depth Z and from the half angle θ formed in the centre of the beam.

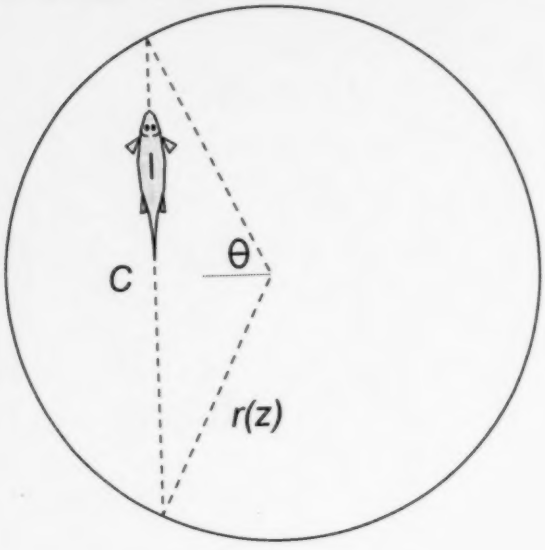

(14) The transect and stationary soundings sample fish with the same characteristics such as speed, size, depth, and orientation. (The validity of this assumption can be promoted by ensuring that the stationary soundings are taken at times that are interspersed spatially and temporally with the transect soundings.)

(15) The target widths of individual fish in the stationary soundings for individual fish are generated independently. (This assumption would be violated if, for example, fish speeds displayed a strong diurnal cycle, and the results were pooled over an entire day. The measured widths of adjacent targets, coming from roughly the same time of day, would then be positively correlated.)

Estimator

The estimator is derived as follows.

(1) Within each stratum, the rate of upstream migration is shown to equal the number of fish per unit upstream distance times the mean upstream speed (formula [4]).

(2) Mean fish speed is obtained from the stationary soundings as the ratio of harmonic mean chord length (distance that fish swim to cross the stationary beam as shown in Fig. 2) to a harmonic mean time. The harmonic mean is the inverse of the average of the inverses (formula [5]).

(3) The harmonic mean target width is shown to equal the paper speed times the harmonic mean time (formula [6]).

(4) The harmonic mean chord length is shown to equal the product of (*i*) the average beam diameter and (*ii*) a correction factor, $2/\pi$, which adjusts for the shorter swimming distances for fish that do not cross the centre of the beam. The factor $2/\pi$ is valid for any beam with circular horizontal cross-sections (formula [13]).

(5) The number of fish migrating upstream per second is then shown to equal the product of (*i*) the correction factor $2/\pi$, (*ii*) the paper speed, and (*iii*) the ratio of expected number of targets per transect to the harmonic mean target width (formula [23]).

(6) The number of fish migrating upstream per second is estimated by

$$\hat{R} = a\sum_i \bar{N}_i \bar{M}_i$$

where

$$a = \frac{2}{\pi} \times \text{paper speed of the recorder}$$

[1] $\bar{N}_i$ = sample average of number of targets per transect in the ith depth stratum

$\bar{M}_i$ = sample average of inverse target widths from the ith depth stratum.

(7) The variance of the estimated numbers of fish migrating per second is estimated by

$$\hat{\mathrm{V}}\mathrm{ar}(\hat{R}) = a^2 \sum_i \left(\frac{s^2_{N_i}}{n} \bar{M}_i^2 + \frac{s^2_{M_i}}{m_i} \bar{N}_i^2 - \frac{s^2_{N_i} s^2_{M_i}}{n m_i} \right)$$

where

n = total number of transect soundings

m_i = total number of targets in depth stratum i from the stationary soundings

[2] $s^2_{N_i}$ = sample variance of the number of targets per transect sounding in depth stratum i

$s^2_{M_i}$ = sample variance of the reciprocals of m_i target widths in depth stratum i from the stationary soundings.

Upstream migration rate

Suppose the water column is divided into several depth strata within each of which the number of fish per unit volume does not vary appreciably with depth. First, consider any depth stratum and assume that target strength is the same for each fish in the depth stratum.

Let R = number of fish migrating upstream per second in the depth stratum: the quantity to be estimated, α = width of the river, z_1 = depth at the top of the depth stratum, z_2 = depth at the bottom of the depth stratum, λ = average number of fish per unit volume in the depth stratum: unknown, and γ = maximum speed of fish (distance per second): an unknown constant.

Next, imagine a barrier across the river. At any given moment, which will be referred to as "the start", fish that are capable of crossing the barrier within one second from the start will be within a distance γ downstream from the barrier. The volume of the river section that contains these fish is $\alpha(z_2 - z_1)\gamma$ and the expected number of fish in this volume is $\lambda\alpha(z_2 - z_1)\gamma$. However, only a fraction of these fish cross the barrier within 1 s from the start because not all fish travel at the maximum speed γ. Let β = probability that a fish will cross the barrier within one second from the start. Then the expected number of fish that will cross the barrier within 1 s is

[3] $R = \lambda\alpha(z_2 - z_1)\gamma\beta.$

Calculation of β

Let D = distance from the fish to the barrier at the start: a random variable, S = speed of the fish: a random variable, and B = time taken by the fish to reach the barrier: a random variable.

Suppose that S has some probability density function $f_S(s)$ whose domain is $[0,\gamma]$. Over the small distance (γ) being considered, D will be essentially uniformly distributed in $[0,\gamma]$. Thus the probability density function of D is

$$f_D(d) = \frac{1}{\gamma}.$$

The variables D and S will also be essentially independent, with joint probability density function

$$\frac{1}{\gamma} f_S(s), \text{ for } d \text{ and } s \text{ both in } [0, \gamma].$$

Note that $B = D/S$, with B then restricted to the range [0,1]. Through standard transformation-of-variables methods, it can be proved that the probability density function of B is

$$f_B(b) = \frac{\mu_S}{\gamma}$$

where $\mu_S = E(S)$ is the mean fish speed. Now,

$$\beta = \Pr(B \le 1) = \int_0^1 f_B(b)db = \int_0^1 \frac{\mu_S}{\gamma} db = \frac{\mu_S}{\gamma}.$$

Substituting u_s/γ for β in formula [3] yields

[4] $R = \lambda\alpha(z_2 - z_1)\mu_S.$

This formula shows that the number of fish passing the barrier per second is equal to the number of fish per unit upstream distance $[\lambda\alpha(z_2 - z_1)]$ times the mean fish speed (μ_S). The next step is to calculate the mean fish speed in terms of quantities associated with stationary soundings.

Calculation of mean fish speed, μ_S

Consider a stationary sounding. Let Z be the random variable representing the depth of a target relative to the transducer. Assume that the horizontal cross section of the beam at depth z is a circle with radius $r(z)$. Now consider the fish that swim through the beam at depth Z. Suppose that S is the speed of the fish, C is the distance that a fish swims through the beam (chord length), and T is the time taken to do so. Speed is distance over time. However, mean fish speed is not equal to mean distance over mean time. Because C and S are independent, the mean speed can be obtained as

[5] $$\mu_S = E(S) = \frac{E\left(\frac{1}{T}\right)}{E\left(\frac{1}{C}\right)}.$$

This formula can also be written as

$$\mu_S = \frac{1/E\left(\frac{1}{C}\right)}{1/E\left(\frac{1}{T}\right)}.$$

This implies that mean fish speed is equal to the ratio of harmonic mean chord length to an harmonic mean time.

The next two subsections are devoted to obtaining expressions for the numerator and the denominator of formula [5].

Calculation of mean reciprocal time, $E(1/T)$

Let W = width of the target record in the echogram: a random variable, and p = paper speed of the recorder. Then, $W = Tp$. For notational convenience in the subsequent sections, let $M = 1/W$. Then,

[6] $$E\left(\frac{1}{T}\right) = pE\left(\frac{1}{W}\right) = pE(M).$$

This formula can also be viewed as

$$\frac{1}{E(1/W)} = \frac{p}{E(1/T)}$$

which means that the harmonic mean target width is equal to the paper speed times the harmonic mean time.

Calculation of mean reciprocal chord length, $E(1/C)$

Let Θ be the half angle that is formed in the centre of the horizontal cross section at depth Z by the chord that a fish travels in the beam (Fig. 2). Then, $C = 2r(Z)\sin(\Theta)$ and hence,

[7] $$E\left(\frac{1}{C}\right) = E\left[\frac{1}{2r(Z)\sin(\Theta)}\right] = E\left[\frac{1}{2r(Z)}\right]E\left[\frac{1}{\sin(\Theta)}\right].$$

Within each depth stratum, fish depths are distributed uniformly (assumption (6)). However, the sampling probability for a fish at depth z is proportional to $r(z)$. Hence for the sampled fish, the probability density function $f_Z(z)$ of Z is

[8] $$f_Z(z) = \frac{1}{\int_{z_1}^{z_2} r(z)dz} r(z).$$

Let

[9] δ = average diameter of the beam

$$= \frac{1}{z_2 - z_1}\int_{z_1}^{z_2} 2r(z)dz.$$

Formulae [8] and [9] lead to

[10] $$f_Z(z) = \frac{2}{\delta(z_2 - z_1)} r(z) \qquad \text{for } z_1 \le z \le z_2.$$

Then,

[11] $$E\left[\frac{1}{2r(Z)}\right] = \int_{z_1}^{z_2} \frac{1}{2r(z)} f_Z(z)dz = \frac{1}{\delta}.$$

Now let $f_\Theta(\theta)$ be the probability density function of Θ. It follows from assumption 9 (that fish do not respond to

the survey vessel) that fish that cross the beam do so along a line that is a uniformly distributed distance away from the beam centre. From this, it follows in turn through a change of variables that $f_\Theta(\theta)$ is proportional to $\sin(\theta)$. Then,

$$f_\Theta(\theta) = \frac{\sin(\theta)}{2}, \qquad \text{for } 0 \le \theta \le \pi$$

and

$$[12] \qquad E\left[\frac{1}{\sin(\Theta)}\right] = \int_0^\pi \frac{1}{\sin(\theta)} f_\Theta(\theta)\,d\theta = \frac{\pi}{2}.$$

Substituting formulae [11] and [12] in formula [7]:

$$[13] \qquad E\left(\frac{1}{C}\right) = \frac{\pi}{2}\frac{1}{\delta}.$$

Formula [13] can be written as $1/E(1/C) = 2\delta/\pi$. That is, the harmonic mean chord length is equal to the product of (i) the average beam diameter and (ii) a correction factor, $2/\pi$, which adjusts for the shorter swimming distances for fish that do not cross the centre of the beam. The factor $2/\pi$ is valid for any beam with circular horizontal cross sections.

Substituting formulae [5], [6], and [13] into formula [4] leads to

$$[14] \qquad R = \frac{2}{\pi} p\lambda\alpha(z_2 - z_1)\delta E(M).$$

This formula still contains quantities that are not readily estimable. The next subsection shows that the quantity $\lambda\alpha(z_2 - z_1)\delta$ is an estimable parameter arising from transect soundings.

Calculation of expected number of fish per transect

Let N = number of targets per transect in the depth stratum. Ignoring river bottom irregularities, edge effects near the shorelines, and fish less than the minimum detection distance from the transducer, the volume of the depth stratum that is ensonified by a transect sounding, v, can be approximated by

$$[15] \qquad v = \alpha\int_{z_1}^{z_2} 2r(z)dz = \alpha(z_2 - z_1)\delta.$$

Now consider an ideal situation where the boat is moving at such a speed that a transect sounding can be considered a snapshot across the river (assumption 8). Then, the expected number of fish that are ensonified during a transect sounding is

$$[16] \qquad E(N) = \lambda v = \lambda\alpha(z_2 - z_1)\delta.$$

However, in practice, there is a maximum feasible speed of the boat. Therefore the assumption of high boat speed introduces a bias to the estimator of $E(N)$ and thereby to the final estimator of R. This is discussed later in the "Bias" section.

Calculation of fish passage per second, *R*

Now we can combine formulae [14] and [16] to obtain R, the number of fish migrating upstream per second, in terms of estimable parameters as

$$[17] \qquad R = \frac{2p}{\pi}\lambda v E(M)$$

and hence

$$[18] \qquad R = \frac{2p}{\pi}E(N)E(M).$$

Extension to unequal target strengths

So far, we have assumed that fish target strength is a constant. Now we allow it to be a random variable and denote it by K. For simplicity, assume that K is a discrete random variable that takes values in a countable set. The result for continuous K is similar, but the proof is technically more complex. Let $R(k)$, $\lambda(k)$, $v(k)$, and $N(k)$ refer to the corresponding quantities above, but for fish of target strength $K = k$. Then,

$$N = \sum_k N(k)$$

$$[19] \qquad E(N) = E\left[\sum_k N(k)\right] = \sum_k E[N(k)].$$

Analogous to formula [16], $E[N(k)] = \lambda(k)v(k)$. Thus, formula [19] can be written as $E(N) = \sum_k \lambda(k)v(k)$.

Let $E(M|K = k)$ be the conditional expectation of M given $K = k$. Then,

$$[20] \qquad E(M) = E[E(M \mid K = k)] = \sum_k E(M \mid K = k)\frac{\lambda(k)v(k)}{\Sigma_k \lambda(k)v(k)}$$

where $[\lambda(k)v(k)]/\sum_k \lambda(k)v(k)$ is the probability mass function of target strengths of fish in the stationary beam. Substitution of $E(N)$ for $\sum_k \lambda(k)v(k)$ in formula [20] yields

$$[21] \qquad E(M) = \frac{1}{E(N)}\sum_k E(M \mid K = k)\lambda(k)v(k).$$

Analogous to formula [17]:

$$[22] \qquad R(k) = \frac{2p}{\pi}\lambda(k)v(k)E(M \mid K = k).$$

Then, formulae [21] and [22] lead to

$$E(M) = \frac{1}{E(N)}\sum_k \frac{\pi}{2p}R(k) = \frac{\pi}{2p}\frac{1}{E(N)}R$$

which again gives formula [18]. This shows that even with fish of unequal target strengths, R can be written in terms of estimable quantities that do not depend on parameters relating to beam shape or target strengths of fish.

Now we attach subscript i to R, N, and M to denote the corresponding quantities for the ith depth stratum. Finally, summing over all depth strata, we can write the total number of fish migrating upstream per second, R, as

$$[23] \qquad R = \sum_i R_i = \frac{2p}{\pi}\sum_i E(N_i)E(M_i).$$

Estimation of fish passage per second, *R*

To estimate R, we first need to estimate $E(N_i)$s and $E(M_i)$s. We use data from transect soundings to estimate $E(N_i)$s

and data from stationary soundings to estimate $E(M_i)$s. Let a, $\bar{N}_i$, and $\bar{M}_i$ be defined as in formula [1]. Then,

$$[24] \quad \hat{R} = a\sum_i \bar{N}_i\bar{M}_i$$

can be used as an estimator for R.

Bias

Boat speed

Assuming that a transect sounding is a snapshot across the river is equivalent to assuming that the boat is travelling infinitely faster than the fish. Since the boat speed is limited in practice, this assumption is false and introduces a bias to the estimate. If the boat speed is not substantially greater than the fish speed during transect soundings, then the beam will ensonify fish that are in the sampled volume when the boat arrives, as well as fish that move into the sampled volume as the boat passes. These latter fish are the source of the bias. For simplicity, we calculate the bias arising from one depth stratum only. The total bias is the sum of these over all strata.

The relative bias (RB) of $\hat{R}$ is

$$\mathrm{RB}(\hat{R}) = \frac{[E(\hat{R}) - R]}{R}.$$

Since from formula [24], $\hat{R}$ for one stratum is $\hat{R} = a\bar{N}\bar{M}$ and from formula [17], $R = a\lambda v E(M)$, the above formula becomes

$$\mathrm{RB}(\hat{R}) = \frac{[E(\bar{N}\,\bar{M}) - \lambda v E(M)]}{\lambda v E(M)}.$$

Recall that $\bar{N}$ is the average target count per transect sounding and is based on mobile soundings, while $\bar{M}$ is the average of reciprocal target widths and is based on stationary soundings. These two quantities are therefore independent. Hence, the above equation simplifies to

$$[25] \quad \mathrm{RB}(\hat{R}) = \frac{[E(\bar{N}) - \lambda v]}{\lambda v} = \frac{[E(N) - \lambda v]}{\lambda v}.$$

Let u = speed of the boat. Then the time taken for one transect is $t = \alpha/u$. Boat speed relative to a fish swimming upstream at speed S is $\sqrt{u^2 + S^2}$. Therefore, the distance that the boat would have travelled relative to the fish during time t is $t\sqrt{u^2 + S^2} = (\alpha/u)\sqrt{u^2 + S^2}$. This corresponds to a volume

$$V = \frac{\alpha}{u}\sqrt{u^2 + S^2}\,\delta(z_2 - z_1) = v\sqrt{1 + \frac{S^2}{u^2}}$$

and

$$[26] \quad E(N) = E(\lambda V) = \lambda v E\left(\sqrt{1 + \frac{S^2}{u^2}}\right).$$

Then, formulae [25] and [26] lead to

$$[27] \quad \mathrm{RB}(\hat{R}) = E\left(\sqrt{1 + \frac{S^2}{u^2}}\right) - 1.$$

As the bias is positive, the effect of low boat speeds is to overestimate R. However, by moving the boat at a high speed relative to fish speed, the bias can be reduced. We can obtain bounds for the relative bias as follows.

From Jensen's inequality (Kotz and Johnson 1983) and the fact that $\sqrt{1 + (S^2/u^2)}$ is convex in S but concave in S^2, one can show that

$$\sqrt{1 + \frac{E^2(S)}{u^2}} - 1 \le E\left(\sqrt{1 + \frac{S^2}{u^2}}\right) - 1 \le \sqrt{1 + \frac{E(S^2)}{u^2}} - 1.$$

That is,

$$[28] \quad \sqrt{1 + \frac{\mu_s^2}{u^2}} - 1 \le \mathrm{RB}(\hat{R}) \le \sqrt{1 + \frac{\mu_s^2 + \mathrm{Var}(S)}{u^2}} - 1.$$

Hence, a lower bound can be placed on the bias if the mean fish speed is known. An upper bound can be added if the variance is also known, and a proper bias adjustment factor can be computed from an estimate of $E\sqrt{1 + (S^2/u^2)}$.

For example, the boat speed was close to 1.5 m·s^{-1}, and Quinn and terHart (1987) reported for sockeye salmon a mean fish speed of 0.66 m·s^{-1}, with a standard deviation of 0.21 m·s^{-1}. With these figures the relative bias would be between 9.3 and 10.1%.

Swimming direction

Fish that deviate from the upstream direction when migrating upriver will also contribute a positive bias. This includes fish that swim downstream, across the flow, or even a few degrees from the true upstream direction. The bias is introduced in the stationary soundings. Results from these soundings are used as if all fish swim directly upstream. The amount of time that fish take to swim through the stationary beam does not depend directly on the direction of travel. However, fish that do not swim directly upstream are not moving upstream as rapidly as the method assumes. The upriver migration rate is therefore overestimated. For fish that swim at an angle, ϕ, off the upstream direction, the upstream component to the velocity will be the fraction, $\cos\phi$, of their overall speed. However, for ϕ close to 0°, $\cos\phi$ is close to 1. Hence, as long as fish movement is strongly directed upriver, this bias will not be serious. If, for example, ϕ is centred at 0°, with a standard deviation of 10°, the bias is approximately 1.5%.

Estimation of variance

The variance of $\hat{R}$ as given in formula [24] can be written as

$$\mathrm{Var}(\hat{R}) = \sum_i \mathrm{Var}(\hat{R}_i) + 2\sum_{i<j} \mathrm{Cov}(\hat{R}_i, \hat{R}_j)$$

where i and j are stratum numbers. Let $\hat{R}_i = R_i + \epsilon_i$ and $\hat{R}_j = R_j + \epsilon_j$. Assume that the errors ϵ_i and ϵ_j are uncorrelated. Then, $\mathrm{Cov}(\hat{R}_i, \hat{R}_j) = \mathrm{Cov}(\epsilon_i, \epsilon_j) = 0$, and

$$[29] \quad \mathrm{Var}(\hat{R}) = \sum_i \mathrm{Var}(\hat{R}_i) = a^2 \sum_i \mathrm{Var}(\bar{N}_i, \bar{M}_i).$$

Recall that $\bar{N}_i$ and $\bar{M}_j$ are independent for all i and j. According to Kendall and Stuart (1977):

Table 1. Summary statistics of the data collected by the Pacific Salmon Commission on August 31, 1993, at Mission, B.C. Also shown are the estimated numbers of fish migrating upriver per second and the corresponding estimated variances.

		Transect observations			Stationary observations			Migration rates	
Depth stratum (i)	Depth range (m)	No. of passes (n)	Avg. count ($\bar{N}_i$)	Var. ($s^2_{N_i}$)	No. of fish (m_i)	Avg. width ($\bar{M}_i$)	Var. ($s^2_{M_i}$)	Est. ($\hat{R}_i$)	Var. ($\hat{\mathrm{Var}}(\hat{R}_i)$)
1	0–5	215	1.20	1.53	77	1.07	0.136	0.39	0.0107
2	5–10	215	6.38	17.4	145	0.76	0.066	1.47	0.0815
3	10–15	215	1.74	2.36	42	0.79	0.130	0.42	0.0164

[30] $$\mathrm{Var}(\bar{N}_i\bar{M}_i) = \mathrm{Var}(\bar{N}_i)\mathrm{Var}(\bar{M}_i) + \mathrm{Var}(\bar{N}_i)E^2(\bar{M}_i) + \mathrm{Var}(\bar{M}_i)E^2(\bar{N}_i).$$

Let n, m_i, $s^2_{N_i}$, and $s^2_{M_i}$ be defined as in formula [2]. Since $s^2_{N_i}/n$ and $s^2_{M_i}/m_i$ are unbiased estimators for $\mathrm{Var}(\bar{N}_i)$ and $\mathrm{Var}(\bar{M}_i)$, respectively, according to Kendall and Stuart (1977), an unbiased estimate of the variance of $\hat{R}$ can be obtained by

[31] $$\hat{\mathrm{Var}}(\hat{R}) = a^2\sum_i\left(\frac{s^2_{N_i}}{n}\bar{M}_i^2 + \frac{s^2_{M_i}}{m_i}\bar{N}_i^2 - \frac{s^2_{N_i}s^2_{M_i}}{nm_i}\right).$$

Numerical example

Data from August 31, 1993, are used to demonstrate the methods described in this paper. Table 1 contains the summary statistics of the data and estimates of the number of fish per second in each depth stratum that migrated upriver, along with the estimated variances. The paper speed of the recorder is 0.478 mm·s^{-1} for these calculations.

The estimated number of fish migrating upriver per second is $\hat{R}$. To estimate total numbers migrating over a time period of duration H, we can use $H\hat{R}$ with estimated variance, $H^2\hat{\mathrm{Var}}(\hat{R})$.

The total daily abundance is estimated with H = 86 400 s·d^{-1} as described above.

$$\text{Estimated abundance} = H\hat{R} = H\sum_{i=1}^{3}\hat{R}_i = 196\,998$$

$$\text{Estimated standad error} = \widehat{\mathrm{SE}}(H\hat{R}) = H\sqrt{\hat{\mathrm{Var}}(\hat{R})} = H\sqrt{\sum_{i=1}^{3}\hat{\mathrm{Var}}(\hat{R}_i)} = 8651$$

$$\text{Estimated coefficient of variation} = \frac{\widehat{\mathrm{SE}}(H\hat{R})}{H\hat{R}} = 4\%.$$

Fish abundance on this day (about 197 000 fish) was about half the largest daily abundance (about 403 000 fish) observed in 1993.

Discussion

The described method for estimating the number of migrating fish in a river using hydroacoustic techniques, originally developed by the IPSFC and now refined by us, has two major advantages over similar methods used in lakes and reservoirs. First, the method is not sensitive to beam shape or dimensions. Second, the exact calculation of the expected reciprocal of the chord length allows the user to avoid the use of the bootstrap to reduce bias caused by using an estimation formula with a random variable in its denominator.

We identified several potential sources of bias inherent in the method. The first, which stems from the speed of the boat being only moderately faster than fish migration speed, tends to result in overestimation of abundance. This bias can be reduced by increasing the boat's speed as much as practically possible, or by estimating a bias adjustment factor that can be extracted from formula [27].

Second, fish swimming off the upstream direction will introduce a positive bias. The stationary soundings estimate overall fish speed, and the upstream component to the velocity will be overestimated. This source of bias can sometimes be reduced by choosing a location, such as the Mission site, where there are limited opportunities for the fish to mill about.

Contrasting with these sources of positive bias are sources of negative bias. Fish that travel in areas of the river that cannot be acoustically sampled, such as close to the surface above the minimum detection depth and close to shore where the echo-sounding boat cannot travel, will be missed. Similarly, fish that sense and avoid the echo-sounding boat will lead to a negative bias. Finally, when the targets of two or more fish overlap on the echogram, so that only one target is apparent, the population will be underestimated. These biases are not considered to be significant for sockeye salmon in the Fraser River.

The estimated variance for the worked example could possibly be reduced further if the day was divided into smaller units of time. This is because a daily cyclical pattern in the abundance of migrating sockeye salmon is ignored in our example. Stratifying each day such that the strata are homogeneous with respect to migration (e.g., into hourly strata) could result in more precise estimates. Daily abundance and variance can then be estimated as the sum of the stratum estimates.

In the example shown, the 264 targets sampled in the stationary soundings provided estimates with reasonable precision. On days with fewer fish in the river, the estimates will have a larger coefficient of variation. A scheme for

optimal allocation of sampling effort between the two types of soundings could substantially reduce the coefficient of variation, particularly on such days.

We do not recommend that approximate confidence limits be calculated in the usual way, by adding and subtracting multiples of standard errors. The estimator, being the sum of products, is not guaranteed to have a sufficiently normal distribution. We are investigating an alternative strategy based on inverting the likelihood ratio test (Madansky 1965) for this purpose.

The method described in this paper has a strong potential to give accurate and precise estimates of fish passage that are robust and comparatively easy to obtain. Methods for promoting and checking the validity of the underlying assumptions are discussed. The method provides a significant tool for managers under pressure to make timely and effective management decisions.

Acknowledgements

We are very grateful to P. Cheng for the analyses and data he provided. Funding was provided by the Pacific Salmon Commission and the Natural Sciences and Engineering Research Council of Canada.

References

Clay, C.S., and Medwin, H. 1977. Acoustical oceanography: principles and applications. Wiley-Interscience, New York, N.Y.

Crittenden, R.N., Thomas, G.L., Marino, D.A., and Thorne, R.E. 1988. A weighted duration-in-beam estimator for the volume sampled by a quantitative echo sounder. Can. J. Fish. Aquat. Sci. **45**: 1249–1256.

Foote, K.G. 1990. Correcting acoustic measurements of scatterer density for extinction. J. Acoust. Soc. Am. **88**: 1543–1546.

Kendall, M., and Stuart, A. 1977. The advanced theory of statistics. Vol. 1. Macmillan, New York, N.Y.

Kieser, R., and Ehrenberg, J.E. 1990. An unbiased, stochastic echo counting model. Rapp. P.-v. Réun. Cons. int. Explor. Mer, **189**: 65–72.

Kotz, S., and Johnson, N.L. (*Editors*). 1983. Encyclopedia of statistical sciences. Vol. 4. John Wiley & Sons, New York, N.Y.

Levy, D.A., Nealson, P.A., and Cheng, P. 1991. Fixed-aspect hydroacoustic estimation of Fraser River sockeye salmon abundance and distribution at Mission, B.C., in 1986. Pac. Salmon Comm. Tech. Rep. No. 4.

MacLennan, D.N., and Simmonds, E.J. 1992. Fisheries acoustics. Chapman and Hall, London.

Madansky, A. 1965. Approximate confidence limits for the reliability of series and parallel systems. Technometrics, **7**: 495–503.

Quinn, T.P., and terHart, B.A. 1987. Movements of adult sockeye salmon (Oncorhynchus nerka) in British Columbia coastal waters in relation to temperature and salinity stratification: ultrasonic telemetry results. *In* Sockeye salmon (*Oncorhynchus nerka*) population biology and future management. *Edited by* H.D. Smith, L. Margolis, and C.C. Wood. Can. Spec. Publ. Fish. Aquat. Sci. 96. pp. 61–67.

Skalski, J.R., Hoffmann, A., Ransom, B.H., and Steig, T.W. 1993. Fixed-location hydroacoustic monitoring designs for estimating fish passage using stratified random and systematic sampling. Can. J. Fish. Aquat. Sci. **50**: 1208–1221.

Thorne, R.E. 1988. An empirical evaluation of the duration-in-beam technique for hydroacoustic estimation. Can. J. Fish. Aquat. Sci. **45**: 1244–1248.

Thorne, R.E., and Dawson, J.J. 1974. An acoustic estimate of the escapement of sockeye salmon (*Oncorhynchus nerka*) into Lake Washington in 1971. J. Fish. Res. Board Can. **31**: 222–225.

Woodey, J.C. 1987. In-season management of Fraser River sockeye salmon (*Oncorhynchus nerka*): meeting multiple objectives. *In* Sockeye salmon (*Oncorhynchus nerka*) population biology and future management. *Edited by* H.D. Smith, L. Margolis, and C.C. Wood. Can. Spec. Publ. Fish. Aquat. Sci. 96. pp. 367–374.

Differences in otolith microstructure between hatchery-reared and wild chinook salmon (*Oncorhynchus tshawytscha*)

Z. Zhang, R.J. Beamish, and B.E. Riddell

Abstract: Otolith microstructure exhibited some characteristic differences between hatchery-reared and wild chinook salmon (*Oncorhynchus tshawytscha*) from the Cowichan River. Daily growth increments that formed in the otoliths of the hatchery-reared chinook salmon after exogenous feeding were more regular in width and contrast than those in the otoliths of wild chinook salmon. In addition, otoliths from hatchery-reared individuals frequently produced a check when the fish were released from the hatchery. Eighty-nine percent of a sample of 67 chinook smolts that had been coded-wire tagged in hatcheries and later captured in the Strait of Georgia were correctly identified as originating from hatcheries based on otolith microstructure. These tagged fish originated from at least 17 different hatcheries, indicating that the method could be used to identify chinook salmon originating from other hatcheries.

Résumé : Nous avons observé des différences caractéristiques dans la microstructure des otolithes entre des saumons quinnats (*Oncorhynchus tshawytscha*) d'élevage et des spécimens sauvages capturés dans la rivière Cowichan. Les marques quotidiennes de croissance qui se formaient dans les otolithes des quinnats d'élevage après le début de l'alimentation exogène étaient plus régulières en largeur et en contraste que celles observées dans les otolithes des quinnats sauvages. De plus, les otolithes des poissons d'élevage présentaient souvent une encoche correspondant au moment où les poissons étaient libérés par l'écloserie. Sur un échantillon de 67 smolts de quinnat qui avaient été marqués en écloserie avec des micromarques codées puis recapturés dans le détroit de Géorgie, 89% ont été correctement identifiés quant à l'origine à partir de la microstructure des otolithes. Ces poissons provenaient d'au moins 17 écloseries différentes, ce qui indique que la méthode pourrait être utilisée pour identifier des quinnats provenant d'autres pisciculturs.
[Traduit par la Rédaction]

Introduction

Chinook salmon (*Oncorhynchus tshawytscha*) is an important fish in the commercial and recreational fisheries of British Columbia. In the Strait of Georgia, where there is a large recreational fishery for chinook salmon, the catches from 1950 to 1992 were highest during 1976–1978. Catches during this period averaged 750 000 individuals, but by the late 1980s they had declined to about 170 000 individuals. As part of an effort to restore the abundance of adults to the late 1970s level, Canadian hatcheries rear and release large numbers of chinook smolts into the Strait of Georgia.

The hatchery-reared chinook salmon smolts mix with wild smolts, but little is known about the impact of one rearing type on the other. It is known that the survival of hatchery-reared chinook salmon declined dramatically (Beamish et al. 1995) as releases from hatcheries increased in the 1980s. It is not known if this decline in survival is the result of increased natural marine mortality or mortality specific to the rearing environment and rearing practices in hatcheries. Furthermore, it is not known if a trend similar to the decline in the survival of hatchery-reared chinook is occurring in wild chinook salmon populations. If it were possible to identify all hatchery-reared and all wild chinook salmon, it would be possible to study the marine survival trends. The information from such a study could be used to identify optimal levels of smolt releases and to compare marine survival trends of hatchery-reared and wild chinook salmon smolts.

The method of acquiring survival information of hatchery-reared chinook salmon has been to tag a percentage of the releases (3–15%) and to recapture these marked fish in the commercial and recreational fisheries or when they return to the hatchery. The tag is a piece of wire with a coded message that is inserted into the cartilage in the nasal area. The adipose fin is removed to indicate that the fish has a tag. The head of a recaptured fish is removed and preserved.

Received January 10, 1994. Accepted August 5, 1994.
J12223

Z. Zhang, R.J. Beamish, and B.E. Riddell. Department of Fisheries and Oceans, Pacific Biological Station, Nanaimo, BC V9R 5K6, Canada.

At a later date, the tag is recovered and decoded. Studies have shown that only a small percentage of the tagged and recaptured fish are returned. Thus, the actual returns must be "expanded" to obtain an estimate of the true number of recaptured fish. This expansion introduces a potential error into any estimate of hatchery production. In addition, the tags have been difficult to apply to wild smolts; hence, it has not been possible to compare marine survival trends of hatchery-reared and wild smolts.

In this study, we identify an inexpensive method of identifying hatchery-reared and wild chinook salmon using patterns in otolith microstructure. Our method is not a replacement for the coded-wire tag, but a procedure for directly assessing the percentage of hatchery-reared and wild chinook salmon in any sample.

Materials and methods

Chinook salmon were reared in groundwater at a constant temperature of 10°C in the Cowichan hatchery, located on the east coast of Vancouver Island, British Columbia. After rearing in the hatchery during the yolk sac stage, fry were transferred to rearing ponds outdoors just before onset of exogenous feeding, which occurred at approximately 900 accumulated temperature units.

Five groups of hatchery-reared chinook salmon were studied: incubated eggs, alevins, pond-reared fry, smolts, and hatchery-reared adults (Table 1). The eggs, alevins, and fry, which were sampled from the hatchery, were used to study checks, which were commonly found in otoliths of both hatchery-reared and wild fish. Smolts, which were collected from the hatchery and the Cowichan River, were used to study the pattern of daily growth increments in otoliths. Adults were used to verify that the otolith microstructural pattern formed at the early life stage is unchangeable for the whole life span. Stomachs of fry sampled from the rearing pond were examined to determine if exogenous feeding had started.

Wild fry (N = 118) were collected in the Cowichan River in 1991 before the release of hatchery-reared fish into the river. The microstructural pattern of the otoliths of these fish was compared with the pattern in the otoliths from hatchery-reared fish.

Fish were frozen before the removal of the otoliths (we used sagittae in this study). Otoliths were washed in 0.1% sodium hydroxide and distilled water to remove soft tissue. Left otoliths from the eggs and alevins were mounted on glass slides using clear fingernail polish and examined without further processing. The left otoliths of fry and smolts were mounted using thermosetting plastic resin. Each otolith was then ground on lapping film of 60 or 30 μm, depending on otolith size, until the primordia were revealed. At this stage, the resin was melted on a hotplate and the otolith was turned over. The other side of the otolith was ground in a similar manner until the microstructure was clearly visible. The otolith was then polished on a lapping film of 0.3 μm to remove scratches caused by the grinding. If the otolith was damaged or the microstructure was not clearly revealed, the right otolith of the pair was used. Otolith microstructure was studied with a compound light microscope using transmitted light.

Table 1. Number and life stages of Cowichan hatchery-reared chinook salmon used in this study.

Year	Eggs	Alevins	Fry	Smolts	Adults
1991	15[a]	39[b]	68[c]	108[d]	59[e]
1992	—	—	—	142[f]	—

[a]Approximately 3 days before hatching.
[b]Composed of 20 and 19 alevins sampled 4 days after hatching and 1 day before transferring to the rearing pond, respectively.
[c]Composed of 25, 20, and 23 fry sampled 3, 6, and 12 days, respectively, after being transferred to the rearing pond.
[d]Composed of 39 fish from the rearing pond and 69 tagged fish captured in the Cowichan River after release of Cowichan hatchery-reared fish.
[e]Coded-wire tagged adults collected in the Cowichan River after they had spawned.
[f]Coded-wire tagged smolts captured in the Cowichan River after release of Cowichan hatchery-reared fish.

All otoliths exhibited a hatching check and most otoliths exhibited a first-feeding check (see Results section for definition of the two checks). In some otoliths, these checks were visible in all areas of the otolith, while in others they were discernible only in some portions of the otolith. The former otoliths were selected from the Cowichan hatchery (reared fry and smolts) and from the Cowichan River (wild fry). The length of the hatching check and first-feeding check in these selected otoliths was measured from the anterior to the posterior end under a compound light microscope.

The widths of daily growth increments in 54 randomly selected otoliths from Cowichan hatchery-reared smolts and 49 randomly selected otoliths from wild fry from the Cowichan River were measured using a Bio-Scan digitizing system. For each otolith, 25–60 daily growth increments that formed after the first-feeding check were measured along the axis intercepting the daily growth increments at their widest portion in the dorso-posterior quadrant.

Otoliths from adults were thinned through decalcification. All decalcification in this study was carried out in 40- or 25-mL beakers with a 1.5-cm-high, close-fitting polyethylene ring at the bottom supporting a close-fitting metal mesh. Resting on the mesh, the otoliths were completely immersed in 8% EDTA ((ethylenedinitrilo)tetraacetic acid, disodium salt) solution, which was stirred with a magnetic stirrer.

The otolith primordia in these fish otoliths are located towards the dorsal edge, which is thinner than the ventral edge. To control the amount of decalcification from the dorsal side, clear fingernail polish was spread carefully along the dorsal edge so that the polish did not extend to the area over the central region. After the polish had set, the otoliths were put into the EDTA solution and decalcified until the hatching check or first-feeding check could be observed under a dissecting microscope using reflected light. These checks are always first revealed from the exterior side, as the otolith primordia are closer to the exterior

Fig. 1. Otolith section from a wild chinook salmon fry presenting an overall view of the internal otolith structure. Note that numerous increments are present within the hatching check (curved arrow), surrounding the fused primordia (white arrow). The rostral primordium (arrowhead) is formed after hatching. The first-feeding check (straight arrow) marks the end of the alevin stage and the beginning of the fry stage. A, anterior end; P, posterior end; D, dorsal side; V, ventral side. Scale bar = 135 μm.

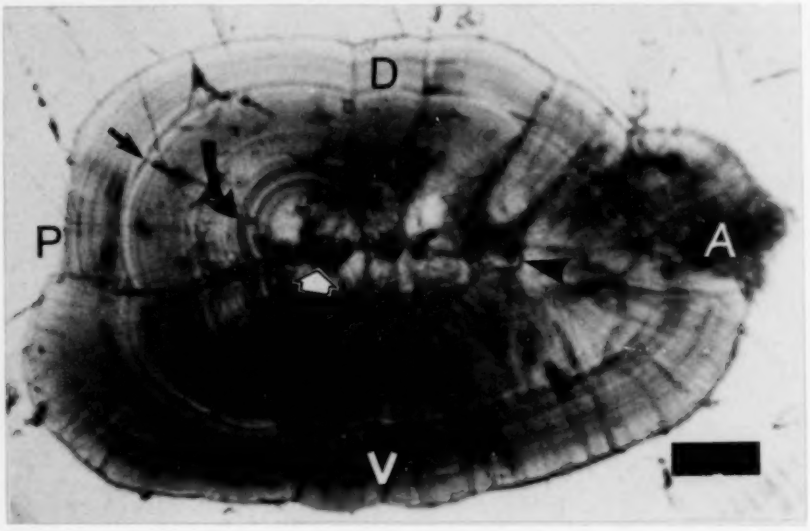

Table 2. Origin of coded-wire-tagged chinook salmon smolts sampled in the Strait of Georgia and Fraser River plume in 1992 and 1993.

Hatchery	Number of hatchery-reared fish	
	1992	1993
Big Qualicum	1	20
Bonoparte	—	1
Bridge River	—	1
Capilano	2	2
Chehalis	1	1
Chilliwack	3	5
Clearwater	13	—
Eagle	3	2
Harrison	—	2
Nicola	—	2
Little Qualicum	—	16
Penny	1	—
Quesnel	1	1
Spius	5	—
Shuswap	—	3
Stuart River	—	1
Tenderfoot	—	1
U.S. hatcheries	—	4
Unknown hatcheries[a]	—	5

[a]Due to loss of tags.

surface. It took 4–14 h to remove sufficient calcareous material, depending on the size of the otolith.

Once the hatching check or first-feeding check was visible from the exterior side, the otolith was dried and carefully placed, exterior side down, on a drop of fingernail polish on a small piece of a broken slide coverslip so that the polish did not overflow onto the interior surface. After the polish had set, the otolith was again put into 8% EDTA solution. The presence of polish prevented any further decalcification from the exterior side. The decalcification was terminated after 6–20 h, when the hatching check or first-feeding check could be observed from the interior side. The processed otolith, which was thin and small, was dried and put into acetone to remove the polish. It was then mounted on a glass slide using thermosetting plastic resin and polished on a lapping film of 30 or 0.3 μm until the primordia were clearly revealed under a light microscope. The otolith was turned over and the other side was also polished until the increments formed after the first-feeding check were clearly revealed.

Samples of a mixture of hatchery-reared and wild chinook salmon smolts were collected using surface beam trawls (R.J. Beamish, unpublished data) from the Strait of Georgia and the Fraser River plume in May, June, and July of 1992 and 1993. Some of these fish had been tagged at the hatchery using coded-wire tags and an adipose fin clip and thus were known to be hatchery-reared fish. Thirty and 67 chinook salmon smolts with coded-wire tags were obtained in 1992 and 1993, respectively. From the coded-wire-tag information, these fish were known to have originated

Fig. 2. Higher magnification of Fig. 1 showing that the appearance of daily growth increments deposited after the first-feeding check (arrow) is more prominent than the appearance of those formed before the first-feeding check. Scale bar = 100 μm.

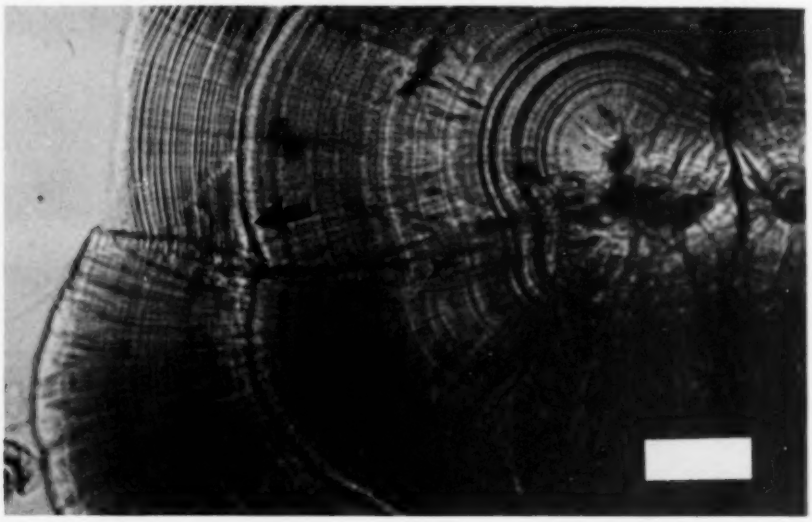

Table 3. Size of hatching check and first-feeding check in the otoliths of Cowichan hatchery-reared chinook salmon and wild chinook salmon from the Cowichan River.

Fish origin	Mean length of hatching check (μm) ± SD	Mean length of first-feeding check (μm) ± SD
Cowichan hatchery	336.07 ± 23.39 (N = 42)	764.34 ± 46.74 (N = 62)
Wild from Cowichan River	347.50 ± 32.05 (N = 67)	814.06 ± 55.65 (N = 81)

from at least 17 different hatcheries (Table 2). Otolith microstructure was examined and compared with the otolith microstructure from the Cowichan hatchery-reared and wild chinook salmon. The accuracy of classification of wild and hatchery-reared chinook salmon was assessed using the 1993 sample of young chinook salmon. The rearing type of the total sample (N = 1264) was classified using the otolith microstructure, without prior knowledge of which fish had coded-wire tags, and the percentage of the known hatchery-reared fish that were correctly identified was determined. The 1992 sample was not used to test the accuracy because the otoliths were known to be from hatchery-reared fish.

Results

Otolith microstructure before exogenous feeding

All otoliths from hatchery-reared and wild chinook salmon contained a prominent hatching check. Within the check, numerous increments surrounded the multiple primordia (Fig. 1). The hatching check was found to be present near the margin of otoliths of fish sampled 4 days after hatching, while the check was not visible in the otoliths of unhatched fish. The mean length of the hatching check in Cowichan hatchery-reared fish was smaller than in Cowichan wild ones, although the difference was not significant (ANOVA, $0.05 < P < 0.1$) (Table 3). A second prominent check was present in most of the otoliths (92.7%). Increments formed before this second check in general appeared less prominent than those deposited after the second check (Figs. 1 and 2). This second check was found in the otolith margin of fish that had just started exogenous feeding and was not present in fish that had not started exogenous feeding. This check is presumably associated with the transition from yolk absorption to exogenous feeding and we referred to it as the "first-feeding check." The average length of this check in the Cowichan hatchery-reared chinook was significantly smaller than in wild chinook from the Cowichan River (ANOVA, $P < 0.005$) (Table 3).

Otolith microstructure in Cowichan hatchery-reared chinook salmon after exogenous feeding

Daily growth increments formed in the hatchery-reared chinook immediately after the first-feeding check were uniform in width and contrast. The average width of increments was 3.97 μm (SE = 0.016, N = 2013) in the dorso-posterior quadrant (Fig. 3). This uniform pattern changed

Fig. 3. Otolith section from a Cowichan hatchery-reared chinook salmon fry showing the regular postfeeding daily growth increments in the dorsoposterior quadrant. Scale bar = 12 μm.

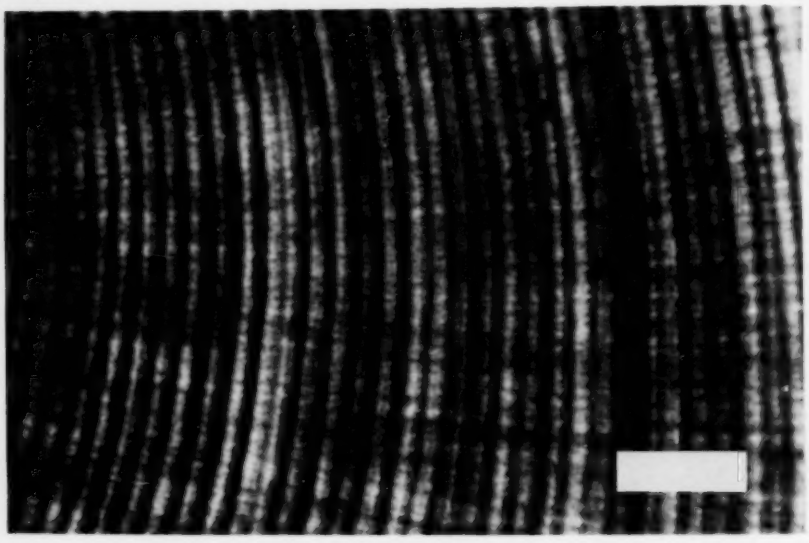

Fig. 4. Otolith section from a Cowichan hatchery-reared chinook salmon smolt caught in the Cowichan estuary showing the transition (arrow) in the dorsoposterior quadrant between regular postfeeding daily growth increments and irregular daily growth increments formed in the wild after release from the hatchery. Scale bar = 30 μm.

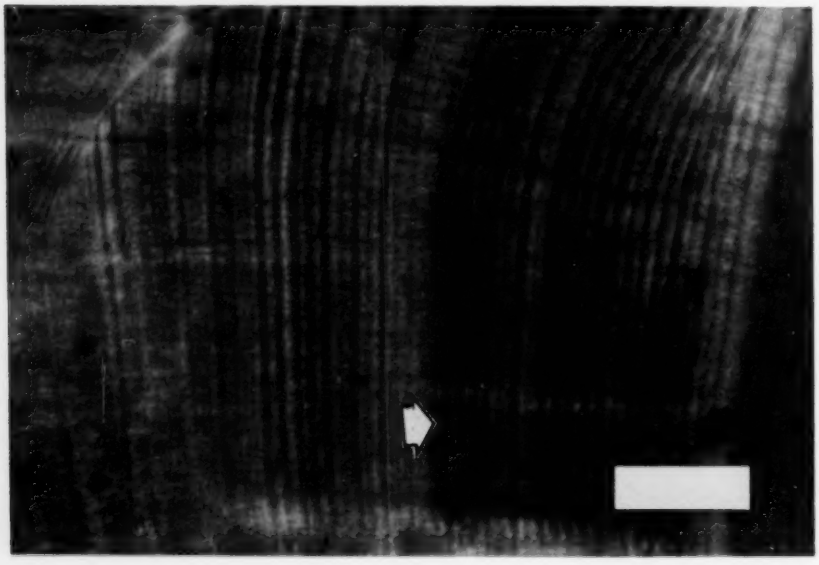

following the release of the fish from the hatchery into the river. Daily growth increments that formed immediately after the release from the hatchery often appeared relatively irregular and narrow. The transition between these two different patterns of daily growth increments frequently (88%) corresponded to the formation of a check that we called a "releasing check". The different appearance in the pattern of daily growth increments before and after release aids in identifying the hatchery-reared fish (Fig. 4).

Otoliths from adults originating from the Cowichan hatchery also exhibited the hatching check and first-feeding check, and daily growth increments following the first-feeding

Fig. 5. Otolith section from a wild chinook salmon fry from the Cowichan River showing the irregular postfeeding daily growth increments in the dorsoposterior quadrant. Scale bar = 12 μm.

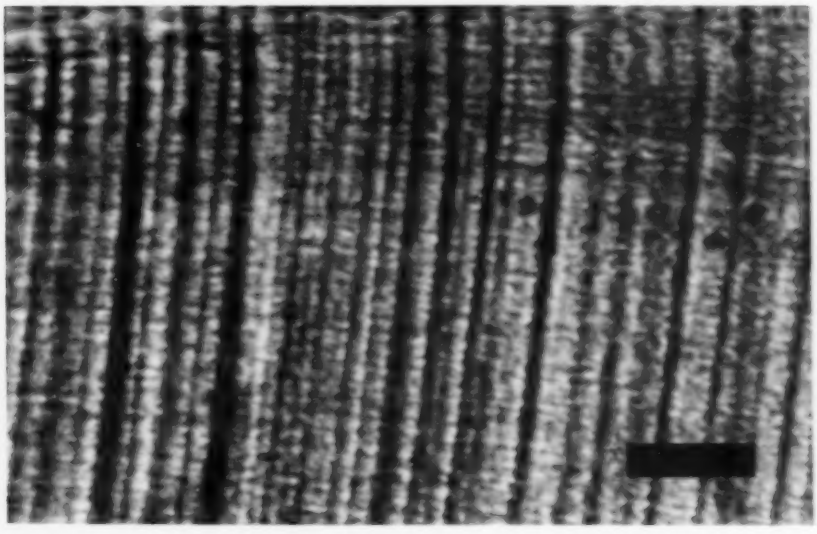

check were regular and wide. These regular and wide daily growth increments were often followed by a releasing check and then relatively narrow and irregular daily growth increments. This microstructural pattern was similar to the pattern found in the otoliths of Cowichan hatchery-reared juvenile chinook salmon.

Otolith microstructure in wild chinook salmon after exogenous feeding

Increments deposited in otoliths from wild fish following the first-feeding check varied a great deal in width and contrast. The average width of the increments was 2.37 μm in the dorsoposterior quadrant, smaller than in the hatchery-reared fish (Fig. 5). The coefficient of variation (standard deviation/mean) of daily growth increments of individual otoliths from the wild and Cowichan hatchery-reared chinook ranged between 0.2504 and 0.4112 and between 0.0614 and 0.1723, respectively. The coefficients of variation for the two rearing types were completely separated (Fig. 6). The coefficient of variation for the wild fish was significantly higher than for the Cowichan hatchery-reared fish (t-test, $P < 0.005$). The wild fish otoliths also did not contain a check equivalent to the releasing check found in the otoliths of most hatchery-reared fish.

Otolith microstructure in chinook salmon from at least 17 different hatcheries

Daily growth increments deposited following the first-feeding check in the otoliths of most of the coded-wire-tagged chinook (92%) were regular in width and contrast (Fig. 7) and considerably different from the daily growth increment pattern found in the otoliths of wild fish from the Cowichan River. Although the daily growth increments in the coded-wire tagged chinook were not as wide as those in the otoliths of Cowichan hatchery-reared fish (an average width of 2.89 μm in the dorsoposterior quadrant), they were wider on average and more regular in their formation than those of wild fish otoliths. Seventy-six percent of the otoliths from these hatchery-reared fish contained a releasing check, immediately after which daily growth increments often appeared relatively irregular (Fig. 7).

Classification accuracy

Among the sample of 1264 chinook salmon smolts collected from the Strait of Georgia in 1993, 633 were identified as wild fish, 620 were identified as hatchery-reared fish, and 11 were unidentified because of crystalline otolith structure or poor otolith preparation. The sample contained 67 fish from various hatcheries identified by the coded-wire tags (Table 2). Approximately 10% of hatchery-reared chinook have coded-wire tags. Thus, in the sample of 1264 fish, the 67 tags would indicate that approximately 670 were of hatchery origin and 594 were wild. Our estimates of hatchery and wild chinook were similar to the expected number. Of the 67 coded-wire tagged fish, 59 were correctly identified, seven were misidentified as wild, and one was not identified because of crystalline otolith structure. Thus, the accuracy of identifying chinook salmon smolts known to have been released from various hatcheries was approximately 89%.

Discussion

It has been verified that increment deposition is daily in otoliths of juvenile chinook salmon (Neilson and Geen 1982; Neilson et al. 1985; Gauldie 1991), although this deposition rate could be affected by fish activity patterns (Neilson and Geen 1982). Hatchery-reared and wild chinook salmon in general have patterns in the otolith microstructure that reflect the rearing environment. The identification

Fig. 6. Standard deviation versus mean of daily growth increment width of individual otoliths from the Cowichan hatchery-reared and wild chinook salmon showing that the daily growth increment width is greater and the variation is smaller for hatchery-reared fish.

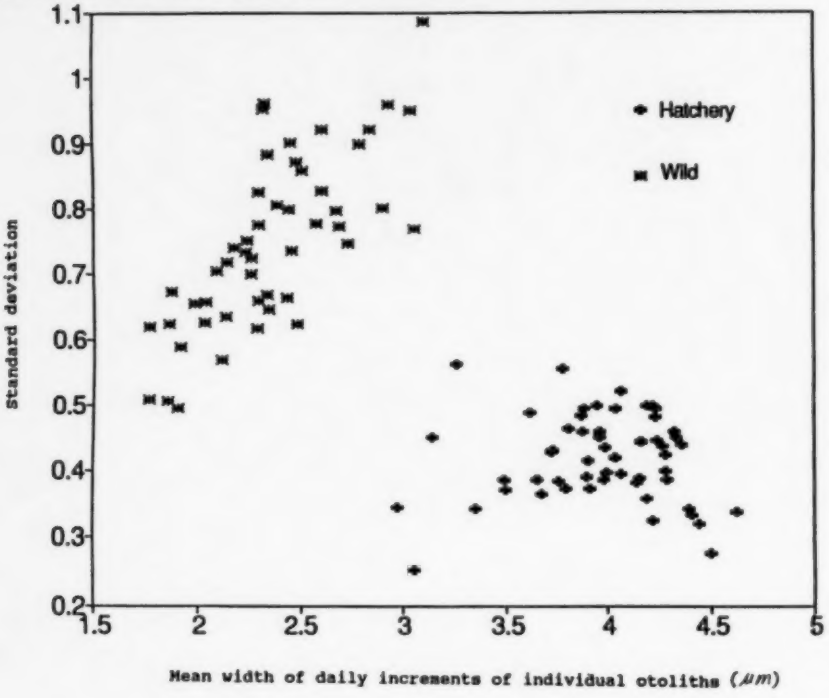

of the two rearing types relies primarily on the difference in the daily growth increment pattern formed immediately after exogenous feeding. The otoliths of hatchery-reared chinook salmon have wider daily growth increments and a more regular pattern of postfeeding daily growth increments than the otoliths of wild fish. The existence of the releasing check and irregular daily growth increments deposited following release from the hatchery provide additional criteria to identify hatchery-reared fish from wild fish. The first-feeding check, which is also present in the otoliths of sockeye salmon (*Oncorhynchus nerka*) (Marshall and Parker 1982), serves as a good bench mark, allowing daily growth increments deposited immediately after the beginning of exogenous feeding to be readily and correctly defined and examined.

Examination of adult chinook salmon of Cowichan hatchery origin indicates that the pattern of early otolith microstructure formation remains constant over the whole life span. While scale resorption is common, resorption of completely formed otolith increments is unlikely to occur except under severe stress (Campana 1983; Mugiya and Takahashi 1985; Mugiya and Uchimura 1989). Although a recent study demonstrates that calcium deposited onto a mineralizing increment may be dissolved at night, the net accumulation of calcium onto the otoliths is significantly greater than net losses each day (Wright et al. 1992). The conservative nature of otolith microstructure enables us, therefore, to identify the origin of adult chinook salmon based on the otolith microstructural pattern formed at the early stage.

Our assumption that the technique can be used to separate chinook salmon of other hatcheries from wild chinook salmon is based on the observations from the hatchery-tagged fish caught in the Strait of Georgia in 1992 and 1993. In the sample of 67 coded-wire tagged smolts, only seven were inaccurately identified. Six fish were incorrectly identified because their otoliths did not contain a regular pattern of daily growth increments following the first-feeding check, as expected in the otoliths of hatchery-reared chinook. The other fish was initially erroneously identified as wild because the otolith was not well prepared and the otolith microstructure was not adequately revealed. A regular pattern of daily growth increments after the first-feeding check was observed in the other otolith of the pair, which was more carefully prepared. The accuracy level for identifying other hatchery-reared chinook is probably not as high as that for identifying Cowichan hatchery-reared chinook among a mixture of Cowichan hatchery-reared and wild chinook salmon, as suggested by Fig. 6. Nonetheless, the high level of accuracy (89%) of identifying tagged fish among the sample collected in 1993 indicates that the determinations were reliable and that the method applies to other hatchery-reared chinook salmon. The ability to identify the rearing type from a large sample of chinook smolts indicates that the method applies for both wild and hatchery-reared chinook.

Fig. 7. Otolith section from a hatchery-reared chinook salmon smolt caught in the Strait of Georgia in 1992 showing the regular postfeeding daily growth increments in the dorsoposterior quadrant and a check (arrow) associated with release from the hatchery into the wild. Daily increments formed after the release are relatively irregular. Scale bar = 60 μm.

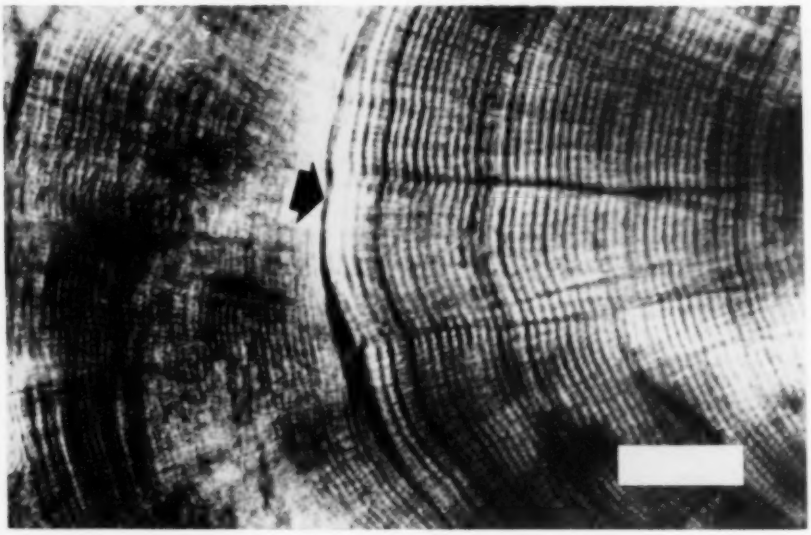

More detailed studies from a selection of these other hatcheries and from more wild stocks must, however, be carried out to verify that the method can be applied to fish reared in other hatcheries and from one year to the next.

Among the whole sample of chinook fry and smolts collected from the hatchery and wild from 1991 to 1993, there was a small percentage (3%) of fish with both otoliths of crystalline structure. When both otoliths were crystalline and the crystalline structure started to develop immediately after exogenous feeding, we could not determine the rearing type, as the microstructure was not clear in the crystalline structure. When crystalline structure of one or both otoliths of a pair developed some time (approximately 40 days or more) after the exogenous feeding, the origin of the fish could still be determined.

Otolith microstructure pattern is known to be closely related to environmental factors, such as temperature and amount of food (Volk et al. 1984; Campan and Neilson 1985; Moksness and Fossum 1991; Wright et al. 1991; Tzeng and Yu 1992; Zhang and Runham 1992). Hatchery-reared chinook salmon in general, and Cowichan hatchery-reared chinook in particular, are well fed and reared in a stable environment, while the wild fish must endure variation in food supply and in the physical environment. Indeed, the postfeeding daily growth increments formed in the hatchery are not only more regular than those in the wild-fish otoliths, but also more regular than daily growth increments formed after the fish are released from the hatchery. The highly uniform and wide daily growth increments in the Cowichan hatchery-reared fish, as compared with other hatchery-reared fish, are possibly due to the constant and high temperature of the rearing water and the abundant food supply.

The formation of the releasing check described in our study was also reported in the otoliths of hatchery-reared kokanee salmon (*O. nerka*) (Paragamian et al. 1992). The physiological mechanism for otolith check formation is unclear, although the check is known to contain a very high concentration of protein (Zhang 1992), and check production has been found to be related to stress (Campana and Neilson 1985). A check was produced when sablefish (*Anoplopoma fimbria*) were transferred from the field to the laboratory (Boehlert and Yoklavich 1985) and when there was an abrupt change in salinity after the transfer (Umezawa and Tsukamoto 1990). Transfer of tilapia (*Oreochromis niloticus*) either from an optimal to a suboptimal condition or from a suboptimal to an optimal condition without evident physical stress also results in check formation (Zhang and Runham 1992), suggesting that adaptation to a new environment itself may be a stressful event to the fish, inducing check production. The releasing check, demarcating the regular increments formed in the hatchery and irregular ones formed after release from the hatchery, was probably due to adaption to a new environment rather than physical stress during the release, as in most hatcheries, fish were released simply by opening the barriers. Otoliths of some hatchery-released chinook salmon did not contain such a releasing mark, possibly because they adapted to the new environment more quickly.

The average length of the hatching check in the otoliths of Cowichan hatchery-reared chinook was less than that of wild chinook from the Cowichan River, although the difference was not significant. The average length of the first-feeding check from the former fish was significantly less than from the wild fish. This indicates that otoliths of the Cowichan hatchery-reared fish, possible upon hatching

and probably upon yolk absorption, were, on average, smaller than those of wild ones. This difference in otolith size perhaps resulted from the different water temperature, as exogenous feeding was not involved. Heming (1982) demonstrated that chinook salmon reared at high temperature were smaller and lighter upon hatching and yolk absorption than those at lower temperature because less energy in the yolk was converted overall for tissue growth. Peterson et al. (1977) also showed that alevins of Atlantic salmon (*Salmo salar*) that hatched at higher temperature were progressively smaller. For a given amount of energy supplied by the yolk, the Cowichan hatchery-reared chinook possibly convert less energy overall for otolith growth, resulting in relatively small otoliths. The difference in size of hatching check and first-feeding check could be used as a supplementary check for identification of Cowichan hatchery-reared and Cowichan wild chinook salmon.

This study identifies a practical and direct method for identifying hatchery-reared and wild chinook salmon, which may be used to study differences in abundance, recruitment, survival, movement, and growth without the need for a large-scale tagging and recovery program. In addition, growth history of individual fish, which is otherwise difficult to obtain, could be studied by using the width of the daily growth increments.

Acknowledgements

We thank Barbara Thomson, Chrys-Ellen Neville, Ray Scarsbrook, Dick Nagtegaal, and John Candy for collecting the fish samples. This study was funded through the Natural Sciences and Engineering Research Council of Canada.

References

Beamish, R.J., Riddell, G.E., Neville, C.M., Thomson, B.L., and Zhang, Z. 1995. Declines in chinook salmon catches in the Strait of Georgia in relation to shifts in the marine environment. Fish. Oceanogr. (In press)

Boehlert, G.W., and Yoklavich, M.M. 1985. Larval and juvenile growth of sablefish, *Anoplopoma fimbria*, as determined from otolith increments. Fish. Bull. **83**: 475–481.

Campana, S.E. 1983. Calcium deposition and otolith check formation during periods of stress in coho salmon, *Oncorhynchus kisutch*. Comp. Biochem. Physiol. **75A**: 215–220.

Campana, S.E., and Neilson, J.D. 1985. Microstructure of fish otoliths. Can. J. Fish. Aquat. Sci. **42**: 1014–1032.

Gauldie, R.W. 1991. The morphology and periodic structures of the otolith of the chinook salmon (*Oncorhynchus tshawytscha*), and temperature-dependent variation in otolith microscopic growth increment width. Acta Zool. (Stockholm), **72**: 159–179.

Heming, T.A. 1982. Effects of temperature on utilization of yolk by chinook salmon (*Oncorhynchus tshawytscha*) eggs and alevins. Can. J. Fish. Aquat. Sci. **39**: 184–190.

Marshall, S.L., and Parker, S.S. 1982. Pattern identification in the microstructure of sockeye salmon (*Oncorhynchus nerka*) otoliths. Can. J. Fish. Aquat. Sci. **39**: 542–547.

Moksness, E., and Fossum, P. 1991. Distinguishing spring- and autumn-spawned herring larvae (*Clupea harengus*) by otolith microstructure. ICES J. Mar. Sci. **48**: 61–66.

Mugiya, Y., and Takahashi, K. 1985. Chemical properties of the saccular endolymph in the rainbow trout, *Salmo gairdneri*. Bull. Fac. Fish. Hokkaido Univ. **36**: 57–63.

Mugiya, Y., and Uchimura, T. 1989. Otolith resorption by anaerobic stress in the gold fish, *Carassius auratus*. J. Fish. Biol. **35**: 813–818.

Neilson, J.D., and Geen, G.H. 1982. Otoliths of chinook salmon (*Oncorhynchus tshawytscha*): daily growth increments and factors influencing their production. Can. J. Fish. Aquat. Sci. **39**: 1340–1347.

Neilson, J.D., Geen, G.H., and Bottom, D. 1985. Estuarine growth of juvenile chinook salmon (*Oncorhynchus tshawytscha*) as inferred from otolith microstructure. Can. J. Fish. Aquat. Sci. **42**: 899–908.

Paragamian, V.L., Bowles, E.C., and Hoelscher, B. 1992. Use of daily growth increments on otoliths to assess stockings of hatchery-reared kokanees. Trans. Am. Fish. Soc. **121**: 785–791.

Peterson, R.H., Spinney, H.C.E., and Sreedharan, A. 1977. Development of Atlantic salmon (*Salmo salar*) eggs and alevins under varied temperature regimes. J. Fish. Res. Board Can. **34**: 31–43.

Tzeng, W.-N., and Yu, S.-Y. 1992. Effects of starvation on the formation of daily growth increments in the otoliths of milkfish, *Chanos chanos* (Forsskal), larvae. J. Fish Biol. **40**: 39–48.

Umezawa, A., and Tsukamoto, K. 1990. Determination of stock origin of the ayu based on the otolith microstructure. Nippon Suisan Gakkaishi, **56**: 1919–1926.

Volk, E.C., Wissmar, R.C., Simenstad, C.A., and Eggers, D.M. 1984. Relationship between otolith microstructure and the growth of juvenile chum salmon (*Oncorhynchus keta*) under different prey rations. Can. J. Fish. Aquat. Sci. 41: 126–133.

Wright, P.J., Rowe, D., and Thorpe, J.E. 1991. Daily growth increments in the otoliths of Atlantic salmon parr (*Salmo salar* L.) and the influence of environmental factors on their periodicity. J. Fish Biol. **39**: 103–113.

Wright, P.J., Talbot, C., and Thorpe, J.E. 1992. Otolith calcification in Atlantic salmon parr, *Salmo salar* L. and its relation to photoperiod and calcium metabolism. J. Fish Biol. **40**: 779–790.

Zhang, Z. 1992. Ultrastructure of otolith increments and checks in the teleost fish *Oreochromis niloticus*. J. Morphol. **211**: 213–220.

Zhang, Z., and Runham, N.W. 1992. Effects of food ration and temperature level on the growth of *Oreochromis niloticus* (L.) and their otoliths. J. Fish Biol. **40**: 341–349.

Effects of aluminum and fluoride on phosphorus acquisition by *Chlamydomonas reinhardtii*

Elaine M. Joseph, François M.M. Morel, and Neil M. Price

Abstract: Al (10 μM) and F (50 μM) added singly or in combination have no effect on growth of *Chlamydomonas reinhardtii* in acid or alkaline media containing organic or inorganic P. Cell surface phosphatase activity, however, is increased in glucose-1-phosphate-amended cultures exposed to Al, but only at low pH. This result is an indirect effect caused by Al binding to the organic P, which inhibits organic P utilization and induces phosphatase synthesis in *C. reinhardtii* as a compensatory response. Phosphatase activity is inversely correlated with lake pH, suggesting that such a mechanism may operate in nature. Al thus appears to enhance phosphatase activity in acidified waters by impeding dissolved organic P catabolism.

Résumé : L'Al (10 μM) et le F (50 μM), ajoutés séparément ou simultanément, n'ont aucun effet sur la croissance du *Chlamydomonas reinhardtii* dans des milieux acides ou alcalins contenant du P organique ou inorganique. L'activité de la phosphatase à la surface de la cellule augmente toutefois dans des cultures enrichies au glucose-1-phosphate et exposées à l'Al, mais seulement à un faible pH. Ce résultat est un effet indirect de la liaison de l'Al au P organique, qui inhibe l'utilisation du P organique et induit la synthèse de la phosphatase chez *C. reinhardtii* comme réaction de compensation. L'activité de la phosphatase est inversement corrélée au pH du lac, ce qui semble indiquer qu'un tel mécanisme peut fonctionner dans la nature. L'Al semble donc augmenter l'activité de la phosphatase dans les eaux acidifiées en entravant le catabolisme du P organique dissous.
[Traduit par la Rédaction]

Introduction

The potential effect of Al on aquatic life is a subject of interest, spurred in part by the release of high Al concentrations in acidified lakes. Besides reports of Al toxicity to fish (Sigel and Sigel 1988; Birchall et al. 1989), there have been a number of reports on the effects of Al on phytoplankton (Folsom et al. 1986; Rueter et al. 1987; Claesson and Törnqvist 1988; Pettersson et al. 1988; Törnqvist 1989; Gensemer 1990, 1991). One such reported effect is the induction of high phosphatase activity in an acidified lake (Jansson 1981), although another study indicated the opposite effect in laboratory cultures (Pettersson et al. 1988).

Recently, researchers studying adenylate cyclase and other G-protein systems have focused attention on the role played by the AlF_4-complex (Chabre 1990). Acting apparently as a structural analog of PO_4^{3-}, AlF_4^- binds to the nucleotide site of the G-protein and in the presence of a suitable guanoside nucleotide (guanosine diphosphate (GDP)) activates the protein. The AlF_4^- complex inhibits some ATPases and phosphatases by interacting with the active site, preventing binding of the substrate (Missiaen et al. 1988; Dupuis et al. 1989), although not all of these enzymes are equally sensitive (Missiaen et al. 1989).

Because fluoro–Al complexes may account for a significant fraction of the monomeric Al species in acidified natural waters (Campbell et al. 1992), the issue of the possible role of Al as an inhibitor of phosphatases in phytoplankton is worth revisiting. Specifically, one may hypothesize that Al would inhibit the utilization of dissolved organic P by phytoplankton through competitive binding of AlF_4^- to the active site of phosphatases, a class of ectoenzymes (Price and Morel 1990). Algal phosphatases are induced by P limitation or when orthophosphate concentrations are low (or when organic P is the sole P source) and consequently have been used to diagnose the P status of algae in natural waters (Healey and Hendzel 1979; Cembella et al. 1984). Here we report that indeed, Al affects phosphatase activity in cultures of the green alga *Chlamydomonas reinhardtii*; however, rather than a direct effect of Al_3^+ or AlF_4^- on the enzymes, the inhibition is the indirect result of Al binding to the organic P substrate as hypothesized by Jansson (1981).

Received January 24, 1994. Accepted July 14, 1994.
J12247

E.M. Joseph,[1] F.M.M. Morel, and N.M. Price.[2]
R.M. Parsons Laboratory, Department of Civil and Environmental Engineering, Massachusetts Institute of Technology, Cambridge, MA 02139, USA.

[1] Present address: Department of Biochemistry and Molecular Biology, 7 Divinity Ave., Harvard University, Cambridge, MA 02138, USA.
[2] Author to whom correspondence should be addressed. Present address: Department of Biology, 1205 Ave. Dr. Penfield, McGill University, Montreal, QC H3A 1B1, Canada.

Materials and methods

Chlamydomonas reinhardtii Dang (UTEX Culture Collection No. 90) was grown in microwave-sterilized Fraquil medium (Morel et al. 1978) containing 0.1 μM H_3BO_3 and 20 μM KCl, but without $Na_2SiO_3 \cdot 9H_2O$. Inorganic phosphate (10 μM Na_2HPO_4) or organic P (10 μM α-D-glucose-1-phosphate (G-1-P)) was added as P source. Alkaline (pH 8.1) and acidic (pH 5.5) media were buffered with 10 mM Tris (tris(hydroxymethyl)aminomethane) and 10 mM MES (2(*N*-morpholino)ethanesulfonic acid), respectively. All stock solutions and media were purified of trace metal contaminants by Chelex-100 resin (Bio-rad). Vitamins and trace metals complexed with ethylenediaminetetraacetic acid (EDTA) were filter-sterilized through sterile, acid-washed 0.2-μm filters (Acrodisc) and then added to sterile medium. Cultures were maintained under continuous light (120 μmol quanta$\cdot m^{-2} \cdot s^{-1}$) at a temperature of 20°C in polycarbonate flasks. Standard procedures for the preparation and handling of trace metal clean media were followed (Price et al. 1988/1989).

In the acidic media, Al ($AlCl_3 \cdot 6H_2O$) and F (NaF) additions were adjusted so that their free ion concentrations remained constant in all treatments: Al-enriched media contained 4.4 μM Al, F-enriched media contained 37.5 μM F, and Al–F-enriched media contained 10 μM Al and 50 μM F. Similar additions were made to alkaline media. Under these conditions, however, the Al concentration exceeded the predicted solubility of inorganic species. The medium thus contained a mixture of dissolved monomeric and polymeric Al species and particulate Al $(OH)_3$(s). Al–EDTA complexes were insignificant at pH 8.1, but were one of the principal forms of Al at pH 5.5: in Al-enriched medium, >99% of total dissolved Al was $AlEDTA^-$ and $(AlOH)EDTA^{2-}$, and in Al–F-enriched medium, 45% of the Al was complexed by EDTA. Equilibrium calculations were performed using MINEQL (Westall et al. 1976) with stability constants for metal– EDTA complexes provided by Ringbom (1963): free-ion concentration of Al^{3+} at pH 5.5 was $10^{-9.04}$. Control media contained no added Al or F.

Phosphatase activity was measured by the methylfluorescein phosphate (3-OMFP) method of Perry (1972), without 0.05 M NaOH. Production of 3-*O*-methylfluorescein (3-OMF) was measured fluorometrically using a Perkin-Elmer LS-5 spectrofluorometer with excitation and emission wavelengths of 472 and 511 nm, with 10-nm slit widths. Standard solutions of 3-OMF were used to calibrate the instrument.

Two types of phosphatase assays were conducted. In long-term exposure experiments, *C. reinhardtii* was grown in Fraquil containing Al, F, Al and F, or no addition and harvested in exponential phase by centrifugation (Beckman TJ-6, 1500*g* for 10 min). Phosphatase activity was determined in cells resuspended in Tris or MES-buffered Fraquil, containing no added Al or F. In short-term exposure experiments, cells were grown in Fraquil containing G-1-P, but no added Al or F, and resuspended and assayed for phosphatase activity in equilibrated, MES-buffered Fraquil (pH 5.5) containing Al, F, Al and F, or no addition. All assays were conducted in 3-mL cuvettes and rates of 3-OMF production were determined over 10-min incubations.

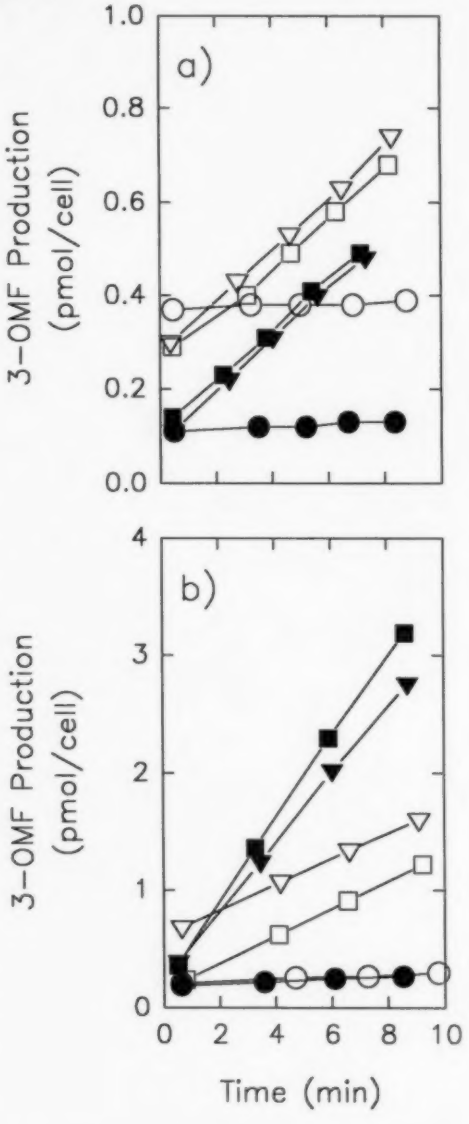

Fig. 1. Phosphatase activity of *C. reinhardtii* grown in (*a*) alkaline medium (pH 8.1) and (*b*) acid medium (pH 5.5) containing PO_4^{3-} or G-1-P as P source with and without Al and F additions: ○, PO_4^{3-}; ●, PO_4^{3-} + Al + F; ▽, G-1-P; ▼, G-1-P + Al; □, G-1-P + F; ■, G-1-P + Al + F. Phosphate-grown cultures were only exposed to a mixture of Al and F. Immediately prior to the phosphatase assay, exponentially growing cells were harvested and resuspended in assay buffer lacking Al and F.

Complexation of Al by G-1-P was examined in the presence of 0.8 mM 8-hydroxyquinoline-5-sulfonate (HQS), using an excitation wavelength of 392 nm (slit width 15 nm) and measuring fluorescence emission between 425 and 600 nm (slit width 10 nm).

Fig. 2. Phosphatase activity of *C. reinhardtii* grown in acid medium (pH 5.5) containing G-1-P as P source. Cells were harvested in exponential phase and resuspended in acid assay buffer containing 4.7 μM Al (●), 37.5 μM F (▽), 10 μM Al and 50 μM F (▼), or no addition (○). In each treatment, the assay buffer was equilibrated for 24 h prior to use.

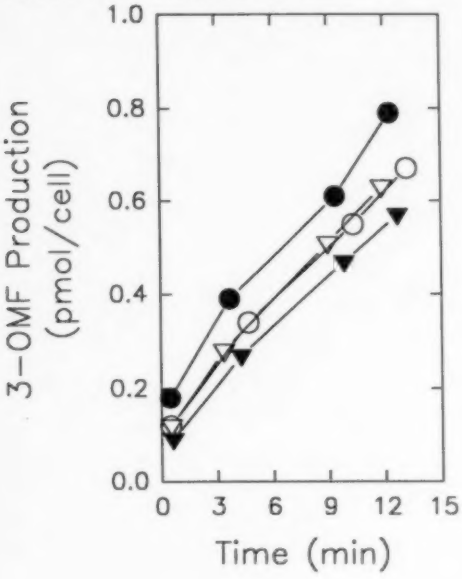

Fig. 3. Relative fluorescence emission of 0.8 mM HQS in acidic solution (pH 4) with 1 mM Al (○) and 1 mM Al and 1 mM G-1-P (●). In the absence of Al with or without G-1-P, HQS did not fluoresce. G-1-P had no effect on the fluorescence of alkaline solutions (pH 7.3) of HQS containing Al.

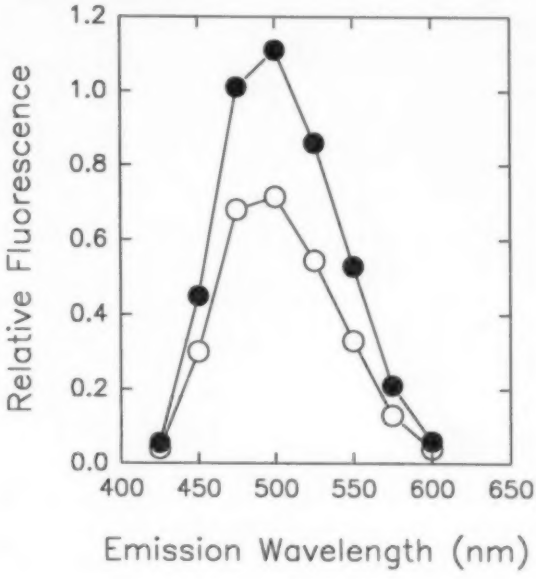

Results and discussion

In batch cultures, *C. reinhardtii* exhibited the same growth rates (0.12 ± 0.01/h: mean of duplicates ± 1 SD) and cell yields when grown on inorganic (PO_4^{3-}) or on organic (G-1-P) P. This result was independent of pH (5.5 or 8.1) and unaffected by the addition of up to 10 μM Al^{3+} and excess F^-.

As expected, phosphatase activity was much higher in cultures grown on G-1-P than in those grown on PO_4^{3-} (Fig. 1). The presence of Al in the growth medium resulted in a further enhancement of phosphatase activity under acidic conditions, but not at high pH. Since this enhancement was independent of the presence or absence of F^-, the AlF_4^- complex was probably not involved. Thus, the results provided no evidence for AlF_4^- inhibition of *C. reinhardtii* cell surface phosphatases which were quantified by our assay. Further, we may rule out both a direct, short-term positive effect of Al on the enzyme and an inhibition of PO_4^{3-} transport (PO_4^{3-} must be taken up after cleavage from the organic moiety) because Al induced neither an enhancement of phosphatase activity nor a decrease in growth rate in cells grown on PO_4^{3-}. The observed enhancement of phosphatase activity in the long-term exposure experiments in acid medium at high Al concentrations, which was also observed under limiting P conditions (results not shown), was probably the result of a compensatory control mechanism. Additional phosphatase was synthesized because P acquisition by *C. reinhardtii* was impeded. Thus, one may postulate either a direct or an indirect Al inhibition of organic phosphate utilization in acid medium.

A direct inhibition of the enzyme was ruled out by the results of short-term exposure experiments. Addition of Al (with or without F^-) to the assay medium had no effect on phosphatase activity (Fig. 2). The organic P concentration used in the assay (0.15 μM 3-OMFP) was below saturation of the phosphatase enzyme, as determined in parallel experiments, and unlikely to mask inhibitory effects through competitive binding. Thus, the most likely explanation for the data is that proposed by Jansson (1981): Al may inhibit organic P utilization through binding of the substrate in the growth medium. This explanation would be consistent with all our data: cells grown on G-1-P (10 μM) in acidic medium at high Al concentration behave exactly as if P were in short supply. Interestingly, the increase in phosphatase activity observed in the long-term experiments fully compensates for the decreased availability of the G-1-P because growth rates are unaltered by Al treatment. Because Al has no effect on phosphatase activity in the short-term exposure experiment, no similar binding of 3-OMFP must be occurring in the assay medium.

Direct support for this substrate-binding hypothesis was obtained from fluorescence measurements of HQS in the presence of Al, with and without G-1-P. The Al–HQS complex fluoresces at 500 nm at both pH 4 and pH 7.3. As seen in Fig. 3, addition of G-1-P to the solution enhances the fluorescence, but only at the low pH. Because there

Fig. 4. In situ phosphatase activity measured at ambient or near ambient pH in acidic and alkaline lakes. Each data point represents the phosphatase activity in an individual lake: data were obtained from Francko (1986) (▼), Hecky et al. (1993) and L.L. Hendzel (personal communication) (□), Jansson (1981) (▽), Olsson (1983) (●), and Olsson (1990) (○). Error bars represent 1 SD of the mean.

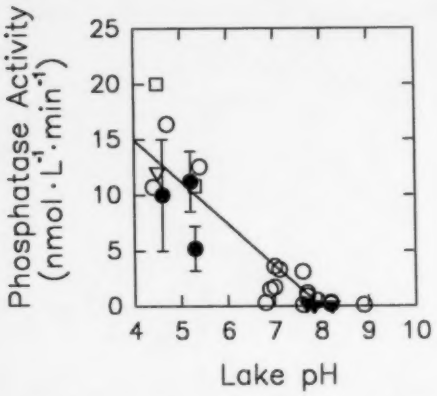

is no fluorescence in the absence of Al, these data indicate formation of a highly fluorescent ternary complex, Al–HQS–(G-1-P), at pH 4 and not pH 7.3. These chemical results are entirely consistent with our biological data which are best explained by the formation of an unavailable Al–(G-1-P) complex at low, but not at high pH.

Elevated Al concentrations are characteristic of all acidified lakes (Dillon et al. 1984) so that the relative concentration of Al – organic P complexes should increase as lake pH decreases. Phosphatase activity should correspondingly increase to compensate for the reduced availability of organic P. Indeed, when literature data were analyzed, we observed a significant inverse correlation between phosphatase activity and lake pH (Fig. 4) (Spearman rank order correlation, $p < 0.005$), suggesting that the Al-binding mechanism may induce high phosphatase activity in acidified, natural waters. Such a mechanism was proposed to account for the elevated phosphatase activity in Lake Gårdsjön (Jansson 1981). The result of our literature analysis implies that high phosphatase activity may be a general characteristic of all acidic lakes caused by the formation of "biologically inert" Al – organic P complexes. Although some acidic lakes contain lower concentrations of P than non-acidic lakes (Blomqvist et al. 1993) and would thus be expected to have higher phosphatase activities (Smith and Kalff 1981), in the lakes we analyzed, total P concentration and pH did not covary (Spearman rank order correlation, $p > 0.05$).

In summary, the chemical and biochemical analyses demonstrate that at acidic pH, Al – organic P complexes are formed which are not accessible to algal cell surface phosphatases. To compensate for the reduction in available organic P, *C. reinhardtii* synthesizes additional phosphatase enzyme. In acidified natural waters, Al may thus complex naturally occurring organic P compounds, reducing their availability and enhancing phosphatase production.

Acknowledgments

Funding was provided by grants from NSF, ONR, and NSERC. We thank Dr. P.G.C. Campbell and M.R. Twiss for providing comments on an earlier version of the manuscript.

References

Birchall, J.D., Exley, C., Chappell, J.S., and Phillips, M.J. 1989. Acute toxicity of aluminium to fish eliminated in silicon-rich acid waters. Nature (Lond.), **338**: 146–147.

Blomqvist, P., Bell, R.T., Olofsson, H., Stensdotter, U., and Vrede, K. 1993. Pelagic ecosystem responses to nutrient additions in acidified and limed lakes in Sweden. Ambio, **22**: 283–289.

Campbell, P.G.C., Hansen, H.J., Dubreuil, B., and Nelson, W.O. 1992. Geochemistry of Quebec North Shore salmon rivers during snowmelt: organic acid pulse and aluminum mobilization. Can. J. Fish. Aquat. Sci. **49**: 1938–1952.

Cembella, A.D., Antia, N.J., Harrison, P.J. 1984. The utilization of inorganic and organic phosphorus compounds as nutrients by eukaryotic microalgae: A multidisciplinary perspective: Part 2. CRC Crit. Rev. Microbiol. **11**: 13–81.

Chabre, M. 1990. Aluminofluoride and beryllofluoride complexes: new phosphate analogs in enzymology. Trends Biochem. Sci. **15**: 6–10.

Claesson, A., and Törnqvist, L. 1988. The toxicity of aluminum to two acido-tolerant green algae. Water Res. **22**: 977–983.

Dillon, P.J., Yan, N.D., and Harvey, H.H. 1984. Acidic deposition: effects on aquatic ecosystems. CRC Crit. Rev. Environ. Control **13**: 167–194.

Dupuis, A., Issartel, J.-P., and Vignais, P.V. 1989. Direct identification of the fluoroaluminate and fluoroberyllate species responsible for the inhibition of the mitochondrial F_1-ATPase. Fed. Eur. Biochem. Soc. Lett. **255**: 47–52.

Folsom, B.R., Popescu, N.A., and Wood, J.M. 1986. Comparative study of aluminum and copper transport in an acid-tolerant freshwater green alga. Environ. Sci. Technol. **20**: 616–620.

Francko, D.A. 1986. Eplimnetic phosphorus cycling: influence of humic materials and iron on coexisting major mechanisms. Can. J. Fish. Aquat. Sci. **43**: 302–310.

Gensemer, R.W. 1990. Role of aluminum and growth rate on changes in cell size and silica content of silica-limited populations of *Asterionella ralfsii* var. *americana* (Bacillariophyceae). J. Phycol. **26**: 250–258.

Gensemer, R.W. 1991. The effects of pH and aluminum on the growth of the acidophilic diatom *Asterionella ralfsii* var. *americana*. Limnol. Oceanogr. **36**: 123–131.

Healey, F.P., and Hendzel, L.L. 1979. Fluorometric measurement of alkaline phosphatase activity in algae. Freshwater Biol. **9**: 429–439.

Hecky, R.E., Campbell, P., and Hendzel, L.L. 1993. The stoichiometry of carbon, nitrogen and phosphorus in particulate matter of lakes and oceans. Limnol. Oceanogr. **38**: 709–724.

Jansson, M. 1981. Induction of high phosphatase activity by aluminum in acid lakes. Arch. Hydrobiol. **93**: 32–44.

Missiaen, L., Wuytack, F., De Smedt, H., Vrolix, M., and Casteels, R. 1988. AlF_4^- reversibly inhibits "P"-type cation transport ATPases, possibly by interacting with the phosphate-binding site of the ATPase. Biochem. J. **253**: 827–833.

Missiaen, L., Wuytack, F., De Smedt, H., Amant, F., and Casteels, R. 1989. AlF_4^--induced inhibition of the ATPase activity, the Ca^{2+}-transport activity and the phosphoprotein-intermediate formation of plasma-membrane and endo(sarco)plasmic-reticulum Ca^{2+}-transport ATPases in different tissues. Biochem. J. **261**: 655–660.

Morel, F.M.M., Westall, J.C., Rueter, J.G., and Chaplick, J.P. 1978. Description of the algal growth media "Aquil and Fraquil". Tech. Note 16, R.M. Parsons Laboratory, M.I.T., Cambridge, Mass.

Olsson, H. 1983. Origin and production of phosphatases in the acid Lake Gårdsjön. Hydrobiologia, **101**: 49–58.

Olsson, H. 1990. Phosphatase activity in relation to phytoplankton composition and pH in Swedish Lakes. Freshwater Biol. **23**: 353–362.

Perry, M.J. 1972. Alkaline phosphatase activity in subtropical central North Pacific waters using a sensitive fluorometric method. Mar. Biol. **15**: 113–119.

Pettersson, A., Hällbom, L., and Bergman, B. 1988. Aluminum effects on uptake and metabolism of phosphorus by the cyanobacterium *Anabaena cylindrica*. Plant Physiol. **86**: 112–116.

Price, N.M., and Morel, F.M.M. 1990. Role of extracellular enzymatic reactions in natural waters. *In* Aquatic chemical kinetics. *Edited by* W. Stumm. John Wiley & Sons, Inc., New York, N.Y. pp. 235–257.

Price, N.M., Harrison, G.I., Hering, J.G., Hudson, R.J., Nirel, P.M.V., Palenik, B., and Morel, F.M.M. 1988/1989. Preparation and chemistry of the artificial algal culture medium Aquil. Biol. Oceanogr. **6**: 443–461.

Ringbom, A. 1963. Complexation in analytical chemistry. Interscience, New York, N.Y.

Rueter, J.G. Jr., O'Reilly, K.T., and Peterson, R.R. 1987. Indirect aluminum toxicity to the green alga *Scenedesmus* through increased cupric ion activity. Environ. Sci. Technol. **21**: 435–438.

Sigel, H., and Sigel, A. (*Editors*). 1988. Metal ions in biological systems — aluminum and its role in biology. Vol. 24.

Smith, R.E.H., and Kalff, J. 1981. The effect of phosphorus limitation on algal growth rates: evidence from alkaline phosphatase. Can. J. Fish. Aquat. Sci. **38**: 1421–1427.

Törnqvist, L. 1989. Ultrastructural changes and altered localization of acid phosphatases in *Monoraphidium* and *Stichococcus* cells (Chlorophyceae) influenced by aluminum. Environ. Exp. Bot. **4**: 457–465.

Westall, J.C., Zachary, J.L., and Morel, F.M.M. 1976. MINEQL, a computer program for the calculation of the chemical equilibrium composition of aqueous systems. Tech. Note 18, R.M. Parsons Laboratory, M.I.T., Cambridge, Mass.

Use of the lateral line in particulate feeding in the dark by juvenile alewife (*Alosa pseudoharengus*)

John Janssen, Warren R. Jones, Audrey Whang, and Philip E. Oshel

Abstract: The alewife (*Alosa pseudoharengus*) is an obligate planktivore which uses a variety of methods for capturing zooplankton. Alewife eat *Mysis relicta*, especially larger individuals, at night during a vertical migration by both predator and prey. We proposed and tested the hypothesis that alewife use the lateral line to sense prey and feed particulately (single prey at a time) in the dark. We used *Daphnia magna* and *Artemia salina* adults as prey. Prey densities were such that they did not elicit filter feeding. Observations using infrared video showed that alewife captured individual prey and bit at a vibrating inert bead. We concluded that under appropriate conditions, alewife were size selective and that streptomycin (which blocks the lateral line sensory cells) eliminated this feeding behavior.

Résumé : Le gaspareau (*Alosa pseudoharengus*) est un planctivore obligé qui utilise des méthodes diverses pour capturer le zooplancton. Le gaspareau consomme des *Mysis relicta*, particulièrement les individus de grande taille, en se nourrissant la nuit au cours d'une migration verticale effectuée à la fois par le prédateur et par sa proie. Nous avons proposé et testé l'hypothèse selon laquelle le gaspareau se servirait de sa ligne latérale pour percevoir la présence des proies et se nourrirait sélectivement (une proie à la fois) dans le noir. Nous avons utilisé comme proies des adultes de *Daphnia magna* et d'*Artemia salina*. Les densités des proies étaient telles qu'elles ne favorisaient pas un mode d'alimentation par filtration. Les observations réalisées à l'aide de la vidéo dans l'infrarouge ont montré que le gaspareau capture une proie à la fois et s'attaque à une perle de matière inerte qui vibre. Nous concluons que, dans des conditions appropriées, le gaspareau sélectionne ses proies en fonction de leur taille. Nous avons également observé que la streptomycine (qui bloque les cellules sensorielles de la ligne latérale) élimine ce comportement d'alimentation.
[Traduit par la Rédaction]

Introduction

The tactics of interactions between fish and zooplankton, predator and prey, are diverse (Lazzaro 1987). Where size-selective feeding is indicated by field dietary studies, it is presumed (generally) that planktivores operate by visually detecting prey. Vertical migration of zooplankton is inferred to minimize predation risk when the upper part of the water column is well lighted. Young and Watt (1993) argued that during the day, zooplankters ought to be deep enough to be visually undetectable and ascend into the phytoplankton-rich zone when it is too dark to be seen. This situation appears to be true for interaction of *Mysis relicta* with the alewife (*Alosa pseudoharengus*). Janssen and Brandt (1980) found that during the day, at a 50-m bottom depth, *Mysis* were on the bottom and unavailable to the alewife because alewife have difficulty feeding on the bottom (Janssen 1978*a*). At night, *Mysis* migrated into the water column and larger individuals were eaten by alewife, although the mechanism by which *Mysis* were detected was unclear. Urban and Brandt (1993) found nocturnal size-selective feeding on microcrustacea by young-of-the-year alewife. Nocturnal conditions should be suboptimal for visual predation. We propose that alewife can use an alternative sense, the hydromechanically sensitive lateral line, to detect and consume zooplankters. Prey used in this study represent two distinct swimming types: "hop and sink" (*Daphnia*) and continuous swimming via metachronal beating of the phyllopods (*Artemia*). *Mysis* uses metachronal swimming which may be similar to *Artemia*. *Artemia* were used as a surrogate for *Mysis* because the latter require very cool water.

Received February 10, 1994. Accepted August 5, 1994.
J12271

J. Janssen, W.R. Jones, and A. Whang. Biology Department, Loyola University, 6525 N. Sheridan, Chicago, IL 60626, USA.
P.E. Oshel. Parmly Hearing Institute, Loyola University, 6525 N. Sheridan, Chicago, IL 60626, USA.

Methods

Alewife were raised from artificially fertilized eggs in 120-L vats in a greenhouse, fed pond plankton, *Artemia salina* metanauplei, and, when fish were large enough, *Daphnia magna* from cultures. Groups of three fish (four in the preliminary experiment), 20–72 mm standard length

(SL), were placed in black-walled 38-L all-glass aquaria in a light-sealed room. Fish ranged in age from about 2 months (earlier experiments) to 5 months (later experiments). An artificial 13 h light : 11 h dark photoperiod was maintained.

Ten experiments testing feeding in the dark were conducted. Experimental prey regimes were exploratory in terms of prey species and density. Before running a feeding experiment in the dark, we fed each group only in the dark for about 1 week on *Daphnia magna* or adult *Artemia salina* (Table 1). *Daphnia* were from a culture; various sizes were sieved on a nitex screen when needed for experiments. Adult *Artemia* were obtained from a pet store. Prey were counted before introduction to the experimental apparatus. A preliminary experiment (PRELIMINARY, see Table 1 for titles of experiments) used only large *Daphnia*, retained on a 2-mm nitex screen. The eight experiments that followed were conducted as pairs; alewife in one experiment per pair had their lateral line function eliminated with streptomycin (10 mM), a means of pharmacologically eliminating lateral line function (Kaus 1987). Blaxter and Fuiman (1989) showed that streptomycin was effective on clupeids. Streptomycin was added 6 h before the experiment, except for experiment DAPHNIA-1 when it was added about 30 h prior to the experiment. One final experiment (experiment ARTEMIA-DAPHNIA-2) was unpaired due to a lack of fish. Paired experiments had the same training and test prey regimes. Paired experiments were tested on a two-night sequence and the experiment tested the first night was randomly determined. For streptomycin-treated fish, a few *Artemia* metanauplei were introduced about 1 h before lights were turned off to determine whether fish would feed visually with the lateral line ablated. For experiment DAPHNIA-1, when the streptomycin was added the day before the experiment, fish were fed in the light 5 h after treatment to confirm that the dosage did not inhibit visual feeding. After feeding for 2 h, fish were killed in ice water, their stomachs removed and preserved in 70% ethanol, and the remaining carcasses preserved in 3% glutaraldehyde. The aquarium was drained and remaining prey preserved in 70% ethanol.

All experiments, except ARTEMIA-DAPHNIA-2, were videotaped with an infrared camera viewing from underneath the aquarium via a mirror. Infrared lighting was from one side of the aquarium so fish were seen as bright on a dark background. For experiment ARTEMIA-DAPHNIA-2, no infrared was used and the aquarium was wrapped in black plastic to insure that fish were not feeding by infrared light or some other source.

Prior to experiment ARTEMIA-DAPHNIA-2, three alewife were used for some lateral videotaping with infrared light to record individual prey captures. Videotaping with an underside view adequately showed fish swimming, but we could not see prey captures. To record prey captures, a side view with the camera close to one aquarium wall was used. This sacrificed the view of most of the aquarium and depth of field was poor, but prey could be resolved and we were able to record a number of captures on video. Prey densities varied from about 50 to 200 *Daphnia* or *Artemia*/test.

We recorded two sessions (experiment DAPHNIA-ARTEMIA-2 fish) with 200 large *Daphnia* and a 4-mm bead attached to a Bruel and Kjeir vibrator. In one session the bead vibrated at 6 Hz with a total displacement of 1.1 mm. In the other session the bead was stationary.

The gross morphology and extent of development of the lateral line system were determined in the sacrificed fish using either scanning electron microscopy (SEM) or filling lateral line canals with India ink. For SEM, fixed specimens were prepared according to conventional protocols (Jones and Janssen 1992). From these specimens, the disposition of the superficial system of neuromasts could be determined. To reveal the extent of the canal system of neuromasts, specimens were bleached for several hours at room temperature in a dilute aqueous solution of hydrogen peroxide to remove skin-associated pigment. The canals were then filled with a dilute solution of India ink introduced into the canals via the pores using a fine capillary pipette.

Results

All fish in the experiments except three (20 mm SL, experiment PRELIMINARY; 20 mm, experiment DAPHNIA-1, streptomycin; 28 mm, experiment DAPHNIA-1, no streptomycin) possessed a postmetamorphic, adult lateral line system. The distribution of both canal and superficial neuromasts conformed, in general, to the pattern characteristic (Bamford 1941; Stevens 1985) of the clupeids (Fig. 1). Canals were confined to the head and just behind the opercle; superficial neuromasts were distributed on both the head and trunk, although they were more numerous on the former. Canals communicated to the exterior by way of an elaborate, racemose system of pores. Superficial neuromasts were minute, averaging 10–25 μm in diameter. On the trunk, superficial neuromasts were arrayed as a longitudinal band one to five scales wide, extending from the dorsal margin of the operculum to the caudal peduncle and onto the anterior margin of the caudal fin. Additional longitudinal bands were observed (1) along the base of the dorsal fin and (2) along the ventral body margin as a band one scale wide extending from the pectoral fin to the posterior margin of the anal fin. The high density of superficial neuromasts flanking the lateral pores of the ethmoid commissure, the anterior maxilla, and the nares is particularly striking (Fig. 2).

Results from fish treated with streptomycin indicated that the lateral line was necessary for feeding in the dark. All 12 alewife exposed to streptomycin had empty stomachs whereas in contrast, only 2 of 19 untreated alewife had an empty stomach. One untreated fish (experiment DAPHNIA-2) which did not feed was small with no canals, and the other (experiment PRELIMINARY) had incompletely developed lateral line canals. One streptomycin-treated fish (20 mm, experiment DAPHNIA-1) was premetamorphic. None of these fish is included in Table 1. All streptomycin-treated fish fed in the light prior to testing in the dark.

Most experiments with *Daphnia* indicated statistically significant ($P < 0.05$) selection for larger prey (Table 1). Statistical analyses comparing *Daphnia* size in stomachs with those introduced into the aquarium as prey were tested using Kruskal–Wallis tests with post-hoc Dunn's multiple

Table 1. Summary and statistics for feeding experiments. Three fish with premetamorphic lateral lines were excluded (see text). For all experiments the null hypothesis was as follows: fish *Daphnia* sizes = available *Daphnia* sizes. For experiments PRELIMINARY, DAPHNIA-1, and DAPHNIA-2, a Kruskal–Wallis test was used followed by Dunn's multiple comparisons test (Hollander and Wolfe 1973). For experiments ARTEMIA-DAPHNIA-1 and ARTEMIA-DAPHNIA-2, *Daphnia* eaten by the fish were combined for a Mann–Whitney test. Fish size is SL in mm, *Daphnia* length (exclusive of tail spine) and *Artemia* length (head plus thorax) are in mm, mean and SD are given; NP = not present, available = sample population introduced to the fish, consumed = prey found in stomachs of experimental fish.

Prey source	Fish		*Daphnia*			*Artemia*	
	Number	Size	Number	Size (SD)	Statistics	Number	Size (SD)
PRELIMINARY (500 mixed size *Daphnia*)							
No streptomycin							
Available			110	2.5 (0.30)		NP	
Consumed	3	34–35	10–15	2.4–2.5 (0.22–0.35)	NS		
DAPHNIA-1 (300 large, 600 small)							
No streptomycin							
Available			69	1.5 (0.77)		NP	
Consumed	2	42–44	28–46	2.2–2.4 (0.56–0.77)	$P < 0.001$		
Streptomycin							
Available			64	1.9 (0.82)			
Consumed	2	37–38	Empty				
DAPHNIA-2 (200 large, 400 small)							
No streptomycin							
Available			80	1.6 (0.71)		NP	
Consumed	3	27–40	15–24	2.2–2.7 (0.39–0.49)	$P < 0.02$		
Streptomycin							
Available			46	1.8 (0.66)		NP	
Consumed	3	35–43	Empty				
ARTEMIA-DAPHNIA-1 (200 *Artemia*, 300 mixed *Daphnia*)							
No streptomycin							
Available			85	1.6 (0.31)		57	3.5 (0.49)
Consumed	3	49–57	1–6	1.8 (0.37)	$P < 0.02$	18	
Streptomycin							
Available			93	1.7 (0.32)		31	3.4 (0.71)
Consumed	3	43–48	Empty			Empty	
ARTEMIA-DAPHNIA-2 (75 *Artemia*, 75 large *Daphnia*)							
No streptomycin							
Available			26	2.6 (0.55)		30	3.6 (0.534)
Consumed	3	56–72	5–6	3.1 (0.58)	$P < 0.01$	3–7	
ARTEMIA (30 *Artemia*)							
No streptomycin							
Available			NP			10	3.3 (0.50)
Consumed	3	42–49				5–8	
Streptomycin							
Available			NP			18	3.2 (0.83)
Consumed	3	44–48				Empty	

Fig. 1. (*a*) Diagrammatic representation of the canal system of early, postmetamorphic alewife, based on India ink canal fills. EC, ethmoid canal; IO, infraorbital canal; MD, mandibular canal. (*b*) India ink canal fill of the infraorbital and mandibular canal showing the extensive branching of the associated pore system. Arrowheads indicate the location of canal neuromasts in the infraorbital canal. Bar = 1 mm.

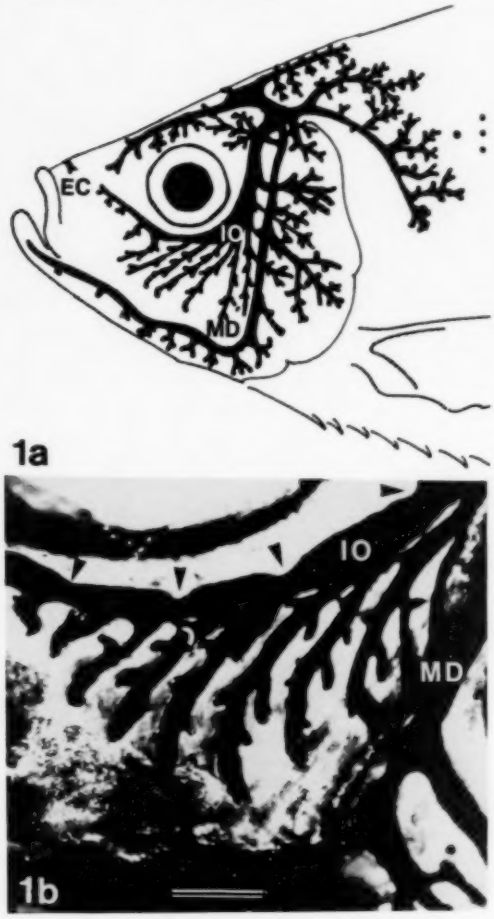

comparisons test (Hollander and Wolfe 1973). Because each fish could feed by particulate feeding or by filtering, each fish was considered and reported separately for the Kruskall–Wallis tests. The exception was the ARTEMIA-DAPHNIA-1 and 2 experiments; there were only a few *Daphnia*, so stomach content data from the three fish were combined and compared with the introduced prey by a Mann–Whitney test. All Kruskal–Wallis and Mann–Whitney analyses, except the PRELIMINARY experiment in which there were only very large *Daphnia*, indicated that fish were size selective, particulate feeding. We could not determine whether there was size selection for *Artemia* because those ingested were partly digested.

Results for mixed prey were ambiguous with regard to whether the "hop and sink" (*Daphnia*) or "metachronal"

Fig. 2. SEM of the snout showing the fields of superficial neuromasts associated with the anterior maxilla, nares (N), and forming ethmoid commissure (arrows). Starred arrow indicates the larger neuromasts of the forming ethmoid commissure. Bar = 250 μm.

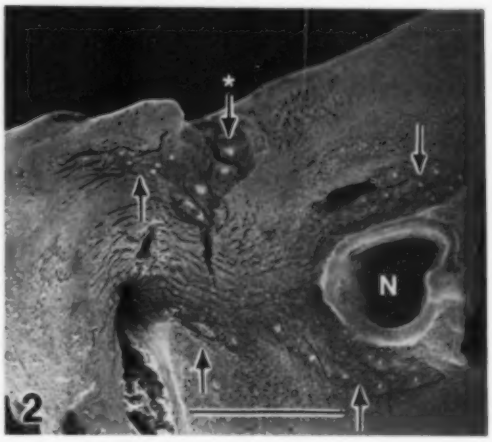

(*Artemia*) prey were more vulnerable. When *Daphnia* were of mixed sizes (experiment ARTEMIA-DAPHNIA-1), each fish diet was mainly *Artemia*; however, when only large *Daphnia* were present with *Artemia* (experiment ARTEMIA-DAPHNIA-2), the diet had about equal numbers of each.

The side views of alewife feeding (fish from experiment ARTEMIA-DAPHNIA-2) also indicated particulate feeding. During five sessions, 10 clear captures of *Daphnia* and 12 clear captures of *Artemia* were recorded. Although the underside views of the other experiments could not resolve actual prey captures, fish swimming was not the exaggerated swimming characteristic of filtering alewife (Janssen 1976, 1978*b*). Instead, fish beat the tail a few strokes and then coasted (about 30–60 mm/s). From the side-view sessions, it appeared that prey were only detected during the coast phase: in all 22 prey captures the bite was associated with a tail beat which altered the course to encounter the prey and hence terminated a coast. Reactive distances could not be clearly measured, but appeared to be only a few millimetres, a distance consistent with the measurements made by Hoekstra and Janssen (1986) for mottled sculpin (*Cottus bairdi*). The vibrating bead experiments also indicated use of the lateral line (fish from experiment ARTEMIA-DAPHNIA-2). The 2-h sessions yielded 15 bites at the vibrating bead and none at the non-vibrating bead. As with live prey, all bites were associated with an orienting tail flick which terminated a coast.

Discussion

Prey produce visual signals useful to fish trying to locate them in well-lighted systems. Vertical migration may make prey less visually obvious to their predators (Young and Watt 1993). Hydromechanical cues in the dark may give a better indication of location than noncontact chemical cues. Support for the use of the lateral line for particulate feeding by alewife in the dark is provided by the following:

(1) feeding in the dark was eliminated by streptomycin, which inhibits hair-cell function (Kaus 1987), (2) size-selective feeding by alewife indicated that they were not filtering prey, and (3) infrared videotaping recorded bites to a vibrating bead and particulate feeding on *Daphnia* and *Artemia*.

Little is known about hydromechanical signals produced by prey. *Artemia* swims with metachronal thoracic limb beating. Appendages oscillate at about 3 Hz; the individual limbs are about 1/9 cycle out of phase (Barlow and Sleigh 1980). These observations of tethered animals might suggest that the signal is a vibration from the appendages. However, the largest signal from a free-swimming animal is a single pulse produced by a pressure wave (Bleckman et al. 1991). We assume that free-swimming *Mysis*, which also swim by metachronal limb-beating, would produce a single pulse signal larger than that for *Artemia* because *Mysis* is larger (about 4–10 mm head plus thorax length, alewife stomachs of Janssen and Brandt 1980). The signal produced by "hop and sink" swimming (a few hertz) of *Daphnia* is a pulse caused by each stroke of the swimming antennae (Kirk 1985).

Other hydromechanical signals, such as schooling conspecifics and the presence of predators, are received by the lateral line. Avoidance responses in the dark to large vibrating inert objects, but no stationary ones, were reported by Blaxter and Batty (1985) for Atlantic herring (*Clupea harengus*). Assuming Atlantic herring and alewife have similar abilities, it would appear that both species could determine the size of the source. As with our experiment, Atlantic herring did not respond to a nonvibrating object.

While it is more difficult to establish the sensory basis for nocturnal feeding by alewife on *Mysis relicta* reported by Janssen and Brandt (1980), we think the case for use of the lateral line is strong. Light levels would be marginal for alewife to see *Mysis* at night. Blaxter (1988) estimated that fishes with no visual specialization for night vision (including clupeids) need 10^{-3} $\mu W/cm^2$ for visually oriented behaviors (such as schooling) with feeding probably requiring more light. Vinyard and O'Brien (1976) found that reactive distance in bluegill (*Lepomis macrochirus*) to large *Daphnia* decreased from 24 to 4 cm as light decreased from 3.2 and 0.7 $\mu W/cm^2$. Two nights from Janssen and Brandt's (1980) study had full moons with *Mysis* and fish concentrated below about 35 m. Based on light intensities for the full moon given by Blaxter (1988) ($<10^{-1}$ $\mu W/cm^2$) and light attenuation estimated at about 1% of surface light at about 33 m (Scavia et al. 1986), we estimated a light intensity slightly less than 10^{-3} $\mu W/cm^2$ near the top of the *Mysis* layer. One night from the Janssen and Brandt (1980) study had a new moon, so the estimated surface light would be about 10^{-4} $\mu W/cm^2$ (Blaxter 1988); in this case, the *Mysis* and fish were in the thermocline, about 5 m below the surface.

Our observation that alewife captured prey at the end of coasting indicates that they altered their swimming to minimize self-generated hydromechanical noise which might interfere with lateral line reception. In the light, actively feeding alewife swim constantly. Janssen et al. (1990) found that mottled sculpin slowed their search movements when the stimulus (water jets) was less detectable. It is interesting that the coasting speed (about 30–60 mm/s) of these alewife is similar to that of the blind cave tetra (*Astyanax jordani*) which exhibit a similar swimming behavior when feeding using their superficial neuromasts (Abdel-Latif et al. 1990). The blind cave tetra apparently detects prey via its superficial neuromasts; alewife could detect their prey either by the canal or superficial neuromasts.

We do not suggest that the lateral line system is the most important sense for feeding alewife. We advocate that the sensory modes used in feeding are diverse for most fishes. The sense which is most useful with depend on conditions that affect prey detectability. We argue that the lateral line is used for foraging by fishes much more that is currently appreciated. Unger et al. (1984) reported nonvisual feeding in an atherinid; they could not identify the sensory system used, but the lateral line is probable. Newman and Waters (1984) found that stream trout were active nocturnal benthos feeders. Light levels were probably sufficient for visual detection of noncryptic prey in clear streams, but many prey are cryptically marked (Feltmate et al. 1992) and difficult to see even with good lighting. Although Newman and Waters (1984) reported that their fish ate larger prey, size selection alone cannot be used as a criterion for visual detection of prey (our results; Lannoo 1986).

We advocate the view that sensory systems are cooperative rather than competitive. When optical conditions are suboptimal, it is likely that fish are first alerted to a prey by one cue, but the cue that finally localizes the prey stimulates another sensory system. A more robust understanding of the sensory basis of fish foraging will come with a better understanding of how fishes integrate their sensory modalities.

Acknowledgements

This research was funded in part by the Illinois–Indiana Sea Grant Program, project No. 91-179, grant No. COMMNA89AA-DSG058, under the National Sea Grant College Program, National Oceanic and Atmospheric Administration, U.S. Department of Commerce.

References

Abdel-Latif, H., Hassan, E.S., and von Campenhausen, C. 1990. Sensory performance of blind Mexican cave fish after destruction of the canal neuromasts. Naturwissenschaften, **77**: 237–239.

Bamford, T.W. 1941. The lateral line and related bones of the herring (*Clupea harengus* L.). Ann. Mag. Nat. Hist. S. **11**(8): 414–438.

Barlow, D.I., and Sleigh, M.A. 1980. The propulsion and use of water currents for swimming and feeding in larval and adult *Artemia*. *In* The brine shrimp *Artemia*. *Edited by* G. Persoone, P. Sorgeloos, O. Roels, and E. Jaspers. Universal Press, Wetteren, Belgium. pp. 61–73.

Blaxter, J.H.S. 1988. Sensory performance, behavior, and ecology of fish. *In* Sensory biology of aquatic animals. *Edited by* J. Atema, R.R. Fay, A.N. Popper,

and W.N. Tavolga. Springer-Verlag, New York, N.Y. pp. 203–232.

Blaxter, J.H.S., and Batty, R.S. 1985. Herring behavior in the dark: responses to stationary and continuously vibrating obstacles. J. Mar. Biol. Assoc. U.K. **65**: 1031–1049.

Blaxter, J.H.S., and Fuiman, L.A. 1989. Function of the free neuromasts of marine teleost larvae. *In* The mechanosensory lateral line. *Edited by* S. Coombs, P. Gorner, and H. Munz. Springer-Verlag, New York, N.Y. pp. 481–499.

Bleckmann, H., Breithaupt, T., Blickhan, R., and Tautz, J. 1991. The time course and frequency content of hydrodynamic events caused by moving fish, frogs, and crustaceans. J. Comp. Phys. B, **168**: 749–757.

Feltmate, B.W., Dudley Williams, D., and Montgomerie, A. 1992. Relationship between diurnal activity patterns, cryptic coloration, and subsequent avoidance of predaceous fish by perlid stoneflies. Can. J. Fish. Aquat. Sci. **49**: 2630–2634.

Hoekstra, D., and Janssen, J. 1986. Lateral line receptivity in the mottled sculpin (*Cottus bairdi*). Copeia, **1986**: 91–96.

Hollander, M., and Wolfe, D.A. 1973. Nonparametric statistical methods. John Wiley, New York, N.Y.

Janssen, J. 1976. Feeding modes and prey size selection in the alewife. J. Fish. Res. Board Can. **33**: 1972–1975.

Janssen, 1978*a*. Feeding behavior repertoire of alewife, *Alosa pseudoharengus*, and the ciscoes *Coregonus hoyi* and *C. artedii*. J. Fish. Res. Board Can. **35**: 249–253.

Janssen, 1978*b*. Will alewives feed in the dark? Environ. Biol. Fishes, **3**: 239–240.

Janssen, J., and Brandt, S.B. 1980. Feeding ecology and vertical migration of adult alewives (*Alosa pseudoharengus*) in Lake Michigan. Can. J. Fish. Aquat. Sci. **37**: 177–184.

Janssen, J., Coombs, S., and Pride, S. 1990. Feeding and orientation of mottled sculpin, *Cottus bairdi*, to water jets. Environ. Biol. Fishes, **29**: 43–50.

Jones, W., and Janssen, J. 1992. Development of the lateral line and its use in feeding in the mottled sculpin (*Cottus bairdi*). Copeia, **1992**: 485–492.

Kaus, S. 1987. The effect of aminoglycoside antibiotics on the lateral line of *Aplocheilus lineatus* (Cyprinodontidae). Acta Otolaryngol. (Stockholm), **103**: 291–298.

Kirk, K. 1985. Water flow produced by *Daphnia* and *Diaptomus*: implications for prey detection by mechanosensory predators. Limnol. Oceanogr. **30**: 679–686.

Lannoo, M.J. 1986. Vision is not necessary for size-selective zooplanktivory in aquatic salamanders. Can. J. Zool. **64**: 1071–1075.

Lazzaro, X. 1987. A review of planktivorous fishes: their evolution, feeding behaviours, selectivities, and impacts. Hydrobiologia, **146**: 97–165.

Newman, R.M., and Waters, T.F. 1984. Size-selective predation on *Gammarus pseudolimnaeus* by trout and sculpins. Ecology, **65**: 1535–1545.

Scavia, D., Fahnenstiel, G.L., Evans, M.S., Jude, D.J., and Lehman, J.T. 1986. Influence of salmonine predation and weather on long-term water quality trends in Lake Michigan. Can. J. Fish. Aquat. Sci. **43**: 435–443.

Stevens, R.R. 1985. The lateral line system of the gizzard shad *Dorosoma cepedianum* Leseuer (Pisces: Clupeidae). Copeia, **3**: 540–556.

Unger, P.A., Lewis, W.M., and McClearn, D.H. 1984. Nonvisual feeding in a visual planktivore, *Xenomelaniris venezuelae*. Oecologia, **64**: 280–283.

Urban, T.P., and Brandt, S.B. 1993. Food and habitat partitioning between young-of-the-year alewives and rainbow smelt in southeastern Lake Ontario. Environ. Biol. Fishes, **36**: 359–372.

Vinyard, G.L., and O'Brien, W.J. 1976. Effects of light and turbidity on the reactive distance of bluegill (*Lepomis macrochirus*). J. Fish. Res. Board Can. **33**: 2845–2849.

Young, S., and Watt, P. 1993. Behavioral mechanisms controlling vertical migration in *Daphnia*. Limnol. Oceanogr. **38**: 70–79.

Analysing differences between two age determination methods by tests of symmetry

J.M. Hoenig, M.J. Morgan, and C.A. Brown

Abstract: A common problem in fisheries science is the comparison of two methods for obtaining ages of individual animals. Often, indices of precision are computed for this purpose. We believe such indices are inappropriate both as measures of precision and for comparative purposes because they do not properly account for age effects or take the experimental design into consideration. We suggest that if the overall level of agreement is low between two ageing methods used on the same sample of fish, then one can use a test of symmetry to look for evidence of systematic disagreement. A χ^2 test is used to determine if the number of fish assigned age i from method 1 and age j from method 2 differs significantly from the number of fish assigned age j from method 1 and age i from method 2. Such a test can also be used to determine the range of nominal ages over which two methods appear to give comparable results.

Résumé : Dans le domaine de l'halieutique se pose souvent le problème de la comparaison de deux méthodes pour obtenir l'âge d'un animal. On calcule souvent à cette fin des indices de précision. Nous pensons que ces indices sont inappropriés tant comme mesure de la précision que comme outils de comparaison parce qu'ils ne rendent pas compte correctement des effets de l'âge et ne tiennent pas compte du protocole expérimental. Nous posons que, si le niveau global de concordance est faible entre deux méthodes de détermination de l'âge employées sur un même échantillon de poisson, on peut avoir recours à un test de symétrie pour rechercher les preuves de divergence systématique. On se sert d'un test χ^2 pour déterminer si le nombre de poissons auxquels la méthode 1 assigne l'âge i et la méthode 2 l'âge j diffère de façon significative par rapport au nombre de poissons auxquels la méthode 1 assigne l'âge j et la méthode 2 l'âge i. Un tel test peut aussi servir à déterminer la plage d'âge nominal dans laquelle les deux méthodes semblent donner des résultats comparables.
[Traduit par la Rédaction]

Introduction

Common methods for evaluating precision or consistency among age determinations are that of Beamish and Fournier (1981) and the modification of their method by Chang (1982). These methods calculate what are called indices of precision for a series of age determinations. A set of determinations with a small index of precision is considered precise. Both Beamish and Fournier (1981) and Chang (1982) suggested that indices of precision are appropriate for comparing two ageing methods or two age readers.

Beamish and Fournier (1981) calculated average percent error (APE) as

$$[1] \quad \mathrm{APE}_{\mathrm{BF}} = 100 \times \frac{1}{N}\sum_{j=1}^{N}\left(\frac{1}{R}\sum_{i=1}^{R}\frac{|X_{ij} - X_j|}{X_j}\right)$$

where N = the number of fish aged, R = the number of times each fish is aged, X_{ij} = the ith age determination for the jth fish, and X_j = the average age calculated for the jth fish.

Chang (1982) calculated APE using the square root of the sum of squared deviations instead of the sum of absolute values:

$$[2] \quad \mathrm{APE}_{\mathrm{C}} = 100 \times \frac{1}{N}\sum_{j=1}^{N}\frac{\sqrt{\sum_{i=1}^{R}\frac{(X_{ij} - X_j)^2}{R-1}}}{X_j}.$$

These methods are based on the assumption that the occurrence of several age groups in the sample is accounted for by expressing the precision in relative terms. It is assumed that in this way the index of precision does not depend on the age of fish and one overall index can be calculated from all of the age groups. However, there may still be differences in precision among ages which these procedures obscure. Brown (1988) calculated an average

Received March 7, 1994. Accepted July 22, 1994.
J12302

J.M. Hoenig and M.J. Morgan. Department of Fisheries and Oceans, P.O. Box 5667, St. John's, NF A1C 5X1, Canada.
C.A. Brown. Rosenstiel School of Marine and Atmospheric Sciences, University of Miami, 4600 Rickenbacker Causeway, Miami, FL 33149, USA.

percent error for each lemon shark (*Negaprion brevirostris*) examined according to the method of Beamish and Fournier (1981) and then plotted these indices against the average age assigned. Ages were determined by counting growth marks in vertebral centra. He found that the APE as well as the variability in APE was much greater for younger lemon sharks than for older ones (Fig. 1).

Kimura and Lyons (1991) concluded that relative precision (equation [2] and minor variations thereof) was independent of age for six species examined and, therefore, that it was appropriate to average an index of precision over fish of different ages. However, if their indices are plotted against age, there are clear trends with age for three of the species they studied (walleye pollock (*Theragra chalcogramma*), Atka mackerel (*Pleurogrammus monopterygius*), and sablefish (*Anaplopoma fimbria*)). Furthermore, the indices were zero for the youngest age for all six species, suggesting that in general the youngest fish are aged with greater relative precision than are the older fish. The possibility of finding trends with age has also been pointed out by Campana and Jones (1992). In a comparison of two age readers, reading different samples, if the two samples contain different proportions of small fish, there will be apparent differences between the readers. This is because there is greater relative precision in ageing young fish than old fish, even after supposedly accounting for age. Thus, indices of precision cannot be averaged across age groups.

The methods of Beamish and Fournier (1981) and Chang (1982) also assume that the variability among observations of individual fish can be averaged over all fish. However, variability in age determinations can come from a variety of sources (i.e., within fish, among fish, among ages, etc.). If the components of the overall variance are not separated, it becomes difficult to interpret the index and to compare index values from different studies that had different experimental designs. An APE from reading two fish 10 times is not comparable with one from reading 10 fish two times. In the first, most of the variability would be within fish whereas in the second, it would be mainly among fish. To account for the different sources of variability properly, one would need to do an analysis of variance and variance components (Kimura et al. 1979). However, because the response variable is observed age, it is inappropriate to do separate analyses for each "nominal" age group as in Kimura et al. (1979). We suggest that separate analyses be conducted by size group (an independent variable correlated with age). This will help ensure that the assumption of homogeneous variances is met.

Finally, we join Campana and Jones (1992) in pointing out that comparisons of precision are only of interest if there is no evidence of systematic disagreement among readers or methods. Unfortunately, this appears to be frequently overlooked. For example, Beamish and Fournier (1981) and Chang (1982) described a study in which two readers aged the same 20 fish three times. They pointed out that reader No. 2 in their example appeared to be less precise than reader No. 1. What this meant in practice was that, for most (13 out of 20) fish, the oldest age assigned differed from the lowest age by 1 year for reader No. 2. In contrast, for most (11 out of 20) fish, the oldest age was

Fig. 1. Plot of APE against average number of circuli in vertebral centra of individual lemon sharks. The number of circuli was counted three times for each shark. Circuli are formed with a lunar periodicity (Brown 1988).

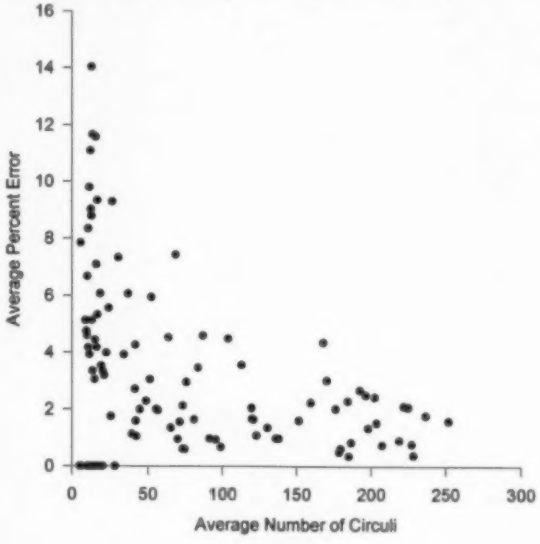

equal to the youngest age for reader No. 1. All other things being equal, we would conclude that reader No. 1 was more precise. However, neither Beamish and Fournier (1981) nor Chang (1982) mentioned the fact that 53% of the time the observation of reader No. 1 was above that of reader No. 2 whereas 8% of the time reader No. 1 was below reader No. 2 (and 38% of the time they agreed). Thus, there is clear evidence that reader No. 1 tended to assign older ages than reader No. 2. The question of which (if either) reader was unbiased seems more important than who was more precise. Furthermore, it is apparent that the first reading for each fish made by reader No. 2 tended to be the highest made by that reader whereas the second reading tended to be lowest. Reader No. 2 appears to have changed criteria over time and there is no way to predict how this reader would perform at other times.

It would seem that these indices tend to oversummarize the data and are hard to interpret. They may lead to false conclusions when used to compare the precision of different readers or methods when the studies compared are based on different experimental designs. The questions that can be addressed by examining measures of precision are not relevant if there are systematic differences among readers or methods, or if performance changes over time. We suggest that a more appropriate approach to comparing age determinations from different structures or readers is a test of symmetry.

In this paper, we describe the test of symmetry developed by Bowker (1948) and show how it can be used to compare two different ageing methods which use either different structures or different readers to determine age. We also show how the test can be extended to determine where differences between methods occur.

A test of symmetry

Valid comparisons of methods can only be made if the methods are used on the same statistical population. Statistical efficiency is attained if the two methods are used on the same individual fish. We assume here that the same fish are aged by two readers or by two methods.

The first step in a comparison of ageing methods would be to determine how often the two methods agree. If agreement is high, there may be no need to proceed further. If, however, there is a considerable amount of disagreement between methods, it is important to know whether this disagreement is simple random error of if there is a systematic difference between methods.

Bowker's (1948) method was designed to test the hypothesis that an $m \times m$ contingency table consisting of two classifications of a sample into categories (e.g., ages given by two readers) is symmetric about the main diagonal. The test statistic is distributed as a chi-square variable with $m(m-1)/2$ degrees of freedom for a table that has no empty cells. The test statistic is

$$[3] \quad X^2 = \sum_{i=1}^{m-1} \sum_{j=i+1}^{m} \frac{(n_{ij} - n_{ji})^2}{n_{ij} + n_{ji}}$$

where n_{ij} = the observed frequency in the ith row and jth column and n_{ji} = the observed frequency in the jth row and ith column.

The summation is over all the cells above the diagonal. These cells are paired with the corresponding cells below the diagonal. If there is a systematic difference between methods, then the test statistic will tend to be large. If, however, the differences are due to simple random error, then the value of n_{ji} will be very similar to that of n_{ij} (the subscripts/readers being essentially interchangeable) and the test statistic will not be significant. The number of degrees of freedom is equal to the number of comparisons. If both cells in a pair (n_{ji} and n_{ij}) are zero, the pair is dropped from the test statistic and the degrees of freedom is reduced by 1.

Example

We consider data from O'Gorman et al. (1987) in which a comparison is made between age determined by otoliths and age determined by scales for alewife (*Alosa pseudoharengus*) from Lake Huron (Table 1A). In O'Gorman et al. (1987), cells with no observations were left blank. To illustrate the pairing of the data, we have explicitly added zeros to those cells needed for calculating the test statistic. Thus, the bottom four rows do not appear in the table presented in O'Gorman et al. (1987).

In Table 1A the number in a cell, n_{ij}, is the number of times a fish was assigned to age j using an otolith when it was assigned to age i using a scale. The numbers are printed in bold typeface in the cells where the two methods agree. The two methods agree only 58% of the time. Differences between the methods should thus be investigated. It is clear that the scale method does not produce ages older than 6 whereas the otolith method yields ages as old as 10. This indicates that a test of symmetry will probably be significant. The test statistic is

$$\begin{aligned} X^2 = {} & \frac{(1-0)^2}{1+0} + \frac{(0-3)^2}{0+3} + \frac{(2-4)^2}{2+4} + \frac{(5-0)^2}{5+0} \\ & + \frac{(4-1)^2}{4+1} + \frac{(2-0)^2}{2+0} + \frac{(1-0)^2}{1+0} + \frac{(2-0)^2}{2+0} \\ & + \frac{(3-0)^2}{3+0} + \frac{(5-0)^2}{5+0} + \frac{(1-0)^2}{1+0} + \frac{(1-0)^2}{1+0} \\ & + \frac{(4-0)^2}{4+0} + \frac{(1-0)^2}{1+0} + \frac{(1-0)^2}{1+0} + \frac{(2-0)^2}{2+0} \\ = {} & 34.47, \text{ df} = 16, p = 0.005. \end{aligned}$$

Here the number of degrees of freedom (16) is equal to the number of comparisons made because the table has pairs of cells which are empty. As expected, the hypothesis of symmetry is rejected presumably because older ages do not occur in the scale readings.

An extension to the test

To determine at which point the two methods begin to differ, the table can be collapsed to form a "plus" group. We compared the two methods with fish greater than or equal to age 4 placed in the ≥4 plus group. To do this, any cell with both subscripts greater than or equal to 4 is added to produce the ≥4 plus group (Tables 1B and 1C). All of the remaining cells with the row subscript greater than 4 are added to the fourth row cell with the same column subscript (e.g., $n_{5,3}$ and $n_{6,3}$ are added to $n_{4,3}$). The same procedure is used for cells with the column subscript greater than 4 (e.g., $n_{3,5}$ and $n_{3,6}$ are added to $n_{3,4}$). In this case, the test statistic is $X^2 = 12.67$, df = 4, $p = 0.013$, and again we reject the hypothesis of symmetry.

This process can be taken a step further, to compare the two methods with a ≥3 plus group (box in Table 1C). Here the test statistic would be $X^2 = 4.7$, df = 3, $p = 0.195$. The hypothesis of symmetry cannot be rejected and we have no significant evidence that scales and otoliths would produce different estimates of age composition if ages are assigned to 0, 1, 2, or ≥3. (Note that the test is based on only 10 fish and 3 degrees of freedom, so it does not have much statistical power.)

Discussion

According to various authors, the percentage agreement statistic is inappropriate and should not be calculated (Beamish and Fournier 1981; Chang 1982). We disagree and find that this statistic is intuitive and important for decision making. If agreement is high, there may be no point in investigating further because the impact of the disagreements on the estimated age composition is minimal. We note, however, that the level of agreement is likely to vary with the age composition of the sample so that the percentage agreement is not interpretable as a property of the species, stock, reader, or method.

Indices of precision can be calculated for individual fish. However, their interpretation becomes problematic if the values are averaged over fish (even if the fish are all of the same nominal age). This is because within-fish and

Table 1. (A) Ages of alewife from Lake Huron as determined from otoliths and scales (from O'Gorman et al. 1987). Bold numbers are where the two methods agree. Numbers with the same superscript are compared in the test of symmetry. In this example, there were no observations below the solid line, which makes asymmetry easily detectable by visual examination of the table. (B) Formation of a table with a ≥4 plus group from the complete table. The UPPER area remains the same when the table is collapsed; in the LOWER area the cells have both subscripts ≥4 and all of these are added to cell 4,4. Cells 5,3 and 6,3 have row subscripts >4 and are added to cell 4,3. Cells 3,5 and 3,6 have column subscripts >4 and are added to cell 3,4. (C) Resulting collapsed table with the ≥4 plus group; also indicated is the way to form a ≥3 plus group.

(A)

Scale age \ Otolith age	0	1	2	3	4	5	6	7	8	9	10
0	**2**	$1^{(1)}$									
1	$0^{(1)}$	**13**	$0^{(2)}$								
2		$3^{(2)}$	**16**	$2^{(3)}$							
3			$4^{(3)}$	**11**	$5^{(4)}$	$2^{(8)}$	$1^{(11)}$				
4				$0^{(4)}$	**12**	$4^{(5)}$	$3^{(9)}$	$1^{(12)}$	$1^{(15)}$		
5				$0^{(8)}$	$1^{(5)}$	**4**	$2^{(6)}$	$5^{(10)}$	$4^{(13)}$		
6				$0^{(11)}$	$0^{(9)}$	$0^{(6)}$	**2**	$1^{(7)}$		$1^{(14)}$	$2^{(16)}$
7					$0^{(12)}$	$0^{(10)}$	$0^{(7)}$				
8					$0^{(15)}$	$0^{(13)}$					
9							$0^{(14)}$				
10							$0^{(16)}$				

(B)

Scale age \ Otolith age	0	1	2	3	4	5	6	7	8	9	10
0	**2**	$1^{(1)}$									
1	$0^{(1)}$	**13**	$0^{(2)}$								
2		$3^{(2)}$	**16**	$2^{(3)}$							
3	UPPER		$4^{(3)}$	**11**	$5^{(4)}$	$\leftarrow 2^{(8)}$	$\leftarrow 1^{(11)}$				
4				$0^{(4)}$	**12**	$4^{(5)}$	$3^{(9)}$	$1^{(12)}$	$1^{(15)}$		
5				$0^{(8)}$	$1^{(5)}$	**4**	$2^{(6)}$	$5^{(10)}$	$4^{(13)}$		
6				$0^{(11)}$	$0^{(9)}$	$0^{(6)}$	**2**	$1^{(7)}$		$1^{(14)}$	$2^{(16)}$
7					$0^{(12)}$	$0^{(10)}$	$0^{(7)}$				
8					$0^{(15)}$	$0^{(13)}$					
9							$0^{(14)}$				
10							$0^{(16)}$		LOWER		

(C)

Scale age \ Otolith age	0	1	2	3	≥4
0	**2**	$1^{(1)}$			
1	$0^{(1)}$	**13**	$0^{(2)}$		
2		$3^{(2)}$	**16**	$2^{(3)}$	
3			$4^{(3)}$	**11**	$8^{(4)}$
≥4				$0^{(4)}$	**43**

Table 2. Hypothetical situation in which asymmetry will be detected by Bowker's χ^2 test but not by two other tests. The marginal row frequencies equal the marginal column frequencies so the hypothesis that the two marginal distributions are equal will not be rejected. The number of observations above the diagonal (40) equals the number of observations below the diagonal so the hypothesis of equal proportions above and below the diagonal will not be rejected by a sign test. Superscripts indicate cells which are paired for Bowker's test.

		Reader A				
	Age	1	2	3	4	Marginal frequency
Reader B	1	**30**	$0^{(1)}$	$20^{(2)}$		50
	2	$20^{(1)}$	**30**		$0^{(3)}$	50
	3	$0^{(2)}$		**30**	$20^{(4)}$	50
	4		$20^{(3)}$	$0^{(4)}$	**30**	50
Marginal frequency		50	50	50	50	

between-fish variability are not distinguished and age effects are ignored.

Our main concern with the use of indices of precision is that they can draw attention away from important trends in the data. For example, in three articles proposing methodology for comparative studies of ageing programs, indices of precision were calculated but the trends in the data across ages and readers were not discussed (Beamish and Fournier 1981; Chang 1982; Kimura and Lyons 1991). Furthermore, indices of precision are often not comparable. Within a species, APEs among samples can differ solely because age compositions differ; the precision of a method is likely to change if readers change, and studies using different designs may have different APEs because of the differences in design rather than inherent differences in precision. Thus, a value of APE reported in the literature is generally not interpretable.

In this paper, we advocate the examination of two-way contingency tables for asymmetry. There are a variety of statistical tests that can be used to test for asymmetry such as a sign test (H_0: proportion of observations above the diagonal equals the proportion below), a test of marginal homogeneity (H_0: age composition according to method 1 equals age composition according to method 2), and the Bowker-type χ^2 test. Some tests are extremely powerful for detecting specific types of asymmetry at the expense of the ability to detect other types of asymmetry. The Bowker-type test, however, is the most general in the sense that it looks at all parts of the table off the diagonal and can detect asymmetries that are not detectable by other methods (Table 2). Additionally, the contribution of different cells of the table to the overall χ^2 test statistic can be examined to determine where differences arise.

Acknowledgements

We thank G. Evans, W. Warren, A.R. Kronlund, and an anonymous reviewer for helpful comments.

References

Beamish, R.J., and Fournier, D.A. 1981. A method for comparing the precision of a set of age determinations. Can. J. Fish. Aquat. Sci. **38**: 982–983.

Bowker, A.H. 1948. A test for symmetry in contingency tables. J. Am. Stat. Assoc. **43**: 572–574.

Brown, C.A. 1988. Validated age assessment of the lemon shark, *Negaprion brevirostris*, using tetracycline labeled vertebral centra. Thesis, University of Miami, Miami, Fla.

Campana, S.E., and Jones, C.M. 1992. Analysis of otolith microstructure data. *In* Otolith microstructure examination and analysis. *Edited by* D.K. Stevenson and S.E. Campana. Can. Spec. Publ. Fish. Aquat. Sci. **117**: 73–100.

Chang, W.Y.B. 1982. A statistical method for evaluating the reproducibility of age determination. Can. J. Fish. Aquat. Sci. **39**: 1208–1210.

Kimura, D.K., and Lyons, J.J. 1991. Between-reader bias and variability in the age-determination process. Fish. Bull. U.S. **89**: 53–60.

Kimura, D.K., Mandapat, R.R., and Oxford, S.L. 1979. Method, validity, and variability in the age determination of yellowtail rockfish (*Sebastes flavidus*), using otoliths. J. Fish. Res. Board Can. **36**: 377–383.

O'Gorman, R., Barwick, D.H., and Bowen, C.A. 1987. Discrepancies between ages determined from scales and otoliths for alewives from the Great Lakes. *In* Age and growth of fish. *Edited by* R.C. Summerfelt and G.E. Hall. The Iowa State University Press, Ames, Iowa. pp. 203–210.

Relating trends in walleye pollock (*Theragra chalcogramma*) abundance in the Bering Sea to environmental factors

Gordon Swartzman, Emily Silverman, and Neal Williamson

Abstract: Generalized additive models (GAM), a nonparametric regression method with less restrictive statistical assumptions than traditional regression methods, were used to model the trend in mean abundance of Bering Sea walleye pollock (*Theragra chalcogramma*) as a function of ocean environmental conditions including water column depth, temperature at 50 m, and depth of the thermocline. Acoustic survey data collected in the summers of 1988 and 1991 were used to test these relationships. In both surveys, mean walleye pollock abundance was highest in areas having a 70–130 m depth range and where the 50-m temperature was close to 2.5°C. Thermocline depth, while not itself significant, had a significant effect on walleye pollock abundance through interactions with both bottom depth and temperature at 50 m. Walleye pollock in the top 50 m of the water column (mostly juveniles) were influenced differently by temperature and thermocline depth than the adult walleye pollock, which were generally deeper in the water column. The depth, temperature, and thermocline preferences of walleye pollock are hypothesized to be linked to food availability which is, in turn, related to temperature regimes or fronts along the Bering Sea shelf slope.

Résumé : Nous avons utilisé des modèles additifs généralisés, méthode de régression non paramétrique fondée sur des hypothèses statistiques moins restrictives que les méthodes de régression traditionnelles, pour modéliser la tendance de l'abondance moyenne de la goberge (*Theragra chalcogramma*) en mer de Béring comme une fonction des conditions environnementales dans l'océan, notamment la hauteur de la colonne d'eau, la température à 50 m et la profondeur de la thermocline. Des données acoustiques recueillies pendant les étés 1988 et 1991 ont servi à tester ces relations. Pendant les deux campagnes, l'abondance moyenne de la goberge était maximale dans les zones dont la fourchette de profondeur était de 70–130 m et où la température à 50 m était d'environ 2,5°C. La profondeur de la thermocline, si elle n'était pas significative en elle-même, avait un effet significatif sur l'abondance de goberges du fait des interactions avec, d'une part, la température au fond et, d'autre part, la température à 50 m. Les goberges se trouvant dans la tranche supérieure de 50 m de la colonne d'eau (principalement des juvéniles) réagissaient différemment à la température et à la profondeur de la thermocline par rapport aux goberges adultes, qui se tenaient généralement plus bas dans la colonne d'eau. Nous posons que les préférences de la goberge en matière de profondeur, de température et de rapport avec la thermocline sont liées à la disponibilité de la nourriture qui, elle-même, varie selon les régimes ou les fronts thermiques le long du talus de la mer de Béring.
[Traduit par la Rédaction]

Introduction

There is abundant evidence in the literature that the spatial distribution of pelagic schooling fish may be influenced by environmental, biotic, and anthropogenic factors. By statistically examining the relationship between pelagic fish abundance and environmental conditions, fisheries scientists have been able to establish significant correlation of abundance to such factors as (1) temperature fronts and eddies (Pacific Saury — Saitoh et al. 1986; Shinomiya and Tameishi 1988; Gulf of Mexico butterfish — Herron et al. 1989; Gulf of Mexico bluefin tuna — Maul et al.

Received January 11, 1994. Accepted July 14, 1994.
J12230

G. Swartzman and E. Silverman. Applied Physics Laboratory HN-10 and Center for Quantitative Science HR-20, University of Washington, Seattle, WA 98105, USA.
N. Williamson. Alaska Fisheries Science Center, National Marine Fisheries Service.

1984; summer Atlantic herring — Sinclair and Iles 1985; coastal Japan — Hanaoka 1983; Atlantic capelin — Rose and Leggett 1990; Kuroshio front — Aoki and Inagaki 1992), (2) depth of the thermocline (yellow sea mackerel — Li 1982; Pacific sardine — Inagake and Hirano 1983), (3) primary and secondary production (Baltic Sea summer herring — Fetter and Davidyuk 1986; Irish coast — Doyle and Ryan 1989), (4) bottom topography–current interaction (coastal Japan — Yamaguchi et al. 1984; dwarf herring — Mochek and Valdes-Munoz 1983), (5) light level (diel patterns for Atlantic menhaden — Kemmerer 1980; coastal Japan — Yamaguchi et al. 1984), and (6) fishing activity (Atlantic menhaden — Kemmerer 1980; Atlantic herring — Fréon et al. 1993; Norwegian Sea herring, mackerel, and sprat — Misund and Aglen 1992).

Our objective was to establish quantitative relationships between the spatial distribution of walleye pollock (*Theragra chalcogramma*) abundance and environmental or biotic factors over a wide geographical area (mesoscale), using acoustic backscatter data for information about fish distribution and oceanic data (collected along with the acoustic survey) for the environmental factors. Advantages of fisheries acoustic surveys for exploring the relationship between fish distributions and environmental factors include the large area covered by the surveys, which allows consideration of mesoscale relationships, the concomitant collection of trawl data for species identification, and the collection of temperature–salinity depth profiles along the survey track. This study is the first, to our knowledge, to quantitatively relate fish abundance distribution to environmental factors over such a wide area using regression without the restrictive linearity assumption.

We related the spatial distribution of Bering Sea walleye pollock in the summers of 1988 and 1991 to bottom depth and the depth–temperature profile. The data used were collected by the National Marine Fisheries Service Alaska Fisheries Science Center (Bakkala et al. 1992) in the summers of 1988 and 1991. The survey tracks in both years covered the eastern Bering Sea shelf between the Aleutian Islands and the U.S.–U.S.S.R. convention line (Fig. 1). These surveys allowed us to examine whether the spatial distribution of walleye pollock during the summer is similar between years and whether the distribution appears to be affected by environmental factors in a similar fashion across years.

A generalized additive model (GAM — Hastie and Tibshirani 1986, 1990; Swartzman et al. 1992) was used to conduct the analysis. GAM is a nonparametric regression technique offering advantages over conventional regression techniques because it is not tied to a particular functional relationship (i.e., linearity) and because it is less restrictive in assumptions about the underlying statistical distribution of the data. A known function of the expected value, called the link function, is modeled as a sum of smooth functions of the covariates. The underlying probability distribution for the data can be any distribution from the exponential family, which includes the normal (used in this case), Poisson, and binomial distributions. A local smoother in GAM replaces the least squares estimate of multiple linear regression. GAM has been used in fisheries to relate the spatial distribution of Bering Sea flatfish, sampled in an annual groundfish survey conducted by the National Marine Fisheries Service, to depth, temperature, and spatial location (Swartzman et al. 1992).

About the data

The Resource Assessment and Conservation Engineering (RACE) division of the Alaska Fisheries Science Center (AFSC) conducts triennial acoustic surveys of the middle shelf, outer shelf, and slope regions of the eastern Bering Sea. The primary objective of the surveys is to estimate walleye pollock abundance. In 1988, the survey was conducted from June 23 to July 28 aboard the chartered vessel *Pelagos*; in 1991, the chartered vessel was the *Continuity* and data was collected from June 30 to August 10. The acoustic systems used in both survey years were echo integration – target strength measurement systems using a 38-kHz split-beam transducer mounted in a dead-weight fin towed behind the vessel. The 1991 acoustic data were summarized into depth intervals of 5-nautical miles (M) and 50 m, while the 1988 data were available as 1-min outputs (~0.2 M at normal transecting speed) for the entire water column (no depth resolution) and were summed to produce 5-M averages. Bottom depth information was recorded along with the acoustic data. Conversion of acoustic backscatter to fish abundance requires an estimate of target strength, a measure of acoustic reflectivity. Target strength is dependent on fish species and size. For walleye pollock, the following target strength (TS) to length (L) relationship was used: $TS = 20 \log L - 66$ (Foote and Traynor 1988). Trawl hauls were conducted to identify echo sign for species composition and to provide biological information (e.g., size composition). In both survey years, water temperature/salinity profile data were collected at trawl locations using a CTD bathythermograph. In 1991, expendable bathythermographs (XBT'S) were also used to provide more complete spatial coverage of temperature data.

Exploratory data analysis

Initial mapping of the 1991 and 1988 data (Fig. 1) used line plots, symbols, and contour plots to show the extend and depth range of the survey. On the computer screen, color was used to enhance contrast between the types of data. Here, we use line boldness and symbols to delineate the data types. As can be seen from Fig. 1, bathytherms were available for only a small subset of the total abundance data locations.

The temperature-depth profiles are multivariate, in that each temperature data point in Fig. 1 represents a vector of values at different depths. We reduced this vector to a small subset of temperature–depth profile measures because the temperatures at similar depths were highly correlated with each other and because we wanted a smaller environmental set to relate to abundance; this facilitated interpretation of results and reduced the run time of the GAM method used. Contour plots of temperature (e.g., Fig. 2) and preliminary GAM runs with several temperature-profile-related parameters included as covariates showed the temperature at 50 m and the depth of the thermocline to be

Fig. 1. Walleye pollock abundance estimates through the water column (thick horizontal lines) along the survey track of the (*a*) 1991 and (*c*) 1988 NMFS Bering Sea summer acoustic surveys. Locations of CTD (○) and XBT (×) data stations for the (*b*) 1991 and (*d*) 1988 surveys are shown along with bottom depth contours.

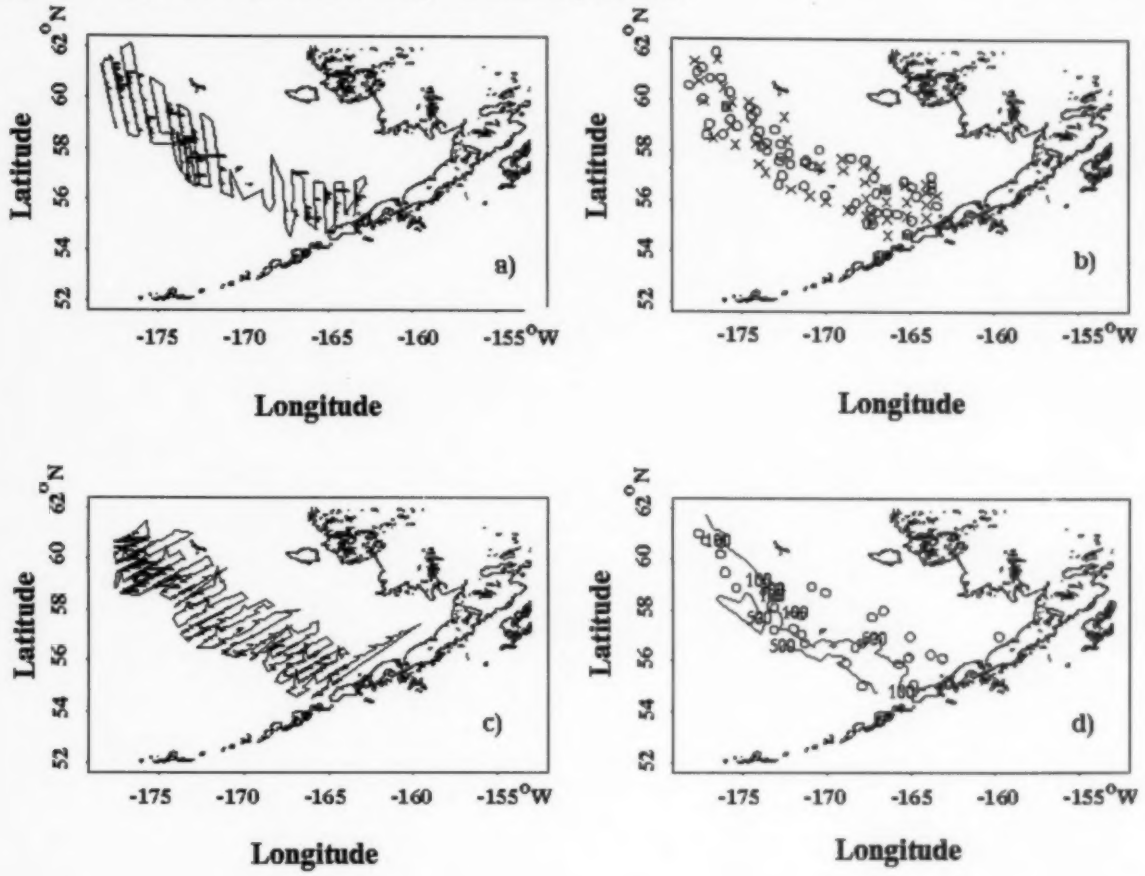

reasonable surrogates for the temperature–depth profile. Sea surface temperatures appeared not to change much over the survey area and were not good predictors of walleye pollock abundance. Temperatures below 50 m changed slowly and were highly correlated with temperatures at 50 m (average $r^2 = 0.723$). We estimated the depth of the thermocline as the depth at which temperature has dropped 90% of the difference between surface and 50-m temperatures, after observing that for almost all casts the thermocline occurred at depths less than 50 m. This definition, although arbitrary, gave a measure of thermocline depth consistent with observation.

To study the relationship between walleye pollock abundance and temperature analytically required estimates of the temperature at 50 m and the depth of the thermocline at each abundance data location. We estimated these parameters by bilinear interpolation based on the data at locations where temperature casts were available. We justify doing this by the relative smoothness of these temperature parameters over space during this season in the Bering Sea (J. Schumacher, Pacific Marine Environmental Laboratory, 7600 Sand Point Way, Seattle, Wa, 98115, personal communication). We had the option of relating walleye pollock abundance to environmental factors only at locations where temperature data were collected. However, we preferred to use the full abundance data set, which was an order of magnitude larger than the number of locations where temperature data were available. We did, however, also use the GAM model described below to estimate mean abundance as a function of environmental conditions using the subset of abundance data collected at locations also having temperature measurements. This analysis gave results similar to those with the full abundance data set.

Generalized additive models

The techniques and theory of GAM's are well described elsewhere (Swartzman et al. 1992) and we refer the reader there for more information. In our model, the expected value of walleye pollock abundance, treated as a random variable, Y is expressed as a sum of smooth functions of the covariates. In this case the covariate X_1 is the logarithm

Fig. 2. Contour plots of temperature at 50 m depth during summer (*a*) 1991 and (*b*) 1988 and of the thermocline depth in (*c*) 1991 and (*d*) 1988.

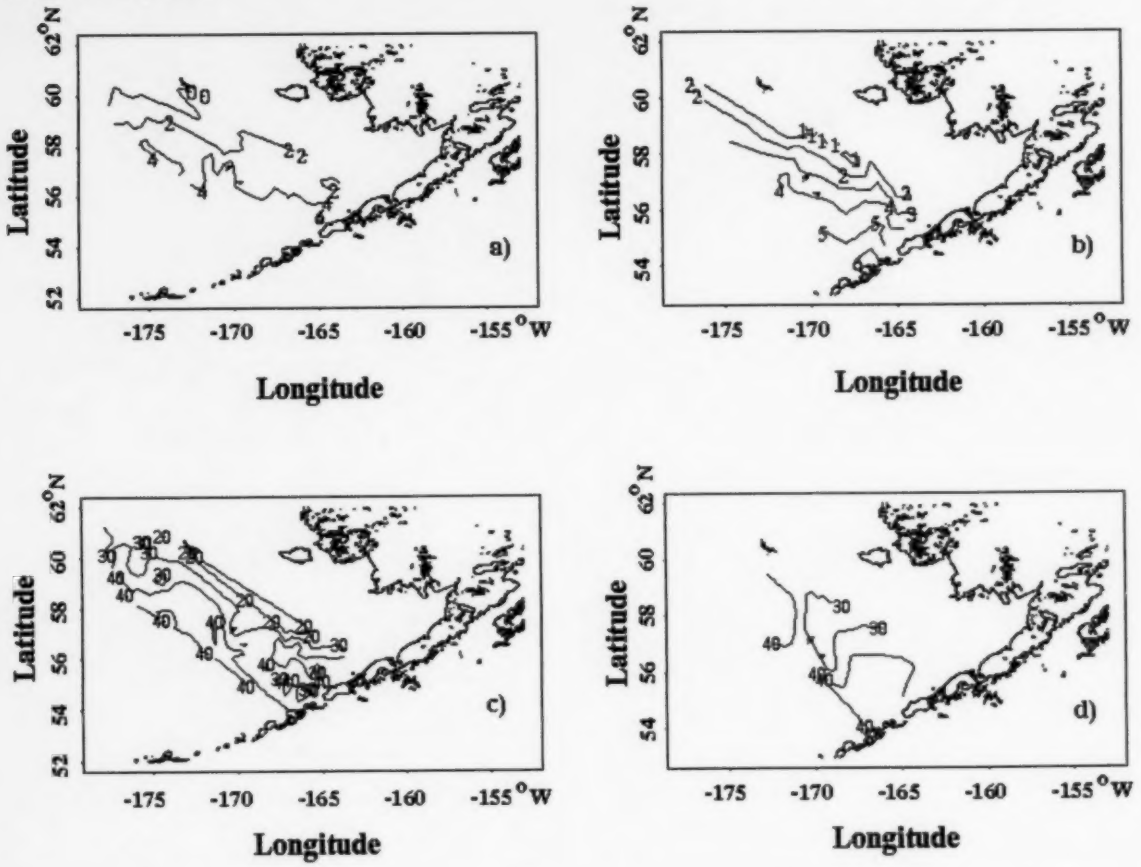

of the depth of the water column, *log(depth)*, X_2 is the depth of the thermocline, *dtherm*, and X_3 is the temperature at 50 m, *temp50*:

$$[1] \quad E(Y|X_1, \ldots) = S_0 + S_1(X_1) + S_2(X_2) + S_3(X_3)$$

where S_j represent smooth, unspecified functions of the covariates. We assumed that the biomass abundance estimates come from a normal distribution. We used the *loess* locally weighted polynomial scatterplot smoother to do the GAM smoothing (Cleveland and Devlin 1988). We chose the logarithm of bottom depth as a covariate instead of depth to avoid having the large range of depth overemphasize the effect of points near the tail of the distribution. In our case, most bottom depths were in the 35–150 m range, while there were few data for depths greater than 200 m and very few for depths greater than 1000 m.

Results

Total walleye pollock abundance through the water column was regressed on the logarithm of bottom depth, the 50-m temperature, and the thermocline depth (bottom depth – thermocline depth and 50-m temperature – thermocline depth interaction terms were also included as covariates) for both the 1988 and 1991 summer walleye pollock surveys. For the 1991 survey, for which abundances by 50-m depth intervals were available, we also ran the model on abundance between 0 and 50 m. While we originally used the explicit survey locations (latitude and longitude) as covariates, we found that using 50-m temperature instead of latitude–longitude interaction provided as significant a relationship. We believe that 50-m temperature can be used as a surrogate for latitude–longitude because in both years, 50-m temperature increased monotonically from the Bering Sea shelf to the basin, from the northeast to the southwest. This suggests that, to the extent that the 50-m temperature is important in affecting Bering Sea shelf summer walleye pollock abundance, it can be used as a surrogate for the explicit spatial location.

Results are similar for the GAM model applied to both 1988 and 1991 data (Table 1). In both surveys, all explanatory variables except thermocline depth are significant at the 0.05 significance level. The explanatory variables are more significant for the 1988 data than for the 1991 data. In both surveys, bottom depth was the most significant explanatory variable, with water temperature at 50 m being

Fig. 3. GAM-derived effects of depth, thermocline depth, and temperature at 50 m on abundance for the 1991 summer Bering Sea walleye pollock survey. Depth and 50-m temperature effects are shown with 2 SE ranges around the estimated effects.

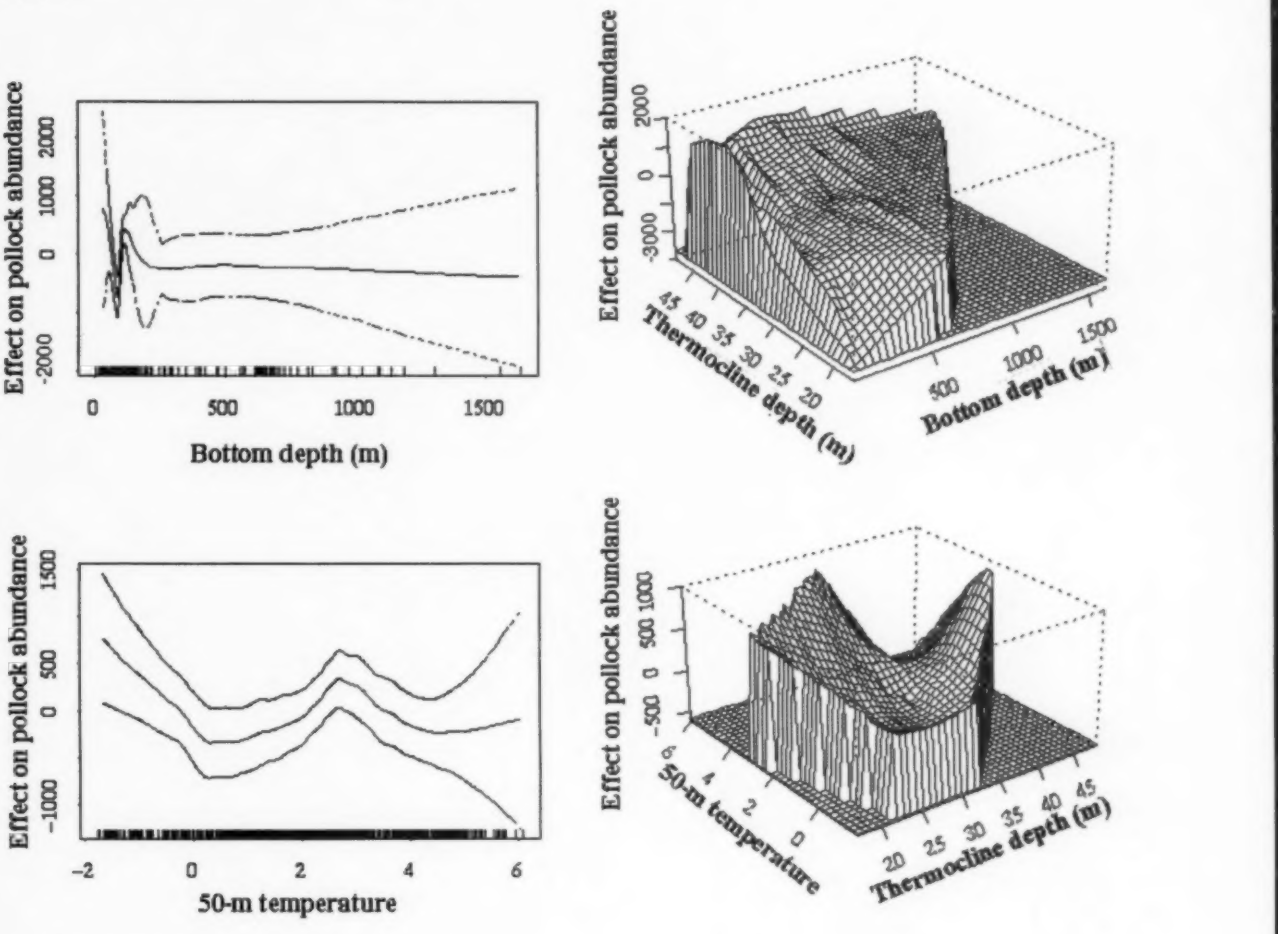

the second most significant explanatory variable for total walleye pollock abundance. The effects of the explanatory variables can be best understood by examining the fitted contribution of each variable to total abundance plotted against the value of the variable. As Figs. 3 and 4 illustrate, depth and temperature at 50 m had similar effects on walleye pollock abundance in the two survey years. Abundances were greatest in the northwest region of the sampling area in both years (Fig. 1). Walleye pollock abundances in both years were, on average, greatest at bottom depths between 60 and 130 m and average abundance was high at a 50-m temperature of about 2.5°C. The density of points for different covariate values is shown by the "rug" under the single covariate effects plots (Figs. 3 and 4). Having fewer points leads to larger standard error ranges. Thus, the apparent high walleye pollock abundance in shallow water (<50 cm) in 1991 has a large standard error range and is not significantly different from the 1988 shallow-water observations of lower average walleye pollock abundance.

Table 1. Significance values (p-levels) for 1988 and 1991 summer survey GAM covariates.

Covariate	1988 summer survey	1991 summer survey
ln(bottom depth)	0.0	0.00016
Temperature at 50 m	0.000000043	0.0017
Thermocline depth	0.227	0.493
Thermocline depth – bottom depth interaction	0.0014	0.0021
Thermocline–temperature interaction	0.0000036	0.0038

One clear difference between the two years was the association of higher average abundance in 1991 with 50-m temperatures of about −2°C (Fig. 3) in addition to having higher abundances at average 50-m temperatures of

Fig. 4. GAM-derived effects of depth, thermocline depth, and temperature at 50 m on abundance for the 1988 summer Bering Sea walleye pollock survey. Depth and 50-m temperature effects are shown with 2 SE ranges around the estimated effects.

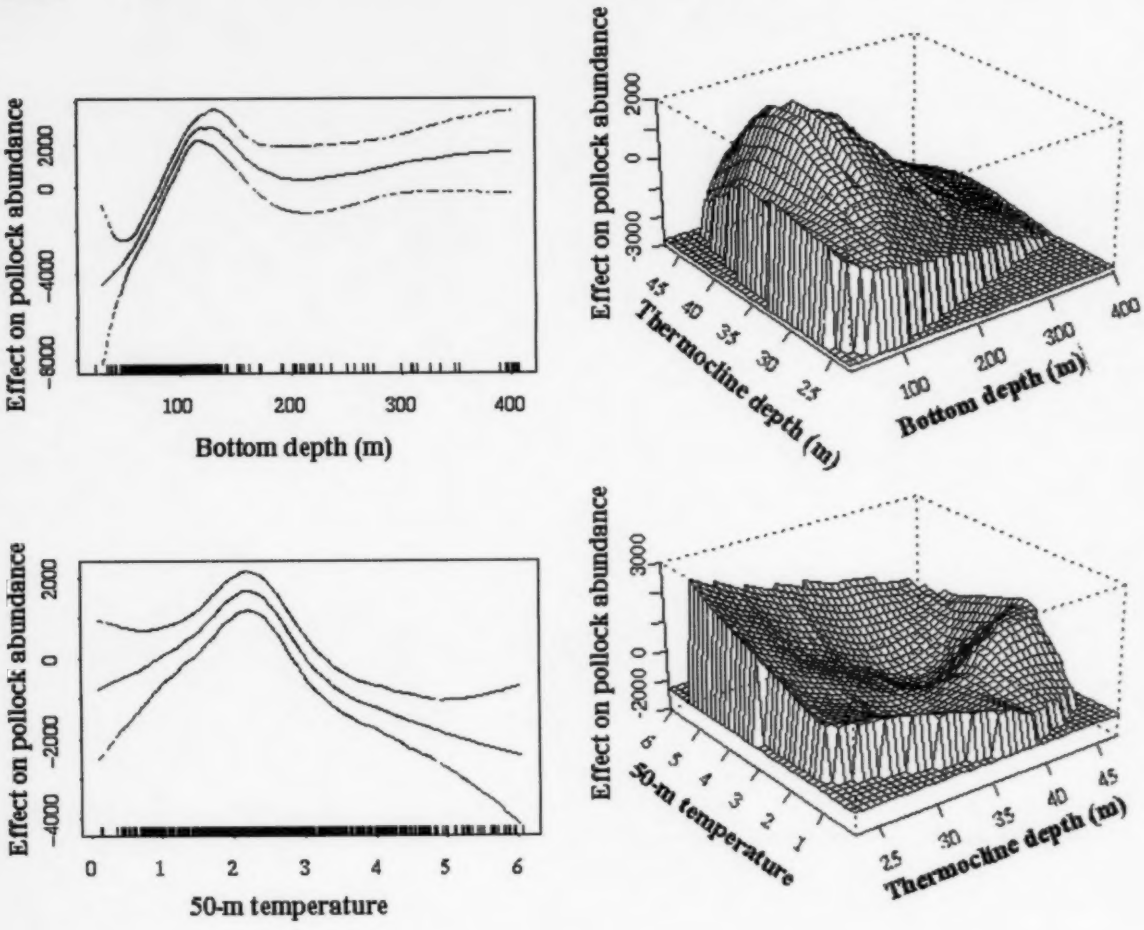

about 2.5°C (which occurred both years). Temperatures at 50 m in 1991 were generally cooler than in 1988 (Fig. 2). This appears to be associated with the 1991 walleye pollock abundance distribution being more southerly in 1991 than in 1988, a year where most high walleye pollock abundance areas were concentrated in the northwest, the region where 50-m temperatures tended to be lowest (Fig. 2).

Table 1 shows significant interactions between thermocline depth and bottom depth on walleye pollock biomass (for both years). For shallow areas (between 60 and 150 m bottom), there was an increase in average walleye pollock abundance with increasing thermocline depth to 45 m. For deeper areas, there was no clear relationship between walleye pollock abundance and thermocline depth. This is evidenced by the relatively flat terrain, for deeper bottom depths (>250 m), with changing thermocline depth, in the bottom depth – thermocline depth perspective plots (Figs. 3 and 4). Therefore, although the thermocline effect was not significant over the entire survey area (Table 1), within the depth range of highest walleye pollock abundance (60–130 m depth), average walleye pollock abundance increased with increasing thermocline depth to 45 m.

The thermocline – 50-m temperature interaction, which was significant in 1991, and highly significant in 1988, differs somewhat between the two years. In both years, higher walleye pollock abundance was associated with deep thermoclines and a 50-m temperature around 2.5°C as well as with shallow thermoclines (about 25 m) and warmer 50-m temperatures. Notice, however, (Fig. 3), that in 1991 there were no areas having both high temperatures and shallow (<20 m) thermoclines. The abundance data can be compared directly with the best-fitting GAM mean predictions using three-dimensional or perspective plots of abundance as a function of location (latitude and longitude). These are given for the 1991 survey in Fig. 5, in which the overall effect of a mean-fitting algorithm like GAM, which flattens and spreads out regions of high abundance, is apparent. The GAM predictions suggest three

regions of high average abundance. These lie along the shelf slope in the northwestern, middle, and southeastern parts of the surveyed Bering Sea area.

Because the 1991 abundance data were available in 50-m depth intervals, we also ran our model using abundance in the 0–50 m interval as the dependent variable. Nor surprisingly, bottom depth had no significant effect on 0–50 m walleye pollock abundance ($p = 0.23$), while 50-m temperature ($p = 0.01$) and thermocline depth ($p = 0.006$) were significant. Walleye pollock abundance in the top 50 m was highest at a 50-m temperature of 2.5°C and at shallow thermocline depths, with a second, smaller peak in 0–50 m abundance for areas with thermocline depth around 42 m (Fig. 6). The highest 0–50 m abundance at shallow thermocline depths may be an artifact of the arbitrary 0–50 m binning of the data because smaller juvenile walleye pollock tend to remain above the thermocline, while adult walleye pollock are generally below it. Thus, if the thermocline is shallow, more adult fish can fit in the 0–50 m depth range and still be below the thermocline. A more detailed examination of the question of the influence of thermocline depth on 0–50 m walleye pollock distributions depends on having higher resolution information about where the fish actually are in the water column and is beyond the scope of this paper.

Note that depth of the thermocline has a more significant effect on 0–50 m walleye pollock abundance than the temperature at 50 m. The differences in the model's fit for the 0–50 m walleye pollock versus total water column walleye pollock abundance are due in part to the differences in the amount of walleye pollock found in each interval. Walleye pollock were present between 50 and 100 m in 88% of the 5-M intervals sampled, but were found within the top 50 m in only 55%. The 50–100 m interval contained 63% of the total recorded walleye pollock biomass, while the 0–50 m interval contained only 11%. In addition, walleye pollock abundance was most variable in the 0–50 m interval with a coefficient of variation of 5.61, compared with 2.40 and 1.62 for the 50–100 and 100–150 m intervals, respectively. The fact that almost half of the 0–50 m intervals contained no walleye pollock may explain much of the increased variability in this interval.

Discussion

The most significant observation from this study is the apparent stability in the relationship between walleye pollock summer spatial distributions and environmental factors from year to year. The key to a testable hypothesis to explain the observed relationships appears to lie in the bottom depth and temperature profile wherein the Bering Sea walleye pollock reside in summer. Oceanographers have divided the eastern Bering Sea shelf into three regions, primarily distinguished by bottom depth range (Coachman 1986). The inner shelf, including bottom depths less than 50 m, is in the northern part of this region. The middle shelf has a bottom depth range of 50–100 m, while the outer shelf includes water columns between 100 and 200 m depth. Both surveys were conducted primarily in the middle and outer shelf regions.

Fig. 5. (*a*) Bering Sea 1991 NMFS summer survey walleye pollock abundance compared with (*b*) GAM estimates of abundance. Abundance estimates for both plots were binned from estimates along the survey track.

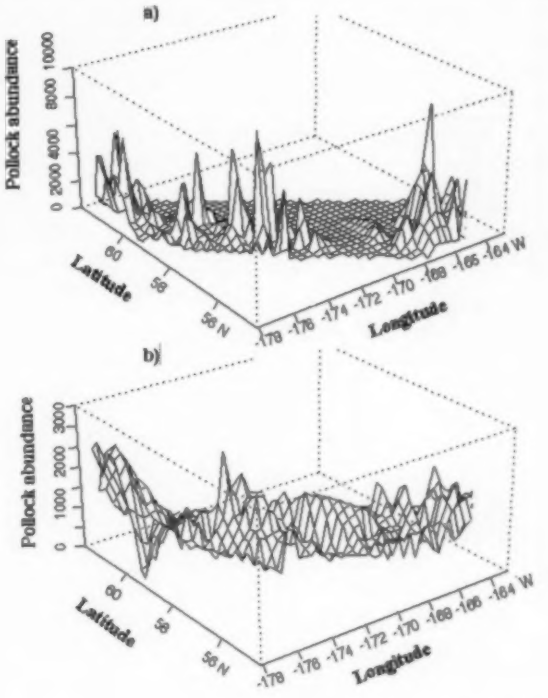

Higher average abundance in areas where the water column is in the 50–130 m range suggests that walleye pollock in summer prefer the middle Bering Sea shelf and the shallow part of the outer shelf to the inner shelf and basin areas. We suggest that higher food abundances attract them to this region. To relate higher food abundance to ocean environment conditions, more discussion of the shelf slope oceanography is in order. The middle shelf region is delineated by two fronts: an inner front at around 50–70 m depth and an outer front at the shelf break around 120–130 m (Coachman 1986). These fronts are broad regions across which there is a relatively large horizontal gradient in the temperature profile. Both north and south of these fronts, there is little change in temperature profile, and the middle shelf region is striking as having weak currents and almost no water transport. On the other hand, there is a relatively strong northwesterly current in the outer shelf region (Hughes et al. 1974). Bering Sea summer zooplankton biomass is concentrated in the top 80 m of the water column with maximum production at around 40 m (Motoda and Minoda 1974). Zooplankton summer production in the Bering Sea is highest along the middle shelf, so it is not surprising that walleye pollock are attracted to this region in summer. The circulation pattern along the shelf slope is from southeast to northwest, which would tend to drift zooplankton toward the northwest and might explain the predominance of walleye pollock in the

Fig. 6. GAM-derived effects of depth, thermocline depth, and temperature at 50 m on walleye pollock abundance in top 50 m of the water column for the 1991 summer Bering Sea acoustic survey.

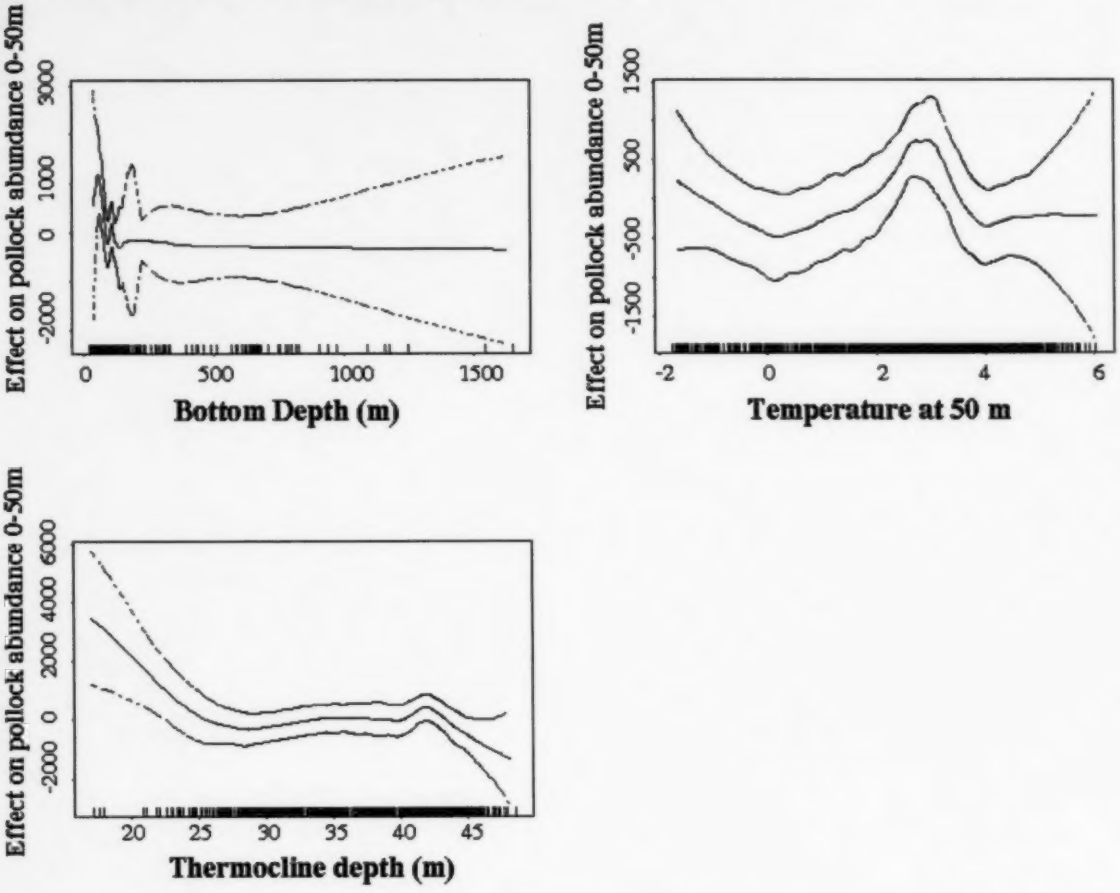

northwest region (Fig. 5). Scrutiny of the CTD and XBT casts on this survey suggests the following commonalities between years (Fig. 7):

(1) Along the inner shelf and shallower parts of the middle shelf (for bottom depths up to 70–80 m; labeled <77 m in Fig. 7), especially in the southeast, the temperature profile generally shows a strongly delineated thermocline, with temperature dropping in a few metres from surface to bottom temperatures.

(2) Beyond the shelf break in basin water (panels labeled >150 m deep in Fig. 7) the temperature drops off relatively slowly with increasing depth to around 80 m.

(3) In the southeast middle shelf region (bottom depths between 77 and 150 m) the temperature profile is intermediate between the inner shelf and basin pattern, especially in 1991, maintaining surface temperatures for the top 10–20 m, dropping initially rapidly and then more slowly to a depth close to 50 m, below which temperature is nearly constant.

(4) In the northwest part of the survey region in 1991, cold temperature (below 0°C) prevailed at depths ranging from 25 to 55 m, below which temperatures were warmer (and water was more saline). This is indicative of residual ice-melt remaining in the area with an intrusion of warmer water below it coming from the basin. Deeper water temperatures in this region were about 2.5°C, the temperature of deeper basin water (Takenouti and Ohtani 1974). In 1988, a similar pattern was seen in the northwestern part of the survey region, but the temperatures were significantly warmer between 25 and 55 m (bottom depths between 77 and 150 m in Fig. 7).

The above generalizations are extracted from bathytherms that display significant variability (Fig. 7). This reflects the large area surveyed and the relatively small number of classes the bathytherms are divided into. Because of the somewhat arbitrary nature of the classes, there are some bathytherms that may appear to belong to another class. We excuse this apparent misclassification because our emphasis is on finding a small set of thermal regions within which bathytherms are similar and not to accurately define the temperature–depth structure in the Bering Sea.

Translating the bathytherms into the thermocline depths, as we defined them, the inner and shallower middle shelf regions had shallow thermoclines, the basin had deeper

Fig. 7. Comparison of bathytherms for 1988 (left panels) and 1991 (right panels) for shelf regions having (from top to bottom) shallow (<77 m), midwater (between 77 and 150 m), in the northwest (NW) and southeast (SE) parts of the survey area, and deeper (>150 m) bottom depths.

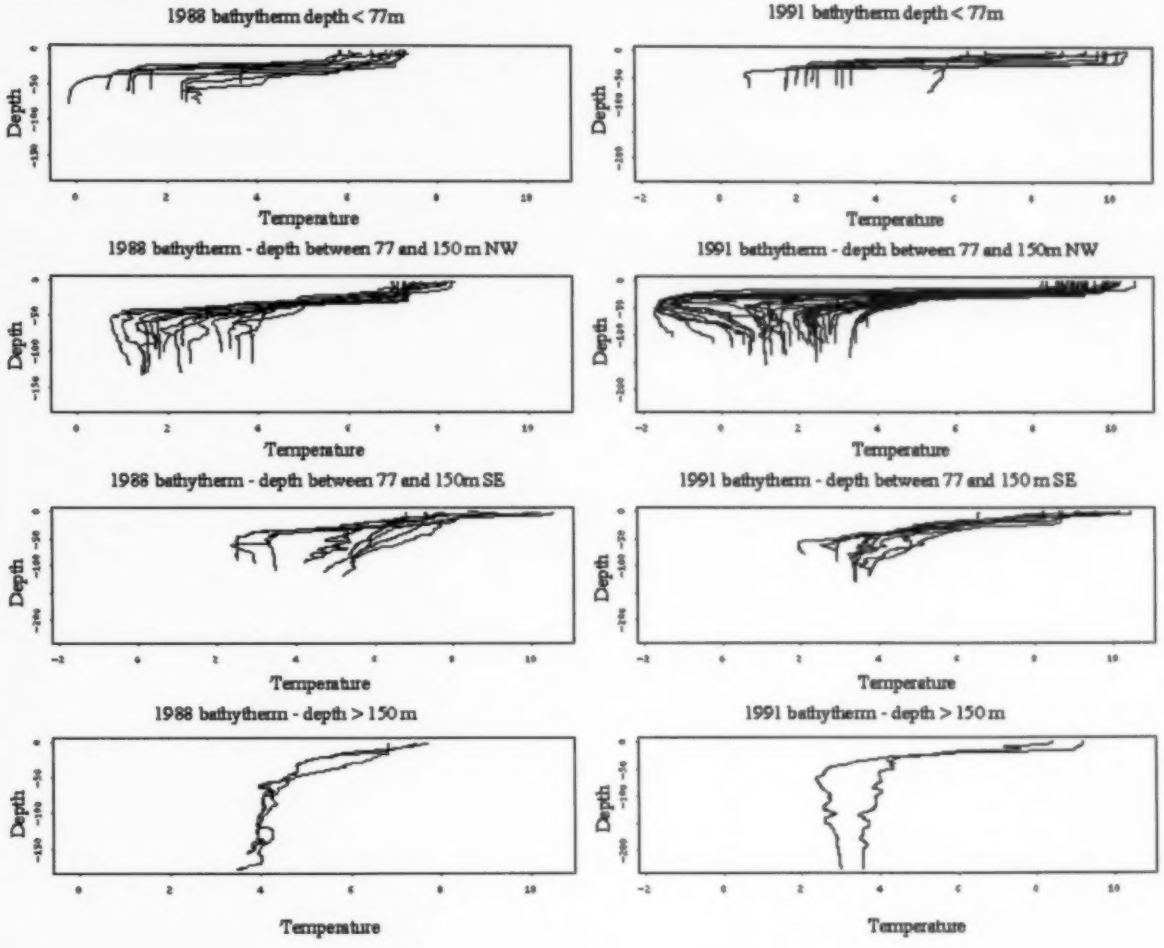
1988 bathytherm depth < 77m
1991 bathytherm depth < 77m
1988 bathytherm - depth between 77 and 150 m NW
1991 bathytherm - depth between 77 and 150m NW
1988 bathytherm - depth between 77 and 150m SE
1991 bathytherm - depth between 77 and 150 m SE
1988 bathytherm - depth > 150 m
1991 bathytherm - depth > 150 m
Depth
Temperature

thermoclines, and the middle region in the southeast had intermediate and more variable thermocline depths. In 1988 the northwest region had deeper thermoclines, while in 1991 the thermocline depth increased with bottom depth, much as in the southeast. Both years showed increased average walleye pollock abundance for 50-m temperatures near 2.5°C and for deeper thermocline depths (up to 45 m) for intermediate-bottom-depth shelf conditions but not for deeper water (basin area). During the summer, Bering Sea basin water below 20 m is almost always warmer than shelf water because the shelf is generally largely ice-covered in winter, while the basin is ice-free. Incursion of this warmer water onto the middle and outer Bering Sea shelf slope appears to create conditions attractive to walleye pollock.

Although we do not know the size–depth distribution of walleye pollock for 1988 and have only a crude estimate (50-m depth bins) for 1991, we can hypothesize from the available evidence that in the northwestern part of the survey region, where there was an incursion of warmer water under cold residual ice-melt water (Fig. 7), most fish remained below the thermocline and avoided the colder water above. Evidence for this is that, although total walleye pollock abundance for the entire water column was high for low 50-m temperatures, which occurred only in the northwest region (<0°C; Fig. 3), the abundance in the top 50 m of the water column was not high under these conditions (Fig. 6). Apparently the northwestern survey region, which had high walleye pollock abundance in both years (Figs. 1 and 5), is attractive to walleye pollock for its high zooplankton production and drift of zooplankton from further south into this area. It is unclear how walleye pollock relate to the colder midwater temperatures when they prevail in this region. Do they move through the colder depths to feed at night or during crepuscular periods or do they remain below the cold water, depending on diel migration of euphausiids and copepods

for their food resources? Unfortunately, we do not know the 1988 walleye pollock depth distribution, 1988 being a year in which warmer midwater temperatures prevailed in the northwest than in 1991 and where the question about avoidance of colder water temperatures by walleye pollock could be addressed.

Shallow thermoclines and higher 50-m temperatures occur in the southeastern part of the survey region and were associated with increased average walleye pollock abundance. Also, average walleye pollock abundance in the top 50 m in 1991 was highest when the thermocline was shallow (Fig. 6). In 1991, many aggregations of the dominant 1989 year class walleye pollock (age 2 juveniles), which tend to be in midwater, were observed in the southeast region (evidence from survey midwater trawl data). Similar juvenile aggregations were not observed in this region in 1988, and 1988 abundances in this region were not as high as in 1991 (Fig. 1). In the eastern Bering Sea, walleye pollock spawning occurs near Bogoslof Island in the basin, north of Unimak Island, and near the Pribilof Islands. These regions are close to the southeastern shelf and may account for the higher incidence of juvenile walleye pollock (up to age 3) in this region in summer (Gershanovich et al. 1974; Walsh and McRoy 1986).

Our analysis suggests that the spatial distribution of walleye pollock in the eastern Bering Sea in summer is associated with temperature and depth conditions. We suggest a food-related hypothesis to account for the given distribution and are left with several additional questions about the relationship of walleye pollock distribution to food resources that cannot be investigated with the available survey data. These questions could be explored through deployment of an acoustic buoy system at a location along the middle Bering Sea shelf front. Having a two-frequency system (e.g., 38 and 120 kHz) would allow observation of both fish and zooplankton. Obtaining the requisite temperature information would require deployment of a second buoy with a temperature-sensing array. Buoy systems of this sort exist and have been demonstrated to be reliable in arctic waters (Ehrenberg et al. 1989).

Walleye pollock are thought to spend the warmwater season along the middle shelf region, while during winter, they are in deeper water in the Bering Sea basin and in spawning areas near Bogoslof Island. During fall and spring, they are more widely distributed over the shelf. An experiment like the one proposed above could also be used to establish a relationship between ice cover and melting, bathytherms, and walleye pollock abundance, indicating what possible temperature conditions could signal the arrival of the walleye pollock onto the shelf slope in the warmwater season. The extensive spatial coverage of surveys such as the one considered here provided an opportunity to uncover mesoscale patterns but could not address temporal issues. For this, similar surveys over a smaller area, such as Dabob Bay, Washington, or a well-studied Norwegian fjord, would be more fruitful.

One potential problem with our use of the thermocline depth as a covariate in the GAM model is the arbitrary nature of our definition. By reducing the depth–temperature information to thermocline depth and 50-m temperature, we may be discarding information about the bathytherm that is important to walleye pollock distribution. An alternative would be to use a classification scheme for bathytherms as discussed by Takenouti and Ohtani (1974), who divided Bering Sea summer bathytherms into four classes, and relating abundance to the bathytherm class. Such a classification could be made using a hierarchical clustering algorithm on existing CTD and XBT data.

Our success in demonstrating a plausible multiyear relationship between Bering Sea walleye pollock abundance in the summer, water column depth, and temperature profile parameters suggests that the methods used here could be fruitfully applied to other pelagic fish such as capelin off the coasts of Iceland and Norway, cod off the Norwegian coast, and the U.S. Pacific coast hake. The ancillary data collected in fisheries surveys are essential to the successes of our methods. Additional ancillary data would also be desirable. Such observations would include currents collected by an acoustic doppler current meter, surface wind velocity, more continuous temperature data so that fine-scale temperature gradients could be considered, and an estimate of primary production.

This fisheries oceanography study is one of few studies spanning the mesoscale in scope with resolution of a few kilometres (Laurs et al. 1984; Mendelssohn and Cury 1987; Svejkovsky 1988; Cury and Roy 1989). We believe that this type of analysis will become more common in fisheries oceanography and presages the need for increased interaction between fisheries biologists and oceanographers. This interaction must involve data transfer, hypothesis formulation, and mutual education. For example, the discussion section of this paper was revised almost completely after meeting with a Bering Sea oceanography team from the Pacific Marine Environmental Laboratory (PMEL). As complex as the walleye pollock spatial distribution is, a clearer understanding of what is known about water circulation in the Bering Sea was needed to shed some light on the observed relationship between walleye pollock distribution in the survey area, depth, and temperature. The water mass hypothesis arose from an observation that the colder water in the northwest region overlaid a more saline water mass that was moving in from the basin area. This warmer water provides a temperature foothold for walleye pollock attracted to the high zooplankton abundance in the area but avoiding temperatures below 2°C. Without the oceanographic information the fish distribution – environment relationship observed becomes an isolated fact, taken out of context. However, the fisheries data have provided a link between an understanding of Bering Sea circulation patterns and how pelagic fish behave in the face of these patterns. The inclusion of higher trophic levels in ocean science is a new frontier, requiring new techniques in sampling, pattern recognition through exploratory data analysis of multivariate data, and imagination to explain the patterns. We will also require further monitoring to evaluate the generality of significant environment – abundance distribution relationships.

Acknowledgments

We thank Jim Traynor, Bill Karp, and Dan Twohig of the Alaska Fisheries Science Center for providing the data,

discussing the concepts, and helping us with interpretation of the analysis. This work was supported by the Washington Sea Grant Program under grant No. NA36RG0071, project R/F-92.

References

Aoki, I., and Inagaki, T. 1992. Acoustic observations of fish schools and scattering layers in a Kuroshio warm-core ring and its environs. Fish. Oceanogr. **1**(2): 137–142.

Bakkala, R.G., Karp, W.A., Walters, G.F., Sasaki, T., Wilson, M.T., Sample, T.M., Shimada, A.M., Adams, D., and Armistead, C.E. 1992. Distribution, abundance, and biological characteristics of groundfish in the eastern Bering Sea based on results of U.S.–Japan bottom trawl and hydroacoustic surveys during June–September 1988. U.S. Dep. Commer. NOAA Tech. Memo. NMFSF/NWC-213.

Cleveland, W.S., and Devlin, S-J. 1988. Locally-weighted regression: an approach to regression analysis by local fitting. J. Am. Stat. Assoc. **83**: 596–610.

Coachman, L. 1986. Circulation, water masses, and fluxes on the southeastern Bering sea shelf. Continental Shelf Res. **5**(1/2): 23–108.

Cury, P., and Roy, C. 1989. Optimal environmental window and pelagic fish recruitment success in upwelling areas. Can. J. Fish. Aquat. Sci. **46**: 670–680.

Doyle, M.J., and Ryan, T.A. 1989. Spatial patterns in a coastal ichthyoplankton community southwest of Ireland. *In* Early life history of fish. *Edited by* J.H.S. Blaxter, J.C. Gamble, and H. von Westernhagen. Rapp. P-v. Réun. Ciem. **191**: 27–84.

Ehrenberg, J.E., Wiebe, P.H., Hanot, W.H., McMichael, H.G., and Miyamoto, R.T. 1989. BIOSPAR: a buoy system for monitoring of biological populations. Proceedings of Oceans 89, Seattle, Wash.

Fetter, M.E., and Davidyuk, A.P. 1986. Seasonal distribution of southern Baltic herring, and environmental factors. Fisheries Research by the GDR and the USSR in the Baltic Sea. Fischerei-Forschung, **24**(2): 16–19.2

Foote, K.G., and Traynor, J.J. 1988. Comparison of walleye pollock target strength estimates determined from in-situ measurements and calculations based on swimbladder form. J. Acoust. Soc. Am. **83**(1): 9–17.

Fréon, P., Gerlotto, F., and Misund, O.A. 1993. Consequences of fish behaviour for stock assessment. ICES Mar. Sci. Symp. 178–183.

Gershanovich, D.E., Fadeev, N.C, Liubimova, T.G., Moiseev, P.A., and Natarov, V.V. 1974. Principal results of Soviet oceanographic investigations in the Bering Sea. *In* Oceanography of the Bering Sea. *Edited by* D.W. Hood and E.J. Kelley. Institute of Marine Science, University of Alaska, Fairbanks, Alaska, pp. 479–506.

Hanaoka, F. 1983. Distribution of fish schools in the Bungo Suido (Channel) determined by acoustic surveys. Bull. Nansei. Reg. Fish. Res. Lab. No. **15**: 13–27.

Hastie, T., and Tibshirani, R. 1986. Generalized additive models. Stat. Sci. **1**: 297–318.

Hastie, T., and Tibshirani, R. 1990. Generalized additive models. Chapman-Hall, London.

Herron, R.C,. Leming, T.D., and Jilong, L. 1989. Satellite-detected fronts and butterfish aggregations in the northwestern Gulf of Mexico. Continental Shelf Res. **9**(6): 569–588.

Hughes, F.W., Coachman, L.K., and Aagaard, K. 1974. Circulation, transport and water exchange in the western Bering Sea. *In* Oceanography of the Bering Sea. *Edited by* D.W. Hood and E.J. Kelley. Institute of Marine Science, University of Alaska, Fairbanks, Alaska. pp. 59–98.

Inagake, D., and Hirano, T. 1983. Vertical distribution of the Japanese sardine in relation to temperature and thermocline at the purse seine fishing grounds east of Japan. Bull. Jpn. Soc. Sci. Fish. **49**(10): 1533–1539.

Kemmerer, A.J. 1980. Environmental preferences and behavior patterns of gulf menhaden (*Brevoortia patronus*) inferred from fishing and remotely sensed data. *In* Fish behavior and its use in the capture and culture of fishes. *Edited by* J.E. Bardach, J.J. Magnuson, R.C. May, and J.M. Reinhart. ICLARM Conf. Proc. No. 5.

Laurs, R.M., Fiedler, P.C., and Montgomery, D.R. 1984. Albacore tuna catch distributions relative to environmental features observed from satellites. Deep-Sea Res. **31**: 1085–1097.

Li, X-D. 1982. Effects of vertical temperature structure of seawater and variation of water temperature with time on fishing grounds. Mar. Fish. Res. **4**: 55–65.

Maul, G.A., Williams, F., Mitchell, R., and Sousa, F.M. 1984. Remotely sensed oceanography patterns and variability of bluefin tuna catch in the Gulf of Mexico. Oceanol. Acta. **7**(4): 469–479.

Mendelssohn, R., and Cury, P. 1987. Fluctuations of a fortnightly abundance index of the Ivoirian coastal pelagic species and associated environmental conditions. Can. J. Fish. Aquat. Sci. **44**: 408–421.

Misund, O.A., and Aglen, A. 1992. Swimming behaviour of fish schools in the North Sea during acoustic surveying and pelagic trawl sampling. ICES J. Mar. Sci. **49**(3): 325–334.

Mochek, A.D., and Valdes-Munoz, E. 1983. Influence of bottom relief on the gregarious behaviour of fish. Cienc. Biol. **9**: 79–85.

Motoda, S., and Minoda, T. 1974. Plankton of the Bering Sea. *In* Oceanography of the Bering Sea. *Edited by* D.W. Hood, and E.J. Kelley. Institute of Marine Science, University of Alaska, Fairbanks, Alaska, pp. 207–410.

Rose, G.A., and Leggett, W.C. 1990. The importance of scale to predator-prey spatial correlations: an example of Atlantic fishes. Ecology, **71**(1): 33–43.

Saitoh, S.I., Kosaka, S., and Iisaka, J. 1986. Satellite infrared observations of Kuroshio warm-core rings and their application to study of Pacific saury migration. Deep-Sea Res. **33**: 11A–12A.

Shinomiya, H., and Tameishi, H. 1988. Discriminant prediction of formation of saury fishing grounds by satellite infrared imageries. Bull. Jpn. Soc. Fish. **54**(7): 1093–1099.

Sinclair, M., and Iles, T.D. 1985. Atlantic herring (*Clupea harengus*) distributions in the Gulf of Maine – Scotian Shelf area in relation to oceanographic features. Can. J. Fish. Aquat. Sci. **42**: 880–887.

Svejkovsky, J. 1988. Remotely sensed ocean features and their relation to fish distributions. *In* Marine organisms as indicators. *Edited by* D.F. Sproule and G.S. Kepple. Springer-Verlag, New York, N.Y. pp. 177–197.

Swartzman, G.L., Huang, C.P., and Kaluzny, S.P. 1992. Spatial analysis of Bering Sea groundfish survey data using generalized additive models. Can.J. Fish. Aquat. Sci. **49**: 1366–1378.

Takenouti, A.Y., and Ohtani, K. 1974. Currents and water masses in the Bering Sea: a review of Japanese work. *In* Oceanography of the Bering Sea. *Edited by* D.W. Hood and E.J. Kelley. Institute of Marine Science, University of Alaska, Fairbanks, Alaska. pp. 33–58.

Walsh, J.J., and McRoy, C.P. 1986. Ecosystem analysis in the southeastern Bering Sea. Continental Shelf Res. **5**(1/2): 259–288.

Yamaguchi, Y., Jinno, T., Ishikura, I., Uchida, M., and Kawamata, S. 1984. Underwater topography and fish schooling dynamics in coastal region of Kumano Nada. Bull. Fac. Fish. Mie Univ. No. **11**: 111–121.

Removal of algae by the zebra mussel (*Dreissena polymorpha*) population in western Lake Erie: a bioenergetics approach[1]

Charles P. Madenjian

Abstract: A bioenergetics model for growth of a zebra mussel (*Dreissena polymorpha*) individual was verified with observations on zebra mussel growth in western Lake Erie. The bioenergetics model was then applied to the zebra mussel population in the western basin of Lake Erie to estimate the removal of phytoplankton by mussels. According to the modeling results, the zebra mussel population consumed 5.0 million tonnes of phytoplankton, while 1.4 million tonnes of phytoplankton was deposited in pseudofeces from the mussels. Thus, a total of 6.4 ± 2.4 million tonnes of phytoplankton was removed from the water column by zebra mussel in western Lake Erie during 1990. Primary production was estimated to be 24.8 million tonnes; therefore, zebra mussel removed the equivalent of 26 ± 10% of the primary production for western Lake Erie.

Résumé : Nous avons vérifié un modèle bioénergétique de la croissance de la moule zébrée (*Dreissena polymorpha*) en fonction des observations de la croissance de ce coquillage dans l'ouest du lac Érié. Nous avons ensuite appliqué le modèle bioénergétique à la population de moules zébrées du bassin occidental du lac Érié pour estimer le prélèvement de phytoplancton par les moules. Selon les résultats de la modélisation, la population de moules zébrées a consommé 5,0 millions de tonnes de phytoplancton, tandis que 1,4 millions de tonnes de phytoplancton était déposée sous forme de pseudofèces produites par les moules. C'est donc un total de 6,4 ± 2,4 millions de tonnes de phytoplancton qui a été retiré de la colonne d'eau par les moules zébrées de l'ouest du lac Érié en 1990. On a estimé la production primaire à 24,8 millions de tonnes; les moules zébrées ont donc prélevé l'équivalent de 26 ± 10 % de la production primaire de l'ouest du lac Érié.
[Traduit par la Rédaction]

Introduction

The zebra mussel (*Dreissena polymorpha*) was first observed in Lake Erie during 1988 (Leach 1993) and quickly established high-density colonies on the reefs (Griffiths et al. 1991). Leach (1993) reported densities as high as 350 000 individuals/m^2 on reefs in the western basin of Lake Erie. Concomitant with the spread of zebra mussel in Lake Erie from 1988 through 1990, chlorophyll concentrations declined (Leach 1993). This decline was attributed, in part, to zebra mussel feeding.

MacIsaac et al. (1992) estimated the filtering impacts of larval and sessile zebra mussel on the western Lake Erie ecosystem. These researchers concluded that settled mussels would graze more than 1000 times the phytoplankton biomass that planktonic veligers would feed upon. Furthermore, their calculations showed that the reef-associated zebra mussel population was theoretically capable of filtering 13.9 times the volume of the western basin in just 1 day. Finally, MacIsaac et al. (1992) argued that the zebra mussel population consumed a larger biomass of phytoplankton than that consumed by herbivorous zooplankton in the western basin, based on a comparison of filtering capabilities and using zebra mussel densities observed on Hen Island Reef.

Comparison of filtering impacts proved useful in gauging the relative potential contributions to phytoplankton grazing by larval and sessile zebra mussel, as well as by zooplankton. Yet, two questions remain to be answered: How much phytoplankton biomass is actually consumed by the zebra mussel population in western Lake Erie? How does the estimate of consumed phytoplankton biomass compare with the primary production estimate? Bioenergetics modeling can serve as a vehicle for estimating the consumption of phytoplankton by zebra mussel in the western basin of Lake Erie.

Bioenergetics models have previously been used to assess the impact of predator populations on prey in the

Received November 16, 1993. Accepted July 18, 1994.
J12162

C.P. Madenjian.[2] National Biological Service, Great Lakes Science Center, Lake Erie Biological Station, 6100 Columbus Avenue, Sandusky, OH 44870, USA.

[1] Contribution 874 of the National Biological Service, Great Lakes Science Center, 1451 Green Road, Ann Arbor, Mich.

[2] Present address: National Biological Service, Great Lakes Science Center, 1451 Green Road, Ann Arbor, MI 48105, USA.

Fig. 1. Proportion of maximum respiration as a function of water temperature used in the modified bioenergetics model for zebra mussel growth.

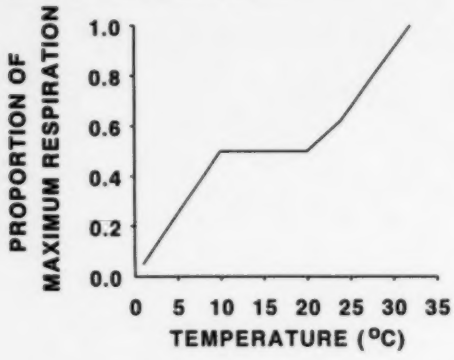

Great Lakes. Stewart et al. (1983) applied a bioenergetics model to estimate annual consumption of alewife (*Alosa pseudoharengus*) biomass by the lake trout (*Salvelinus namaycush*) population of Lake Michigan. Similarly, Hartman and Margraf (1992) employed a bioenergetics approach to estimate prey fish consumption by the dominant piscivore, the walleye (*Stizostedion vitreum*), in western Lake Erie. Bioenergetics modeling has also been used to estimate zooplanktivory by fish (Hewett and Stewart 1989; Rudstam et al. 1992) and by mysid shrimp (*Mysis mixta*) (Rudstam et al. 1992). Given this history of model application, the bioenergetics approach should be appropriate for answering the first of the two questions posed above.

The objectives of this study are to (1) verify that a bioenergetics model adequately explains growth of zebra mussel in Lake Erie, (2) apply the bioenergetics model to the zebra mussel population in western Lake Erie to calculate the consumption of phytoplankton, and (3) discuss the implications for the western Lake Erie ecosystem.

Methods

Bioenergetics model

I modified a zebra mussel bioenergetics model originally developed by Schneider (1992) by updating values of a few model parameters, restructuring the respiration component, and simplifying the egestion component. First, the intercept value for maximum consumption, a_c, was changed from 0.031 to 0.027 $g \cdot g^{-1} \cdot d^{-1}$ to correct for differences in wet weight carbon content between zebra mussel and diatoms. The original value for a_c was taken from Walz (1978*a*); however, this value was reported in terms of carbon mass rather than biomass. The adjustment was made to express the ratio on a biomass basis, which is the appropriate currency for the model.

The respiration component was restructured according to the results of recently completed studies on zebra mussel respiration rates. In these studies, the mussels were allowed to acclimate to the incubation temperatures, and consequently confounding effects due to lack of acclimation were eliminated. Acclimation to a particular water temperature has a huge effect on zebra mussel respiration rate (Bayne et al. 1976; Payne and Aldridge 1994). Quigley et al. (1993) did not find a significant difference in zebra mussel respiration rate between 10 and 20°C; therefore, I assumed that respiration rate was constant within this temperature range (Fig. 1). In a recent experiment, zebra mussel respiration rate increased three- or fourfold between 20 and 32°C, with a disproportionately higher increase between 24 and 32°C than between 20 and 24°C (D. Aldridge, North Carolina A&T State University, Greensboro, N.C., personal communication). In this experiment, the mussels exposed to the higher water temperatures were slightly smaller than those at the cooler temperatures. Specific respiration rate has been shown to increase dramatically with decreasing zebra mussel size (Quigley et al. 1993). But even taking into account the mussel size differences, respiration rate at 32°C was at least twice as great as that at 20°C. I therefore assumed that respiration rate doubled between 20 and 32°C, with only 25% of the increase realized between 20 and 24°C and the rest between 24 and 32°C (Fig. 1). To complete the picture, I assumed that the proportion of maximum consumption was only 0.05 (the value used by Schneider (1992)) at 1°C, but increased linearly from to 1 to 10°C (Fig. 1). For purposes of this modeling application to western Lake Erie, the respiration rate at 32°C will be considered the maximum respiration rate.

Quigley et al. (1993) showed that the specific respiration rate of zebra mussel decreased as body weight increased. Using respiration data presented in the Quigley et al. (1993) study, the following regression equation was developed:

$$\text{spcresp} = 0.00059W^{-0.605}$$

where spcresp = specific respiration rate (grams of oxygen per gram per day) and W = zebra mussel wet weight (grams). Because the respiration rate in the 10–20°C range was assumed to be one half the rate at 32°C, the equation for maximum specific respiration rate is

$$\text{spcresp} = 0.00118W^{-0.605}$$

Respiration rate was converted from units of oxygen consumption to body mass units as outlined by Schneider (1992).

I simplified the egestion component of the bioenergetics model because food assimilation efficiency by zebra mussel has not been directly measured. Walz (1978*a*) estimated a food assimilation efficiency by zebra mussel of 35.2% using the Conover method, an indirect approach in which the assumptions may not always be met (Bayne et al. 1976). Furthermore, applying the ratio of consumption to pseudofeces production given in Walz (1978*a*) to the waste (pseudofeces and feces) production of zebra mussel measured directly by Stańczykowska et al. (1976) yields an assimilation efficiency estimate of 100%. Given the great disparity in the indirect estimates of zebra mussel assimilation efficiency, I opted to use an average assimilation efficiency of 82% taken from studies on other species of mussels (Winter 1969; Vahl 1973). This choice for the assimilation efficiency is supported by the work of Reeders and bij de Vaate (1992), who estimated that roughly 90% of the waste produced by zebra mussel was pseudofeces, with true feces constituting the remainder of the waste. If pseudofeces productivity did not exceed double the value of the consumption rate (Walz 1978*a*), then assimilation

efficiency would be approximately 80%. Lower food assimilation efficiency by the marine mussel *Mytilus edulis* at high food concentrations has been documented by Bayne et al. (1976); however, with no direct measurement of food assimilation efficiency by zebra mussel, I decided to use the simplest approach of a constant assimilation efficiency.

Schneider (1992) simulated spawning of zebra mussel in his bioenergetics model by assuming a 5% decrease in body weight on the spawning day, as estimated by Walz (1978*b*) on a dry weight basis. Nalepa et al. (1993) estimated the wet weight loss in spawning zebra mussel from Lake St. Clair to be 33%, and this proportion was used in the modified bioenergetics model.

Specific dynamic action (S) has not been measured in zebra mussel, but S is typically set equal to 0.172 times the food assimilation rate in fish bioenergetics model applications. I used this approach in the modified bioenergetics model. Schneider (1992) reasoned that, under normal conditions, S (including the energetic cost of feeding) in the zebra mussel would be substantially less than 57% of consumption that has been reported in actively feeding specimens of *M. edulis*, and he arbitrarily assigned S a value of 28.5% of consumption. For lack of better information, I used the typical approach from fish applications.

The zebra mussel bioenergetics model is summarized in the appendix.

Model verification

The modified bioenergetics model, like the original model by Schneider (1992), was tested with Lake Constance growth data. The water temperature and P-value regimes, as well as the initial zebra mussel wet weights, used in the modified model simulations were identical to those presented by Schneider (1992). Here, P-value refers to the proportion of maximum consumption that is realized by the mussel (Schneider 1992). See the appendix for more details on the calculation of the specific consumption rate.

In the present study, newly settled zebra mussel were considered to represent the age-0 cohort from the time of settlement in late summer through December 31. From 1 January through 31 December of the following year, these individuals were placed in the age-1 cohort; finally, the mussels belonged to the age-2 cohort during the subsequent year. Thus, the age-1 and age-2 cohorts in the present study corresponded to the young-of-the-year (YOY) and age-1 cohorts of the Schneider (1992) study.

Next, predictions by the modified bioenergetics model were compared with zebra mussel growth observations by Dermott et al. (1993) on a reef in eastern Lake Erie during 1990. These researchers measured mean length of the age-1 zebra mussel cohort from May through November 1990 at monthly intervals. Water temperature was also monitored and a regression of zebra mussel wet tissue weight as a function of shell length formulated. I used this length–weight regression to convert from shell length to tissue wet weight. Initial wet weight in the bioenergetics model application was assigned the observed weight on 2 May. The temporal pattern in lipid content suggested that spawning by the age-1 zebra mussel cohort occurred by early August (Dermott et al. 1993). In the bioenergetics simulation, spawning occurred on 1 August.

Chlorophyll *a* observations in the eastern basin of Lake Erie indicated that phytoplankton biomass was relatively high during late April 1990 (R. Dermott, Great Lakes Laboratory for Fisheries and Aquatic Sciences, Burlington, Ont., personal communication). Because phytoplankton biomass data were unavailable for the eastern basin in 1990, phytoplankton biomass was assumed to be greater than 1.25 mg/L during May 1990 and was assumed to be 0.525 mg/L for June–November. Schneider (1992) calculated the P-value by dividing phytoplankton biomass by 1.25 mg/L for phytoplankton biomasses less than 1.25 mg/L and let the P-value equal 1 for phytoplankton biomasses equal to or exceeding 1.25 mg/L. Therefore, the P-values used in the bioenergetics application were 1.0 for May and 0.42 for June–November. The value of 0.525 mg/L represents the average phytoplankton biomass between June and November in eastern Lake Erie over the years 1983–1985 (Makarewicz 1987, 1988; Makarewicz et al. 1989).

Finally, the modified bioenergetics model was verified with zebra mussel length–frequency distributions during April and October 1990 from Sunken Chicken Reef, located in the central portion of the western basin of Lake Erie; these data were provided by J. Leach (Ontario Ministry of Natural Resources, Wheatley, Ont.). Water temperature data were also furnished by the Ontario Ministry of Natural Resources (S. Nepszy, Ontario Ministry of Natural Resources, Wheatley, Ont., unpublished data); water temperature was monitored from April through November 1990 on Hen Island Reef, which is within 5 km and at approximately the same depth (4.4 m) as Sunken Chicken Reef.

Phytoplankton biomass observations were not available for the western basin during 1990, so the following scenario was used to model zebra mussel food availability. Phytoplankton biomass was assumed to exceed 1.25 mg/L in late April and May 1990. From June through October during 1983–1985, phytoplankton biomass in the western basin averaged 1.66 mg/L (Makarewicz 1987, 1988; Makarewicz et al. 1989). Leach (1993) reported a 54% decrease in chlorophyll *a* concentrations in the western basin from 1988 to 1990. Given that chlorophyll *a* is strongly correlated with phytoplankton biomass during summer and fall months (Munawar and Burns 1976), the summer and fall phytoplankton biomass was estimated to be 0.76 mg/L. Consequently, the P-value used in the western basin simulations was set equal to 1.0 for late April and May and to 0.61 for the summer and fall months.

Again, the length–weight regression from Dermott et al. (1993) was used to convert from shell lengths to tissue wet weights. An average individual from both the age-1 and age-2 cohorts was simulated from 20 April through 22 October 1990, which corresponds to the period between the length–frequency observations. The simulated mussel from either cohort spawned on 1 August. Observations from a reef near South Bass Island in western Lake Erie indicated that, on the average, age-2 mussels spawn twice between June and September, with the spawnings roughly 1 month apart (D. Garton, Indiana University, Kokomo, Ind., personal communication); therefore, simulated age-2 mussels also spawned on 1 July. These simulated spawning times correspond to the peak abundance of zebra mussel

larvae observed during July and August 1990 in western Lake Erie (Leach 1993). The initial weight of the age-1 and age-2 simulated zebra mussel was assigned the estimated observed weight on the starting date.

Growth of the "average" age-0 zebra mussel from the western basin was also simulated. Simulated growth began on 15 September and ended on 22 October 1990. 15 September was chosen as the starting day because almost all of the mussel larvae in the western basin had settled by then (Fraleigh et al. 1993; Leach 1993). Based on observations by Martel (1993), the average shell length of age-0 zebra mussel by mid-September would be between 1.5 and 2 mm. A shell length of 1.75 mm converts to a tissue wet weight of 0.6 mg, and this value was the chosen initial weight for the simulation.

Pseudofeces production

As pointed out by Schneider (1992), pseudofeces production must be taken into account to fully evaluate the impact of zebra mussel on phytoplankton. For consumption, zebra mussel prefer particles in the 15- to 40-μm range (Sprung and Rose 1988). There is a tendency for larger particles to be bonded by mucus and to accumulate as pseudofecal pellets, which are ejected through the inhalant siphon (Morton 1993). Thus, some phytoplankton may be removed from the water column by the filtering action of zebra mussel and then be ejected in pseudofeces. Some phytoplankton may still be viable after being ejected in a pseudofecal pellet (R. Lowe, Bowling Green State University, Bowling Green, Ohio, unpublished data); however, the exact proportion has yet to be quantified. For my simulations, I assumed that all phytoplankton ejected in the pseudofeces were permanently removed from the water column. The ingestion of pseudofeces by zebra mussel was not addressed because this feeding behavior apparently has not been documented in western Lake Erie, although D. McNaught (University of Minnesota, Minneapolis, Minn., personal communication) has suggested that pseudofeces may serve as a food source of zebra mussel.

D. Schneider (University of Illinois, Urbana-Champaign, Ill., personal communication) has developed an equation, using data from Walz (1978*a*), to calculate pseudofeces production by zebra mussel as a function of mussel body size and food availability; food availability was represented by the *P*-value described by Schneider (1992). I used this equation in my simulation runs to estimate pseudofeces production by zebra mussel (see the appendix for more details). Not all of the pseudofeces consists of phytoplankton and mucus (D. Culver, Ohio State University, Columbus, Ohio, personal communication), but the proportion of nonphytoplankton material in pseudofeces has not been measured. I assumed that the proportion of phytoplankton in pseudofeces was equal to the proportion of phytoplankton in particulate material suspended in western Lake Erie water. Based on suspended solid measurements for western Lake Erie conducted from June through October for 1981–1983 (P. Richards, Heidelberg University, Tiffin, Ohio, unpublished data), and on phytoplankton biomass measurements over a similar range in months during 1983–1987 (Makarewicz 1993), living phytoplankton constituted approximately 20% of the particulate matter suspended in western Lake Erie water. Thus, the pseudofeces production estimate was multiplied by 0.2 to arrive at the phytoplankton removed from the water column by zebra mussel via incorporation into pseudofeces.

In the present paper, the amount of phytoplankton removed from the water column by a zebra mussel is defined as the sum of the biomass of phytoplankton actually consumed by the mussel and the biomass of phytoplankton ejected in the pseudofeces.

Simulations of zebra mussel population in western Lake Erie

Using the length–frequency distributions from Sunken Chicken Reef, mortality of the age-1 and age-2 zebra mussel cohorts from April through October 1990 was estimated to be 90 and 43%, respectively. Survival was modeled as decaying exponentially between April and October (see Stewart et al. 1983). Zebra mussel density on the reef on 20 April 1990 was estimated to be 138 160 mussels/m^2. These mussels were divided into two age groups based on their lengths: shell lengths of 1–9 mm represented the age-1 cohort and constituted 94% of the population, while the larger mussels were classified as belonging to the age-2 cohort. The age-3 cohort was not included in the population simulations because few zebra mussels in western Lake Erie are believed to survive beyond their third birthday (D. Garton, personal communication; J. Leach, personal communication).

The age-0 cohort was included in the population simulations by back-calculating the density of newly settled mussels on 15 September 1990 from the population density estimate of 269 725 age-0 zebra individuals/m^2 on 22 October 1990. The instantaneous mortality rate derived for the age-1 cohort was applied to the age-0 cohort to yield a population density estimate of 428 722 newly settled mussels/m^2 on 15 September 1990.

Hartman (1973) reported a surface area of 3276 km^2 for western Lake Erie and estimated that 13% of the bottom was hard bottom (bedrock, gravel, or clay). For the simulations, bottom area was set equal to surface area, and mussels inhabited only 13% of the available bottom.

Zebra mussel density on Sunken Chicken Reef is suspected of being relatively high compared with other reef areas in western Lake Erie during 1990 because it affords highly suitable habitat (D. Schloesser, National Biological Survey, Ann Arbor, Mich., personal communication). Garton and Haag (1993) estimated zebra mussel densities on a reef near South Bass Island in western Lake Erie to be 30 000 mussels/m^2. A density of 50 000 individuals/m^2 may be representative of hard substrate in the western basin (Fisher et al. 1993).

Population simulations were conducted to determine the ingestion of phytoplankton by zebra mussel in western Lake Erie. I performed 11 sets of population simulations corresponding to initial zebra mussel densities of 10, 20, 30, 36.19, 40, 50, 60, 70, 80, 90, and 100% of the reference density of 138 160 individuals/m^2, which was reported for Sunken Chicken Reef on 20 April 1990. Multiplying the reference density by 0.3619 yields 50 000 individuals/m^2, which presently may be the best estimate for the average zebra mussel density on hard bottom in western Lake Erie

Fig. 2. Standard error of zebra mussel mean density as a function of zebra mussel mean density. Mussel densities were estimated for Chickenolee Reef, Little Chicken Island Reef, Hen Island Reef, and Sunken Chicken Reef in western Lake Erie, 1990–1992 (Leach 1993; J. Leach, personal communication). Standard errors were based on a sample size of between 6 and 12 observations.

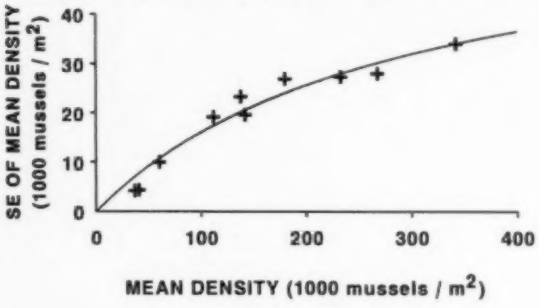

Fig. 3. Observed and predicted zebra mussel growth in Lake Constance, Switzerland, during 1974 and 1975. Observations were taken from Schneider (1992), and predictions were based on the modified bioenergetics model for zebra mussel growth.

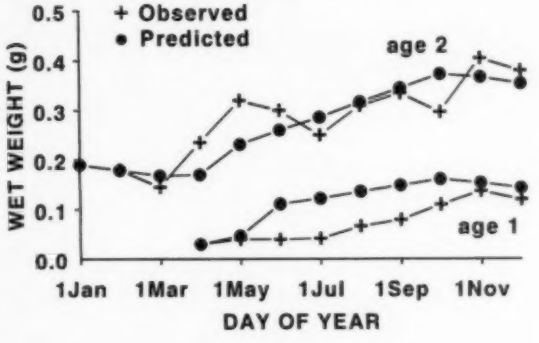

Fig. 4. Observed and predicted zebra mussel growth in eastern Lake Erie during 1990. Observations were taken from Dermott et al. (1993), and predictions were based on the modified bioenergetics model for zebra mussel growth.

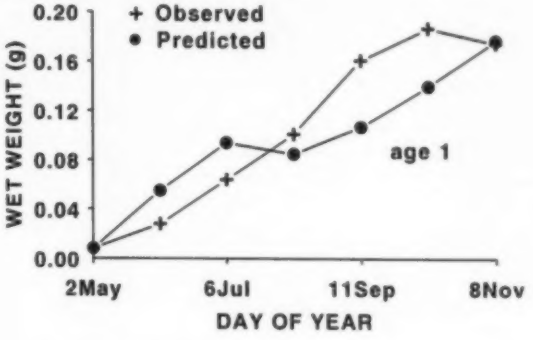

Fig. 5. Observed and predicted zebra musssel growth for age-1 and age-2 cohorts in western Lake Erie during 1990. Observations were taken from the Ontario Ministry of Natural Resources (J. Leach, unpublished data), and predictions were based on the modified bioenergetics model for zebra mussel growth.

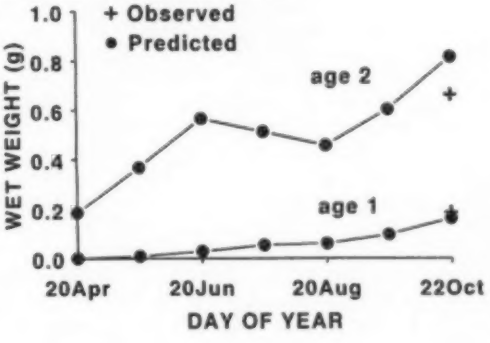

during 1990. The age-0, age-1, and age-2 cohorts were simulated at each fraction of the reference density. Initial density for each of the three age groups was determined using the abundance proportions described above. Total removal of phytoplankton by zebra mussel included phytoplankton biomass actually consumed as well as the biomass of phytoplankton deposited in pseudofeces.

In these simulations, it was assumed that zebra mussel diet consisted exclusively of phytoplankton, which seemed reasonable judging from the zebra mussel stomach contents reported by Ten Winkel and Davids (1982).

Uncertainty in zebra mussel density

Bioenergetics models are generally robust to uncertainties in metabolic parameters, especially when the model is calibrated with observed growth (Stewart et al. 1983). Far greater uncertainties are associated with estimates of population parameters, such as population size and mortality rates (Stewart et al. 1983). Probably the biggest source of uncertainty in the bioenergetics model application would be the error in the estimate of the mean zebra mussel density. I plotted standard error of mean zebra mussel density against mean zebra mussel density in order to estimate error bounds on the representative density of 50 000 mussels/m^2 (Fig. 2). Fitting a Michaelis–Menten curve to the data yielded the following equation:

$$SE = \frac{63461D}{294903 + D}$$

where SE is the standard error of the mean density of zebra mussels (number per square metre) and D is the mean zebra mussel density (number per square metre). At a mean density of 50 000 mussels/m^2, the standard error of the mean was 9200 mussels/m^2.

Upper and lower error bounds were calculated by adding and substracting 2 standard errors from the mean density of 50 000 mussels/m^2. The error bounds about the estimate of mean zebra mussel density were then translated into error bounds about the estimate of algal biomass removal by zebra mussel in western Lake Erie during April–October 1990.

Fig. 6. Observed and predicted zebra mussel growth for the age-0 cohort in western Lake Erie during 1990. Observations were taken from the Ontario Ministry of Natural Resources (J. Leach, unpublished data), and predictions were based on the modified bioenergetics model for zebra mussel growth.

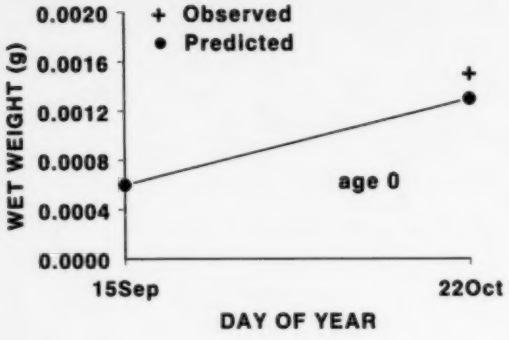

Fig. 7. Predicted phytoplankton biomass that would be removed from the water column by the zebra mussel population in western Lake Erie from late April through late October 1990 as a function of the average zebra mussel density on hard-bottom areas of western Lake Erie. Predictions were based on the modified bioenergetics model applied to the zebra mussel population in western Lake Erie.

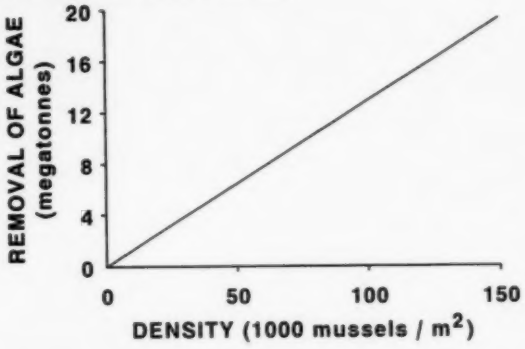

Results

The modified bioenergetics model performed as well as the original model developed by Schneider (1992) in describing growth of Lake Constance zebra mussel. Predictions of final weight by the modified model were within 19 and 7% of observed weight for the age-1 and age-2 zebra mussels, respectively (Fig. 3).

In addition, the modified model described zebra mussel growth adequately in eastern Lake Erie (Fig. 4). Final zebra mussel weight was accurately predicted by the model, although predicted weight showed relatively large deviations from actual weight during late summer and fall. Larger deviations may be expected due to lack of temporal resolution for estimation of *P*-values. Recall that observations on phytoplankton biomass for eastern Lake Erie were not available for 1990, and therefore, an average *P*-value, based on average observed phytoplankton biomass during the years 1983–1985, for the summer and fall months was used in the bioenergetics application.

The modified bioenergetics model furnished estimates of zebra mussel growth western Lake Erie that were fairly close to observed values. Predictions of final weight of age-1 and age-2 mussels were within 13 and 23%, respectively, of the observed wet weights (Fig. 5). The decline in predicted wet weight of age-2 mussels during July and August was attributed to scheduled spawnings. Similarly, the slower growth rate predicted for age-1 mussels in August was due to a scheduled spawning on 1 August. Observed growth of newly settled age-0 zebra mussel was closely matched by growth predicted by the bioenergetics model (Fig. 6).

According to the model, zebra mussel covering the hard-bottom areas of western Lake Erie at an average density of 50 000 individuals/m^2 ingested 6.4 megatonnes (10^{12} g = 1 Mt) of phytoplankton during the period from 20 April to 22 October 1990 (Fig. 7). Of the 6.4 Mt ingested, 5.0 Mt of phytoplankton was actually consumed by the zebra mussel, while 1.4 Mt of phytoplankton was deposited in pseudofeces. Of the three age groups, the age-1 cohort was responsible for the bulk of the ingestion. The age-1 cohort removed 3.4 Mt whereas the age-2 and age-0 cohorts removed 2.5 and 0.5 Mt, respectively.

The upper and lower error bounds for the mean zebra mussel density were 68 400 and 31 600 individuals/m^2. Incorporating this uncertainty into the estimate of algae removal by zebra mussel yielded upper and lower error bounds of 8.8 and 4.0 Mt of phytoplankton removed from the water column.

Discussion

Using the modified bioenergetics model, I estimated that zebra mussel in the western basin of Lake Erie during 1990 removed 6.4 ± 2.4 Mt of phytoplankton. The implications for the western Lake Erie ecosystem may be addressed by comparing the amount of phytoplankton ingested by zebra mussel with the net primary production in the western basin. Apparently, the most recent available estimate of primary production for western Lake Erie was for 1970. Glooschenko et al. (1974) estimated primary production in western Lake Erie from late April through mid-December to be 1.016 Mt of fixed carbon, based on a surface area of 3276 km2 (Hartman 1973). Two of the five stations sampled were technically not in the western basin as defined by Hartman (1973). Including just the three "true" western basin stations, and production from late April to late October, yields an estimate of primary production equal to 1.143 Mt of carbon. Assuming a carbon to dry weight ratio for phytoplankton of 0.36 and a dry weight to wet weight ratio for phytoplankton of 0.25 (Bierman et al. 1980), the primary production estimate for 1970 would be 12.7 Mt of phytoplankton.

However, Verduin (1960) and Welch (1968) have concluded that primary production is underestimated by bottle incubations; Verduin (1960) showed that the estimate by the free-water method was 2.4 times greater than that by bottle incubations in Lake Erie. Thus, correcting for bottle

incubations results in a primary production estimate of 30.5 Mt of phytoplankton for 1970. Wallen and Botek (1984) sampled 18 different stations in western Lake Erie and showed a high degree of spatial heterogeneity in primary productivity. Perhaps the sampling of only three western basin stations in 1970 by Glooschenko et al. (1974) led to an underestimate of primary production. However, a strong spatial bias was not apparent because the mean productivity for the basin based on sampling 18 sites was approximately equal to mean productivity estimated by sampling just the three stations selected by Glooschenko et al. (1974).

Regulations by the U.S. Environmental Protection Agency resulted in a 67.5% decrease in western Lake Erie phosphorus loadings from 1970 to the late 1980s (Dolan 1993; D. Dolan, International Joint Commission, Windsor, Ont., personal communication). Most of the decrease took place during the 1970s whereas annual loadings have levelled off during the mid- and late 1980s. Vollenweider et al. (1974), using Laurentian Great Lakes data, presented an empirical relationship between primary production and phosphorus loading. According to their regression equation, the 67.5% decrease in phosphorus loading would result in an 18.5% decrease in primary production; therefore the estimate of primary production for western Lake Erie immediately prior to the zebra mussel invasion would be 24.8 Mt. In the absence of any contradictory information, I will assume that zebra mussels do not alter annual primary production, and therefore, I will use 24.8 Mt as the 1990 primary production estimate for western Lake Erie.

From an ecosystem perspective, 24.8 Mt of phytoplankton was available for consumption by higher trophic levels in western Lake Erie during 1990. According to the bioenergetics model application, zebra mussel removed 6.4 ± 2.4 Mt of phytoplankton from the water column between April and November 1990, and this amount is equivalent to 26 ± 10% of the primary production.

Hartman and Margraf (1992) applied a bioenergetics model to the walleye population in western Lake Erie to estimate consumption of prey fish. The annual average consumption of prey fish between the years 1986 and 1988 was 88 200 t. Assuming an average gross growth efficiency of 16.5% for prey fish consuming zooplankton (Mills and Forney 1981; Stewart and Binkowski 1986; Hewett and Johnson 1992; Rudstam et al. 1994), and assuming an average gross growth efficiency of 20% for zooplankton consuming phytoplankton (Paffenhöfer 1976; Urabe and Watanabe 1991), the phytoplankton biomass needed to support the walleye population in western Lake Erie would be 2.7 Mt. Therefore, the modeling results indicated that the zebra mussel population ingested more phytoplankton during 1990 than the phytoplankton biomass needed to support an "average" walleye population.

Because the filtering rate of the settled zebra mussel population was substantially higher than that for zooplankton or zebra mussel veligers, MacIsaac et al. (1992) concluded that zebra mussel played an important role in the phytoplankton standing stock decrease observed in the western basin of Lake Erie from 1988 through 1990. The results of this bioenergetics application support this conclusion. Considering that the population removed roughly one quarter of the primary production during 1990, the zebra mussel was one of the dominant herbivores in the western Lake Erie ecosystem during that time. The bioenergetics approach calculated the zebra mussel population impact based on measurements of their growth and their population characteristics. Extent of water column mixing need not be considered in the bioenergetics methodology, but this effect was a consideration for the filtering impact approach. On the other hand, the filtering impact approach was not dependent on a suite of metabolism parameters, unlike the bioenergetics approach. The conclusions from both approaches agreed that zebra mussel played an important role as a major consumer of phytoplankton in the western Lake Erie ecosystem.

Preliminary findings on zebra mussel respiration rate at higher temperatures were incorporated into the modified bioenergetics model developed in this study; thus, the model may have to undergo further refinement as more information becomes available.

According to the model application to western Lake Erie, the major mechanism whereby zebra mussel remove algae from the water column is by ingestion rather than by deposition in pseudofeces. Nevertheless, the proportion of pseudofecal material that is actually composed of phytoplankton has yet to be measured under field conditions. Such an investigation would be useful in validating the assumption that this proportion equals the proportion of phytoplankton biomass constituting the total suspended solids of the water column.

This study has exposed some of the weaknesses in our understanding of the western Lake Erie ecosystem. Uncertainty in the estimate of average zebra mussel density in the western basin of Lake Erie is one of the biggest sources of error in the estimation of the proportion of primary production removed from the water column by the zebra mussel population. However, the precision of the estimate of removed phytoplankton can be improved upon as more data become available. Observations should include length–frequency distributions at the various reef sites, as well as total zebra mussel densities. A new primary production survey for western Lake Erie would also be helpful in further resolving the extent of the zebra mussel impact. The results of such a survey could serve to verify the projected estimate of present-day primary production in the western basin. There is no reason to believe that the relationship between the free-water estimate of primary production and the bottled-^{14}C estimate has changed since the last time these estimates were compared, but an up-to-date comparison would also be useful.

Acknowledgments

J. Leach and S. Nepszy provided the zebra mussel length–frequency data and water temperature data. D. Garton shared his insights on the population biology of zebra mussels in western Lake Erie. D. Schneider developed the equation for pseudofeces production. This paper was greatly enhanced by conversations with D. Culver, R. Dermott, D. McNaught, P. Meier, S. Millard, T. Nalepa, S.J. Nichols, R. Pontius, D. Schneider, and W.G. Sprules. I thank P. Ferreri, D. Garton, M. Hansen, J. Leach, H. MacIsaac,

K. Muth, S. Nepszy, D. Schloesser, graduate students and faculty from the EDIT group at the Ohio State University Aquatic Ecology Laboratory, and two anonymous reviewers for reviewing the manuscript.

References

Bayne, B.L., Thompson, R.J., and Widdows, J. 1976. Physiology: I. *In* Marine mussels: their ecology and physiology. International Biological Programme 10. *Edited by* B.L. Bayne. Cambridge University Press, Cambridge, pp. 121–206.

Bierman, V.J. Jr., Dolan, D.M., Stoermer, E.F., Gannon, J.E., and Smith, V.E. 1980. The development and calibration of a spatially simplified multi-class phytoplankton model for Saginaw Bay, Lake Huron. Great Lakes Environmental Planning Study, Contribution 33, Great Lakes Basin Commission, Ann Arbor, Mich.

Dermott, R., Mitchell, J., Murray, I., and Fear, E. 1993. Biomass and production of zebra mussels (*Dreissena polymorpha*) in shallow waters of northeastern Lake Erie. *In* Zebra mussels: biology, impacts, and control. *Edited by* T.F. Nalepa and D. Schloesser. Lewis Publishers, Chelsea, Mich. pp. 399–413.

Dolan, D.M. 1993. Point source loadings of phosphorus to Lake Erie: 1986–1990. J. Great Lakes Res. **19**: 212–223.

Fisher, S.W., Gossiaux, D.C., Bruner, K.A., and Landrum, P.F. 1993. Investigations of the toxicokinetics of hydrophobic contaminants in the zebra mussel (*Dreissena polymorpha*). *In* Zebra mussels: biology, impacts, and control. *Edited by* T.F. Nalepa and D. Schloesser. Lewis Publishers, Chelsea, Mich. pp. 465–490.

Fraleigh, P.C., Klerks, P.L., Gubanich, G., Matisoff, G., and Stevenson, R.C. 1993. Abundance and settling of zebra mussel (*Dreissena polymorpha*) veligers in western and central Lake Erie. *In* Zebra mussels: biology, impacts, and control. *Edited by* T.F. Nalepa and D. Schloesser. Lewis Publishers, Chelsea, Mich. pp. 129–142.

Garton, D.W., and Haag, W.R. 1993. Seasonal reproductive cycles and settlement patterns of *Dreissena polymorpha* in western Lake Erie. *In* Zebra mussels: biology, impacts, and control. *Edited by* T.F. Nalepa and D. Schloesser. Lewis Publishers, Chelsea, Mich. pp. 111–128.

Glooschenko, W.A., Moore, J.E., Munawar, M., and Vollenweider, R.A. 1974. Primary production in lakes Ontario and Erie: a comparative study. J. Fish. Res. Board Can. **31**: 253–263.

Griffiths, R.W., Schloesser, D.W., Leach, J.H., and Kovalak, W.P. 1991. Distribution and dispersal of the zebra mussel (*Dreissena polymorpha*) in the Great Lakes region. Can. J. Fish. Aquat. Sci. **48**: 1381–1388.

Hartman, W. 1973. Effects of exploitation, environmental changes, and new species on the fish habitats and resources of Lake Erie. Great Lakes Fish. Comm. Tech. Rep. **22**.

Hartman, K.J., and Margraf, F.J. 1992. Effects of prey and predator abundances on prey consumption and growth of walleyes in western Lake Erie. Trans. Am. Fish. Soc. **121**: 245–260.

Hewett, S.W., and Johnson, B.L. 1992. Fish bioenergetics model 2. Univ. Wis. Sea Grant Inst. WIS-SG-92-250.

Hewett, S.W., and Stewart, D.J. 1989. Zooplanktivory by alewives in Lake Michigan: ontogenetic, seasonal, and historical patterns. Trans. Am. Fish. Soc. **118**: 581–596.

Leach, J.H. 1993. Impacts of the zebra mussel (*Dreissena polymorpha*) on water quality and fish spawning reefs in western Lake Erie. *In* Zebra mussels: biology, impacts, and control. *Edited by* T.F. Nalepa and D. Schloesser. Lewis Publishers, Chelsea, Mich. pp. 381–397.

MacIsaac, H.J., Sprules, W.G., Johannsson, O.E., and Leach, J.H. 1992. Filtering impacts of larval and sessile zebra mussels (*Dreissena polymorpha*) in western Lake Erie. Oecologia, **92**: 30–39.

Makarewicz, J.C. 1987. Phytoplankton and zooplankton composition, abundance and distribution: Lake Erie, Lake Huron and Lake Michigan: 1983. EPA-905/2-87-002. U.S.E.P.A. Great Lakes National Program Office, Chicago, Ill.

Makarewicz, J.C. 1988. Phytoplankton and zooplankton in Lake Erie, Lake Huron and Lake Michigan: 1984. EPA-905/3-88-001. U.S.E.P.A. Great Lakes National Program Office, Chicago, Ill.

Makarewicz, J.C. 1993. Phytoplankton biomass and species composition in Lake Erie, 1970 to 1987. J. Great Lakes Res. **19**: 258–274.

Makarewicz, J.C., Lewis, T., and Bertram, P. 1989. Phytoplankton and zooplankton composition, abundance and distribution and trophic interactions: offshore region of Lake Erie, Lake Huron and Lake Michigan, 1985. EPA-905/3-90-003. U.S.E.P.A. Great Lakes National Program Office, Chicago, Ill.

Martel, A. 1993. Dispersal and recruitment of zebra mussel (*Dreissena polymorpha*) in a nearshore area in west-central Lake Erie: the significance of postmetamorphic drifting. Can. J. Fish. Aquat. Sci. **50**: 3–12.

Mills, E.L., and Forney, J.L. 1981. Energetics, food consumption, and growth of young yellow perch in Oneida Lake, New York. Trans. Am. Fish. Soc. **110**: 479–488.

Morton, B. 1993. The anatomy of *Dreissena polymorpha* and the evolution and success of the heteromyarian form in the Dreissenoidea. *In* Zebra mussels: biology, impacts, and control. *Edited by* T.F. Nalepa and D. Schloesser. Lewis Publishers, Chelsea, Mich. pp. 185–215.

Munawar, M., and Burns, N.M. 1976. Relationships of phytoplankton biomass with soluble nutrients, primary production, and chlorophyll *a* in Lake Erie, 1970. J. Fish. Res. Board Can. **33**: 601–611.

Nalepa, T.F., Cavaletto, J.F., Ford, M., Gordon, W.M., and Wimmer, M. 1993. Seasonal and annual variation in weight and biochemical content of the zebra mussel, *Dreissena polymorpha*, in Lake St. Clair. J. Great Lakes Res. **19**: 541–552.

Paffenhöfer, G.-A. 1976. Feeding, growth, and food conversion of the marine planktonic copepod *Calanus helgolandicus*. Limnol. Oceanogr. **21**: 39–50.

Payne, B.S., and Aldridge, D. 1994. Acclimation response of zebra mussels to laboratory testing. U.S. Army Corps Eng. Tech. Note ZMR-1-13. U.S. Army Engineer Waterways Experiment Station, Vicksburg, Miss.

Quigley, M.A., Gardner, W.S., and Gordon, W.M. 1993. Metabolism of the zebra mussel (*Dreissena polymorpha*) in Lake St. Clair of the Great Lakes. *In* Zebra mussels: biology, impacts, and control. *Edited by* T.F. Nalepa and D. Schloesser. Lewis Publishers, Chelsea, Mich. pp. 295–306.

Reeders, H.H., and bij de Vaate, A. 1992. Bioprocessing of polluted suspended matter from the water column by the zebra mussel (*Dreissena polymorpha* Pallas). Hydrobiologia, **239**: 53–63.

Rudstam, L.G., Hansson, S., Johansson, S., Larsson, U. 1992. Dynamics of planktivory in a coastal area of the northern Baltic Sea. Mar. Ecol. Prog. Ser. **80**: 159–173.

Rudstam, L.G., Binkowski, F.P., and Miller, M.A. 1994. A bioenergetics model for analysis of food consumption patterns of bloater in Lake Michigan. Trans. Am. Fish. Soc. **123**: 344–357.

Schneider, D.W. 1992. A bioenergetics model of zebra mussel, *Dreissena polymorpha*, growth in the Great Lakes. Can. J. Fish. Aquat. Sci. **49**: 1406–1416.

Sprung, M., and Rose, U. 1988. Influence of food size and food quantity on the feeding of the mussel *Dreissena polymorpha*. Oecologia, **77**: 526–532.

Stańczykowska, A., Ławacz, W., Mattice, J., and Lewandowski, K. 1976. Bivalves as a factor effecting circulation of matter in Lake Mikolajskie (Poland). Limnologica, **10**: 347–352.

Stewart, D.J., and Binkowski, F.P. 1986. Dynamics of consumption and food conversion by Lake Michigan alewives: an energetics-modeling synthesis. Trans. Am. Fish. Soc. **115**: 643–661.

Stewart, D.J., Weininger, D., Rottiers, D.V., and Edsall, T.A. 1983. An energetics model for lake trout, *Salvelinus namaycush*: application to the Lake Michigan population. Can. J. Fish. Aquat. Sci. **40**: 681–698.

Ten Winkel, E.H., and Davids, C. 1982. Food selection by *Dreissena polymorpha* Pallas (Mollusca: Bivalvia). Freshwater Biol. **12**: 553–558.

Urabe, J., and Watanabe, Y. 1991. Effect of food concentration on the assimilation and production efficiencies of *Daphnia galeata* G.O. Sars (Crustacea: Cladocera). Funct. Ecol. **5**: 635–641.

Vahl, O. 1973. Pumping and oxygen consumption rates of *Mytilus edulis* L. of different sizes. Ophelia, **12**: 45–52.

Verduin, J. 1960. Phytoplankton communities of western Lake Erie and the CO_2 and O_2 changes associated with them. Limnol. Oceanogr. **7**: 372–380.

Vollenweider, R.A., Munawar, M., and Stadelmann, P. 1974. A comparative review of phytoplankton and primary production in the Laurentian Great Lakes. J. Fish. Res. Board Can. **31**: 739–762.

Wallen, D.G., and Botek, C. 1984. Heterogenous patterns of primary productivity in western Lake Erie. Verh. Int. Ver. Limnol. **22**: 495–503.

Walz, N. 1978*a*. The energy balance of the freshwater mussel *Dreissena polymorpha* Pallas in laboratory experiments and in Lake Constance. I. Pattern of activity, feeding and assimilation efficiency. Arch. Hydrobiol. Suppl. **55**(1): 83–105.

Walz, N. 1978*b*. The energy balance of the freshwater mussel *Dreissena polymorpha* Pallas in laboratory experiments and in Lake Constance. IV. Growth in Lake Constance. Arch. Hydrobiol. Suppl. **55**(2): 142–156.

Welch, H.E. 1968. Use of modified diurnal curves for the measurement of metabolism in standing water. Limnol. Oceanogr. **13**: 679–687.

Winter, J.E. 1969. Über den Einfluß der Nahrungskonzentration und anderer Faktoren auf Filtrierleistung und Nahrungsausnutzung der Muscheln *Arctica islandica* und *Modiolus modiolus*. Mar. Biol. **4**: 87–135.

Appendix

Bioenergetics model for growth of a zebra mussel. This model represents a modification of the original model developed by Schneider (1992).

Symbol	Parameter description	Parameter value
	Consumption	
a_c	Intercept for maximum consumption ($g \cdot g^{-1} \cdot day^{-1}$)	0.027
b_c	Exponent for maximum consumption	−0.39
Q	Lower temperature at which consumption is k_1·maximum	2°C
T_0	Lower temperature at which consumption is 0.98·maximum	12°C
T_m	Higher temperature at which consumption is 0.98·maximum	21°C
T_1	Higher temperature at which consumption is k_4·maximum	32°C
k_1	Empirical coefficient for Q	0.1
k_4	Empirical coefficient for T_1	0.02

$C = a_c W^{b_c} \cdot f(t) \cdot P$-value

Appendix (*concluded*).

Symbol	Parameter description	Parameter value
	where C is the daily specific consumption by the zebra mussel ($g \cdot g^{-1} \cdot day^{-1}$), W is the wet weight (g) of the soft body of the mussel, and $f(t)$ and P-value are multipliers ranging from 0 to 1 for the temperature dependence of consumption and the proportion of maximum consumption realized, respectively (see Hewett and Johnson (1992) and Schneider (1992) for more details on $f(t)$). For Great Lakes applications, P-value was calculated by dividing the observed algal biomass (mg/L) in the lake by 1.25 mg/L (see Schneider (1992) for more details). Caloric content of the zebra mussel was set equal to 580 cal/g wet weight, and the caloric content of algae was set equal to 1000 cal/g wet weight (Schneider 1992) (1 cal = 4.1855 J)	
	Respiration	
a_r	Intercept for maximum standard respiration (g O_2/day)	0.00118
b_r	Exponent for maximum standard respiration	−0.605
	$R = a_r W^{b_r} \cdot f(t)$	
	where R is the daily specific respiration rate ($g\ O_2 \cdot g^{-1} \cdot day^{-1}$) and $f(t)$ is the multiplier ranging from 0 to 1 for the temperature dependence of respiration. $f(t)$ is calculated from the relationship presented in Fig. 1 (see the bioenergetics model section for more details). Specific respiration rate was converted to a caloric rate using the oxycalorific coefficient of 3240 cal/g O_2 (Stewart et al. 1983) and to a rate in terms of body weight by using a zebra mussel caloric density of 580 cal/g	
	Egestion, excretion, and SDA	
α_f	Proportion of consumed food egested	0.18
α_u	Proportion of assimilated food excreted	0.064
SDA	Proportion of assimilated food used in specific dynamic action	0.172
	$F = \alpha_f \cdot C$	
	$U = \alpha_u \cdot (C - F)$	
	$S = \text{SDA} \cdot (C - F)$	
	where F, U, and S are the egestion, excretion, and specific dynamic action costs ($g \cdot g^{-1} \cdot day^{-1}$), respectively, realized by the zebra mussel	
	Growth	
	Daily specific growth, dW/dt ($g \cdot g^{-1} \cdot day^{-1}$), is given by the following equation:	
	$dW/dt = C - (R + F + U + G + S)$	
	where G is the energetic cost of reproduction (see the bioenergetics model section for more details on G)	
	Pseudofeces production	
α	Pseudofeces coefficient	1.79
a_k	Intercept for weight dependence of pseudofeces production	1.346
b_k	Exponent for weight dependence of pseudofeces production	−0.4
a_i	Intercept for weight dependence in P-value component of pseudofeces production	0.247
b_i	Exponent for weight dependence in P-value component of pseudofeces production	0.4
	$\text{Pfeces} = \alpha(1 - e^{a_k W^{b_k}(a_i W^{b_i} - P\text{-value})})$	
	where Pfeces is pseudofeces production expressed as a proportion of consumption by the zebra mussel. The pseudofeces production equation was furnished by D. Schneider (personal communication). In western Lake Erie during 1990, it was assumed that phytoplankton comprised 20%, by weight, of the pseudofeces (see pseudofeces production section for more details)	

Age determination and growth of orange roughy (*Hoplostethus atlanticus*): a comparison of annulus counts with radiometric ageing

David C. Smith, Gwen E. Fenton, Simon G. Robertson, and Stephen A. Short

Abstract: Ages of orange roughy (*Hoplostethus atlanticus*) determined by two methods (counting annuli on the surface of whole and in longitudinally sectioned otoliths) were similar up to maturity. Beyond maturity, age estimates from sectioned otoliths exceeded those from whole otoliths. Maximum recorded age was 125 years for an individual 41 cm standard length (SL), and age at maturity was estimated to be 25 years (30–32 cm SL). These are consistent with ages estimated previously by radiometric methods. Results demonstrated a two-stage linear relationship between otolith weight and age that confirmed the two-stage otolith mass growth model previously used in radiometric ageing. However, in the radiometric analyses the reduction in otolith growth was arbitrarily estimated at 45% of the immature rate whereas annuli data demonstrated a reduction after maturity to 62% of the immature rate. The new estimates of otolith mass growth rate were incorporated into the radiometric data and ages recalculated, which reduced age estimates for 38–40 cm SL fish from 77–149 to 59–101 years. The radiometric data were also recalculated using only the percentage reduction in otolith growth after maturity, giving the radiometric age of 125 ± 9 years for the oldest fish.

Résumé : Nous avons déterminé l'âge de spécimens d'hoplostète orange (*Hoplostethus atlanticus*) par deux méthodes (comptage des anneaux à la surface des otolithes entiers et sur des coupes longitudinales), et les résultats étaient les mêmes jusqu'à la maturité. Au-delà de la maturité, les estimations effectuées à partir des sections d'otolithes dépassaient celles obtenues sur les otolithes entiers. L'âge maximum enregistré était de 125 ans pour un individu mesurant 41 cm de longueur standard (LS), et l'âge à la maturité a été estimé à 25 ans (30–32 cm LS). Ces résultats concordent avec des estimations réalisées antérieurement par radiométrie. Les résultats montrent une relation linéaire en deux phases entre le poids de l'otolithe et l'âge, ce qui a confirmé le modèle de croissance de la masse de l'otolithe en deux stades utilisé auparavant dans la datation radiométrique. Toutefois, dans les analyses radiométriques, on a estimé arbitrairement que la réduction de la croissance des otolithes correspondait à 45% du taux de croissance chez les immatures, tandis que les données fournies par les anneaux de croissance ont montré que cette réduction après la maturité serait de 62% du taux de croissance chez les immatures. On a intégré les nouvelles estimations du taux de croissance de la masse des otolithes aux données radiométriques et l'on a recalculé les âges, ce qui a permis de réduire les estimations de l'âge des poissons de 38–40 cm LS de 77–149 ans à 59–101 ans. On a aussi recalculé les données radiométriques en se servant seulement du pourcentage de réduction de la croissance des otolithes après la maturité, ce qui a donné pour le poisson le plus âgé l'âge radiométrique de 125 ± 9 ans.

[Traduit par la Rédaction]

Received October 28, 1993. Accepted July 14, 1994.
J12137

D.C. Smith and S.G. Robertson. Victorian Fisheries Research Institute, Department of Conservation and Natural Resources, P.O. Box 114, Queenscliff, Victoria 3225, Australia.
G.E. Fenton. Department of Zoology, University of Tasmania, G.P.O. Box 252C, Hobart, Tasmania 7001, Australia.
S.A. Short. Environmental Radiochemistry Laboratory, Australian Nuclear Science and Technology Organisation, Private Mail Bag 1, Menai, N.S.W. 2234, Australia.

Introduction

Orange roughy (*Hoplostethus atlanticus*) are widely distributed on the midslope region of temperate waters. They occur off southern Australia, New Zealand, and southern Africa and are widespread in the Mediterranean Sea and Atlantic Ocean (Last et al. 1983). Orange roughy is the major species in the Australian South East Fishery (SEF), and the 1989–1990 catch of 40 000 t was the largest finfish catch in Australia. The species is also an important constituent of the New Zealand deepwater trawl fishery with catches of about 50 000 t recorded during the mid-1980s (Annala 1993). Catches have fallen in both countries following the introduction of management measures designed to stabilise catches at sustainable yields. Commercial catches of orange roughy are taken, by demersal trawling, in depths from 800 to 1200 m.

Accurate age estimates are fundamental to the management of the orange roughy fishery. There have been several attempts to age orange roughy using otoliths but these produced a range of ages that led to considerably different estimates of growth rate and longevity (Kotylar 1980; van den Broek 1983; Gauldie et al. 1989). Gauldie (1987, 1988, 1990), from an examination of otolith microstructure and surface morphology, questioned the interpretation of annuli being formed annually. However, Mace et al. (1990) provided the first validated ages for orange roughy. They showed that the first three translucent zones on the otoliths from very small (<10 cm standard length (SL)) orange roughy are formed annually by relating them to the progression of length–frequency modes in a population of juveniles in New Zealand waters. Examining the surface of whole otoliths, they estimated a maximum age of 42 years and an age at maturity of about 20 years. However, beyond the first 3 years the ages were not validated. Smith and Robertson (1992) argued that surface ageing of whole otoliths appeared to be unreliable because it was difficult to identify annuli in the relatively thicker otoliths of larger fish. They suggested that examination of sectioned otoliths may be the most useful method.

Fenton et al. (1991) demonstrated by radiometric analysis (^{210}Pb:^{226}Ra disequilibria) of whole otoliths that orange roughy were long-lived. They estimated radiometric ages of 77–149 years for 38–40 cm SL fish, which is close to the maximum length (45 cm SL) of orange roughy from the major fishery in Australia (Lyle 1994). In deriving their age estimates from the ^{210}Pb:^{226}Ra activity ratios, it was necessary for them to model the mass growth of the otoliths. Ages estimated using a linear model of mass growth indicated that there was a difference in otolith growth before and after maturity. It was evident from the radiometric data that there was a reduction in otolith growth after maturity, but the actual amount of this reduction could only be approximated. Therefore, the ages were then calculated using a two-stage linear growth model in which they assumed that the otolith mass growth rate after maturity reduced to 45% of the prematurity rate. An independent source of otolith mass growth rate was needed to provide more accurate ages.

In this paper, a method to reliably age orange roughy, using sectioned otoliths, is described and results compared with the radiometric ages of Fenton et al. (1991). Otolith mass growth rates for immature and mature fish are estimated from the relationship of otolith weight and annulus count and fish age recalculated from the ^{210}Pb:^{226}Ra activity ratios previously reported by Fenton et al. (1991). A further check on radiometric ageing is made by assessing the stable lead concentrations in juvenile and adult otoliths.

Methods

Collection of otoliths

Sagittal otoliths were removed from orange roughy caught during trawl surveys off southern Australia between January 1987 and June 1989 and from commercial landings (Smith et al. 1988). In addition, samples of small fish were provided by other Australian research institutions (CSIRO Division of Fisheries, Department of Sea Fisheries Tasmania, details are given in Smith and Robertson 1992, table 1). Otoliths were stored dry in envelopes on which the locality, standard length (millimetres), weight (grams), and sex were recorded. In all cases, the SL of orange roughy was measured to the nearest millimetre and weight was measured to the nearest gram.

Description and preparation of otoliths

Whole otoliths

Orange roughy otoliths have an unusual shape which increases in complexity in older fish (Fig. 1). Alternating translucent and opaque zones are evident on the distal surface.

Prior to examination, each pair of otoliths was coded to enable annuli to be determined without reference to fish size. Otoliths were immersed in water and viewed, using a dissecting microscope (low power ×6 to ×10), against a black background with reflected light. Under these conditions, translucent zones appear dark and opaque zones appear white (Fig. 1). Some otoliths from larger fish required brief soaking in water to clarify the inner zones, but prolonged soaking reduced clarity at the edge. Annuli were counted along the anterior–posterior axis in the posterior portion of the otolith.

Annuli were determined with the aid of a semiautomatic measuring system. Initially, each otolith was measured using a 22 × 28 cm digitising pad and a LED cursor linked to a microcomputer using customised software. A camera-lucida was used to superimpose the LED image on the microscope field of view. Later, an image analysis system was used to give an on-screen digitising capability. Data were written automatically to files for later analysis.

Otolith weight was measured to the nearest milligram. A comparison of the weight of left and right otoliths using a paired *t*-test showed no significant difference at the 0.05 level.

Sectioned otoliths

Commonly, otoliths are sectioned transversely (e.g., Jearld 1983; Pentilla and Dery 1988). However, preliminary results indicated that sections of orange roughy otoliths along the anterior–posterior axis were the clearest and most useful.

Fig. 1. Distal face of whole orange roughy otoliths viewed with reflected light. (A) 13.4 cm, 8 years; (B) 18.8 cm, 11 years; (C) schematic representation of otolith from 27.0 cm fish, aged at 16 years. v, ventral; d, dorsal; a, anterior; p, posterior; arrows mark the line of section.

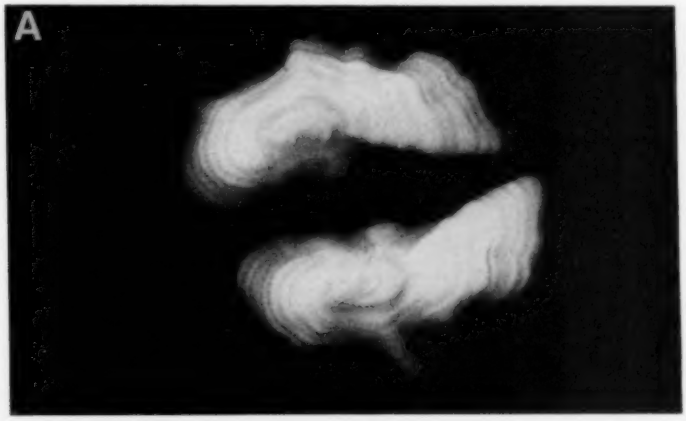

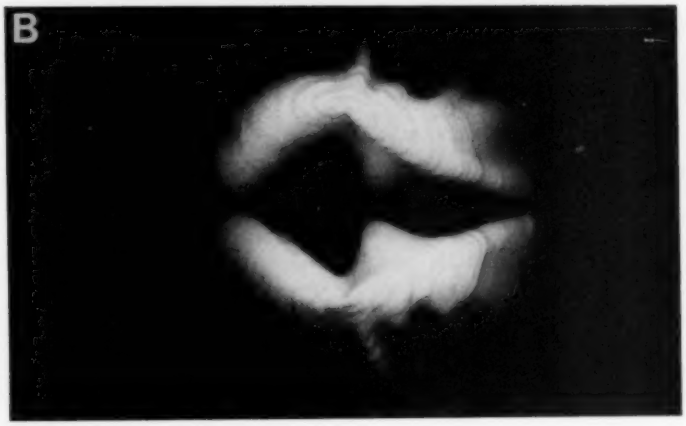

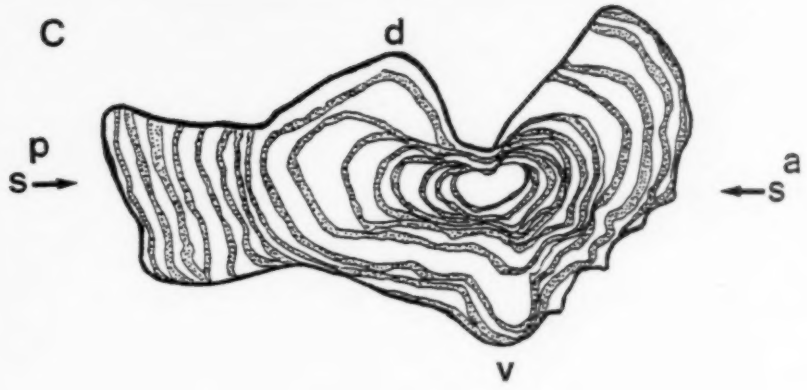

Table 1. Radiometric age determination of orange roughy otoliths (calculations from Fenton et al., 1991). Errors expressed are ±1 SD.

Sample No.	Mean fish SL (cm)	No. of otoliths	Mean otolith mass (mg)	^{210}Pb:^{226}Ra activity	Linear otolith age (years)	Two-stage growth otolith age (years)
LH752	10.87	135	7.6	0.063±0.061	0.9+4.4, −0.9	—
LH753	14.20	102	13.9	0.134±0.045	6.1+3.6, −3.3	—
LH569	16.51	54	21.0	0.193±0.097	10.7+8.9, −7.6	—
LH751	25.40	16	66.1	0.333±0.067	23.4+8.9, −6.9	—
LH664	33.90	8	137.9	0.427±0.093	36+14, −11	—
LH1240	37.30	6	175.1	0.499±0.065	47+12, −9	47.5±5
LH570	38.90	4	241.2	0.755±0.202	122+inf, −65	92±24
LH666	39.05	4	185.3	0.814±0.132	163+inf, −73	77±12
LH748	39.20	4	270.6	0.867±0.085	230+inf, −91	118±11
LH750	39.30	4	338.8	0.746±0.068	117+46, −28	127±11
LH668	40.30	2	224.0	0.830±0.163	179+inf, −94	94±18
LH749	40.40	4	367.5	0.806±0.069	156+inf, −44	149±12

Annuli were revealed by tranverse section but it was not possible to relate them to those seen on whole otoliths. We regarded this as important because it is only the first three annuli seen on whole otoliths that have been validated.

From a random subsample of paired otoliths, one was read whole and the other sectioned. For sectioning, otoliths were embedded, initially in three rows, in a block of clear polyester resin and cut, longitudinally, along the anterior–posterior axis, using a Gemmasta circular saw with a diamond blade of 0.15 mm thickness. Subsequently, otoliths were sectioned individually. Although more time consuming, it ensured that the number of poor preparations was reduced. Sections were approximately 0.3 mm thick. No further preparation was required other than to mount them on slides with a clear mountant and coverslip. In most cases, three sections were taken through each otolith to ensure that sections were through the primordium. Annuli were counted using a compound microscope at magnifications of ×40 – ×100 t. A sample was read twice by the primary reader and also by a secondary reader to enable estimates of precision; intra- and intervariability in estimated age.

Radiometric determination of fish age

Radiometric analysis

^{210}Pb:^{226}Ra activity ratios were analysed by Fenton et al. (1991) in samples of female orange roughy otoliths from the west coast of Tasmania. The samples of juveniles (LH752 and LH753) also included some Kangaroo Island and Tasmanian east coast fish. Further details of the samples and analysis are given in Fenton et al. (1991). For convenience to the reader, the activity ratios and ages estimated using the linear and two-stage otolith mass growth models reported in Fenton et al. (1991) are given here in Table 1.

Calculation of fish age

Orange roughy ages have been calculated from the activity ratios given by Fenton et al. (1991), using the two-stage growth model essentially as derived by Bennett et al. (1982):

$$A\,e^{-\lambda_R t} = \frac{t_1 G_1}{M_t}\left[1-(1-R)\left(\frac{1-e^{-\lambda_P t_1}}{\lambda_P t_1}\right)e^{-\lambda_P (t-t_1)}\right] + \frac{(t-t_1)G_2}{M_t}\left\{1-(1-R)\left[\frac{1-e^{-\lambda_P (t-t_1)}}{\lambda_P (t-t_1)}\right]\right\}$$

where $A = (^{210}\text{Pb}:^{226}\text{Ra})_t$ = activity ratio at time t, $R = (^{210}\text{Pb}:^{226}\text{Ra})_0$ = initial activity ratio at time of deposition, λ_P = decay constant for ^{210}Pb (0.03114·year^{-1}), λ_R = decay constant for ^{226}Ra (0.00043·year^{-1}), G_1 = otolith mass-growth rate until maturity (milligrams per year), G_2 = otolith mass-growth rate after maturity (milligrams per year), t_1 = age at maturity (years), and M_t = otolith mass at age t. The extra term $e^{-\lambda_R t}$ accounts for the minor decay of ^{226}Ra from the specific activity laid by the aragonite at time of deposition.

To improve the estimation of orange roughy age the variables R, G_1, G_2, and t_1 are reexamined.

Estimation of R

An assumption of radiometric analysis is that the ratio of uptake of ^{210}Pb relative to ^{226}Ra remains constant throughout life (i.e., the R value) and that increasing levels of ^{210}Pb are due to the decay of ^{226}Ra in the otolith. Fenton and Short (1992) pointed out that by examining the lead content of juvenile and adult otoliths, it should be possible to detect any change in the uptake rate of allogenic ^{210}Pb (nonradiogenic ^{210}Pb) from the environment. To test this, inductively coupled plasma mass spectrometry (ICPMS) determinations of stable lead concentration in carefully decontaminated orange roughy otoliths, from juvenile fish from the same region, were made.

Estimation of G_1 and G_2

The earlier estimate of G_1 derived by regressing the linear radiometric age estimate from Fenton et al. (1991) against otolith mass is 3.94 mg·year^{-1}. New values of G_1 and G_2 were estimated by regressing otolith mass against fish age determined from otolith sections.

Fig. 2. Longitudinal sections of orange roughy otoliths viewed with transmitted light. (A) 36.8 cm, 70 years; (B) tip of Fig. 2A at higher magnification; annuli designated by closed circles; (C) 41.0 cm, 125 years; (D) tip of Fig. 2C at higher magnification.

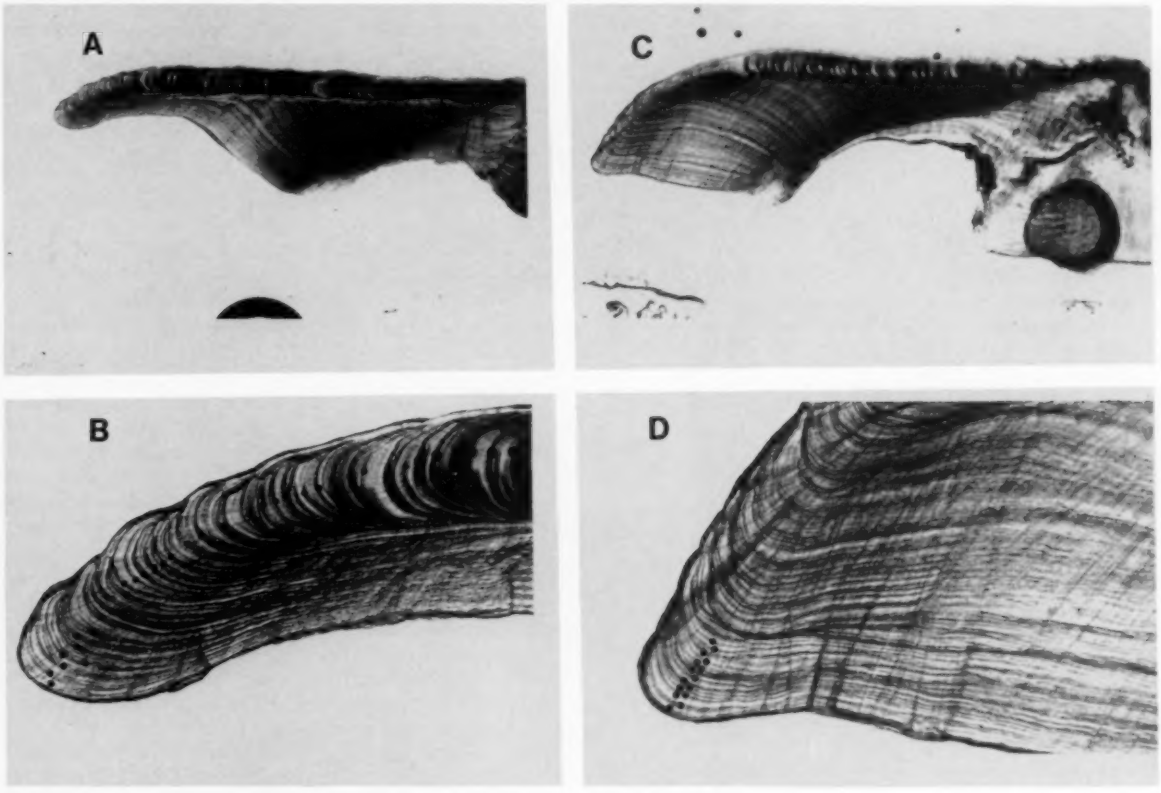

Table 2. Number of otoliths examined (*N*) per 5 cm (SL) length class and number and percentage for which estimates could not confidently be obtained (unread and %, respectively).

	Length class (cm)						
	<20	21–25	26–30	31–35	36–40	>40	Total
Whole otoliths							
N	96	88	168	110	189	21	672
Unread	0	2	12	12	12	3	41
%	0	2.3	7.1	10.9	6.3	14.3	6.1
Sectioned otoliths							
N	13	35	123	68	135	12	386
Unread	0	4	16	10	30	4	64
%	0	11.4	13.0	14.7	22.2	33.3	16.6

Estimation of maturity

An age of maturity (of 50% of the population) was estimated from the radiometric analysis in Fenton et al. (1991) at 32 years. A new estimate of age at maturity was determined from the relationship of fish length and age determined from otolith sections.

Three different combinations of value of G_1, G_2, and maturity have been used in the calculation of age for comparative purposes: (*i*) Age calculated using new estimates of G_1, G_2, and maturity derived from the present study of otolith sections. (*ii*) Age calculated using G_1 estimated from the linear radiometric age model, i.e., 3.94 mg·year^{-1}.

Fig. 3. Relationship of sectioned otolith and whole otolith annulus counts for (A) all sizes and (B) orange roughy less than 30 cm (SL).

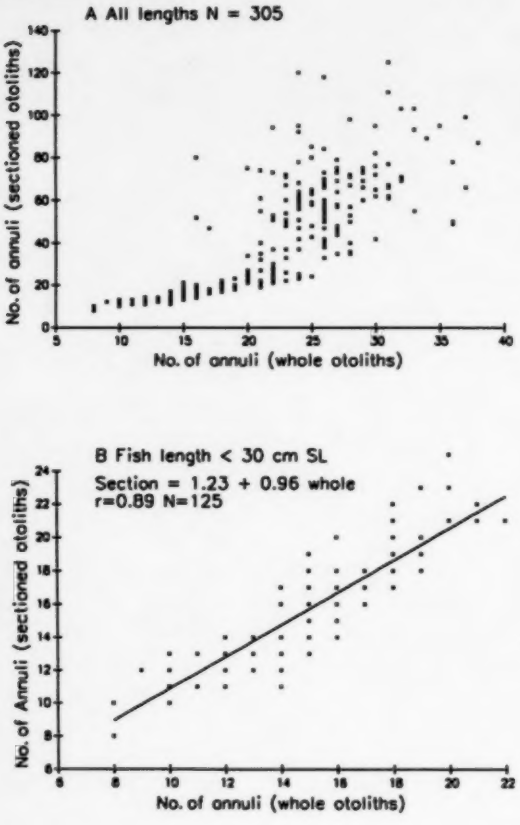
A All lengths N = 305
No. of annuli (sectioned otoliths)
No. of annuli (whole otoliths)
B Fish length < 30 cm SL
Section = 1.23 + 0.96 whole
r=0.89 N=125
No. of Annuli (sectioned otoliths)
No. of annuli (whole otoliths)

The estimate of G_2 used was the percentage reduction in otolith mass-growth rate after maturity, determined here in the present study of otolith annuli. The age at 50% maturity was determined from the linear radiometric age model in Fenton et al. (1991) as 32 years. (*iii*) Age calculated using the G_1 and G_2 values used in (*ii*), but using maturity estimated from the present study of otolith annuli.

Results and discussion

Comparison of age estimates from whole and sectioned otoliths

Whole otoliths from 672 orange roughy ranging in size from 7 to 43 cm SL were examined. Age estimates could not be confidently obtained from 41 (6.1%). Otoliths from smaller fish were easier to interpret than those from larger fish (Table 2). Annuli counts ranged from 2 (for a 7.2 cm SL fish) to 38 (for a 39.1 cm SL fish).

In sectioned otoliths, annuli seen on the surface of whole otoliths are evident along the posterior axis. Towards the tip of the otolith, however, these annuli become less distinct. Sections of otoliths from older fish revealed numerous fine annuli at the tip which are not visible on the surface of whole otoliths (Fig. 2). These annuli were assumed to be formed annually.

Otoliths from 386 fish ranging in size from 18 to 42 cm SL were sectioned. Of these, 64 (16.6%) were unreadable. As in whole otoliths, sectioned otoliths from younger fish were easier to interpret. The number of unreadable sectioned otoliths, however, increased as a function of fish size (Table 2). This was in part due to difficulty in interpretation, but also reflected an increasing problem with preparation caused by the complex shape of otoliths from large fish.

There is a rapid divergence in annuli counts between sectioned and whole otoliths after about 20 annuli (Fig. 3A). For fish less than 30 cm SL, however, ages estimated by either method were equivalent ($t = 0.778$, df = 123, $0.50 > p > 0.20$) (Fig. 3B). The ages estimated from sectioned otoliths ranged from 8 (for a 20.4 cm SL fish) to 125 years (for a 41.3 cm SL fish).

The maximum ages determined from sectioned otoliths are consistent with those of Fenton et al. (1991). This, together with the validation of the first three zones on whole otoliths (Mace et al. 1990), supports the interpretation that annuli seen in sectioned otoliths are formed annually.

Smith and Robertson (1992) showed a linear relationship between otolith length and fish length, but otolith weight increased rapidly in larger fish due to thickening of otoliths. This increase in otolith weight has been shown for other species (Williams and Bedford 1974; Beamish 1979, Boehlert 1985; Anderson et al. 1992). It is due to the continued deposition on the internal (proximal) face of the otolith even though the growth in length of the otolith (and fish) has slowed or stopped. It is particularly evident in long-lived, slow-growing species (Nedreaas 1990). For orange roughy, we used the distal face for age determination, but it was the thickening of the tip that provided the additional information.

We have shown that surface counts on whole otoliths are inadequate for ageing mature orange roughy. This may, in part, explain the inconsistencies in the ages estimated by earlier workers. It is also possible that the early interpretations reflected preconceptions about fish growth that, for example, fish species mature at much younger ages than determined in the present study.

Notwithstanding these considerations, there is no doubt that orange roughy are difficult to age using otoliths. However, our interpretation is repeatable. For the primary reader, 76% of repeated annuli counts from sectioned otoliths were within ±5 counts and 94% ± 10 counts. The Beamish and Fournier (1981) index of average precision was 3.7%. Between-reader variability was slightly higher with 60 and 90% of the second reader's annuli counts within ±5 and ±10, respectively. The index of average precision was 4.4%. These precision estimates compare favourably with the literature, but because orange roughy are so long-lived, Beamish and Fournier's index gives precision estimates that are, perhaps, better than expected.

Relationship between otolith weight and age

The otolith mass growth rate (milligrams per year) was computed by regressing otolith weight against age. This was done separately for immature and mature fish based on both

Fig. 4. Otolith weight versus age for immature and mature orange roughy. Maturity is based on (A) length and (B) age.

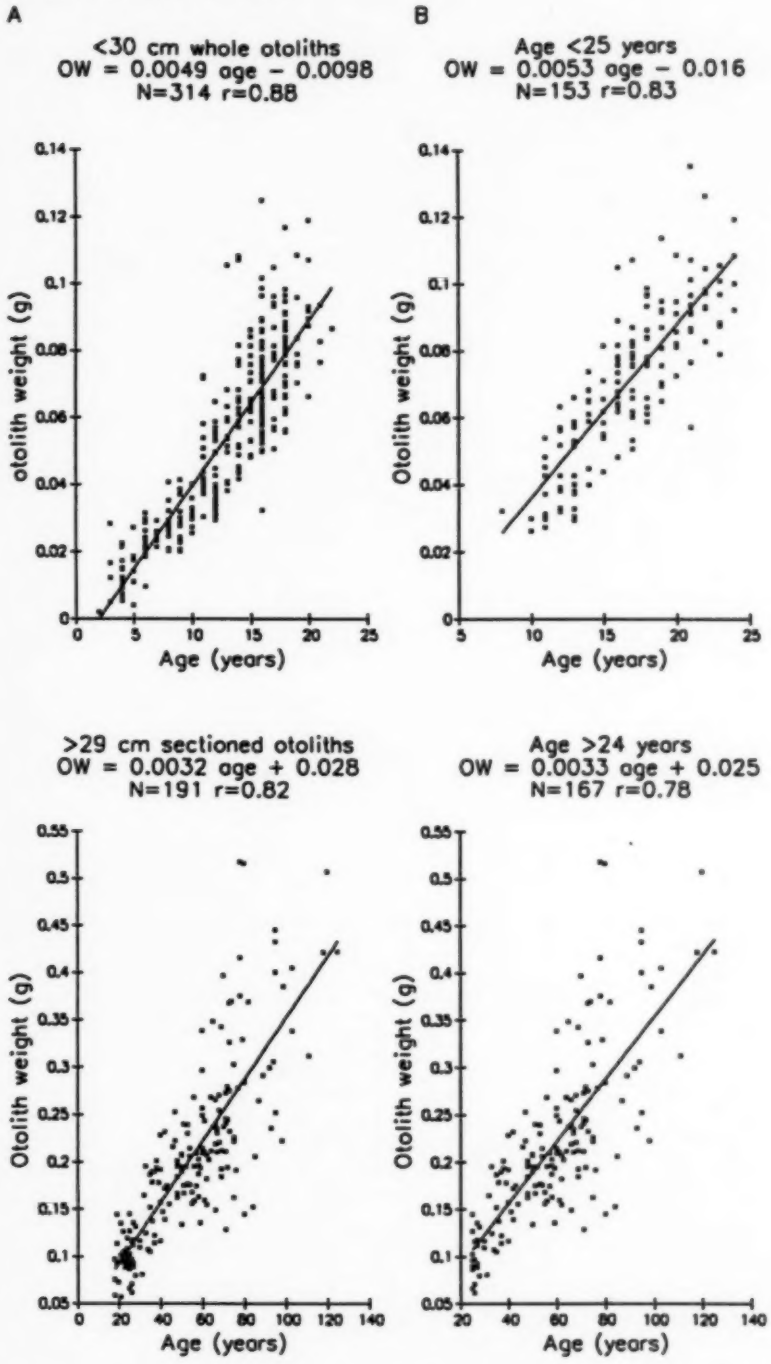

their length and their estimated age to determine the validity of the Fenton et al. (1991) two-stage linear growth model.

The size at which 50% of orange roughy are mature is 30–32 cm (Bell et al. 1992), which, from our results, is equivalent to an age of about 25 years (e.g., see Fig. 6). For maturity based on fish length (set at 30 cm), ages used

Table 3. Remodelling of radiometric ages for mature orange roughy. Errors expressed are ±1 SD.

Sample No.	Mean fish SL (cm)	No. of otoliths	Mean otolith mass	^{210}Pb:^{226}Ra activity ratio	Otolith age (years) Annuli (*i*)	Otolith age (radiodata) Maturity 32 years (*ii*)	Otolith age (radiodata) Maturity 25 years (*iii*)
LH664	33.90	8	137.9±28.2	0.427±0.093	29±4	35±5	36±5
LH1240	37.30	6	175.1±4.1	0.499±0.065	39±4	46±4	48±15
LH570	38.90	4	241.2±64.0	0.755±0.202	68±15	82±19	86±19
LH666	39.05	4	185.3±3.8	0.814±0.132	59±8	70±9	74±10
LH748	39.20	4	270.6±15.2	0.867±0.085	83±7	102±9	106±9
LH750	39.30	4	338.8±17.3	0.746±0.068	89±7	109±9	112±9
LH668	40.30	2	224.0±19.7	0.830±0.163	69±11	84±14	87±14
LH749	40.40	4	367.5±16.5	0.806±0.069	101±7	125±9	129±9

for immature fish were estimated from whole otoliths and ages used for mature fish were estimated from sectioned otoliths. For maturity estimated from fish age, ages were derived from sectioned otoliths. In both cases the relationships were linear although there was considerable variability (Fig. 4).

The otolith mass growth rate, equivalent to the slope of the regression, of mature fish was significantly lower than that for immature fish: 64 and 62% of immature fish based on size (df = 1,487, $F = 17.56$, $p = 0.0001$) or age (df = 1,315, $F = 4.22$, $p = 0.0408$) at maturity, respectively. These results provide independent support for the two-stage model used by Fenton et al. (1991).

Linear relationships between otolith weight and age have been shown before (e.g., Fletcher 1991; Anderson et al. 1992). The need for a reliable and quick predictor of age for fish populations has resulted in many attempts at scaling, i.e., relating the size of structures to age. Brander (1974) suggested that otolith weight may be directly related to age. Two recent experimental studies designed to examine the effects of somatic growth on otolith size in guppies (*Poecilia reticulata*) and striped bass (*Morone saxatilis*), respectively, both indicated the value of otolith weight as a predictor of age (Reznick et al. 1989; Secor and Dean 1989). Recently, Fletcher (1991) showed that it was possible to age pilchards (*Sardinops neopilchardus*) directly from otolith weight alone. These studies, however, are based on young or short-lived species. For orange roughy the variability of the otolith weight – age relationship precludes its use as a basis for predicting age directly. Francis and Smith (1995) have also shown that, for orange roughy, although mean otolith weight is a useful index of biomass depletion, it is no more sensitive than fish length.

Remodelling of radiometric data

Uptake of allogenic Pb

The assumption that the ratio of uptake of ^{210}Pb relative to ^{226}Ra remains constant throughout life (i.e., the R value) and that specific activities of ^{210}Pb are due to decay of ^{226}Ra in the otoliths was tested by measuring concentrations of stable lead in a large sample of juvenile otoliths. The mean lead concentration of otoliths from juvenile orange roughy was 0.13 ± 0.19 $\mu g \cdot g^{-1}$ (N = 24 otoliths). Edmonds et al. (1991) reported that the lead concentration in otoliths of mature orange roughy from the same geographic regions ranged from 0.00 to 2.40 $\mu g \cdot g^{-1}$ with a mean value of 0.50 ± 0.45 $\mu g \cdot g^{-1}$ (N = 51 otoliths). The ratio of lead concentration in adults (using the mean value determined by Edmonds et al. (1991)) compared with juveniles is 3.8 ± 6.6. This indicates that there may be some increase in lead uptake rate over the lifetime of orange roughy. However, there is a large variation in the lead content of both juvenile and adult otoliths leading to poor precision in the estimate of any increase. The concept of normalising the R value to stable lead discussed in Fenton and Short (1992) shows promise but requires further investigation.

As a test of the effect that an increase in R would have on the age estimates, we recalculated the ages of the mature orange roughy samples. In the calculations, we chose a value of $R = 0.5$ for fish beyond maturity. Thus, above an otolith mass of 125 mg (i.e., approximate mass where 50% are mature) the value of R increased 10-fold (i.e., the maximum increase indicated from the ICPMS data 3.8 + 6.6) from the juvenile rate of $R = 0.05$. This only reduced the ages of the mature fish by 10–20 years. However, given the large error associated with the estimated increase in R, it is difficult to assess whether there really is a significant increase in uptake of lead as the orange roughy grow older. Therefore, an increased R value for postmaturity fish was not included in the new age calculations (Table 3).

Otolith mass growth G_1 and G_2

The prematurity otolith mass growth rate (G_1) determined from the sectioned otoliths was 5.3 $mg \cdot year^{-1}$ and the postmaturity (G_2) was 3.3 $mg \cdot year^{-1}$; therefore, G_2 = 62% of G_1. The original estimate of G_1 in Fenton et al. (1991) derived by regressing age calculated with a linear mass growth model against otolith mass was similar but slightly lower, i.e., $G_1 = 3.94$. Fenton et al. (1991) correctly identified a reduction in the mass growth of the otolith beyond maturity, but the extent of the reduction was arbitrarily estimated to be 45% of G_1.

Age of maturity M_t

The age at which 50% of the population is mature corresponding to length 30–32 cm SL in the present study of sectioned otoliths was 25 years compared with an age of

Fig. 5. Otolith mass growth rate models. Model (*i*) (solid line), 5.3/3.3 mg·year^{-1} (25 years); model (*ii*) (dotted line), 3.94/2.47 mg·year^{-1} (32 years); model (*iii*) (dashed line), 3.94/2.47 mg·year^{-1} (25 years); Fenton et al. (1991) model (dash-dotted line), 3.94/1.77 mg·year^{-1} (32 years).

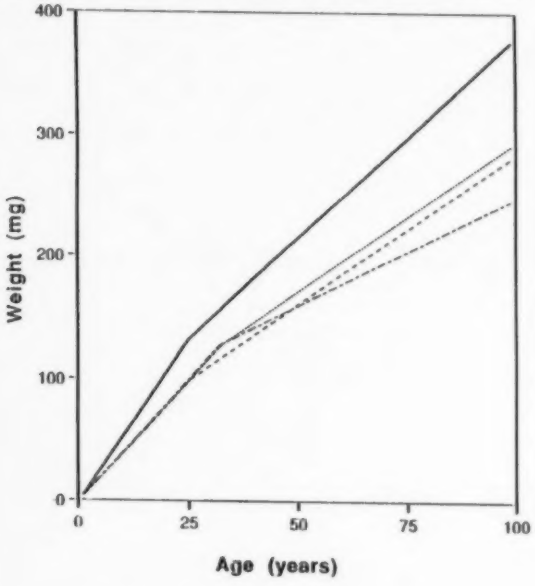

32 years estimated in the radiometric study of Fenton et al. (1991).

Calculation of age

Ages estimated using three combinations of G_1, G_2, and M_t in the two-stage growth model are presented in Table 3. The otolith mass-growth models are shown in Fig. 5. For the oldest fish which was originally estimated to be 149 ± 12 in Fenton et al. (1991) the effect of each calculation in turn changes the ages to (*i*) 101 ± 7 (G_1 = 5.3 mg·year^{-1}; G_2 = 3.3 mg·year^{-1}; M_t = 25 years), (*ii*) 125 ± 9 (G_1* = 3.94 mg·year^{-1}; G_2 = 62% of G_1; M_t = 32 years), and (*iii*) 129 ± 9 (G_1* = 3.94 mg·year^{-1}; G_2 = 62% of G_1; M_t = 25 years). Estimates from Fenton et al. (1991) are indicated with an asterisk.

Age at maturity has relatively small effect on the calculation of age, since the estimates in (*ii*) and (*iii*) are not statistically different. As expected, the ages calculated using the radiometrically derived value of G_1 = 3.94 mg·year^{-1} gave higher ages than those estimated using the higher G_1 = 5.3 mg·year^{-1} estimated from the sectioned otoliths. The latter juvenile otolith mass growth rate is likely to be more accurate, since the data collection was done individually compared with the pooled samples used to drive the radiometric ages which included 135 otoliths for the smallest length class. The remodelling of the radiometric data from Fenton et al. (1991) has, therefore, refined the estimates of age given in that study.

Growth

The growth of orange roughy was well described by the von Bertalanffy growth curve (Fig. 6). The curve was fitted

Fig. 6. von Bertalanffy growth curves for orange roughy derived from otoliths (solid line) and radiometric ages (dashed line). Individual data points are annulus counts (less than 30 cm: whole otoliths; greater than 30 cm: sectioned otoliths).

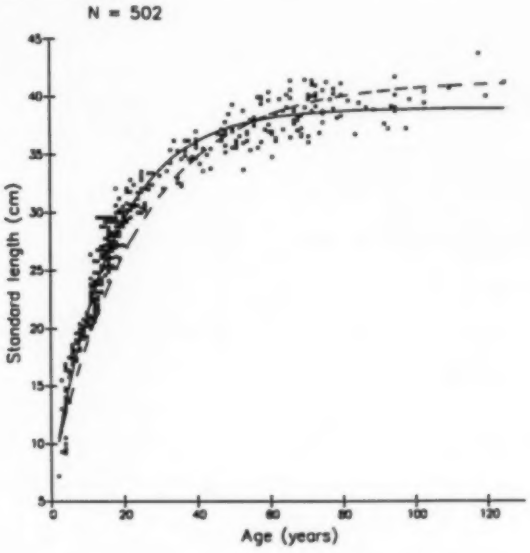

to individual observations using nonlinear least squares. To include the greatest number of observations, ages estimated from whole otoliths were used for fish under 30 cm SL and those from sectioned otoliths for the remainder. The parameters of the curve (standard errors in parenthesis) were L_{inf} = 39.06 (1.89), K = 0.06 (0.001), and t_0 = −3.18 (013). The postmaturity radiometric data of Fenton et al. (1991) were remodelled using the otolith mass growth rate estimates derived from sectioned otoliths: immature 5.3 mg·year^{-1} and mature 3.3 mg·year^{-1} (i.e., calculation (*i*)). The parameters of the resulting growth curve (Fig. 6) were L_{inf} = 41.36, K = 0.04, and t_0 = −4.9 (r^2 = 0.92).

Conclusions

We present a method to age orange roughy using sectioned otoliths. The estimated ages are broadly consistent with those derived by Fenton et al. (1991), using radiometric methods, and independently confirm their two-stage linear model of otolith mass growth rate. The similarity of ages from both methods was used to justify using the otolith mass growth rates derived from annulus counts to remodel the radiometric results. This reduced the radiometric ages from the 77–149 years given in Fenton et al. (1991) to 59–101 years for 38–40 cm SL fish compared with a maximum of 125 years (41 cm SL) from annulus counts. If the otolith mass growth data from the linear radiometric model are used together with G_2 = 62% G_1, the ages of these fish range from 70 to 125 years (maturity 32 years) or from 74 to 129 years (maturity 25 years).

We realise that these comparisons do not provide validation in the strict sense of the term. The comparison of independent methods presented here confirms that orange

roughy are extremely long-lived and have a great age-at-maturity but does not confirm that each zone is formed annually. In addition, an outcome of the remodelling of radiometric data is that, although methods are not independent, the maximum age estimates converge.

Our results have profound implications for stock productivity and hence optimum harvest rates. They indicate that natural mortality (M) must be extremely low, considerably lower than that given by Mace et al. (1990) who estimated M to be under 0.1, using a maximum age of 50. Recent assessments in Australia and New Zealand use M = 0.04, but estimates of M are currently being reexamined by workers in both countries.

Acknowledgments

Otolith collection was coordinated by Ken Smith and David McKeown. Kerry Frlan prepared the otolith schematic. Dr. Jeremy Lyle, Tasmanian Division of Sea Fisheries, and Dr. Nick Elliot and Cathy Bulman, CSIRO Division of Fisheries, provided additional otoliths. Owen Farrell of CSIRO Division of Coal and Energy Technology made ICPMS lead analyses. They are all thanked for their cooperation. Sandy Morison and Bryce Stewart provided helpful comments on the manuscript. The significant contribution of two referees is acknowledged. This study was partially funded by the Fishing Industry Research and Development Council and the Fisheries Development Trust Account.

References

Anderson, J.R., Morison, A.K., and Ray, D.J. 1992. Age and growth of Murray cod, *Maccullochella peelii* (Perciformes: Percichthyidae), in the lower Murray–Darling Basin, Australia, from thin-sectioned otoliths. *In* Age determination and growth in fish and other aquatic animals. *Edited by* D.C. Smith. Aust. J. Mar. Freshwater Res. **43**: 983–1013.

Annala, J.H. (*Comp.*) 1993. Report from the Fishery Assessment Plenary, May 1993: stock assessments and yield estimates. (Available from MAF Fisheries Greta Point Library, Wellington, New Zealand).

Beamish, R.J. 1979. Differences in the age of pacific hake (*Merluccius productus*) using whole otoliths and sections of otoliths. J. Fish. Res. Board Can. **36**: 141–151.

Beamish, R.J., and Fournier, D.A. 1981. A method for comparing the precision of a set of age determinations. Can. J. Fish. Aquat. Sci. **38**: 982–983.

Bell, J.D., Lyle, J.M., Bulman, C.M., Graham, K.J., Newton, G.M., and Smith, D.C. 1992. Spatial variation in reproduction, and occurrence of non-reproductive adults, in orange roughy, *Hoplostethus atlanticus* Collett (*Trachichthyidae*), from south-eastern Australia. J. Fish Biol. **40**: 107–122.

Bennett, J.T., Boehlert, G.W., and Turekian, K.K. 1982. Confirmation of the longevity in *Sebastes diploproa* (Pisces: Scorpaenidae) from ^{210}Pb:^{226}Ra measurements in otoliths. Mar. Biol. **71**: 209–215.

Boehlert, G.W. 1985. Variability in age estimates in *Sebastes* as a function of methodology, different readers and different laboratories. Calif. Fish Game, **70**: 210–224.

Brander, K. 1974. The effect of age reading error on the statistical reliability of marine fishery modelling. *In* The ageing of fish. Unwin Brother Ltd., The Gresham Press, Old Woking, England. pp. 181–191.

Edmonds, J.S., Moran, M.J., Caputi, N., and Morita, M. 1991. Stock discrimination by trace-element analysis of otoliths of orange roughy (*Hoplostethus atlanticus*), a deep-water marine teleost. Aust. J. Mar. Freshwater Res. **42**: 383–389.

Fenton, G.E., and Short, S.A. 1992. Fish age validation by radiometric analysis of otoliths. *In* Age determination and growth in fish and other aquatic animals. *Edited by* D.C. Smith. Aust. J. Mar. Freshwater Res. **43**: 913–922.

Fenton, G.E., Short, S.A., and Ritz, D.A. 1991. Age determination of orange roughy *Hoplostethus atlanticus* (Pisces: Trachichthyidae) using ^{210}Pb:^{226}Ra disequilibria. Mar. Biol. **109**: 197–202.

Fletcher, W.J. 1991. A test for the relationship between otolith weight and age for the pilchard *Sardinops neopilchardus*. Can. J. Fish. Aquat. Sci. **48**: 35–38.

Francis, R.I.C.C., and Smith, D.C. 1995. Mean length, age, and otolith weight as potential indicators of biomass depletion for Chatham Rise orange roughy. N.Z. Fish. Assess. Res. Doc. 95/3.

Gauldie, R.W. 1987. The fine structure of check rings in the otolith of the New Zealand orange roughy (*Hoplostethus atlanticus*) N.Z., J. Mar. Freshwater Res. **21**: 261–274.

Gauldie, R.W. 1988. The effect of surface sculpturing on the interpretation of opaque and hyaline zones in the orange roughy otolith. J. Appl. Ichthyol. **4**: 140–146.

Gauldie, R.W. 1990. Phase differences between check ring locations in the orange roughy otolith (*Hoplostethus atlanticus*). Can. J. Fish. Aquat. Sci. **47**: 760–765.

Gauldie, R.W., West, L.F., and Davies, N.M. 1989. *K*-selection characteristics of orange roughy stocks in New Zealand waters. J. Appl. Ichthyol. **5**: 127–140.

Jearld, J.A. 1983. Age determination. *In* Fisheries techniques. *Edited by* L.A. Nielsen and D.L. Johnson. American Fisheries Society, Bethesda, Md. pp. 301–324.

Kotlyar, A.N. 1980. Age and growth speed of the bigheads, *Hoplostethus atlanticus* Collett and *H. mediterraneus* Cuvier (Trachichthydae, Beryciformes). *In* Fishes of the open ocean. *Edited by* P.V. Shirston. Moscow Institute of Oceanography, Moscow. pp. 68–88.

Last, P.R., Scott, E.O.G., and Talbot, F.H. 1983. Fishes of Tasmania. Tasmanian Fisheries Development Authority, Hobart.

Lyle, J.M. 1994. Orange roughy (*Hoplostethus atlanticus*). *In* A scientific review of the south east fishery with particular reference to quota management. *Edited by* R.D.J. Tilzey. Bur. Resour. Sci. Bull., Australian Government Printer, Canberra.

Mace, P.M., Fenaughty, J.M., Coburn, R.P., and Doonan,

I.J. 1990. Growth and productivity of orange roughy (*Hoplostethus atlanticus*) on the north Chatham Rise. N.Z. J. Mar. Freshwater. Res. **24**: 105–119.

Nedreaas, K. 1990. Age determination of Northeast Atlantic *Sebastes* species. J. Cons. int. Explor. Mer, **47**: 208–230.

Pentilla, J., and Dery, M. (*Editors*). 1988. Age determination methods for Northwest Atlantic species. NOAA Tech. Rep. NMFS 72.

Reznick, D., Lindbeck, E., and Bryga, H. 1989. Slower growth results in larger otoliths: an experimental test with guppies (*Poecilia reticulata*). Can. J. Fish. Aquat. Sci. **46**: 108–112.

Secor, D.H., and Dean, J.M. 1989. Somatic growth effects on the otolith – fish size relationship in young pond-reared striped bass, *Morone saxatilis*. Can. J. Fish. Aquat. Sci. **46**: 113–121.

Smith, D.C., and Robertson, S.G. 1992. The problem of ageing orange roughy. *In* The measurement of age and growth in fish and shellfish. *Edited by* D.A. Hancock. Australian Society for Fish Biology Workshop, Lorne, 22-23 August 1990. Bur. Rural Resour. Proc. No. 12, Bureau of Rural Resources, Canberra.

Smith, D.C., Huber, D., and Withell, A.F. 1988. Western Bass Strait trawl fishery assessment. Progress Rep. No. 2. Orange roughy. *Prepared for* Demersal and Pelagic Fish Research Group Workshop on Orange Roughy, Adelaide, 3 July 1988. Mar. Sci. Lab. Int. Rep. **164**.

Van Den Broek, W.L.F. 1983. Ageing deepwater fish species: report of a visit to the United Kingdom, – September–November 1982. N.Z. MAFFish Misc. Ser.

Williams, T., and Bedford, B.C. 1974. The use of otoliths for age determination. *In* Ageing of fish. *Edited by* T.B. Bagenal. Unwin Brothers, Old Woking, England. pp. 114–123.

Implications of trip regulations for high-grading: a model of the behavior of fishermen

Darren M. Gillis, Randall M. Peterman, and Ellen K. Pikitch

Abstract: We developed a simulation model, based on observations of the actions of fishermen, to determine how regulations on trips by management agencies may influence discarding behavior at sea. Our model employed the results of a separate dynamic optimization model and data from the Oregon groundfish trawl fishery to predict quantitative patterns of high-grading expected across a range of regulatory limits on both fishing effort and the quantity of landings per trip (trip quota). In all cases, the total seasonal landings were assumed to be constant. High-grading was predicted to be greatest when there is a high probability of the catch exceeding the trip quotas, as when effort limits are high and trip quotas are low. Our evaluation of regulations also considered indicators such as expected economic value of the trip, proportion of trip landing limit attained, and the number of trips made in a season. A combination of large trip landing limits and intermediate trip effort limits best satisfied the multiple goals typically used by management agencies.

Résumé : En nous fondant sur des observations des comportements des pêcheurs, nous avons élaboré un modèle de simulation afin de déterminer comment la réglementation des campagnes de pêche par les organismes de gestion peut influer sur le comportement de rejet des prises en mer. Notre modèle employait les résultats d'un modèle différent d'optimisation dynamique et des données tirées de la pêche du poisson de fond au chalut en Oregon pour prédire les profils quantitatifs de rejet sélectif auxquels on peut s'attendre avec une gamme de limites réglementaires portant à la fois sur l'effort de pêche et sur le volume des débarquements par campagne (quota par campagne). Dans tous les cas, on posait que les débarquements saisonniers totaux étaient constants. On a prédit que le rejet sélectif serait maximal lorsqu'il y a une forte probabilité que les prises dépassent les quotas par campagne, par exemple quand les limites fixées pour l'effort sont élevées tandis que les quotas sont faibles. Dans notre évaluation de la réglementation, nous avons aussi considéré des indicateurs comme la valeur économique prévue de la campagne, la proportion dans laquelle la limite de débarquement est atteinte et le nombre de campagnes accomplies par saison. Une combinaison de limite de débarquement élevée par campagne et de limite intermédiaire de l'effort de pêche par campagne était ce qui satisfaisait le mieux aux buts multiples que se fixent typiquement les organismes de gestion.
[Traduit par la Rédaction]

Introduction

The incidental by-catch of unwanted marine life during fishing is one of the major political and biological issues of modern fisheries. Fish in the by-catch often consist of species and sizes that are unmarketable, illegal, or have lower values than the target species. The less desirable components of the by-catch are usually disposed of at sea, and their capture is reported poorly, if at all. In some fisheries such as shrimp (*Penaeus* spp.) trawling, discarded individuals may constitute the majority of the catch biomass (Slavin 1982). In other fisheries, a significant amount of the target species may be discarded because of their small size, such as 68% of the American plaice (*Hippoglossoides platessoides*) caught by trawling in the Gulf of St. Lawrence (Halliday et al. 1989) or 25% the North Atlantic cod (*Gadus morhua* caught by trawling (Kulka and Stevenson 1986). Furthermore, these figures may underestimate the actual amount of discarding occurring if fishermen are reluctant to discard in the presence of observers (Kulka and Stevenson 1986). However, discarding will be of little consequence if the discarded individuals are unaffected by the catch and discarding process.

There are few direct studies on the ability of fish to survive discarding. It is generally believed that the mortality of discarded fish is high, and that few discarded individuals survive to be caught again (Caddy 1982). Powles (1969)

Received June 25, 1993. Accepted July 14, 1994.
J11986

D.M. Gillis.[1] Department of Biological Sciences, Simon Fraser University, Burnaby, BC V5A 1S6, Canada.
R.M. Peterman. School of Resource and Environmental Management, Simon Fraser University, Burnaby, BC V5A 1S6, Canada.
E.K. Pikitch. Fisheries Research Institute, School of Fisheries, WH-10, University of Washington, Seattle, WA 98195, USA.

[1] Present address: Department of Zoology, University of Manitoba, Winnipeg, MB R3T 2N2, Canada.

studied the survival of juvenile American plaice on the decks of commercial fishing trawlers and concluded that over 95% of the discarded individuals were dead when they were returned to the water. Ricker (1976) cited discarding mortality estimates of between 1.9 and 86% for different Pacific salmon (*Oncorhynchus*) species and fishing methods (seine, gill net, troll), with most of the estimates falling between 30 and 50%. For Pacific halibut (*Hippoglossus stenolepis*), the mortality of discards varies among gears and regions. Estimates of the discarding mortality of Pacific halibut in the Bering Sea have ranged from 12% for individuals caught in groundfish pots to 100% in the trawl fisheries (Hoag 1975; IPHC 1991). These studies indicate that the potential mortality of discarded fish is high, especially in trawl fisheries. If so, unreported discarding by fishermen would make fishery statistics unreliable sources for estimates of fishing mortality. This would clearly create difficulties in stock assessment procedures and evaluations of regulations. In this paper, our objective is to show how behavioral models could be used to assess the potential impact of proposed regulations on discarding practices at sea.

Management regulations

The management of a multispecies fishery, where the selectivity of harvesting methods among species is limited, is a difficult problem. Managers must often make trade-offs between the local welfare of certain species and the current economic value of the main fishery (May 1984; Pikitch 1988). The problem is made more complicated because simple regulations do not always have the desired effects. For example, regulations limiting the landing of certain fish may result in large unreported fishing mortalities of other fish due to discarding rather than the avoidance of the protected individuals by fishermen. This appears to be true in the Oregon trawl fishery, where fishermen claim that much of their discarding is due to regulations (Pikitch et al. 1988; Pikitch 1991).

Generally, agencies attempt to manage fisheries through regulation of the amount of fish that can be legally landed and the nominal fishing effort applied in a region. The amount of fish landed is often set by a single total allowable catch (TAC) for a fishery within a year. This limit is then divided among several components of the fishery, often representing vessels with different gear types or nationalities (e.g., the Atlantic groundfish management plan, 1991–1993, Department of Fisheries and Oceans 1990). The limitation of nominal fishing effort, often advocated on theoretical grounds, is difficult in practice. Generally, effort limitation has focused upon regulation of the size of the fleet (through licensing policy), the type and sizes of gear used (such as mesh size restrictions), and restrictions on where and when fishing is allowed (Gulland 1974). Regulations are often designed to extend the fishery temporally in order to stabilize the incomes of fishermen and to give all of them equal access to the resource.

Recently, limits on individual fishing trips have become the focus of management regulations in both the Canadian and American Pacific coast trawl fleets (e.g., West coast groundfish management plan, 1992, Department of Fisheries and Oceans 1991; also see Pikitch 1987*a*, Pikitch et al. 1988). By regulating individual trips, a better control of the temporal allocation of effort and a more equitable division of the resource within the fleet could be obtained. However, our discussions with members of various sectors of the trawl fisheries suggest that these regulatory measures may increase the amount of fish discarded.

Discarding creates several problems. The marketable fish that are discarded due to regulations result in an immediate loss in revenue to the fishermen. Also, unreported fishing mortality can lead to poor estimates of future stock productivity. Discarded, dead fish will obviously not contribute directly to future catches and their potential reproductive contribution is also lost. When discards include the juveniles of the target species, the effects on future harvest can be severe (IPHC 1991). Even when the discarded fish are members of an unmarketable species, they may be important predators, prey, or competitors for the commercial species (Garcia 1988). Ignoring the mortality of nontarget species and size classes may thus make it difficult to understand changes in the marine community that result from fishing activities, and the subsequent effects on the commercial fishery.

Causes of discarding

Discarding can have many different causes. Regulations limiting the quantity or species composition of fish landed are commonly given by fishermen as the reasons for disposing of fish at sea. Marketability, and occasionally storage limitations (hold capacity), can also result in discarding. Any combination of these factors may act together to create the pattern of catch disposition that is observed in a particular trip. We have chosen to categorize discarding according to the pattern (and bias) that it will create in the landings rather than the factors causing it.

The simplest form of discarding is *exclusion*. In this case, all individuals of a species or size class will be removed from the catch during the fishing trip. This may be due to the lack of a market or regulations preventing the landing of the discarded fish.

The second form of discarding is *capacity-discarding*. When the hold of a vessel is full, or when a regulatory landing limit is reached, all additional individuals that are caught will be discarded. On average, the species and size-class composition of the discards will be the same as the catch. In a single-species fishery, capacity-discarding should only occur during the last haul of the trip, and its overall effect on fishing mortality will probably be slight. However, if the amount of one species landed is restricted in a multispecies fishery, the discarding will continue as the vessel fishes for other legally landable species. The additional unreported fishing mortality that occurs for the regulated species during the latter part of such a trip could be quite large.

The final form of discarding is *high-grading*. In this case, fishermen selectively discard marketable fish in favor of more valuable ones. The retained fish may be in the same haul as the discards, or they may be expected to appear in future hauls before the trip is over. The ultimate goal of high-grading is to maximize the value of the total amount of fish that will be landed. High-grading may occur long before the hold is full or before the trip landing limit

is reached, although it should be more common toward the end of the trip when the amount of fish in storage is close to the maximum that can be landed. The species and size-class composition of discards resulting from high-grading behavior will be biased toward less valuable individuals and could include members of the juvenile age classes of the target species.

Theoretical framework

There is presently very little formal theory regarding discarding (see Hilborn 1985 for a discussion of the problem). This paper focuses on high-grading because it represents a modification of fishing effort that results from decisions made by fishermen at sea. The amount of discarding caused by exclusion and capacity-discarding could be estimated from a knowledge of catch composition, vessel characteristics, market conditions, and regulations. However, high-grading is the result of decisions made by fishermen in response to their natural and economic environments.

The question of when to high-grade is similar to the problem of optimal diet choice for natural predators, an active research topic in behavioral ecology (see Stephens and Krebs 1986 for a general review). In the optimal diet choice problem, a predator is faced with several prey types, each with a different energetic or nutrient value and different abundances. The choice of which prey to keep in order to maximize energetic benefits depends on the dominant constraints faced by the forager (such as the handling time for a prey item or the gut capacity of the predator, Charnov 1976; Kaspari 1990). Using these principles from behavioral ecology, we previously developed a model using dynamic programming (Bellman 1957; Mangel and Clark 1988) that considered the fishing vessel as a predator attempting to maximize the value of its landed catch while limited by the maximum length of the trip and the amount of fish that could be landed (Gillis et al. 1995). The parameters of the model were estimated from field data on the contents of hauls and trip characteristics collected from the Oregon trawl fleet (Pikitch et al. 1988). The dynamic program predicted when (within a trip) high-grading would occur for the case of a single-species fishery for sablefish (*Anoplopoma fimbria*), which has three distinct market classes of fish based on size. Comparison of the results of the model with additional data on catch disposition at sea showed a qualitative agreement between the predictions of high-grading in the model and the patterns of discarding observed in the field: (1) discarding increased with the availability of fish when regulations limited the amount of sablefish landed and (2) discarding increased as trips progressed in cases where landing limits were present but never attained (Gillis et al. 1995).

However, the contribution of high-grading to discard rates and its effect on the reliability of fishery statistics cannot be determined from the output of the dynamic program. That model's output is in the form of state-dependent predictions of the discarding decisions that will be made during fishing trips, given prescribed conditions. In order to generate predictions of high-grading frequency in a fishery, we built a second model. This model simulated a fishery during one season, where the fleet was composed of fishing vessels whose behavior was generated by the state-dependent optimal decisions arising from our dynamic program. This second model is the subject of the current paper.

The purpose of this study was to determine how the high-grading resulting from within-trip regulations on effort and landings can affect landing statistics, the economic value of fishing trips to fishermen, and the allocation of effort among fishing trips. Our study was based on the relatively novel approach noted above of simulating the behavior of fishermen using the principles of behavioral ecology in conjunction with field data. The resulting model begins to address the concerns raised by Hilborn (1985) by explicitly including the dynamics of fishing effort within a season in the evaluation of fishery regulations.

Methods

Fishery

The data used to estimate the parameters of our model were taken from records of the Oregon trawl fishery, which employs a wide variety of trawling gears and strategies. We focused our work on a subcatch of this fishery, the sablefish. These fish are marketed by size class, with larger size classes receiving higher prices per kilogram. There are four size classes for sablefish: <1.36, 1.36–2.27, 2.27–3.18, and >3.18 kg. Because the two largest size classes were relatively rare in the catch, they were combined into a single large class to simplify our analysis. Thus, there were three size classes in our model: the largest fish (X), the medium fish (Y), and the smallest fish (Z). In this fishery, regulatory limits on the amount of fish landed from a trip did not distinguish among the different size classes (above a minimum length of 56 cm, which was roughly equivalent to the small size category). Thus, if a fisherman's catch exceeded the amount of fish that could be legally landed, it may have been more profitable to retain only the larger fish from the catch. Therefore, in this fishery, high-grading was more likely to occur when regulatory limits on the tonnage of allowable landings were low or the abundance of larger size classes was high.

Data for this fishery came from an observer program conducted from 1985 to 1987 (Pikitch et al. 1988). The data collected by researchers in this program included information about samples from the hauls, the amount of discarding occurring, and the prices received for each size class. In addition, the program obtained details about the management regulations that limited the landing of sablefish during the study.

Model

Overview

We used simulation modeling to evaluate the potential consequences of different management regulations on the amount of discarding expected due to high-grading and the success of fishing trips for the fishermen. The model assumed that the fishing abilities were equivalent among all vessels and therefore, it used individual fishing trips as the unit of fleet dynamics. These fishing trips were composed of a series of separate hauls. At the beginning of each haul, a decision was made about how much of each size class of fish would be discarded, if any. These discarding decisions were based on the amount of space

Fig. 1. Flow chart of the simulation of a fishing season, including simulation of discarding activity during each trip. TAC, TEL, and TLL are abbreviations for TAC, total allowable catch (tonnes); TEL, trip effort limit (number of hauls); TLL, trip landing limit (tonnes). The notation *f*( ) means "a function of ( )".

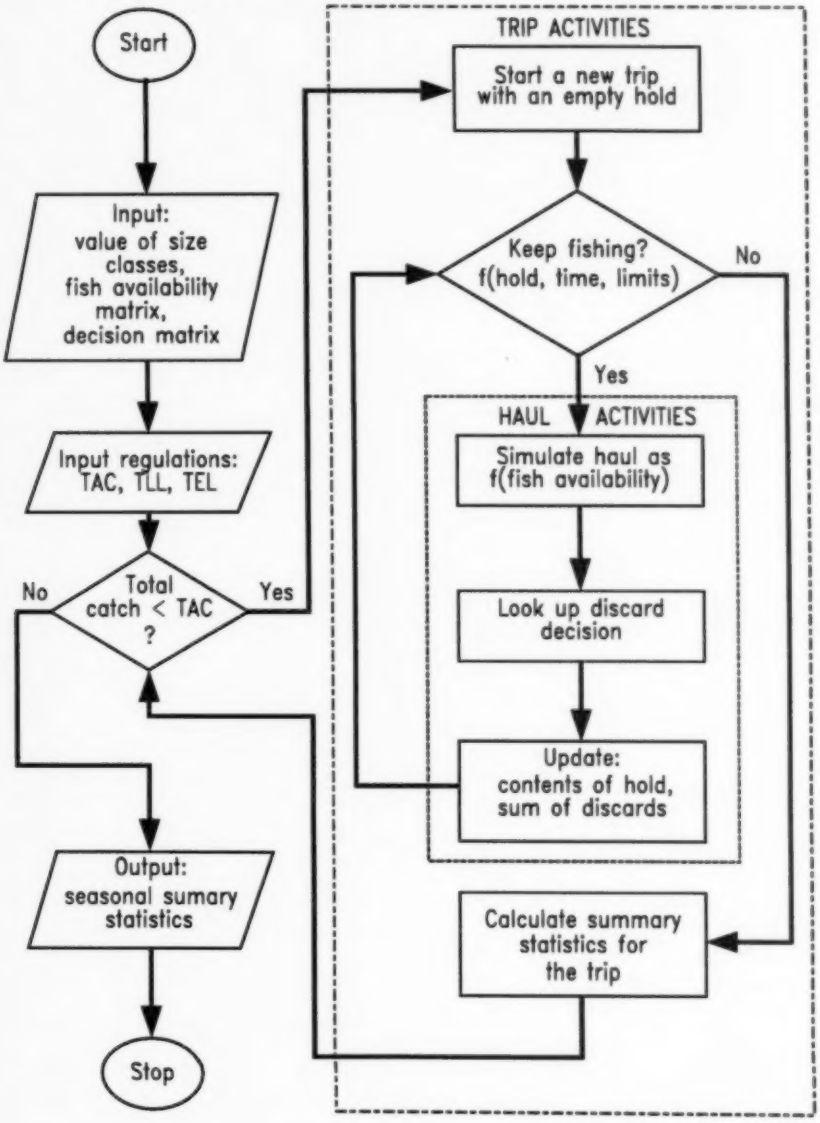

remaining in the hold, the expected availability of each size class in the haul, the time left until the end of the trip, and other factors, as described in detail below. Basing the discarding decisions in this simulation on the expected contents of a haul is equivalent to assuming that fishermen base their decisions on the average haul rather than the contents of the current haul. This situation could occur if fishermen have poor knowledge about the contents of a haul until after they have chosen which fish to retain from it. For a species like sablefish, which is dumped on deck as a component of a mixed-species catch, this is a reasonable assumption. Fishing trips were simulated until a predefined TAC for the season was landed. This TAC, as in most fisheries, referred to the catch that was landed and did not include discarded fish. The steps involved in simulating a season are summarized in Fig. 1. We quantified the influence of different management regulations on discarding behavior and other measures of performance by repeating these seasonal simulations using the same TAC and different regulations on individual trips.

State variables and input parameters

The present model used results from our previous dynamic programming model of fishermen's discarding decisions in a single trip (Gillis et al. 1995) to determine the expected cumulative outcome of a series of trips. Consequently, the form of many of the variables and parameters in the present model was dictated by our previous model. In general, a stochastic dynamic program determines a set of optimal decisions for a system that depends on the state of the system when a decision is being made and the time that the decision occurs (Mangel and Clark 1988). The optimization is based on the probability of moving from one state to another in a unit time interval and the value of each of the possible states at the final time period. In the numerical form of this procedure that we employed, both the values of the states and the time intervals were defined in discrete units in order for the optimal set of decisions to be found.

In both the simulation model and our previous dynamic program, all vessels in a fleet were considered identical. The state of a vessel at a particular time during a trip was defined by the amount of each size class of sablefish in the hold. Time within a trip was measured in terms of the number of completed hauls, progressing in unit increments from the beginning of the trip to its end. We set a maximum of 14 hauls for a trip in our models, based on the mean of 7.5 hauls per trip (ranging from 1 to 21) that was observed to target on the assemblage of fish containing sablefish in the field data. The hold of a vessel was discretized into thirty-one 226.8-kg (500-lb.) units, with a maximum capacity of 6803.8 kg. The actual hold capacities of the vessels involved in the Oregon fishery were larger than 6803.8 kg, but the regulated limits on landings used in the Oregon fishery, when in effect, were less than this maximum. This discretization represented the possible contents of a hold as elements in a $31 \times 31 \times 31$ matrix. However, not all elements in this matrix were potential states because the total hold contents could not exceed the hold limit. Thus, only 5456 of the 29 791 elements of the state matrix represented possible states for a simulated hold. Each simulated trip began with the first haul and an empty hold. In addition to the hold contents at each time, the amount of each size class discarded during a trip was also recorded to quantify the amount of discarding occurring.

The simulation model's input parameters and variables (Fig. 1) were estimated from field data or simulations based on field data. These parameters were (1) the market value of each size class, (2) the estimates of the amount of each size class that would be caught in a single haul (fish availability), (3) the discarding decisions that would be made by the fishermen, and (4) the management regulations on the fishery. The potential consequences of management regulations are the focus of this study, so we will examine the regulations chosen in a separate section.

The value of each size class was estimated from the prices paid for fish landed from 23 trips landing sablefish from all size classes during the Oregon trawl study. The value of a size class per kilogram was defined as the average price paid for that size class across all of these trips. As described above, the relative scarcity of larger fish in the catch forced us to combine the two largest market size classes into the large size class of our model and to use the average price for those two classes from the data. Thus, in our model the value of large sablefish was \$1.41/kg, medium sablefish was \$0.99/kg, and small sablefish was \$0.61/kg.

The availability of fish was represented as the probability that a haul would contain discrete amounts of each of the three size classes of sablefish. The observed size class distribution from 50 hauls of the Oregon trawl fishery was used to estimate the availability of each of the size classes used in the simulated catch. The occurrence of each size class in the observed data was 49 of 50 hauls (mean amount in haul = 146.3 kg, SD = 176.4 kg) for the small size class, 42 of 50 hauls (mean = 168.6 kg, SD = 189.2 kg) for the medium size class, and 35 of 50 hauls (mean = 76.4 kg, SD = 102.2 kg) for the large size class. The amount of each size class in a haul was not independent of the other size classes. When two or more size classes were present in a haul, a linear regression between the logarithms of the catches provided reasonable fits ($P < 0.001$) when the zero points were removed. However, the catch could not be simulated by only logarithmic regressions between the size classes because there were numerous cases where one or more size classes were missing from a haul. The presence of the two largest size classes in a haul was predicted by logit models using the amount of the smaller size class (or size classes) in the haul as the independent variable(s). When a larger size class occurred in a haul, the amount of the larger size class present was estimated with the logarithmic regression on the amounts of the smaller size classes in the haul. For example, to simulate the amount of medium-sized fish in a haul, we began by randomly selecting the amount of the small fish in that haul from the field data. The amount of small fish was used as the predictor variable in a logit model, based on the field data, to estimate the probability that medium-sized fish were also in the haul. This probability and a uniform random number determined whether any medium-sized fish were present in the simulated haul. The mean amount of medium-sized fish present, if not zero, was predicted by the logarithmic regression on the amount of small fish in a haul that was estimated from the field data. Variation around this predicted value was generated by adding a randomly selected residual from the fit of the field data to the logarithmic regression line. A similar procedure was followed for the largest size class using the two smaller, but more abundant, size classes as predictor variables. In this manner, we were able to simulate the contents of hauls based on the original data. One thousand hauls were simulated in order to generate the range of variability that was indicated by the data but not realized in the field due to the limited sample size.

In order to match the amounts in a haul to the states of our modeled vessels, we discretized the weights of each size class in a haul into five categories, based on 226.8-kg increments, ranging from 0 to 907.2 kg. The probability that a haul would contain a given categorical amount of the three size classes was calculated from our simulated hauls. We chose to assign a zero value to all simulated hauls containing between 0 and 113.3 kg. This introduced a slight negative bias into the estimates of the probability of capture for each

size class (compared with the original data), but it represented capture more accurately because hauls that did not catch sablefish had not been used in calculating these probabilities. For example, the probability of a haul containing between 113.4 and 340.2 kg (represented in the model as the 226.8-kg category) of each of the three size classes was estimated as 0.043 because 43 of the 1000 simulated hauls contained that combination of size classes. The frequencies of each size class in these simulated hauls are summarized in Table 1. With five categories of haul weights for each of the three size classes of sablefish, there was a total of $5 \times 5 \times 5 = 125$ possible combinations of haul contents to be considered. The probabilities of these combinations became the entries of a $5 \times 5 \times 5$ matrix that reflected both the relative availability of the size classes of sablefish and the degree to which the abundances of the size classes were correlated. The sum of all of these probabilities, representing all possible contents of a haul, was 1. This fish availability matrix, together with a uniform random number generator, was used to simulate compositions of hauls in our model so that they were similar to those experienced in the Oregon fishery.

The decision rules regarding which size classes to discard were derived from our earlier dynamic programming model (Gillis et al. 1995). This program determined the discarding behavior of fishermen that would yield the highest expected gross profit when the value of the size classes, the fullness of hold, the maximum amount of time left in the trip, and the availability of fish were all known. In the notation of Mangel and Clark (1988), the equations describing our dynamic program are

$$[1.1] \quad F(x,y,z,T,T) = \Phi\,(x,y,z)$$

$$[1.2] \quad F(x,y,z,t,T) = \operatorname{Max}_{d} \sum_{ijk} \mathbf{A}_{ijk} \cdot F(x'_d,y'_d,z'_d,t+1,T)$$

$$[2] \quad \Phi(x,y,z) = (x \cdot V_X) + (y \cdot V_Y) + (z \cdot V_Z) \quad \text{if } x + y + z \le \text{TLL}$$
$$= 0. \quad \text{if } x + y + z > \text{TLL}.$$

In equations 1.1 and 1.2, the $F(\ )$ notation indicates that the dynamic program solution was a function of the current hold contents (the amount of x, y, and z), the current time (t), and the final time or maximum duration of the trip (T). $\mathbf{A}$ was the $5 \times 5 \times 5$ matrix of probabilities of capture for each of the three size classes that was described above. The indices i, j, and k corresponded to the possible discretized amounts of each of the size classes that could be in a haul. The d subscript represented a discarding decision and x'_d, y'_d, and z'_d were the expected amounts of the three size classes that would be in the hold after decision d was made. The function $\Phi(\ )$ determined the value of the hold contents at the end of the trip; V_X, V_Y, and V_Z were the ex-vessel values of the size classes and TLL was the trip landing limit. The solution of this dynamic program was the set of decisions (d) that maximized the value of the dynamic program for each possible state (x, y, and z) and time period (t). For example, if the hold contained the maximum amount of fish (the state) at any time during the trip, then no additional hauls would be made and the trip would end (the decision). If the hold contained no fish during the penultimate time step, then all size classes would be retained from the haul. With an intermediate amount of fish in the hold, the discarding of some of the size classes might occur, if that discarding could be expected to result in a higher value for the final landed catch. Thus, in our dynamic program the amount of a size class that would be discarded due to high-grading depended on (1) the amount of more valuable fish available (which determined if discarding would occur for a particular time and fullness of the hold) and (2) the amount of the size class in the haul (which was the amount discarded when high-grading took place). Our previous dynamic program also considered the effect of risk of damage to the gear and injuries to the crew on discarding decisions, but due to lack of data, we did not include this factor in the current study. For a more detailed discussion and interpretation of the dynamic program, see Gillis et al. (1995).

Table 1. Probability of obtaining different amounts of each size class in a haul simulated using the data from 50 observed hauls. For our fishery model, the amount of a size class in a haul was discretized into five categories. When the simulated amount of a size class was within a category's range, that amount was set equal to the model value for that category. The model value was the midpoint of the category's range, except for the lowest category which was set to zero. The distribution of categories shown here indicates the mean availability of each size class in a single haul from our model. This summary does not indicate the interdependence among the size classes caught, which is described in the text.

Categories of amount in haul		Probability of amounts for each size class		
Range (kg)	Model value (kg)	Small	Medium	Large
0.0–113.3	0.0	0.590	0.550	0.709
113.4–340.2	226.8	0.320	0.300	0.270
340.3–567.0	453.6	0.055	0.107	0.020
567.1–793.8	680.4	0.035	0.033	0.001
793.9–1020.6	907.2	0.0	0.010	0.0

The output from our dynamic program (Gillis et al. 1995) was a matrix containing the 14×5456 time- and state-dependent decisions that indicated which size classes to discard from a haul with a given amount of fish in the hold at any time during a trip. These decisions are not easily presented or interpreted in their matrix form. However, in Fig. 2, we present some of the behavior generated in simulated vessels using the decisions from the dynamic program. Briefly, high quotas on trip landings resulted in more discarding as trips progressed, while more restrictive quotas resulted in frequent discarding at the beginning of the trips.

Simulation of a haul, a trip, and a season

The simulation of the events in a haul involving the capture, selection, and storage of fish was done in three steps (Fig. 1). First, the contents of a haul were randomly created

Fig. 2. Proportion of vessels that discarded fish as simulated fishing trips progressed through consecutive hauls. The trip landing limit (TLL) was the total weight of fish that could be landed. The proportion was calculated as a fraction of the vessels that were still fishing during a particular haul. The number of vessels filled their TLLs and stopped fishing. When the TLL was high the proportion of vessels discarding increased throughout the trip; however, when the TLL was low, discarding was more common at the beginning of a trip. (Adapted from Gillis et al. 1995).

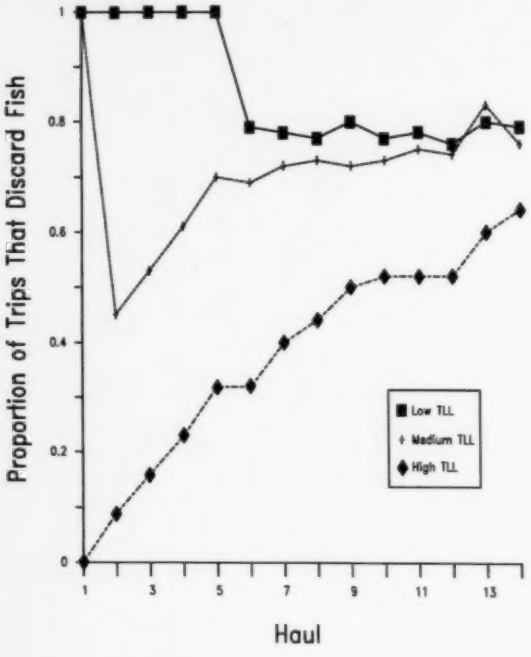

using the fish availability matrix described above. The choice of which size classes in the catch to keep was taken directly from the output of the dynamic program (the decision matrix), according to the current contents of the hold and the time remaining before the end of the trip (represented by the number of hauls which had already been made). Finally, the contents of the hold and the sum of the amount of each size class that was discarded were updated, based on the discarding decision and the fish that were caught. As stated above, a trip was simply a series of hauls, beginning with an empty hold and finishing when either the limit of fish that could be landed in a trip or the maximum duration of a trip had been reached. The value of the landed catch at the end of the trip was calculated from the amount and value of each size class that was landed. The value of discarded fish was calculated in a similar manner. A fishing season was simulated as a series of consecutive trips and the season ended when the total amount of fish landed from the trips equalled or exceeded the TAC. The actual number of trips in a season could vary, depending on the amount of fish that was landed per trip. The analysis of the model focused upon variables that were measured at the end of the trips and at the end of a season. In order to reduce the influence of rare stochastic events on the interpretation of model results, 1000 seasons were simulated for each set of management options considered. The performance indicators that we used to evaluate the management options were averaged across these 1000 simulated seasons.

Performance indicators

We chose variables to be produced by our model that could be important to fishermen, managers, or both. These variables were (1) the number of trips in a season, (2) the number of hauls in a trip, (3) the proportion of the maximum legal landing that was taken, (4) the market value of the fish discarded during a trip, (5) the market value of the fish landed at the end of a trip, (6) the total weight of fish discarded during a season, (7) the proportion (by weight) of caught fish that were discarded during a season, and (8 and 9) the weight of each of the two smallest size classes of fish discarded during a season. Our goal was to provide a set of indices that would allow decision makers to compare the potential effects of varying regulations on different aspects of the fishery.

For example, both managers and fishermen are interested in the number of trips per season and the average length of a trip (measured here as the number of hauls). Regulations that lead to an increased number of trips will increase the importance of travel costs (such as fuel) to seasonal net profits, especially if the number of hauls per trip and the resulting catch per trip are reduced. However, such regulations will also tend to extend the fishing season. Developing regulations that maintain fishing throughout the year is often a goal of managers that is also favored by fishermen.

Fishermen are also likely to be concerned with the economic value of a trip, the proportion of the allowable landing quota that can be taken, and the market value of the fish that they have discarded. By definition, the gross value of the landed catch will have a direct influence on the trip's net profit. The proportion of the quota that can be landed will influence the fishermen's opinion of the skill of the managers in choosing the regulations and potentially their future cooperation with regulatory agencies. For instance, if only a small portion of this quota can be landed, fishermen will begin to doubt that managers adequately understand the system that they are controlling. Finally, the market value of discarded fish could cause concern and frustration in the fleet. Although fishermen are the ones who high-grade, they often perceive themselves as responding to market and regulatory conditions that have been forced upon them. In our experience, few fishermen favor of discarding, especially when the discarded fish have little chance of surviving to contribute to future catches. Regardless of the long-term effects, it is important to know the immediate economic losses arising from discarding.

In addition to the conditions relevant to fishermen that result from regulations, managers are also concerned with the restriction of discarding-induced mortality and the distribution of that mortality among age classes for the reasons discussed in the introduction. These aspects of the simulated fishery are represented by the total weight discarded per season, the proportion of weight initially caught that is

Fig. 3. Number of trips required to achieve the total allowable catch (TAC) of a season for two different trip landing limits (TLLs) and several trip effort limits (TELs).

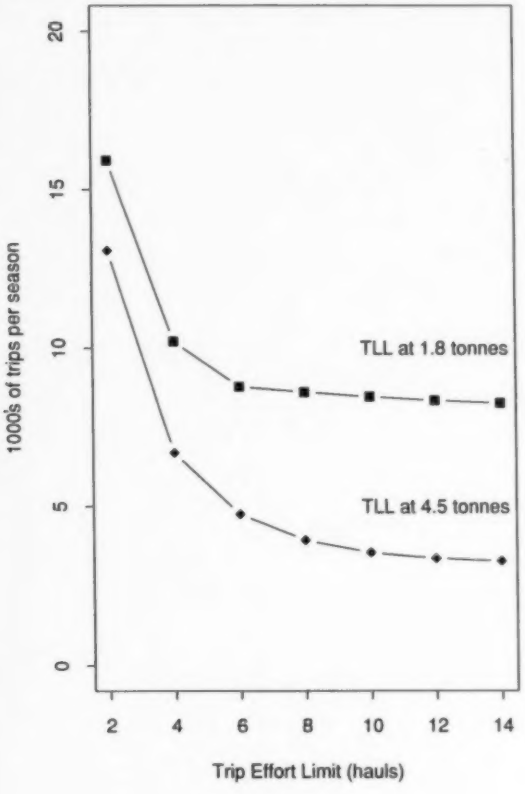

Fig. 4. Number of trips required to achieve the total allowable catch (TAC) of a season for a range of trip landing limits (TLLs) and trip effort limits (TELs). Each contour represents a set of conditions that result in the same number of trips in a season.

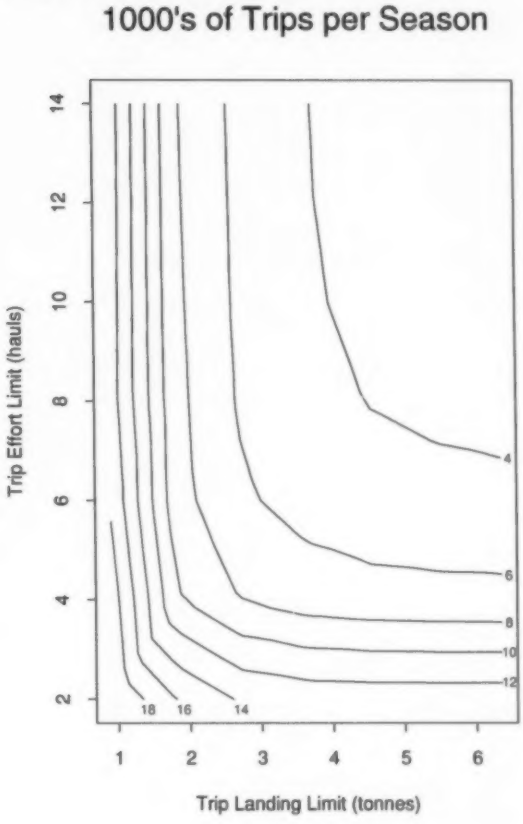

discarded per season, and the weight of each size class discarded per season.

Management regulations examined

We examined the sensitivity of our model to a range of management conditions based on those regulating the Oregon trawl fishery for sablefish between 1985 and 1987. During these years the TLLs on sablefish ranged from complete exclusion to no limit and often included special provisions for size and the proportion of the total catch that was landed as sablefish. When TLLs were applied to sablefish of all size classes, they ranged from 2721.6 to 5443.1 kg (6000–12 000 lb). We used TLLs of 907.2, 1814.4, 2721.6, 3628.7, 4535.9, 5443.1, and 6350.3 kg, which we will refer to as 0.9, 1.8, 2.7, 3.6, 4.5, 5.4, and 6.3 t, respectively. We chose to represent the limitation of effort within a trip (TEL) by the number of hauls allowed, rather than a maximum trip duration, because although time limits would probably be used in practice, our model was based on data from individual hauls rather than time at sea. Due to the presence of other commercial species in the trawl fishery, more study would be required to equate the number of sablefish hauls to total fishing time. The range of TEL values used was based on the maximum of 14 sablefish hauls per trip in our model. The TELs explored were 2, 4, 6, 8, 10, 12, and 14 hauls. In all cases, a TAC of 14 000 t was used to delimit a season of fishing in the simulation model. We simulated 1000 seasons for each of the 49 possible combinations of these TLLs and TELs in order to evaluate the sensitivity of high-grading behavior (and the associated indicators) to management regulations. The response of an indicator variable to each combination of TEL and TLL was presented as a contour plot. The contours representing the value of the response variable were based on the indicator values for each of the 49 combinations of TELs and TLLs examined; contours were drawn using the "contour" function of the S-plus statistical package (Statistical Sciences, Inc., 1700 Westlake Ave. N, Seattle, WA 98109-9891, 1993).

Sensitivity analysis

We analyzed the sensitivity of simulated high-grading behavior to a range of management conditions, but the computational requirements of our model were high and

Fig. 5. Variation in the nine performance indicators under a variety of management options. TLL, trip landing limit; TEL, trip effort limit. The response of each indicator to the different regulations is shown using isopleth diagrams. In Figs. 5*h* and 5*i*, Y refers to the medium-valued size class and Z refers to the lowest-valued size class.

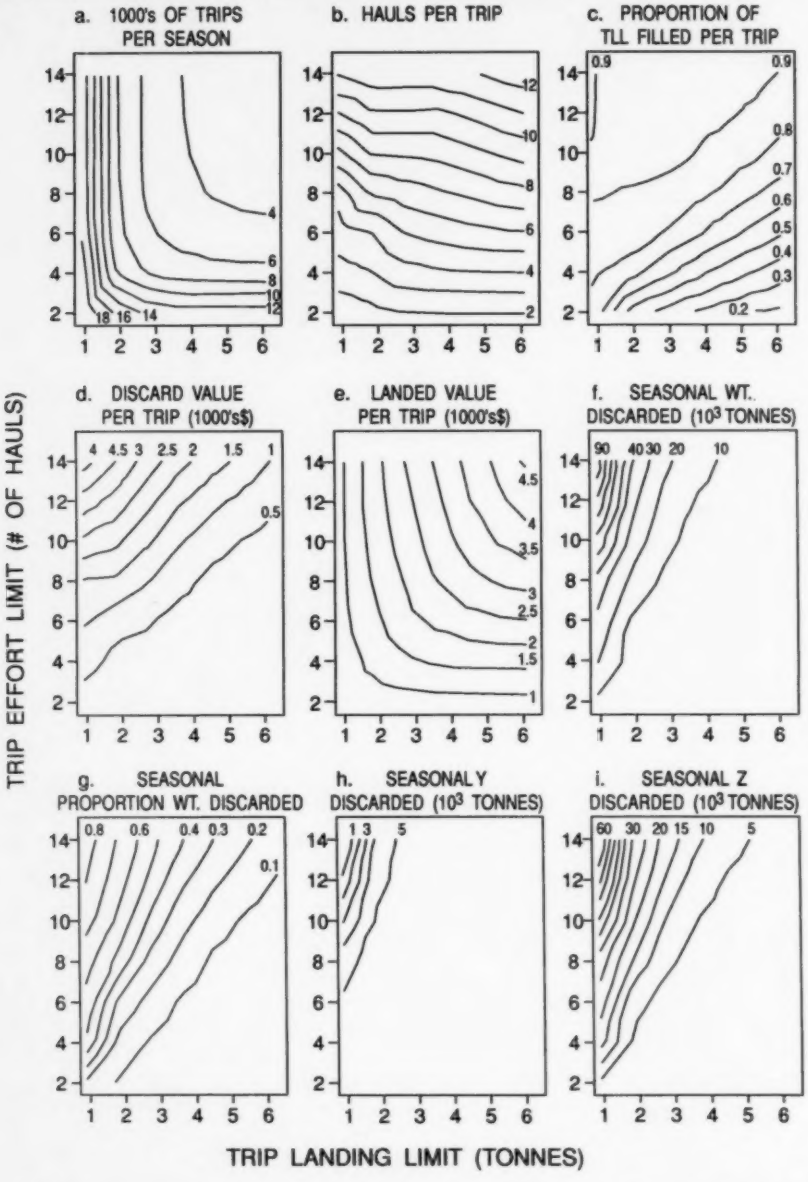
a. 1000's OF TRIPS PER SEASON
b. HAULS PER TRIP
c. PROPORTION OF TLL FILLED PER TRIP
d. DISCARD VALUE PER TRIP (1000's$)
e. LANDED VALUE PER TRIP (1000's$)
f. SEASONAL WT. DISCARDED (10³ TONNES)
g. SEASONAL PROPORTION WT. DISCARDED
h. SEASONAL Y DISCARDED (10³ TONNES)
i. SEASONAL Z DISCARDED (10³ TONNES)
TRIP EFFORT LIMIT (# OF HAULS)
TRIP LANDING LIMIT (TONNES)

a full sensitivity analysis was not feasible. For instance, each run of the seasonal simulation model for all 49 different management conditions took up to a week to complete on an IBM RS6000/530 computer. This precluded extensive sensitivity analyses on the other parameters that were estimated from the historical data, such as fish availability and the economic value of size classes. However, two additional runs were performed using higher and lower fish availabilities; these were created by multiplying the expected amount of small fish in a haul (estimated from the data) by a constant factor (2 or 0.5) and recalculating the fish availability matrix as previously described.

Results and discussion

Effects of regulations

The indicators varied with all of the combinations of TELs and TLLs used. For example, Fig. 3 uses two superimposed

plots to show that the number of trips per season decreased as the TEL increased and that the number of trips was higher with a 1.8-t TLL than with a 4.5-t TLL. Because of the number of management conditions examined, the effects of both TEL and TLL on each indicator variable are best illustrated by an isopleth plot with TELs and TLLs on the axes and with contours through equal values of the indicator. For example, the number of trips per season is shown as a function of TELs and the full range of TLLs in Fig. 4, where the contours connect equal numbers of trips per season. Figure 3 can be viewed as two vertical cross-sections through Fig. 4, one at TLL = 1.8 t and the second at TLL = 4.5 t.

The number of trips per season was greatest at low TELs and TLLs (the lower left corner of Fig. 4), which was expected with a fixed TAC. More trips were required to land the same amount of fish when there was less opportunity to catch fish in a trip, due to either low TLLs or low TELs. The upper right corner of the graph indicates that the number of trips per season was lower and relatively insensitive to variation in TELs and TLLs when both regulatory limits were high. In the upper left corner of Fig. 4, representing high TELs and low TLLs, the number of trips per season was highly sensitive to changes in the TLL, but not to changes in the TEL. The sensitivity of the number of trips to changes in the TLL suggests that this value was significantly limiting the amount of fish that could be landed from a trip in this region of the graph. The TEL did not obviously influence the number of trips in a season until it dropped below 8–10 hauls per trip. For cases where the TEL was at its lowest and the TLL was high, the contours of equal numbers of trips per season were nearly horizontal (lower right of Fig. 4), indicating that in those cases the TEL had become the limiting factor for trip landings.

To summarize Fig. 4 (also Fig. 5*a*), when the TLL was greater than 4 t and the TEL was greater than eight hauls per trip, changes in regulations had little effect on the number of trips required to catch the TAC in a season. However, below these values the number of trips required increased. The number of trips per season was most sensitive to changes in the more severe of the two regulations. When landings and effort were both strongly limited, the number of trips was equally sensitive to changes in either regulation.

The contours of equal value on the isopleth graphs for the other eight indicators (Figs. 5*b*–5*i*) can be interpreted similarly to show the sensitivity of these indicators to the different combinations of effort and landing regulations that we examined.

The number of hauls per trip (Fig. 5*b*) increased only slightly with increasing TLL. In contrast, the number of hauls per trip was very sensitive to TEL. For a given TLL, the average number of hauls per trip increased with increasing TEL, but was always less than the TEL. The difference between the TEL and the number of hauls was due to the stochastic nature of the catch, which resulted in some simulated vessels filling their quotas before their TEL was reached. These trends indicate that trips tended to go on as long as possible, high-grading the hauls to avoid exceeding the TLL, and finally terminating when the TLL was reached.

For a given TEL, the proportion of the TLL filled within a trip generally decreased as the TLL increased (Fig. 5*c*) because for a given availability of fish, there was a lower probability of reaching a landing limit as the limit increased. Conversely, for a given TLL, increases in the TELs resulted in a greater proportion of the TLL being filled, due to the increased opportunity to fill the landing limit through more hauls. However, there is a plateau in the upper left region of Fig. 5*c* which represents cases with high TELs and low TLLs. The height of this plateau, where less than all of the TLL was filled, was the result of high-grading behavior. Without high-grading, we would have expected the proportion of the TLL filled to continue up to form a plateau at 1.0 because with low TLLs and high TELs, there was ample opportunity to fill the landing limit. However, discarding some of the catch in favor of more valuable fish in future hauls resulted in some trips that did not fill their TLL. The stochastic nature of the availability of fish in our model contributed to this shortfall in the landings by creating situations where catches of higher quality fish did not occur before the end of the trip. This does not mean that high-grading was a poor decision (the decisions in this model are optimal by definition of the decision rules in our previous model analysis), but instead it means that *on average* it was more profitable to leave room for a possible catch of high-quality fish than to always land the full TLL. The tendency to leave space in the hold became extreme for the combination of the lowest TLL (0.9 t) and the highest TEL (12 and 14 hauls), causing the proportion of the TLL filled to drop below the plateau to values similar to those associated with higher TLLs. Here, where the opportunity to catch more high-quality fish was greatest, the strongest high-grading occurred, which can be seen clearly in Fig. 5*d*.

The economic value of the fish discarded during a trip (Fig. 5*d*) increased when TEL was increased, reflecting the greater amount of high-grading that occurred when there was more opportunity to catch fish. In contrast, when the TLL was increased, the total value of the discarded fish decreased because of the decrease in high-grading that accompanied less restrictive TLLs. The greatest total value of discarded fish, because of the greatest amount of high-grading, occurred for limits of 0.9 t on landings and 14 hauls on effort.

Not surprisingly, the value of a trip to a fisherman (Fig. 5*e*) is greatest when the TLL and the TEL are greatest; both regulatory actions appear equally effective at causing a change in that value. However, when either TEL or TLL was low, the value of a trip was unresponsive to changes in the other regulatory measure. Like Fig. 5*a*, Fig. 5*e* suggests that low values of either regulatory action could limit the maximum economic value of a trip. Unlike Fig. 5*a*, the value of a trip could still be increased by increasing either of the limits when both regulatory measures had high values. In short, both regulations limited the gross profits from a trip and the trip value was maximized when regulatory actions were minimal.

The trends in the value of the fish landed from a trip and the value of the fish discarded provided an insight into an interesting contrast that could occur in a real fishery. Comparing Figs. 5*d* and 5*e* shows that the combinations of regulations that led to extreme high-grading often resulted

in the value of fish discarded exceeding the value of fish landed (e.g., for a TEL of 14 and a TLL of 1, the value of discarded fish exceeded $4000, while the value of the fish landed was less than $1000). Even though the value of fish being landed from a trip was maximized by the discarding decisions, it is unlikely that either fishermen or managers would be content with a situation that was so obviously wasteful.

All indices of discarding over the entire season (Figs. 5*f*–5*i*) shared the same pattern as the economic value of the discards during a trip (Fig. 5*d*); they increased when the TEL was increased and they decreased when the TLL was increased. However, unlike Fig. 5*d*, the rate of change in the weight of fish discarded during a season, indicated by the distance between the contours (Figs. 5*f*, 5*h*, 5*i*), was not constant. This rate accelerated towards the upper left corner of the graphs, indicating that the sensitivity of the weight discarded to changes in regulations increased when TEL was high and TLL was low. The increased sensitivity of discarding to regulations would be expected with the onset of high-grading behavior, which occurred during conditions that allowed a vessel to catch more fish than it could keep (i.e., low TLLs and moderate to high TELs). The total weight of fish discarded from all size classes varied greatly with the combination of regulations in effect, ranging from less than 10 000 t to over 90 000 t. The majority of the discards were from the least valuable size class, Z (Fig. 5*i*), because high-grading discriminates against the less valuable size classes in favor of retaining the more valuable fish. Within this size class, the seasonal discards ranged from less than 5000 t to over 60 000 t (Fig. 5*i*). Some of the second most valuable size class (Y) was discarded under conditions favoring high-grading (Fig. 5*h*). The most valuable size class was never discarded in our model because discarding them could not improve the value of the landed catch.

The range in the proportion of the catch discarded per season (by weight) varied over the range of regulations studied from less than 0.1 to over 0.8 (Fig. 5*g*) and corresponds to the patterns in high-grading behavior that were discussed previously. The potential for TELs and TLLs to result in discarding over 80% of the total weight of fish caught in a season emphasizes the potential sensitivity of high-grading behavior to trip regulations implemented by management agencies.

Varying the total availability of fish by a constant factor did not change the general results observed in Fig. 5. There were some quantitative differences among the runs. For example, when the availability of fish was halved, the maximum proportion of the catch that was discarded was between 0.7 and 0.8, rather than over 0.8 as in the base case and the case where the availability of fish was doubled. Overall, the differences among the runs were minor and do not warrant further discussion.

In summary, Fig. 5 quantifies, to our knowledge for the first time, the potential effects of regulatory limits on trip effort and landings per trip on numerous relevant indicators. These results clearly illustrate that the manner in which regulations are imposed can strongly influence the extent of discarding arising specifically from high-grading behavior. The differences among the effects of regulations occur even though the availability of fish and TAC were constant. This modeling approach, based on the available data and incorporating the behavioral responses of fishermen who maximize trip value, provides a useful method for evaluating the potential consequences of proposed regulatory actions.

Management implications

We have not defined the relative importance of the indicators in Fig. 5; this would need to be done in a final analysis of any proposed regulations. Many different response variables can be considered in a multiattribute analysis of decisions (Keeney and Raiffa 1976). A formal presentation of this technique is beyond the scope of the present work, but it essentially involves weighting each indicator variable and then combining them through an objective function into a single utility value which is to be maximized.

In practice, managers may want to weight various indicators based on regional social needs or the expected long-term biological consequences of the regulations (Smith 1980; Wooster 1988; Department of Fisheries and Oceans 1990). For example, managers may want to minimize discarding (Fig. 5*g*) while attempting to keep both the economic value of a trip (Fig. 5*e*) and the proportion of the landing limits that are filled (Fig. 5*c*) high. The model indicates that these management goals would be met by large TLLs and TELs, corresponding to the upper right region of the graphs in Fig. 5. This region has the most desirable values, according to the stated objectives, for each of the three indicators under consideration.

Additionally, managers may want to include another factor in their objectives: to spread fishing effort more evenly throughout a season by increasing the number of trips required to land the TAC (Fig. 5*a*). This is a common reason for the implementation of TLLs in fisheries (e.g., Pikitch 1987*a*; Department of Fisheries and Oceans 1990). Our model indicates that this could be achieved by decreasing either the TLLs or the TELs from the levels discussed above, but both approaches will result in less desirable values for some of the indicators. The reduction of either limit will cause similar reductions in trip revenues (Fig. 5*e*), the reduction of the TLL alone will result in increased discarding (Fig. 5*g*), and the reduction of TEL alone will result in a smaller proportion of the TLL being filled in a trip (Fig. 5*c*). If both TEL and TLL were reduced, there would be little effect on either the proportion of the catch that was discarded (Fig. 5*g*) or the proportion of the TLL filled during a typical trip (Fig. 5*c*). The best combination of TEL and TLL regulations for the fishery will depend on the weights that the managers assign to each of these indicator variables in their objective function.

Our analysis in its present form does not provide valid recommendations for sablefish management in the Oregon trawl fleet. It is only a general analysis of the discarding process based on a small subset of data from that fleet. To justify specific application to the Oregon situation, further refinements of the model in many areas would be required. For instance, a definition of effort in the model which provided a closer approximation to actual time at sea would be necessary. This will be especially difficult in a multispecies fishery, such as this one, where entire

trips may catch the regulated species as a by-catch while pursuing other target species.

Factors omitted

There were many factors that we could not consider in this work due to lack of data or the amount of time that would be required to rerun both the dynamic program and the simulation model. The market values for the size classes, the relative availabilities of the size classes, and the influence of the costs of fishing on high-grading are all examples of factors that would require a complete reanalysis to study the effects of changing their values. However, there are reasons to believe that the results of our model are at least qualitatively robust to many of these factors.

For instance, the results of the model should be robust to different values per kilogram for the three size classes as long as the values can be ranked in the same order, because the model maximizes the value of the landed catch. With availabilities of the three size classes similar to those in our simulation model, keeping more of the most valuable size class will still give a greater value to the landed catch, regardless of the magnitude of the differences between the values. However, if the values of the size classes became approximately equal, the stochastic nature of fishing would probably make it unlikely that fishermen would distinguish between them, and high-grading would be less likely to occur.

The relative availability of the three size classes is not as important to high-grading behavior in our model as the absolute availability of the more valuable size classes. The important factor in the decision to high-grade is whether enough of the most valuable size class can be caught within the time constraints to justify discarding the other classes. Generally, as the more valuable size classes become more abundant, we would expect high-grading to become more common for any management regime. This was studied briefly in the simulation runs with higher and lower availabilities of fish that we discussed previously. However, our examination of the effects of fish availability on our results was limited; similar models should be built with fish availability estimates from other times or fisheries in order to make predictions about discarding behavior in those new situations.

The relationship between storage time and landed value was not examined in our work. Generally, the deterioration of stored fish should tend to reduce trip length and therefore reduce high-grading due the lower probability of filling the TLL. However, additional data would be required to test for and quantify this effect. This is a potential area for future research; such a study could provide new information about the potential impact of changing technologies (such as the introduction of freezers) on discarding practices in developing fisheries.

Fixed costs, such as the travel costs of going to and from the fishing grounds, should have little effect on our results under the patterns of fish availability explored. They will only offset the final landed value of the catch by a fixed amount and will not change the fact that increased profit is expected from high-grading behavior. However, variable costs related to fishing activities, such as fuel costs while trawling or the risk of gear damage during a haul, could reduce the expected benefit of waiting for more valuable fish in future hauls. If the costs associated with making additional hauls exceed the expected increase in profit from high-graded hauls, then high-grading will result in an economic loss and should not occur. Pikitch (1987*b*) estimated vessel operating costs off the Oregon coast as about $36.42 per trawling hour. With an average of four or five hauls in a day, these variable costs are small relative to many of the values of the landings per trip being considered (Fig. 5*e*), but not relative to those values for the cases where high-grading was most severe (at low TLLs and high TELs). Thus, the present model may overestimate high-grading behavior and the duration of trips when the limits on the amount of fish landed are low and the limits on effort are high or nonexistent. However, the inclusion of variable costs should cause little departure from our model's predictions when TLLs are large and TELs are low, nor will variable costs have a substantial influence on behavior when the gross profits are large.

Although we present a seasonal model, we do not consider temporal variation in costs or expected catches that could result in changing trip policies within seasons. For example, if some decrease in costs or increase in fish availability is expected due to seasonal or tidal distributions, then a current trip may be extended or a vessel may delay its departure in order to obtain better catch rates at sea. The temporal concentration of fish availability could make our model underestimate the discarding associated with a specific trip limit. In contrast, we would expect temporal variation in fixed costs to have little influence on the high-grading unless the resulting temporal concentration of effort influences the availability of fish experienced by the fleet. Seasonal patterns in variable costs may cause temporal variation on high-grading due to their influence on trip duration, favoring longer trips and high-grading when costs are low. Additional data and analysis, focusing on temporal variations in catch and costs for sablefish, will be necessary to develop a model incorporating these seasonal dynamics.

The simulation of a fishing season as a series of consecutive trips does not account for complexities that may exist in a fishery when many vessels are fishing concurrently and delivering their catch to one or a few processors. In these cases the discarding decisions at sea may be based on the capacity of processing plants rather than a vessel's hold or TLL. If discarding decisions are caused by processing constraints, then our model may provide a poor indication of high-grading practices. Given the interaction between the economic, biological, and social aspects of fishery systems, the effect of processing and marketing factors on discarding is an obvious area for further research.

Finally, the key assumption of our model, that fishermen maximize the value of their landed catch (profit) from each trip, may be false. Alternatively, they may maximize their rate of profit (profitability or landed catch per unit effort) while fishing. In both cases, we expect fishermen to attempt to maximize their profit over a season. Our focus on the final landed value from a trip is similar to the assumption often made by fisheries economists that "...for a fishing vessel, total revenue from a trip is more important than the marginal revenue created by a unit of output"

(Doll 1988). There are also other financial strategies, such as minimizing potential losses, which could dominate the system and make high-grading less likely than our model would suggest. In addition to economic goals, it is possible that noneconomic factors, such as the desire to be at sea, may play a role in determining the actual value of a fishing trip to fishermen and result in economically suboptimal behavior (Smith 1974, 1981). Identifying the goals used by fishermen in a particular situation is an important step in applying any model of fishermen's behavior to a fishery. We have made assumptions that we feel are reasonable based on available data, but a more detailed analysis with additional data would be required to determine the accuracy of those assumptions.

Conclusions

Our model, although extremely simplified in relation to the processes it represents, still provides important insights into how fishermen's behavior may respond to management actions and produce undesirable, but potentially predictable, results. Presently, regulations that focus on fishing trips are becoming a common management tool (Pikitch 1991; Department of Fisheries and Oceans 1991), while concerns about the influence of discarding on the reliability of catch and effort data are leading to the development of statistical means of estimating it (e.g., Tallman 1990). However, evaluations of alternative management plans and fisheries statistics in general may be misleading if they do not include considerations of fishermen's behavior (Hilborn 1985; Lane 1988). Modeling behavior will never fully reflect the dynamic and complex conditions influencing fishery systems; thus, models will never replace direct interactions by managers with members of the fleet. However, the value of a given method can only be measured by comparison with the other methods that are available. Presently, there is little formal methodology for the quantitative consideration of the effect of fishermen's behavior on the effectiveness of new regulations that can be used by management agencies. We suggest that explicitly evaluating the potential reactions of fishermen to management actions through modeling with the available data could be a better approach than current methods. If so, this will result in regulations that better achieve their goals while minimizing conflicts between managers and the fleet.

Acknowledgments

We are grateful to the many people who contributed to this paper. Colin Clark, Larry Dill, Dan Lane, Mike Lapointe, Bernard Roitberg, Ross Tallman, Al Tyler, and Ron Ydenberg commented on various versions of the manuscript. In addition, Larry Dill provided both work space and numerous constructive comments throughout the work. Dan Erickson coordinated sampling and collected most of the data in the original observer study; John Wallace organized and maintained the resulting data base. R.B. Fisher, commercial fishermen, and other members of the fishing industry made the original observer study possible. In addition to these specific tasks, all of the above also provided invaluable assistance through informal discussions, as did John Emlen and Nev Venables. The original observer study was supported by the Oregon Department of Fish and Wildlife, the National Marine Fisheries Service (grant Nos. NA86-86-ABH-00035 and NA88-ABH-00017), and the NOAA Office of Sea Grant (grant No. NA86AA-D-SG044). This study was supported by an NSERC scholarship and Simon Fraser University Postgraduate Awards to D.M. Gillis, an NSERC operating grant to R.M. Peterman, and a grant to E.K. Pikitch from the NOAA Office of Sea Grant (grant No. NA89AA-D-SG022).

References

Bellman, R. 1957. Dynamic programming. Princeton University Press, Princeton, N.J.

Caddy, J.F. 1982. Management of shrimp fisheries. *In* Fish by-catch — bonus from the sea: report of a technical consultation on shrimp by-catch utilization held in Georgetown, Guyana, 27–30 October 1981. IDRC, Ottawa, Ont. pp. 120–123.

Charnov, E.L. 1976. Optimal foraging: attack strategy of a mantid. Am. Nat. **110**: 141–151.

Department of Fisheries and Oceans. 1990. 1991 Atlantic groundfish multi-year management plan (1991–1993). Ottawa, Ont.

Department of Fisheries and Oceans. 1991. Pacific groundfish trawl management plan 1992. Ottawa, Ont.

Doll, J.P. 1988. Traditional economic models of fishing vessels: a review with discussion. Mar. Res. Econ. **5**: 99–123.

Garcia, S. 1988. Tropical penaeid prawns. *In* Fish population dynamics. 2nd ed. *Edited by* J.A. Gulland. John Wiley & Sons, New York, N.Y. pp. 219–250.

Gillis, D.M., Peterman, R.M., and Pikitch, E.K. 1995. Dynamic discarding decisions: foraging theory for high-grading in a trawl fishery. Behav. Ecol. **6**: 146–154.

Gulland, J.A. 1974. The management of marine fisheries. University of Washington Press, Seattle, Wash.

Halliday, R.G., Hay, D.E., and Metuzals, K.I. 1989. Wastage of American plaice (*Hippoglossoides platessoides* (Fabricus)) in the southern Gulf of St. Lawrence fishery in the 1970's. Can. Tech. Rep. Fish. Aquat. Sci. 1663.

Hilborn, R. 1985. Fleet dynamics and individual variation: why some people catch more fish than others. Can. J. Fish. Aquat. Sci. **42**: 2–13.

Hoag, S.H. 1975. Survival of halibut released after capture by trawls. International Pacific Halibut Commission, Seattle, Wash., Scientific Report No. 57.

IPHC. 1991. Annual report, 1990. International Pacific Halibut Commission, Seattle, Wash.

Kaspari, M. 1990. Prey preparation and the determinants of handling time. Anim. Behav. **40**: 118–126.

Keeney, R.L., and Raiffa, H. 1976. Decisions with multiple objectives: preferences and value tradeoffs. John Wiley & Sons, New York, N.Y.

Kulka, D.W., and Stevenson, S.C. 1986. Trends in discarding of divisions 2J3KL cod by the Newfoundland offshore fleet for 1981–1986, with particular reference to size of fish. CAFSAC Res. Doc. 86/101.

Lane, D.E. 1988. Investment decision making by fishermen. Can. J. Fish. Aquat. Sci. **45**: 782–796.

Mangel, M., and Clark, C.W. 1988. Dynamic modeling in behavioral ecology. Princeton University Press. Princeton, N.J.

May, R.M. [*Editor*]. 1984. Exploitation of marine communities. Springer-Verlag, Berlin.

Pikitch, E.K. 1987*a*. Impacts of management regulations on the catch and utilization of rockfish in Oregon. Proceedings of the International Rockfish Symposium, University of Alaska Sea Grant Report 87-2. pp. 369–382.

Pikitch, E.K. 1987*b*. Use of a mixed-species yield-per-recruit model to explore the consequences of various management policies for the Oregon flatfish fishery. Can. J. Fish. Aquat. Sci. **44**(Suppl. 2): 349–359.

Pikitch, E.K. 1988. Objectives for biologically and technically interrelated fisheries. *In* Fishery science and management. *Edited by* W.S. Wooster. Springer-Verlag, New York, N.Y. pp. 107–135.

Pikitch, E.K. 1991. Technological interactions in the US west coast groundfish trawl fishery and their implications for management. ICES Mar. Sci. Symp. **193**: 253–263.

Pikitch, E.K., Erickson, D.L., and Wallace, J.R. 1988. An evaluation of the effectiveness of trip limits as a management tool (preliminary report). NWAFC processed report 88-27, NOAA, U.S. Department of Commerce.

Powles, P.M. 1969. Size changes, mortality, and equilibrium yields in an exploited stock of American plaice (*Hippoglossoides platessoides*). J. Fish. Res. Board Can. **26**: 1205–1235.

Ricker, W.E. 1976. Review of the rate of growth and mortality of Pacific salmon in salt water, and noncatch mortality caused by fishing. J. Fish. Res. Board Can. **33**: 1483–1524.

Slavin, J.W. 1982. Utilization of the shrimp by-catch. *In* Fish by-catch — bonus from the sea: report of a technical consultation on shrimp by-catch utilization held in Georgetown, Guyana, 27–30 October 1981. IDRC, Ottawa, Ont. pp. 21–28.

Smith, C.L. 1974. Fishing success in a regulated commons. Ocean Dev. Int. Law J. **1**: 369–382.

Smith, C.L. 1980. Management provoked conflicts in the fisheries. Environ. Manage. **4**: 7–11.

Smith, C.L. 1981. Satisfaction bonus from salmon fishing: implications for economic evaluation. Land Econ. **57**: 181–194.

Stephens, D.W., and Krebs, J.R. 1986. Foraging theory. Princeton University Press, Princeton, N.J.

Tallman, R. 1990. Reduction of uncertainty caused by discarding in the fisheries of the Gulf of St. Lawrence. NAFO Sci. Counc. Stud. **16**: 39–48.

Wooster, W.S. 1988. Biological objectives of fisheries management. *In* Fishery science and management. *Edited by* W.S. Wooster. Springer-Verlag, New York, N.Y. pp. 1–6.

Relation of algal biovolume to chlorophyll *a* in selected lakes and wetlands in the north-central United States

James W. LaBaugh

Abstract: Algal chlorophyll *a* is commonly used as a surrogate for algal biomass. Data from three lakes in western Nebraska, five wetlands in north-central North Dakota, and two lakes in north-central Minnesota represented a range in algal biovolume of over four orders of magnitude and a range in chlorophyll *a* from less than 1 to 380 $mg \cdot m^{-3}$. Analysis of these data revealed that there was a linear relation, $\log_{10}$ algal biovolume = 5.99 + 0.09 chlorophyll *a* ($r^2 = 0.72$), for cases in which median values of chlorophyll *a* for open-water periods were less than 20 $mg \cdot m^{-3}$. There was no linear relation in cases in which median chlorophyll *a* concentrations were larger than 20 $mg \cdot m^{-3}$ for open-water periods, an occurrence found only in shallow prairies lakes and wetlands for years in which light penetration was the least.

Résumé : On utilise souvent la chlorophylle *a* des algues à la place de la biomasse algale. Les données de biovolume algal recueillies dans trois lacs de l'ouest du Nebraska, cinq terres humides du centre-nord du Dakota du Nord et deux lacs du centre-nord du Minnesota étaient réparties sur une fourchette de plus de quatre ordres de grandeur, tandis que la fourchette pour la chlorophylle *a* variait de moins de 1 à 380 $mg \cdot m^{-3}$. L'analyse de ces données a révélé une relation linéaire, $\log_{10}$ du biovolume algal = 5,99 + 0,09 de chlorophylle *a* ($r^2 = 0,72$), dans les cas où les concentrations médianes de chlorophylle *a* pour les périodes d'eau libre étaient inférieures à 20 $mg \cdot m^{-3}$. Il n'y avait pas de relation linéaire dans les cas où les concentrations médianes de chlorophylle *a* étaient supérieures à 20 $mg \cdot m^{-3}$ pour les périodes d'eau libre, phénomène observé seulement dans les lacs peu profonds des prairies et dans les terres humides les années où la pénétration de la lumière était la plus basse.

[Traduit par la Rédaction]

Introduction

Algal chlorophyll *a* commonly is used as a surrogate for algal biomass, to define the central tendency in algal biomass as an average of values for a specific period (Nicholls and Dillon 1978), to identify seasonal patterns for algal biomass (Marshall and Peters 1989), or to determine spatial variation in algal biomass (Cloern et al. 1992). Few investigations include independent analysis of both algal chlorophyll and algal biomass, measured either as wet weight or biovolume, because chlorophyll *a* is assumed to be a reasonable estimate of biomass and because wet weight or biovolume is not determined as readily as chlorophyll *a*. Statistically significant correlation between chlorophyll *a* and algal biomass has been reported by Desortova (1981) and Canfield et al. (1985). However, in both of those studies, chlorophyll *a* content varied considerably per unit phytoplankton biovolume. Tolstoy (1979) found good agreement between chlorophyll *a* and phytoplankton volume in some but not all lakes that were part of that study; the weakest relation was found in an oligotrophic lake and attributed to methodological error. Statistically significant linear relations between chlorophyll *a* and dry weight varied with season and taxa as reported by Bailey-Watts (1978). From the rare studies which have included measurement of both algal chlorophyll *a* and algal biomass, as biovolume or weight, it is obvious that chlorophyll *a* can be an approximation of algal biomass. Yet, the variability in that approximation has not been quantified using data derived from common methods of analysis for a variety of aquatic environments.

Chlorophyll *a* has been used as an estimate of algal biomass in several studies relating various environmental factors to algal biomass (Dillon and Rigler 1974; Hoyer and Jones 1983; Prepas and Trew 1983; Molot and Dillon 1991). Empirical phosphorus–chlorophyll *a* relations have been used as a basis for management of algal biomass in lakes (Hutchinson et al. 1991), but the variation in data used to derive such empirical relations is large (Knowlton et al. 1984) and has been the focus of subsequent study

Received January 11, 1994. Accepted July 14, 1994.
J12226

J.W. LaBaugh. U.S. Geological Survey, Water Resources Division, Mail Stop 413, Denver Federal Center, Lakewood, CO 80225, USA.

to evaluate the sources of variability in the relation (Molot and Dillon 1991). One source of variability is the fact chlorophyll content of algae can vary as a function of light and nutrient levels, leading to some debate over the suitability of using chlorophyll *a* as an estimate of algal biomass (Watson et al. 1992). Watson et al. (1992) found similar sigmoid relations between phosophorus and algal chlorophyll and phosphorus and algal biovolume, indicating that the relation between phosphorus and biomass was not a function of the choice of chlorophyll *a* as an estimator of biomass. Direct quantification of the relation between algal chlorophyll *a* and algal biomass over the wide range of available published data, determined using a variety of methods, was not part of the analyses presented by Watson et al. (1992). Comparison of algal chlorophyll *a* with algal biomass, as either biovolume or weight, over a large range in values for each, where methodological differences are not a factor, could prove useful in the debate concerning use of chlorophyll *a* as an estimate of algal biomass.

Algal chlorophyll *a* and algal biovolume determinations have been an integral part of limnological investigations from 1985 to 1990 at a group of wetlands and lakes in the north-central United States (Fig. 1). The study sites were selected as being representative of different hydrogeologic settings, where numerous lakes and wetlands are located, and lying within a climate gradient in midcontinent (Siegel and Winter 1980; Winter and Carr 1980; Winter 1986). Research at these sites was designed to examine how hydrologic processes affect the chemical and biological characteristics of these water bodies. The large range in values for chlorophyll *a* and algal biovolume at these sites, and the fact that uniform analytical methods were used, provided the opportunity to examine the relation between algal chlorophyll *a* and algal biovolume in these aquatic environments, which represent a large range in limnological conditions. The purpose of this article is to determine how well chlorophyll *a* estimates algal biovolume as a measure of the central tendency in algal biomass for open-water periods, and as a measure of seasonal changes of algal biovolume in these lakes and wetlands.

Study sites

The three study sites are different in geologic setting, vegetation, and climate. The Crescent Lake National Wildlife Refuge is in the Nebraska sand hills, an area of large, stable dunes composed of dune sand. The sand hills comprise Great Plains short-grass prairie where annual average lake evaporation exceeds annual average rainfall by 70 cm (Winter 1986). At the Cottonwood Lake National Waterfowl Production Area in central North Dakota, the tall-grass prairie is underlain by clayey, silty till of the large glacial drift complex of the Missouri Coteau and is in an area where average annual evaporation exceeds rainfall by about 50 cm (Winter and Carr 1980). Mixed deciduous–coniferous forest characterizes the Shingobee River watershed of north-central Minnesota, where evaporation is equal to rainfall based on annual averages and silty, sandy till typifies the glacial outwash plain the watershed lies within (Siegel and Winter 1980).

Lakes and wetlands at the study sites are also different based on size, depth, and chemical characteristics, but are similar with respect to controls on water balances. Lakes and wetlands at the prairie study sites were less than 2 m deep whereas the lakes at the Minnesota site were 8.5–10 m deep. With respect to surface area, the largest water bodies (50–300 ha) were the three lakes in Nebraska, the smallest were among the five wetlands in North Dakota (<1–40 ha), and the two Minnesota lakes were intermediate in size (36–66 ha). Chemical characteristics of water in the lakes and wetlands of the study were quite varied (LaBaugh 1988), ranging from fresh to mesosaline, circumneutral to alkaline, mesotrophic to hypertrophic, and with dominant anions either bicarbonate or sulfate. Seepage of groundwater into these lakes and wetlands, inputs from rain and snow, seepage of water from these lakes and wetlands to groundwater, and loss by evapotranspiration controlled the water balances of these water bodies, except for Shingobee Lake. Most of the lakes and wetlands in the study did not have channelized surface-water inlets or outlets. Only Shingobee Lake, Minnesota, had a surface-water inlet and outlet. Wetland P8 in North Dakota had an intermittent outlet.

Materials and methods

Water samples were collected approximately once each month between 1986 and 1987 when the three study lakes were ice-free at the Crescent Lake National Wildlife Refuge. At the Cottonwood Lake National Waterfowl Production Area, water samples were collected approximately once each month between 1985 and 1987 when the five study wetlands were ice-free. At the Shingobee River watershed site, samples were collected from two lakes every 2 weeks when lakes were ice-free and monthly when the lakes were covered with ice. Sample collection procedures at the prairie sites are described in LaBaugh (1988). At the Minnesota site, sample collection was done by combining water collected just below lake surface with water collected by use of a van Dorn bottle at 1-m intervals through the photic zone, defined as twice the Secchi disk transparency.

At all sites, sample processing was the same once water samples were obtained. A 1-L bottle was filled with sample water and preserved with 10 mL of Lugol's solution for phytoplankton analysis. Species identification, enumeration, and biovolume determinations for algae were performed by R. Dufford, Ft. Collins, Colorado, using standard inverted microscope techniques with a Leitz phase-contrast inverted microscope with 12.5 oculars. Counts were made according to the procedure in APHA et al. (1980). Measurements of algal cells were made by microscopy and biovolume was determined using the methods and equations found in Willen (1976), Sicko-Goad et al. (1977), and Tikkanen (1986). For chlorophyll *a* analysis, a known volume of water was pumped through a Gelman A-E glass fiber filter. The filter was placed into a glass vial and shipped in ice to the U.S. Geological Survey National Laboratory in Arvada, Colorado, for determination of chlorophyll *a* by the liquid chromatographic and fluorometric technique described in Britton and Greeson (1988). In this method, glass fiber filters are homogenized in

Fig. 1. Location of study sites.

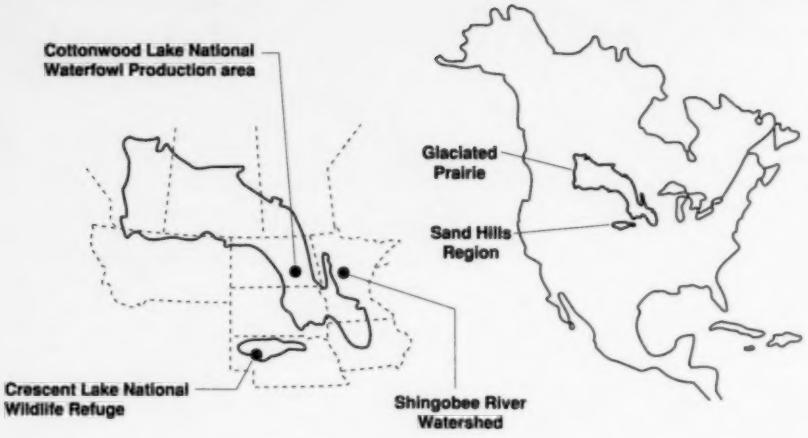

dimethyl sulfoxide, mixed with diethyl ether, centrifuged, ether separated from this mixture and combined with acetone, and injected into a high-pressure liquid chromatograph to separate pigments which are then measured by fluorometry.

Samples for chemical analyses also were collected concurrently by using sample collection procedures described in LaBaugh (1988) and those described above. Sample processing and analytical procedures for water collected for determination of total phosphorus and calculation of total nitrogen from determination of total Kjeldahl nitrogen, nitrate, and nitrite were the same as described in LaBaugh (1991).

Parametric statistical analyses were done using SAS[1] (SAS Institute Inc. 1990) on a workstation computer. Data used in these statistical analyses were from samples collected when the lakes and wetlands were not covered by ice. In general, this period of open water was between April and November. Regression analyses were done using data from the period 1985–1987 when data were available for more than one site. Robust nonparametric regression analyses were done using locally weighted scatter plot smoothing, also known as LOWESS (Cleveland 1979; Cleveland and McGill 1984). LOWESS uses weighted least squares to determine the pattern of the dependence of variable y on variable x.

Results

Data from all of the study sites included a large range in values (Table 1), four orders of magnitude for algal biovolume and from less than 1 to 380 mg·m^{-3} for chlorophyll *a*. For individual water bodies, larger ranges in values occurred at the prairie sites and smaller ranges occurred at the Minnesota site. A major use of chlorophyll *a* data is to provide an estimate of the central tendency in algal biomass for the period of most growth. Data in Table 1 provide the opportunity to examine the assumption that the central tendency in chlorophyll *a* data is related to the central tendency in algal biovolume data. Before this assumption can be addressed, it is necessary to determine what is an appropriate measure of the central tendency in these data.

Algal biovolume data from each lake or wetland were not representative of a sample from a normal distribution based on the Shapiro–Wilk test (SAS Institute Inc. 1990) at the 95% confidence level. With the exception of data from Goose Lake, chlorophyll *a* data also were not representative of a normal distribution. Algal biovolume and chlorophyll *a* data for all lakes and wetlands had sufficient disparity between the number of larger values and the number of smaller values that the arithmetic mean was a misleading measure of the central tendency of the data for open-water periods. Thus, median values for data from each year from each lake or wetland were used to make comparisons between the central tendencies in algal biovolume and chlorophyll *a* data from this study.

Two different patterns emerged from the median values for open-water periods of each year for which data were available for more than one site (1985–1987): an apparent linear relation for cases where median chlorophyll *a* concentrations were smaller than 20 mg·m^{-3} and no apparent relation for cases where median chlorophyll *a* concentrations were larger than 20 mg·m^{-3} (Fig. 2). The pattern in the relation between algal biovolume and chlorophyll *a* determined by LOWESS regression analysis (f = 0.5) confirmed that there was a linear increase in algal biovolume as chlorophyll *a* increased when median values of chlorophyll *a* were less than 20 mg·m^{-3} (Fig. 2). LOWESS analysis also indicated that for median values of chlorophyll *a* greater than 20 mg·m^{-3}, larger median values of chlorophyll *a* did not correspond to larger median values of algal biovolume.

The correspondence between increases in chlorophyll *a* and algal biovolume for cases in which median values of chlorophyll *a* were less than 20 mg·m^{-3} was quantified using parametric statistical analyses. Correlation analysis requires data from a normal distribution (Steel and Torrie 1980). Base 10 logarithms of chlorophyll *a* and algal

[1] Any use of trade, product, or firm names is for descriptive purposes only and does not imply endorsement by the U.S. Government.

Table 1. Median and range of values of algal biovolume and chlorophyll *a* for the period of open water from 1985 to 1990.

Study site	Year	Algal biovolume, millions of $\mu m^3 \cdot mL^{-1}$			Chlorophyll *a*, $mg \cdot m^{-3}$		
		Median	Minimum	Maximum	Median	Minimum	Maximum
Crescent Lake National Wildlife Refuge, Nebraska							
Goose Lake	1986	9.11	1.76	117	62	0.9	110
	1987	21.7	3.64	74.1	14	7.1	51
Island Lake	1986	11.0	4.77	274	28.5	6.8	78
	1987	14.6	4.36	95.9	11	3.7	22
Roundup Lake	1986	13.3	2.18	72.2	55.5	10	114
	1987	31.7	4.36	269	59	14	220
Cottonwood Lake National Waterfowl Production Area, North Dakota							
Wetland P1	1985	0.786	0.443	3.09	1.8	0.7	3.9
	1986	1.75	0.244	6.69	2.7	0.8	7.7
	1987	2.41	0.237	12.87	2.9	0.6	11
Wetland P8	1985	1.10	0.191	25.1	2.1	0.4	17
	1986	3.18	0.340	10.2	2.2	0.4	15
	1987	1.62	0.097	34.4	2.3	0.6	14
Wetland P11	1985	8.68	0.256	37.7	7.2	0.8	220
	1986	3.98	0.148	36.4	10	1.2	110
	1987	0.615	0.057	33.7	1.9	0.3	46
Wetland T3	1985	28.5	18.7	39.7	16	13	230
	1986	3.17	1.19	91.0	47	4.8	380
	1987	10.6	0.828	28.2	32	2.6	81
Wetland T8	1985	4.78	1.41	13.2	4.1	2.3	7.2
	1986	5.53	2.02	8.60	7.4	5.9	8.3
	1987	1.74	0.353	36.0	7.8	1.4	140
Shingobee River Watershed, Minnesota							
Shingobee Lake	1989	4.65	0.494	12.1	8.6	5.2	14
	1990	7.70	0.533	22.8	6.6	3.7	13
Williams Lake	1985	3.43	0.584	19.9	3.55	1.7	7.9
	1986	1.90	0.701	4.97	6.2	1.9	15
	1987	3.38	0.864	8.44	3.85	1.9	12
	1988	2.72	1.70	8.57	4.75	0.8	13
	1989	1.88	0.644	4.64	4.7	2.3	8.7
	1990	3.27	1.00	7.10	3.45	1.6	14

biovolume data were representative of a sample from a normal distribution based on the Shapiro–Wilk test at the 95% confidence level. There was a significant correlation, at the 95% level of significance, between algal biovolume and chlorophyll *a* ($r = 0.83$) for logarithmically transformed data.

Parametric least-squares regression analysis only requires dependent data to be from a normal distribution (Steel and Torrie 1980). The parametric least-squares regression equation for the relation shown in Fig. 3 is $\log_{10}$ (median algal biovolume) = 5.99 + 0.09 (median chlorophyll *a*). The coefficient of determination (r^2) for this regression was 0.72. The 95% prediction interval for the regression line is included in Fig. 3.

The regression equation above was determined using data from the years 1985–1987 for which data were available for more than one site, and included the widest range in both chlorophyll *a* and algal biovolume. Data for open-water periods from 1988 to 1990 were available from Williams Lake and for 1989–1990 from Shingobee Lake,

Fig. 2. Comparison of median values of algal biovolume and chlorophyll *a* for the period of open water in each year for each lake and wetland from which data were collected from 1985 to 1987, including the relation of algal biovolume and algal chlorophyll *a* based on the LOWESS regression line.

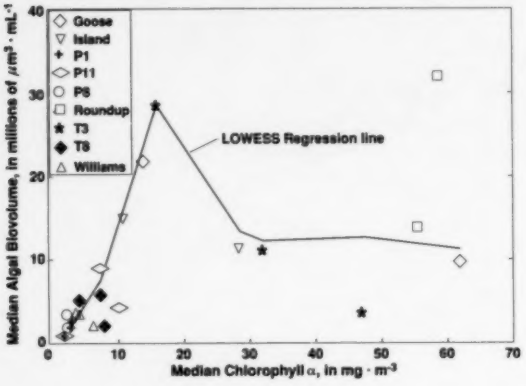

Fig. 3. Relation to the $\log_{10}$ median of algal biovolume to median chlorophyll *a* based on 1985–1987 data in which median chlorophyll *a* was less than 20 mg·m^{-3}, including the 95% prediction interval and data for 1988–1990.

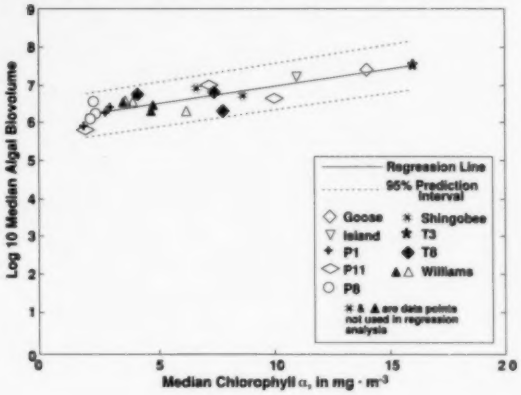

data not used to determine the regression line. Median values for open-water periods for the years 1988–1990 from these two lakes were within the prediction interval of the regression line (Fig. 3), verifying the regression model. Therefore, chlorophyll *a* provided a reasonable estimate of median algal biovolume in a variety of lakes and wetlands when median values of chlorophyll *a* for an open-water period of a year were less than 20 mg·m^{-3}.

Examination of the relation of chlorophyll *a* content per unit algal biovolume to absolute chlorophyll *a* concentration did not reveal any distinct patterns when all water bodies were considered. Yet, for individual water bodies, Goose and Island lakes, wetland T3, and Shingobee and Williams lakes, there was more chlorophyll *a* per unit algal biovolume at larger concentrations of chlorophyll *a*. Larger concentrations of chlorophyll *a*, median values greater than 20 mg·m^{-3}, and larger ratios of chlorophyll *a* per algal biovolume were found in Goose and Island lakes and wetland T3 in years in which light penetration was the least and turbidity the greatest. In contrast with Shingobee and Williams lakes, in which Secchi disk transparency values were greater than 2 m, values in the Nebraska lakes commonly were less than 0.5 m. Secchi disk transparency was not measured at the North Dakota site, but the wetlands were as turbid as the Nebraska lakes when chlorophyll *a* concentrations were large and the bottom sediments of the wetlands were visible when chlorophyll *a* concentrations were small.

Decreased light penetration and increased turbidity can explain the change in the relation of chlorophyll *a* to algal biovolume when median chlorophyll *a* values were larger than 20 mg·m^{-3}; however, the relation could be affected by other factors such as nutrient content of water or taxonomic composition of the algal community. Some of the variation in chlorophyll *a* content per unit biovolume was consistent with changes in either total phosphorus or total nitrogen in individual water bodies. The amount of chlorophyll *a* per unit biovolume, based on open-water period medians, increased as total phosphorus increased in Goose Lake and in wetland T8 (Table 2). Chlorophyll *a* content of algal biovolume increased as total nitrogen increased in Roundup Lake. These relations were unique to each water body in which they occurred; there was no common relation that could be quantified for a group of water bodies.

The fact that some of the variation in chlorophyll *a* content of the algae varied with taxamonic composition was evident from wetland T3 and Roundup Lake. In wetland T3, diatoms constituted the largest fraction of total algal biovolume, greater than 75%, when the ratio of chlorophyll to biovolume was the least whereas when the ratio was largest, diatoms generally were less than 25%. Similarly, in Roundup Lake, during periods of larger chlorophyll *a* concentrations, the ratio was smaller when diatoms were abundant and the ratio was larger when diatoms were less abundant and cyanobacteria were most abundant. However, the difference in the relation of chlorophyll *a* to algal biovolume between cases when the median concentration of chlorophyll *a* was less than or greater than 20 mg·m^{-3} could not be explained by taxonomic composition of the algal communities. For example, cyanobacteria were most abundant in Goose Lake, typically representing greater than 50% of total algal biovolume. Yet the relation between algal biovolume and chlorophyll *a* was not the same in each year of the study (Table 1, Fig. 2).

Water bodies in the study were not uniform with respect to the percent composition of total algal biovolume represented by major taxa. Chlorophyta constituted the largest fraction of algal biovolume in wetland T8 in 1985 and 1987 and in wetland P11 in 1985 and 1986. Diatoms were prominent in wetland P11 in 1987, wetland T3 in 1985, Roundup Lake in 1987, and Island Lake in 1986. Cyanobacteria represented 50% of algal biovolume in Shingobee Lake in 1990. Dinoflagellates were most common in Williams Lake. In wetlands P1 and P8, cryptophyta usually were the most abundant algae.

Data presented in Fig. 3 established the relation between open-water period medians; of additional interest is the

Table 2. Median values for the ratio of chlorophyll *a* to algal biovolume (millions of $\mu m^3 \cdot mL^{-1}$), total phosphorus, and total nitrogen for the period of open water from 1985 to 1990.

Study site	Year	Median		
		Ratio of chlorophyll *a* to algal biovolume	Total phosphorus, $\mu mol \cdot L^{-1}$	Total nitrogen, $\mu mol \cdot L^{-1}$
Crescent Lake National Wildlife Refuge, Nebraska				
Goose Lake	1986	6.1	20	1000
	1987	1.3	5	1070
Island Lake	1986	2.0	2	168
	1987	0.4	2	207
Roundup Lake	1986	3.6	23	538
	1987	1.9	26	326
Cottonwood Lake National Waterfowl Production Area, North Dakota				
Wetland P1	1985	1.6	2	282
	1986	1.9	1	197
	1987	1.0	1	162
Wetland P8	1985	2.1	4	226
	1986	2.1	2	169
	1987	1.2	3	175
Wetland P11	1985	2.1	5	336
	1986	5.2	3	324
	1987	3.7	6	210
Wetland T3	1985	0.4	6	342
	1986	9.1	9	406
	1987	2.9	3	309
Wetland T8	1985	0.5	7	228
	1986	1.3	13	299
	1987	3.9	25	232
Shingobee River Watershed, Minnesota				
Shingobee Lake	1989	1.9	0.7	55
	1990	0.8	1	57
Williams Lake	1985	0.6	0.4	42
	1986	3.5	0.3	44
	1987	1.7	0.4	51
	1988	1.5	0.2	49
	1989	2.1	0.3	51
	1990	1.0	0.3	50

relation of the seasonal pattern of change in algal biovolume to that of chlorophyll *a* in individual water bodies. Data from Roundup Lake did not fall in the region of Fig. 3 defined by a linear relation between biovolume and chlorophyll *a*. Median values for each year from Roundup Lake were larger than 20 $mg \cdot m^{-3}$. However, on a seasonal basis, changes in biovolume were reflected by changes in chlorophyll *a*, although the changes were not strictly parallel (Fig. 4). For other water bodies in this study, results were similar; seasonal changes in biovolume based on individual observations were generally reflected by changes in chlorophyll *a*. Best agreement, based on correlation coefficients for logarithmically transformed data, occurred in wetland P11 ($r = 0.78$, $P > |r| = 0.0001$) and Roundup Lake ($r = 0.74$, $P > |r| = 0.001$); least agreement, based on no statistically significant correlation, occurred in Goose

Fig. 4. Seasonal changes in algal biovolume and chlorophyll *a* in Roundup Lake, based on individual observations.

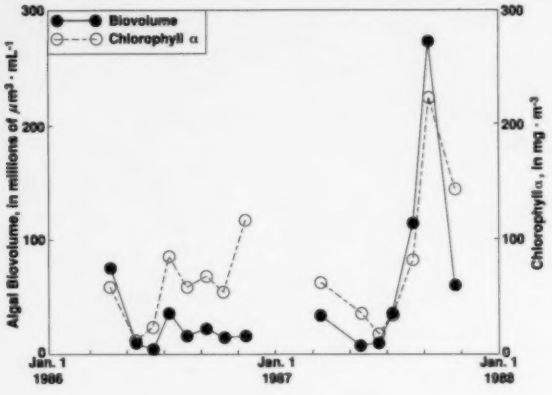

Fig. 5. Seasonal changes in algal biovolume and chlorophyll *a* in Williams Lake, based on LOWESS analyses using data for the period 1985–1990.

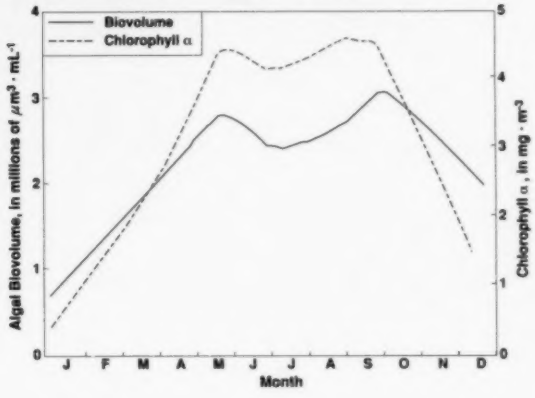

and Island lakes. In Williams Lake, availability of multiyear (1985–1990) data enabled determination of a general seasonal pattern by using LOWESS analysis (Fig. 5). Multiyear data from Williams Lake also made it possible to calculate a median value for each month of the year by combining data from all years for each month. Use of monthly median data provided better agreement between seasonal changes in biovolume and chlorophyll *a* ($r = 0.90$, $P > |r| = 0.0001$) than for individual observations from Williams Lake ($r = 0.56$, $P > |r| = 0.0001$).

Discussion

Chlorophyll *a* has been considered to be a measure of algal biomass in many investigations, although there are relatively few studies that have quantified the relation between chlorophyll *a* and some other independent measure of algal biomass, such as algal biovolume or wet weight. The few studies that have made this comparison have focused on individual water bodies (Nicholls 1976) or a set of water bodies in a particular region (Tolstoy 1979; Canfield et al. 1985). Some of these studies have used literature values from other investigations of individual lakes or limnological regions to document variability in chlorophyll *a* content per unit algal biovolume (Nicholls and Dillon 1978; Tolstoy 1979) while recognizing the fact that differences in analytical methods between investigations can contribute to some of the variation in the ratio. In the investigation of water bodies from three distinct limnological settings in the north-central United States presented here, common methods were used, enabling comparisons between water bodies and regions without the confounding effects of methodological differences. Even so, there was considerable variation in the relation between chlorophyll *a* and algal biovolume, based on seasonal correlations and comparison of open-water medians.

Light is one of the factors that have been related to variations in chlorophyll *a* content per unit algal biomass. Jones and Ilmavirta (1978), Nicholls and Dillon (1978), and Desortova (1981) found that decreased availability of light was related to increased chlorophyll *a* content per unit algal biovolume. In the case of the prairie lakes and wetlands having the larger median values of chlorophyll *a*, increased chlorophyll *a* content per unit algal biovolume was associated with increased turbidity or decreased light penetration except for Roundup Lake, which had less year-to-year variation in light penetration. In Roundup Lake, increased chlorophyll *a* per unit algal biovolume was related to differences in total nitrogen instead. Canfield et al. (1985) reported that nitrogen affects chlorophyll *a* content of algal biomass but found no relation of the ratio to differences in light penetration.

The fact that nutrient content is another important factor affecting the ratio of chlorophyll *a* to algal biovolume has been documented by previous studies. In addition to Canfield et al. (1985) noting that increased total nitrogen was associated with increased chlorophyll *a* per unit algal biomass, Nicholls and Dillon (1978) reviewed the relation of nitrogen to the ratio found in the literature and came to a similar conclusion. The effect of nitrogen on the chlorophyll *a* to algal biovolume ratio is not universal, as demonstrated by data presented here. In some cases, increases in the ratio were coincident with increases in total phosphorus, or not clearly related to either nitrogen or phosphorus.

Another factor that could affect the chlorophyll *a* to algal biomass ratio is the relative abundance of different taxonomic groups. Tolstoy's (1979) study of several lakes indicated that the smallest ratios were characteristic of Bacillariophyceae. Similarly, in the study presented here, the smallest ratio of chlorophyll *a* to algal biovolume in wetland T3 occurred in the year diatoms were most abundant. Nicholls and Dillon (1978) and Tolstoy (1979) cited several studies to demonstrate that there are differences between taxa with respect to chlorophyll *a* content per unit algal biomass. Despite the differences between chlorophyll content of various taxa, both Nicholls and Dillon (1978) and Tolstoy (1979) indicated that other factors such as light and nutrients could have a larger effect on the chlorophyll *a* to algal biovolume ratio. Desortova (1981) found little effect of taxonomic composition on chlorophyll *a* contents

of the algae. Canfield et al. (1985) noted the chlorophyll *a* content of cyanobacteria was less than that in other taxa but concluded that taxonomic differences could not explain differences in the chlorophyll *a* to algal biovolume ratios in their study. The lakes and wetlands selected for the study presented here encompass much variety in the relative abundance in different taxa, both between water bodies and within water bodies from year to year. Yet no clear relation was evident with respect to relative taxonomic abundance and chlorophyll *a* content of the algal community, a finding consistent with previous studies.

Few studies have been done that include analysis of both chlorophyll *a* and some other measure of algal biomass to examine the assumption that chlorophyll *a* is a representative measure of algal biomass (Nicholls and Dillon 1978; Tolstoy 1979; Desortova 1981; Canfield et al. 1985). The study reported here found that median values of chlorophyll *a* could be used to estimate the median of algal biovolume over a range of three orders of magnitude in biovolume, with a prediction interval of approximately one order of magnitude, but only when cases were considered for median chlorophyll *a* concentrations less than 20 $mg \cdot m^{-3}$.

The absence of data sets including both algal biomass and chlorophyll *a* to determine how well seasonal changes in the algal biomass can be examined by use of the chlorophyll *a* has forced some investigators to use indirect comparisons (Marshall and Peters 1989). Concurrent determination of algal biovolume and chlorophyll *a* in this study allowed for direct comparison of the data for a wide range of water bodies. Although there was general agreement between seasonal changes in chlorophyll *a* and algal biovolume in the individual water bodies in the study, this agreement was not uniform.

Evidence from this study demonstrates that there can be considerable variation in the relation between chlorophyll *a* and algal biomass across a wide range of limnological conditions, variation that is not method dependent. There is no doubt that chlorophyll *a* will continue to be used instead of direct microscopic determinations of algal biomass because of its widespread use in empirical models (Hutchinson et al. 1991), even though Nicholls and Dillon (1978) suggested that direct determinations of algal biomass could lead to improved empirical relations, a finding disputed by Canfield et al. (1985). Results presented here reinforce the fact that chlorophyll *a* is an approximation of algal biomass, and as an approximation is likely a factor affecting variation in empirical relations between environmental characteristics, such as nutrients, and chlorophyll *a* concentrations. The lack of a relation between median values of chlorophyll *a* and algal biovolume for median chlorophyll *a* concentrations greater than 20 $mg \cdot m^{-3}$ also points out the usefulness of having alternative measures of algal biomass in waters containing large quantities of algae and where light penetration is limited.

Acknowledgements

I thank Ted McConnaughey, David Mueller, Jack Jones, and an anonymous reviewer for their reviews of previous versions of the manuscript. I appreciate the invaluable assistance of George Swanson at the Cottonwood Lake site, whose work there made possible the data used in this article.

References

American Public Health Association (APHA), American Water Works Association (AWWA), and Water Pollution Control Federation (WPCF). 1980. Standard methods for the examination of water and wastewater. 15th ed. Washington, D.C.

Bailey-Watts, A.E. 1978. A nine-year study of the phytoplankton of the eutrophic and non-stratifying Loch Leven (Kinross, Scotland), J. Ecol. **66**: 741–771.

Britton, L.J., and Greeson, P.E. (*Editors*). 1988. Methods for collection and analysis of aquatic biological and microbiological samples. Tech. Water-Resources Invest. U.S. Geol. Surv. Book 5, Chap. A4, Lakewood, Colo.

Canfield, D.E. Jr., Linda, S.B., and Hodgson, L.M. 1985. Chlorophyll–biomass–nutrient relationships for natural assemblages of Florida phytoplankton. Water Resour. Bull. **21**: 381–391.

Cleveland, W.S. 1979. Robust locally weighted regression and smoothing scatterplots. J. Am. Stat. Assoc. **74**: 829–836.

Cleveland, W.S., and McGill, R. 1984. The many faces of a scatterplot. J. Am. Stat. Assoc. **79**: 807–822.

Cloern, J.E., Alpine, A.E., Cole, B.E., and Heller, T. 1992. Seasonal changes in the spatial distribution of phytoplankton in small, temperate-zone lakes. J. Plankton Res. **14**: 1017–1024.

Desortova, B. 1981. Relationship between chlorophyll *a* concentration and phytoplankton biomass in several reservoirs in Czechoslovakia. Int. Rev. Gesamten Hydrobiol. **66**: 153–169.

Dillon, P.J., and Rigler, F.H. 1974. The phosphorus–chlorophyll relationship in lakes. Limnol. Oceanogr. **19**: 767–773.

Hoyer, M.V., and Jones, J.R. 1983. Factors affecting the relation between phosphorus and chlorophyll *a* in midwestern reservoirs. Can. J. Fish. Aquat. Sci. **40**: 192–199.

Hutchinson, N.J., Neary, B.P., and Dillon, P.J. 1991. Validation and use of Ontario's Trophic Status model for establishing lake development guidelines. Lake Reservoir Manage. **7**: 13–23.

Jones, R.I., and Ilmavirta, V. 1978. Vertical and seasonal variation of phytoplankton photosynthesis in a brown-water lake with winter ice cover. Freshwater Biol. **8**: 561–572.

Knowlton, M.F., Hoyer, M.V., and Jones, J.R. 1984. Sources of variability in phosphorus and chlorophyll and their effects on use of lake survey data. Water Resour. Bull. **20**: 397–407.

LaBaugh, J.W. 1988. Relation of hydrogeologic setting to chemical characteristics of selected lakes and wetlands within a climate gradient in the north-central United States. Verh. Int. Ver. Limnol. **23**: 131–137.

LaBaugh, J.W. 1991. Spatial and temporal variation in chemical characteristics of groundwater adjacent to selected lakes and wetlands in the north-central United States. Verh. Int. Ver. Limnol. **24**: 1588–1594.

Marshall, C.T., and Peters, R.H. 1989. General patterns in the seasonal development of chlorophyll *a* for temperate lakes. Limnol. Oceanogr. **34**: 856–867.

Molot, L.A., and Dillon, P.J. 1991. Nitrogen/phosphorus ratios and the prediction of chlorophyll in phosphorus limited lakes in Central Ontario. Can. J. Fish. Aquat. Sci. **48**: 140–145.

Nicholls, K.H. 1976. Nutrient–phytoplankton relationships in the Holland Marsh, Ontario. Ecol. Monogr. **46**: 179–199.

Nicholls, K.H., and Dillon, P.J. 1978. An evaluation of phosphorus–chlorophyll–phytoplankton relationships for lakes. Int. Rev. Gesamten Hydrobiol. **63**: 141–154.

Prepas, E.E., and Trew, D.O. 1983. Evaluation of the phosphorus–chlorophyll relationship for lakes off the Precambrian Shield in western Canada. Can. J. Fish. Aquat. Sci. **40**: 27–35.

SAS Institute Inc. 1990. SAS procedures guide version 6, 3rd edition. SAS Institute Inc., Cary, N.C.

Sicko-Goad, L., Stoemer, E.F., and Lakewski, B.G. 1977. A morphometric method for correcting phytoplankton cell volume estimates. Protoplasma, **93**: 147–163.

Siegel, D.I., and Winter, T.C. 1980. Hydrologic setting of Williams Lake, Hubbard County, Minnesota. U.S. Geol. Surv. Open-File Rep. 80-403. St. Paul, Minn.

Steel, R.G.D., and Torrie, J.H. 1980. Principles and procedures of statistics. 2nd edition. McGraw-Hill, New York, N.Y.

Tikkanen, T. 1986. Kasviplanktonopas. Suomen Luonnonsuojelun Tuki Oy, Helsinki.

Tolstoy, A. 1979. Chlorophyll *a* in relation to phytoplankton volume in some Swedish lakes. Arch. Hydrobiol. **85**: 133–151.

Watson, S., McCauley, E., and Downing, J.A. 1992. Sigmoid relationships between phosphorus, algal biomass, and algal community structure. Can. J. Fish. Aquat. Sci. **49**: 2605–2610.

Willen, E. 1976. A simplified method of phytoplankton counting. Phycol. J. **11**: 265–278.

Winter, T.C. 1986. Effect of ground-water recharge on configuration of the water table beneath sand dunes and on seepage in lakes in the Sandhills of Nebraska, U.S.A. J. Hydrol. **86**: 221–237.

Winter, T.C., and Carr, M.R. 1980. Hydrologic setting of wetlands in the Cottonwood Lake area, Stutsman County, North Dakota. U.S. Geol. Surv. Water-Resources Invest. Rep. 80-99, Denver, Colo. 42 p.

Population dynamics, growth, and production of the Asiatic clam, *Corbicula fluminea*, in a blackwater river[1]

David L. Stites, Arthur C. Benke, and David M. Gillespie

Abstract: In a sixth-order blackwater river (Lower Coastal Plain of Georgia, USA), the average life span of *Corbicula fluminea* (Müller) was 3–4 years, with shell length reaching only 18–20 mm by the third year. Mean density was usually <200/m^2 over a 43-month period, but >1000/m^2 in population centers. Mean biomass (dry mass of soft tissue) was consistently 1–5 g/m^2, but averaged 11 g/m^2 in population centers. Biomass growth rates of clams reared in situ were highest in late spring and were inversely related to clam mass. Production ranged from 0.18 g·m^{-2}·year^{-1} at a main-channel site to 3.2 in a backwater and averaged 1.2–1.7 for 2 consecutive years. In population centers, production reached 9–23 g·m^{-2}·year^{-1}. Production was highest in spring and fell to zero in winter when growth ceased. Annual production/biomass values were about 4–8 for first-year individuals, but ranged from 0.51 to 1.78 overall. Individual size, growth rates, and production all indicated that this blackwater river was a stressful environment for *Corbicula*, probably due to low alkalinity (<30 mg/L as $CaCO_3$). Unlike its effect in many other systems, the clam appears to play a minor role in the trophic dynamics of this river.

Résumé : Dans une rivière d'eau noire de sixième ordre (basse plaine côtière de Géorgie, États-Unis), la durée de vie moyenne de la *Corbicula fluminea* (Müller) était de 3–4 ans, la longueur de la coquille n'atteignant que 18–20 mm la troisième année. La densité moyenne était généralement de < 200/m^2 sur une période de 43 mois, mais de > 1 000/m^2 dans les zones de concentration. La biomasse moyenne (masse sèche de tissus mous) était régulièrement de 1–5 g/m^2, mais atteignait en moyenne 11 g/m^2 dans les zones de concentration. Les taux de croissance de la biomasse de coquillages élevés sur place atteignaient un sommet à la fin du printemps et étaient inversement proportionnels à la masse des coquillages. La production se situait entre 0,18 g·m^{-2}·a^{-1} dans un site du chenal principal et 3,2 dans un bras dormant, et atteignait en moyenne 1,2 à 1,7 pendant 2 années consécutives. Dans les zones de concentration, la production atteignait 9–23 g·m^{-2}·a^{-1}. La production était maximale au printemps et tombait à zéro en hiver lorsque la croissance cessait. Les valeurs de production annuelle et de biomasse étaient d'environ 4–8 pour les individus de première année, mais variaient de 0,51 à 1,78 dans l'ensemble. La taille des individus, les taux de croissance et la production indiquaient que cette rivière constituait pour la *Corbicula* un milieu difficile, probablement en raison de sa faible alcalinité (< 30 mg/L de $CaCO_3$). Contrairement à ce qui se passe dans de nombreux autres systèmes, ce coquillage semble jouer ici un rôle mineur dans la dynamique trophique de la rivière.

[Traduit par la Rédaction]

Introduction

Corbicula fluminea is a well-known exotic freshwater bivalve introduced to the west coast of North America in the 1920's (e.g., Counts 1986). It has spread to at least 33 of the 49 continental states (Counts 1986) and into Northern and Central Mexico (Hillis and Mayden 1985), apparently limited in its geographic distribution only by low (<2°C) winter temperatures (e.g., Mattice and Dye 1976; McMahon 1983). *Corbicula fluminea* occurs in both

Received February 9, 1994. Accepted August 5, 1994.
J12265

D.L. Stites.[2] Department of Biology, Emory University, Atlanta, GA 30322, USA.
A.C. Benke.[3] A-122 Bevill Building, Department of Biological Sciences, University of Alabama, Tuscaloosa, AL 35487-0206, USA.
D.M. Gillespie. Graduate School and Research, University of Guam, UOG Station, Mangilao, Guam 96913.

[1] Contribution No. 215, University of Alabama Aquatic Biology Program.
[2] Present address: St. Johns River Water Management District, P.O. Box 1429, Palatka, FL 32078-1429, USA.
[3] Author to whom reprints requests should be addressed.

Fig. 1. Location of section transect sites on the Ogeechee River, Georgia.

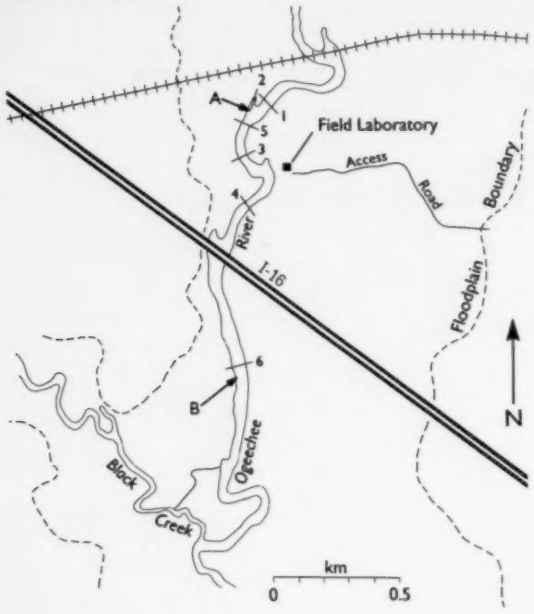

lentic and lotic habitats in its native southeast Asia (e.g., Morton 1986) and has been particularly successful in well-oxygenated, flowing waters of North America (Counts 1986). During the 1960's and 1970's, *Corbicula* dispersed widely throughout the southeastern United States, where it has become a major component of the benthic communities in most freshwater environments (McMahon 1983; Counts 1986). *Corbicula* originally attracted considerable attention as an economically important fouling organism in irrigation and drainage canals and water distribution and industrial water use systems (e.g., Isom 1986; Potter and Liden 1986). However, its ecological influence in natural lotic systems has become a major concern and requires basic population studies of factors affecting its growth, bioenergetics, and production dynamics.

Population studies of *Corbicula* in North America have often focused on artificial or disturbed habitats including irrigation/drainage canals (Heinson 1958; Eng 1979; Marsh 1985), oligohaline environments (Heinson 1958; Diaz 1974), and reservoirs (Dreier 1977; Aldridge and McMahon 1978; Abbott 1979; Williams and McMahon 1986). Growth studies of individuals and populations have been made in reservoirs (Britton et al. 1979; Buttner and Heidinger 1980) and dammed, dredged, or otherwise disturbed rivers (Kraemer 1976; Welch and Joy 1984). Less research has been done on populations in undisturbed medium to large rivers (Sickel 1976; Rodgers et al. 1977; Lauritsen and Mozley 1983).

In comparison with most freshwater bivalves, *Corbicula* is reported to have high growth rates, a short life span of only 3 years or less, and densities of >1000/m^2 (e.g., Britton et al. 1979; McMahon and Williams 1986; Belanger et al. 1990). It also appears to have relatively high annual production of >20 g dry mass (DM)/m^2 in some environments (e.g., Aldridge and McMahon 1978; Marsh 1985) and has been reported to filter seston at rates >10 L·h^{-1}·g DM^{-1} (e.g., Lauritsen 1986*a*). Such characteristics have led many to speculate that *Corbicula* has the capacity to alter the trophic and nutrient dynamics of aquatic systems (e.g., Cohen et al. 1984; Lauritsen and Mozley 1989) and to displace native bivalves (e.g., Gardner et al. 1976; Kraemer 1979; Belanger et al. 1990; Leff et al. 1990).

We have studied the population dynamics, growth, and production of *Corbicula* in the Ogeechee River, an unpolluted and relatively undisturbed blackwater river in the lower Coastal Plain of Georgia, USA. *Corbicula*'s presence in the Ogeechee River was first observed in 1974 (Counts 1986), shortly after its presence was documented in the Savannah River in 1972 (Fuller and Powell 1973) and in the Altamaha River in 1971 (Sickel 1973), two larger rivers to the north and south, respectively.

Our analyses were done as part of an ecosystem study of carbon flow dynamics, including the distribution of secondary production of the entire invertebrate community. Although several bivalve species are known to occur in the Ogeechee River (e.g., Sepkowski and Rex 1974), *Corbicula fluminea* was the only species of any importance at our sites. Our analysis of *Corbicula* extended over a relatively long time frame of 43 months, beginning in 1981, less than 10 years after its introduction. We were thus able to examine multiyear patterns of this introduced species within the context of the entire invertebrate community.

Study sites

The study site was a 2-km reach of the Ogeechee River located 63 km from the Atlantic Ocean in the lower Coastal Plain of Georgia, USA. The river flows 394 km through the Piedmont and Coastal Plain physiographic provinces before reaching its mouth south of Savannah, Georgia. At our study site, the Ogeechee is a low-gradient (0.02%), sixth-order river with coarse shifting sands in the main channel, overlain by mud and organic matter in backwaters and depositional areas (10–20% of the total area). The river has a mean width of 33 m and meanders within a wide floodplain (Fig. 1). The waters are chemically soft (alkalinity = 23 mg/L as $CaCO_3$), slightly acidic (pH = 6.6–7.2), and fairly high in dissolved organic carbon (12.7 mg C/L) (Meyer 1986, 1992). Average water temperature is 18.5°C, commonly ranging between 2 and 32°C over a year (Benke and Meyer 1988; Benke and Parsons 1990). Mean discharge is 66.8 m^3/s (47-year period of record), tending to be highest during winter floods (floodplain inundation), declining in the spring, and reaching relatively stable low water levels during the late summer and fall (Benke and Meyer 1988; Benke and Parsons 1990). Species richness of invertebrate taxa is high, suggesting little pollution (e.g., Benke et al. 1991).

Materials and methods

Field studies

In order to estimate densities and biomass for the entire river reach, representative sections were selected. Each section was divided into left, center, and right strata. Section 1 was a straight run, with relatively shallow water overlaying

shifting sand (Fig. 1). Section 2 was a backwater slough, with strata from the back, middle, and mouth. Section 3 was at the middle of a river bend, with strata going from a large sandbar to a deep area on the outside of the bend. Two 15 × 15 cm ponar grab samples were collected in each stratum of each section approximately every 4 weeks from December 1981 to December 1982 (n = 18/date).

Three additional main channel sections were established in January 1983 to include a larger range of microhabitats. Each section was stratified as before. Section 4 was on a straight run directly downstream of a river bend (Fig. 1). Section 5 was on a main channel depositional area located between sections 1 and 3, and section 6 was approximately 1 km downstream, where the river becomes broader (55 m) and slower. Two samples were collected in each stratum of all six sections every 4 weeks between January and December 1983 (n = 36/date). Section samples were also collected in June and December 1984 and monthly from February through June 1985 to examine density trends over a longer period of time (total of 43 months).

It became apparent after sampling began that samples from the river sections may not have sufficient representation of all year classes on each date. Therefore, a separate sampling effort was initiated in May 1983 to improve our understanding of cohort structure and life history. Two small, localized sites were discovered where *Corbicula* was present in much higher densities than in the section samples and in a wider and more complete range of sizes. Site A was located directly below a point bar near sections 1 and 2, and site B was just below section 6 (Fig. 1). Twelve ponar grab samples were collected monthly from site A, the larger of the two sites, but only six from site B to reduce the chance of significantly depleting numbers at the latter. These sites, hereafter called "population centers", were sampled monthly from May to December 1983, bimonthly in 1984, and monthly from February through June 1985, covering a 25-month span.

Each sample was placed in a bucket and rinsed through a 2-mm sieve. Greatest anterior-to-posterior length of each animal was measured to the nearest millimetre and the data recorded as the number of individuals in each millimetre size class for each sample. In contrast with our samples from the main channel sections, samples from each population center site were collected in a single container and then processed like section samples. This time-saving procedure was used for the population center samples because they were collected principally to determine size distributions. Empty shells with little or no apparent dissolution were also measured and recorded as death assemblages. It became apparent late in our study that the 2-mm sieve was not effectively retaining clams <4 mm shell length. Thus, during the final year of sampling (June 1984 – June 1985), material passing through the 2-mm sieve was saved and elutriated onto a 250-μm sieve to collect these small individuals.

The seasonal relationship between shell dimensions and soft tissue mass was analyzed from live clams collected from the river in March, June, September, and December 1982. Individuals representing the range of available sizes were placed on ice and returned to the laboratory. Length, height, and width were measured to the nearest 0.05 mm with Vernier calipers. Each clam was then opened and all soft tissue scraped onto a preweighed aluminum pan. Tissues were then dried at 60°C for 36 h, cooled to room temperature in a desiccator, and weighted to 0.01 mg. Individual dry mass was regressed against shell length. Size-specific biomass values in each field sample were calculated as the product of length-specific densities and individual mass from a length/mass regression and then summed to obtain total biomass per sample. Because a certain amount of organic matter is stored in the shell rather than the soft tissue, all our biomass and production estimates are conservative, perhaps underestimating actual values by about 25% (e.g., Patterson 1985).

Growth studies and production

Growth of individual clams was measured using in situ chambers during two periods: May 1983 – January 1984 and February–June 1985. Growth chambers were Plexiglas box frames, 30 cm on each side, 16 cm deep, and open at the top. Nitex mesh (243-μm openings) formed the sides and bottom of the box. This mesh size was sufficient to prevent the loss of the coarse sediments (median grain size >1 mm; Stites 1986). The top was covered with 2.54-cm-mesh hardware wire to prevent predation by large fishes (e.g., McMahon 1983; Sickel 1986; D.L. Stites, personal observation).

Initially, clams were collected from the river and allowed to dry for 1 h. The greatest anterior–posterior length of each clam was measured to the nearest 0.05 mm and an identification number painted on one valve. Thirty individuals from 5 to 24 mm in length were then placed in each of three separate chambers containing washed river sediments. Initial densities in the chambers (300/m^2) were somewhat greater than usually found in section samples and considerably lower than found in population center sites (see below).

During the 1983 growth experiments, three chambers were suspended from a float to a depth of 1 m. They were anchored from the bottom of the chamber on an eddy line between the main channel and a backwater, downstream of an accreting sandbar, where congregations of *Corbicula* were often found. Individuals placed in the chambers in May 1983 were measured at monthly intervals for 3 months and then replaced with a new set of clams from the river. This procedure was followed for two additional 90-day periods for a total of 270 days. In February 1985, individuals were placed in each of two chambers and were measured monthly until June without population replacement. However, any missing or dead individuals were replaced with individuals of the same size class during this period.

Growth rates for each clam were calculated according to the formula

$$g = \ln(DM_{t+\Delta t}/DM_t)/\Delta t$$

where DM is dry mass, t is time in days, and Δt is length of the growth interval. All individual growth rates calculated for each monthly period were then regressed against the geometric mean mass of each clam. Regressions from different months were then compared using analysis of

Fig. 2. Size–frequency histograms of total population center collections from May 1983 through June 1985. Shell length is greatest anterior–posterior length. Lines connecting histograms follow mean cohort sizes as determined by visual analysis and verified with Bhattacharya's (1967) graphical method of cohort analysis when possible. Numbers above each histogram are the total number of clams measured on each date.

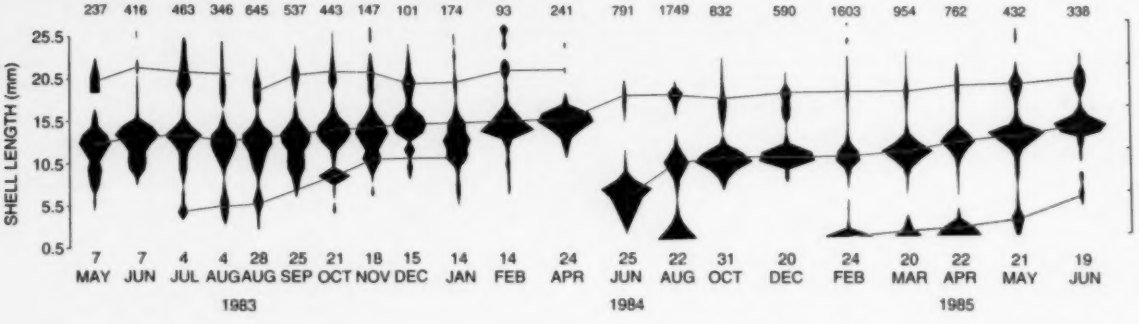

covariance and statistical comparisons of slope (Neter and Wasserman 1974). If the regressions were not significantly different ($p > 0.05$), the data were pooled and a single regression equation calculated for the entire period. This was repeated until the test failed, thus defining seasonal growth dynamics.

Mean daily production was estimated for section and population center data by the instantaneous growth method. Production was initially calculated for each size class in each sample as

$$P_i = g_i B_i$$

where P_i = production of size class i (grams DM per sample per day), g_i = growth rate of size class i determined from growth/mass regression (milligrams per milligram per day), and B_i = biomass of size class i (grams DM per sample).

Total sample production was calculated as the sum of size-specific estimates and converted to production per unit area. Daily production means were then calculated for each section separately and across all sections to obtain a mean for the river. It was assumed that the daily production calculated on a specific sampling date occurred for a period defined from one half the number of days since the last sample to one half the number of days to the next sample (typically 2 weeks before and after a sample). Thus, the monthly pattern of daily production was estimated for 2 consecutive years (December 1981 – December 1983), and annual production was the sum of daily production values calculated in this way for an entire year. Statistical analyses were implemented with the Statistical Analysis System (SAS Institute Inc. 1982).

Results

Life history

Cohort recruitment, growth, and life span were analyzed with size–frequency histograms of population center collections (Fig. 2). Lines connecting the histograms indicate changes in cohort mean size and describe a continuous progression of cohort growth. Three size groups (cohorts) were present on most dates, providing an initial indication that maximum life span was at least 3 years (Fig. 2). Over the 2-year period from May 1983 to June 1985, new individuals were recruited both in winter and summer. Clams <4 mm were not effectively sampled until a 250-μm sieve was used (beginning in June 1984). In February 1985, a new cohort was present at a mean size of <1 mm. The cohorts observed first at 4.5 mm in early July 1983 and at 6.1 mm in June 1984 were each probably recruited the previous winter, as documented for 1985. The summer cohort that appeared on 22 August 1984 (but was not observed in 1983) did not appear to survive to the next sampling date (21 October). Clearly, the major recruitment period occurs in the winter.

Individuals from a typical cohort grew to between 9 and 10 mm length in the first year of life. The first-year cohorts from 1983 and 1984 each reached this size by December (Fig. 2). The new cohort in February 1985 grew to approximately 5 mm by June when sampling was discontinued. The second year of growth from the weak 1983 year class was somewhat more difficult to distinguish, as the cohort appeared to merge with the strong third-year cohort (1982 year class). It began at approximately 10 mm and appeared to reach 14–17 mm length. A distinct second-year cohort in 1985 grew from almost 10 mm in February to 13 mm by June.

Events of the third year were also difficult to discern. The largest cohort from 1983 (presumably in their third year) mostly disappeared in early 1984 at sizes ranging from 20 to 25 mm. The second- and third-year cohorts cannot be distinguished during 1984. This size group from 1984 then became the largest size class for 1985 (presumably in their third year) and reached only 18 mm by June. Considering all years, it appeared that by the end of the third year, mean individual size only reached 18–20 mm. Very few individuals reached 21–26 mm in length and may represent those able to achieve atypically high growth rates or survive a fourth year of life in a favorable location.

Individual size and growth relationships

Of the four seasonal length/mass regressions, only the June equation was significantly different from the others (Table 1, analysis of covariance, $p < 0.05$). Individuals collected in June were significantly heavier for a given length than those in September or December 1982. March regression parameters were intermediate between June values and

Table 1. Comparison of length/mass regression equations for *Corbicula fluminea* in the Ogeechee River and other systems. Length (L) is greatest anterior–posterior shell length (mm), DM is usually dry mass of soft tissue (mg), and logarithm is base 10. For Foe and Knight (1985), DM is ash-free dry mass.

System	Equation	n	r^2	Source
Ogeechee River, Georgia				
March	$\log DM = -1.67 + 2.46 \log L$	44	0.95	This study
June	$\log DM = -1.77 + 2.64 \log L$	45	0.96	This study
September	$\log DM = -1.66 + 2.36 \log L$	46	0.93	This study
December	$\log DM = -1.66 + 2.31 \log L$	50	0.91	This study
Mean	$\log DM = -1.69 + 2.45 \log L$	185	0.91	This study
Altamaha River, Georgia	$\log DM = -2.26 + 3.18 \log L$	66	0.99	Sickel 1976
Lake Arlington, Texas	$\log DM = -2.11 + 3.12 \log L$	20	0.99	Aldridge and McMahon 1978
Sacramento – San Joaquin Delta, California				
Spring	$\log DM = -2.05 + 3.34 \log L$	26	0.97	Foe and Knight 1985
Summer	$\log DM = -2.24 + 3.45 \log L$	18	0.99	Foe and Knight 1985
Chowan River, Virginia – North Carolina				
Spring	$\log DM = -1.85 + 3.01 \log L$	21	0.97	Lauritsen and Mozley 1983
Summer	$\log DM = -1.68 + 2.77 \log L$	35	0.87	Lauritsen and Mozley 1983

others, but no additional equations were significantly different. Although there was some evidence for seasonal changes in length/mass regressions, we used the composite regression for all seasons (Table 1) to estimate biomass from length in field samples on all dates (below). We felt this was appropriate because it was uncertain whether the June relationship could be extrapolated to adjacent months, or whether the patterns were consistent from one year to the next. For example, changes in mass among seasons may be related in part to reproductive state (Kennedy and Van Huekelen 1985; Williams and McMahon 1989) or food abundance, either of which may vary in its time pattern from year to year. We also used the composite regression to calculate biomass change for the in situ growth estimates. However, variation in growth rates obtained from the different length/mass regressions would be slight because growth rates are based on a relative, rather than absolute, change in mass.

Regressions of daily growth rate (milligrams per milligram per day) versus individual mass were estimated from the clams grown in suspended chambers for each 30-day period. From mid-November through mid-February, when temperatures were consistently below 15°C, clams showed no growth. During other months, there was always a strong relationship between growth rate and body mass. Regressions for all 30-day periods fell into three groups, within which there were no significant differences: March–April 1985 ($n = 228$, $r^2 = 0.73$); May 1985, May and June 1983 ($n = 118$, $r^2 = 0.72$); July–October 1983 ($n = 234$, $r^2 = 0.69$). However, composite regressions among these periods were significantly different (Fig. 3). The highest growth rates were clearly seen in late spring (May and June) when temperatures usually ranged from 20 to 24°C (e.g., Benke and Parsons 1990). Growth was significantly lower than this in the summer (July–October), when temperatures usually range from 26 to 30°C, and in early spring (March and April), when temperatures vary from 12 to 20°C.

Fig. 3. Regressions predicting daily growth rate from dry mass for *Corbicula fluminea* during different times of the year in the Ogeechee River. Growth rates were zero from mid-November through February.

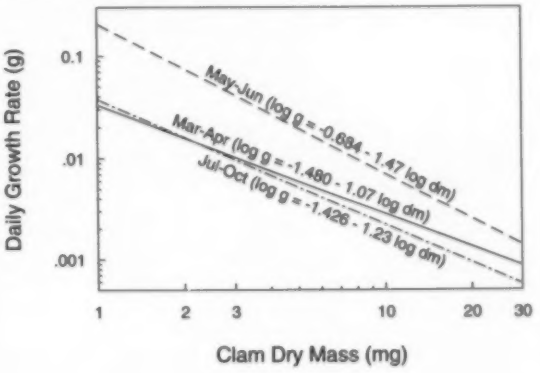

Average growth rates over a 300-day growing season were approximated for each year class in the population centers from the histograms (Fig. 2) and were compared with those calculated from the chamber growth equations (Fig. 3). Growth rates estimated from the regression bracketed histogram values in most cases, indicating that growth within chambers and from the field was reasonably consistent (Table 2).

Production dynamics

Corbicula densities averaged across all sections consistently were less than 200/m^2 and showed relatively little annual variation (Fig. 4*a*). Although there were only two sample dates in 1984, and sampling in 1985 was limited to February–June, it is clear that densities were very stable for over 3.5 years. There was some seasonal variation with

Table 2. Comparison of growth rates ($mg \cdot mg^{-1} \cdot day^{-1}$) calculated from histogram analysis (field, Fig. 2) and growth rates estimated from regression equations (chambers, Fig. 3).

Year class	Length (mm)	Growth rates	
		Histograms	Chambers
0–1	0.5–9.5	0.014	0.0048–0.34
1–2	9.5–15.5	0.004	0.0078–0.020
2–3	15.5–18.5	0.002	0.0013–0.0024

highest values in winter when recruitment occurred. However, due to inefficiency in sampling clams <4 mm, these winter densities were underestimated and the seasonal variation in density was undoubtedly greater than actually observed. Declines during the fall were accompanied by death assemblages (measured empty shells) sufficient to account for approximately 80% of the summertime densities. Markedly different mean annual densities were found among the sections, particularly in 1983 (Table 3). The highest densities for two years were found at the backwater site (section 2), especially at the mouth of the backwater, near one of the population centers (see below). One of the main-channel sites (section 6) also had relatively high densities and it was near the second population center. The average density for two years in the backwater ($282/m^2$) was higher than in the main channel ($160/m^2$). However, excluding section 6, the main channel sites averaged only $81/m^2$.

Biomass patterns were similar to those of density, showing relatively little variation across years, and no long-term trend (Fig. 4*b*). Mean monthly biomass consistently ranged from 1 to 5 g DM/m^2. The peak in April 1982 was due to the collection of numerous large clams (>20 mm length), and biomass declines in the fall were associated with the high mortality mentioned above. As with density, mean annual biomass values were extremely different among sections (Table 3). The difference between *Corbicula* biomass in the backwater (6.97 g/m^2) and the channel (1.41 g/m^2) was even more pronounced than with density, since the backwater contained larger clams. Excluding section 6, all other main-channel sections averaged only 0.6 g/m^2. The use of a composite length/mass regression for estimating biomass may have produced some bias in seasonal patterns (Fig. 4*b*), but it is unlikely to have substantially affected mean annual biomass. If we had used season-specific length/mass regressions, it would have elevated biomass values by about 34% in late spring and reduced biomass about 14% in summer and fall. These would not have substantially altered the annual pattern.

Unlike density and biomass which showed relatively little seasonal and annual variation, production displayed distinct seasonal patterns (Fig. 4*c*) because growth rates were very season-specific (Fig. 3). The highest production occurred in the spring of both years, with no production in early winter. If we had used season-specific length/mass regressions to estimate biomass rather than the composite regression, it would have accentuated the seasonal production patterns observed, making spring peaks higher and the summer/fall values lower. Annual production would be little affected, since the seasonal differences would tend to cancel out.

First-year individuals accounted for 51% of the total 1982 production (Fig. 4*c*, Table 4). In 1983, this same cohort (1982 year class) again composed more than half of the total annual production. First- and third-year classes contributed equal amounts to the total in 1983. Thus, there appeared to be an alternation of strong and weak year classes based on production (i.e., the 1980 and 1982 year classes were strong, with 1981 and 1983 weak). Age-specific annual production/biomass (*P/B*) values reflected the average growth rates of each age class, declining with age, and these values were relatively consistent between years (Table 4). Large production differences occurred among sections reflecting the same density and biomass differences seen above (Table 3). With the exception of section 6, production was highest in the backwater (section 2) each year (mean = 2.87 g $DM \cdot m^{-2} \cdot year^{-1}$). Annual production averaged 0.98 $g \cdot m^{-2} year^{-1}$ across the main-channel sandy habitats, but only 0.54 if section 6 was excluded.

Although population centers were sampled primarily for life history information, it was possible to estimate production for comparison with river section sampling (Table 5). Biomass and production were typically an order of magnitude higher than the mean values from the river sections. Clearly, there are localized areas within the river that create much more highly favorable conditions than found in most sections. Annual *P/B* values in population centers (0.92–1.78) were substantially higher than in the river sections (0.55–0.57), reflecting the greater concentration of small animals in the first year class.

Discussion

Although many investigators have suggested that the spread of *Corbicula* throughout North America has had profound effects on aquatic ecosystems, its potential influence in the Ogeechee River does not appear to be dramatic, at least in our 2-km area of study. In fact, *Corbicula*'s life history pattern, individual growth characteristics, population density, and production all suggest that the Ogeechee River represents a stressful environment for this species. Furthermore, less than a decade after its invasion, the population was relatively stable over an almost 4-year period.

Life history and growth characteristics

The *Corbicula* population from the Ogeechee River appears to have at least a 3-year life span, with most individuals reaching no more than 20 mm in length after 3 years of growth. This represents a very modest growth pattern compared with many North American populations which reach 16–35 mm in the first year alone, with a total life span of only 1.5–2 years (e.g., McMahon and Williams 1986). However, life spans of 3 or more years have sometimes been reported for other populations (e.g., Morton 1977; Eng 1979; Fritz and Lutz 1986; Mattice and Wright 1986). In a survey of streams in Mississippi, Payne et al. (1989) found that while six streams had three cohorts present simultaneously (and apparently 3-year life spans), eight

Fig. 4. Mean density, biomass, and daily production of *Corbicula fluminea* from December 1981 through December 1983. Error bars are ±1 SE. Mean daily production is partitioned among three year classes. Mean density and biomass are also shown for less frequent samples taken during 1984–1985.

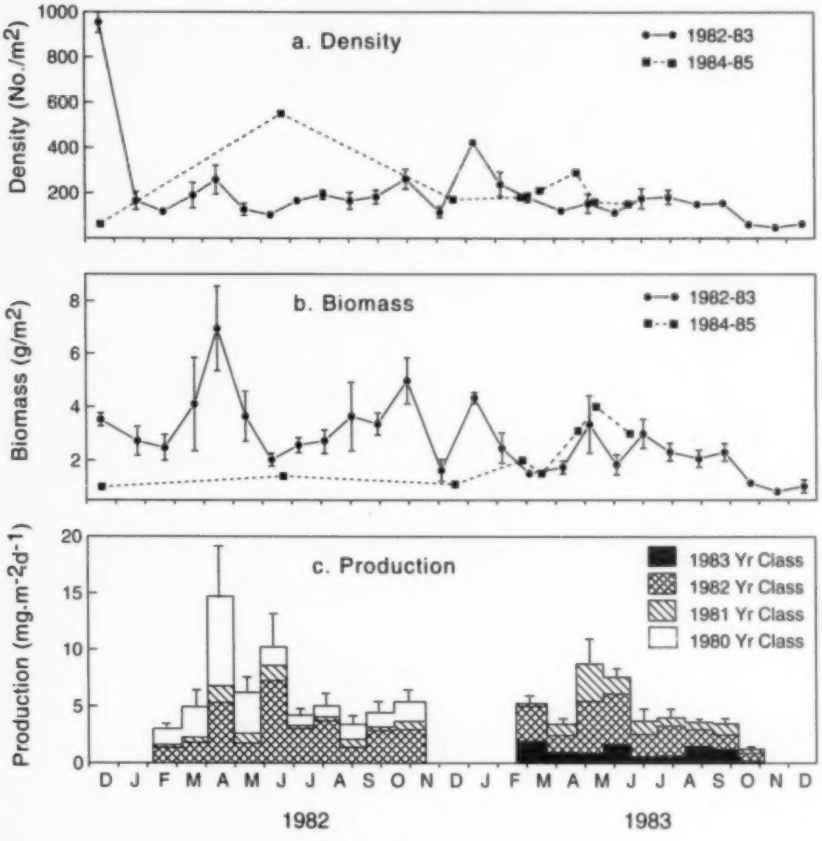

streams consisted of only a single dominant year class <20 mm in length. In contrast with other long-lived populations that show stready increases in individual size, the Ogeechee population had long periods of little apparent change (Fig. 2).

Coinciding with the long life span was a slow increase in linear shell growth for clams in the Ogeechee River. First-year individuals (<10 mm) averaged about 0.75 mm/month and older individuals <0.5 mm/month. Most previous studies have shown shell growth to be considerably higher. For clams <10 mm, it is common to find that shell length increases by >2 mm/month (e.g., O'Kane 1976; Dreier 1977; McMahon and Williams 1986). However, instances of slow shell growth have been found in other systems (e.g., Trama 1982; Fritz and Lutz 1986; Belanger et al. 1990; Hornbach 1992).

Although there are a few instances of only a single reproductive period per year for *Corbicula* (Hornbach 1992), most studies have shown two distinct periods, regardless of estimated life span (e.g., Kraemer and Galloway 1986; McMahon and Williams 1986; Williams and McMahon 1986; Hornbach 1992). In the Ogeechee River, there was some evidence for two reproductive periods, but only the winter cohort appeared to be successful in producing clams surviving past the first few months. This somewhat unusual recruitment pattern again suggests the possibility of stress.

The seasonal differences in length/mass relationships with highest values in the spring (Table 1) are consistent with the findings of others (Foe and Knight 1985; Lauritsen and Mozley 1989; Doherty et al. 1990). However, even the highest mass per unit length relationship in the Ogeechee (June) produced lower estimates of mass than found from a broad range of aquatic systems in which *Corbicula* has been found, including the nearby Altamaha River (Table 1), again suggesting a stressful environment for this species.

Biomass growth rates (milligrams per milligram per day) were highest in late spring, with no growth during early winter, and slow growth in early spring, summer, and fall (Fig. 3). This seasonal pattern of growth rate is consistent with the seasonal pattern of length/mass relationships which also shows a springtime maximum. Some studies of *Corbicula* have shown that maximum growth rate usually occurs between 20 and 25°C (e.g., Joy 1985;

Table 3. Comparison of mean annual density (N), biomass (B), and production (P) of *Corbicula* within different river sections. Note that section 2 occurred in a backwater with substantial organic deposition. All other sections occurred in the main channel with a shifting sand substratum. Numbers in parentheses are ±1 SE.

	1982			1983		
Section	N (no./m^2)	B (g/m^2)	P (g·m^{-2}·year^{-1})	N (no./m^2)	B (g/m^2)	P (g·m^{-2}·year^{-1})
1	128.1 (8.6)	0.32 (0.08)	0.28	51.9 (5.1)	0.26 (0.04)	0.51
2	277.7 (20.0)	7.59 (0.54)	3.24	285.9 (20.8)	6.35 (0.57)	2.44
3	284.8 (20.8)	2.32 (0.46)	1.66	79.5 (7.2)	1.21 (0.20)	0.76
4				22.6 (4.0)	0.14 (0.02)	0.18
5				29.3 (4.2)	0.22 (0.03)	0.38
6				477.5 (37.2)	4.67 (0.37)	2.73
Channel	206.5	1.32	0.97	132.2	1.30	0.91
River	230.2	3.41	1.72	157.8	2.14	1.18

Table 4. Comparison of annual production (g DM·m^{-2}·year^{-1}) and annual P/B from sampling sections for each of three year classes.

	1982		1983	
Year class	P	P/B	P	P/B
0–1	0.88	3.46	0.28	2.38
1–2	0.19	1.14	0.63	0.78
2–3	0.66	0.24	0.28	0.25
Total	1.72	0.51	1.18	0.55

Table 5. Biomass (B), production (P), and P/B for population center data (Fig. 1) by year class. The first year of data (1983–1984) was from samples taken from May 1983 to April 1984, and the second year (1984–1985) was from June 1984 to June 1985. Percentage of production for each year class is shown in parentheses.

Year class	B (g/m^2)	P (g·m^{-2}·year^{-1}) (%)	P/B
1983–1984			
0–1	0.36	3.01 (32)	8.45
1–2	5.72	5.21 (55)	0.91
2–3	4.27	1.24 (13)	0.29
Total	10.35	9.45	0.92
1984–1985			
0–1	2.39	15.75 (69)	6.58
1–2	4.40	5.15 (22)	1.17
2–3	6.18	2.04 (9)	0.33
Total	12.94	22.94	1.78

Foe and Knight 1986; Mattice and Wright 1986) whereas others have shown no suppression of growth up to 30°C (McMahon and Williams 1986). Our results are more consistent with the evidence suggesting maximum growth between 20 and 25°C, about the temperature usually found in late spring in the Ogeechee River. Furthermore, most studies indicate that growth declines rapidly as temperature falls below 15°C, as we observed in the Ogeechee River (Joy 1985; Mattice and Wright 1986). Thus, the low biomass growth rates of *Corbicula* in the Ogeechee River during the summer and the lack of growth in midwinter were probably at least partly due to temperature. These observations are somewhat in conflict with the findings of Williams and McMahon (1989) for *Corbicula* in Lake Arlington, who found that maximum shell growth appeared to be associated with minimal tissue accumulation in the summer whereas energy appeared to be diverted from shell growth into tissue accumulation during the winter.

Most previous studies of *Corbicula* considered absolute increase of shell length per unit time (e.g., millimetres per month) as a measure of growth, rather than instantaneous biomass growth rates (milligrams per milligram per day). However, Sickel (1976) examined both increase in length and biomass growth rate in the Altamaha River and found that each was substantially higher than occurred in the Ogeechee River. Not only did Altamaha individuals grow to approximately 14 mm in the first year (versus 10 in the Ogeechee) and 22 mm in the second year (versus 15 in the Ogeechee), but they attained approximately twice the mass per unit length by the second year of life (Table 1). Thus, biomass growth rates were much higher than found in the Ogeechee, especially for the second year class.

Density, biomass, and production

Corbicula densities in the Ogeechee River from the section transects were highest in spring as a result of recruitment

Table 6. Mean annual biomass (B, g DM/m^2), annual production (P, g DM·m^{-2}·year^{-1}), life span, and annual P/B for *Corbicula fluminea* in the Ogeechee River and other sites.

River	Date	B	P	Life span (years)	P/B	Source
Ogeechee River, Georgia						
River section means	1982–83	2.1–3.4	1.2–1.7	3	0.51–0.55	This study
Population centers	1983–85	10.3–12.9	9.5–22.9	3	0.92–1.78	This study
Altamaha River, Georgia	1975	11–16	15–16	2	1.0–1.3	Sickel 1976
Drainage canal, Arizona	1984	9.5	25.6	2	2.7	Marsh 1985
Lake Arlington, Texas	1975	5[a]	20.7[a]	1–1.5	4.1	Aldridge and McMahon 1978

[a]Estimated from data reported as grams carbon.

in the winter and were lowest after sudden mortality in the fall. Overall, densities were relatively low (<200/m^2), but stable over the 43-month period of study. Such characteristics are in sharp contrast with many *Corbicula* populations which often exceed 1000/m^2 and fluctuate widely within and between years (e.g., Gardner et al. 1976; Cohen et al. 1984; Belanger et al. 1990; Leff et al. 1990; Hornbach 1992). Gardner et al. (1976) and Sickel (1979) have both described *Corbicula* densities to commonly range from a few hundred to >1000/m^2 in the nearby Altamaha River. Only in our population centers were densities sometimes >1000/m^2, but these small areas were not at all representative of this reach of the Ogeechee River. Some populations have shown a steady increase in density over a few years from <100/m^2 to well over 1000/m^2, followed by a crash (Gardner et al. 1976; Cohen et al. 1984). Lauritsen and Mozley (1983) have found densities most similar to ours in the Chowan River, averaging about 200/m^2 over about 82 km of river length. However, other longitudinal analyses of *Corbicula* populations have shown that densities can vary greatly from zero in some locations to >1000/m^2 in others (e.g., Belanger et al. 1990; Leff et al. 1990). Our own data showed large variation in densities between sections that is related to habitat rather than longitudinal trends.

Biomass values in the Ogeechee River were also relatively stable, usually varying from 1 to 5 g DM/m^2. Again, biomass varied greatly among sections, being greatest in the backwater. Such biomass values are relatively high in comparison with other benthic invertebrates and comprise about 80% of total benthic biomass in the Ogeechee River (Stites 1986). However, they are low in comparison with most environments where *Corbicula* has become established. For example, biomass in the Altamaha River ranged from 4.4 to 26.2 g DM/m^2 between 1973 and 1977 (Sickel 1979). Mean biomass was 12.2 g DM/m^2 for the Chowan River (Lauritsen and Mozley 1983) and 9.5 g DM/m^2 in an Arizona drainage canal (Marsh 1985). Only sections 2 and 6 and population center estimates were comparable with these high values.

In spite of many *Corbicula* studies, there have been surprisingly few estimates of secondary production. Nonetheless, production of *Corbicula* from the Ogeechee River (1.2–1.7 g DM/m^2) was much less than that reported for the few other systems from which production has been estimated (Table 6, 15–26 g DM/m^2). Production in the population centers was similar to that found by others, but represented a very small fraction of the total bottom area along 2 km of river length. Considering the high biomass (e.g., Cohen et al. 1984) and growth rates (e.g., McMahon and Williams 1986) found in other systems, it seems certain that *Corbicula* production in some systems will be considerably higher than has been measured to date.

Annual P/B values from the section production estimates were surprisingly low (0.51–0.57, Tables 3 and 4) for a population with a 3- to 4-year life span. Annual P/B values from population centers (0.92–1.78, Table 5) were more consistent with P/B values of about 1–2 that would be expected for a population with a 3-year life span (Benke 1984). The low P/B for the mean of sections was primarily influenced by sections 2 (backwater), 3, and 6 which had a relatively low fraction of first-year clams in comparison with sections 1, 4, and 5 and population centers (Tables 3–5). A combination of hydrologic and behavioral factors was probably responsible for the differences in size distributions and thus P/B values between sections. Smaller, younger individuals are more likely than large, older clams to migrate (Prezant and Chalermwat 1984), presumably to more acceptable microhabitats after having been redistributed during hydrologic events. Larger, older individuals were thus oversampled after they had collected and remained at specific sites (outside bend, front of backwater, and along wide slow reach). These sites yielded the highest densities and greatest numbers of large (>15 mm) individuals, while other sites contained lower densities of smaller, younger individuals. Increases in density in the population center between recruitment events (Fig. 2) suggest that individuals were migrating toward population centers and away from other sites. The larger individuals were less likely to move and therefore remained at sites other than the population centers. This resulted in a skewed distribution of individuals, and hence a skewed P/B values.

Potential limitations to *Corbicula* growth and production

The most likely factors involved in creating a stressful environment for *Corbicula* are temperature, pH/calcium, and food. As discussed above, *Corbicula* seems to grow well only in a fairly narrow range of temperatures (18–25°C). In the Ogeechee River, temperatures fall below 15°C for roughly 3 months, and they are consistently 26–30°C for another 3 months.

Another factor that has been shown to contribute to physiological stress in molluscs is lack of calcium. The Ogeechee River has somewhat lower alkalinity (as $CaCO_3$) than the Altamaha, with values falling below 10 mg/L in the winter and rising to >30 mg/L in the summer (Meyer 1992). Values of pH are also somewhat less in the Ogeechee River (6.6–7.2, Meyer 1992). Dissolution of the umbo has been implicated as the cause of death of *Corbicula* in chemically soft waters (Kat 1982) and implied as the cause of death in Savannah River populations (Geisy and Dickson 1981). Very few shells in the samples collected for this study showed severe umbonal erosion, and no freshly dead shells were found with holes through the umbo. Although pH and alkalinity are not greatly different between the Ogeechee and Altamaha rivers, the differences among the *Corbicula* populations are suggestive that limiting conditions are near the Ogeechee values (Burky 1983). In rivers significantly lower in pH/alkalinity throughout the southeast (e.g., Satilla River, St. Marys River), the presence of *Corbicula* has not been reported (Counts 1986). Similarly, Black Creek, a low-alkalinity, low-pH tributary of the Ogeechee River near our study sites (Fig. 1), contains no *Corbicula*.

Food quality and quantity may also play a role in limiting *Corbicula* in the Ogeechee River, since these clams have particularly high growth rates and densities in environments with high algal concentrations (e.g., Aldridge and McMahon 1978; Foe and Knight 1985). The Ogeechee River, on the other hand, is strongly heterotrophic (Edwards and Meyer 1987), and the highest fraction of seston consists of microbially enriched amorphous detritus (Edwards 1987; Wallace et al. 1987). While this seston composition results in high growth rates for various aquatic insects such as black flies (Hauer and Benke 1987), mayflies (Benke and Jacobi 1986; Benke et al. 1992), and midges (Stites and Benke 1989; Hauer and Benke 1991), it may not be sufficient for maximum growth of *Corbicula*.

Potential influence of *Corbicula* in the Ogeechee River

Some investigators have attempted to determine the capability of *Corbicula* to remove seston from the water column. Using filtration rates per individual clam, *Corbicula* has been estimated to be able to clear seston from overlying water in 1–4 days (Cohen et al. 1984; Lauritsen 1986*a*; Leff et al. 1990). For comparison, we have estimated the amount of seston removed by *Corbicula* in the Ogeechee River with two approaches: (1) using the production estimate and assuming bioenergetic efficiencies (as done with black flies by Benke and Parsons 1990) and (2) using estimated filtration rates and applying them to biomass estimates (Cohen et al. 1984; Lauritsen 1986*a*; Leff et al. 1990).

Corbicula annual production was estimated to be 1.7 g DM/m^2, which converts to a mean daily value of 4.7 mg·m^{-2}·day^{-1} in 1982. Assuming a mean channel width of 33 m, this is equivalent to 0.0018 mg·m river length^{-1}·s^{-1}. Consumption can be estimated from production using the procedure of Benke and Wallace (1980), as applied by Wallace et al. (1987). Wallace et al. (1987) examined the gut contents of *Corbicula* from the Ogeechee River and found that about 90% was amorphous detritus and 10% diatoms. Assuming that assimilation efficiencies were 10% for detritus and 30% for diatoms, they estimated that 73.6% of production would be attributed to consumption of detritus and 23.5% to diatoms. Assuming these same assimilation efficiencies and a net production efficiency of 0.5, a production of 0.0018 mg·m^{-1}·s^{-1} translates to a total consumption of 0.0295 mg·m^{-1}·s^{-1} (0.0266 for detritus and 0.0028 for diatoms). These efficiencies are lower than found by Foe and Knight (1986) and Lauritsen (1986*b*), but they used algal cultures as food, rather than the microbially enriched amorphous detritus found in the Ogeechee River. Since mean discharge in 1982 was 50.7 m^3/s (Benke and Parsons 1990), and mean seston concentration was 1.1 mg ash-free DM/L, seston flow rate was estimated to be 55.8 g/s. The fraction of seston filtered by *Corbicula* can be calculated as the seston filtration rate (0.0295 mg·m^{-1}·s^{-1}) divided by the seston flow rate (55.8 g/s) to yield 0.000053% removed/m river length (5.3%/100 km) or 0.99%/day.

Using published filtration rates per unit body mass (Prokopovich 1969; Cohen et al. 1984) and appropriate conversion factors (e.g., Joy 1985), we independently estimated seston removal to be 0.023 mg·m^{-1}·s^{-1}, very similar to the bioenergetic estimate. Although both estimates are based on several untested assumptions (i.e., assimilation efficiency, filtration rate, etc.) and should not be considered highly accurate, they strongly suggest a relatively low utilization of total seston, perhaps two orders of magnitude less than found in other systems (Cohen et al. 1984; Lauritsen 1986*a*; Leff et al. 1990). The removal rate for *Corbicula* was very similar to that estimated for black flies (0.02 mg·m^{-1}·s^{-1}) in the Ogeechee River (Benke and Parsons 1990).

Production by *Corbicula* (<2 g DM·m^{-2}·year^{-1}) represents only a small fraction of invertebrate production in the Ogeechee River. Although *Corbicula* is the major filtering collector in the benthic habitats, production by small gathering collectors such as aquatic insects (mostly chironomids) and oligochaetes was roughly 10 times higher (Stites 1986, 1987). The most productive invertebrate habitat in natural Coastal Plain rivers is submerged wood, or snags (e.g., Benke et al. 1984). A preliminary estimate of invertebrate production on snags in the Ogeechee River is over 50 g DM·m^{-2}·year^{-1}, a substantial fraction of which is filtering collectors such as black flies (Benke and Parsons 1990), Tanytarsini midges, and hydropsychid caddisflies (Wallace and Benke 1984; A.C. Benke, unpublished data). Thus, although *Corbicula* constitutes much of the benthic biomass, it contributes a relatively small amount to total invertebrate production and filtering capacity.

Acknowledgements

Support for this research was provided by grants DEB-8104427 and BSR-8406630 from the National Science Foundation, the Emory University Department of Biology, and the Department of Biological Sciences, University of Alabama. M. Mayer, J. Mizner, and K. Parsons assisted in various aspects of the field sampling program. We thank T. Richardson, T. Waters, and an anonymous reviewer for several helpful suggestions on the manuscript.

References

Abbott, T.M. 1979. Asiatic clam (*Corbicula fluminea*) vertical distributions in Dale Hollow Reservoir, Tennessee. *In* Proc. 1st Int. *Corbicula* Symp. *Edited by* J.C. Britton. Texas Christian University Research Foundation, Fort Worth, Tex. pp. 111–118.

Aldridge, D.W., and McMahon, R.F. 1978. Growth, fecundity and bioenergetics in a natural population of the asiatic freshwater clam *Corbicula manilensis* Phillipi from north central Texas. J. Molluscan Stud. **44**: 49–70.

Belanger, T.V., Annis, C.G., and VanEpps, D.D. 1990. Growth rates of the Asiatic clam, *Corbicula fluminea*, in the upper and middle St. Johns River, Florida. Nautilus, **104**: 4–9.

Benke, A.C. 1984. Secondary production of aquatic insects. *In* The ecology of aquatic insects. *Edited by* V.H. Resh and D.M. Rosenberg. Praeger Publishers, New York, N.Y. pp. 289–322.

Benke, A.C., and Jacobi, D.I. 1986. Growth rates of mayflies in a subtropical river and their implications for secondary production. J. N. Am. Benthol. Soc. **5**: 107–114.

Benke, A.C., and Meyer, J.L. 1988. Structure and function of a blackwater river in the southeastern U.S.A. Verh. Int. Ver. Limnol. **23**: 1209–1218.

Benke, A.C., and Parsons, K.A. 1990. Modelling black fly production dynamics in blackwater streams. Freshwater Biol. **24**: 167–180.

Benke, A.C., and Wallace, J.B. 1980. Trophic basis of production among net-spinning caddisflies in a southern Appalachian stream. Ecology, **61**: 108–118.

Benke, A.C., Van Arsdall, T.C., Gillespie, D.M., and Parrish, F.K. 1984. Invertebrate productivity in a subtropical blackwater river: the importance of habitat and life history. Ecol. Monogr. **54**: 25–63.

Benke, A.C., Parsons, K.A., and Dhar, S.M. 1991. Population and community patterns of invertebrate drift in an unregulated Coastal Plain river. Can. J. Fish. Aquat. Sci. **48**: 811–823.

Benke, A.C., Hauer, F.R., Stites, D.L., Meyer, J.L., and Edwards, R.T. 1992. Growth of snag-dwelling mayflies in a blackwater river: the influence of temperature and food. Arch. Hydrobiol. **125**: 63–81.

Bhattacharya, C.G. 1967. A simple method of resolution of a distribution into gaussian components. Biometrics, **45**: 115–135.

Britton, J.C., Coldiron, D.C., Evans, L.P., Golightly, C., O'Kane, K.D., and TenEyck, J.R. 1979. Reevaluation of the growth pattern in *Corbicula fluminea*. *In* Proc. 1st Int. *Corbicula* Symp. *Edited by* J.C. Britton. Texas Christian University Research Foundation, Fort Worth, Tex. pp. 177–192.

Burky, A.J. 1983. Physiological ecology of freshwater bivalves. *In* The Mollusca. Vol. 6. Ecology. *Edited by* W.D. Russell-Hunter. Academic Press, Orlando. Fla. pp. 281–327.

Buttner, J.K., and Heidinger, R.C. 1980. Seasonal variations in growth of the asiatic clam *Corbicula fluminea* (Bivalvia: Corbiculidae) in a southern Illinois fish pond. Nautilus, **94**: 8–10.

Cohen, R.R.H., Dresler, P.V., Phillips, E.J.P., and Cory, R.L. 1984. The effect of the Asiatic clam *Corbicula fluminea* on phytoplankton of the Potomac River, Maryland. Limnol. Oceanogr. **29**: 170–180.

Counts, C.L. 1986. The zoogeography and history of the invasion of the United States by *Corbicula fluminea* (Bivalvia: Corbiculidae). Am. Malacol. Bull. Spec. Ed. No. **2**: 7–39.

Diaz, R.J. 1974. Asiatic clam *Corbicula manilensis* (Phillipi) in the tidal James River, Virginia. Chesapeake Sci. **15**: 118–120.

Doherty, F.G., Cherry, D.S., and Cairns, J. 1990. Multiseasonal tissue growth trends in *Corbicula fluminea* (Bivalvia: Corbiculidae) from the New River, Virginia. Nautilus, **104**: 10–15.

Dreier, H. 1977. Study of *Corbicula manilensis* in Lake Sangchris. *In* The annual report for fiscal year 1976, Lake Sangchris project. Illinois Natural History Survey, Urbana, Ill. pp. 7.1–7.52.

Edwards, R.T. 1987. Sestonic bacteria as a food source for filtering invertebrates in two southeastern blackwater rivers. Limnol. Oceanogr. **32**: 221–234.

Edwards, R.T., and Meyer, J.L. 1987. Metabolism of a subtropical low gradient blackwater river. Freshwater Biol. **17**: 251–263.

Eng, L.L. 1979. Population dynamics of the Asiatic clam *Corbicula fluminea* (Müller) in the concrete lined Delta-Mendota Canal of central California. *In* Proc. 1st Int. *Corbicula* Symp. *Edited by* J.C. Britton. Texas Christian University Research Foundation, Fort Worth, Tex. pp. 39–68.

Foe, C., and Knight, A. 1985. The effect of phytoplankton and suspended sediment on the growth of *Corbicula fluminea* (Bivalvia). Hydrobiologia, **127**: 105–115.

Foe, C., and Knight, A. 1986. A thermal energy budget for juvenile *Corbicula fluminea*. Am. Malacol. Bull. Spec. Ed. No. **2**: 143–150.

Fritz, L.W., and Lutz, R.A. 1986. Environmental perturbations reflected in internal shell growth patterns of *Corbicula fluminea* (Mollusca: Bivalvia). Veliger, **28**: 401–417.

Fuller, S.L.H., and Powell, C.E. 1973. Range extensions of *Corbicula manilensis* (Philippi) in the Atlantic drainage of the United States. Nautilus, **87**: 59.

Gardner, J.A., Woodall, W.R., Staats, A.A., and Napoli, J.F. 1976. The invasion of the asiatic clam (*Corbicula manilensis* Philippi) in the Altamaha River, Georgia. Nautilus, **90**: 117–125.

Geisy, J.P., and Dickson, G.W. 1981. The effect of season and location on phosphoadenylate concentrations and adenylate energy charge in 2 species of freshwater clams. Oecologia, **49**: 1–7.

Hauer, F.R., and Benke, A.C. 1987. Influence of temperature and river hydrograph on black fly growth rates in a subtropical blackwater river. J. N. Am. Benthol. Soc. **6**: 251–261.

Hauer, F.R., and Benke, A.C. 1991. Rapid growth of snag-dwelling chironomids in a blackwater river: the influence of temperature and discharge. J. N. Am. Benthol. Soc. **10**: 154–164.

Heinson, G.E. 1958. Life history and ecology of the freshwater clam *Corbicula fluminea*. M.S. thesis, University of California, Santa Barbara, Calif.

Hillis, D.M., and Mayden, R.L. 1985. Spread of the Asiatic clam *Corbicula* (Bivalvia: Corbiculacea) into the new world tropics. Southwest. Nat. **30**: 454–456.

Hornbach, D.J. 1992. Life history traits of a riverine population of the Asian clam *Corbicula fluminea*. Am. Midl. Nat. **127**: 248–257.

Isom, B.G. 1986. Historical review of Asiatic clam (*Corbicula*) invasion and biofouling of waters and industries in the Americas. Am. Malacol. Bull. Spec. Ed. No. **2**: 1–6.

Joy, J.E. 1985. A 40-week study on growth of the Asian clam, *Corbicula fluminea* (Müller), in the Kanawha River, West Virginia. Nautilus, **99**: 110–116.

Kat, P.W. 1982. Shell dissolution as a significant cause of mortality for *Corbicula fluminea* (Bivalvia: Corbiculidae) inhabiting acidic waters. Malacol. Rev. **15**: 129–134.

Kennedy, V.S., and Van Huekelen, L. 1985. Gametogenesis and larval production in a population of the introduced Asiatic Clam *Corbicula* sp. (Bivalvia: Corbiculidae) in Maryland. Biol. Bull. **168**: 50–60.

Kraemer, L.R. 1976. An evaluation of the effects of dredging within the Arkansas River Navigation System. Vol. 4. The effects upon the benthic associations. Arkansas Water Resources Center Publication No. 46, University of Arkansas, Fayetteville, Ark.

Kraemer, L.R. 1979. *Corbicula* (Bivalvia: Sphaeriacea) vs. indigenous mussels (Bivalvia: Unionacea) in U.S. rivers: a hard case for interspecific competition? Am. Zool. **19**: 1085–1096.

Kraemer, L.R., and Galloway, M.L. 1986. Larval development of *Corbicula fluminea* (Müller) (Bivalvia: Corbiculacea): an appraisal of its heterochrony. Am. Malacol. Bull. **4**: 61–79.

Lauritsen, D.D. 1986*a*. Filter-feeding in *Corbicula fluminea* and its effect on seston removal. J. N. Am. Benthol. Soc. **5**: 165–172.

Lauritsen, D.D. 1986*b*. Assimilation of radiolabeled algae by *Corbicula*. Am. Malacol. Bull. Spec. Ed. No. **2**: 219–222.

Lauritsen, D.D., and Mozley, S.C. 1983. The freshwater asian clam *Corbicula fluminea* as a factor affecting nutrient cycling in the Chowan River, N.C. Water Resources Research Institute of the University of North Carolina UNC-WRRI-83-192, Raleigh, N.C.

Lauritsen, D.D., and Mozley, S.C. 1989. Nutrient excretion by the Asiatic clam *Corbicula fluminea*. J. N. Am. Benthol. Soc. **8**: 134–139.

Leff, L.G., Burch, J.L., and McArthur, J.V. 1990. Spatial distribution, seston removal, and potential competitive interactions of the bivalves *Corbicula fluminea* and *Elliptio complanata*, in a coastal plain stream. Freshwater Biol. **24**: 409–416.

Marsh, P.C. 1985. Secondary production of introduced Asiatic clam *Corbicula fluminea* in a central Arizona canal. Hydrobiologia, **24**: 103–110.

Mattice, J.S., and Dye, L.L. 1976. Thermal tolerance of adult Asiatic clam. ERDA Symp. Ser. **40**: 130–135.

Mattice, J.S., and Wright, L.L. 1986. Aspects of growth of *Corbicula fluminea*. Am. Malacol. Bull. Spec. Ed. No. **2**: 167–178.

McMahon, R.F. 1983. Ecology of an invasive pest bivalve, *Corbicula*. *In* The Mollusca. Vol. 6. Ecology. *Edited by* W.D. Russell-Hunter. Academic Press, New York, N.Y. pp. 505–561.

McMahon, R.F., and Williams, C.J. 1986. A reassessment of growth rate, life span, life cycles and population dynamics in a natural population and field caged individuals of *Corbicula fluminea* (Müller) (Bivalvia: Corbiculacea). Am. Malacol. Bull. Spec. Ed. No. **2**: 151–166.

Meyer, J.L. 1986. DOC patterns of two subtropical black water rivers. Arch. Hydrobiol. **108**: 119–134.

Meyer, J.L. 1992. Seasonal patterns of water quality in blackwater rivers of the Coastal Plain, southeastern United States. *In* Water quality in North American river systems. *Edited by* D.C. Becker and D.A. Neitzel. Battelle Press, Columbia, Ohio. pp. 249–276.

Morton, B. 1977. The population dynamics of *Corbicula fluminea* (Bivalvia: Corbiculidae) in Plover Cove, Hong Kong. J. Zool. Lond. **181**: 21–42.

Morton, B. 1986. *Corbicula* in Asia - an updated synthesis. Am. Malacol. Bull. Spec. Ed. No. **2**: 113–124.

Neter, J., and Wasserman, W. 1974. Applied linear statistical analysis. Richard D. Irwin, Homewood, Ill.

O'Kane, K.D. 1976. A population study of the exotic bivalve *Corbicula manilensis* (Phillipi) in selected Texas reservoirs. M.S. thesis, Texas Christian University, Fort Worth, Tex.

Paterson, C.G. 1985. Biomass and production of the unionid, *Elliptio complanata* (Lightfoot) in an old reservoir in New Brunswick, Canada. Freshwater Invertebr. Biol. **4**: 201–207.

Payne, B.S., Miller, A.C., Hartfield, P.D., and McMahon, R.F. 1989. Variation in size demography of lotic populations of *Corbicula fluminea* (Müller). Nautilus, **103**: 78–82.

Potter, J.M., and Liden, L.H. 1986. *Corbicula* control at the Potomac River steam electric station Alexandria, Virginia. Am. Malacol. Bull. Spec. Ed. No. **2**: 53–58.

Prezant, R.S., and Chalermwat, K. 1984. Flotation of the bivalve *Corbicula fluminea* as a means of dispersal. Science (Wash., D.C.), **225**: 1491–1493.

Prokopovich, N.P. 1969. Deposition of clastic sediments by clams. J. Sediment. Petrol. **39**: 891–901.

Rodgers, J.H., Cherry, D.S., Clark, J.R., Dickson, K.L., and Cairns, J. 1977. The invasion of Asiatic clam, *Corbicula manilensis* in the New River, Virginia. Nautilus, **91**: 43–46.

SAS Institute, Inc. 1982. SAS users guide: basics, 1982 ed. SAS Institute Inc., Cary, N.C.

Sepkowski, J.J., and Rex, M.A. 1974. Distribution of freshwater mussels: coastal rivers as biogeographic islands. Syst. Zool. **23**: 165–188.

Sickel, J.B. 1973. New record of *Corbicula manilensis*

(Philippi) in the southern Atlantic slope region of Georgia. Nautilus, **87**: 11–12.

Sickel, J.B. 1976. An ecological study of the Asiatic clam, *Corbicula manilensis* (Phillipi, 1841), in the Altamaha River, Georgia, with emphasis on population dynamics, productivity and control methods. Ph.D. dissertation, Emory University, Atlanta, Ga.

Sickel, J.B. 1979. Population dynamics of *Corbicula* in the Altamaha River, Georgia. *In* Proc. 1st Int. *Corbicula* Symp. *Edited by* J.C. Britton. Texas Christian University Research Foundation, Fort Worth, Tex. pp. 69–88.

Sickel, J.B. 1986. *Corbicula* population mortalities: factors influencing population control. Am. Malacol. Bull. Spec. Ed. No. **2**: 89–94.

Stites, D.L. 1986. Secondary production and productivity in the sediments of blackwater rivers. Ph.D. dissertation, Emory University, Atlanta, Ga.

Stites, D.L. 1987. Population and production dynamics of an enchytraeid worm in a subtropical blackwater river. Can. J. Fish. Aquat. Sci. **44**: 1469–1474.

Stites, D.L., and Benke, A.C. 1989. Rapid growth rates of chironomids in three habitats of a subtropical blackwater river and their implication for *P:B* ratios. Limnol. Oceanogr. **34**: 1278–1289.

Trama, F.B. 1982. Occurrence of the Asiatic clam *Corbicula fluminea* in the Raritan River, New Jersey. Nautilus, **96**: 6–8.

Wallace, J.B., and Benke, A.C. 1984. Quantification of wood habitat in subtropical coastal plain streams. Can. J. Fish. Aquat. Sci. **41**: 1643–1652.

Wallace, J.B., Benke, A.C., Lingle, A.H., and Parsons, K. 1987. Trophic pathways of macroinvertebrate primary consumers in subtropical blackwater streams. Arch. Hydrobiol. (Suppl.), **74**: 423–451.

Welch, K.J., and Joy, J.E. 1984. Growth rates of the Asiatic clam, *Corbicula fluminea* (Müller), in the Kanawha River, West Virginia. Freshwater Invertebr. Biol. **3**: 139–142.

Williams, C.J., and McMahon, R.F. 1986. Power station entrainment of *Corbicula fluminea* (Müller) in relation to population dynamics, reproductive cycle and biotic and abiotic variables. Am. Malacol. Bull. Spec. Ed. No. **2**: 99–111.

Williams, C.J., and McMahon, R.F. 1989. Annual variation of tissue biomass and carbon and nitrogen content in the freshwater bivalve *Corbicula fluminea* relative to downstream dispersal. Can. J. Zool. **67**: 82–90.

1995

Annual Subscription Rates / Abonnements annuels*†‡

Publication	Volume	Code	Canada ($CAN) Institutional/ Collectif (CI)	Canada ($CAN) Personal/ Personnel (CP)	Foreign / Étranger ($US) Institutional/ Collectif (FI)	Foreign / Étranger ($US) Personal/ Personnel (FP)	Foreign / Étranger ($US) Air mail / Par avion Add / ajouter
Monthly / Mensuelle							
Biochemistry and Cell Biology / Biochimie et biologie cellulaire	73	44	242	88	242	90	75
Canadian Journal of Botany / Revue canadienne de botanique	73	45	417§	162	417§	174	150
Canadian Journal of Chemistry / Revue canadienne de chimie	73	46	477	146	477	155	150
Canadian Journal of Earth Sciences / Revue canadienne des sciences de la Terre	32	47	398	128	398	134	150
Canadian Journal of Fisheries and Aquatic Sciences / Journal canadien des sciences halieutiques et aquatiques	52	261	365	130	395	145	150
Canadian Journal of Forest Research / Revue canadienne de recherche forestière	25	54	366	119	366	123	75
Canadian Journal of Microbiology / Revue canadienne de microbiologie	41	48	279	110	279	115	75
Canadian Journal of Physics / Revue canadienne de physique	73	49	296	94	296	96	75
Canadian Journal of Physiology and Pharmacology / Revue canadienne de physiologie et pharmacologie	73	50	347	112	347	119	75
Canadian Journal of Zoology / Revue canadienne de zoologie	73	51	449	166	449	175	150
Bimonthly / Bimestrielle							
Canadian Journal of Civil Engineering / Revue canadienne de génie civil	22	52	287	92	287	97	75
Genome / Génome	38	70	262	108	262	116	75
Canadian Geotechnical Journal / Revue canadienne de géotechnique	32	53	226	88	226	95	50
Quarterly / Trimestrielle							
Environmental Reviews/ Dossiers environnement	3	244	163	57	163	63	25

*Price of regular single issues of all journals: institutional, $45.00; personal, $20.00. / Prix des numéros réguliers de toutes les revues : collectif, 45,00 $; personnel, 20,00 $.

†Rates include second-class postage. Canadian customers please include additional 7% GST (GST No. R121491807). In Quebec please add a further 6.5% QST to the total price including GST (QST No. 1006178088). / Affranchissement de deuxième classe compris. Clients canadiens veuillez ajouter 7% pour la TPS (N° de TPS R121491807). Au Québec veuillez ajouter un 6,5% de plus pour la TVQ au montant total incluant la TPS (N° de TVQ 1006178088).

‡Special rates apply for members of Canadian scientific and engineering societies if they subscribe through their respective societies. / Les tarifs spéciaux sont offerts aux membres des sociétés scientifiques et des sociétés de génie au Canada, s'ils s'abonnent par l'intermédiaire de leur société respective.

§Institutional subscriptions include a supplementary issue containing the *Proceedings of the Fifth International Mycological Congress*. / Les abonnés collectifs recevront un supplément où seront publiés les *Comptes rendus du Fifth International Mycological Congress*.

Subscriptions, renewals, requests for single or back numbers, and all remittances should be sent to Subscription Office, Research Journals, National Research Council of Canada, Ottawa, ON K1A 0R6, Canada. Remittances should be made payable to the Receiver General for Canada, credit National Research Council of Canada.
Enquiries: Helen Goulet: 613-993-9084; Fax No.: 613-952-7656; E-mail: research.journals@nrc.ca.

Subscriptions are entered for the calendar year. There are no refunds on cancelled subscriptions once delivery has begun.

Change of address - Send change of address information (complete old address, customer code, and new address) to Subscription Office, Research Journals, National Research Council of Canada, Ottawa, ON K1A 0R6, Canada.

Claims for missing numbers should be made within four months (North America) or six months (outside North America) following the date of publication. The publisher expects to supply missing numbers only when losses have been sustained in transit and when the reserve stock will permit.

Abonnements - Pour toutes les questions d'abonnements, paiements, demandes de vieux numéros de la revue, etc., on doit s'adresser au Bureau d'abonnements, Revues scientifiques, Conseil national de recherches du Canada, Ottawa, ON K1A 0R6, Canada. Les chèques et mandats seront formulés à l'ordre du Receveur général du Canada, au crédit du Conseil national de recherches du Canada.
Renseignements : Helen Goulet : 613-993-9084; N° de télécopieur : 613-952-7656 ; Courrier électronique : research.journals@nrc.ca.

La durée des abonnements correspond à l'année civile. Les abonnements annulés ne pourront être remboursés une fois que le premier numéro sera envoyé.

Changement d'adresse - Faire parvenir tous renseignements (ancienne adresse, code du client et nouvelle adresse) au Bureau d'abonnements, Revues scientifiques, Conseil national de recherches du Canada, Ottawa, ON K1A 0R6, Canada.

Les réclamations de numéros manquants doivent être adressées dans les quatre mois (en Amérique du Nord) ou les six mois (à l'étranger) suivant la date de publication. L'éditeur s'engage à remplacer les numéros manquants seulement lorsque les pertes ont été subies en transit et lorsque ses réserves le permettent.

Contents (concluded) / Table des matières (suite et fin)

Sarath G. Banneheka, Richard D. Routledge, Ian C. Guthrie, and James C. Woodey	**335–343**	Estimation of in-river fish passage using a combination of transect and stationary hydroacoustic sampling
Z. Zhang, R.J. Beamish, and B.E. Riddell	**344–352**	Differences in otolith microstructure between hatchery-reared and wild chinook salmon (*Oncorhynchus tshawytscha*)
Elaine M. Joseph, François M.M. Morel, and Neil M. Price	**353–357**	Effects of aluminum and fluoride on phosphorus acquisition by *Chlamydomonas reinhardtii*
John Janssen, Warren R. Jones, Audrey Whang, and Philip E. Oshel	**358–363**	Use of the lateral line in particulate feeding in the dark by juvenile alewife (*Alosa pseudoharengus*)
J.M. Hoenig, M.J. Morgan, and C.A. Brown	**364–368**	Analysing differences between two age determination methods by tests of symmetry
Gordon Swartzman, Emily Silverman, and Neal Williamson	**369–380**	Relating trends in walleye pollock (*Theragra chalcogramma*) abundance in the Bering Sea to environmental factors
Charles P. Madenjian	**381–390**	Removal of algae by the zebra mussel (*Dreissena polymorpha*) population in western Lake Erie: a bioenergetics approach
David C. Smith, Gwen E. Fenton, Simon G. Robertson, and Stephen A. Short	**391–401**	Age determination and growth of orange roughy (*Hoplostethus atlanticus*): a comparison of annulus counts with radiometric ageing
Darren M. Gillis, Randall M. Peterman, and Ellen K. Pikitch	**402–415**	Implications of trip regulations for high-grading: a model of the behavior of fishermen
James W. LaBaugh	**416–424**	Relation of algal biovolume to chlorophyll *a* in selected lakes and wetlands in the north-central United States
David L. Stites, Arthur C. Benke, and David M. Gillespie	**425–437**	Population dynamics, growth, and production of the Asiatic clam, *Corbicula fluminea*, in a blackwater river

National Research Council Canada
Ottawa, Canada K1A 0R6

Conseil national de recherches Canada
Ottawa, Canada K1A 0R6

Postage paid at Ottawa
Publications mail
Registration pending

Port payé à Ottawa
Poste-publication
Enregistrement en cours

Canadian Journal of Fisheries and Aquatic Sciences

Volume 52, Number 2, February 1995

Journal canadien des sciences halieutiques et aquatiques

Volume 52, numéro 2, février 1995

D.G. Worthington, P.J. Doherty, and A.J. Fowler	**233–242**	Variation in the relationship between otolith weight and age: implications for the estimation of age of two tropical damselfish (*Pomacentrus moluccensis* and *P. wardi*)
Åse I. Berge, Arne Berg, Hans Jørgen Fyhn, Trygg Barnung, Tom Hansen, and Sigurd O. Stefansson	**243–251**	Development of salinity tolerance in underyearling smolts of Atlantic salmon (*Salmo salar*) reared under different photoperiods
You-Gan Wang, Mervyn R. Thomas, and Ian F. Somers	**252–259**	A maximum likelihood approach for estimating growth from tag–recapture data
David A. Somerton and Bert S. Kikkawa	**260–267**	A stock survey technique using the time to capture individual fish on longlines
Claude B. Renaud, Klaus L.E. Kaiser, and Michael E. Comba	**268–275**	Historical versus recent levels of organochlorine contaminants in lamprey larvae of the St. Lawrence River basin, Québec
Claude B. Renaud, Klaus L.E. Kaiser, Michael E. Comba, and Janice L. Metcalfe-Smith	**276–282**	Comparison between lamprey ammocoetes and bivalve molluscs as biomonitors of organochlorine contaminants
Richard K. Booth, James D. Kieffer, Kevin Davidson, Alex T. Bielak, and Bruce L. Tufts	**283–290**	Effects of late-season catch and release angling on anaerobic metabolism, acid–base status, survival, and gamete viability in wild Atlantic salmon (*Salmo salar*)
Shane W. Frederick and Randall M. Peterman	**291–306**	Choosing fisheries harvest policies: when does uncertainty matter?
Moira M. Ferguson, Arunas P. Liskauskas, and Roy G. Danzmann	**307–314**	Genetic and environmental correlates of variation in body weight of brook trout (*Salvelinus fontinalis*)
R.J. Miller and J.T. Addison	**315–324**	Trapping interactions of crabs and American lobster in laboratory tanks
William W. Hsieh, Daniel M. Ware, and Richard E. Thomson	**325–334**	Wind-induced upwelling along the west coast of North America, 1899–1988

Continued on inside back cover / Suite au verso

Canada

Printed in Canada by / Imprimé au Canada par
University of Toronto Press, Inc.
Typesetting by / Typographie par
Aubut & Nadeau Services Inc.

0706-652X(199502)52:2;1-K